Advanced Sulfur Control Concepts

Final Report

Work Performed Under
Contract No.: **DE- AC21-94MC31258**

Prepared by

Apostolos A. Nikolopoulos
Santosh K. Gangwal
William J. McMichael
Jeffrey W. Portzer
Center for Energy Technology
RTI
P.O. Box 12194
Research Triangle Park, NC 27709-2194

Submitted to

U.S. Department of Energy
National Energy Technology Laboratory
3610 Collins Ferry Road
P.O. Box 880
Morgantown, WV 26507-0880

January 2003

Advanced Sulfur Control Concepts

Final Report

Work Performed Under
Contract No.: **DE- AC21-94MC31258**

Prepared by

Apostolos A. Nikolopoulos
Santosh K. Gangwal
William J. McMichael
Jeffrey W. Portzer
Center for Energy Technology
RTI
P.O. Box 12194
Research Triangle Park, NC 27709-2194

Submitted to

U.S. Department of Energy
National Energy Technology Laboratory
3610 Collins Ferry Road
P.O. Box 880
Morgantown, WV 26507-0880

January 2003

RTI INTERNATIONAL

DISCLAIMER

ABSTRACT

Conventional sulfur removal in integrated gasification combined cycle (IGCC) power plants involves numerous steps: COS (carbonyl sulfide) hydrolysis, amine scrubbing / regeneration, Claus process, and tail-gas treatment. Advanced sulfur removal in IGCC systems involves typically the use of zinc oxide-based sorbents. The sulfided sorbent is regenerated using dilute air to produce a dilute SO_2 (sulfur dioxide) tail gas. Under previous contracts (DE-AC21-93MC30010, DE_AC21-90MC27224), RTI (Research Triangle Institute) and the U.S. Department of Energy / National Energy Technology Laboratory (DOE/NETL) have developed the highly effective first generation Direct Sulfur Recovery Process (DSRP) for catalytic reduction of this SO_2 tail gas to elemental sulfur. This process is currently undergoing field-testing.

In this project, advanced concepts were evaluated to reduce the number of unit operations in sulfur removal and recovery. Substantial effort was directed towards developing sorbents that could be directly regenerated to elemental sulfur in an Advanced Hot Gas Process (AHGP). Development of this process has been described in detail in Appendices **A-F**. RTI began the development of the Single-step Sulfur Recovery Process (SSRP) to eliminate the use of sorbents and multiple reactors in sulfur removal and recovery. This process showed promising preliminary results and thus further process development of AHGP was abandoned in favor of SSRP.

The SSRP is a direct Claus process that consists of injecting SO_2 directly into the quenched coal gas from a coal gasifier, and reacting the H_2S-SO_2 mixture over a selective catalyst to both remove and recover sulfur in a single step. The process is conducted at gasifier pressure and 125 to 160°C. The proposed commercial embodiment of the SSRP involves a liquid phase of molten sulfur with dispersed catalyst in a slurry bubble-column reactor (SBCR).

From micro fixed bed reactor experiments, a total sulfur conversion of 99% with 35 ppm COS formation was achieved. Increasing pressure had a positive effect on sulfur removal. The SSRP process concept was found to be feasible in liquid sulfur medium. The liquid sulfur was shown to be inactive for direct reaction with reducing gases in coal gas. The process was scaled up to 50 cc of catalyst dispersed in 400 cc of molten sulfur in a continuous stirred tank reactor (CSTR). Conversion, as expected, was lower (up to 97%) in the CSTR compared to the fixed-bed reactor. COS formation up to 500 ppm occurred, but it could be reduced to 75 ppm by increasing the total flow and steam concentration and reducing the operating temperature.

A preliminary economic evaluation of SSRP with amine-based sulfur removal process showed that SSRP had the potential of reducing the cost of electricity in a 400 MWe IGCC plant by about 5%. It is recommended that the SSRP be tested with actual coal gas to evaluate the effect of coal gas contaminants. Further work is needed to mitigate COS slip in SSRP, e.g. by using a Claus catalyst with COS hydrolysis functionality. Kinetics of the SSRP reactions should be evaluated and solubility of sulfur gases and major coal gas components in molten sulfur should be measured to enable modeling of the SBCR based commercial embodiment. Following development of dual function catalysts, the process should be scaled up to a pilot-scale SBCR.

TABLE OF CONTENTS

Section **Page**

LIST OF FIGURES

LIST OF FIGURES (continued)

LIST OF FIGURES (continued)

Figure **Page**

LIST OF TABLES

LIST OF TABLES (continued)

ABBREVIATIONS AND ACRONYMS

%	percent
°C	degree Celcius
°F	degree Farenheit
A	Feed Procedure: SO_2 followed by coal gas (no steam)
A'	Feed Procedure: coal gas followed by SO_2 (no steam)
AHGP	Advanced Hot-Gas Process
AII	Adjustment for Interest and Inflation
ASU	Air Separation Unit
B	Feed Procedure: steam addition after Procedure A
B'	Feed Procedure: steam addition after Procedure A'
BET	Brunauer-Emmett-Teller
C	Feed Procedure: SO_2 followed by steam and then by coal gas
C'	Feed Procedure: coal gas followed by steam and then by SO_2
cc, cm^3	cubic centimeter
CGCU	Cold Gas Cleanup Unit
Cl	Chlorine
CO	Carbon Monoxide
CO_2	Carbon Dioxide
COE	Cost of Electricity
COR	Contracting Officer's Representative
COS	Carbonyl Sulfide
CSC	Convective Syngas Cooler
CSTR	Continuous Stirred Tank Reactor
D	Feed Procedure: steam followed by SO_2 and then by coal gas
D*	Feed Procedure: steam followed by simultaneous SO_2 & coal gas addition
D'	Feed Procedure: steam followed by coal gas and then by SO_2
DOE	Department of Energy
DSRP	Direct Sulfur Recovery Process
E-alumina	Engelhard alumina
Fe_2O_3	Iron Oxide
FPC	Fractional Process Contingency
G	Feed stream: H_2S-containing coal-derived synthesis gas
G'	Feed Procedure: coal gas followed by steam (no SO_2)
h, h^{-1}	hour, inverse hour
H_2	Hydrogen
H_2O	Water, steam
H_2S	Hydrogen Sulfide
Hg	Mercury
HGCU	Hot Gas Cleanup Unit
HGD	Hot Gas Desulfurization
HHV	high heating value
IC	Installed Cost
IGCC	Integrated Gasification Combined Cycle
L	liter
Lb	pound

ABBREVIATIONS AND ACRONYMS (continued)

Lb/D	pounds per day
LHV	low heating value
LP	Mechanical and/or Electrical Power
MDEA	Methyl Diethanolamine
MWe	Mega Watt electric
NC	North Carolina
NETL	National Energy Technology Laboratory
NH_3	Ammonia
NOC	Net Operating Cost
O	Feed stream: O_2 in N_2
OX	Operating Expenses
P	pressure
P.O.	Post Office
PPC	Process Plant Cost
ppm	parts per million
PSDF	Power Systems Development Facility
psia, psig	pounds per square inch (absolute, gage)
RSC	Radiant Syngas Cooler
RTI	Research Triangle Institute
S	Feed stream: SO_2 in N_2
SBCR	Slurry Bubble Column Reactor
scc	standard cubic centimeter
SCOT	Shell Claus Offgas Treating
SLPM	standard liters per minute
SO_2	Sulfur Dioxide
SSRP	Single-step Sulfur Recovery Process
SV	space velocity
Syngas	synthesis gas
T	temperature, ton
T/D	ton per day
TCR	Total Capital Requirement
TGA	Thermogravimetric Analysis
TPC	Total Plant Cost
TPI	Total Plant Investment
U.S.	United States
W	Feed stream: water in the form of steam
WV	West Virginia
X	Conversion
ZnO	Zinc Oxide

ACKNOWLEDGEMENTS

This research was supported by the National Energy Technology Laboratory (NETL) of the U.S. Department of Energy, under Contract No. DE-AC21-94MC31258.

RTI gratefully acknowledges the assistance and guidance of the current NETL contracting officer's representative (COR) on this project, Mr. Suresh Jain, and that of the former CORs, Mr. Daniel C. Cicero and Mr. Thomas P. Dorchak.

Valuable contributions to this work were provided by
Dr. Raghubir P. Gupta
Dr. James J. Spivey
Dr. Brian S. Turk
Mr. K. David Carter
Mr. David T. Coker
Mr. Gary B. Howe
Mr. Daryl D. Smith

EXECUTIVE SUMMARY

Background

Gasification of heavy feedstock (e.g. coal, petcoke, resid, biomass, and others) produces a raw syngas that must be cleaned before it can be used to produce electricity in a integrated gasification combined cycle (IGCC) power plant and/or synthetic liquid fuel using Fischer-Tropsch synthesis. The commercially proven process for gas cleaning involves quenching the gas to remove particulates and trace contaminants. Then a complex multi-step highly equipment intensive amine-based process consisting of an amine scrubber, regenerator, Claus plant, and tail-gas treatment plant to remove hydrogen sulfide (H_2S) and recover elemental sulfur follows. Also, conventional amine systems cannot effectively remove COS, and thus it needs to be hydrolyzed to H_2S first in a separate reactor.

To reduce the cost of electricity and increase efficiency of IGCC systems, research has been conducted on solid sorbent-based desulfurization systems for the past two decades. Advanced sulfur removal in IGCC systems involves typically the use of zinc oxide-based sorbents in a two-reactor system to reduce the H_2S and COS in syngas to below 10 ppmv:

$$\mathbf{ZnO + H_2S\ (or\ COS) \rightarrow ZnS + H_2O\ (or\ CO_2)} \qquad \textbf{(sulfidation)}$$

$$\mathbf{ZnS + 3/2\ O_2 \rightarrow ZnO + SO_2} \qquad \textbf{(regeneration)}$$

Due to the highly exothermic regeneration a dilute air stream is used. Unfortunately, this results in a problematic dilute SO_2 tail-gas that must be properly disposed. Conversion of this SO_2 to elemental sulfur is the most attractive disposal option. RTI has developed the highly effective first generation Direct Sulfur Recovery Process (DSRP) for catalytic reduction of the SO_2 tail-gas to elemental sulfur using a small slip stream of the syngas:

$$\mathbf{SO_2 + 2\ H_2\ (or\ 2\ CO) \rightarrow 1/n\ S_n + 2\ H_2O\ (or\ 2\ CO_2)}$$

The combined sorbent / DSRP process is slated to begin undergoing field-testing in 2003 under a separate DOE contract (DE-AC26-99FT 40675).

Project Goal

The ultimate goal of this project is to develop a simple economically attractive process to remove and recover elemental sulfur from raw syngas that can be easily integrated with the gasifier. To this end advanced concepts were evaluated to reduce the complexity of conventional and advanced sulfur removal/recovery process.

Advanced Hot Gas Process (AHGP)

The problematic dilute SO_2 tail gas produced by air regeneration not only needs disposal but also consumes 2 mol of valuable reducing component in syngas for every mol of SO_2 that is

converted to elemental sulfur. To alleviate this problem, substantial effort was directed towards an Advanced Hot Gas Process (AHGP) that uses a bimetallic zinc-iron sorbent. It aimed to eliminate the problematic SO_2 tail-gas using a two-stage regeneration reactor in which the sulfided sorbent flows down counter current to a regenerating gas containing SO_2 and O_2. The iron sulfide portion of the sorbent is regenerated by SO_2 in the upper stage whereas the zinc sulfide portion of the sorbent is regenerated by O_2 in the lower stage to provide heat and SO_2 for the upper stage:

$$\mathbf{FeS + \tfrac{1}{2}\, SO_2 \rightarrow FeO + \tfrac{3}{4}\, S_2 \text{ (upper stage)}}$$

$$\mathbf{ZnS + \tfrac{1}{2}\, O_2 \rightarrow ZnO + SO_2 \text{ (lower stage)}}$$

The effluent SO_2 and S_2 mixture is cooled to condense elemental sulfur, and the SO_2 is recycled. Following lab-scale feasibility studies, multi-cycle bench-scale tests were conducted at high-temperature, high-pressure conditions, to demonstrate quantitative elemental sulfur recovery. Preparations were made for a field test of the process at Southern Company Services Power Systems Development Facilities in early 2000. However, research emphasis had shifted toward lower temperature desulfurization due to the difficulty of trace containment (NH_3, Cl, Hg) removal at high temperature.

RTI began the development of a lower temperature Single Step Sulfur Recovery Process (SSRP). This process showed promising preliminary results and thus further process development of AHGP was abandoned in favor of SSRP. Complete details of the AHGP work are provided in Appendices **A-F** and the rest of this summary is dedicated to SSRP.

Single-Step Sulfur Recovery Process (SSRP)

Process Description

Unlike the amine-based process, the SSRP is a direct Claus process consisting of injecting SO_2 directly into the syngas to oxidize H_2S selectively on a suitable catalyst to both remove and recover sulfur in a single step.

$$\mathbf{2\, H_2S + SO_2 \rightarrow 3/n\, S_n + 2\, H_2O \qquad (Claus\ Reaction)}$$

The key differences between SSRP and the traditional Claus process are: a) in SSRP the catalytic oxidation of H_2S by SO_2 (Claus reaction) occurs selectively in a highly reducing atmosphere containing the highly reactive H_2 and CO fuel gas components, and b) the reaction is carried out at the pressure of the fuel gas (300-1200 psig). Higher pressures favor conversion due to more favorable thermodynamics. The temperature of the SSRP reactor is between 125°C (257°F, where sulfur liquefies) and 160°C (320°F, where liquid sulfur viscosity starts to increase rapidly). The SSRP uses a catalyst that is highly selective for the oxidation of H_2S as opposed to the undesirable oxidation of H_2 and CO that is present in great excess in the syngas.

Commercial Embodiment

The proposed commercial embodiment of the SSRP involves a liquid phase of molten sulfur with dispersed catalyst in a slurry bubble-column reactor (SBCR) as shown in Figure ES-1; it is currently under development. The advantages of this embodiment are: a) ease of scale-up and excellent temperature control; and b) the potential to eliminate the Claus plant, amine regenerator, and COS hydrolyzer, by removing COS in addition to H_2S in a single step.

Furthermore, the molten sulfur can act to:

- Moderate the reaction, minimize side reactions, and control the temperature; and
- Dissolve sulfur formed on the catalyst surface, thereby achieving recovery of product as well as a potential shift in thermodynamic limitations on sulfur formation.

Experimental

The SSRP was studied in a 5-cc micro fixed-bed reactor, a 1-cc molten sulfur bubbler and a 2.0-liter continuous stirred tank reactor containing up to 50 cc of catalyst and 400 cc of sulfur. Most of the experiments were conducted using an Engelhard alumina catalyst. Blank reactors and molten sulfur without catalyst were also evaluated.

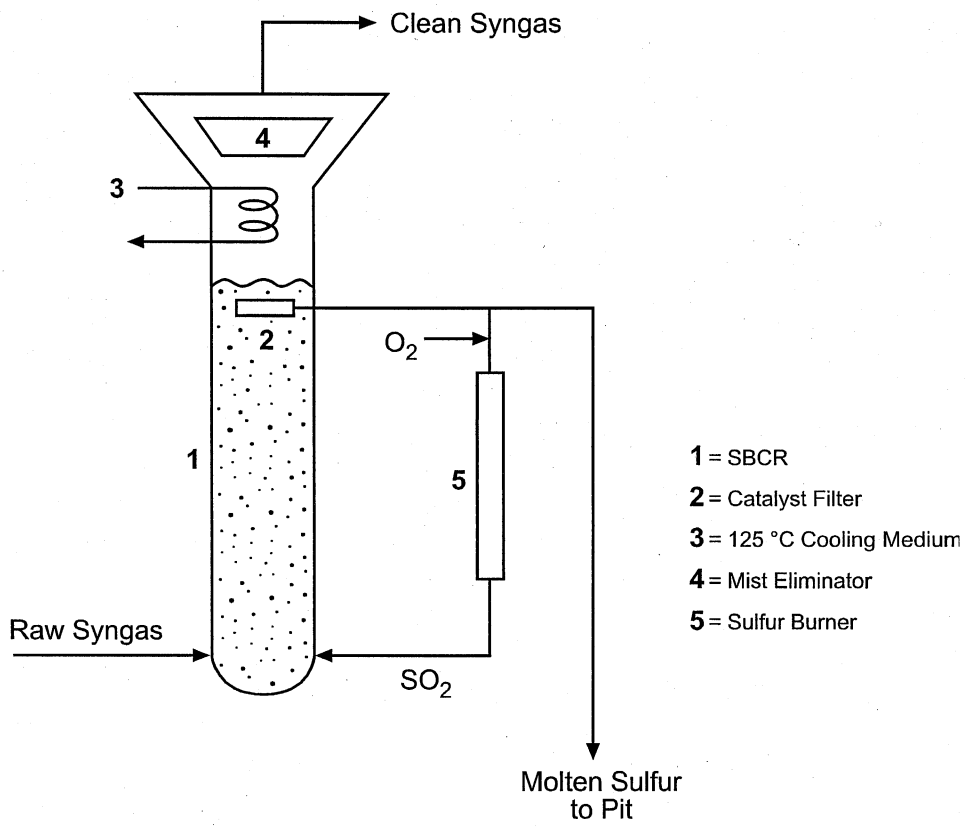

Figure ES-1. Proposed commercial embodiment of the Single-step Sulfur Recovery Process (SSRP)

Results and Accomplishments

- From micro fixed-bed reactor experiments, a total sulfur conversion of 99% with 35 ppm COS formation was achieved.
- The SSRP concept was shown to be feasible in the liquid sulfur medium.
- The process was scaled up to 50 cc of catalyst dispersed in 400 cc of molten sulfur in a continuous stirred tank reactor (CSTR).
- The liquid sulfur was shown to be inactive for direct reaction with reducing gases (H_2 and CO) in coal gas, but was shown to be active for the Claus reaction.
- Conversion, as expected, was lower in the CSTR (up to 97%) compared to fixed-bed reactor (up to 99%).
- COS formation up to 500 ppm occurred in the CSTR, but it could be reduced to 75 ppm by increasing the total feed flow and steam inlet concentration and reducing the reaction temperature.
- Runs over 100 hours duration demonstrated no deactivation of the catalyst. This suggested that the sulfur formed on the catalyst surface dissolved into the molten sulfur medium.
- A patent was filed on the process and papers were presented at the Pittsburgh Coal Conference (September 2002) and AIChE Meeting (November 2002).
- A preliminary economic comparison of the SSRP with a conventional amine-based process showed the potential to reduce the installation cost, operating cost, and cost of electricity of a 400 MWe IGCC plant by about 5%.

Recommendations for Future Work

Further work is needed to minimize COS formation in SSRP by (1) preventing COS formation during SSRP and (2) promoting COS hydrolysis and hydrogenation during SSRP. Fundamental research is needed to develop proper catalysts by combining Claus and COS conversion functionalities. Kinetics of the SSRP reactions should be evaluated. The solubility of sulfur gases and major coal gas components in molten sulfur should be measured to enable modeling of the SBCR commercial embodiment. The process should be scaled up to a pilot-scale SBCR.

1. INTRODUCTION

1.1. Background

Gasification of heavy feedstock (e.g. coal, petcoke, resid, biomass, and others) produces a raw syngas that must be cleaned before it can be used to produce electricity in an IGCC power plant and/or synthetic liquid fuel using Fischer-Tropsch synthesis. The commercially proven process for gas cleaning involves quenching the gas to remove particulates and trace contaminants. Then a complex multi-step highly equipment intensive amine-based process consisting of an amine scrubber, regenerator, Claus plant and tail gas treatment plant to remove H_2S and recover elemental sulfur follows. Also conventional amine systems cannot effectively remove COS which needs to be hydrolyzed first in a separate reactor.

To reduce the cost of electricity and increase efficiency of IGCC systems, research has been conducted on solid sorbent-based desulfurization systems for the past two decades (*Cicero et al., 1999; Gangwal et al., 1997; Thambimuthu, 1993*). This research and development effort has been spear headed by the Department of Energy's (DOE) National Energy Technology Laboratory (NETL) and its predecessor agencies since 1980.

Sorbent-based desulfurization typically use a zinc-oxide-based sorbent and is carried out in a two-reactor system consisting of a desulfurizer and an air-regenerator:

$$\mathbf{ZnO + H_2S \rightarrow ZnS + H_2O} \qquad \textbf{(desulfurization)}$$

$$\mathbf{ZnS + 3/2\ O_2 \rightarrow ZnO + SO_2} \qquad \textbf{(regeneration)}$$

Early developments emphasized fixed-bed reactors. The highly exothermic regeneration led to a move away from fixed beds toward moving beds (*Ayala et al., 1995*) and fluidized-beds (*Gupta and Gangwal, 1992*) fluidized-bed reactors, in particular transport reactors, are currently receiving the maximum emphasis (*Gangwal et al., 2002*[a]) due to several potential advantages including smaller foot print (lower cost), ability to continuously add and remove sorbent and ability to control the highly exothermic regeneration. However an attrition-resistant sorbent that can withstand stresses induced by fluidization, transport, chemical transformation, and rapid temperature swings must be developed.

Air regeneration leads to a problematic dilute SO_2 tail gas that must be disposed. Converting to a salable product- sulfuric acid or elemental sulfur- is an attractive option. Elemental sulfur is particularly attractive because it is the smallest volume sulfur product and because it can be stored easily, transported over long distances, readily disposed, or sold. Direct Sulfur Recovery Process (DSRP), a promising process, is currently in an advanced development stage to treat the SO_2 tail gas (*Gangwal and Portzer, 2002*). In this process, the SO_2 is catalytically reduced to elemental sulfur at the pressure and temperature condition of the tail gas using a small slipstream of the syngas:

$$\mathbf{SO_2 + 2\ H_2S\ (or\ 2\ COS) \rightarrow 1/n\ S_n + 2\ H_2O\ (or\ 2\ CO_2)}$$

The combined sorbent/DSRP process is slated to begin undergoing field-testing this year under a separate DOE contract with RTI (DE-AC26-99FT 40675). In this contract, a promising zinc-oxide sorbent called RTI-3 (*Gangwal et al., 2002*[a]) will be tested using a KBR transport reactor system at the ChevronTexaco Montebello 3 ton/day gasifier. DSRP will be tested on the full tail gas flow of about 2200 scfh.

1.2. Objective

The original goal of this project was the development of simpler and economically superior processing of known regenerable sorbents used for sulfur control in advanced IGCC systems. The major objective was to produce an elemental-sulfur by product. Through contract modification the goal was broadened to also include a novel approach to produce elemental sulfur. These modifications directed an investigation into direct catalytic oxidation of H_2S to elemental sulfur in the presence of the raw syngas components including H_2, CO, H_2O and CO_2.

1.3. Project Tasks and Chronology

The original project Tasks were as follows:

Task 1. Assessment of Concepts
Task 2. Evaluation of Selected Concepts
Task 3. Laboratory Development
Task 4. Feasibility Demonstration
Task 5. Process Performance, Evaluation, and Economics

Work on the first two tasks above led to the Advanced Hot-Gas Process (AHGP) concept, which aimed to avoid the problematic SO_2 tail gas from regeneration. AHGP was developed through laboratory and bench-scale testing in Tasks 3 and 4, and developed to the point of field-testing. A process model was developed and an economic evaluation was conducted in comparison to DSRP in Task 5. Section 2 describes the AHGP and its development in more detail.

As mentioned above, contract modifications directed an investigation into direct catalytic oxidation of H_2S. This work lead to the discovery of a highly promising process called Single-step Sulfur Recovery process (SSRP). This process works at lower temperature following quench of the high-pressure syngas. As the quench removes most of the trace contaminants and complies better with the DOE's Vision 21 plant, DOE's emphasis changed towards lower-temperature operation. As a result, the field test of the high-temperature AHGP was abandoned and project resources were directed toward development of SSRP. The SSRP work was conducted under the following Tasks:

Task 1. Literature Review
Task 2. Lab-Scale Testing
Task 3. Bench-Scale Testing
Task 4. Preliminary Economic Evaluation

Tasks 1 to 3 of SSRP are described in detail in Section 3. Task 4 is described in Section 4.

2. ADVANCED HOT GAS PROCESS (AHGP)

2.1. Introduction

As mentioned in Section 1, DSRP results in a problematic dilute SO_2 tail gas that needs to be disposed and results in the energy penalty of consumption of 2 mol of reductants in syngas for every mol of sulfur. AHGP is a second-generation process that regenerates the sulfided sorbent directly to elemental sulfur using SO_2. Thus a dilute SO_2 tail gas is not produced and potentially the energy penalty is avoided. SO_2 regeneration involves the reaction of nearly pure SO_2 with sulfided sorbent at elevated temperature and pressure. Under these conditions, elemental sulfur is the only product predicted from thermodynamics.

Some H_2S sorbents based on metal oxides other than zinc oxide—iron oxide, for example—can be regenerated following sulfidation using SO_2 to directly produce the desirable elemental sulfur byproduct according to the following sulfidation and regeneration reactions:

$$\mathbf{FeO + H_2S \rightarrow FeS + H_2O}$$

$$\mathbf{2\ FeS + SO_2 \rightarrow 2\ FeO + 3/2\ S_2}$$

Based on a theoretical evaluation of a number of potential sorbent candidates, iron- and zinc-based regenerable sorbents were chosen for experimental evaluation. Iron oxide was considered the most promising candidate based on a combination of factors—desulfurization efficiency, SO_2 regenerability, cost, and knowledge base. Zinc oxide is a leading candidate due to its excellent desulfurization efficiency, its extensive knowledge base, and its low cost.

Although zinc sulfide (ZnS) shows essentially no SO_2 regenerability at temperatures of interest, zinc oxide can act as a polishing agent when combined with iron oxide to remove H_2S down to very low levels. Advantageously, the ZnS can be regenerated using air to produce the SO_2 needed for regeneration of the iron sulfide (FeS).

2.2. Process Description

Based on a feasibility study, initial laboratory testing, and successful bench-scale testing of several sorbent formulations, AHGP was conceptualized as shown in Figure 2.1. The primary elements of the process are a single desulfurization reaction stage, but two stages of regeneration: an SO_2 regeneration stage, and an oxygen regeneration stage. The sulfided sorbent flows counter-currently to an internally recirculating regeneration gas (high concentration SO_2). The desulfurization of the coal gas (sulfidation of the sorbent) takes place at about 450°C at the pressure of the coal gas (typically 2.0 MPa) in the desulfurization reactor. This would most likely be a "transport" type fluidized-bed reactor, resulting in a research focus on attrition-resistant sorbents.

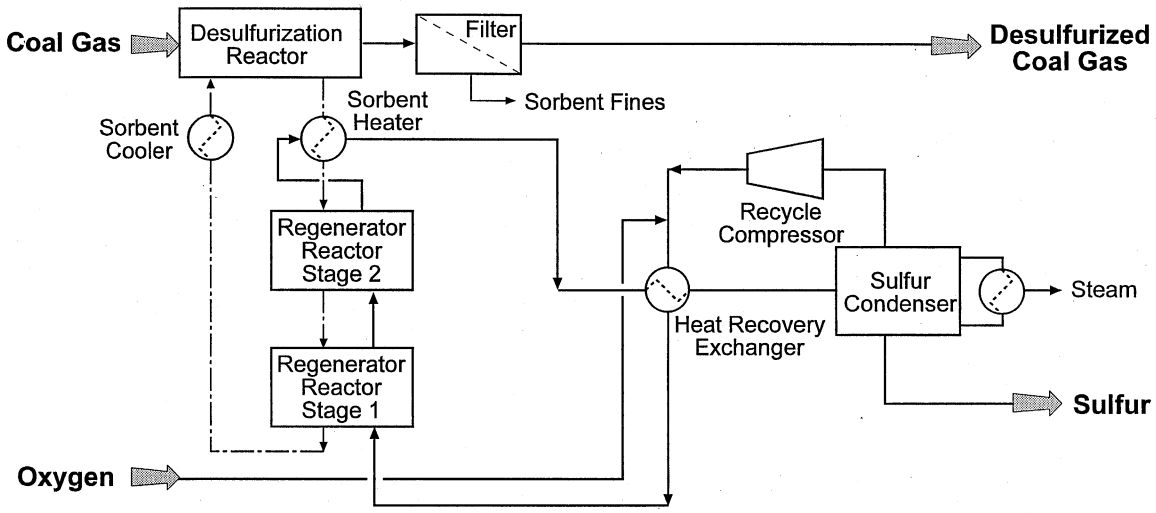

Figure 2.1. Conceptualized Advanced Hot Gas Process (AHGP)

The sulfided sorbent enters a multistage reaction vessel to be heated to 600°C using waste heat from the regenerated sorbent. This reactor is envisioned to be a bubbling-type fluidized bed. The heated sorbent passes to Stage 2 of the regenerator to contact the re-circulating SO_2 gas stream. The elemental sulfur formed exits in the gaseous state. The partially regenerated sorbent then passes into Stage 1 (the lowest stage) of the regenerator, where oxygen is added to the regeneration gas. In this heat-integrated process, the energy from the exothermic O_2 regeneration is used to drive the endothermic SO_2 regeneration. The regenerated sorbent is then cooled and re-circulated to the desulfurization reactor.

The regeneration off-gas exiting from Stage 2 is cooled to condense out the sulfur, which is removed as a molten product. The exit gas from the sulfur condenser is then compressed slightly (to recover the pressure drop losses from re-circulation) and is reheated by countercurrent exchange with the hot regeneration off-gas. With control of the ratio of iron and zinc in the sorbent, and by balancing the amount of oxygen supplied to Stage 1 with the amount of elemental sulfur that is actually being produced, the SO_2 material balance of the re-circulation loop can be maintained. For startup purposes, an external supply of liquid SO_2 could be used to charge the re-circulation loop.

2.3. Development of AHGP

The development of AHGP was carried out under the following Tasks:

Task 1. Assessment of Concepts
Task 2. Evaluation of Selected Concepts
Task 3. Laboratory Development
Task 4. Feasibility Demonstration
Task 5. Process Performance, Evaluation and Economics

Work under Tasks 1 and 2 is described in detail in Appendix **A**. Concepts to recover sulfur (as elemental sulfur) from sulfided sorbents without producing the problematic SO_2 tail gas were assessed and evaluated. The following alternative regeneration concepts were evaluated for the sulfided sorbent:

- Partial oxidation.
- Steam regeneration.
- SO_2 regeneration.

Based on this evaluation, all alternative regeneration concepts were eliminated except for SO_2 regeneration. Laboratory development of the SO_2 regeneration concept was conducted under Task 3 using thermogravimetric analysis (TGA) and a high-pressure lab-scale reactor as shown in Appendix **A**. Zinc and iron sorbents were chosen as the primary candidates for the SO_2 regeneration concept, based on literature information and thermodynamic calculations. Several sorbents were prepared and screened. Laboratory tests of SO_2 regeneration of a promising zinc-iron sorbent (R-5) showed that the iron portion of the sorbent could be completely regenerated with SO_2. The zinc portion was regenerated using O_2. This two-step regeneration led to the concept of the AHGP (Figure 2.1).

A high-temperature, high-pressure (HTHP) bench-scale reactor system was commissioned to test the AHGP under Task 4. Numerous test cycles were conducted for candidate sorbents as described in Appendix **B**. This led to the development of a proprietary R-5-58 sorbent, which was tested for 50 cycles as described in detail in Appendices **C** and **D**. The SO_2 regeneration step accounted for 55 to 70% of the total regeneration of the sorbent compared to a theoretical limit of 80% based on complete regeneration of the iron component by SO_2.

Sorbent improvement studies to further improve both reactivity and attrition-resistance were conducted as detailed in Appendix **D**. Numerous sorbents were prepared and tested. The total active metal component of R-5-58 was 20 wt% ($ZnO + Fe_2O_3$) on an inert support. Attempts were made to prepare attrition resistant sorbents with higher ZnO and Fe_2O_3 (closer to 90% total) and a silica-based binder. Cyclic tests of these sorbents showed that although attrition resistance was improved, the reactivity was reduced due to the reaction of the silica with the zinc and iron.

Simultaneous to these studies, an engineering and economic comparison of AHGP with DSRP was conducted under Task 5 as detailed in Appendices **E** and **F**. Aspen Plus process simulations of DSRP and AHGP revealed the complexity of both HGD process. The capital cost of AHGP was higher than that of DSRP but operating costs were lower. For high sulfur coal (>3%), a preliminary comparison shows that the total cost of implementing AHGP will be less than that of DSRP after just 2 years of operation. AHGP however is more complex as a process.

Plans were made for a field test of AHGP at the Power System Development Facility (PSDF). At about this time, a more promising process called SSRP was discovered and field test plans for AHGP were abandoned in favor of SSRP. SSRP development is described in detail in the next section. The rest of this report is dedicated to SSRP.

3. SINGLE-STEP SULFUR RECOVERY PROCESS (SSRP)

3.1. Introduction

As an alternative to AHGP (described in the previous section), the Single-Step Sulfur Recovery Process (SSRP) is being developed as a simple, economically attractive process to remove and recover sulfur from raw syngas that can be integrated with coal-based integrated gasification combined cycle (IGCC) power generation. The SSRP involves the direct catalytic oxidation of hydrogen sulfide (H_2S) to elemental sulfur using sulfur dioxide (SO_2) in the presence of >60vol% of highly reducing fuel gas components such as hydrogen (H_2) and carbon monoxide (CO).

RTI has conducted research on SSRP and developed it to the point that a patent application was recently filed (*Gangwal et al., 2002*[b]). Based on the promising results of SSRP testing in a lab-scale fixed-bed micro-reactor, a bench-scale 2-liter continuous stirred tank reactor (CSTR) with the catalyst suspended in molten sulfur was used to scale up the process. Results demonstrated the feasibility of sulfur recovery from syngas in a molten sulfur / catalyst slurry. Optimization of reaction conditions (temperature, pressure, feed composition, contact time) and catalyst (type, activation procedure) are critical for enhanced sulfur removal and suppressing the undesirable formation of carbonyl sulfide (COS).

3.2. Process Description

The SSRP is a direct Claus process that consists of injecting SO_2 directly into the quenched coal gas from a coal gasifier, and reacting the H_2S-SO_2 mixture over a selective catalyst to both remove and recover sulfur in a single step:

$$\mathbf{2\ H_2S + SO_2 \rightarrow {}^{3}/_{n}\ S_n + 2\ H_2O} \qquad (3.1)$$

The key differences between SSRP and the traditional Claus process are: a) in SSRP the catalytic oxidation of H_2S by SO_2 (Claus reaction) occurs selectively in a highly reducing atmosphere containing the highly reactive H_2 and CO fuel gas components, and b) the reaction is carried out at the pressure of the fuel gas (300-1200 psig). The catalyst used needs to be highly selective for the Claus reaction (1) in order to minimize undesirable side reactions such as:

$$3\ H_2 + SO_2 \rightarrow H_2S + 2\ H_2O \qquad (3.2)$$
$$2\ H_2 + SO_2 \rightarrow {}^{1}/_{n}\ S_n + 2\ H_2O \qquad (3.3)$$
$$H_2 + {}^{1}/_{n}\ S_n \rightarrow H_2S \qquad (3.4)$$
$$CO + SO_2 \rightarrow COS + O_2 \qquad (3.5)$$
$$2\ CO + SO_2 \rightarrow {}^{1}/_{n}\ S_n + 2\ CO_2 \qquad (3.6)$$
$$CO + H_2S \rightarrow COS + H_2 \qquad (3.7)$$
$$CO + {}^{1}/_{n}\ S_n \rightarrow COS \qquad (3.8)$$
$$CO_2 + H_2S \rightarrow COS + H_2O \qquad (3.9)$$

The temperature range of the SSRP is 125°C (257°F) to 160°C (320°F). The lower limit is to prevent solidification (at about 121°C) and the upper limit is because of a rapid increase in liquid sulfur viscosity above 160°C. The operating pressure for SSRP can be the same as the coal gas pressure. In fact, as shown below, higher pressure favors higher sulfur conversion in SSRP. Texaco gasifiers typically operate from 300 up to 1200 psig.

The proposed commercial embodiment of the SSRP involves a liquid phase of molten sulfur with dispersed catalyst in a slurry bubble-column reactor (SBCR, Figure 3.1) and is currently under development (*Gangwal et al, 2002*[b]).

The advantages of this embodiment are: a) ease of scale-up and excellent temperature control; and b) the potential to eliminate the Claus plant, amine regenerator, and COS hydrolyzer, by removing COS in addition to H_2S in a single step.

The molten sulfur can act to:

- Moderate the reaction, minimize side reactions, and control the temperature; and
- Dissolve sulfur formed on the catalyst surface, thereby achieving recovery of product as well as a potential shift in thermodynamic limitations on sulfur formation.

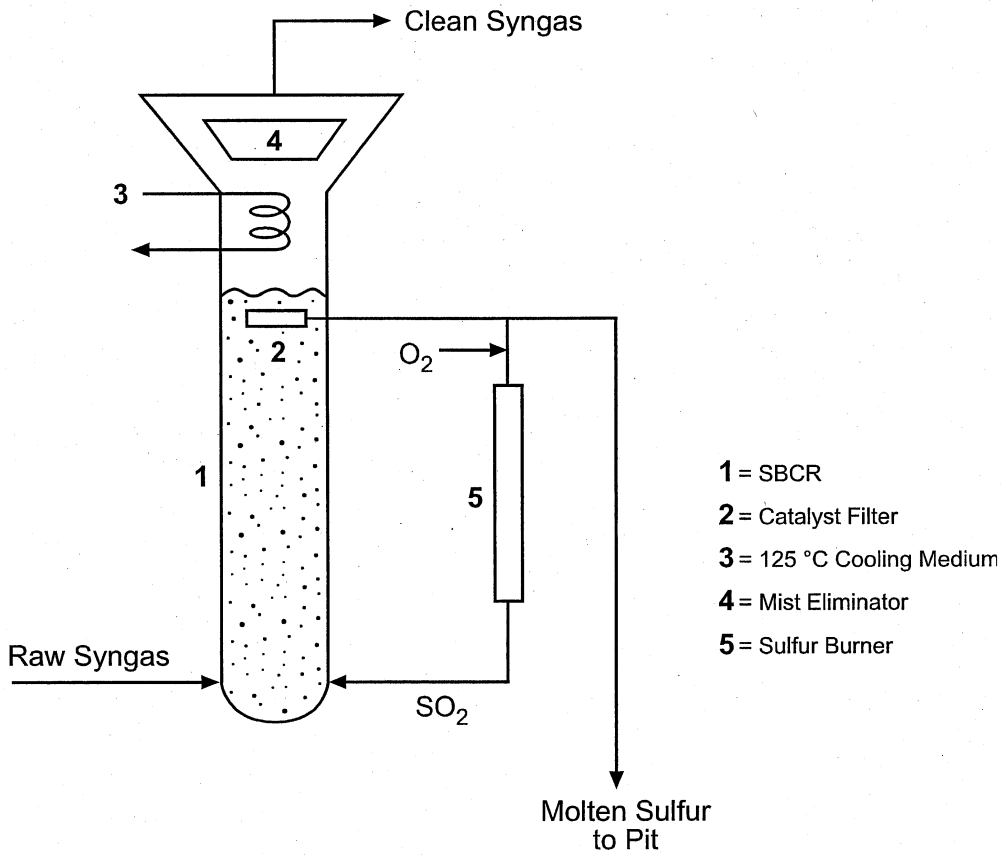

Figure 3.1. Proposed commercial embodiment of the Single-step Sulfur Recovery Process

3.3. SSRP Development

The development of SSRP was conducted under 4 tasks:

Task 1. Literature Review

This task involved a literature review on candidate processes and materials for the direct catalytic oxidation of H_2S in coal-derived synthesis gas. It is presented in Appendix **G**. The review of the literature did not identify any studies in which the Claus reaction was carried out in the presence of large concentrations of CO and H_2. *Pearson (1976)* studied the Claus reaction at temperatures between 135°C and 175°C using a Claus tail gas containing ca. 3vol% CO+H_2. Conversion of H_2S+SO_2 was 96-98% until his active alumina catalyst reached 60% sulfur loading in the pores. The conversion then declined rapidly to 31%.

Even though the SSRP was counter-intuitive (Claus reaction in the presence of high levels of H_2 and CO), it was decided to go ahead with the initial lab-scale work, since no studies appeared in the literature, especially at high pressure. The very high level of the desirable Claus reaction that was observed in the first experiment undertaken encouraged the accelerated development of SSRP.

Task 2. Lab-Scale Testing

This task included an extensive catalyst screening study on the Claus reaction in the presence of syngas in the feed, using a fixed-bed micro-reactor, and the evaluation of the concept of performing SSRP in a molten sulfur medium, using a micro-bubbler reactor. The lab-scale testing was conducted in a small fixed-bed reactor and a micro-bubbler. These reactor systems and their results are described in detail in Sections 3.3.1 and 3.3.2.

Task 3. Bench-Scale Testing

This task involved a scale-up of the SSRP in molten sulfur using the best catalyst from the screening studies of the previous Task, using a 2-liter continuous stirred tank reactor (CSTR). This apparatus and its results are described in Section 3.3.3.

Task 4. Preliminary Economic Evaluation

This task included a preliminary economic evaluation of SSRP in comparison to amine scrubbing for removing H_2S and recovering sulfur from a coal-derived synthesis gas produced by a Texaco gasifier. The preliminary economic evaluation of the SSRP is described in Section 4.

3.3.1. Catalyst screening: SSRP in a fixed-bed micro-reactor

The SSRP reaction was studied in a 0.5-inch fixed-bed micro-reactor at 125-160°C (257-320°F) and 200-350 psig, over various commercial catalysts such as alumina, a precipitated iron oxide, and a silica gel. The stainless steel reactor was coated with silica to minimize reactions on its walls. The reactant feed consisted of a simulated Texaco coal gas stream (containing 50.8% CO, 35.7% H_2, 12.5% CO_2, and 1.0% H_2S), and a 2.5% SO_2/N_2 stream. A syringe pump provided a constant flow of steam (through water evaporation) into the coal gas line.

A typical reaction composition included ca. 8400 ppm H_2S, ca. 4200 ppm SO_2, 10% steam, and a balance of simulated Texaco gasifier gas (N_2, CO_2, H_2, and CO). A back-pressure-control valve, located downstream of the condenser, controlled the reactor and condenser pressure.

The outlet gases were analyzed in a gas chromatograph with a thermal conductivity detector (TCD) and a flame photometric detector (FPD), for high (above 500 ppm) and low (down to single-digit ppm) sulfur-gas concentrations, respectively. A schematic of the SSRP reaction system is shown in Figure 3.2.

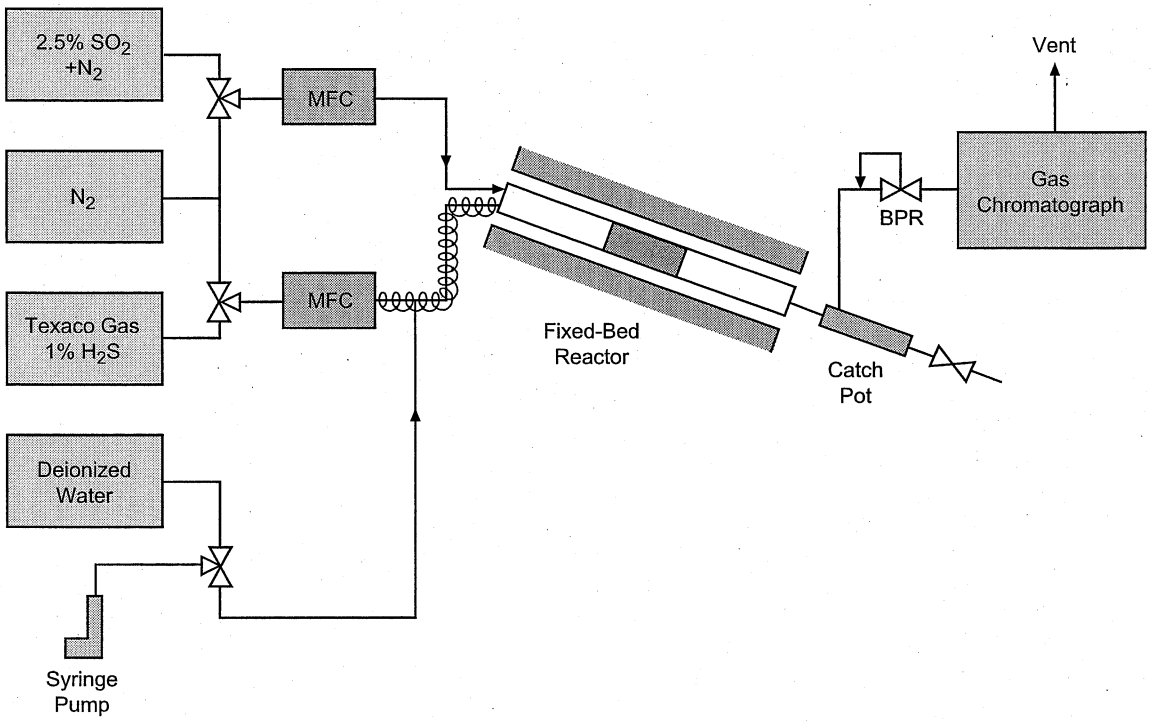

Figure 3.2. Schematic of the SSRP micro-reactor system for catalyst screening

Preliminary reaction experiments involved evaluating the intrinsic activity of the silica-coated (silanized) micro-reactor of Fig. 3.2 in the absence of a catalyst; only inert quartz-wool was loaded instead. The blank reactor activity was measured as a function of temperature under a dry feed (no steam addition), 3950 ppm SO_2 and 8750 ppm H_2S ($H_2S/SO_2 = 2.2$), and feed flow of 270 sccm at 200 psig. After establishing pseudo steady state at 60°C, the reaction temperature was increased to 120°C in 20°C steps, then to 140°C and finally to 160°C in 10°C steps.

The effect of temperature on the blank reactor activity is given in Figure 3.3. The measured H_2S and SO_2 conversions were less than 6% at any temperature within the 60-160°C range, indicating a minimal reactivity of the blank reactor. All conversions decreased with increasing reaction temperature, suggesting an adsorption-controlled reaction on the reactor walls (homogeneous, and kinetically-controlled or desorption-controlled heterogeneous reaction would be favored with increasing temperature). The formation of COS was also minimal (less than 30 ppm).

The effect of reaction pressure on the blank reactor activity was then examined at 160°C with a feed H_2S/SO_2 ratio of 2.0. The reaction pressure was increased from 200 psig to 300 and then to 400 psig. The results are given in Table 3.1. The sulfur removal activity (expressed as H_2S+SO_2 conversion) increased from ca. 4% to ca. 7%, and the COS formation from 30 ppm to 60 ppm. Thus, under the examined reaction conditions and within the pressure range of interest, the blank silanized reactor exhibits only minimal activity for both the Claus and COS formation reaction.

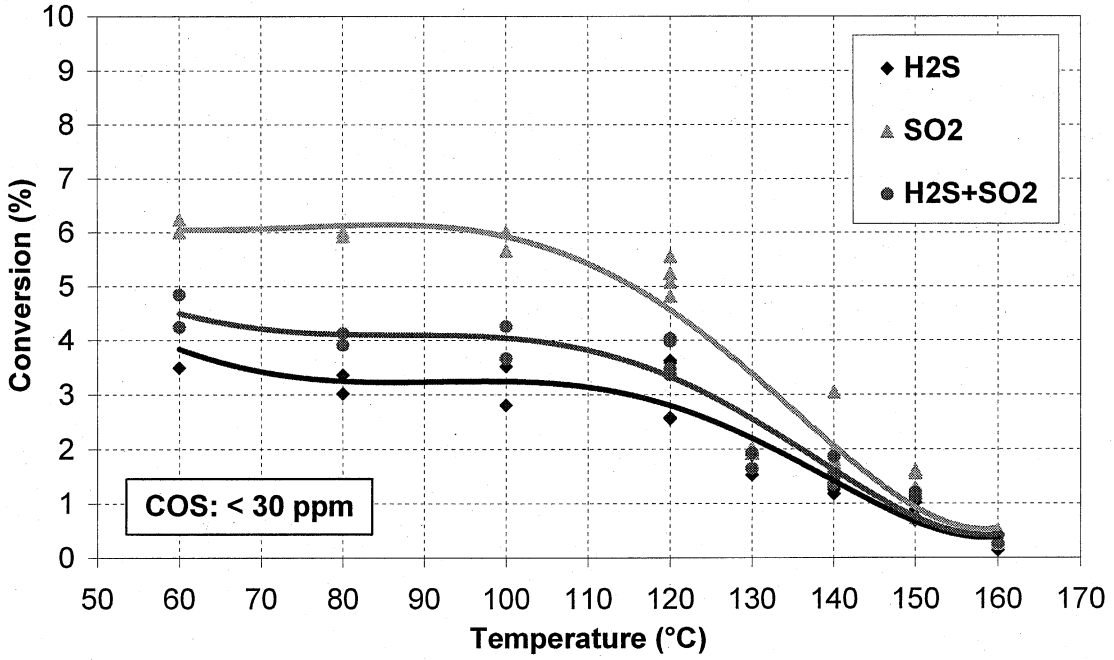

Figure 3.3. Effect of reaction temperature on H_2S, SO_2, and H_2S+SO_2 conversion, and COS formation for SSRP in blank reactor; P: 200 psig; F: 270 sccm; H_2S: 8750±150 ppm; SO_2: 3950±150 ppm; steam: 0%

Table 3.1. Effect of pressure on H_2S, SO_2, and H_2S+SO_2 conversion, and COS formation, for SSRP in blank reactor; T: 160°C; H_2S: 8500 ppm; SO_2: 4300 ppm; steam: 0%

	Conversion (%)			COS formation
Pressure (psig)	**H_2S**	**SO_2**	**H_2S+SO_2**	**(ppmv)**
200	3.8	3.5	3.7	30
300	4.9	5.3	5.0	40
400	6.9	6.1	6.7	60

The effect of addition of 10% steam on the blank reactor activity at 160°C was also examined. After establishing a pseudo steady state under a feed flow of 270 sccm with a feed H_2S/SO_2 ratio of 2.0 (dry feed) 30 sccm of steam were fed into the reactor, thus increasing the total feed flow to 300 sccm, while maintaining the reaction temperature and pressure. The comparative results are given in Table 3.2. The addition of 10% steam in the feed enhanced the sulfur removal activity of the blank reactor extensively (from ca. 4% to ca. 52%). The formation of COS increased only to a much lesser extent (from 30 ppm to 60 ppm).

The strong promotional effect of steam onto the H_2S+SO_2 reaction could be related to an enhancement in the adsorption of the reactant species onto the reactor walls, possibly through decoking of the reactor surface, or through formation of a reaction complex. Under conditions of industrial interest the H_2S-containing synthesis gas would typically be saturated with steam. Thus, the reactor intrinsic sulfur removal activity can be significant and should not be overseen.

Since the impact of steam addition on the activity of the blank reactor was found to be significant, the effect of reaction pressure on the blank reactor activity was also examined in the presence of steam in the feed. After reaching a pseudo-steady state at 156°C and 200 psig, under a total feed flow of 200 sccm with 10% steam and a feed H_2S/SO_2 of 2.2, the reaction pressure was increased to 300 psig and then to 380 psig. The results are shown in Table 3.3. Higher reaction pressures enhance the adsorption of the reactant species onto the reactor walls, thus promoting the heterogeneous H_2S+SO_2 reaction. The formation of COS was again maintained at low levels (30 ppm or lower).

Table 3.2. Effect of 10% steam addition on H_2S, SO_2, and H_2S+SO_2 conversion, and COS formation, for SSRP in blank reactor; T: 160°C; H_2S: 8500 ppm; SO_2: 4300 ppm

	Conversion (%)			COS formation
Steam (%)	**H_2S**	**SO_2**	**H_2S+SO_2**	**(ppmv)**
0 (dry feed)	3.8	3.5	3.7	30
10 (steam addition)	50.7	54.3	51.9	60

Table 3.3. Effect of pressure on H_2S, SO_2, and H_2S+SO_2 conversion, and COS formation, for SSRP in blank reactor; T: 156°C; H_2S: 8500 ppm; SO_2: 4300 ppm; steam: 10%

	Conversion (%)			COS formation
Pressure (psig)	**H_2S**	**SO_2**	**H_2S+SO_2**	**(ppmv)**
200	59.2	62.3	60.2	< 30
300	69.7	78.3	72.3	< 30
380	73.8	89.1	78.5	30

Prior to the experiments with the blank silanized reactor, another series of preliminary experiments was conducted using a similar stainless steel reactor that was not silanized. The sulfur removal activity (measured as H_2S+SO_2 conversion) of the blank stainless steel non-silanized reactor was compared to that of the blank silanized reactor at 156°C and 300 psig. The total feed flow was 86 sccm and 200 sccm, respectively. The SO_2 feed concentration was 4500ppm and 3800ppm, and the H_2S concentration was 9300ppm and 8500ppm, respectively, all other concentrations being the same. The comparative results are given in Table 3.4. The sulfur removal activity of the two reactor types was apparently the same, within the uncertainty of the different total flow. The formation of COS, however, was lower by more than one order of magnitude in the case of the silanized reactor.

The SSRP reaction experiments were then conducted by loading the silica-coated reactor with 5 cm^3 of an alumina catalyst (**E-alumina**). For this reactor system, the efficiency for sulfur removal was evaluated in relation to the procedure under which the reactive gases were fed into the reactor, at other conditions (temperature, pressure) constant.

Initially 4300ppm of SO_2 in inert gas (N_2) was fed into the reactor at a feed flow of 540 sccm and the system was allowed to reach pseudo-steady state. Then, a part of the inert gas flow was substituted by an equal syngas flow so as to get a ratio of H_2S/SO_2 of ca. 2 in the absence of steam (Procedure **A**). The activity for sulfur removal declined from ca. 71% to ca. 42% in a time period of 132 min, as shown in Figure 3.4. The measured COS outlet concentration at 132 min on stream was 575ppm.

Table 3.4. Sulfur removal activity in blank non-silanized reactor vs. blank silanized reactor at 156°C and 300 psig; steam: 10%

	Temperature	Flow	H_2S/SO_2	Conversion (%)	COS formation
Reactor	**(°C)**	**(sccm)**	**Ratio (-)**	**H_2S+SO_2**	**(ppmv)**
Non-Silanized	156	86	2.1	83.0	550
Silanized	156	200	2.2	72.3	< 30

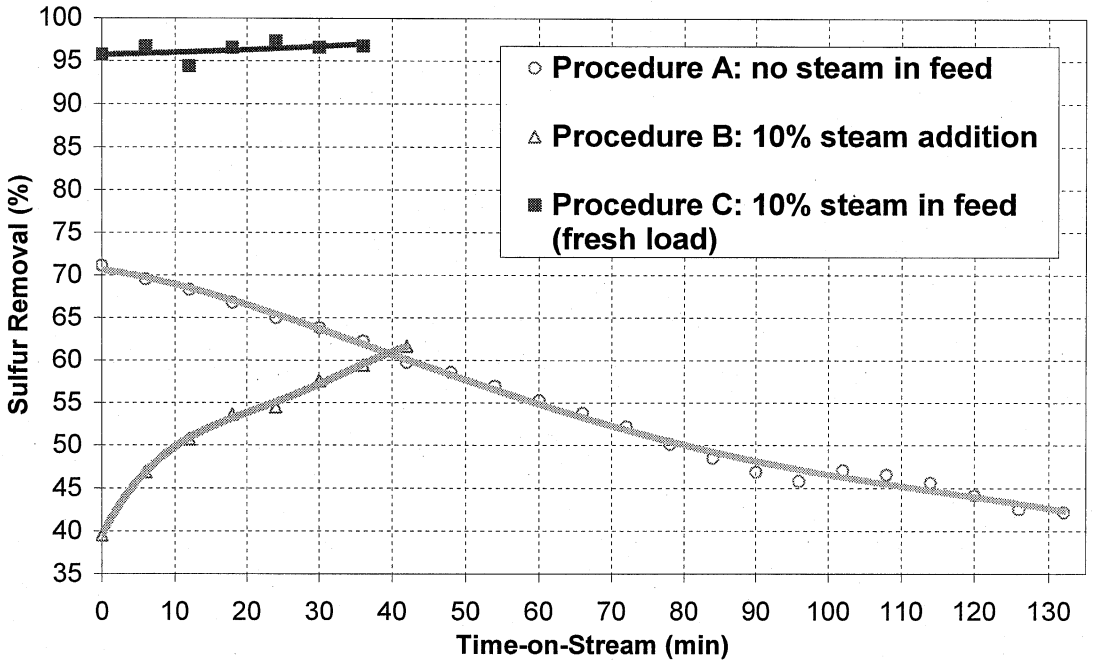

Figure 3.4. Effect of feed procedure on sulfur removal activity for SSRP on E-alumina; T: 154°C; P: 200 psig; F: 600/500 sccm; H_2S: 8550±100 ppm; SO_2: 4300±100 ppm

Then, steam was fed into the reactor at a feed rate of 60 sccm (Procedure **B**), thus increasing the total flow to 600 sccm, while maintaining the reaction temperature and pressure. The sulfur removal activity (H_2S+SO_2 conversion) increased from ca. 40% to ca. 62% within 42 min, at which point the experiment was terminated without allowing for the reaction to reach a pseudo steady state (Fig. 3.4). The formation of COS declined rapidly down to 15 ppm after the addition of steam and was maintained below 10 ppm for the duration of this run.

A fresh batch of $5cm^3$ E-alumina was loaded into the reactor which was then heated and pressurized under inert gas (N_2), until attaining the reaction conditions (temperature, pressure) as described above. Initially 4300 ppm of SO_2 in inert gas (N_2) was fed into the reactor at a feed flow of 500 sccm and the system was allowed to reach pseudo steady state. Then, 50 sccm of the inert gas flow were substituted by an equal flow of steam (10% steam addition). After a time period of 30 min, another part of the inert gas flow was substituted by an equal syngas flow so as to get a ratio of H_2S/SO_2 of ca. 2 in the presence of steam, while maintaining the reaction temperature and pressure (Procedure **C**). The reaction reached pseudo steady state within 20 min. The sulfur removal activity was 96% and remained constant for a period of 36 min (Fig. 3.4). The COS formation was constant at 22 ppm.

These results illustrate the importance of the order in which reactants should be fed into the reactor, as well as the importance of the presence of steam in the feed. The addition of steam prior to exposure of the catalyst to the H_2S-containing syngas results in a stable, very high sulfur removal activity (more than 96%), with minimal formation of COS (less than 25 ppm).

The impact of the feed procedure on the performance of the E-alumina catalyst for the oxidation of H_2S by SO_2 was further examined. One such run involved feeding H_2S-containing syngas only (no SO_2, no steam) at 125°C and 200 psig. The formation of 500 ppm COS was observed (corresponding to a decrease in H_2S from 8500 ppm to 8000 ppm), as shown in the time-on-stream plot of Figure 3.5. Addition of ca. 4300 ppm SO_2 (Procedure **A'**) while maintaining the reaction temperature, pressure, and total feed flow, resulted in a significant decrease in the outlet H_2S concentration (due to the H_2S+SO_2 reaction) and a complete suppression in the formation of COS (Fig. 3.5).

Later in the same run, the syngas flow was substituted by inert (N_2) leaving the SO_2 to reach a steady state outlet value of 4300 ppm. Then, the H_2S_containing syngas flow was again introduced, still in the absence of steam (Procedure **A**). The outlet SO_2 concentration declined to essentially zero, and then the outlet H_2S gradually increased to ca. 6500 ppm, as shown in Figure 3.6. The data of the H_2S curve in Fig. 3.6 correspond to those of the "Procedure **A**" curve of Fig. 3.4. Under this procedure, the sulfur removal activity was very low.

Continuing on the same run (Procedure **A**), the effect of SO_2 removal from the feed on the sulfur removal activity of E-alumina is shown in Figure 3.7. The outlet H_2S concentration increased to ca. 13500 ppm temporarily and at was restored to its inlet value of ca. 8500 ppm at steady state. Interestingly, the outlet COS increased gradually from ca. 500 ppm to more than 7500 ppm before starting to decline with time on stream. This COS appears to be formed by the reaction of CO with the sulfur that was formed by the H_2S+SO_2 reaction prior to removing the $SO_2$from the reactant feed.

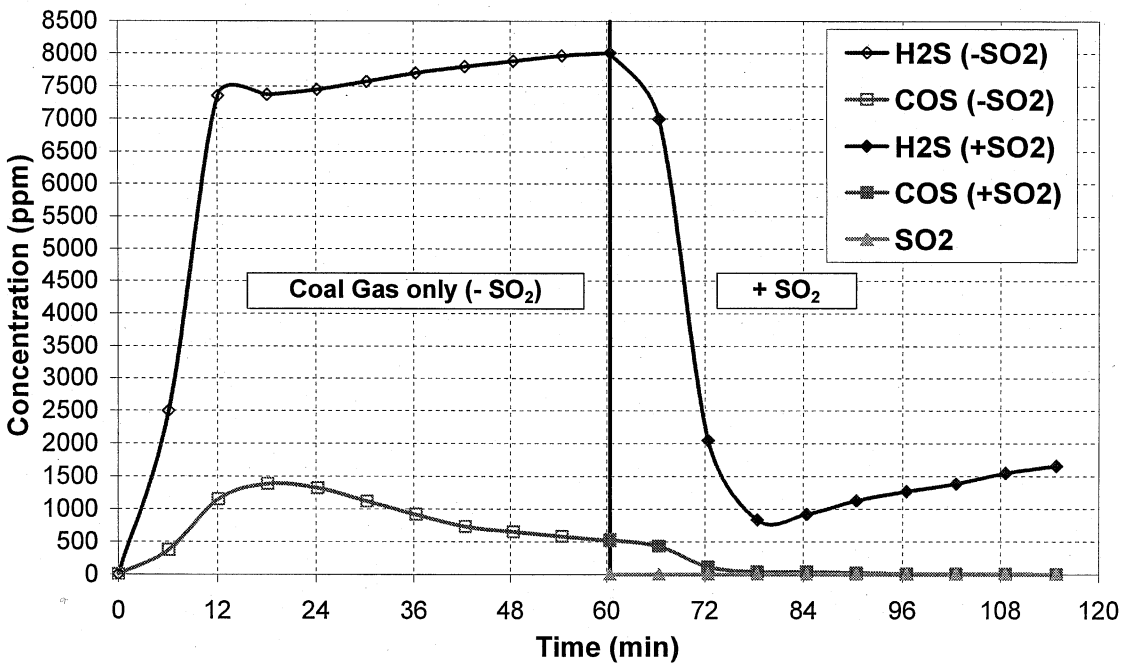

Figure 3.5. Effect of SO_2 addition on sulfur removal activity and COS formation for SSRP on E-alumina (Procedure **A'**); T: 125°C; P: 200 psig; F: 270 sccm; H_2S: 8500±50 ppm; SO_2: 4300±50 ppm; steam: 0%

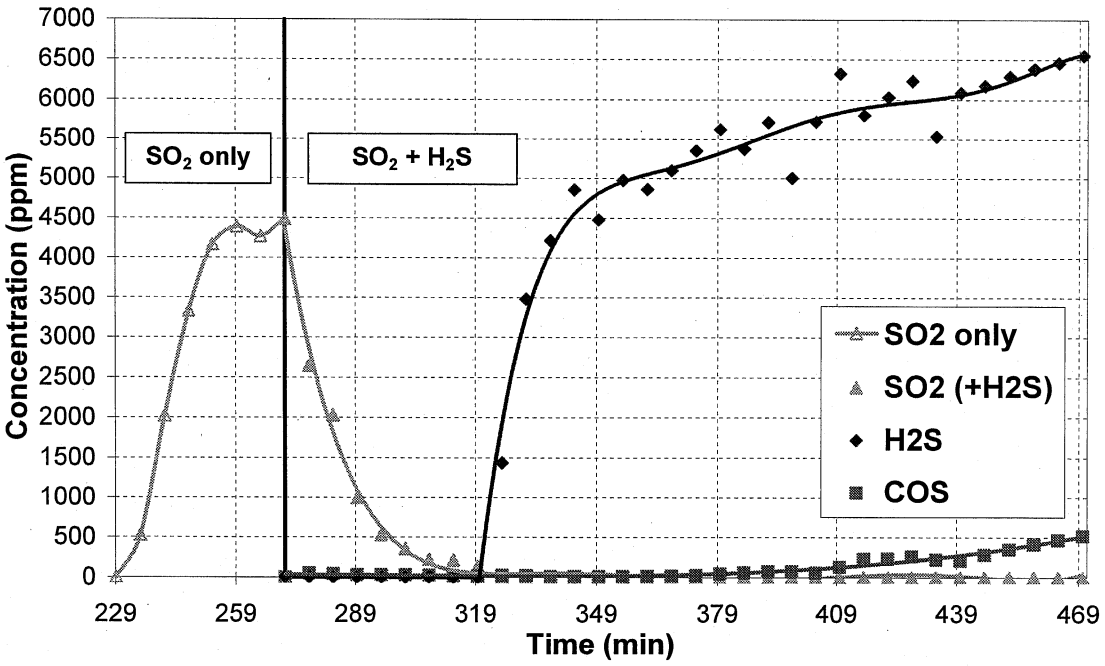

Figure 3.6. Effect of H_2S addition on sulfur removal activity and COS formation for SSRP on E-alumina (Procedure **A**); T: 125°C; P: 200 psig; F: 270 sccm; H_2S: 8500±50 ppm; SO_2: 4300±50 ppm; steam: 0%

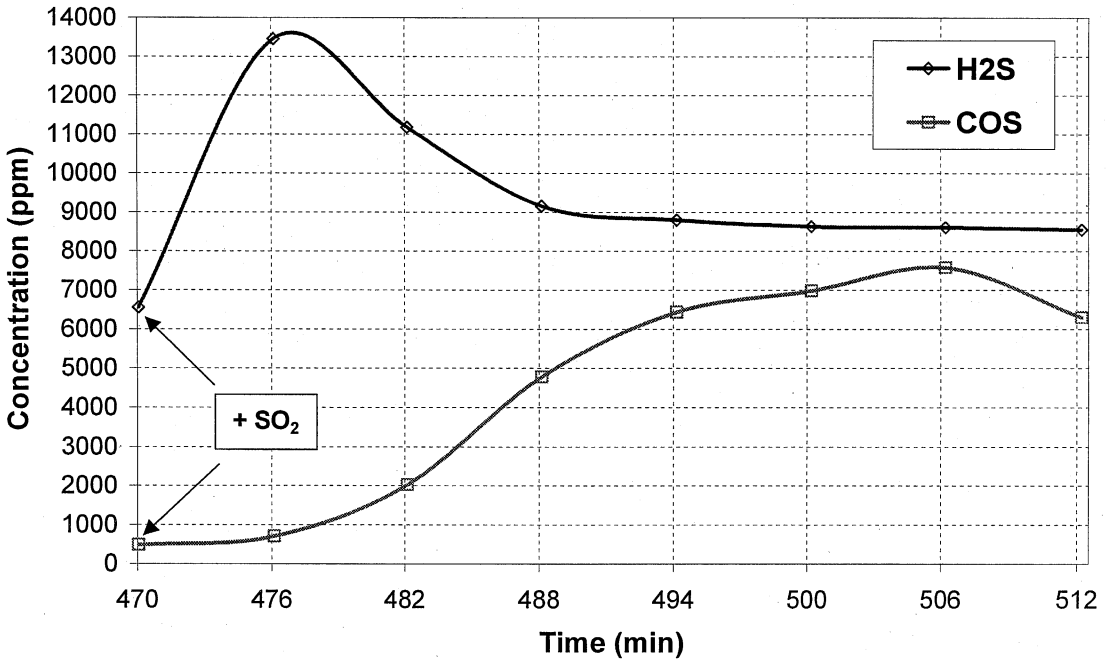

Figure 3.7. Effect of SO_2 removal on sulfur removal activity and COS formation for SSRP on E-alumina (Procedure **A**); T: 125°C; P: 200 psig; F: 270 sccm; H_2S: 8500±50 ppm; SO_2: 4300±50 ppm; steam: 0%

The effect of SO_2 removal on the sulfur removal performance of E-alumina was also examined under feed Procedure **B**. Referring to Fig. 3.4, after the final data point shown in the "Procedure **B**" curve the SO_2 feed was substituted by inert gas (N_2) feed, while keeping the total flow as well as the reaction temperature and pressure constant. The time-on-stream data for the effect of SO_2 removal under Procedure **B** are shown in Figure 3.8. In clear contrast to the data of Procedure **A** (shown in Fig. 3.7), the outlet H_2S concentration increased to ca. 17000 ppm, which was double its inlet concentration of ca. 8500 ppm. The outlet COS was minimal (less than 10 ppm). Thus, under Procedure **B** the sulfur that was formed by the H_2S+SO_2 reaction prior to removing the SO_2 from the reactant feed appears to form the excess H_2S in the outlet. The presence of steam (the difference between Procedures **A** and **B**) appears to shift the major product in the absence of SO_2 from COS to H_2S.

The effect of SO_2 removal on the sulfur removal performance of E-alumina was finally examined under feed Procedure **C**. Referring to Fig. 3.4, after the final data point shown in the "Procedure **C**" curve the SO_2 feed was again substituted by inert gas (N_2) feed, while keeping the total flow as well as the reaction temperature and pressure constant. The time-on-stream data for the effect of SO_2 removal under Procedure **C** are shown in Figure 3.9. In contrast to the results of Procedure **A** as well as Procedure **B**, the outlet H_2S concentration at steady state was essentially equal to that in the reactor inlet, i.e., ca. 8800 ppm, whereas the outlet COS was limited to ca. 80 ppm or less. Therefore, based on the results presented in Figures 3.4-3.9, the comparison of the various examined feed procedures (**A**, **A'**, **B**, and **C**) indicates that Procedure **C** gave the highest sulfur removal activity along with minimal COS formation for the SSRP on E-alumina.

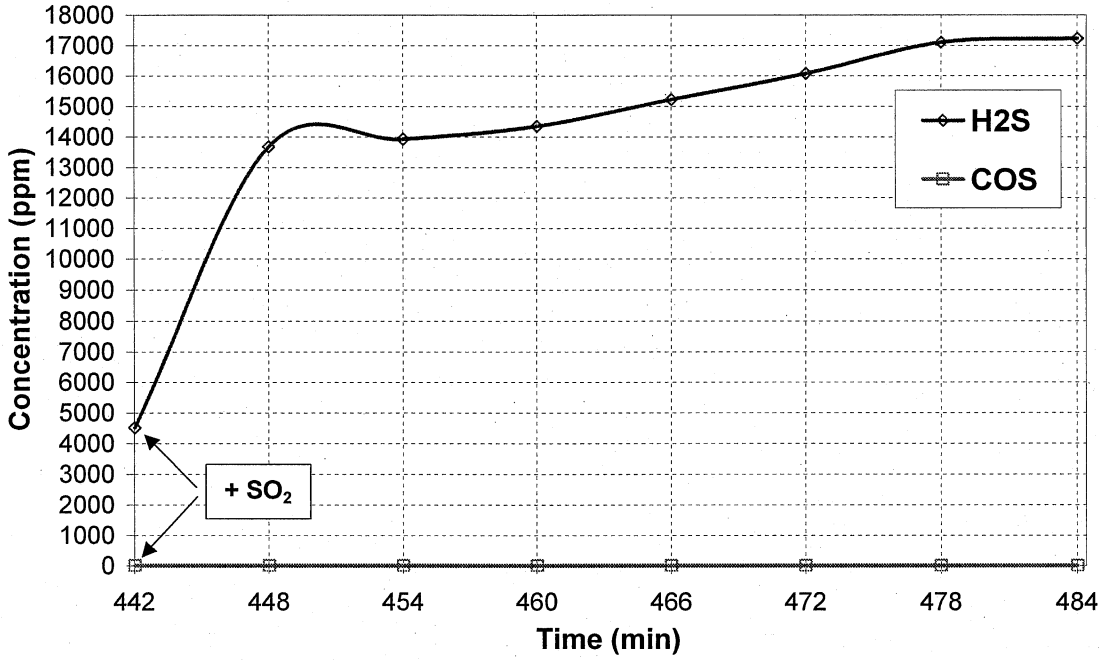

Figure 3.8. Effect of SO_2 removal on sulfur removal activity and COS formation for SSRP on E-alumina (Procedure **B**); T: 154°C; P: 200 psig; F: 590 sccm; H_2S: 8500±50 ppm; SO_2: 4300±50 ppm; steam: 10%

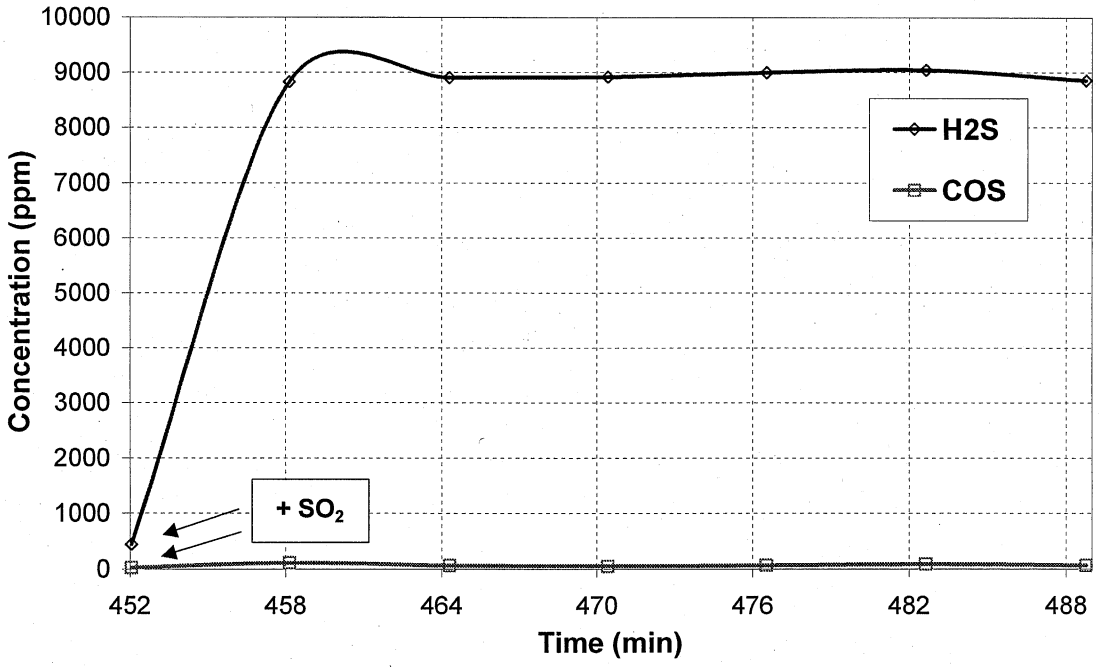

Figure 3.9. Effect of SO_2 removal on sulfur removal activity and COS formation for SSRP on E-alumina (Procedure **C**); T: 154°C; P: 200 psig; F: 500 sccm; H_2S: 8800±100 ppm; SO_2: 4300±50 ppm; steam: 10%

The efficiency of E-alumina for sulfur removal under Procedure **C** (SO_2 feed, steam feed, H_2S feed) was compared to that of two other procedures: one where 10% steam was first fed into the reactor, followed by SO_2 feed, and finally by H_2S-containing syngas feed (Procedure **D**), and another, where the steam feed was followed by H_2S-containing syngas feed and then by SO_2 feed (Procedure **D'**). The total feed flow was maintained at 100 sccm and 300 sccm, respectively, and all other reaction conditions were the same, to facilitate the comparison. The results are given in Table 3.5. Procedures **C** and **D** gave essentially identical results. Procedures **C** and **D'** also gave essentially identical results with respect to the sulfur removal activity. The COS formation was slightly higher under Procedure **D'** compared to Procedure **C**. Unless otherwise indicated, all the following experiments were performed under one of these three feed procedures.

Table 3.5. Sulfur removal activity and COS formation as function of feed procedure on E-alumina; T: 154°C; P: 200 psig; F: 100 sccm / 300 sccm; steam: 10%

Procedure	Conversion (%) H_2S+SO_2	COS formation (ppmv)
C (SO_2 feed, steam feed, coal gas feed) @ 100 sccm	98.5	20
D (steam feed, SO_2 feed, coal gas feed) @ 100 sccm	98.6	20
C (SO_2 feed, steam feed, coal gas feed) @ 300 sccm	98.4	34
D' (steam feed, coal gas feed, SO_2 feed) @ 300 sccm	98.9	85

A new series of SSRP reaction experiments was conducted by loading the silica-coated reactor with 5 cm^3 of E-alumina, then heating to 154°C (309°F) and pressurizing to 200 psig (14.4 bar) under an inert gas flow of 100sccm. 15sccm SO_2/N_2 (corresponding to ca. 3800 ppm SO_2) were fed into the reactor, followed by feeding 10 sccm steam, substituting an equal flow of N_2. Upon reaching a pseudo steady state, simulated coal gas with H_2S was fed into the reactor (giving ca. 8400 ppm H_2S), at a constant total feed flow of 100 sccm. The total sulfur (H_2S+SO_2) conversion was 86.5%, with less than 20 ppm COS formation.

The effect varying the SO_2 inlet concentration was examined by increasing the SO_2/N_2 flow from 15 to 18 to 20 sccm while keeping the coal gas and steam flows constant, thus increasing the total flow from 100 to 103 to 105 sccm, respectively. The results are shown in Figure 3.10. Upon increasing the SO_2 inlet concentration the conversion of H_2S increased up to 99.5%, while the conversion of SO_2 decreased from essentially 100% down to ca. 87%. Thus the H_2S+SO_2 conversion showed a maximum at an intermediate SO_2 concentration. This implies reaction of SO_2 with H_2S only, and not with H_2 or CO which are in great excess, at least to any appreciable rate. The COS formation was only about 20 ppm.

The effect of space velocity was studied by varying the total wet feed flow from 100 sccm to 500 sccm (space velocity of 1200 h^{-1} to 6000 h^{-1}) while keeping the other reaction parameters (temperature, pressure, feed composition) constant. This fivefold increase in space velocity resulted in only a minor decrease (from 98.5% to 96%) in H_2S+SO_2 conversion. The formation of COS was again only about 20 ppm. Thus the SSRP reaction is very active and selective even at significantly short contact times.

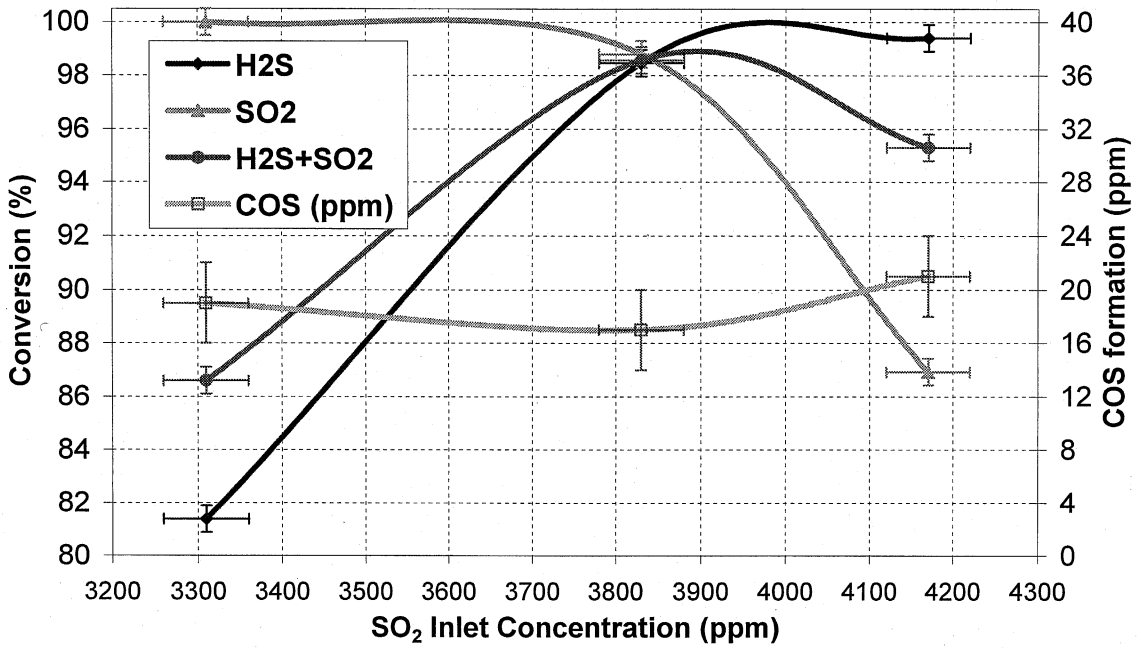

Figure 3.10. Effect of SO_2 inlet concentration on H_2S, SO_2, and H_2S+SO_2 conversion, and COS formation for SSRP on E-alumina; T: 154°C; P: 200 psig; SV: 1200-1260 h^{-1}; H_2S: 8400-8000 ppm; steam: 10%

The effect of pressure was examined by increasing the reaction pressure from 200 psig to 350 psig at 300 sccm total feed flow while keeping the other reaction parameters (temperature, feed composition) constant. The results are given in Table 3.6. The combined H_2S+SO_2 conversion was found to increase up to 99.0%. Higher pressures favor the reaction in terms of thermodynamic equilibrium, so they would be expected to further increase the measured H_2S + SO_2 conversion. The amount of formed COS was below 40 ppm.

Table 3.6. Effect of pressure on H_2S, SO_2, and H_2S+SO_2 conversion, and COS formation, for SSRP on E-alumina; T: 154°C; H_2S: 8400 ppm; SO_2: 4200 ppm; steam: 10%

	Conversion (%)			COS formation
Pressure (psig)	**H_2S**	**SO_2**	**H_2S+SO_2**	**(ppmv)**
200	98.9	97.3	98.4	34
240	98.9	98.4	98.7	34
300	99.0	99.0	99.0	36
350	98.8	99.3	99.0	38

The effect of temperature was examined by varying the reaction temperature from 154°C (309°F) down to 125°C (257°F). The H_2S+SO_2 conversion was only minimally affected (from 98.6% down to 98.0%), indicating that the reaction has reached thermodynamic equilibrium at these conditions.

The effect of catalytically oxidizing H_2S in the presence of excess H_2 and CO by an oxidant other than SO_2 (such as O_2) was also examined on alumina at 154°C, 200 psig, and a total flow of 100 sccm. After addition of 10% steam for 30 min, $2\%O_2/N_2$ was fed into the reactor, producing ca. 4300 ppm O_2 in the feed, at a total flow of 105 sccm. Then, coal gas was fed to get a ratio of H_2S/O_2 of ca. 2 and the reaction reached a pseudo steady state. Finally, the O_2 flow was substituted by a flow of SO_2 producing ca. 4300 ppm of SO_2 in the feed (H_2S/SO_2 ratio of ca. 2) and the reaction reached a new pseudo steady state.

The results for the effect of O_2 vs. SO_2 in the feed are given in Figure 3.11. Oxygen is much less selective for the oxidation of H_2S compared to SO_2 and also allows for enhanced undesirable formation of COS. There appears to be a clear unselective consumption of O_2 by H_2 and/or CO of the syngas, thus limiting its availability for the desirable selective reaction with H_2S.

Besides the E-alumina catalyst, three other commercially available catalysts were also examined for SSRP using the previously described fixed-bed micro-reactor: a) another alumina, named P-alumina, with different physical properties (surface area, pore volume) compared to E-alumina, b) a silica gel, and c) a precipitated iron oxide which was treated *in-situ* overnight with the H_2S-containing simulated Texaco coal gas and was thus transformed to iron sulfide. Table 3.7 summarizes the physical properties of these catalysts. Table 3.8 gives a comparison of these 4 catalysts in terms of sulfur removal activity (H_2S+SO_2 conversion) and selectivity (minimized undesirable formation of COS).

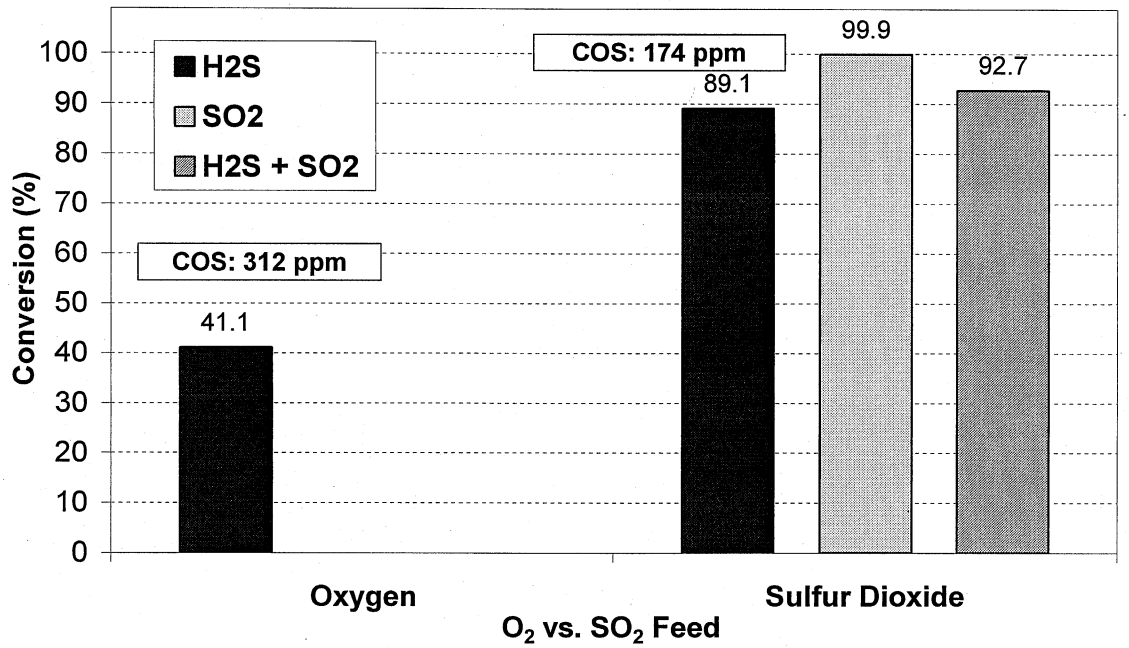

Figure 3.11. Effect of O_2 vs. SO_2 feed on H_2S, SO_2, and H_2S+SO_2 conversion, and COS formation for SSRP on E-alumina; T: 154°C; P: 200 psig; H_2S: 8400 ppm; O_2 (SO_2): 4300 ppm; steam: 10%

Table 3.7. Physical properties of catalysts examined for SSRP

Designation	Type	BET Surface Area (m^2/g)	Pore Volume (cm^3/g)
E	Alumina	227	0.62
P	Alumina	288	0.14
F	Precipitated Iron Oxide*	153	0.17
S	Silica gel	233	1.05

* *in-situ* sulfided by H_2S-containing simulated Texaco goal gas into iron sulfide

Table 3.8. Comparative ranking of catalysts for SSRP in terms of H_2S+SO_2 conversion, and COS formation; T: 154°C; P: 200 psig; F: 300 sccm; steam: 10%

Catalyst	S Removal Activity (H_2S+SO_2 conv. %)		Catalyst	S Removal Selectivity (COS formation, ppm)
E-alumina	98.4-98.9		E-alumina	35-85
Iron sulfide	96.9-98.4		P-alumina	45
P-alumina	95.6		Silica gel	115-170
Silica gel	87.4-90.7		Iron sulfide	8900-14000

The comparative results of Table 3.8 indicate that E-alumina was the best catalyst for SSRP under the examined conditions, followed closely by P-alumina. Silica gel showed lower activity and higher selectivity for COS formation. Iron sulfide was very active but transformed all the H_2S into COS. Therefore, E-alumina was chosen for all subsequent studies of SSRP.

The effect of oxidizing H_2S by oxygen vs. SO_2 was also examined on the silica gel. At 154°C, 200 psig and 300 sccm, 10% steam was added, followed by SO_2/N_2 to achieve 4450 ppm SO_2 in the feed, and then by H_2S-containing syngas to achieve 8200 ppm H_2S (Procedure **D**). After reaching pseudo steady state, the SO_2/N_2 flow was substituted by a flow of $2\%O_2/N_2$ to produce ca. 4450 ppm O_2 in the feed (the total feed flow increased to 314 sccm). Finally, the O_2/N_2 flow was back-substituted with SO_2/N_2 flow (the total flow returned to 300sccm).

The results of the SO_2 to O_2 to SO_2 switch are given in Table 3.9. In agreement to results with E-alumina (Fig. 3.11), oxygen was significantly less selective for the oxidation of H_2S (implied by the lower conversion of H_2S) and also showed enhanced formation of COS. Again, there appears to be an unselective consumption of O_2 by the H_2 and/or CO of the syngas, thus limiting its availability for the selective reaction with H_2S.

Table 3.9. Sulfur removal activity as function of O_2 vs. SO_2 in the feed on silica gel; T: 154°C; P: 200 psig; F: 300 sccm; steam: 10% (Procedure **D**)

	Conversion (%)			COS formation
Oxidant (ppmv)	**H_2S**	**SO_2**	**H_2S+SO_2**	**(ppmv)**
SO_2 (4450)	93.8	85.0	90.7	140
O_2 (4450)	31.8	-	-	510
SO_2 (4450)	92.7	83.3	89.4	180

The sulfur that was generated on the catalyst during the SSRP was retained within the catalyst pores (the collected water condensate was clear). Normally in low temperature fixed-bed Claus-type processes, the catalyst is reversibly poisoned by the sulfur plugging its pores (Pearson (1976)). The catalyst would have to be heated to high temperatures to remove the sulfur. The commercial embodiment suggested in Figure 3.1 appears attractive in this context, as the sulfur formed should dissolve into the molten sulfur, thereby facilitating its removal and recovery. The reactor system is analogous to a slurry-bubble column Fischer-Tropsch reaction in which wax is formed in the catalyst pores and is removed by the liquid wax medium.

Some of the most important results of the SSRP experiments on E-alumina described above have been presented in the 19th Annual International Pittsburgh Coal Conference (see Appendix **H**, Nikolopoulos and Gangwal, 2002). The processed data of the micro-reactor SSRP catalyst screening study, from which the figures and tables presented above were generated, are included in Appendix **I**. The main conclusions from the overall catalyst screening in the fixed-bed micro-reactor are presented in Section 5.

3.3.2. Concept evaluation: SSRP in a micro-bubbler reactor

The SSRP reaction was also studied in a 0.5-inch micro-bubbler with a 10ml glass liner containing 1 cm^3 of E-alumina and 5 cm^3 of sublimed sulfur.. A 1/8-inch stainless steel tube was closed at its bottom and was drilled with $1/21000^{th}$ inch bits within 1 inch from its bottom to create a gas distributor. It was then adjusted to the bubbler top with a reducer and a tee and was inserted to the bubbler so that its bottom was positioned at about half the height of the sulfur powder and catalyst mixture. This 1/8-inch tube was used as the feed line to the bubbler, whereas the gas outlet was connected to the outlet gas line in the same manner as the fixed-bed reactor shown in Fig. 3.2.

The reactor was fed with 125 sccm of N_2 and was heated to 140°C and pressurized to 150 psig. The heat added to the reactor caused the sulfur powder to melt and thus form a molten sulfur bath where the catalyst particles would be suspended (due to similar density of the molten sulfur and the catalyst) and the bubbles of the N_2 feed gas would produce sufficient agitation so as to assume the molten sulfur bath as essentially homogenized. A schematic of this micro-bubbler reactor is given in Figure 3.12.

The effect varying the SO_2 inlet concentration was examined at a reaction pressure of 150 psig by increasing the SO_2/N_2 flow while keeping the coal gas and steam flows constant. The results are shown in Figure 3.13. In agreement with the fixed-bed reactor results, the sulfur removal activity (H_2S+SO_2 conversion) showed a maximum of 80.9% at an intermediate SO_2 concentration. The amount of COS formed (400-450 ppm) was essentially unaffected by the variation in SO_2 concentration, but was one order of magnitude greater than in the corresponding fixed-bed run (Fig. 3.10), implying possible reaction of CO with the molten sulfur vapor.

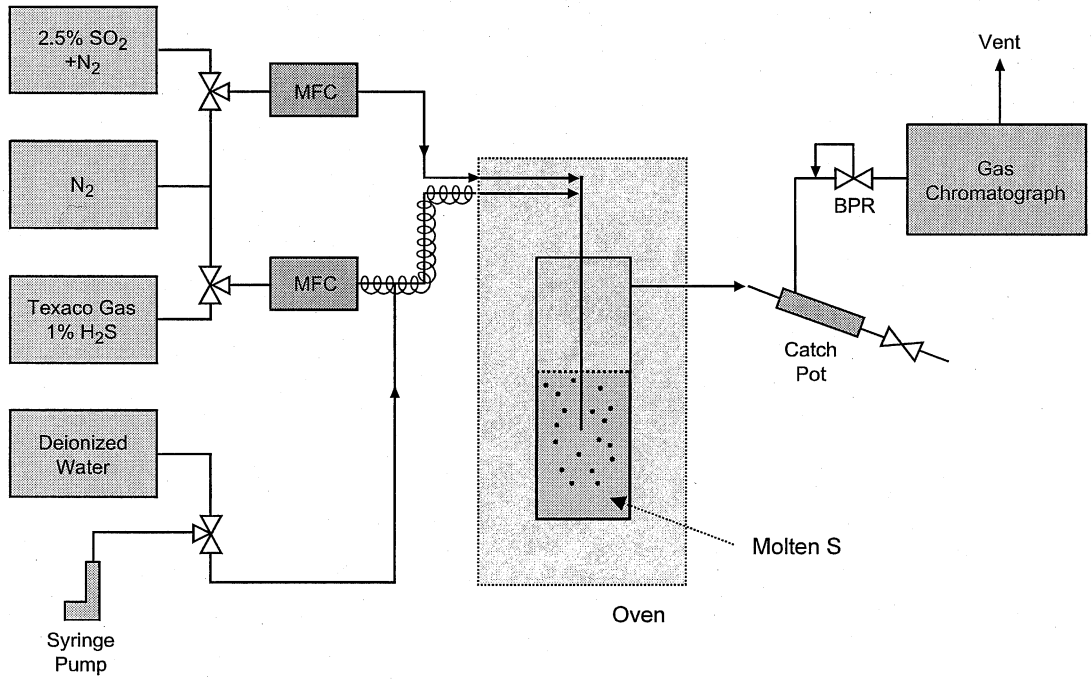

Figure 3.12. Schematic of the SSRP micro-bubbler reactor system for concept evaluation

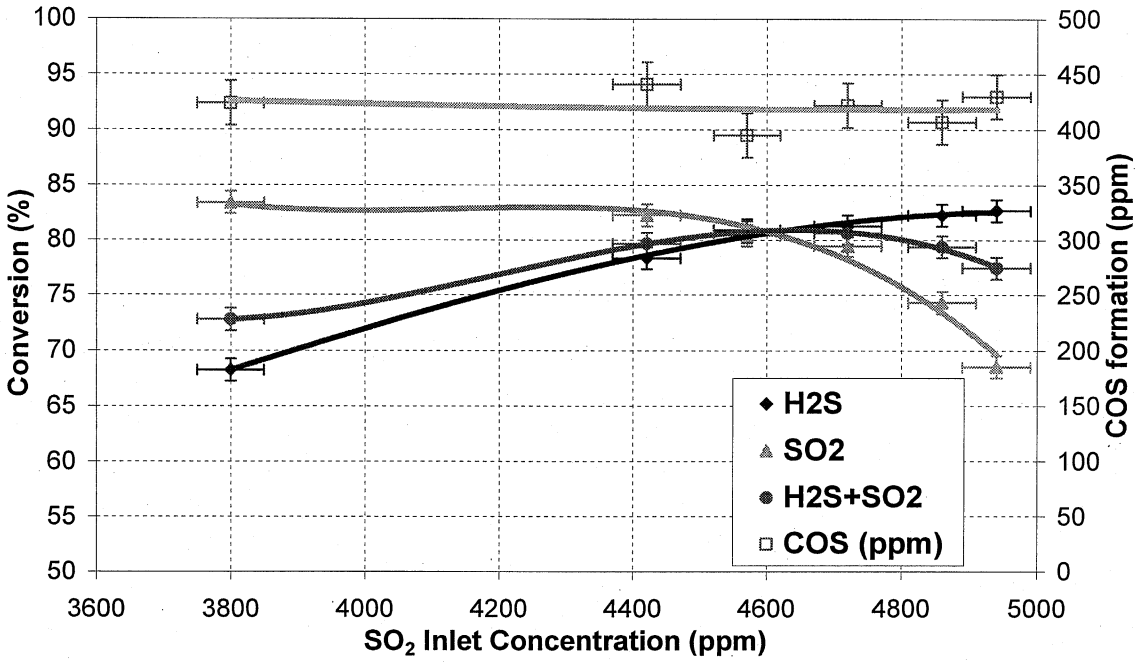

Figure 3.13. Effect of SO_2 inlet concentration on H_2S, SO_2, and H_2S+SO_2 conversion, and COS formation for SSRP on E-alumina in Molten Sulfur; T: 140°C; P: 150 psig; SV: 7500-8100 h^{-1}; H_2S: 8900-8400 ppm; steam: 10%

The effect of pressure was examined by increasing the reaction pressure from 150 psig to 300 psig at 135 sccm total feed flow while keeping the other reaction parameters (temperature, feed composition) constant. The results are shown in Figure 3.14. The H_2S+SO_2 conversion was found to increase from 80.9% to 92.8% with increasing pressure, in agreement with the results of the fixed-bed reactor (Table 3.6). The amount of formed COS increased only moderately with doubling the reaction pressure (from 400 ppm to 475 ppm).

The significantly higher amounts of COS that were measured at the outlet of the micro-bubbler compared to the fixed-bed micro-reactor clearly identify the significance of minimizing the formation of COS during SSRP. A preliminary attempt to investigate the pathways for COS formation involved substituting the H_2S-containing coal gas feed with a pure CO feed, thus simplifying the matrix of possible reactions substantially.

By feeding pure CO only (no SO_2) into the bubbler containing the molten sulfur and E-alumina mixture at 154°C and 300 psig for a brief period of time, a very large amount of COS (ca. 11000 ppm) was measured at the outlet. Addition of SO_2 resulted in strong suppression of COS formation (< 1250 ppm). The inlet and outlet SO_2 concentrations were essentially equal after reaching steady state. After purging the system with N_2, SO_2 was fed (no CO feed) and no reaction was observed (no SO_2 consumption, and no COS formation). Addition of CO in huge excess (80% compared to < 6000 ppm SO_2) gave rise to only 230 ppm COS. Again, the inlet and outlet SO_2 concentrations were essentially equal after reaching steady state.

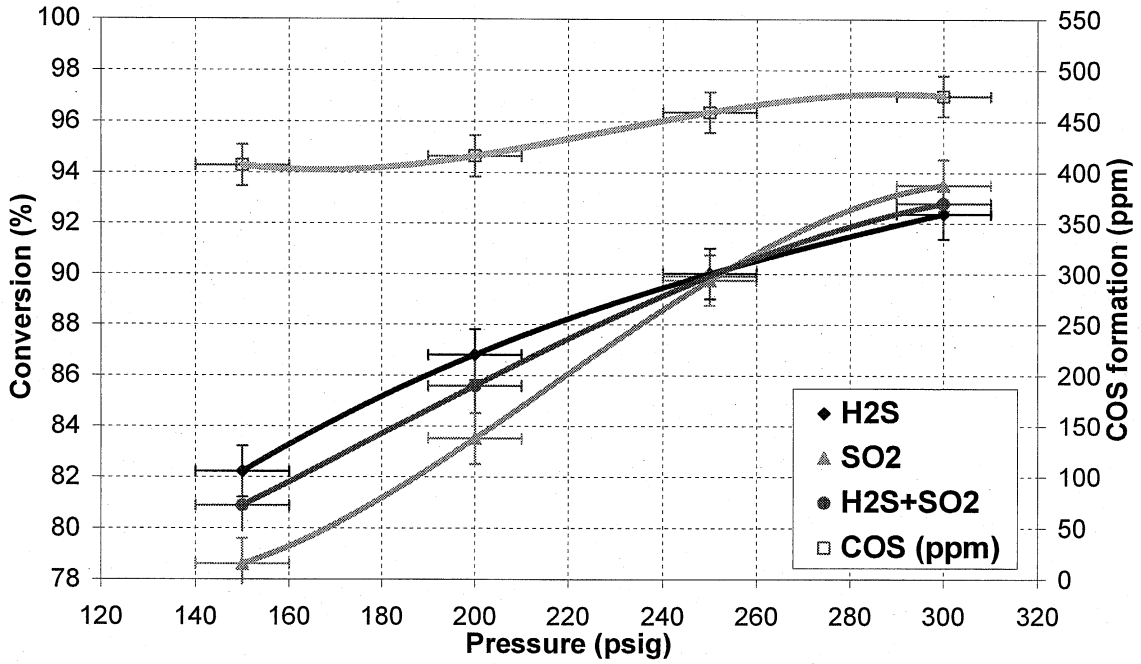

Figure 3.14. Effect of pressure on H_2S, SO_2, and H_2S+SO_2 conversion, and COS formation for SSRP on E-alumina in Molten Sulfur; T: 140°C; SV: 8100 h^{-1}; H_2S: 8400 ppm; SO_2: 4900 ppm; steam: 10%

Furthermore, a decrease in SO_2 inlet concentration (by 22%) resulted in a significant increase in COS formation (from 230 ppm to 420 ppm, an 82% increase). This correlation was found to be reversible, i.e., returning the SO_2 inlet concentration to its original value also caused the COS amount to return to a value close to its original one (200 ppm). Also, these transients were independent of the presence or absence of steam (0% or 10% steam in the feed).

The results of the experiments with the pure CO feed instead of the H_2S-containing syngas feed suggest that the formation of COS was not resulting from any direct reaction involving SO_2 and was negatively correlated with SO_2 concentration. This strong negative correlation implies that COS did not form via direct reaction of CO with molten sulfur, although some CO reaction with adsorbed molten S vapor cannot be excluded based solely on the present evidence. It appears that COS was formed by reaction of CO with an active form of sulfur located at the catalyst sites responsible for sulfur formation during SSRP.

The processed data of the micro-bubbler SSRP experiments, from which the figures and tables presented above were generated, are included in Appendix **J**. The main conclusions from the SSRP concept evaluation study in the micro-bubbler reactor are presented in Section 5.

3.3.3. Process evaluation: SSRP in a bench-scale continuous stirred tank reactor

The SSRP reaction was studied in a 2-liter continuous stirred tank reactor (CSTR) equipped with a glass liner containing 716 g sublimed sulfur (400 cm^3 of molten sulfur at 155°C) and typically 22.5g (25 cm^3) E-alumina. The stainless steel reactor and the feed tubing inside it were teflonized to minimize reactions on their walls. The reactant feed was the same as that for the reaction systems previously described: a simulated Texaco coal gas stream containing 50.8% CO, 35.7% H_2, 12.5% CO_2, and 1.0% H_2S, a 2.5% SO_2/N_2 stream, and a steam stream generated by evaporation of water supplied from a constant-flow syringe pump. A back-pressure-control valve, located downstream of the condenser, controlled the reactor and condenser pressure. The reactor was pressurized to 300 psig under inert gas flow and heated to 155°C. The sulfur melted at about 125°C and the catalyst was suspended in the molten sulfur phase by stirring the liquid, typically at 1000 RPM. The outlet gases were analyzed as previously described (Section 3.2.1). A schematic of the bench-scale SSRP reaction system is shown in Figure 3.15.

Preliminary SSRP reaction experiments involved evaluating the intrinsic activity of the teflonized CSTR of Fig. 3.15 in the absence of both catalyst and molten sulfur (empty glass liner only). After heating to 155°C and pressurizing to 200 psig under inert gas flow of ca. 1.5 SLPM (standard liters per minute), the H_2S-containing syngas was fed into the reactor (no SO_2, no steam feed). The blank reactor showed minimal activity under these conditions, with only ca. 15 ppm COS formation (see Table 3.10). Addition of SO_2 only (no steam feed, Procedure **A'**) led to an increase in COS formation to 75 ppm, with very low sulfur removal activity (less than 4%). Reaction of CO with active sulfur formed by the SSRP reaction (as discussed in Section 3.3.2) is the most likely path for this limited increase in COS formation. These observations are in agreement with results from the blank silanized micro-reactor (see Appendix **I**).

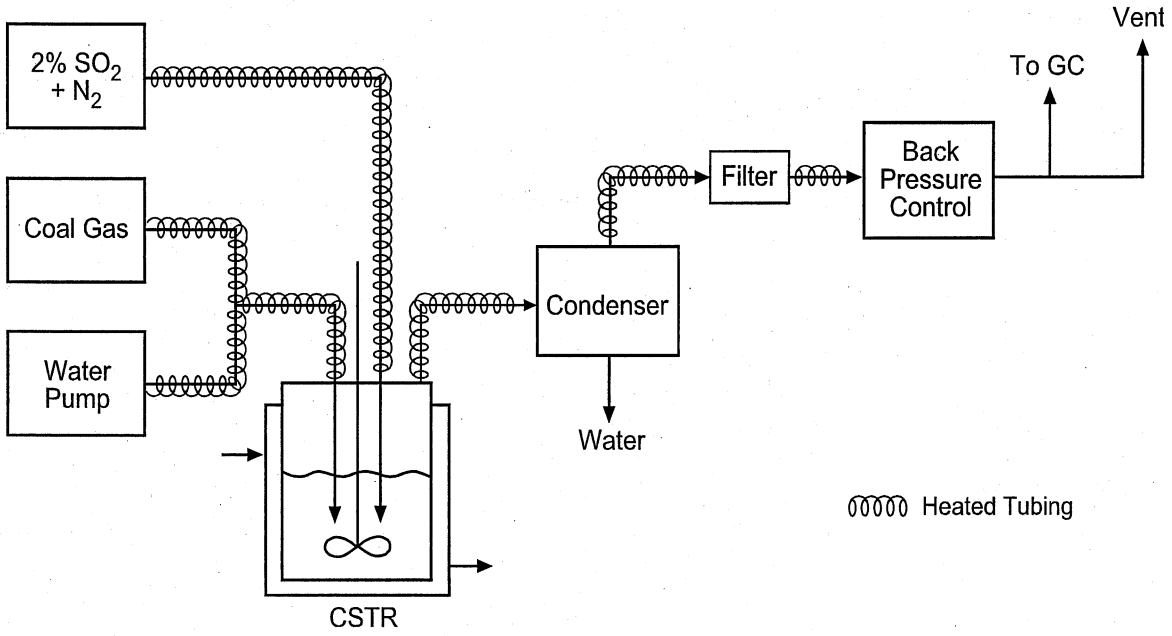

Figure 3.15. Schematic of the SSRP continuous stirred tank reactor (CSTR) system

Table 3.10. Effect of SO_2 addition on sulfur removal activity and COS formation, for SSRP in blank reactor; T: 155°C; P: 200 psig; H_2S: 8350 ppm; steam: 0% (Procedure **A'**)

	Conversion (%)			COS formation
SO_2 inlet (ppm)	**H_2S**	**SO_2**	**H_2S+SO_2**	**(ppmv)**
0 (H_2S feed only)	0.4	-	-	15
4800 (H_2S+SO_2 feed)	3.7	3.4	3.6	75

Continuing in the same run, the effect of adding 10% steam in the feed was examined (Procedure **B'**). Steam was fed into the reactor at 150 sccm, thus increasing the total inlet flow to 1.65 SLPM, while maintaining all other reaction parameters. As shown in Table 3.11, the addition of 10% steam enhanced the sulfur removal activity of the blank reactor significantly (from ca. 4% to ca. 51%). This result is in excellent agreement with the corresponding one for the blank micro-reactor (see Table 3.2). The formation of COS was only minimally affected by the steam addition (a decrease from 75 ppm to 55 ppm, whereas in the blank micro-reactor it had increased from 30 ppm to 60 ppm, in either case being insignificant compared to ca. 6500 ppm of sulfur that was removed).

Table 3.11. Effect of 10% steam addition on sulfur removal activity and COS formation, for SSRP in blank reactor; T: 155°C; P: 200 psig; H_2S: 8350 ppm; SO_2: 4800 ppm

	Conversion (%)			COS formation
Steam (%)	**H_2S**	**SO_2**	**H_2S+SO_2**	**(ppmv)**
0 (dry feed)	3.7	3.4	3.6	75
10 (steam addition)	51.2	50.6	51.0	55

Another set of preliminary experiments involved loading the CSTR with sulfur only (no catalyst), in order to evaluate this configuration in terms of its sulfur removal activity. The glass liner was loaded with 716 g of sublimed sulfur powder and was placed inside the reactor. Upon heating up beyond the melting point of sulfur (ca. 121°C) the reactor contained ca. 400 cc of molten sulfur (MS). The reactor was then heated to 155°C and pressurized to 300 psig under inert gas flow of 0.9 SLPM. A steam flow of 0.1 SLPM was added (i.e., 10% steam) followed by substituting part of the inert gas flow with an equal flow of H_2S-containing syngas (no SO_2 feed). After attaining steady state, the total feed flow was increased from 1 SLPM up to 4 SLPM in 1 SLPM steps by proportionally increasing both the syngas and steam flows. The effect of feed flow variation on H_2S conversion and COS formation is shown in Figure 3.16. A four-fold increase in flow caused a decrease in H_2S conversion (from ca. 7% to ca. 5%) and a significant decrease in COS formation (from 520 ppm to 115 ppm). By interpolation of the COS curve, the COS values for flows of 1.1 SLPM and 1.3 SLPM were 480 ppm and 420 ppm, respectively.

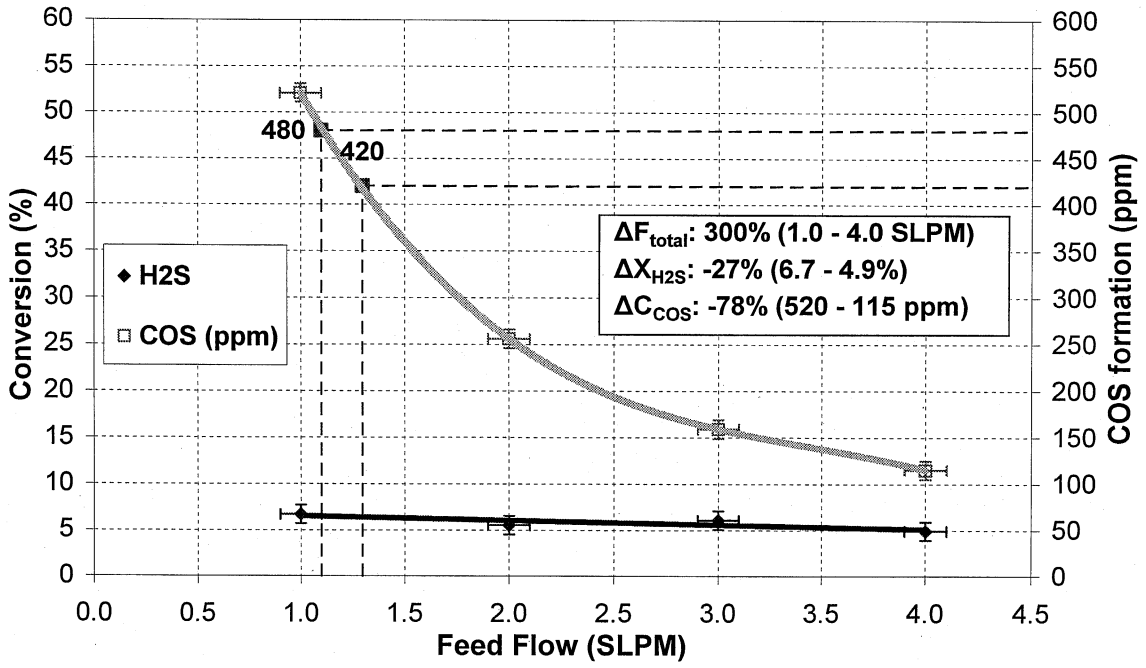

Figure 3.16. Effect of feed flow on H_2S conversion and COS formation for SSRP in Molten Sulfur; T: 155°C; P: 300 psig; H_2S: 9000 ppm; steam: 10%

Continuing in the same run, the syngas and inert flow were then restored to 0.9 SLPM while the steam flow was kept at 0.4 SLPM, thus decreasing the total feed flow from 4 SLPM to 1.3 SLPM and increasing the steam concentration from 10% to 30.8%, all other parameters being the same. The effect of steam concentration variation was then examined by decreasing the steam flow from 0.4 SLPM to0.2 SLPM and finally to its original value of 0.1 SLPM. This decrease in steam concentration from 30.8% back to 10% led to an increase in H_2S conversion from ca. 4% to ca. 6.5%, and in COS formation from 420 ppm to 520 ppm (see Figure 3.17).

The results of Fig. 3.17 seem to indicate that increasing the steam feed concentration resulted in a decrease in the undesirable formation of COS. Yet, besides the variation in steam concentration, the total feed flow was also varied. As demonstrated in Fig. 3.16, an increase in total feed flow also decreased the COS formation. The data of Fig. 3.17 were plotted vs. the total feed flow in Figure 3.18, in order to identify which of these two variables (feed flow vs. steam concentration) was actually responsible for the observed decrease in COS formation. The COS formation curve from Fig. 3.16 (dashed line) was also plotted for a direct comparison.

The two COS formation curves of Fig. 3.18 almost coincide, with two data point pairs being exactly equal to each other, and the third (middle) data point pair with minimal deviation (460 ppm vs. the interpolated value of 480 ppm). The data on the continuous curve correspond to a variation in both feed flow and steam concentration, whereas the ones on the dashed curve to a variation in feed flow only. Therefore, the presence of steam in the feed apparently did not impede the formation of COS (possibly via COS hydrolysis); the COS formation was simply inversely correlated with the total feed flow.

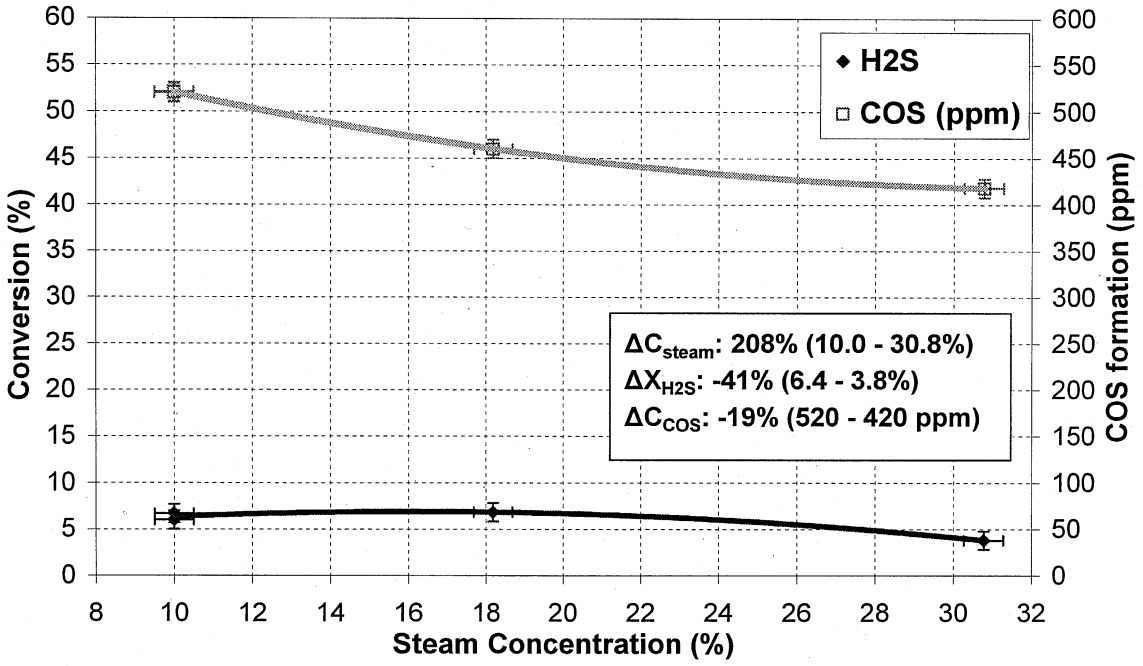

Figure 3.17. Effect of steam feed concentration on H_2S conversion and COS formation for SSRP in Molten Sulfur; T: 155°C; P: 300 psig; H_2S: 9000 ppm; F: 1.0-1.3 SLPM

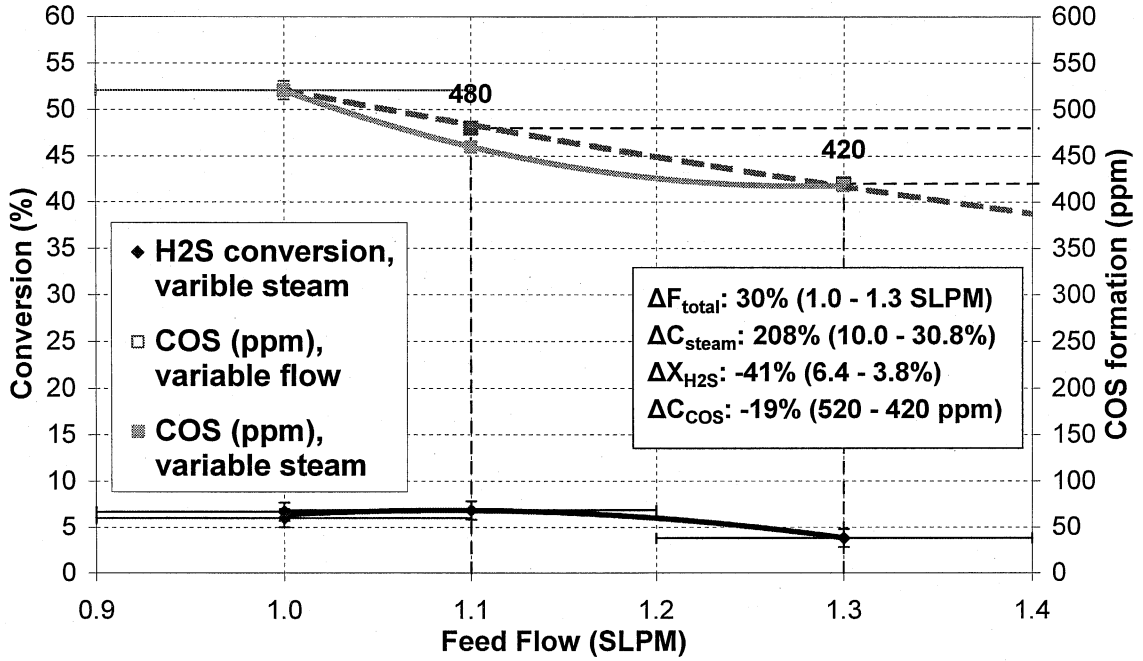

Figure 3.18. Effect of feed flow & steam feed concentration on H_2S conversion and COS formation for SSRP in Molten Sulfur; T: 155°C; P: 300 psig; H_2S: 9000 ppm; steam: 10%-30.8%

The effects of total feed flow and steam feed concentration variation were also examined in the Molten Sulfur configuration under the full SSRP feed (i.e., in the presence of SO_2). As before, after feeding 10% steam (0.1 SLPM in a 1 SLPM total feed), the H_2S-containing syngas was fed into the reactor at 155°C, 300 psig, and 1 SLPM. After reaching steady state, the H_2S conversion was ca. 7% and the outlet COS was ca. 665 ppm. Then, SO_2 was added (ca. 4400 ppm, Procedure **D'**) and the reaction system reached a new steady state. The conversion of H_2S increased to ca. 91% due to the H_2S+SO_2 reaction, and the formation of COS increased to ca. 830 ppm. This increase in the outlet COS by SO_2 addition is apparently related to the creation of an alternative pathway for COS formation, i.e., the reaction between CO and active sulfur (not molten sulfur) formed by the H_2S+SO_2 reaction, as also discussed previously.

The effect of feed flow on the Molten Sulfur activity under Procedure **D'** was examined by increasing the total (steam and syngas and SO_2) feed flow from 1 SLPM to 2 and finally 3 SLPM, all other reaction parameters remaining constant. As shown in Figure 3.19, this three-fold increase in feed flow resulted in a decrease in both sulfur removal activity (from ca. 93% to ca. 84%) and in the formation of COS (from ca. 830 ppm to ca. 255 ppm). Thus, high feed flows offer the advantage of suppressing the undesirable formation of COS, but also decrease the sulfur removal activity. The total outlet sulfur-gas concentration (sum of unreacted H_2S and SO_2 and formed COS) was found to increase with increasing feed flow. Also, it is interesting to note that the outlet H_2S/SO_2 ratio was found to increase with increasing feed flow, possibly implying a significantly different diffusivity of these compounds in the molten sulfur medium.

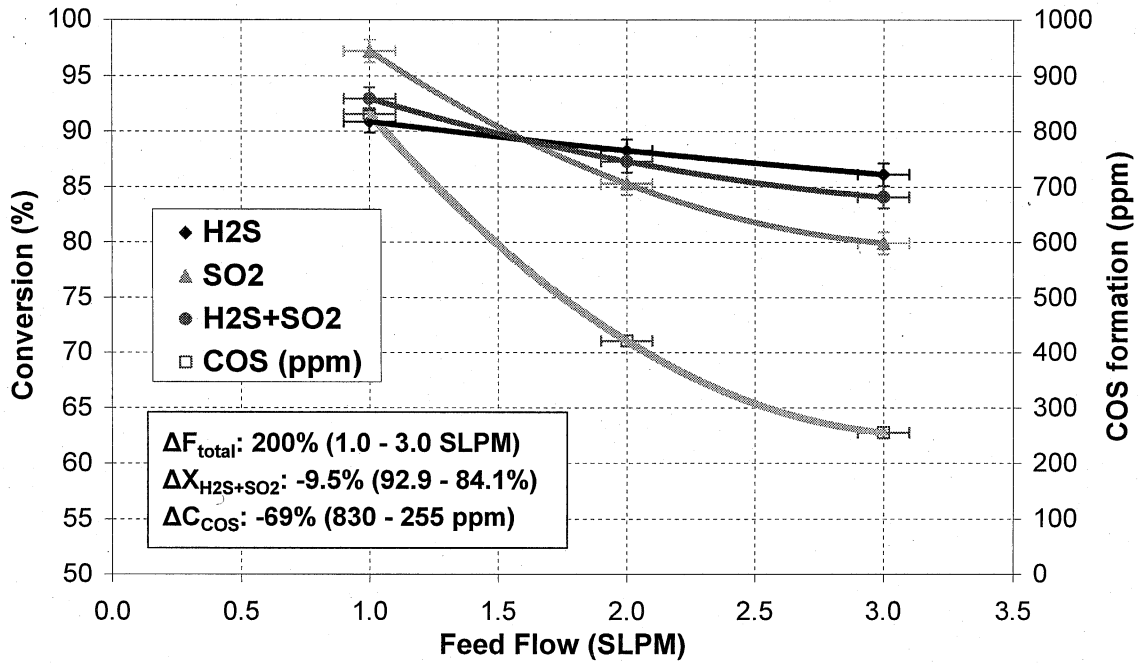

Figure 3.19. Effect of feed flow on sulfur removal activity and COS formation for SSRP in Molten Sulfur; T: 155°C; P: 300 psig; H_2S: 9000 ppm; SO_2: 4400 ppm; steam: 10%

Continuing in the same run, the syngas + SO_2 flow was restored to 0.9 SLPM while the steam flow was kept at 0.3 SLPM, thus decreasing the total feed flow from 3 SLPM to 1.2 SLPM and increasing the steam concentration from 10% to 25%, all other reaction parameters being the same. The sulfur removal activity (H_2S+SO_2 conversion) remained essentially constant (from ca. 3% to ca. 92.5%), whereas the COS formation decreased from 830 ppm to 620 ppm by this increase in steam concentration.

Again, in order to decouple the effect of variable steam feed concentration and total feed flow on the sulfur removal activity and COS formation, the results of the previous paragraph were plotted vs. the corresponding feed flow in Figure 3.20, along with parts of the H_2S+SO_2 and COS curves of Fig. 3.19. The two H_2S+SO_2 curves essentially coincide. The COS data point at 1.2 SLPM (620 ppm) deviated measurably from the predicted value of the continuous COS curve (ca. 730 ppm). Despite this deviation, it appears that also in the presence of SO_2, the presence of steam in the feed apparently did not extensively impede the formation of COS; the COS formation was again inversely correlated with the total feed flow, as seen above.

The effect of the H_2S inlet concentration on the formation of COS in the absence of SO_2 was examined in the Molten Sulfur configuration at 155°C, 300 psig, 10% steam in the feed, and a total feed flow of 2 SLPM. The H_2S concentration was varied from 8500 ppm down to 4250 ppm while keeping the total flow, the steam flow, and all other reaction parameters constant. The results are shown in Figure 3.21.

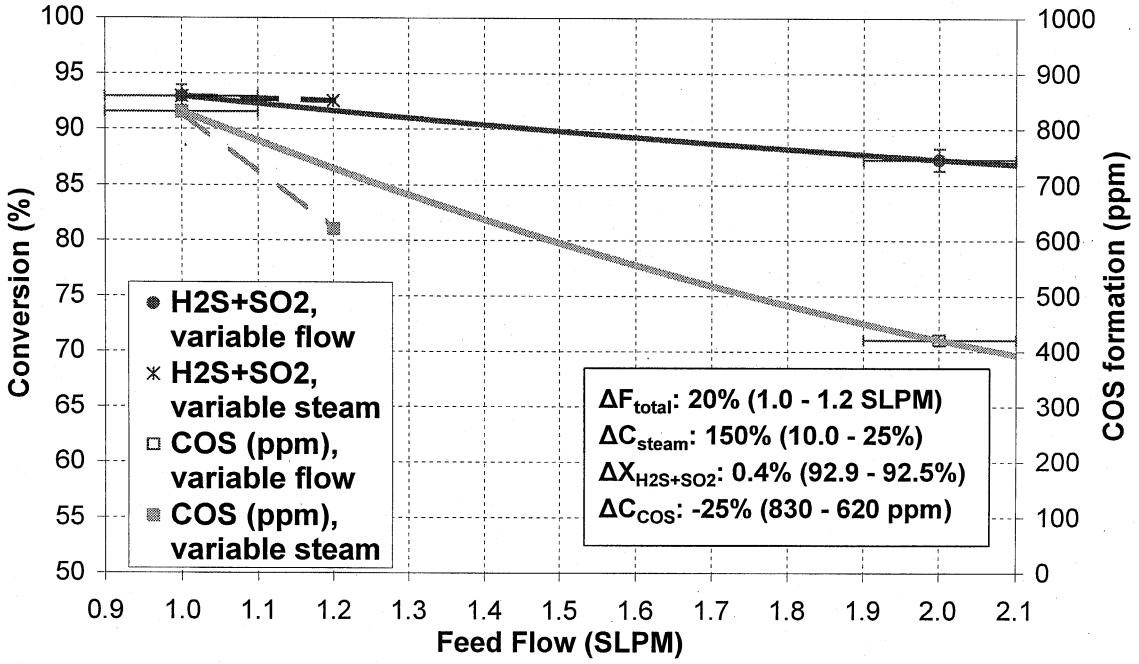

Figure 3.20. Effect of feed flow and steam feed concentration on sulfur removal activity and COS formation for SSRP in Molten Sulfur; T: 155°C; P: 300 psig; H_2S: 9000 ppm; SO_2: 4400 ppm; steam: 10%

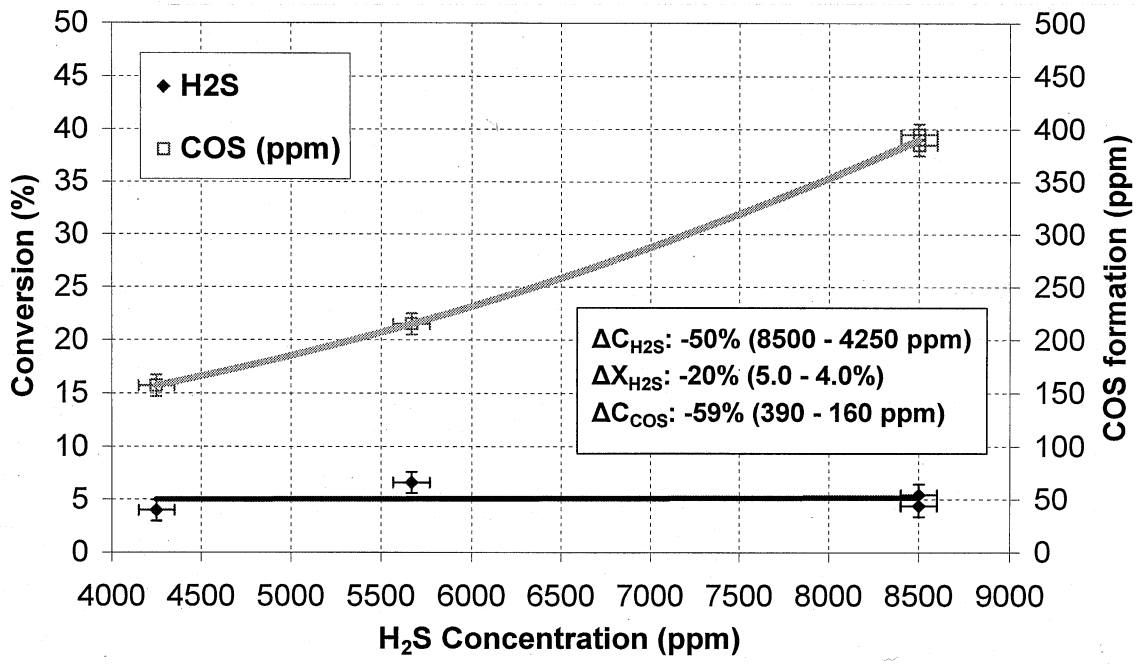

Figure 3.21. Effect of H_2S inlet concentration on H_2S conversion and COS formation for SSRP in Molten Sulfur; T: 155°C; P: 300 psig; F: 2 SLPM; steam: 10%

The conversion of H_2S was essentially constant (between 5% and 4%) upon decreasing the H_2S inlet concentration by half (from 8500 ppm to 4250 ppm), while the COS formation decreased by ca. 60% (from 390 ppm to 160 ppm). These results are indicative of an apparent first-order reaction of H_2S into COS with respect to the inlet concentration of H_2S (the expected apparent reaction order with respect to CO would be zero, due to the great excess of CO in the feed, ca. 50% vs. less than 1% H_2S). These results, however, could not indicate unequivocally whether the formation of COS was controlled by intrinsic kinetics or by diffusion of the reactant H_2S through the molten sulfur medium.

After restoring the H_2S inlet concentration to 8500 ppm, SO_2 was added at an inlet concentration of. 4330 ppm (Procedure **D'**), and a new steady state was attained at 155°C, 300 psig, and a total feed flow of 2 SLPM. The H_2S+SO_2 conversion was ca. 90.5% and the outlet COS was ca. 475 ppm. These results fit quite well with those of Fig. 3.19 at 2 SLPM, indicating that the steady-state reactivity of the system is the same, regardless of whether the addition of SO_2 took place prior to or after a reaction parameter variation (total feed flow in the former case and H_2S inlet concentration in the latter).

The effect of the steam inlet concentration was examined once again at 155°C and 300 psig, under a different feed procedure: steam feed followed by SO_2 feed and finally by the H_2S-containing syngas feed (Procedure **D**). Due to an error in the syngas flow, the H_2S/SO_2 inlet ratio was only ca. 1.36 as opposed to the target value of 2. The results of varying the steam feed concentration from 11.8% to 21.1% (with a corresponding increase in the total feed flow from 1.7 to 1.9 SLPM, with all other reaction parameters constant) are shown in Figure 3.22.

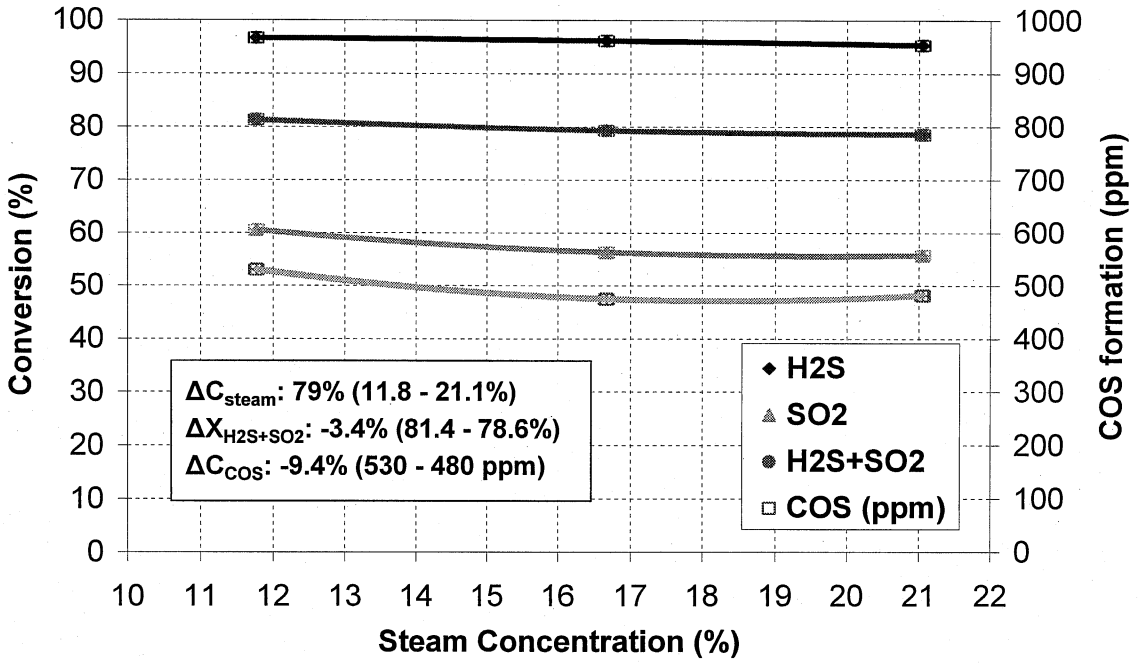

Figure 3.22. Effect of steam feed concentration on sulfur removal activity and COS formation for SSRP in Molten Sulfur; T: 155°C; P: 300 psig; inlet H_2S/SO_2: 1.36; F: 1.7-1.9 SLPM

The significant difference between the H_2S and SO_2 conversion at every examined steam concentration was due to the low H_2S/SO_2 inlet ratio, which is a good indication that the Claus (H_2S+SO_2) reaction is the major reaction under these conditions. Despite this difference in the conversion of the two reactants as shown in Fig. 3.22, the effect of variable steam concentration was minimal for both the sulfur removal activity (ca. 81.5% to 78.5%) and COS formation (ca. 530 ppm to 480 ppm).

Continuing in the same run, the stirring speed was varied from the standard value of 1000 RPM to 1500, 750, and finally 500 RPM, in order to examine its effect on the sulfur removal activity. The results of the variable stirring speed study are shown in Figure 3.23. A three-fold variation in stirring speed (from 500 to 1500 RPM) had minimal effect on sulfur removal activity and COS formation, suggesting the absence of significant mass transfer limitations under the examined reaction conditions.

The effect of varying the reaction temperature was examined at 300 psig, 10% steam in the feed, and a total feed flow of 2 SLPM. After feeding 200 sccm of steam (10% in 2 SLPM), SO_2 was fed followed by H_2S-containing syngas (Procedure **D**) and the system reached steady state. The reaction temperature was decreased from 155°C to 145°C, 136°C, and finally 128°C, with all other reaction parameters constant. As shown in Figure 3.24, the sulfur removal activity decreased from ca. 83.5% to ca. 79.5%, and the outlet COS from ca. 495 ppm to ca. 165 ppm. The total outlet sulfur-gas concentration (sum of unreacted H_2S and SO_2 and formed COS) was found to increase with decreasing temperature, indicating that the efficiency of SSRP is favored at the higher temperatures within the examined range (i.e., 145-155°C).

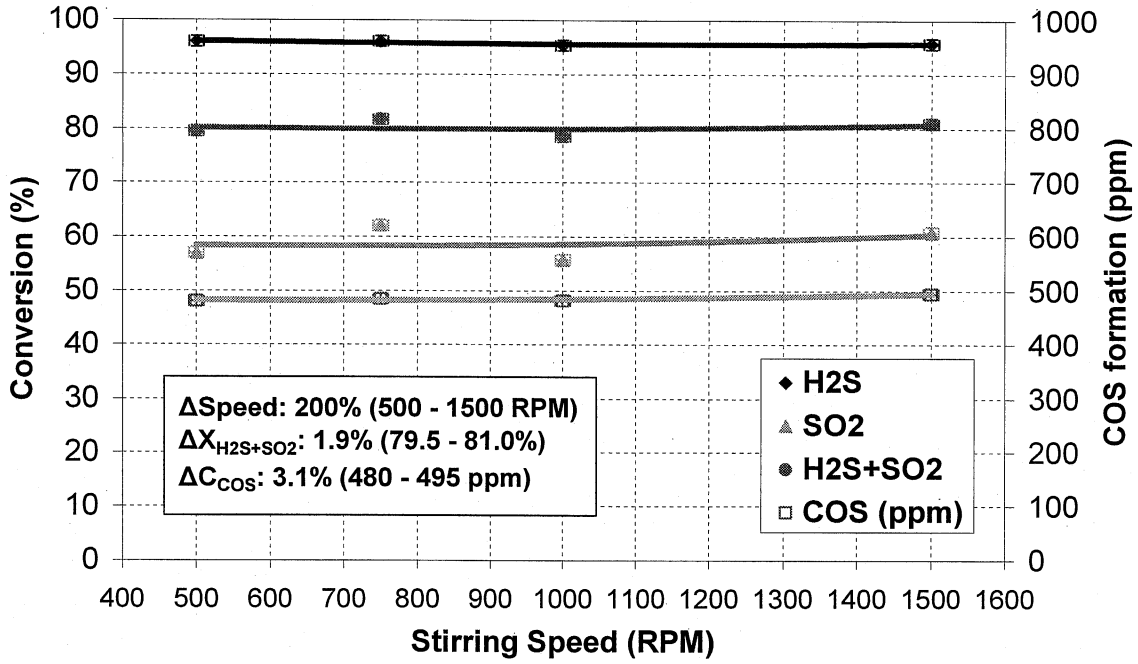

Figure 3.23. Effect of stirring speed on sulfur removal activity and COS formation for SSRP in Molten Sulfur; T: 155°C; P: 300 psig; inlet H_2S/SO_2: 1.36; F: 1.9 SLPM; steam: 21.1%

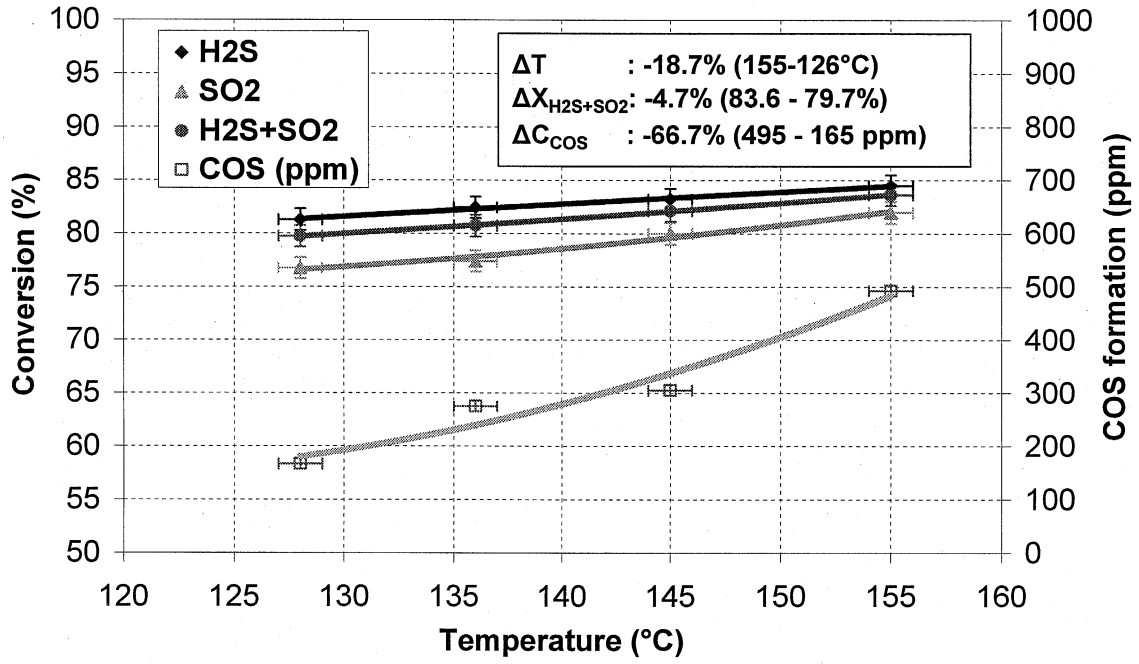

Figure 3.24. Effect of reaction temperature on sulfur removal activity and COS formation for SSRP in Molten Sulfur; P: 300 psig; H_2S: 8500 ppm; SO_2: 4380 ppm; F: 2 SLPM; steam: 10%

A new set of SSRP reaction experiments involved loading the glass liner with ca. 22.5 g (ca. 25 cc) E-alumina and ca. 716 g sublimed sulfur powder and placing it inside the reactor. Upon heating up beyond the melting point of sulfur (ca. 121°C) the reactor contained ca. 400 cc of molten sulfur (MS) into which the catalyst was suspended under stirring. The reactor was then heated to 155°C and pressurized to 300 psig under inert gas flow of 0.9 SLPM. A steam flow of 0.1 SLPM was added (i.e., 10% steam) followed by substituting part of the inert gas flow with an equal combined flow of SO_2 and H_2S-containing syngas, that were fed at the same time (reactant co-feed).

After reaching steady state at a feed flow of 1 SLPM, the flow of each one of the three feed components (steam, SO_2, and H_2S-containing syngas) was decreased by 50%, thus making the total feed flow 0.5 SLPM. The results of this variation in total feed flow are given in Table 3.12. A decrease in feed flow by half (i.e., doubling the residence time) resulted in an increase in both sulfur removal activity (from ca. 91% to ca. 94%) and in the formation of COS (from ca. 745 ppm to ca. 950 ppm). The total outlet sulfur-gas concentration (sum of unreacted H_2S & SO_2 and formed COS) was found to decrease with decreasing feed flow. Therefore, higher residence times appear to enhance the efficiency of SSRP, despite the observed increase in the unfavorable formation of COS.

Table 3.12. Effect of feed flow on sulfur removal activity and COS formation, for SSRP in E-alumina + Molten Sulfur; T: 155°C; P: 300 psig; H_2S/SO_2: 1.85; steam: 10%

Feed Flow	**Conversion (%)**			**COS formation**
(SLPM)	**H_2S**	**SO_2**	**H_2S+SO_2**	**(ppmv)**
1.0	98.4	77.2	90.9	745
0.5	99.1	84.8	94.0	950

In a new run at 155°C following the same feed procedure as above (reactant co-feed) and at a total feed flow of 1 SLPM, steady state was attained at a pressure of 300 psig. Then, the effect of varying the reaction pressure to 400 psig, then to 350 psig, and finally to 250 psig, on the sulfur removal activity of the E-alumina + MS (molten sulfur) configuration was examined. The results of this pressure variation study are shown in Figure 3.25. An increase in reaction pressure from 250 psig to 400 psig resulted in an increase in sulfur removal activity (from ca. 94.5% to ca. 97.5%), as well as in COS formation (from ca. 600 ppm to ca. 730 ppm). The total outlet sulfur-gas concentration (sum of unreacted H_2S & SO_2 and formed COS) was found to increase with increasing pressure, indicating that the efficiency of SSRP is enhanced at higher pressures, which are favored in a commercial application involving gasifier-syngas.

It is also interesting to note that the difference in conversion between H_2S and SO_2 was found to decrease with increasing pressure (the conversion curves appeared to merge above 350 psig). This observation is apparently related to the different effect of pressure on the diffusivity and solubility of these two compounds in molten sulfur.

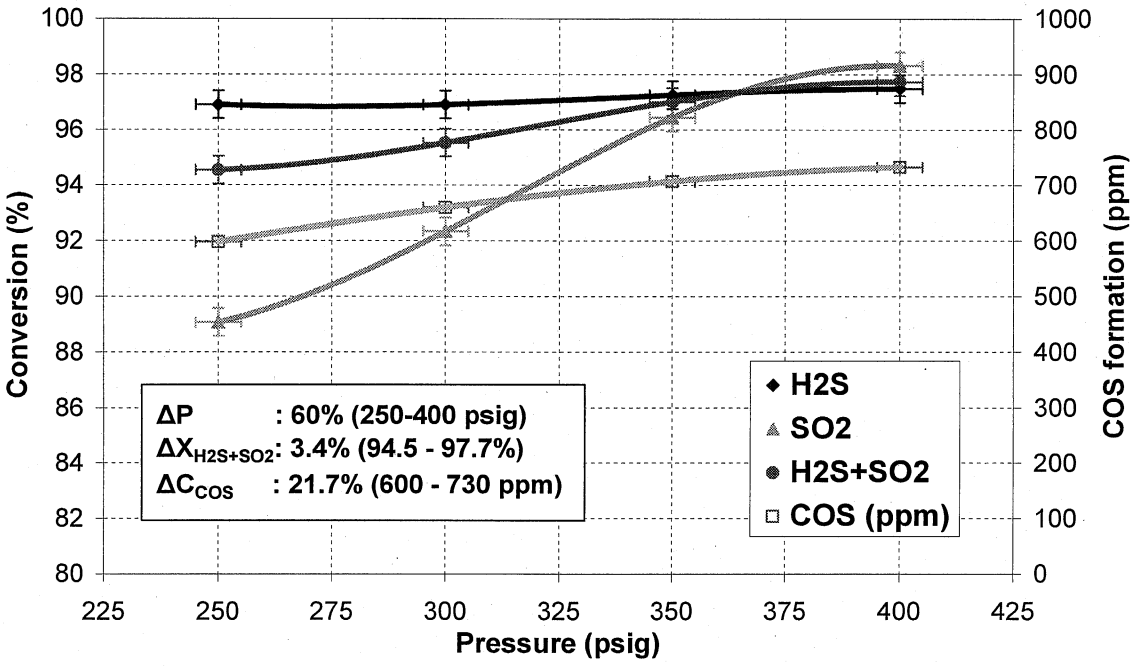

Figure 3.25. Effect of reaction pressure on sulfur removal activity and COS formation for SSRP on E-alumina + Molten Sulfur; T: 155°C; H_2S: 8800 ppm; SO_2: 4600 ppm; F: 1 SLPM; steam: 10%

After completing the pressure study and with the reaction being at steady state at 155°C and 250 psig, the SO_2 was removed from the feed while maintaining the total feed flow and all other reaction parameters constant. As shown in Table 3.13, the removal of SO_2 from the feed resulted in a significant increase in COS formation (from ca. 600 ppm to ca. 930 ppm). This is in clear contrast to the observed trends for the blank CSTR and the Molten Sulfur only (no catalyst) configurations, where addition of SO_2 increased and removal of SO_2 decreased the outlet COS. Furthermore, the H_2S conversion in the present case was minimal (ca. 0.4%), implying that less than ca. 1/10th of the measured COS was formed from H_2S. Therefore, in the presence of the E-alumina catalyst, addition of SO_2 apparently shifts the pathway for COS formation from the (inevitable for H_2S-containing syngas feed) CO+H_2S reaction to that of CO with active sulfur generated by the H_2S+SO_2 reaction, at least to a major extent.

Table 3.13. Effect of SO_2 removal on sulfur removal activity and COS formation, for SSRP on E-alumina + Molten Sulfur; T: 155°C; P: 300 psig; H_2S: 8500 ppm; steam: 10%; F: 1 SLPM

	Conversion (%)			COS formation
SO_2 (ppm)	**H_2S**	**SO_2**	**H_2S+SO_2**	**(ppmv)**
4600 (SO_2 present)	96.9	89.1	94.5	600
0 (SO_2 removed)	0.4	-	-	930

A comparison between the Molten Sulfur only (no catalyst) and the E-alumina + Molten Sulfur configuration with respect to their sulfur removal activity and COS formation, is given in Table 3.14. The reaction parameters were 155°C, 300 psig, 1 SLPM, and 10% steam in the feed. The presence of the E-alumina catalyst appears to enhance the sulfur removal activity (from ca. 93% to ca. 95.5%), while decreasing the undesirable formation of COS (from ca. 830 ppm to 660 ppm). The total outlet sulfur-gas concentration (sum of unreacted H_2S & SO_2 and formed COS) decreased significantly (by more than 500 ppm) with the E-alumina catalyst. More efficient catalysts (especially in terms of further suppressing the formation of COS, possibly via COS hydrolysis) would further improve the performance of SSRP in terms of sulfur removal.

Table 3.14. Effect of the presence of E-alumina on the sulfur removal activity and COS formation, for SSRP in Molten Sulfur; T: 155°C; P: 300 psig; H_2S/SO_2: 1.9-2.0; steam: 10%; F: 1 SLPM

	Conversion (%)			COS formation
Configuration	**H_2S**	**SO_2**	**H_2S+SO_2**	**(ppmv)**
Molten Sulfur only	90.9	97.2	92.9	830
MS +E-alumina	96.9	92.3	95.5	660

A new set of SSRP reaction experiments involved loading the glass liner with a fresh batch of ca. 22.5 g (ca. 25 cc) E-alumina and ca. 716 g sublimed sulfur powder and placing it inside the reactor. Upon heating up beyond the melting point of sulfur (ca. 121°C) the reactor contained ca. 400 cc of molten sulfur (MS) into which the catalyst was suspended under stirring. The reactor was then heated to 155°C and pressurized to 300 psig under inert gas flow of 0.9 SLPM. A steam flow of 0.1 SLPM was added (i.e., 10% steam) followed by substituting part of the inert gas flow with SO_2/N_2 to achieve 4400 ppm SO_2 in the feed. Then, the remaining N_2 flow was substituted by an equal coal gas flow, thus achieving 8800 ppm H_2S in the feed and a total feed flow of 1 SLPM. The measured H_2S+SO_2 conversion was ca. 90.5% and the outlet COS was ca. 645 ppm (Figure 3.26).

As expected, the conversion was lower in the CSTR than the fixed-bed micro-reactor that more closely simulates a plug-flow reactor (PFR) and whose results were discussed in Section 3.3.1. This is because in a CSTR the conversion (rate) is determined by the outlet concentration. The commercial embodiment (Fig. 3.1) is conceived to be a slurry bubble column reactor in which the conversion should be closer to that of the fixed-bed reactor.

The effect of feed flow variation on sulfur removal activity and COS formation was examined by increasing the total (steam + SO_2 + H_2S-containing syngas) flow from 1 SLPM to 2 and finally 3 SLPM, all other reaction parameters remaining constant. As shown in Figure 3.26, a three-fold increase in feed flow caused a decrease in H_2S+SO_2 conversion (down to ca. 86.5%) and an almost 60% decrease in COS formation (down to ca. 265ppm). These results are in good agreement with those of Table 3.12 (for 0.5-1 SLPM) and Fig. 3.19 (for Molten Sulfur only).

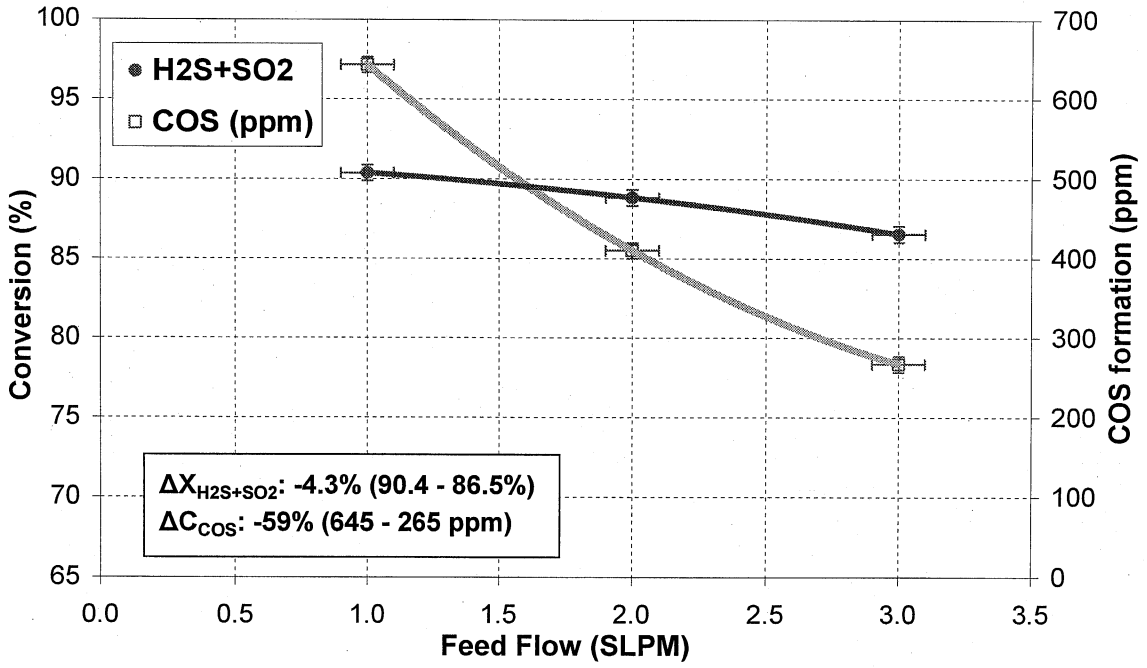

Figure 3.26. Effect of feed flow on sulfur removal activity and COS formation for SSRP on E-alumina + Molten Sulfur; T: 155°C; P: 300 psig; H_2S: 8800 ppm; SO_2: 4400 ppm; steam: 10%

The effect of pressure on sulfur removal activity and COS formation was examined at 155°C and a feed flow of 2.8 SLPM, by varying the reaction pressure from 350 psig to 400 psig and then down to 300, 275, and finally 250 psig. A decrease in pressure from 400 psig to 250 psig resulted in a decrease in sulfur removal activity (the H_2S+SO_2 conversion decreased from ca. 91% to ca. 87%) and only a small decrease in COS formation (from ca. 345 ppm to ca. 290 ppm), as shown in Figure 3.27. These results are in good qualitative agreement with those of Fig. 3.25. The lower H_2S+SO_2 conversion and COS formation values in the present case compared to the corresponding ones of Fig. 3.25 are due to the higher total feed flow (2.8 SLPM vs. 1 SLPM). Therefore, higher reaction pressures enhance the sulfur removal efficiency of SSRP while only moderately increasing the undesirable formation of COS.

After completing the pressure variation study, the reaction was maintained at steady state at 155°C, 250 psig, and a total feed flow of 2.8 SLPM. Then, the SO_2/N_2 flow was substituted by an equal flow of N_2, thus maintaining the reaction pressure and total feed flow into the reactor. In the absence of SO_2 the conversion of H_2S decreased drastically (down to 5% or less), and the formation of COS increased from ca. 290 ppm to ca. 410 ppm. These results are in very good qualitative agreement with those of Table 3.13. The lower COS formation values in both the presence and absence of SO_2 in the present case compared to the corresponding ones of Table 3.13 are due to the higher feed flow (2.8 SLPM vs. 1 SLPM). Thus, removal of SO_2 appears to shift the pathway for COS formation back to the $CO+H_2S$ reaction.

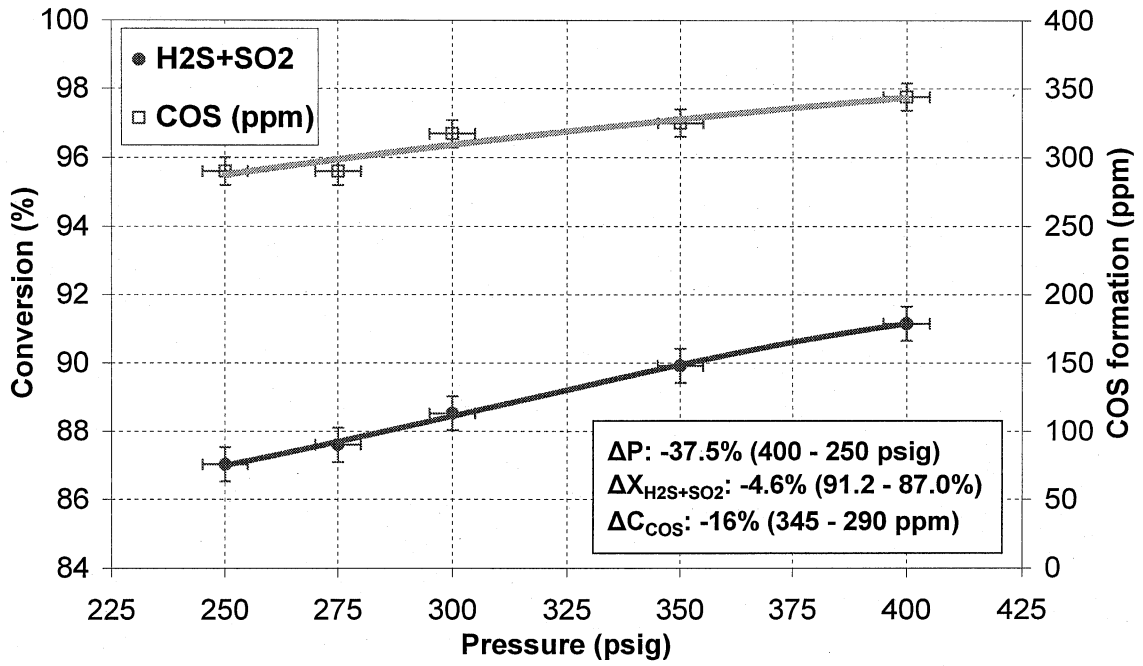

Figure 3.27. Effect of pressure on sulfur removal activity and COS formation for SSRP on E-alumina + Molten Sulfur; T: 155°C; H_2S: 8800 ppm; SO_2: 4400 ppm; steam: 10.7%; F: 2.8 SLPM

In a similar manner, the SSRP reaction was examined at a reaction temperature of 125°C, a reaction pressure of 350 psig, and a feed flow of 2.8 SLPM. After achieving a pseudo steady state under these conditions, the SO_2/N_2 flow was again substituted by an equal flow of N_2, thus maintaining the reaction pressure and total feed flow into the reactor. In the absence of SO_2 the conversion of H_2S decreased from ca. 93.5% down to ca. 1% (corresponding to ca. 90 ppm of converted H_2S), whereas the formation of COS remained essentially constant (from ca. 95 ppm to ca. 85ppm). Thus, the same observation is valid for these two experiments, despite the differences in reaction temperature (155°C and 125°C) and pressure (250 psig and 350 psig): the good agreement between the amount of converted H_2S and formed COS appears to suggest that in the absence of SO_2 the formation of COS is the result of the reaction between CO (and/or CO_2) and H_2S (reactions 3.7 and 3.9).

The effect of steam concentration was examined at 125°C, 300 psig, and an initial feed flow of 2 SLPM, by varying the steam feed flow from 0.2 SLPM to 0.3 and then to 0.4 SLPM, while keeping all other reaction parameters constant. The corresponding feed concentration of steam was 10%, 14.3%, and 18.2%, respectively. As shown in Figure 3.28, the sulfur removal activity was not affected by this variation in feed steam concentration (H_2S+SO_2 conversion of ca. 90.5%). On the other hand, the formation of COS decreased from ca. 115 ppm to ca. 75 ppm, the lowest achievable outlet COS concentration. This 35% decrease in COS could be partially due to a 10% increase in total feed flow (from 2.2 SLPM to 2.4 SLPM). Reaction temperature, inlet steam concentration, and total feed flow, appear to be important parameters in limiting the formation of COS, without significantly affecting the sulfur removal efficiency of SSRP.

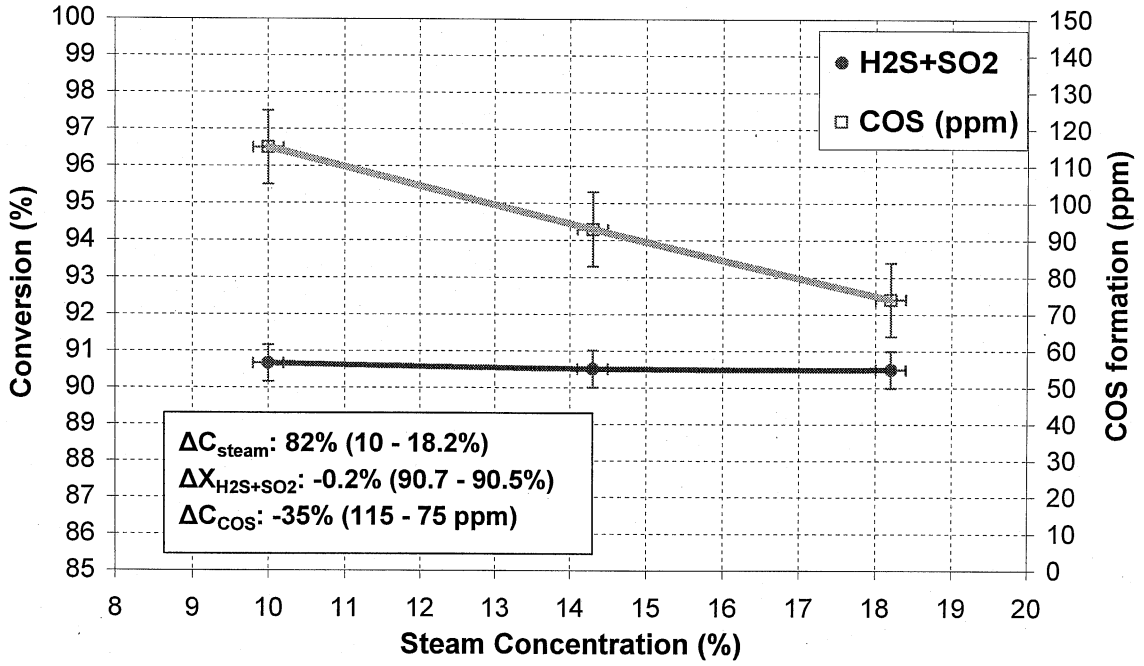

Figure 3.28. Effect of steam inlet concentration on sulfur removal activity and COS formation for SSRP on E-alumina + Molten Sulfur; T: 125°C; P: 300 psig; H_2S: 8480 ppm; SO_2: 3800 ppm; F: 2.0-2.4 SLPM

The final set of SSRP reaction experiments involved loading the glass liner with ca. 45 g (ca. 50 cc) E-alumina and ca. 716 g sublimed sulfur powder and placing it inside the reactor. The scope of these experiments with double the amount of catalyst but same amount of sulfur as above was to evaluate the effect of a higher catalyst load onto the sulfur removal activity of the catalyst + Molten Sulfur configuration in the CSTR. Upon heating up beyond the melting point of sulfur (ca. 121°C) the reactor contained ca. 400 cc of molten sulfur (MS) into which the catalyst was suspended under stirring. The reactor was then heated to 155°C and pressurized to 300 psig under inert gas flow of 1.8 SLPM. A steam flow of 0.2 SLPM was added (i.e., 10% steam) followed by substituting part of the inert gas flow with an equal flow of SO_2 and then with H_2S-containing syngas (Procedure **D**).

After attaining steady state under these conditions, the SO_2 and H_2S-containing syngas flow were decreased by half (from 1.8 SLPM to 0.9 SLPM) while the steam flow was maintained at 0.2 SLPM, thus giving a new total feed flow of 1.1 SLPM with a steam feed concentration of 18.2%. The effect of steam feed concentration was examined by increasing the steam feed flow to 0.3 SLPM (total feed flow of 1.2 SLPM, steam concentration of 25%); then by decreasing it to 0.1 SLPM (total fee flow of 1.0 SLPM, steam concentration of 10%). The results of the steam concentration variation study are shown in Figure 3.29. An increase in steam inlet concentration from 10% to 25% had essentially no effect on sulfur removal activity (H_2S+SO_2 conversion of ca. 95.5%), whereas the formation of COS decreased from ca. 630 ppm to ca. 535 ppm. These results are in very good agreement with those of Fig. 3.28. The decrease in COS formation (less prominent percentage-wise than that in Fig. 3.28), is again apparently related to both the increase in steam concentration and increase in total feed flow.

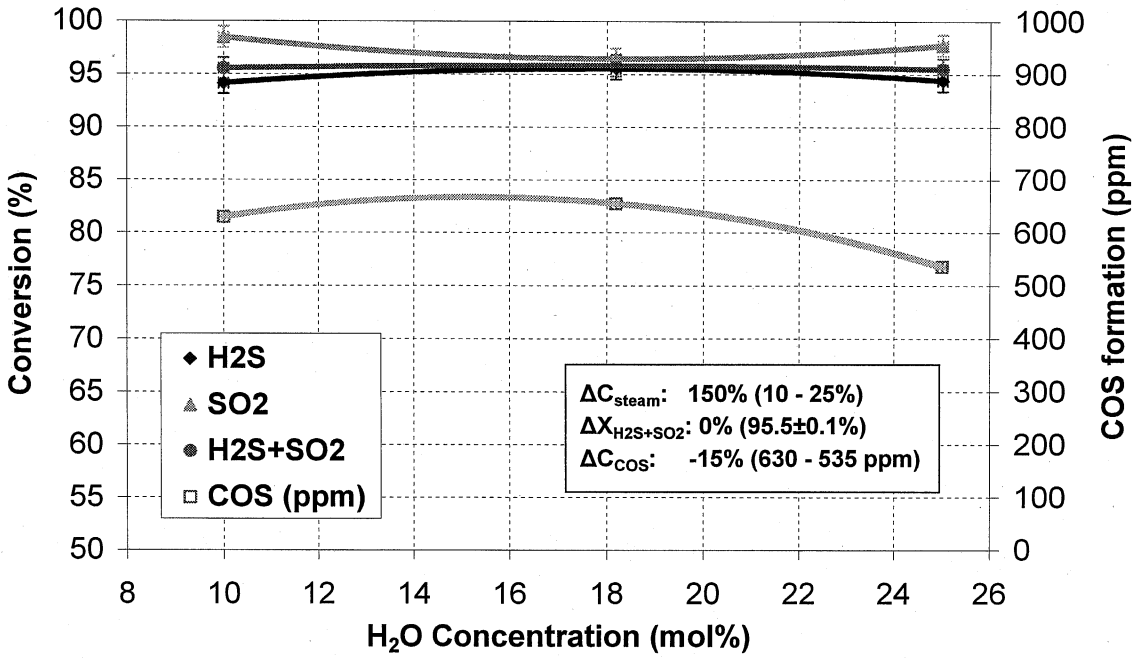

Figure 3.29. Effect of steam inlet concentration on sulfur removal activity and COS formation for SSRP on E-alumina + Molten Sulfur; T: 155°C; P: 300 psig; H_2S: 8500 ppm; SO_2: 4040 ppm; F: 1.0-1.2 SLPM

The effect of feed flow variation under constant steam inlet concentration was examined by comparing the results of the first and last stages of the above run; with a total feed flow of 2.0 SLPM and 1.0 SLPM, respectively, and a steam inlet concentration of 10% in both cases. The results of this comparison are given in Table 3.15. A decrease in the total feed flow by half resulted in a measurable increase in H_2S+SO_2 conversion (from ca. 92% to ca. 95.5%) and in COS formation (from ca. 575 ppm to ca. 630 ppm). These results are in very good agreement with those in Table 3.12 (for 1.0-0.5 SLPM), in Fig. 3.26 (for 1.0–3.0 SLPM), and in Fig. 3.19 (for 1.0-3.0 SLPM, Molten Sulfur only). As seen before, the total outlet sulfur-gas concentration (sum of unreacted H_2S & SO_2 and formed COS) was found to decrease with decreasing feed flow. Therefore, higher residence times again appear to enhance the efficiency of SSRP, despite the observed increase in the unfavorable formation of COS.

Table 3.15. Effect of feed flow on sulfur removal activity and COS formation, for SSRP in E-alumina + Molten Sulfur; T: 155°C; P: 300 psig; H_2S/SO_2: 2.1; steam: 10%

Feed Flow	Conversion (%)			COS formation
(SLPM)	H_2S	SO_2	H_2S+SO_2	(ppmv)
2.0	95.2	85.2	92.0	575
1.0	94.1	98.5	95.5	630

The effect of varying the SO_2 inlet concentration at 155°C and 300 psig was examined by varying the SO_2/N_2 flow while keeping the syngas and steam flows constant. The concentration of $SO_2$was varied from 4550 ppm down to 3200 ppm, then up to 3900 ppm, and finally to 5150 ppm. As shown in Figure 3.30, the H_2S+SO_2 conversion exhibited a maximum of ca. 94% at an intermediate SO_2 inlet concentration. The formation of COS was only minimally affected by this variation (outlet COS from 570 ppm to 480 ppm). These results are in very good agreement with those in Fig. 3.10 (fixed-bed micro-reactor) and in Fig. 3.13 (micro-bubbler).

In a new run at 155°C and 300 psig, 0.2 SLPM steam were fed into the reactor under a total feed flow of 2 SLPM, followed by introducing the H_2S-containing syngas feed (no SO_2 feed). Upon attaining steady state, SO_2 was added in the feed (Procedure **D'**) while keeping the total feed flow at 2 SLPM and all other reaction parameters constant. The results of the addition of SO_2 are given in Table 3.16. The outlet COS concentration decreased from 560 ppm to 465 ppm, in very good agreement with the results of Table 3.13 (for SO_2 removal).

Continuing in the same run, the syngas and SO_2 flows were decreased by half whereas the steam feed flow was maintained at 0.2 SLPM, thus making the total feed flow 1.1 SLPM. The results of this variation in feed flow were qualitatively very similar to those of Table 3.15. At these new conditions, the effect of reaction temperature on sulfur removal activity and COS formation was examined by decreasing the temperature from 155°C to 145°C and then to 135°C, while keeping all other reaction parameters constant. The results of this temperature variation study are shown in Figure 3.31.

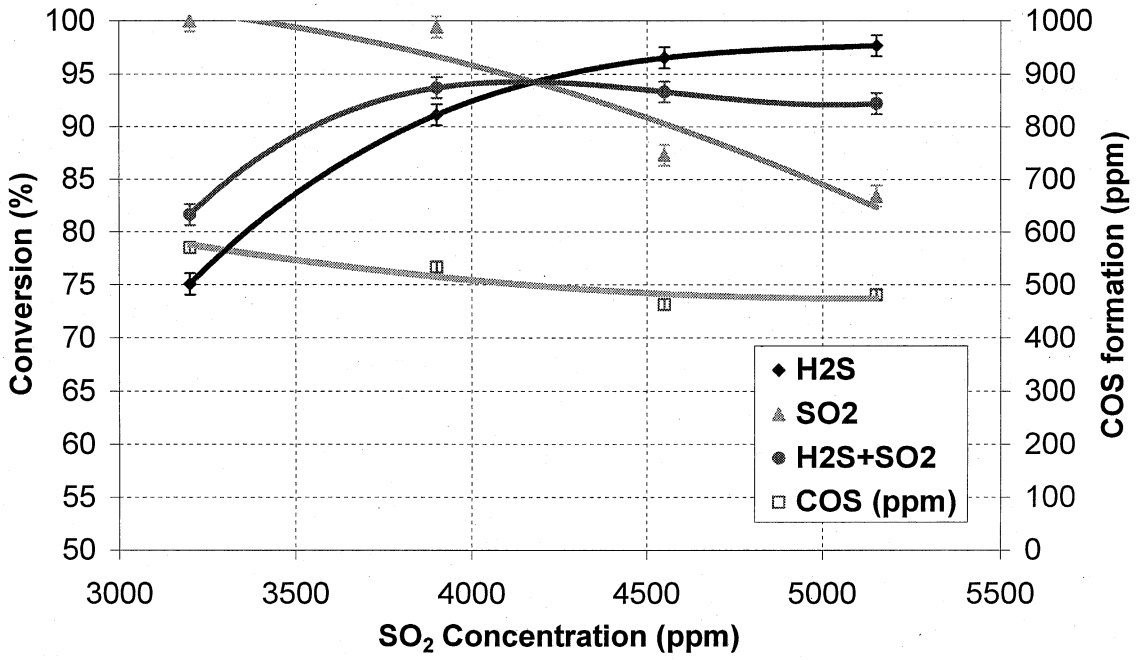

Figure 3.30. Effect of SO_2 inlet concentration on sulfur removal activity and COS formation for SSRP on E-alumina + Molten Sulfur; T: 155°C; P: 300 psig; H_2S: 9000-8270 ppm; steam: 9.75-10.25%; F: 1.90-2.05 SLPM

Table 3.16. Effect of SO_2 removal on sulfur removal activity and COS formation, for SSRP on E-alumina + Molten Sulfur; T: 155°C; P: 300 psig; H_2S: 8760 ppm; steam: 10%; F: 2 SLPM

	Conversion (%)			COS formation
SO_2 (ppm)	H_2S	SO_2	H_2S+SO_2	(ppmv)
4600 (SO_2 present)	96.9	89.1	94.5	600
0 (SO_2 removed)	0.4	-	-	930

A decrease in reaction temperature from 155°C to 135°C was found to have essentially no effect on the sulfur removal activity of the E-alumina + Molten Sulfur configuration (H_2S + SO_2 conversion of ca. 96.5-97%). The outlet COS concentration decreased from ca. 720 ppm to 510 ppm. The total outlet sulfur-gas concentration (sum of unreacted H_2S & SO_2 and formed COS) was found to decrease with decreasing temperature; thus, the overall efficiency of SSRP is favored at lower reaction temperatures. This result is in contrast to that for the Molten Sulfur without a catalyst, where the H_2S+SO_2 conversion decreased with reaction temperature along with COS formation (see Fig. 3.24), making the overall efficiency of SSRP to be favored at higher reaction temperatures. It is obvious that the presence of the E-alumina catalyst changes the relative progress of the H_2S+SO_2 reaction and the COS formation, thus making lower temperatures more favorable for SSRP.

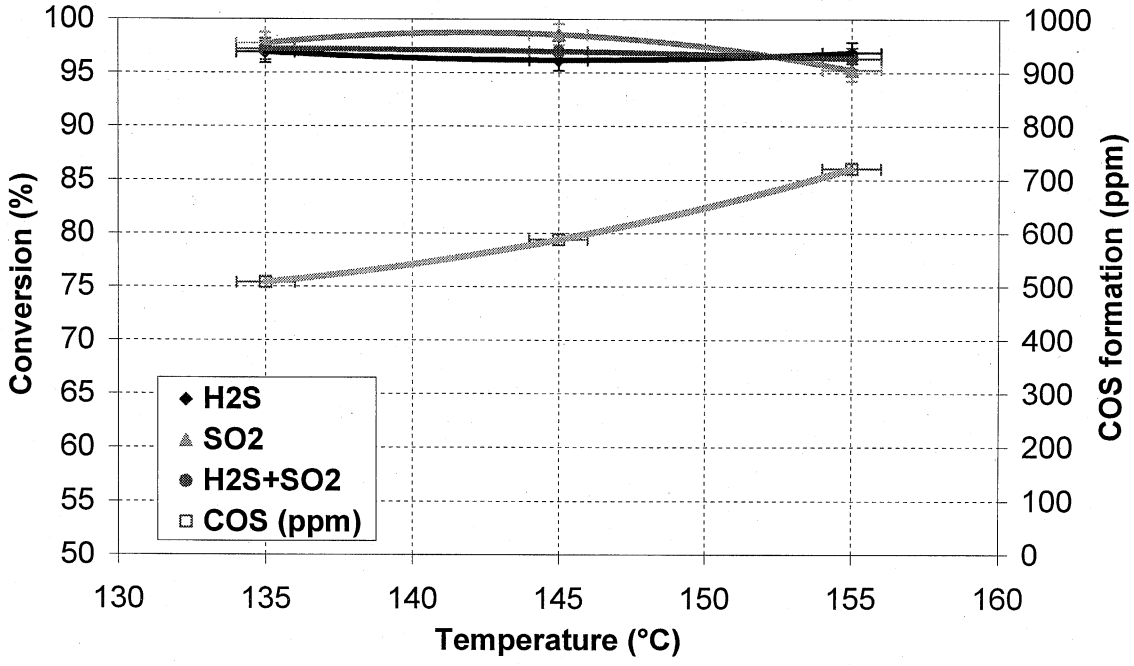

Figure 3.31. Effect of reaction temperature on sulfur removal activity and COS formation for SSRP on E-alumina + Molten Sulfur; P: 300 psig; H_2S: 8760 ppm; SO_2: 4400 ppm; steam: 18.2%; F: 1.1 SLPM

The effect of steam addition was examined at 135°C and 300 psig by adding 0.2 SLPM steam to a flow of SO_2+H_2S-containing syngas of 0.9 SLPM, thus making the total feed flow 1.1 SLPM and the steam inlet concentration from 0% to 18.2%. The results of the steam addition on sulfur removal activity and COS formation are given in Table 3.17. The addition of steam resulted in a measurable increase in sulfur removal activity (H_2S+SO_2conversion from ca. 94% to ca. 95.5%), and a decrease in COS formation from ca. 450 ppm to ca. 405 ppm. The observed decrease in COS formation was most likely the result of the corresponding increase in total feed flow along with the addition of steam.

Table 3.17. Effect of steam addition on sulfur removal activity and COS formation, for SSRP on E-alumina + Molten Sulfur; T: 135°C; P: 300 psig; H_2S: 8760 ppm; SO_2: 4700 ppm; F: 0.9-1.1 SLPM

	Conversion (%)			COS formation
Steam (%)	**H_2S**	**SO_2**	**H_2S+SO_2**	**(ppmv)**
0 (steam absent)	98.8	85.5	94.2	450
18.2 (steam added)	98.3	90.2	95.5	405

Continuing in the same run, after the addition of steam the feed flow of the SO_2 and H_2S-containing syngas streams was doubled (from 0.9 SLPM to 1.8 SLPM), thus making the total feed flow increase from 1.1 SLPM to 2.0 SLPM. The corresponding steam inlet concentration was decreased from 18.2% down to 10% by this increase in feed flow. The effect of this flow increase on sulfur removal activity and COS formation are given in Table 3.18 (the first row of which is the same as the last one of Table 3.17). As expected, an increase in the total feed flow led to a decrease in sulfur removal activity (H_2S+SO_2 conversion from ca. 95.5% to ca. 93%) and in COS formation by almost half (from ca. 405 ppm down to ca. 215 ppm). Inspection of the results of Tables 3.17 and 3.18 indicated that the formation of COS (decreasing) was affected by the total feed flow (increasing) rather than by the steam inlet concentration (increasing and then decreasing). On the other hand, the sulfur removal activity was apparently influenced by both these two reaction parameters, in good agreement with previous observations on the importance of steam in the feed for SSRP (see Fig. 3.4).

Table 3.18. Effect of feed flow on sulfur removal activity and COS formation, for SSRP on E-alumina + Molten Sulfur; T: 135°C; P: 300 psig; H_2S: 8760 ppm; SO_2: 4700 ppm; steam: 18.2%-10.0%

Feed Flow	Conversion (%)			**COS formation**
(SLPM)	**H_2S**	**SO_2**	**H_2S+SO_2**	**(ppmv)**
1.1 (steam: 18.2%)	98.3	90.2	95.5	405
2.0 (steam: 10.0%)	97.0	85.0	92.8	215

In a new run at 135°C, 300 psig, and a total feed flow of 2 SLPM, 0.2 SLPM (i.e. 10%) of steam were fed into the reactor, followed by SO_2 feed and finally by H_2S-containing syngas feed (Procedure **D**). After reaching steady state, the reaction pressure was increased to 450 psig in 50 psig steps, and then decreased to 375 psig and finally to 325 psig. The effect of reaction pressure variation on sulfur removal activity and COS formation is shown in Figure 3.31. The H_2S+SO_2 conversion increased from ca. 93% to ca. 95% as a result of the increase in reaction pressure from 300 psig to 450 psig. On the other hand, the formation of COS was essentially unaffected (ca. 230-220 ppm). The total outlet sulfur-gas concentration (sum of unreacted H_2S & SO_2 and formed COS) was found to decrease with increasing pressure; thus, the overall efficiency of SSRP is favored at higher reaction pressures, as was also observed before (see Figs. 3.25 and 3.27).

The effect of reaction pressure was also examined at 135°C under the same procedure (Procedure **D**), but at a total feed flow of 1 SLPM (instead of 2 SLPM) and a steam inlet concentration of 18.2% (instead of 10%). The reaction pressure was increased from 300 psig to 350 and finally to 400 psig, and the results are shown in Figure 3.33. The observed trends in sulfur removal activity and COS formation are the same as those of Fig. 3.32. The absolute values for both H_2S+SO_2 conversion and outlet COS were higher than those of Fig. 3.32, due to the lower total feed flow (1 SLPM vs. 2 SLPM), the effect of which (i.e., the feed flow) has been clearly demonstrated above. It is interesting to note that the beneficial effect of pressure on the sulfur removal activity of E-alumina + Molten Sulfur appears to be more prominent at lower reaction temperatures.

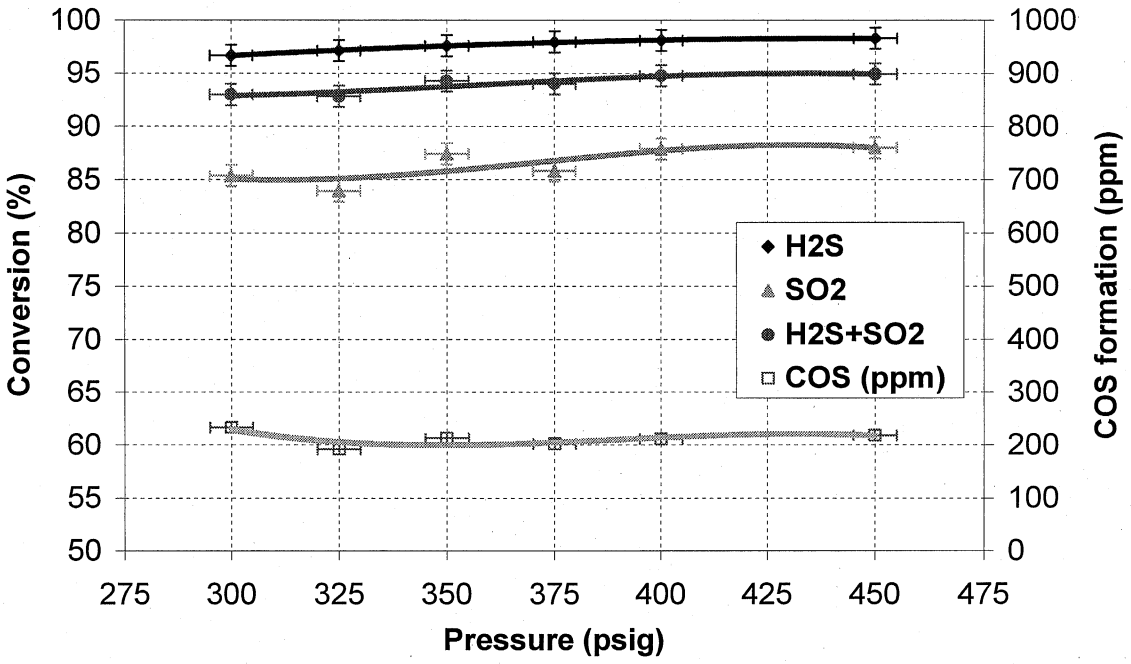

Figure 3.32. Effect of reaction pressure on sulfur removal activity and COS formation for SSRP on E-alumina + Molten Sulfur; T: 135°C; H_2S: 8700 ppm; SO_2: 4200 ppm; steam: 10%; F: 2 SLPM

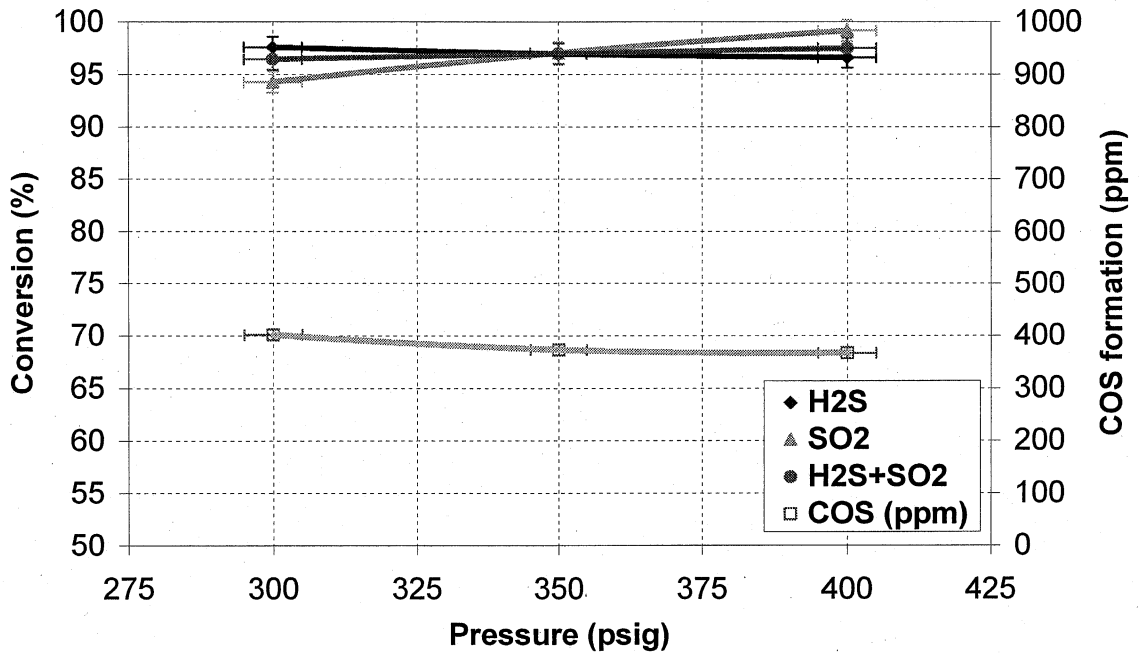

Figure 3.33. Effect of reaction pressure on sulfur removal activity and COS formation for SSRP on E-alumina + Molten Sulfur; T: 135°C; H_2S: 8400 ppm; SO_2: 4400 ppm; steam: 18.2%; F: 1 SLPM

A total of 17 runs were performed using the 45 g (50 cc) of E-alumina in Molten Sulfur. This catalyst was exposed to at least one of the two reactants (H_2S and SO_2) for ca. 145 hours, and to both reactants for ca. 100 hours. Assuming an average total feed flow of 1 SLPM (which is an underestimate) and a total inlet sulfur concentration of 12500 ppm (typically ca. 8400 ppm H_2S and 4200 ppm SO_2), then, on a time basis of 100 hours on stream:

1 SLPM * 1000 scc/L* 60 min/h * 100 h * 12500 ppm S = 75000 scc S
75000 scc S / 22400 (scc/mol) = 3.35 mol S, and 3.35 mol S * 32 (g/mol) = 107 g S

Assuming that the produced sulfur has the density of liquid sulfur at 155°C (which is ca. 1.79 g/cc), the total volume of produced sulfur during 100 hours on stream is ca. 60 cc. The pore volume of 45 g E-alumina is ca. 28 cc (see Table 3.7), i.e., less than half of the sulfur produced during this experiment. If even one fifth of the produced sulfur were to remain in the pores of E-alumina, it would have blocked almost 50% of them, causing a very rapid deactivation, which was definitely not observed in the described experiment. These calculations clearly indicate that the majority of the produced sulfur is indeed dissolved into the molten sulfur medium; thus, the SSRP can be performed in molten sulfur with high efficiency and no apparent deactivation.

The processed data of the bench-scale CSTR experiments on SSRP, from which the figures and tables presented above were generated, are included in Appendix **K**. The main conclusions from the process evaluation study for SSRP in the bench-scale CSTR are presented in Section 5.

4. ECONOMIC EVALUATION OF SSRP

4.1. Introduction

Over the past three years RTI has been investigating the Single-step Sulfur Recovery Process (SSRP). The SSRP (Figure 3.1) is an alternative to the conventional amine-Claus-SCOT process in which H_2S is removed from syngas and converted to elemental sulfur. In the SSRP, H_2S laden syngas is mixed with a quantity of SO_2 containing gas such that the ratio of H_2S to SO_2 in the syngas is 2.0. This mixture is then passed to a slurry bubble column reactor (SBCR) where the gas is contacted with a slurry of SSRP catalyst in liquid sulfur at about 300°F and at near the gasification pressure. In the SBCR, the H_2S and SO_2 react via the Claus reaction and produce liquid elemental sulfur. An amount of sulfur equivalent to the yield of sulfur produced by the Claus reaction is withdrawn from the SBCR. Approximately 1/3 of this yield is burned with air to produce the SO_2 that is mixed with the untreated syngas prior to passage into the SBCR. The remaining 2/3 of the elemental sulfur is product which can be sold. Experiments carried out at RTI which simulate the SSRP, have shown that it is possible to remove 99% of the inlet sulfur passed to the catalytic reactor. About 1% of the sulfur as SO_2, H_2S and a small fraction as COS remain in the treated syngas. Thus in a single catalytic reactor supported by an external sulfur burner, the SSRP accomplishes the same job as the amine-Claus-SCOT which involves numerous columns and catalytic reactors. This observation indicates that the SSRP may be a cost effective alternative to the amine-based scrubbing process and can potentially make power generation by IGCC less capital intensive.

An economic evaluation of the SSRP as applied to IGCC power generation was carried out and compared to a cost analysis carried out by EG&G (*Shelton and Lyons, 1998*) for IGCC power generation using a Texaco gasifier and an amine-Claus-SCOT process for sulfur control. DOE's objective in sponsoring this work at EG&G was "to establish base cases for commercially available (or nearly available) power systems having a nominal size of 400 megawatts (MWe)." Thus it is an excellent analysis upon which to base an economic evaluation of the SSRP and can also serve as a source of economic evaluations of IGCC processes using various sulfur control technologies to which IGCC - SSRP can be compared.

4.2. Selection of IGCC Base Case

In the EG&G Report, three base cases are presented. For each case, fairly detailed material and heat balances are presented. In addition capital and operating cost are computed for each base case. The three cases are summarized in Table 4.1. The major differences between the three base cases are the mode of gas cooling following the Texaco gasifier and the gas cleanup systems. In Case 1 the gasifier is operated at a pressure of 615 psia with raw gas cooling being accomplished by quenching the raw gas with liquid water. The quenched and partially cooled syngas is then passed through a COS hydrolysis unit to convert COS to H_2S. H_2S is removed by first cooling the syngas to 103°F, and then scrubbing it with MDEA to remove approximately 99% of H_2S from syngas. The MDEA scrubbing unit is supported by Claus and SCOT units to recover the absorbed H_2S as elemental sulfur.

Table 4.1. Texaco Gasifier IGCC Base Cases Summary

	CASE 1	CASE 2	CASE 3
Gasifier	Texaco	Texaco	Texaco
Gasifier Pressure, psia	615	475	475
Cooling Mode	Quench	RSC + CSC	RSC + CSC
Sulfur Removal	CGCU	CGCU	HGCU
Gas Turbine Power (MWe)	271.9	272.5	271.2
Steam Turbine Power (MWe)	154.1	192.4	184.9
Misc/Aux Power (MWe)	44.4	54.5	49.2
Total Plant Power (MWe)	381.7	410.4	406.9
Efficiency, HHV (%)	39.6	43.4	46.3
Efficiency LHV (%)	41.1	45.0	48.1
Total Capital Requirement, ($1,000)	519,625	596,033	593,871
$/KW	1,361	1,452	1,459
Net Operating Cost ($1,000)	57,128	69,832	70,836
COE (mills/kwh)	47.2	48.1	48.8

RSC: Radiant Syngas Cooler
CSC: Convective Syngas Cooler
CGCU: Cold Gas Cleanup → Amine & Claus & SCOT
HGCU: Hot Gas Cleanup → transport desulfurization

Case 2 of the EG&G Report is similar in operation to Case 1 except in Case 2 attempts are made to recover the heat of the raw gas more efficiently than Case 1 by radiant and convective cooling of the syngas to raise steam for power generation. In Case 2, H_2S is removed from the syngas as elemental sulfur via the DMEA-Claus-SCOT. In Case 3 of the EG&G Report, radiative and convective cooling of the syngas is used to raise steam for power generation. In Case 3, however, H_2S is removed from the syngas at high temperature using a solid sorbent in a circulating fast fluidized bed reactor system. The absorbed sulfur is eventually recovered as sulfuric acid.

As shown in Table 4.1, Case 1 has the lowest total capital requirements and lowest cost of electricity (COE); however, it is the least thermally efficient process of the three cases. Since RTI proposes to compare the SSRP with an amine process to remove H_2S from the syngas, Case 3, which uses a circulating solid sorbent for this purpose, is eliminated from consideration as a choice of base case against which to compare the SSRP. Because Case 1 operates at the highest process pressure of the remaining cases, RTI has chosen to use Case 1 as a basis for comparing the amine based removal of H_2S versus SSRP to remove H_2S. The elevated pressure of Case 1 more nearly matches the preferred operating pressure of the SSRP than does the operating pressure of Case 2.

4.3. Base Case 1: Texaco-IGCC-Amine

A simplified flow sheet of the Base Case 1 is shown in Figure 4.1. Illinois #6 coal is crushed and mixed with water to produce a coal / water slurry containing roughly 33% water. This slurry is pumped into the Texaco gasifier along with oxygen. The gasifier operates at about 615 psia in a down flow-entrained mode at temperatures in excess of 2300°F. The coal's sulfur is converted to mostly H_2S with some COS being formed. The raw syngas leaves the gasifier at 2300 to 2700°F along with molten ash and unburned carbon particles. This stream is then passed to a large water pool, which cools the gas and removes solidified ash particles. As shown in Fig. 4.1, the cooled raw gas enters a gas scrubbing section to remove additional fine solids before the gas is passed to the Gas Cooling Section.

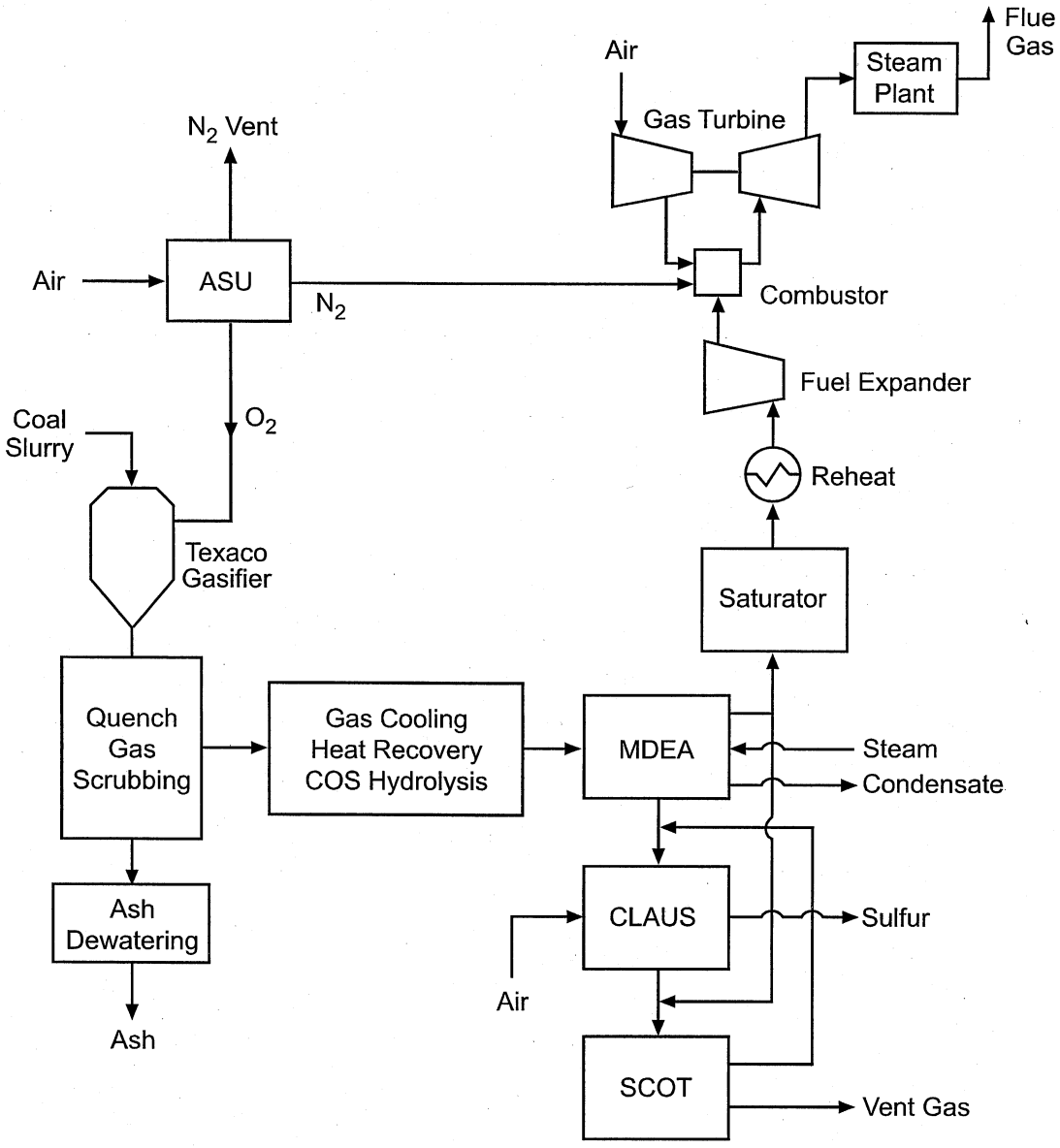

Figure 4.1. Simplified flow sheet for the Texaco-IGCC using an amine-base H_2S to elemental sulfur process

In the Gas Cooling Section the raw syngas in cooled from 425°F to 103°F in a series of heat exchangers. Heat recovered in this heat exchange network is used to generate low-pressure steam for the HRSG. Low quality heat is used for BFW heating. Condensate produced in the heat exchange is used to resaturate the clean syngas after it leaves the amine scrubber unit. The Gas Cooling Section also contains a catalytic hydrolyzer in which COS is converted to H_2S. This is necessary because COS will pass through the amine scrubber and would significantly increase the sulfur load in the cleaned syngas if COS were not converted to H_2S prior to the amine scrubber.

The MDEA/Claus/SCOT process is used for cold syngas cleanup and elemental sulfur recovery. As shown in Fig. 4.1, the cooled gas from Gas Cooling Section is passed to the MDEA absorber where it is contacted with a lean, with respect to H_2S and CO_2 content, MDEA solvent. Almost all of the H_2S and a portion of the CO_2 in the syngas are removed in the MDEA scrubber. The H_2S-rich MDEA solvent exits the absorber and is heated by H_2S lean solvent from the H_2S/MDEA stripper in a heat exchanger before entering the stripper column. Acid gases exiting the MDEA stripper are sent to the Claus/SCOT units for sulfur recovery. The lean MDEA solvent exiting the stripper column is cooled and eventually recycled to the scrubbing column. Approximately 98.5% of the cleaned syngas from the MDEA scrubber is sent to the gas turbine whereas 1.5% of the cleaned syngas is mixed with the Claus off gas prior to being fed to the SCOT tail gas treatment unit.

The Claus process is carried out in two steps. In the first stage about one-quarter of the gases from the amine stripper column are mixed with the recycle acid gases from the SCOT unit as shown in Figure 4.1 and burned in air in a furnace. The remaining acid gas from the amine stripper is mixed with this combustion gas in the second stage of the Claus process which is a sequence of catalytic reactors were H_2S and SO_2 react to form elemental sulfur. Following each catalytic reactor the gas is cooled to condense out elemental sulfur and reduce the inlet temperature of the catalytic reactor to improve the thermodynamic favorability of the Claus reaction.

The tail gas from the last Claus reactor, which contains elemental sulfur, SO_2, H_2S and COS, is sent to the SCOT unit where in the presence of the 1.5% of the cleaned syngas, as mentioned previously, SO_2 is converted to H_2S with the aid of a cobalt-molybdate catalyst. The effluent is cooled before being sent to an absorber column where H_2S is removed. The H_2S rich stream is sent to a regenerator where H_2S is released. The acid gas from the regenerator is recycled to the inlet of the Claus unit as shown in Fig. 4.1.

The portion of the clean syngas leaving the amine scrubber that is sent to the gas turbine combustor is humidified with high pressure condensate generated in the Gas Cooling Section, as shown in Fig.4.1, to increase mass flow rate through the gas turbine and the fuel expander. This humidification reduces the amount of nitrogen feed to the gas turbine from the air separation unit that is needed to fully load the gas turbine unit.

4.4. Texaco-IGCC-SSRP System

Basically the flow sheet for the Texaco-IGCC-SSRP system is the same as that for the Base Case 1 flow sheet shown in Fig.4.1 except the SSRP is inserted between the Gas Cooling Section and the Gas Saturation Unit. In the case of H_2S being removed by the SSRP, all of the treated syngas is sent to the Gas Saturator, whereas in Base Case 1, about 1.5% of the clean syngas is consumed in the SCOT unit. As a consequence of 100% of the clean syngas going to the gas turbine, and because it is assumed that the production rate of electrical power will be held constant in the comparison of the Texaco-IGCC processes using the two H_2S-to-sulfur removal options, the rate at which coal is gasified and the flow rate of raw syngas will be 1.5% less in the case of the SSRP H_2S removal process versus the amine-based process. This translates into reduced equipment and operating costs of the units upstream of the SSRP in comparison to the costs associated with the amine-based process. The methods used to evaluate these costs will be described below following a brief description of the SSRP unit.

A simplified flow sheet of the SSRP unit is shown in Figure 4.2. This may be an unduly complicated version of the SSRP, in that, fine adjustments to the ratio of H_2S to SO_2 in the inlet gas to the SBCR are made by vaporizing liquid SO_2, which is produced and stored for this purpose. The ratio of H_2S to SO_2 in the raw syngas at the inlet of the SBCR is maintained at 2.0. This is accomplished in part by liquid SO_2 as mentioned above and in large part by burning product sulfur in air to produce SO_2 as shown in Fig. 4.2. The raw fuel gas enters the SBCR at approximate 260°F and 600 psia and is saturated with water vapor. A small amount of supplemental steam and/or saturated liquid water can be supplied to the SBCR as needed to control the slurry temperature at approximately 300°F (150°C) and the water vapor content at 10%. In the SBCR, the raw gas with a H_2S to SO_2 ratio of 2.0 is contacted with a slurry of liquid elemental sulfur and a catalyst, which has been shown by RTI to promote the Claus reaction in the presence of liquid sulfur. Approximately 99% of the H_2S and SO_2 entering the SBCR will be converted to elemental sulfur. As mentioned above, the gas from the Gas Cooling Section is passed to the SBCR at 260°F (127°C). Thus the Gas Cooling Section will require less heat exchange equipment than the Gas Cooling Section associated with using the amine-based unit for H_2S removal. In calculating the capital cost of the Gas Cooling Section associated with the use of the SSRP unit to remove sulfur the decrease in the exchange surface area was not taken into consideration. The cost of the Gas Cooling Section was based simply on the total syngas throughput of the Gas Cooling Section as will be described below. Thus the capital cost of Gas Cooling Section associated with the use of the SSRP will be highly conservative.

The Gas Cooling Section also contains a COS hydrolysis reactor due to the fact that COS will pass through the amine scrubber. For the Gas Cooling Section associated with the use of the SSRP this catalytic reactor may not be necessary in that the SSRP may be able to convert COS to elemental sulfur in the SBCR by adding a COS hydrolysis functionality to the SSRP catalyst or by admixing hydrolysis catalyst with the SSRP catalyst in the SBCR catalyst slurry. The fate of COS in the SSRP will be one of the subjects of the future research on the SSRP.

As shown in Fig. 4.2, liquid sulfur is withdrawn from the SBCR and passed through a filter to separate the SSRP catalyst from the liquid sulfur. The separated SSRP catalyst is returned to the SBCR. Also, the sulfur product is withdrawn after the filter. The SSRP catalyst is assigned a highly conservative active life of about 6 months.

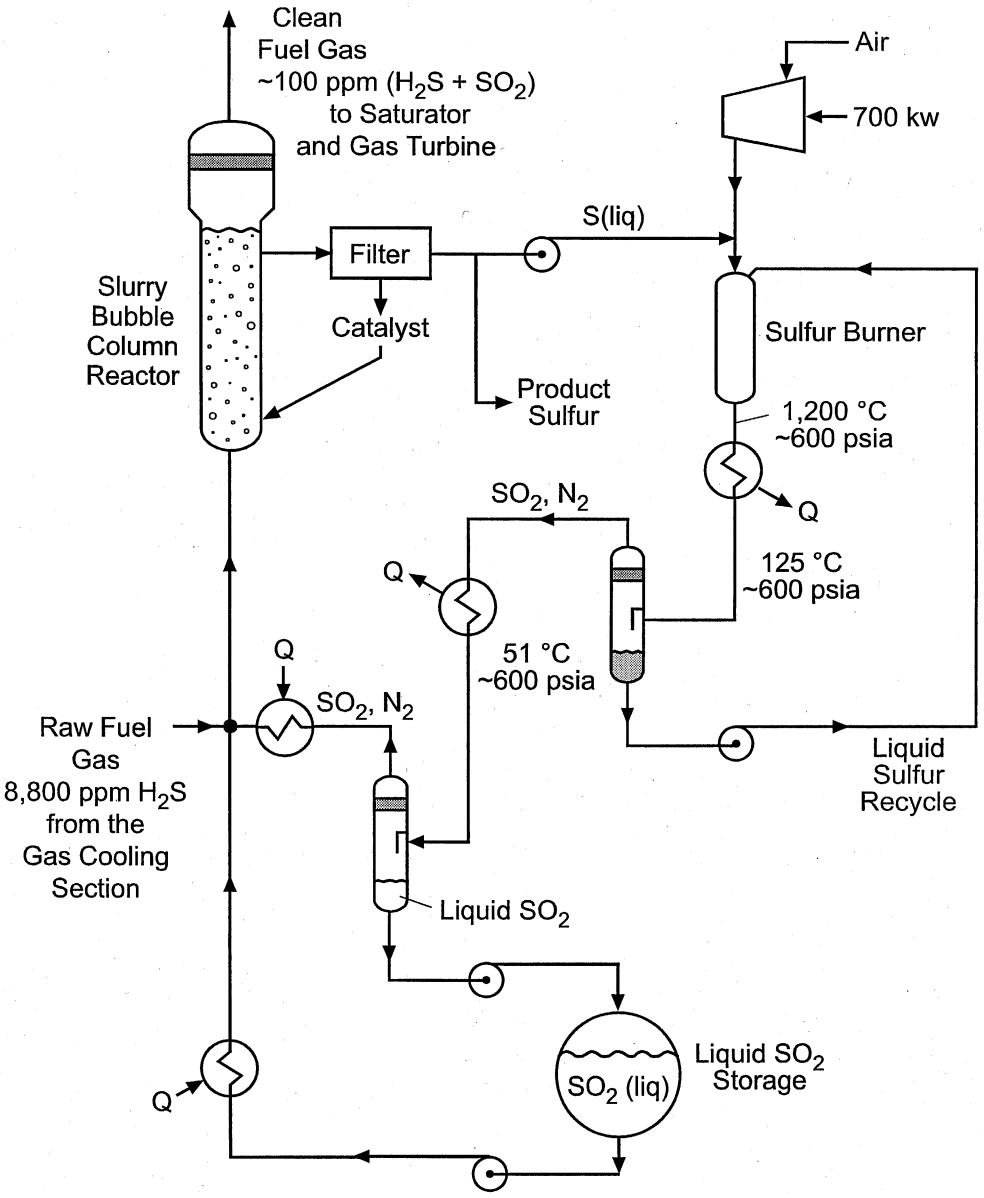

Figure 4.2. Simplified SSRP flowsheet

About 1/3 of the sulfur produced in the SBCR will be burned with a stoichiometric amount of air at approximately 600 psia. The sulfur burner is anticipated to be spray-type burner. Liquid sulfur in excess of the amount burned will be sprayed into the burner to help control the temperature at 1200°C (2200°F). The vaporized sulfur, sulfur dioxide and nitrogen produced in the sulfur burner will be cooled to approximately 125°C (257°F) and the SO_2 and N_2 will be separated from the unreacted liquid sulfur as shown in Fig.4.2. The condensed sulfur will be recycled to the burner. The SO_2/N_2 mixture will be further cooled to about 50°C (122°F) to partially condense SO_2. The condensed SO_2 will be stored and used intermittently by quickly adjust the H_2S/SO_2 ratio in the inlet of the SBCR to 2.0.

While the SSRP flow sheet shown in Fig.4.2 is complex, most of the complexity can be attributed to maintaining a ratio of H_2S to SO_2 of 2.0 in the inlet of the SBCR. The complexity of this support equipment could be sealed back by not accumulating liquid SO_2 as shown in Fig.4.2 and simply adjusting the flow of oxygen to the burner to give the proper flow of gaseous SO_2 in the SO_2/N_2 mixture so that the ratio of H_2S to SO_2 in the inlet of the SBCR is 2.0. The flow sheet for the SSRP shown in Fig.4.2 is complex; but the complexity pales in comparison to the DMEA-Claus-SCOT process. The SSRP eliminates numerous catalytic reactors, inter-stage cooling exchangers and separation devices.

4.5. Comparison of Base Case 1 with SSRP

In comparing the Texaco-IGCC power generation system using the amine based processes for removing H_2S from syngas to produce elemental sulfur with the SSRP to do the same job, the two H_2S removal alternatives must be compared in the context of being part of the Texaco-IGCC process. The reason for this is that the amine-Claus-SCOT process consumes about 1.5% of the syngas, which is then not available for power production whereas the SSRP does not consume syngas and the full production of syngas is available for power generation. Thus the Texaco-IGCC using the SSRP can generate the same level of electrical power as the Texaco-IGCC using amine-based H_2S removal using smaller, less expensive gasifier and gas cooling equipment and fewer resources, such as highly purified oxygen and coal. These savings associated with the use of the SSRP will then allow more to be spent on the SSRP than the amine-based process and have the same COE, or as will be shown in the discussion below, a reasonably priced SSRP unit will yield a significantly reduced COE for the Texaco-IGCC than a Texaco-IGCC process using amine-based H_2S removal.

Two basic approaches can be taken. One, the amount of coal used in the gasifier could be held constant in the two alternatives. Thus, because the SSRP des not consume valuable fuel gas, whereas the DMEA-Claus-SCOT process consumes 1.5% of the clean syngas, the SSRP can generate about 1.5% more electrical power than the system that uses the DMEA-Claus-SCOT for H_2S removal from the syngas and elemental sulfur production. Given the scenario of similar coal feed rates for the two alternatives then the amount of capital and operating expenses available for the SSRP that would give the same COE as the Base Case 1 could be computed. The estimated capital and operating expenses of the SSRP could then be compared to the permissible, COE breakeven capital and operating expense to determine if the SSRP is competitive with the amine-based option.

Another way of comparing the two H_2S removal options and the one used by RTI was to hold the amount of power generated constant and adjust the amount of coal that was fed to the Texaco-IGCC to generate the same level of power as the Base Case 1. The permissible levels of capital and operating expenses that could be utilized in the SSRP to give the same COE as Base Case 1 was calculated and compared to estimates for the SSRP in order to determine if the SSRP would be economically competitive with the amine based H_2S removal process.

For the Texaco-IGCC-Amine based power generation system, Base Case 1, the capital requirements and annual operating costs are shown in Tables 2 and 3, respectively.

Table 4.2. Installed costs of equipment and total capital requirement for the Texaco-IGCC using two alternative H_2S removal processes

Plant Section	Texaco-IGCC with Amine H_2S Removal			Texaco-IGCC with SSRP H_2S Removal		
	Process Cont, %	Process Cont, k$	1Q 1997 Cost, k$ w/o Cont	Process Cont %	Process Cont, k$	1Q 1997 Cost, k$ w/o Cont
Coal Slurry Preparation	0	$0	$27,191	0	$0	$26,911
Oxygen Plant	0	$0	$67,357	0	$0	$66,821
Texaco Gasifier (Quench)	15	$3,605	$24,032	15	$3,572	$23,815
Low Temperature Gas Cooling/Gas Saturation	0	$0	$17,237	0	$0	$17,061
MDEA	0	$0	$5,313	0	$0	$0
Claus	0	$0	$9,968	0	$0	$0
SCOT	0	$0	$4,216	0	$0	$0
SSRP	0	$0	$0	50	$2,650	$5,300
Gas Turbine System	10	$5,400	$53,996	10	$5,400	$53,996
HRSG/Steam Turbine	0	$0	$45,211	0	$0	$45,211
	Subtotal, Installed Equipment Cost		**$245,521**			**$239,115**
Bulk Plant Items						
Water Systems	0	$0	$18,071	0	$0	$16,977
Civil/Structural/Architectural	0	$0	$23,416	0	$0	$21,999
Piping	0	$0	$18,0712	0	$0	$16,977
Control/Instrumentation	0	$0	$6,618	0	$0	$6,217
Electrical	0	$0	$20,362	0	$0	$19,129
	Subtotal, Process Plant Cost		**$341,059**			**$320,414**
Engineering Fees			$34,106			$32,041
Process Contingency (Using Process contingency listed above)			$9,004			$11,622
Project Contingency, 15% Process Plant Cost			$51,159			$48,062
	Total Plant Cost (TPC)		**$435,329**			**$412,139**
Plant Construction Period, 4.0 Years (1 or more)						
Construction Interest Rate, 12.7%						
Adjustment for Interest and Inflation			$57,551			$54,485
	Total Plant Investment		**$492,879**			**$466,624**
Prepaid Royalties			$1,705			$1,602
Initial Catalyst and Chemical Inventory			$76			$75
Startup Costs			$13,693			$13,009
Spare Parts			$2,177			$2,061
Working Capital			$7,794			$7,634
Land, 200 Acres			$1,300			$1,300
	Total Capital Requirement (TCR)		**$519,625**			**$492,305**
		$/kW	1361			1290

Table 4.3. Annual operating costs for the Texaco-IGCC using two alternative H_2S removal processes

Cost Item	Unit $ Price	Texaco-IGCC with Amine H_2S Removal		Texaco-IGCC with SSRP H_2S Removal	
		Quantity	Annual Cost, k$	Quantity	Annual Cost, k$
Coal (Illinois #6)	$30.60 /T	3,385 T/D	$32,136	3,334 T/D	$31,654
Consumable Materials					
Water	$0.19 /T	4,333 T/D	$255	4,268	$252
MDEA Solvent	$1.45 /Lb	403.2 Lb/D	$181	0	0
Claus Catalyst	$470	0.01 T/D	$1	0	0
SCOT Activated Alumina	$0.67 /Lb	15.9 Lb/D	$3	0	0
SCOT Cobalt Catalyst			$5	0	0
SCOT Chemicals			$16	0	0
SSRP Catalysis	$470 /T	0	$0	0.4 T/D	$58
Ash/Sorbent Disposal Costs	$8.00/T	634 T/D	$1,574	625 T/D	$1,551
Plant Labor					
Oper Labor (incl benef)	$34.00 /Hr.	22 Men/shift	$6,535	22 Men/shift	$6,552
Supervision & Clerical			$3,684		$3,598
Maintenance Costs 3.3%			$14,366		$13,601
Insurance & Local Taxes			$8,707		$8,243
Royalties			$321		$317
Other Operating Costs			$1,228		$1,199
	Total Operating Costs		**$69,014**		**$67,025**
By-Product Credits					
Sulfur	$75.00 /T	81.0 T/D	$1,886	79.1 T/D	$1,841
	Total By-Product Credits		**$1,886**		**$1,841**
	Net Operating Costs		$67,128		$65,184

Capacity Factor = 85%

These cost figures are those that were summarized in the EG&G Report. The corresponding cost figures derived by RTI for the Texaco-IGCC-SSRP are also shown in Tables 4.2 and 4.3. The derivation of these costs will be described below.

4.6. Cost Calculation Details

In the case where the SSRP is used to remove H_2S from the raw syngas and the level of power generation is the same for the two alternative H_2S removal processes presently under consideration, the capacity of the equipment upstream of the SSRP unit will be 1.5% less than the capacity of the equipment needed to support the same level of power generation while utilizing the amine based H_2S removal unit. Thus the installed cost of the Coal Slurry Preparation, Oxygen Plant, Texaco Gasifier and the Gas Cooling Section of the process as summarized in Table 2 where computed by the methods listed at upper portion of Table 4.4. Basically it was assumed that the installed cost-capacity relation was given in the form:

$$\left[\text{Installed Cost of Equipment i}\right] = A_i\left[\text{Capacity of Equipment i}\right]^{n_i} \qquad (4.2)$$

where A_i and n_i are constants unique to equipment i.

For the Coal Slurry Preparation and Oxygen Plant units the capacity exponents $\mathbf{n_i}$ shown in Table 4.4 were determined by the least square fit of the cost/capacity data in the form given by Equation 4.2 for the three cases given in the EG&G Report. This could not be done for the Texaco gasifier quench unit and the Gas Cooling Section due to the radically different nature of these units in the three base cases discussed in the EG&G Report. Therefore the exponent in Equation 4.2 and as shown in Table 4.4 for the Texaco gasifier/quench unit was assumed to be n=0.6 which is a rule of thumb exponent that is often assumed in the absence of hard cost/capacity data. The Texaco gasifier used in the EG&G Report had a nominal capacity of 3,000 tons of coal per day. One might ponder then why the variation of capacity of 1.5% would even be a consideration in the cost of the gasifier since surely there must be turn-up or turn-down capacity built into the nominal capacity of the Texaco gasifier. The reason the small variation in gasifier capacity on the cost of the gasifier/quench unit was even considered, is based on analogy to how DOE handled the small changes in capacity of the gas turbine for the three base cases in the EG&G Report. Here, all three cases utilized the W501G gas turbine, which would be expected to have some turn- down or –up capacity, yet variation in the cost of the turbine was considered even for minute changes in capacity among the three base cases.

For the Gas Cooling Section the exponent in Equation 4.2 and as shown in Table 4.4 was assumed to be n=0.68, which is the figure suggested by *Garrett (1989)* for heat exchange equipment. Using the cost scaling formula shown in Table 4.4 the Gas Cooling Sections should yield highly conservative cost estimates for the Gas Cooling Section for the SSRP based IGCC in that the raw gas needs to be cooled only to 260°F rather than 103°F for the process using the amine-based H_2S removal unit. The cost savings due to the higher allowable inlet temperature for the SSRP was not determined due to scant details and the black box nature of the Gas cooling Section given in the EG&G Report.

Table 4.4. Details of Costing Plant Sections and Bulk Plant Items

Costing of Plant Sections	
Coal Surry Preparation	$Cost2=Cost1\cdot(Capacity2/Capacity1)^{0.6844}$
Oxygen Plant	$Cost2=Cost1\cdot(Capacity2/Capacity1)^{0.5288}$
Texaco Gasifier	$Cost2=Cost1\cdot(Capacity2/Capacity1)^{0.6}$
Low Temperature gas cooling and Gas Saturation	$Cost2=Cost1\cdot(Capacity2/Capacity1)^{0.68}$
Gas Turbine Section	Same as Case 1 of The EG&G Report
HRSG/Steam Turbine Section	Same as Case 1 of the EG&G Report

Costing of Bulk Plant Items	
Bulk Plant Item	% of Installed Equipment Cost
Water Systems	7.1
Civil/Structural/Architectural	9.2
Piping	7.1
Control and Instrumentation	2.6
Electrical Systems	8.0
Total	**34.0**

The installed cost of the SSRP unit shown in Table 4.2 is based on the observation that the SSRP basically consists of a single high pressure scrubber-like column such as might be used for the DMEA scrubber of Case 1. While the SSRP has other minor supporting equipment, such as the sulfur burner, these are well developed and should add a minimum of cost. Therefore, the installed cost of the SSRP was assumed to be approximately the cost of the DMEA unit of Case 1 even though the cost of the DMEA unit includes the cost of two large column: the amine scrubbing and stripping columns. This qualitative cost of the SSRP was used due to the fact that the engineering details of SBCR have not been researched as of yet. For example the sizing of the SBCR in the SSRP is highly dependent on the solubility of SO_2 and H_2S in liquid sulfur; however, nothing is known of these solubilities. What is known though is that 99% conversion of the H_2S and SO_2 entering the SSRP can be achieved at quite reasonable space velocities. Due to the uncertainly of the sizing of the SBCR in the SSRP and consequently the installed cost of the SSRP as shown in Table 4.2, RTI has assigned a large process contingency to the SSRP unit of 50%.

As stated above the generating capacity of the gas turbine and steam turbines have been assumed the same for the Texaco-IGCC using either the amine-base H_2S removal or the SSRP. Thus the installed costs of these power generators are the same for the two H_2S removal alternatives as shown in Table 4.2.

The method of costing of the bulk plant items is also shown in Table 4.4. These are based on set percentages of the installed equipment cost as prescribed by DOE. Other factors that contribute to the total capital requirement as listed in Table 4.2 are shown in Table 4.5. These cost factors, like the bulk plants items are based on set percentages of the Process Plant Cost (PPC), Total Plant Cost (TPC), and the Total Plant Investment (TPI). In Table 4.5 listed under Start-up costs is a category labeled "Operating Costs." This cost is not explicitly defined in the text of the EG&G Report and therefore for the purposes comparing in Table 4.2 the capital requirements for the Texaco-IGCC using either amine based H_2S removal or SSRP the following estimate was used to determine the operating cost category of the Start-up Costs.

Start-up Costs

$$\text{Operating Cost} = \frac{\text{Total Operating Cost - Coal Cost}}{365} \times 30 \qquad (4.3)$$

A second cost item listed in Table 4.2 that is insufficiently defined in the EG&G Report to calculate is the Working Capital. Working Capital is divided into three costs as shown in Table 4.5. Two of the three costs are straight forward; however, the third "Direct Expenses" is not defined in any manner in the EG&G Report and was calculated for the SSRP-based case by the using assuming the fraction of Direct Expense of the Net Operating Cost were similar for the Texaco-IGCC using the two alternative H_2S removal process. Thus,

Working Capital

$$\text{Direct Expenses (SSRP)} = \text{Direct Expenses (DMEA)} \times \frac{\text{Net Operating Cost (SSRP)}}{\text{Net Operating Cost (DMEA)}} \qquad (4.4)$$

The third cost item listed in Table 4.2 that was not explicitly defined in the EG&G Report was the Adjustment for Interest and Inflation (AII). This cost as applied to the SSRP case was assumed to be the same fraction of the Total Plant Cost (TPC) as that for the Base Case 1, the amine-based H_2S removal process. Thus,

Adjustment for Interest and Inflation (AII)

$$\text{AII (SSRP)} = \text{AII (DMEA)} \times \frac{\text{TPC (SSRP)}}{\text{TPC (DMEA)}} \qquad (4.5)$$

Based on the cost calculations listed in Tables 4.4 and 4.5 and suing Equations 4.3 through 4.5, the Total Capital Requirement (TCR) for the Texaco-IGCC with the SSRP H_2S removal option can be calculated as shown in Table 4.2. Examination of Table 4.2 shows that the TCR for the two alternative processes are \$1,361/kw and \$1,290/kw for the amine and SSRP H_2S removal options, respectively. Thus the SSRP option gives over a 5% reduction in TCR over the amine option.

Table 4.5. Capital Cost Assumptions

General Facilities	0
Engineering Fee	10% of PPC
Project Contingency	15% of PPC
Construction Period	4 Years
Inflation Rate	4%
Discount Rate	12.7
Prepaid Royalties	0.5% of PPC
Catalyst and Chemical Inventory	30 Days
Spare Parts	0.5% of TPC**
Land	200 Acres@ $6,500/Acre
Start-Up Costs	
Plant Modifications	2% of TPI***
Operating Costs	30 Days
Fuel Costs	7.5 Days
Working Capital	
Coal	60 Days
By-Product Inventory	30 Days
Direct Expenses	30 Days

*PPC=Process Plant Cost
**TPC=Total Plant Cost
***TPI=Total Plant Investment

In order to determine the effect of the two H_2S removal options on the Cost of Electricity (COE), the annual operating cost must be determined for the two options. Once the annual operating costs are determined they can be combined with the Total Capital Requirement (TCR) given in Table 4.2 to yield the Cost of Electricity.

The annual operating cost for the Texaco-IGCC using amine-based H_2S removal (Base Case 1) has been reported previously in Table 4.3. On the right-hand side of this table the operating costs associated with the SSRP option are also reported. The method of calculating each operating cost item listed in Table 4.3 is outlined in Table 4.6. Examination of Table 4.3 shows that the SSRP H_2S removal option reduces the net operating costs by about $2 million/yr or about 3% over the DMEA-Claus-SCOT H_2S removal option.

4.7. Calculation of the Cost of Electricity (COE)

The EG&G Report on the Texaco-IGCC base cases does not explicitly describe the accounting procedures by which the Cost of Electricity is calculated; however sensitivity analysis of the COE to increments in the Net Operating Costs and Total Capital Requirement carried out by DOE shows that COE is consistent with the following functional relationship:

Table 4.6. Operating and Maintenance Assumptions

Consumable Material Prices	
Illinois #6 Coal	$30.60/Ton
Raw Water	$0.19/Ton
MDEA Solvent	$1.45/Lb
Claus Catalyst	$470/Ton
SCOT Activated Alumina	$0.067/Lb
SSRP Catalyst	$470/Ton
Off-Site Ash/Sorbent Disposal Costs	$8.00/Ton
Operating Royalties	1% of Fuel Cost
Operator Labor	$34.00/hour
Number of Shifts for Continuous Operation	4.2
Supervision and Clerical Labor	30% of O&M Labor
Maintenance Costs	3.3% of TPC
Maintenance Labor	40% Maintenance Cost
Insurance and Local Taxes	2% of TPC
Miscellaneous Operating Costs	10% of O&M Labor
Capacity Factor	85%

$$COE = \left[\frac{NOC \times 10^3}{P \times 365 \times 0.85 \times 24}\right] + B\left[\frac{TCR \times 10^3}{P \times 365 \times 0.85 \times 24}\right] \quad (4.6)$$

where: COE is the Cost of Electricity, mils/kWh,
NOC is the Net Operating Cost, $/yr
TCR is the Total Capital Requirement, $,
P is the Power produced by the Plant, kW,
and B is the constant which depends on accounting procedure, interest rates, etc., hr^{-1}.

The denominator of each term of the right-hand side of the Equation 4.6 represents the kWh of power produced per year by the Texaco-IGCC process. The EG&G Report on the Texaco-IGCC base cases lists the Cost of Electricity as well as the Total Capital Requirement and Net Operating Costs for each of the three base cases. This information is reproduced in Table 4.1 of this report. Using the data in Table 4.1 to obtain at least square fit of the data in the form of Equation 4.6 yields

$$B = 0.1304\ hr^{-1} \quad (4.7)$$

Applying Equation 4.6 and 4.7 to the TCR and NOC shown in Tables 4.2 and 4.3 shows that the cost of Electricity for the SSRP H_2S removal option is

$$COE_{SSRP} = 45.5\ mils/kWh \quad (4.8)$$

The Cost of Electricity for the DMEA-Claus-SCOT H_2S removal option (Case 1) as shown in Table 4.1 is

$$COE_{Amine} = 47.2 \text{ mils/kWh} \tag{4.9}$$

Thus the SSRP option will reduce the Cost of Electricity by 3.6%, a significant saving.

4.8. COE Sensitivity Analysis

The COE of 45.5 mils/kWh for the SSRP option is highly dependent on the installed cost of the SSRP unit and the process contingency assigned to the unit. While every effort was made to assign reasonable installed costs and process contingency to the SSRP, it is informative to calculate the installed cost of the SSRP that might be assumed and yield the same COE as the amine based option, and see how the installed cost of $5,300,000 used in the calculation of the entrees of Tables 2 and 3 compares to this COE breakeven installed cost of the SSRP.

To calculate COE breakeven cost of the SSRP, the Total Capital Requirement as computed in Table 2 can be computed for the Texaco-IGCC-SSRP system in terms of an unknown SSRP Installed cost given by IC and yet to be prescribed Fractional Process Contingency, FPC, for the SSRP. If the cost computations indicated in Table 4.2 are carried out the following result is obtained:

$$TCR = 478826 + (1.9593 + 1.1657*FPC)*IC \tag{4.10}$$

where: TCR is the Total Capital Requirement, K$,
FPC is the Fractional Process Contingency for the SSRP, dimensionless,
and IC is the Installed Cost of the SSRP, K$

Similarly if the operating cost calculations indicated in Table 4.3 are carried out the following is obtained:

$$NOC = 64452 + OX + (0.0976 + 0.0583 * FPC)*IC \tag{4.11}$$

where NOC is the Net Operating Cost, K$/yr,
and OX is the Operating expenses of the SSRP unit, K$/yr,

Letting LP represent the mechanical and/or electrical power consumed by the SSRP, substituting Equations 4.10 and 4.11 into Equation 4.6 and setting the Cost of Electricity, COE, equal to the COE for the amine based Texaco-IGCC process of 47.2 mils/kWh gives, after simplification:

$$IC = \frac{21246 - 2.83* OX - LP}{1 + 0.6 * FPC} \tag{4.12}$$

where IC is Installed Cost, K$, of the SSRP that will yield a COE for the Texaco-IGCC equal to the COE for the Texaco-IGCC-Amine process,
OX is Operating Costs for the SSRP, K$/yr

LP is the Mechanical and/or Electrical Power consumed by the SSRP, kW

For the Texaco-IGCC-SSRP case considered in Tables 4.2 and 4.3

OX = $58k/yr
LP = 700kW
and FPC = 0.5.

Substituting these values into Equation 4.12 gives

IC = $15,760k

Thus the estimated Installed Cost of the SSRP unit is roughly

$$\frac{5300}{15760} \text{ or one-third}$$

the maximum Installed Cost that could be spent on the SSRP unit and still give an estimated Cost of Electricity for the Texaco-IGCC-SSRP equal to the Texaco-IGCC-Amine process.

4.9. Summary

An economic comparison of using the DMEA-Claus-SCOT process or the SSRP to remove H_2S and convert it to elemental sulfur for the Texaco-IGCC has been made. The procedures used to calculate the Total Capital Requirement and Net Operating Cost for the Texaco-IGCC using the two H_2S removal alternatives were as prescribed by the EG&G Report on the Texaco-IGCC base cases or in the absence of explicit procedures, the costs were estimated.

The installed cost of the SSRP was estimated based on engineering judgment to be about the cost of the DMEA unit alone. Unlike the DMEA-Claus-SCOT H_2S removal unit the SSRP does not require the consumption of syngas; and therefore, if the net power generated by the Texaco-IGCC using the two alternatives is assumed to be the same, the units upstream of the SSRP will process 1.5% less material than the Texaco-IGCC process using the DMEA-Claus-SCOT H_2S removal process. The Total Capital Requirement and Net Annual Operating Costs for the two alternative processes are summarized in Table 4.2 and 4.3, respectively.

The total Capital Requirement for the IGCC process using the SSRP alternative is thought to be conservative due to the fact that the raw syngas only needs to be cooled to 260°F rather than 103°F in the case of the amine-based H_2S removal alternative and due to the lack of details of Gas Cooling Unit this difference could not be taken into consideration. Also the COS hydrolysis unit necessary in the amine-based H_2S removal process may not be needed in the SSRP, but this conjecture needs to be researched.

A summary of the economic calculations performed and described above is given in Table 4.7. It can be seen that the use of the SSRP gives significant reductions in the Total Capital Requirement, Net Operating Costs and Costs of Electricity over the three base cases. The use of the SSRP also improves the thermal efficiency of the over all Texaco-IGCC process over the efficiency of Base Case 1.

Table 4.7. Summary of the economic comparison of the Texaco-IGCC using various raw gas cooling and H_2S removal schemes

	CASE 1	**SSRP**	**CASE 2**	**CASE 3**
Gasifier	Texaco	Texaco	Texaco	Texaco
Cooling Mode	Quench	Quench	RSC + CSC	RSC + CSC
Sulfur Removal	CGCU	SSRP	CGCU	HGCU
Total Plant Power (MWe)	381.7	381.7	410.4	406.9
Efficiency, HHV (%)	39.6	40.2	43.4	46.3
Efficiency, LHV (%)	41.1	41.7	45.0	48.1
Total Capital Requirement, ($1,000)	519,625	492,299	596,033	593,781
$/KW	1,361	1,290	1,452	1,459
Net Operating Costs ($1,000)	67,128	65,182	69,832	70,836
COE (mills/kWh)	47.2	45.5	48.1	48.8

5. CONCLUSIONS AND RECOMMENDATIONS

The major conclusions from the **fixed-bed micro-reactor catalyst screening** for SSRP are:

- A total sulfur conversion of 99% with only 35ppm COS formation was achieved at 300psig and 154°C (309°F) on a commercial alumina catalyst (E-alumina).
- Sulfur conversion is limited only by thermodynamic equilibrium from reaching 100%.
- Higher reaction pressures shift the thermodynamic equilibrium toward higher conversion, thus sulfur removal activity increases with increasing pressure.
- Catalyst activation and feed procedure are critical for enhanced selectivity of sulfur removal (minimized COS formation).
- SO_2 is more selective than O_2 for the catalytic oxidation of H_2S in the presence of excess reducing gases (H_2, CO) on two different catalysts (alumina and silica gel) under the examined reaction conditions.

The major conclusions from the **micro-bubbler concept evaluation study** for SSRP are:

- The selective catalytic oxidation of H_2S by SO_2 in the presence of excess reducing gases (CO, H_2) is feasible in a molten sulfur medium.
- Higher pressures and an intermediate SO_2 concentration enhance sulfur removal.
- Reaction of CO with an active form of sulfur is the major pathway for COS formation.
- Molten sulfur appears to be inactive for direct reaction with CO.

The major conclusions from the **bench-scale process evaluation study** for SSRP are:

- A 97.5% sulfur conversion with 365 ppm COS formation was achieved at 400 psig and 135°C (275°F) on E-alumina suspended in molten sulfur.
- Conversions under comparable residence times, as expected, are lower in a CSTR compared to a fixed-bed reactor. The data trends, however, were identical. The SBCR commercial embodiment is expected to achieve conversions of fixed-bed reactor levels with proper design.
- COS formation was reduced to 75ppm without affecting the sulfur removal activity, by increasing the steam feed content to 18% at 125°C.
- Reaction temperature, inlet steam concentration, and total feed flow, appear to be important parameters in limiting the formation of COS, without significantly impeding the sulfur removal efficiency of SSRP.
- The overall sulfur removal efficiency of SSRP (minimization of outlet S concentration) is enhanced by higher residence times, and by higher reaction pressures; higher reaction pressures are favored in industrial applications involving gasifier-syngas.
- The beneficial effect of higher reaction pressure on sulfur removal activity appears to be more prominent at lower reaction temperatures.
- The overall sulfur removal efficiency is favored at lower reaction temperatures in the presence of the E-alumina catalyst, but at higher reaction temperatures in Molten Sulfur only (no catalyst). The presence of catalyst changes the relative progress of the H_2S+SO_2 reaction vs. COS formation, making lower temperatures more favorable for SSRP.

- Addition of SO_2 suppresses the formation of COS in the presence of the E-alumina catalyst, in contrast to the blank reactor and Molten Sulfur only (no catalyst) systems. In the presence of the catalyst, addition of SO_2 apparently shifts the pathway for COS formation from the (inevitable for H_2S-containing syngas feed) CO + H_2S reaction to that of CO with active sulfur formed by the Claus reaction, at least to a major extent.
- No catalyst deactivation was observed after running for more than 100 hours, indicating that the formed sulfur was recovered by the molten sulfur medium. In other words, a self-regenerable catalyst system was established. This is a major accomplishment since in fixed-bed reactors conversion will drop due to pore plugging.
- Molten sulfur is inactive for direct reaction with reducing gases (H_2 and CO), but is itself shown to be an active catalyst (or medium) for the Claus reaction.
- Addition of catalyst to molten sulfur enhances its catalytic activity for SSRP, while decreasing the undesirable formation of COS.

The major conclusions from the **economic evaluation of SSRP** are:

- Even with highly conservative assumptions, SSRP gives significant reductions in the total capital requirements, operating costs, and COE, over conventional amine systems.
- The COS hydrolysis reactor may not be needed for SSRP as opposed to amine systems. Also, gas-cooling requirements for SSRP are lower than amine systems.

Based on the **experimental results on SSRP** described in Section 3, it is recommended to focus the future work on SSRP in the following:

- The formation of COS as the main undesirable reaction during SSRP should be prevented or minimized. The effect of various reaction parameters (temperature, pressure, total flow, steam concentration, catalyst to Molten Sulfur ratio) in minimizing the formation of COS (as opposed to maximizing the Claus reaction) has to be examined.
- The role of steam as an active participant in the Claus and COS formation reactions (in both the presence and absence of SO_2, and in both the presence and absence of catalyst) must be elucidated.
- The COS hydrolysis or hydrogenation during SSRP should be promoted through use of suitable catalysts. Evaluation of various catalysts in terms of their activity for these reactions in relation to the Claus reaction needs to be performed.
- Evaluation of SSRP as a process for the potential removal of COS in the absence of H_2S (using an active COS hydrolysis or hydrogenation catalyst) should be conducted.
- Evaluation of SSRP and optimization of reaction parameters for a combined H_2S and COS removal from coal-derived synthesis gas must be performed.

Based on the **economic calculations** and the discussion of the various Texaco-IGCC alternatives the following recommendations are made:

- More precise engineering data needs to be collected, concerning the solubility and diffusivity of H_2S and SO_2 in liquid elemental sulfur.
- The kinetics of the formation of elemental sulfur and COS in liquid sulfur and for the liquid sulfur/SSRP catalyst system should be elucidated in more detail.

- A more detailed analysis of the Gas Cooling Section should be carried out using ASPEN.
- The fate of COS entering the SSRP SBCR should be investigated. Experiments should be carried out to determine if COS can be controlled in the SSRP by imparting COS hydrolysis functionality to the SSRP catalyst or by simply mixing COS hydrolysis catalyst into the SSRP sulfur/catalyst slurry.

6. REFERENCES

Ayala, R.E., Feitelberg, A.S., Furman, A.H., "*Development of a High-Temperature Moving-Bed Coal Desulfurization System*", Proc. 12th Annual Int. Pittsburgh Coal Conf., Pittsburgh, 1053 (September 11-15, 1995).

Cicero, D.C., Gupta, R.P., Turk, B.S., Portzer, J.W., and Gangwal, S.K., "*Recent Developments in Hot-Gas Desulfurization*", High-Temperature Gas Cleaning, A. Dittler, G. Hemmer, and G. Kasper, Eds., Institut fur Mechanische Verfahrenstechnik und Mechenik der Universitat Karlsruhe (TH), 522-544 (1999).

Gangwal, S.K. and Portzer, J.W., "*Bench-Scale Demonstration of Hot-Gas Desulfurization Technology*", Final Report, DOE Contract No. DE-AC21-93MC30010, (April 2002).

Gangwal, S.K., Nikolopoulos, A.A., and Dorchack, T.P., "*Method of Removing and Recovering Elemental Sulfur from Highly Reducing Gas Streams Containing Sulfur Gases*", US Patent applied for (July 2002).

Gangwal, S.K., Portzer, J.W., Gupta, R., and Turk, B.S., "*Sulfur Recovery in Advanced IGCC Systems*", Proc. 12th Korea-US Joint Workshop on Energy and Environment, KIER and FETC, Taejon, Korea, 186 (October 1997).

Gangwal, S.K., Turk, B.S., and Gupta, R.P., "*Development of Fluidized-Bed Sorbent for Desulfurization of ChevronTexaco Quench Gasifier Syngas*", CD-ROM, 19th Annual. In. Pittsburgh Coal Conf., Pittsburgh (September 23-27, 2002).

Garrett, D.E., "*Chemical Engineering Economics*", Van Nostrand Reinhold, New York (1989).

Gupta, R. and Gangwal, S.K., "*Enhanced Durability of Desulfurization Sorbents for Fluidized-Bed Applications – Development and Testing of Zinc Titanate Sorbents*", DOE/MC/25006-3271 (1992).

Nikolopoulos, A.A. and Gangwal, S.K., "*Single-step Sulfur Recovery Process (SSRP)*", CD-ROM, 19th Annual Int. Pittsburgh Coal Conference, Pittsburgh (September 23-27, 2002).

Pearson, M.J., "*Catalyst Performance in Low-Temperature Claus* Process", Energy Processing / Canada, 38-42 (July-Aug. 1976).

Shelton, W. and Lyons, J., "*Texaco Gasifier IGCC Base Cases*," Report PED-IGCC-98-001 prepared by EG&G and issued by the Department of Energy, FETC, Office of Systems Engineering and Analysis, Process Engineering Division, July (1998).

Thambimuthu, K.V., "*Gas Cleaning for Advanced Coal Based Power Generation*", IEA Coal Research Rpt., IEA CR/53, UK (1993).

APPENDIX A Advanced Sulfur Control Concepts: Proceedings of the Advanced Coal-Fired Power Systems '95 Review Meeting

7A.5 Advanced Sulfur Control Concentration

CONTRACT INFORMATION

Contract Number	DE-AC21-94MC31258
Contractor	Research Triangle Institute P.O. Box 12194 Research Triangle Park, NC 27709-2194 Telephone: (919) 541-8033 Facsimile: (919) 541-8000
Other Funding Sources	None
Contractor Project Manager	Santosh K. Gangwal
Principal Investigators	Brian S. Turk Raghubir P. Gupta
METC Project Manager	Thomas P. Dorchak
Period of Performance	March 21, 1994 to March 20, 1997

Schedule and Milestones

FY94-96 Program Schedule

	J	A	S	O	N	D	J	F	M	A	M	J	J	A	S	O	N	D
Concept Assessment	———																	
Laboratory Development				———	———	———	———	———	———	———	———	———	———	———	———			
Feasibility Demonstration																———	———	———

OBJECTIVES

Regenerable metal oxide sorbents, such as zinc titanate, are being developed to efficiently remove hydrogen sulfide (H_2S) from coal gas in advanced power systems. Dilute air regeneration of the sorbents produces a tailgas containing a few percent sulfur dioxide (SO_2). Catalytic reduction of the SO_2 to elemental sulfur with a coal gas slipstream using the Direct Sulfur Recovery Process (DSRP) is a leading first-generation technology. Currently the DSRP is undergoing field testing at gasifier sites. The objective of this study is to develop

second-generation processes that produce elemental sulfur without coal gas or with limited use.

Novel approaches that were evaluated to produce elemental sulfur from sulfided sorbents include (1) sulfur dioxide (SO_2) regeneration, (2) substoichiometric (partial) oxidation, (3) steam regeneration followed by H_2S oxidation, and (4) steam-air regeneration. Preliminary assessment of these approaches indicated that developing SO_2 regeneration faced the fewest technical and economic problems among the four process options. Elemental sulfur is the only likely product of SO_2 regeneration and the SO_2 required for the regeneration can be obtained by burning a portion of the sulfur produced. Experimental efforts have thus been concentrated on SO_2-based regeneration processes.

BACKGROUND INFORMATION

Leading Hot-Gas Desulfurization Technologies

Hot-gas desulfurization research has focused on air-regenerable mixed-metal oxide sorbents such as zinc titanate and zinc ferrite that can reduce the sulfur in coal gas, present primarily as H_2S, to <20 ppmv and that can be regenerated in a cyclic manner with air for multicycle operation.

The sulfidation/regeneration cycle can be car ried out in fixed-, moving-, and fluidized-bed reactor configurations. The regeneration reaction is highly exothermic, requiring the use of large volumes of diluent to control the temperature and results in a dilute SO_2-containing tailgas that must be further treated. Under contracts with the U.S. Department of Energy/ Morgantown Energy Technology Center (DOE/METC), many approaches have been evaluated for treatment of the tailgas. These include adsorption of SO_2 using calcium-based sorbents followed by landfilling of calcium sulfate as well as conventional methods such as Wellman-Lord coupled with high-temperature syngas reduction and augmented Claus for converting the SO_2 to elemental sulfur. There are two leading advanced approaches that DOE/METC is currently sponsoring to convert the SO_2 tailgas to useful byproducts. These include the General Electric (GE) moving-bed process and the DSRP.

In the GE moving-bed process (Cook et al., 1992), the H_2S in coal gas is removed by moving a bed of sorbent countercurrent to the upward gas flow. The sulfided sorbent is transferred to a moving-bed regenerator below the moving-bed absorber using a lock-hopper arrangement. In the regenerator, SO_2 recycle and limited air are used to control the temperature of the exothermic reactions, producing a tailgas containing 10- to 13-vol% SO_2. The regenerated sorbent is lifted back to the absorber using a bucket elevator arrangement. The 10- to 13-vol% SO_2 is a suitable feed for a sulfuric acid plant. The GE moving-bed process has undergone a series of pilot-scale tests and has been selected for demonstration in a Clean Coal Technology project.

In the DSRP (Dorchak et al., 1991; Gangwal et al., 1993), the SO_2 tailgas is reacted with a slipstream of coal gas over a fixed bed of a selective catalyst to directly produce elemental sulfur at the high-temperature, high-pressure (HTHP) conditions of the tailgas and coal gas. Major reactions involved are shown below:

$$2\ H_2 + SO_2 \rightarrow (1/n)\ S_n + 2\ H_2O$$

$$2\ CO + SO_2 \rightarrow (1/n)\ S_n + 2\ CO_2$$

$$H_2 + (1/n)\ S_n \rightarrow 4\ H_2S.$$

The DSRP was originally envisioned as a two-stage process. Recent results, however, indicate that sufficient selectivity (>99 percent or better) to elemental sulfur can be achieved in a single stage

by careful control of the inlet stoichiometry to maintain a reducing gas (H_2 + CO) to SO_2 mole ratio of 2.0. The DSRP integrates well with zinc titanate fluidized-bed desulfurization (ZTFBD) (Gupta et al., 1992), as opposed to fixed- or moving-bed desulfurization because of the relative ease of achieving a constant concentration of SO_2 in the tailgas using the fluidized-bed desulfurization-regeneration system. Both ZTFBD and DSRP have been demonstrated at bench scale using simulated gases and are being demonstrated in an integrated manner using a slipstream of actual coal gasifier gas under another contract awarded to the Research Triangle Institute (RTI) by DOE/ METC.

Economic evaluations of the GE moving-bed process coupled to a sulfuric acid plant and fluidized-bed desulfurization coupled to DSRP have been conducted by Gilbert Commonwealth for DOE. These evaluations show that the two approaches are closely competitive, with costs within 1 percent of each other, cost of electricity basis.

Need for Simpler Processing

Production of a sulfuric acid byproduct, e.g., using the GE moving-bed process, is site specific, requiring a nearby sulfuric acid plant and a ready market because sulfuric acid cannot be stored in bulk for long periods of time and cannot be transported over long distances. Another inherent problem with the GE moving-bed process has been that, in spite of several attempts, a steady (constant) level of SO_2 has not been achieved in the tailgas, which could present operation problems for converting to sulfuric acid in the downstream sulfuric acid plant. A number of other problems have been encountered in the operation of the GE moving-bed process, e.g., control of temperature in the regenerator and corrosion in the SO_2 recycle system.

Elemental sulfur is the desired sulfur byproduct because it is easily stored, transported, or sold. It is also the preferred choice of utilities. DSRP has the advantage that it produces elemental sulfur and is also significantly cheaper than conventional processes to reduce SO_2 to elemental sulfur.

Nevertheless, simpler processes that can be more fully and economically integrated with regenerable sorbents are needed because the DSRP requires a small portion of the fuel gas (i.e., coal gas) to reduce SO_2 to elemental sulfur and, thus, imposes an inherent efficiency and economic penalty on the overall system. For every mole of SO_2 converted to elemental sulfur in DSRP, approximately 2 mols of reducing gas (H_2 + CO) are consumed. As the sulfur content of the coal fed to the gasifier increases, obviously the proportion of the reducing gas required in the DSRP will increase as will the cost associated with it. A greater incentive thus exists for developing alternative processing schemes for higher sulfur coals that eliminate or minimize the use of coal gas.

PROJECT DESCRIPTION

This project seeks to recover sulfur (as elemental sulfur) from sulfided sorbents using alternative regeneration reactions/process schemes that do not result in the production of a dilute SO_2-containing tailgas requiring coal gas for reduction to sulfur (as in DSRP). The project is divided into three tasks shown in the Schedule and Milestones. Task 1, Concept Assessment, is complete; Task 2, Laboratory Development, is currently ongoing; and Task 3, Feasibility Demonstration, will not begin until 1996.

Based on a concept assessment, the alternative regeneration techniques listed in order of increasing potential are partial oxidation, simultaneous steam and air regeneration, steam regeneration with direct oxidation of H_2S, and SO_2 regeneration.

Partial oxidation is attractive due to lack of thermodynamic limitations, thereby allowing the choice of sorbent purely on its ability to remove H_2S. The challenge, however, is to inhibit subsequent oxidation of elemental sulfur to SO_2 which is rapidly catalyzed by the sorbent as the sulfur attempts to escape its pores. Possible remedies include reducing reaction rates by reducing temperature, limiting the oxygen supply, and reducing sorbent and sulfur contact. However, none of these are complete solutions or achievable in practice without a great deal of difficulty. Lower temperatures would reduce the rate of sulfur vapor diffusions out of the sorbent. Oxygen concentrations at all points in the reactor must be at a level to control the sequential reaction, sorbent $\rightarrow$ sulfur $\rightarrow$ SO_2, to make sulfur but prevent SO_2 formation. This would require highly complex reactor designs. Reducing contact between sorbent and sulfur will require modifying sorbents to have a wide pore structure without altering attrition resistance. Thus, significant barriers exist to development of partial oxidation for direct sulfur production during regeneration.

The use of steam for regeneration involves the reaction that is simply the reverse of the sulfidation reaction. Thus, an immediate barrier to steam regeneration is that any sorbent capable of removing H_2S down to ppm levels will only release ppm levels of H_2S during steam regeneration. The ppm H_2S release will increase with steam concentration but only weakly (e.g., linearly, depending on sorbent stoichiometry). Higher steam concentrations and temperatures assist the regeneration but could result in severe sorbent sintering. Both steam regeneration followed by H_2S oxidation to sulfur and simultaneous steam and air regeneration followed by Claus reaction face additional technical problems. Mixtures of steam and SO_2 are corrosive. Effective condensation of sulfur occurs at a lower temperature than steam at HTHP conditions. A large heat duty is required to generate steam from condensed process steam or fresh water.

Based on detailed thermodynamic calculations and the barriers presented above, all alternative regeneration concepts, other than dry-SO_2 regeneration, were eliminated from further immediate consideration. Assessment and laboratory results of SO_2 regeneration are described in the Results section. Laboratory experiments to test the SO_2 regeneration concept were carried out using an atmospheric pressure thermogravimetric analyzer (TGA), a high-pressure TGA, and a high-pressure lab-scale reactor. The high-pressure lab-scale reactor system is shown in Figure 1. The reactor is made of a ½-in. stainless steel tube capable of operation at 750 °C and 200 psig. Provision is made for sulfiding the sorbent with simulated coal gas, or regenerating the sorbent with up to 15 vol% SO_2. The gas exiting the reactor passes through heated tubing into a 130 °C convective oven where a 0.1-micron filter is used to collect sulfur. A sample of the exit gas is analyzed by gas chromotography (GC) to measure H_2S breakthrough. The gas finally vents through a back-pressure regulator.

Zinc and iron containing sorbents have been the primary candidates that have been tested. The atmospheric pressure and high-pressure TGA experiments have involved cyclic tests using simulated coal gas for sulfidation and up to 15 vol% SO_2 for regeneration. The concept of SO_2 regeneration followed by air regeneration has also been evaluated.

RESULTS

Assessment of SO_2 Regeneration

Like steam regeneration, SO_2 regeneration has thermodynamic constraints as the thermodynamic calculations presented later show. However, high-pressure conditions are anticipated to enhance

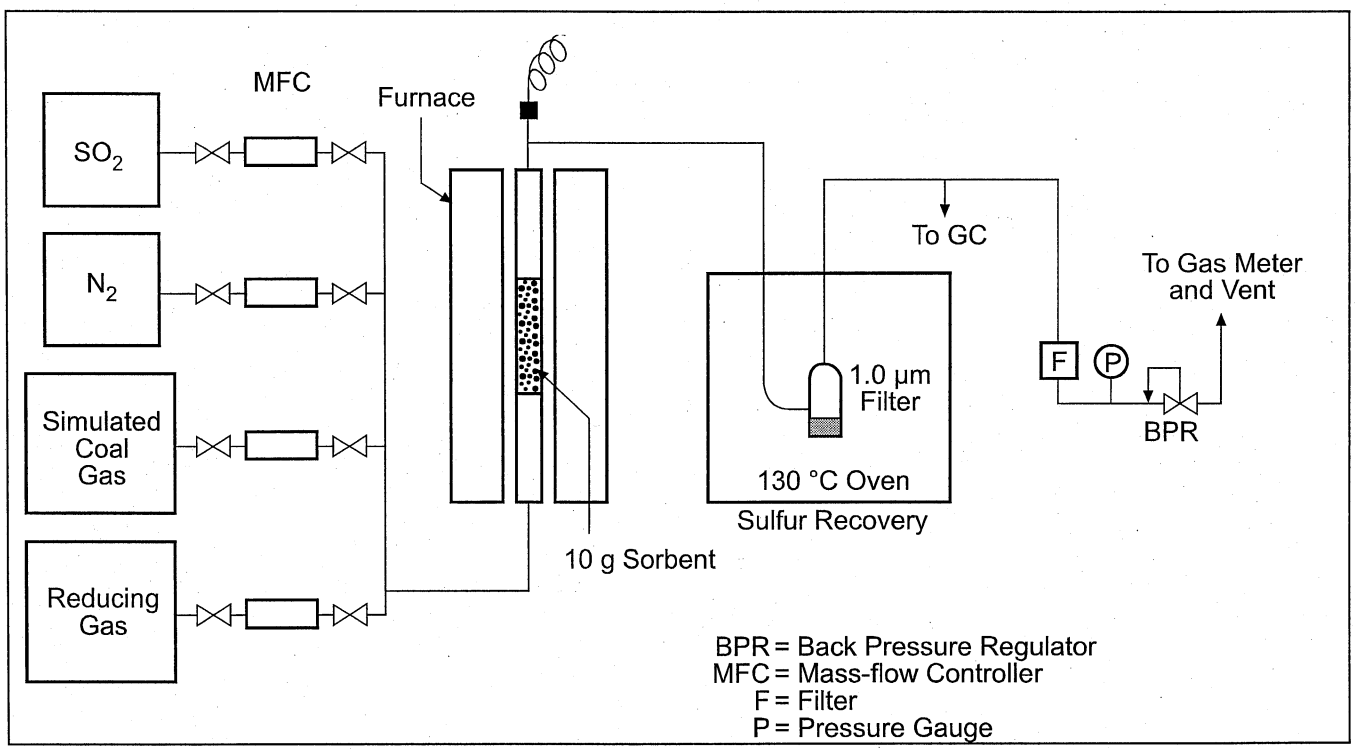

Figure 1. Laboratory-Scale SO_2 Regeneration Test System

elemental sulfur formation. Based on Le Chatalier's principle, high pressure favors formation of fewer gaseous products. Since formation of sulfur oligomers larger than S_3 result in few moles of gaseous products, high pressure should favor formation of higher oligomers. Also, nonideal behavior of sulfur oligomers could lead to increased yield at higher pressures.

Unlike thermodynamic limitations for steam regeneration, development of sorbents for SO_2 regeneration may benefit from the thermodynamic limitations. Regeneration with SO_2 will require SO_2 and heat because SO_2 regeneration is endothermic. Oxygen regeneration, which is rapid and extremely exothermic, produces SO_2 and heat. By balancing the amounts of SO_2 and O_2 regeneration, it may be possible to achieve complete regeneration, convert all sulfur species into elemental sulfur, and balance heat requirements. Since SO_2 regeneration is slow, achieving this balance requires increasing SO_2 regeneration rates. Increasing temperature will increase reaction rates, but the maximum temperature is limited by sorbent sintering and materials of construction available for reactor and process heat integration. Any temperature effects on the thermodynamic equilibrium constant will be further augmented by the increase in reaction rate. Although pressure effects on reaction rate constants are generally assumed insignificant, research with DSRP found rate constants, specifically for the H_2-SO_2 reaction, increased with pressure while all other conditions were kept constant. Thus HTHP conditions offer considerable potential for effective SO_2 regeneration.

With SO_2 regeneration, sulfate formation, a major cause of sorbent decrepitation, does not occur. Absence of sulfate formation during SO_2 regeneration should increase mechanical stability and extend life expectancy for sorbents. Sulfur

dioxide regeneration allows simple separation of SO_2 and elemental sulfur and dry SO_2 is much less corrosive than a SO_2 and steam mixture. The endothermic nature of SO_2 regeneration may require additional heat in spite of extensive heat recovery from the sulfidation unit and O_2 regenerator. Although a certain amount of sorbent optimization will be needed, SO_2 regeneration has a much greater potential for rapid process development than any of the other alternative regeneration techniques.

Sorbent Metal-Oxide Selection

A number of sorbent metal-oxide formulations were assessed on the basis of literature information and thermodynamic calculations. A review of the literature indicated regenerable sorbents based on oxides of cerium, copper, cobalt, iron, manganese, molybdenum, tin, and zinc individually and in combinations. These metal or mixed metal oxides have been investigated both without as well as combined with a secondary oxide, typically silica, alumina, titania, and chromia. The roles of these secondary oxides include support for strengthening mechanical structure, as stabilizers against reduction of the metal oxide to metal in a reducing environment, and/or as modifiers of thermodynamic properties of the metal oxide to enhance elemental sulfur formation during regeneration.

Based on the evaluations, sorbents based on cerium, cobalt, cobalt, molybdenum and tin were found to be poor desulfurizing agents, costly, or not easily regenerated with SO_2. Some had a combination of these deficiencies. Thus, they were eliminated from further consideration. Of the remaining metal oxides, namely oxides of manganese, iron, and zinc, due to the similarity of reduction and desulfurizing properties of manganese and iron, iron was chosen for further consideration because more is known about iron.

Also zinc remained a candidate for further consideration due to its very high desulfurization efficiency even though it showed very poor thermodynamics for SO_2 regeneration. In combination with iron, zinc could act as a polishing agent for H_2S which could be regenerated using air to produce SO_2 needed for SO_2 regeneration. Thus, the laboratory work concentrated on iron and zinc-based sorbents.

Thermodynamic and Process Evaluation of SO_2 Regeneration

As stated earlier, SO_2 regeneration also shows thermodynamic constraints as seen from thermodynamic calculations shown in Table 1. Results are relevant only for zinc- and iron-based sorbents and thus Table 1 is limited to these sorbents. It is noted that, as the sorbent becomes less effective for H_2S removal, it becomes thermodynamically more easily regenerated by SO_2. This suggests that a sorbent combination from the top and bottom parts of the table may be necessary for an effective SO_2 regeneration process.

The SO_2 regeneration could be followed by air or O_2 regeneration to complete the regeneration before returning the sorbent to the sulfider as shown conceptually in Figure 2. Of course, alternative process schemes employing various combinations of SO_2 and O_2 regeneration are also possible but are not discussed here in the interest of space.

Test Results

A number of sorbents based on iron and zinc oxides were prepared and tested for SO_2 regeneration using the TGAs and the laboratory reactor system. The benchmark zinc titanate and zinc ferrite sorbents were ZT-4 and L-7. These sorbents have been developed for fluidized-bed desulfurization incorporating air regeneration under a previous DOE contract. The ZT-4 sorbent (based purely on ZnO as the active sorbent) and other ZnO-only-based sorbents showed essentially no

Table 1. Thermodynamic Calculations for Sulfidation and SO_2 Regeneration

Sorbent	Sulfidation Equilibrium H_2S Concentration with 20% Steam at 800 K (ppm)	Equilibrium Constants for SO_2 Regeneration			
		800 K		1,000 K	
		S_2 ($x10^{-4}$)	S_8 ($x10^{-4}$)	S_2 ($x10^{-4}$)	S_8 ($x10^{-4}$)
ZnO	3	0.17	0.51	3.3	1.1
$ZnO-TiO_2$	3	0.19	0.56	3.7	1.2
FeO	107	6.2	19.0	55.0	18.0
$ZnO-A1_2O_3$	1,055	61.0	183.0	316.0	100.0
$FeO-A1_2O_3$	3,484	202.0	605.0	717.0	227.0

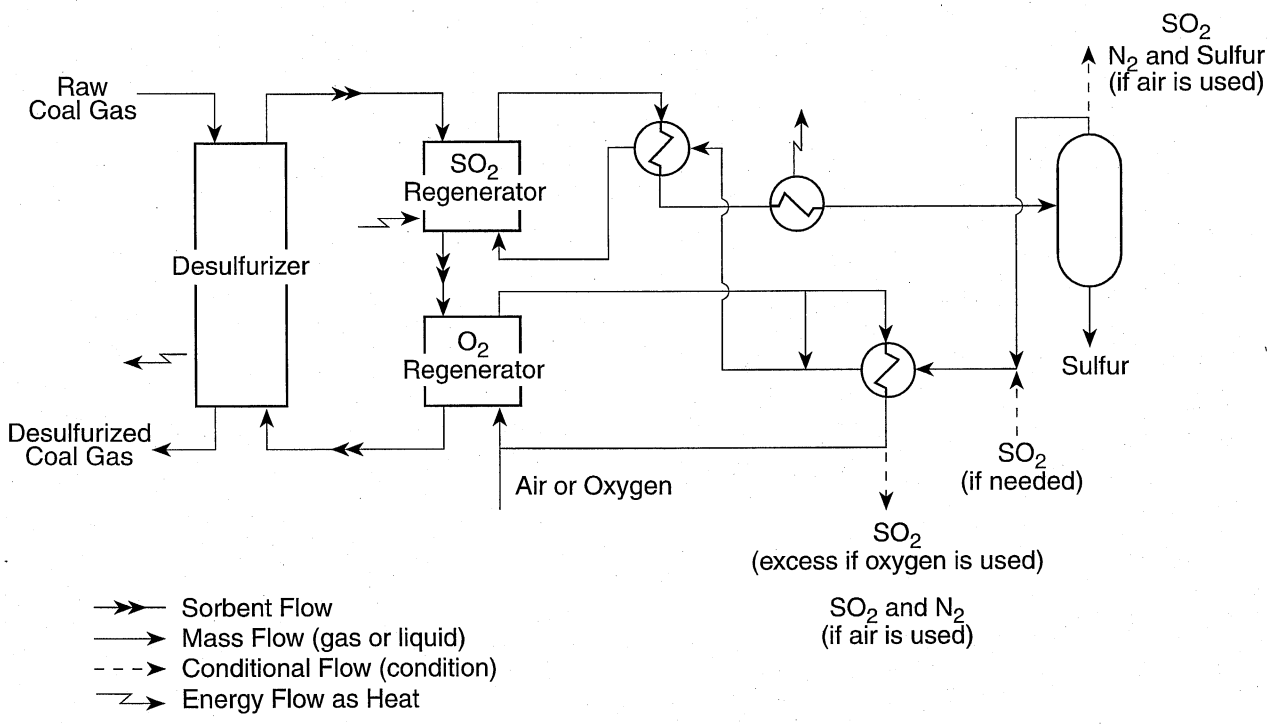

Figure 2. Three Reactor Systems for SO_2 Regeneration Followed by O_2 Regeneration

regeneration with 3.3 percent SO_2 in N_2 at up to 800 °C and 10 atm. However, iron- and zinc-iron-based sorbents showed good regeneration with SO_2. The rates of regeneration of the various sorbents depended on how they were prepared. Due to the proprietary nature of the preparations, no data related to the sorbent's preparation or pore structure are presented. Average regeneration rates (expressed in terms of sulfur production rate) are presented in Table 2 along with average sulfidation rates and conditions. The sulfidations were conducted using a 0.5 vol% H_2S containing simulated coal gas. The results suggest that SO_2 regeneration is a feasible approach for iron-based sorbents. Significant potential for increased SO_2-regeneration rates is possible by increasing the SO_2 concentration and pressure and by modifying sorbent properties.

Table 2. Comparison of Sulfidation and SO_2 Regeneration for Several Sorbents (3.3 percent SO_2, 10 atm)

Sorbent Designation	Sorbent Type (P = proprietary additive)	Sulfidation Temperature (°C)	Regeneration Temperature (°C)	Sulfidation Rate ($x10^{-4}$) (g sulfur/g sorbent/min)	Regeneration Rate ($x10^{-4}$) (g sulfur/g sorbent/min)
L-7	Zn+Fe	550	800	10.8	2.0
RTI-3	Fe+P	450	800	19.2	18.2
FE-90	Fe	400	800	34.0	4.6
R-2	Zn+Fe	550	700	24.0	2.2
R-3	Re+P	500	700	3.8	5.8
R-4	Fe+P	500	700	2.0	4.4
R-5	Zn+Fe+P	460	00	13.4	4.4

The L-7, R-2, and R-5 sorbents did not show complete regeneration in SO_2 because the zinc portion of the sorbent did not regenerate. The iron-only-based sorbents completely regenerated in SO_2. To test the potential of SO_2 regeneration (with higher SO_2 concentrations) followed by air regeneration for zinc-iron-based sorbents, the R-5 sorbent was subjected to three cycles at 10 atm, each consisting of a sulfidation at 460 °C, a SO_2 regeneration with 3.3 to 15 percent SO_2 at 650 to 700 °C, and finally an air regeneration with 2 percent O_2 at 700 °C.

The sorbent showed consistent behavior over the three cycles of operation. The rates of sulfidation, SO_2 regeneration, and air regeneration are compared in Table 3. Results show that as SO_2 concentration is increased, regeneration can be carried out effectively at lower temperatures. Also, the various rates are not widely different and thus system design difficulty would not be very formidable.

Table 3. Comparison of Sulfidation, SO_2-Regeneration and Air-Regeneration Rates for R-5 Sorbent (Pressure = 10 atm)

Reactant	Temperature (°C)	Rate g sulfur/ (g sorbent/min)
Simulated Coal Gas (0.5% H_2S)	460	13.4
SO_2		
3.3%	700	4.4
3.3%	650	0.22
15%	650	3.7
2% O_2 in N_2	700	5[a]

[a] Result probably limited by mass transfer

Laboratory-scale tests of SO_2 regeneration were carried out with the R-5 sorbent. About 5 g of the sorbent was loaded in the reactor and fully sulfided using simulated coal gas. SO_2 regeneration was then started at 7.8 atm and 700 °C with 15 percent SO_2 in N2. Samples were withdrawn after 5.5 h and 10 h of regeneration for TGA analysis. The TGA analysis showed, as expected, that the zinc portion of the sorbent was not regenerated.

However, the iron portion of the sorbent regenerated at a rate of 2.1×10^{-4} g sulfur/ (g sorbent/min). This result is the same order of magnitude as most TGA results presented in Table 3 at 10 atm. After 10 h of operation, sulfur plugging downstream of the reactor occurred. The sulfur was removed and examined. It was found to be yellow without any kind of odor.

Based on the results, the concept of SO_2 regeneration processes shows significant promise for development as an effective hot-gas desulfurization system with sulfur recovery.

FUTURE WORK

Laboratory scale tests and TGA experiments will continue to narrow the choices for sorbents for the SO_2 regeneration concept. Feasibility demonstration with a larger reactor system will begin in the next fiscal year. Process evaluations will be carried out using the lab-scale and larger-scale data.

REFERENCES

Cook, C.S., et al. 1992. "Integrated Operation of a Pressurized Fixed Bed Gasifier and Hot Gas Desulfurization System." In *Proceedings of the 12th Annual Gasification Gas Stream Cleanup Systems Contractors' Review Meeting*. Vol. 1, DE93000228, p. 84.

Dorchak, T.P., S.K. Gangwal, and W.J. McMichael. 1991. "The Direct Sulfur Recovery Process." *Environmental Progress* 10(2):68.

Gangwal, S.K., W.J. McMichael, and T.P. Dorchak. 1992. "The Direct Sulfur Recovery Process for Refinery Gas Processing." AIChE Meeting, New Orleans, March.

Gangwal, S.K., et al. 1993. "DSRP, Direct Sulfur Production." In *"Proceedings of the Coal Fired Power Systems 93—Advances in IGCC and PFCB Review Meeting"*. DOE/METC, Morgantown, WV. June.

Gupta, R., and S.K. Gangwal. 1992. "Enhanced Durability of Desulfurization Sorbents for Fluidized-Bed Applications–Development and Testing of Zinc Titanate Sorbents." Topical Report to DOE/METC. Report No. DOE/MC/ 25006-3271. DOE/METC, Morgantown, WV.

APPENDIX B Advanced Sulfur Control Processing: Proceedings of the Advanced Coal-Fired Power Systems '96 Review Meeting

Advanced Sulfur Control Processing

Santosh K. Gangwal (skg@rti.org; 919-541-8033)
Jeffrey W. Portzer (jwp@rti.org; 919-541-8025)
Brian S. Turk (bst@rti.org; 919-541-8024)
Raghubir Gupta (gupta@rti.org; 919-541-8023)
Research Triangle Institute
P.O. Box 12194
Research Triangle Park, NC 27709-2194

Introduction

Advanced integrated gasification combined cycle (IGCC) power plants call for hot particulate removal and hot-gas desulfurization (HGD) following gasification in order to achieve high thermal efficiency. The Morgantown Energy Technology Center's (METC's) HGD research program has focused on the development of regenerable metal oxide sorbents to remove hydrogen sulfide (H_2S) from coal gas. Leading sorbents such as zinc titanate can reduce the H_2S in coal gas to low parts-per-million levels and can be regenerated using air for multicycle operation. The sulfidation-regeneration cycle for a generic metal oxide (MO) is as follows:

$$MO + H_2S \rightarrow MS + H_2O \qquad \text{(sulfidation)}$$
$$MS + {}^3/_2O_2 \rightarrow MO + SO_2 \ . \qquad \text{(regeneration)}$$

Because the regeneration reaction is highly exothermic, temperature control is required to prevent overheating and sorbent sintering. One way to control the temperature is to use a highly dilute air stream, typically containing up to 3 vol% oxygen. This would result in a tail gas containing up to 2 vol% sulfur dioxide (SO_2). More elegant methods to control exothermicity of air regeneration that could potentially produce up to 14 vol% SO_2 are being developed (Cook et al., 1992; Campbell et al. 1995). In any event, a problematic tail gas containing 2 to 14 vol% SO_2 is produced that must be disposed of. The most desirable treatment option for the tail gas is to convert the SO_2 to elemental sulfur. METC is sponsoring the development of the Direct Sulfur Recovery Process (DSRP) (Gangwal and Portzer, 1995) that uses the reducing components (H_2, CO) of coal gas to directly and efficiently reduce the SO_2 to elemental sulfur in the presence of a catalyst in one step:

$$SO_2 + 2H_2 \text{ (or } 2CO) \rightarrow 2H_2O \text{ (or } 2CO_2) + \tfrac{1}{2}S_2 \ .$$

In the DSRP, for every mole of SO_2, 2 mol of reducing components are used. DSRP is a leading first generation technology and is undergoing field testing at gasifier sites. This study seeks to develop more advanced HGD approaches leading to elemental sulfur recovery in IGCC systems.

Research sponsored by the U.S. Department of Energy's Morgantown Energy Technology Center, under Contract DE-AC21-93MC31258, with Research Triangle Institute, 3040 Cornwallis Road, Research Triangle Park, NC 27709, telefax: 919-541-8000.

Objectives

The objective of this study is to develop a second generation HGD process that produces elemental sulfur without or with minimal use of coal gas and has better overall economics than DSRP when integrated with the overall IGCC system.

Approach

Direct production of elemental sulfur during sorbent regeneration was chosen as the approach for development of the required second generation HGD process. Concepts that were evaluated to produce elemental sulfur from sulfided sorbent included:

1. SO_2 regeneration

$$2MS + SO_2 \rightarrow 2MO + {}^3/_2S_2$$

2. Substoichiometric oxidation

$$2MS + O_2 \rightarrow 2MO + S_2$$

3. Steam regeneration followed by H_2S oxidation

$$MS + H_2O \rightarrow MO + H_2S$$
$$H_2S + \tfrac{1}{2}O_2 \rightarrow H_2O + \tfrac{1}{2}S_2$$

4. Steam-air regeneration followed by Claus reaction

$$MS + H_2O \rightarrow MO + H_2S$$
$$MS + {}^3/_2O_2 \rightarrow MO + SO_2$$
$$2H_2S + SO_2 \rightarrow 2H_2O + {}^3/_2S_2 \ .$$

Preliminary assessment of these concepts indicated that Concept 1, SO_2 regeneration faced the fewest technical and economic problems among the four options (Gangwal et al., 1995). Elemental sulfur is the only likely product of SO_2 regeneration and the SO_2 required for the regeneration can be obtained by burning a portion of the sulfur produced. With SO_2 regeneration, sulfate formation, a major cause of sorbent decrepitation, does not occur. This should result in longer sorbent life. At high pressure, dry SO_2 is also simpler to separate from elemental sulfur than steam. Thus, recycle of unused SO_2 to the regenerator would be possible and this would be much less energy intensive than the use of steam. Efforts have thus concentrated on SO_2 regeneration.

Based on a theoretical evaluation of a number of potential sorbent candidates, iron- and zinc-based regenerable sorbents were chosen for experimental evaluation in this study (Gangwal et al., 1995). The selection criteria included desulfurization efficiency, SO_2 regenerability, cost, and knowledge base. Iron was considered to be the most promising candidate among numerous metals based on the above selection criteria. Also zinc remained a candidate for consideration (primarily in combination with iron) due to its excellent desulfurization efficiency, its extensive knowledge base, and its low cost, even though ZnS showed essentially no SO_2 regenerability at temperatures of interest. In combination with iron, zinc can act as a polishing agent to remove

H_2S down to very low levels and can be regenerated using air to produce SO_2 needed for regeneration of the iron sulfide. Thermogravimetric analyzer (TGA) and lab-scale reactor testing of a number of iron-zinc sorbents demonstrated the feasibility of direct regeneration of these sorbents using SO_2 to produce elemental sulfur (Gangwal et al., 1995). This year the experimental work has progressed to the bench-scale. A number of sorbents were prepared and tested at the bench-scale over multiple cycles. Work on development and multicycle testing of attrition-resistant zinc and iron sorbents is continuing. Based on results of bench-scale testing of promising sorbents, an economic evaluation for a 300 MWe plant is to be conducted next year.

Project Description

Summary of Previous Experiments

Laboratory experiments to test the SO_2 regeneration concept were carried out using a high-pressure TGA and a high-pressure lab-scale reactor (Gangwal et al., 1995). The reactor was made of a ½-in. stainless steel tube capable of operation at 750 °C and 200 psig. Provision was made for sulfiding up to 10 g of sorbent with simulated coal gas and regenerating the sulfided sorbent with up to 15 vol% SO_2. The gas exiting the reactor passed through heated tubing into a 130 °C convective oven where a 0.1-μm filter was used to collect sulfur. The gas finally vented through a back pressure regulator.

A number of proprietary sorbents based on iron and zinc oxides were prepared and tested for SO_2 regeneration. The benchmark zinc titanate and zinc ferrite sorbents were ZT-4 and L-7. These sorbents have been developed for fluidized-bed desulfurization incorporating air regeneration under a previous DOE contract. The sulfided ZT-4 sorbent which was based purely on ZnO as the active sorbent showed essentially no regeneration with 3.3 percent SO_2 in N_2 at up to 800 °C and 10 atm. However, sulfided iron- and zinc-iron-based sorbents showed good regeneration with SO_2. TGA rates of SO_2 regeneration ranged from 2.2×10^{-4} to 5.8×10^{-4} g sulfur/g sorbent/min with 3.3 vol% SO_2 at 700 °C and 10 atm.

A zinc-iron sorbent designated R-5 showed promising results and was tested further using the high-pressure lab-scale reactor. About 5 g of the sorbent was loaded in the reactor and fully sulfided using simulated coal gas. SO_2 regeneration was then started at 7.8 atm and 700 °C with 15 vol% SO_2 in N_2. Samples were withdrawn after 5.5 h and 10 h of regeneration for TGA analysis. As expected, the TGA analysis showed that the zinc portion of the sorbent was not regenerated but the iron portion of the sorbent regenerated at a rate of 2.1×10^{-4} g sulfur/g sorbent/min. This result is similar to rates with the high-pressure TGA. At the end of 10-h, sulfur plugging occurred and solid yellow sulfur was recovered downstream of the reactor.

The R-5 sorbent was also tested for SO_2 regeneration as a function of SO_2 concentration and for air regeneration. The SO_2 regeneration rate, as measured by the high pressure TGA, increased from 2.2×10^{-5} to 3.7×10^{-4} g sulfur/g sorbent/min at 650 °C and 10 atm when SO_2 concentration was increased from 3.3 to 15 vol%. The air regeneration rate at 10 atm and 700 °C was around 5×10^{-4} g sulfur/g sorbent/min with 2 vol% O_2 in N_2.

Process Concept

Based on the results presented above, the concept of SO_2 regeneration with iron- and zinc-based sorbents showed significant promise for development as an effective HGD system resulting in sulfur recovery with limited use of coal gas. A number of HGD processes could be conceptualized using alternative combinations of SO_2 and air regeneration. The similarity of air and SO_2 regeneration rates and the significant increase in SO_2 regeneration rate with SO_2 concentration were highly encouraging. It suggested that, with further increase in SO_2 concentration to 90 to 100 vol%, rates could be increased sufficiently to allow the use of even lower regeneration temperatures around 600 °C. This temperature is closer to the expected sulfidation temperature of iron sorbents which is around 450 °C. A conceptual three-reactor process based on sulfidation of iron-zinc sorbents followed by SO_2 regeneration followed by air regeneration is shown is Figure 1. The SO_2 regeneration produces sulfur from the iron portion of the sorbent and the air regeneration regenerates the zinc portion of the sorbent.

In this process concept, the sorbent from the sulfider at around 450 °C would have to be heated to around 600 °C for SO_2 regeneration. The required heat could be obtained using indirect heat exchange with coal gas which is being cooled to 450 °C, by injecting a small amount of O_2 along with SO_2 in the SO_2 regenerator, by indirect heat exchange with the sorbent being returned from the air regenerator to the sulfider, or using a convenient combination of these approaches. An alternative process concept with partial air (or O_2) regeneration of the sorbent to effect the required temperature increase and some zinc regeneration prior to SO_2 regeneration can also be visualized. A number of other process combinations are also possible but are not presented here in the interest of space.

Bench-Scale Testing

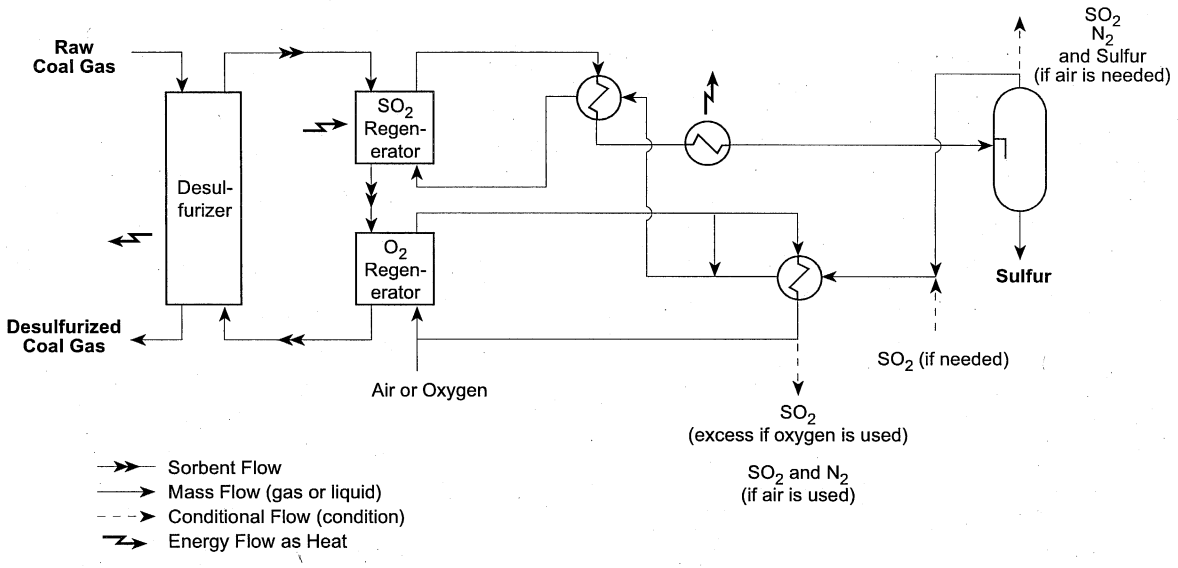

Figure 1. Three-Reactor System for SO_2 Regeneration Followed by O_2 Regeneration

Efforts this year have concentrated on scale-up of the R-5 sorbent preparation to

attrition-resistant fluidizable form, construction and commissioning of a high-temperature, high-pressure (HTHP) bench-scale unit and multicycle HTHP testing of the iron-zinc sorbents simulating the conceptualized three-reactor process of Figure 1.

The bench-scale reactor system which was built by modifying an existing unit is shown in Figure 2. The system has the capability of simulating a complex coal gas mixture using a set of mass flow controllers for gaseous components and a positive displacement pump for water to generate steam. The reactor can operate either as a fluidized-bed or as a fixed-bed with up to a 3-in. inside diameter sorbent cage. The pressure and temperature rating of the reactor is 400 psig at 750 °C and it is Alon-processed to reduce corrosion of the stainless steel. Reactor throughput up to 400 slpm of gas can be processed and sorbent up to 1.0 liter can be tested.

For SO_2 regeneration, pure SO_2 or SO_2 mixed with N_2 can be fed to the reactor by displacement of liquid SO_2 from a tank using a head pressure of nitrogen. Air regeneration (air line not shown in the figure) can also be carried out. Two separate reactor exits and downstream vent systems are utilized. SO_2 regeneration is conducted through a hot exit line with a sulfur condenser, catch pot, and a hot pressure control valve. This line is maintained hot to prevent sulfur plugging. Sulfidation and air regeneration are conducted through the other exit line. Gas samples are analyzed continuously for H_2S during sulfidation and SO_2 during air regeneration using Ametek continuous analyzers. Oxygen during air regeneration is measured continuously using a fuel cell-based analyzer and H_2S, COS, and SO_2 are measured intermittently during

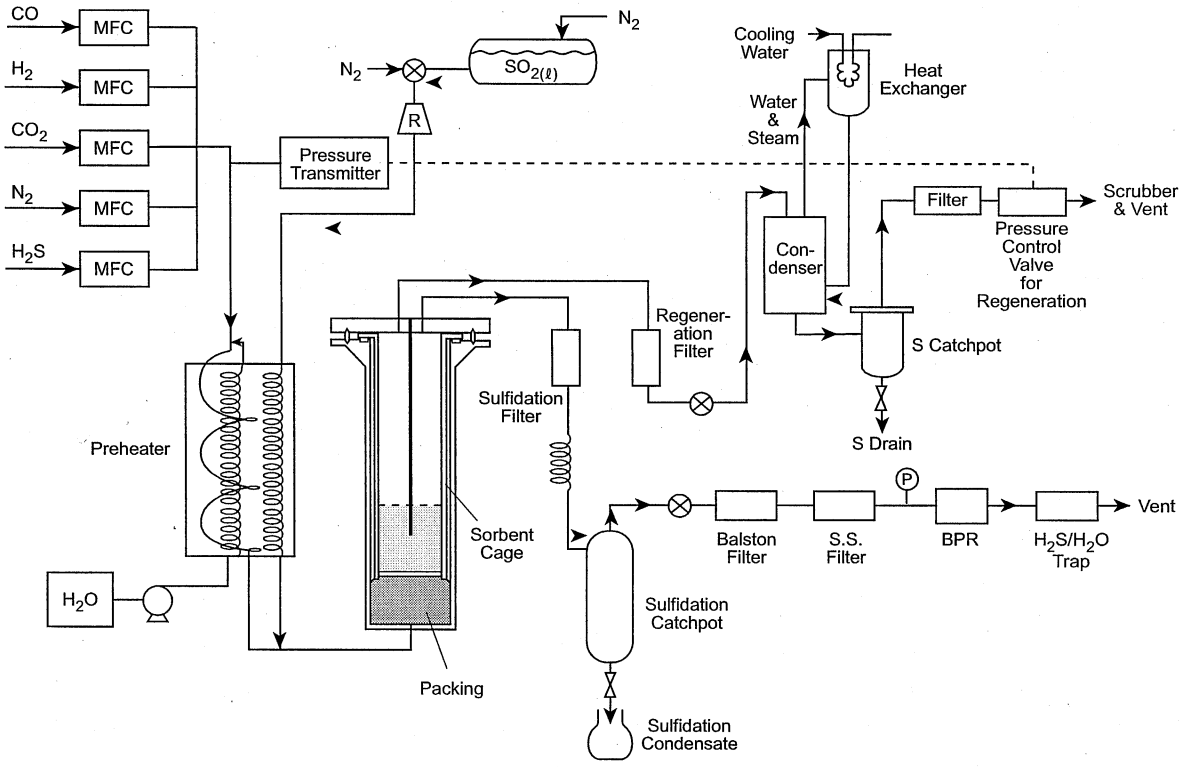

Figure 2. Bench-Scale Reactor System

sulfidation using a gas chromatograph with a flame photometric detector.

Results

Iron- and zinc-based sorbents were tested at HTHP conditions for multiple cycles. The sorbent preparation is proprietary and a patent application is pending, thus any information that could result in revealing the chemical composition and structure of the sorbents such as breakthrough curves and physical properties will not be presented. The R-5 sorbent recipe was scaled up to kilogram quantities of fluidizable attrition-resistant form with the help of a catalyst manufacturer. Two separate scale-up procedures were attempted. Using the first procedure, sorbents R-5-AWB, R-5-B, and R-5-C were produced in kilogram quantities. Using the second procedure, sorbents R-5-52, R-5-57, and R-5-58 were prepared in kilogram quantities.

R-5-B had poor attrition resistance and was immediately rejected. R-5-AWB, R-5-C, R-5-52, and R-5-58 were tested over multicycles simulating the three-reactor process of Figure 1 (R-5-57 is yet to be tested). The nominal test conditions for these multicycle tests are shown in Table 1.

The cycles typically consisted of sulfidation until breakthrough, followed by two types of regeneration. The first type of regeneration was a full air regeneration (up to 60 min) whereas the second type consisted of SO_2 regeneration (for 30 to 120 min followed by air regeneration for up to 60 min. Since a procedure for directly measuring elemental sulfur in a gas stream containing large amounts of SO_2 is yet to be developed, the amount of elemental sulfur produced during SO_2 regeneration was determined by actual measurement of the elemental sulfur that was collected or by the difference between the SO_2 produced by the two types of regeneration.

A total of 40 cycles have been run. The number of cycles completed with the various sorbents is shown in Table 2.

Table 1. Bench-Scale Test Conditions

Pressure:	275 psig	Coal gas composition (vol%)	
Flow rate:	18-75 slpm	CO:	15
Sorbent amount:	270-350 g	H_2:	10
Temperature (°C)		N_2:	Balance
Sulfidation:	420-460	CO_2:	10
SO_2 regeneration:	625	H_2O:	10-15
Dilute air regeneration:	600-650	H_2S:	0.3
SO_2 gas (vol%)		Oxidizing gas (vol%)	
SO_2:	50-65	O_2:	1-2
N_2:	Balance	N_2:	Balance

Because of the proprietary nature of the sorbents, the results presented here are of a general nature while patent protection is being sought. Generally each of the sorbents was able to reduce the H_2S to below 100 ppmv and was regenerable over multiple cycles. Also, measurable (several grams) quantities of elemental sulfur were produced during SO_2 regeneration of each of the sorbents. As much as 60 to 80 percent of the sulfur adsorbed by the sorbents has been recovered as elemental sulfur. However, the sorbents produced by the first procedure, namely R-5-AWB and R-5-C, underwent excessive loss in reactivity with cycles. In addition, they underwent significant attrition, as measured by a three-hole attrition tester, following cyclic testing. On the other hand, the sorbents prepared by the second procedure, namely R-5-52 and R-5-58, showed no loss in reactivity over the cyclic operation and also very low attrition, comparable to FCC catalysts, as measured both before and after cyclic testing by the three-hole attrition tester. In fact, the reactivity of both R-5-52 and R-5-58 improved with cycling.

Table 2. No. of Cycles Completed

Sorbent	Active metal	No. of cycles
R-5-AWB	Zn, Fe	5
R-5-C	Zn, Fe	17
R-5-52	Fe	10
R-5-58	Zn, Fe	8

Applications

As briefly discussed, the HGD process envisioned in Figure 1 or other similar processes that could result in direct production of elemental sulfur during regeneration have potential advantages over existing process options if they can be economically integrated with IGCC. The other options are production of undesirable calcium waste, production of sulfuric acid, or production of elemental sulfur using DSRP. Production of sulfuric acid is attractive if a market is readily available nearby. It may be difficult to find several such sites for IGCC plants. Elemental sulfur is the preferred option and DSRP is a highly efficient process but, as discussed earlier, requires the use of a small portion of the coal gas that results in an energy penalty to the power plant. Application of reactive and attrition-resistant sorbent such as R-5-58 to an IGCC with the capability to undergo direct SO_2 regeneration to elemental sulfur, where the SO_2 can be obtained by burning a portion of the elemental sulfur product, is a process option that needs to be developed further.

Future Activities

Approximately 15 cycles will be completed with sorbents R-5-58 and R-5-57 each. Then one of these sorbents will be tested for up to 50 cycles to demonstrate sorbent and process durability. Based on the results of testing, an economic evaluation for a 300 MWe plant will be conducted.

Acknowledgments

The authors would like to gratefully acknowledge the assistance and guidance of the METC Contracting Officer's Representative, Mr. Thomas P. Dorchak. The contract period of performance is from March 21, 1994, to March 20, 1997. United Catalyst, Inc., is assisting with preparation of zinc- and iron-based sorbents. Texaco is following the work on the project and will provide their existing nonproprietary data to assist in the economic evaluation.

References

Cook, C.S., et al. 1992. Integrated Operation of a Pressurized Fixed-Bed Gasifier and Hot Gas Desulfurization System. In *Proceedings of the 12th Annual Gasification and Gas Stream Cleanup System Contractors' Review Meeting.* Vol. 1, DE93000228, p. 84.

Campbell, W.M. et al. 1995. Hot-Gas Desulfurization Using Transplant Reactors. In *12th International Pittsburgh Coal Conference Proceedings,* pp. 1059-1064. September

Gangwal, S.K., and J.W. Portzer. 1995. Slipstream Testing of Hot-Gas Desulfurization with Sulfur Recovery. In *Proceedings Advanced Coal-Fired Power Systems' 95 Review Meeting,* pp. 220-228, DOE/METC-95/1018 Vol. 1. NTIS/DE 95009732. Springfield, VA.

Gangwal, S.K., B.S. Turk, and R. Gupta. 1995. Advanced Sulfur Control Concepts. In *Proceedings Advance Coal-Fired Systems' 95 Review Meeting,* pp. 622-630, DOE/METC-95/1018, Vol. 2, NTIS/DE 95009733. Springfield, VA.

APPENDIX C Hot Gas Desulfurization with Sulfur Recovery: Proceedings of the Advanced Coal-Based Power and Environmental Systems '97 Conference

Hot-Gas Desulfurization with Sulfur Recovery

Jeffrey W. Portzer (jwp@rti.org; 919-541-8025)
Ashok S. Damle (adamle@rti.org; 919-541-6146)
Santosh K. Gangwal (skg@rti.org; 919-541-8033)
Research Triangle Institute
3040 Cornwallis Road
Research Triangle Park, NC 27709

Introduction

Advanced integrated gasification combined cycle (IGCC) power plants require advanced particle filters and hot-gas desulfurization (HGD) following gasification in order to achieve high thermal efficiency. The Federal Energy Technology Center's (FETC's) research program is focusing on the development of regenerable metal oxide sorbents, such as zinc titanate, for efficient removal of hydrogen sulfide (H_2S) from coal gas. During regeneration of these sorbents, there is the opportunity to produce elemental sulfur (S_x) as a valuable byproduct. Currently, the leading technologies use air or dilute-air regeneration of the sorbents to produce a tail gas containing mostly nitrogen plus 2 to 14 vol% sulfur dioxide (SO_2). This tail gas must be treated further to avoid release of SO_2. One option is the catalytic reduction of SO_2 with a coal gas slipstream using the Direct Sulfur Recovery Process (DSRP), a leading first- generation technology to produce elemental sulfur.

The FETC is sponsoring the development of the DSRP (Dorchak et al., 1991; Portzer and Gangwal, 1995), a single-step catalytic process that uses the reducing components (H_2 and CO) of coal gas to directly and efficiently reduce the SO_2 to elemental sulfur:

$$SO_2 + 2H_2 \text{ (or } 2CO) \rightarrow 2H_2O \text{ (or } 2CO_2) + 1/nS_n \, .$$

In the DSRP, for every mole of SO_2, two moles of reducing gas are used, leading to a small but noticeable consumption of coal gas. Although the DSRP continues to show promise and has undergone field testing at gasifier sites (Portzer et al., 1996), alternative or improved processing is still possible.

Objective

The objective of this study is to develop a second generation HGD process that regenerates the sulfided sorbent directly to elemental sulfur using SO_2, with minimal consumption of coal gas. The goal is to have better overall economics than DSRP when integrated with the overall IGCC system.

Approach

Direct production of elemental sulfur during sorbent regeneration, using SO_2 as an oxidizing agent, was chosen as the approach for development of the second-generation HGD process

(Gangwal et al., 1995, 1996). SO_2 regeneration involves the reaction of nearly pure SO_2 with sulfided sorbent at elevated temperature and pressure. Under these conditions, elemental sulfur is the only product predicted from thermodynamics. Based on a theoretical evaluation of a number of potential sorbent candidates, iron- and zinc-based regenerable sorbents were chosen for experimental evaluation in this study (Gangwal et al., 1995). Iron is considered the most promising candidate based on a combination of factors—desulfurization efficiency, SO_2 regenerability, cost, and knowledge base. Zinc is a leading candidate, primarily in combination with iron, due to its excellent desulfurization efficiency, its extensive knowledge base, and its low cost. Although zinc sulfide (ZnS) shows essentially no SO_2 regenerability at temperatures of interest, zinc can act as a polishing agent when combined with iron to remove H_2S down to very low levels. Advantageously the ZnS can be regenerated using air to produce the SO_2 needed for regeneration of the iron sulfide (FeS). The key chemical reactions of interest are as follows:

1. Sulfidation

$$Fe_2O_3 + 2H_2S + H_2 \rightarrow 2FeS + 3H_2O$$

$$ZnO + H_2S \rightarrow ZnS + H_2O$$

2. SO_2 regeneration

$$4\ FeS + 3SO_2 \rightarrow 2Fe_2O_3 + 7/2\ S_2$$

3. O_2 regeneration

$$2FeS + 7/2\ O_2 \rightarrow Fe_2O_3 + 2SO_2$$

$$ZnS + 3/2\ O_2 \rightarrow ZnO + SO_2\ .$$

The feasibility of SO_2 regeneration of iron- and zinc-based sorbents was demonstrated using high-pressure thermogravimetric analysis (TGA) and high-pressure, small-scale lab reactors. A number of sorbents were prepared and tested at the bench scale over multiple cycles. Attrition-resistant zinc and iron formulations were developed, and the most promising material was tested for 50 cycles of alternating sorption and regeneration. Computer flowsheet simulation of a conceptual process design is proceeding in preparation for a preliminary economic evaluation of a commercial embodiment (nominal 250 MWe [net] scale plant).

Project Description

Summary of Previous Experiments

In previously reported work, microreactor-scale experiments were conducted at elevated pressure (10 atm) and temperatures up to 750 °C to test the concept of SO_2 regeneration. Concentrations up to 15 vol% SO_2 were used (Gangwal et al., 1995). An iron-zinc sorbent designated R-5 showed promising results, with solid sulfur being recovered from the lab-scale system or condenser. Following this initial success, four different iron- and zinc-based fluidizable sorbents,

manufactured by two different methods, were chosen for scale-up, These were prepared in larger batches (350 g) suitable for fluidized-bed testing.

An existing 3-in. diameter, high-temperature, high-pressure (HTHP), bench-scale, fluidized-bed reactor system was modified to enable SO_2 regeneration as well as air regeneration, plus elemental sulfur recovery. The reactor system is described by Gangwal et al. (1996) and was operated for the multicycle HTHP testing of the iron-zinc sorbents. For each test cycle (conducted at 20 atm), sulfidation of the sorbent at 450 °C was accomplished using a synthetic coal-gas mixture containing 3,000 ppm of H_2S. Figure 1 shows the several combinations of conditions that were used for regeneration of each cycle. The SO_2 regeneration was accomplished by vaporizing liquid SO_2 into a heated nitrogen stream (at 450 to 630 °C). Concentrations up to 75 vol% were used. Oxygen regeneration was typically conducted following the SO_2 regeneration step. The procedure was convenient from the experimental standpoint, as the instrumentation for the evolved SO_2 of the O_2 regeneration step gave an independent measure of the amount of sulfur still in the sorbent following SO_2 regeneration. In addition, some O_2 regeneration half-cycles were run with the air mixed with the N_2-SO_2 stream to simulate the O_2 + SO_2 regeneration. These conditions are present in the conceptualized three-reactor process described later in which SO_2 regeneration of the iron component of the sorbent **is** followed by O_2 regeneration of the zinc component using a single recirculation loop of regeneration gas consisting mainly of SO_2.

50-Cycle Bench-Scale Testing

One highly attrition-resistant formulation was selected for a long-duration, 50-cycle test. Table 1 shows the conditions used for that test.

In the HTHP testing, the candidate sorbent demonstrated H_2S removal down to the 50 to 100 ppm levels with stable desulfurization activity over the duration. Attrition resistance of the sorbent is excellent. Other characterizations show a small loss of surface area and pore volume after 50 cycles of testing.

In the 50-cycle test campaign, considerable effort was expended to verify the degree of SO_2 regeneration to elemental sulfur that actually occurred. The amount of sorbent regeneration occurring during the SO_2 regeneration portion of the cycles was typically determined by mass in balance based on gas analyses during the sulfidation step and the air-regeneration step. The amount of sulfur loaded on the sorbent in each cycle was calculated by integrating the metered gas flows of H_2S into the reactor, minus the outlet concentration as determined by gas

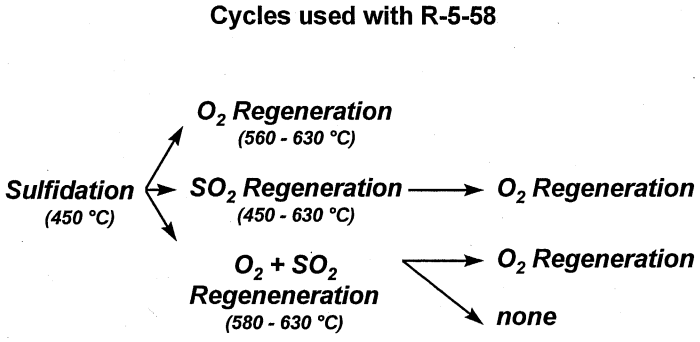

Figure 1. 50-cycle bench-scale test.

Table 1. 50-Cycle Test Conditions

Pressure:	20 atm	Coal gas composition (vol%)	
Flow rate:	36 slpm	CO:	15
Sorbent amount:	250 g	H_2:	10
Temperature (°C)		N_2:	55
Sulfidation:	450	CO_2:	10
SO_2 regeneration:	450–630	H_2O:	10
Dilute air regeneration:	560–630	H_2S	3,000 ppm
SO_2 regeneration gas (vol%)		Oxidizing gas (vol%)	
SO_2	25–75	O_2	2
N_2	balance	N_2	98

chromatography and continuous H_2S analyzer. During SO_2 regeneration, no reliable gas analysis was possible, due to the high concentration of SO_2. During O_2 (dilute air) regeneration, the evolved SO_2 was metered using a continuous analyzer, giving a measure of the amount of absorbed sulfur from the sulfidation step that was not regenerated by the SO_2. The difference (after discounting any obvious experimental error) represents the production of elemental sulfur.

The weight of elemental sulfur recovered in a downstream trap confirmed the degree of SO_2 regeneration. In the earlier experiments, elemental sulfur was produced, but no material balance was obtained probably because of poor collection efficiency. With some redesign of the outlet piping and a sulfur trap design, more reliable sulfur recovery was obtained for the later runs in the 50-cycle test.

Process Conceptualization and Simulation

A three-reactor, fluidized-bed HGD process involving sulfidation (absorption), SO_2 regeneration, and O_2/SO_2 regeneration was conceptualized for direct elemental sulfur production (see Figure 2). In this Advanced Hot Gas Desulfurization (AdvHGD) process, the two stages of regeneration could likely be contained in a single reactor vessel. The desulfurization of the coal gas (sulfidation of the sorbent) takes place at about 450 °C at the pressure of the coal gas (typically 20 atm). The sulfided sorbent is heated to 600 °C using waste heat from the regenerated sorbent and enters Stage 2 of the regenerator to contact the recirculating SO_2 gas stream. The elemental sulfur formed exits in the gaseous state. The partially regenerated sorbent then passes into Stage 1 of the regenerator where oxygen will be added to the regeneration gas. In a fully heat-integrated process, the energy from the exothermic O_2 regeneration will be used to drive the endothermic SO_2 regeneration. The regenerated sorbent is then cooled and recirculated to the desulfurization reactor.

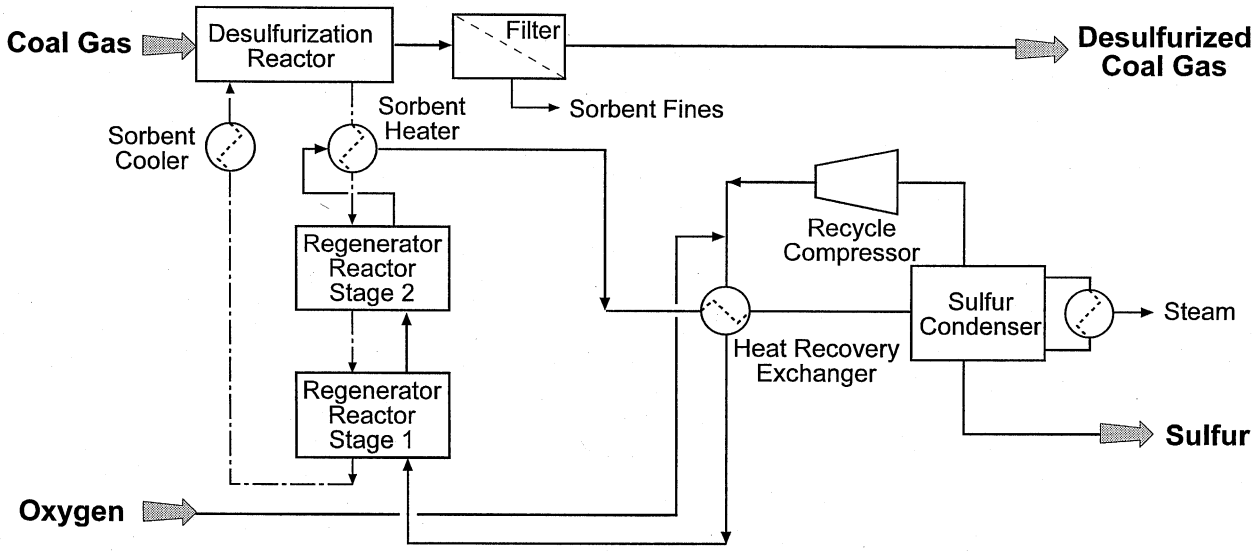

Figure 2. Advanced hot gas desulfurization.

The recirculation loop for the regeneration gas functions as follows: the regeneration off-gas exiting from Stage 2 is cooled to condense out the sulfur, which is removed as a molten product. The exit gas from the sulfur condenser is then compressed slightly (to recover the pressure drop losses from recirculation) and is reheated by countercurrent exchange with the hot regeneration off-gas. With control of the ratio of iron and zinc in the sorbent, and by balancing the amount of oxygen supplied to Stage 1 with the amount of elemental sulfur that is actually being produced, the SO_2 material balance of the recirculation loop can be maintained. For startup purposes, an external supply of liquid SO_2 is required to charge the recirculation loop.

Because of the need for transfer of sorbent from the sulfidation reactor to the multistage regenerator, fluidized-bed reactors are envisioned. However, a detailed configuration has not been proposed. Heat transfer from fluidized-bed reactors is also expected to be more straightforward than with fixed beds. The recirculation rate of the SO_2 stream is fixed by the gas velocity needed in the regeneration reactors for proper fluidization of the sorbent. However, the production of sulfur is a function of the sorbent circulation rate and is thus somewhat independent of the regeneration gas flow rate. It should be noted that the concentration of the elemental sulfur in the regeneration loop is dependent on the engineering design of the system; it is not inherent to the chemistry of the regeneration process.

For comparison, Figure 3 presents an HGD process based on using the DSRP to produce elemental sulfur. The sulfidation takes place at about 600 °C and at the pressure of the coal gas (20 atm). The sulfided sorbent passes to the regenerator where it is contacted with preheated, compressed air. The off-gas from the regenerator (ROG), containing approximately 14 vol% SO_2, is the feed to the DSRP reactor. In this reactor, the ROG is contacted with a slipstream of the coal gas to produce a gas stream containing mostly nitrogen plus elemental sulfur. The DSRP reactor

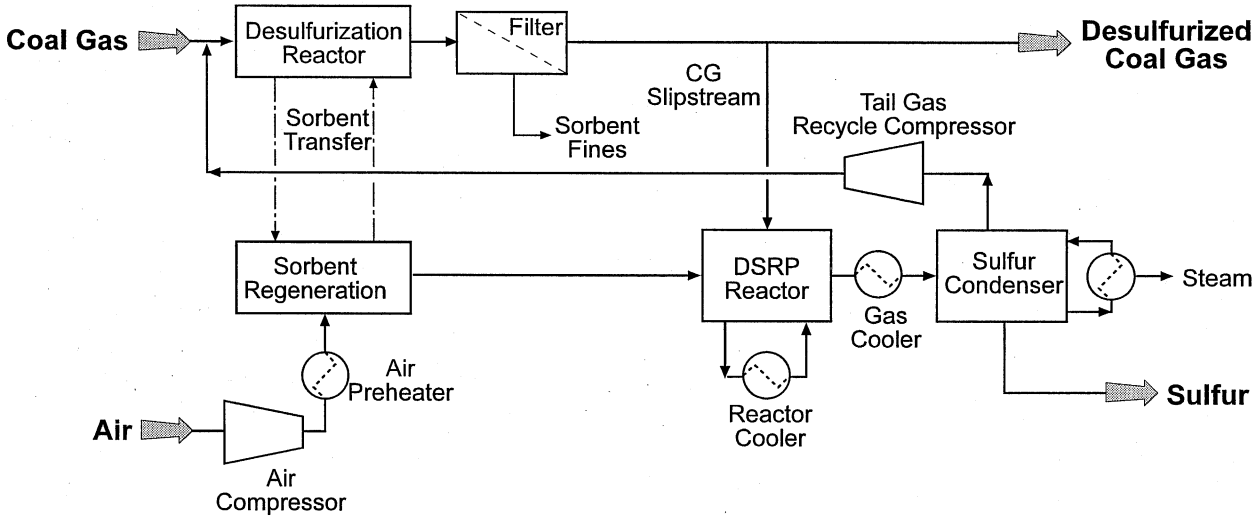

Figure 3. Hot-gas desulfurization with DSRP.

effluent is then cooled to recover the sensible heat, and the sulfur is condensed while producing low-pressure steam. The gas stream from the condenser, DSRP tail gas, contains some sulfur compounds (H_2S and SO_2). Most likely it cannot be discharged, so in this process conceptualization, the tail gas is recompressed slightly and recycled to the desulfurizer. An economic analysis comparing the conceptualized AdvHGD process with this conceptualized DSRP-based scheme is under way.

Results/Accomplishments

Experimental

In the HTHP testing, sorbent R-5-58 demonstrated H_2S removal down to the 50 to 100 ppm levels with stable desulfurization activity over the duration. Figure 4 shows the sulfidation breakthrough curves for selected cycles covering the full test period. Interestingly, the sulfidation performance, as measured by time to breakthrough, improved considerably after the first few cycles. Figure 5 plots the steady-state concentration of H_2S in the sulfidation reactor outlet. One can see that in several cycles the concentration was <50 ppm and that, in general, the concentration was 100 ppm or better. However, a successful commercial embodiment would require consistent removal of H_2S to 20 ppm or less. Additional sorbent development is required to achieve this level of performance while maintaining the ability to be regenerated with SO_2.

Based on the gas analysis "difference" methodology described above, the SO_2 regeneration step accounted for as much as 55 to 70 percent of the total regeneration of the sorbent. This compares to a theoretical limit of approximately 80 percent, assuming complete regeneration by SO_2 of the iron component. Many of the cycles had lower percent regeneration because the test conditions were intentionally set at nonoptimal levels.

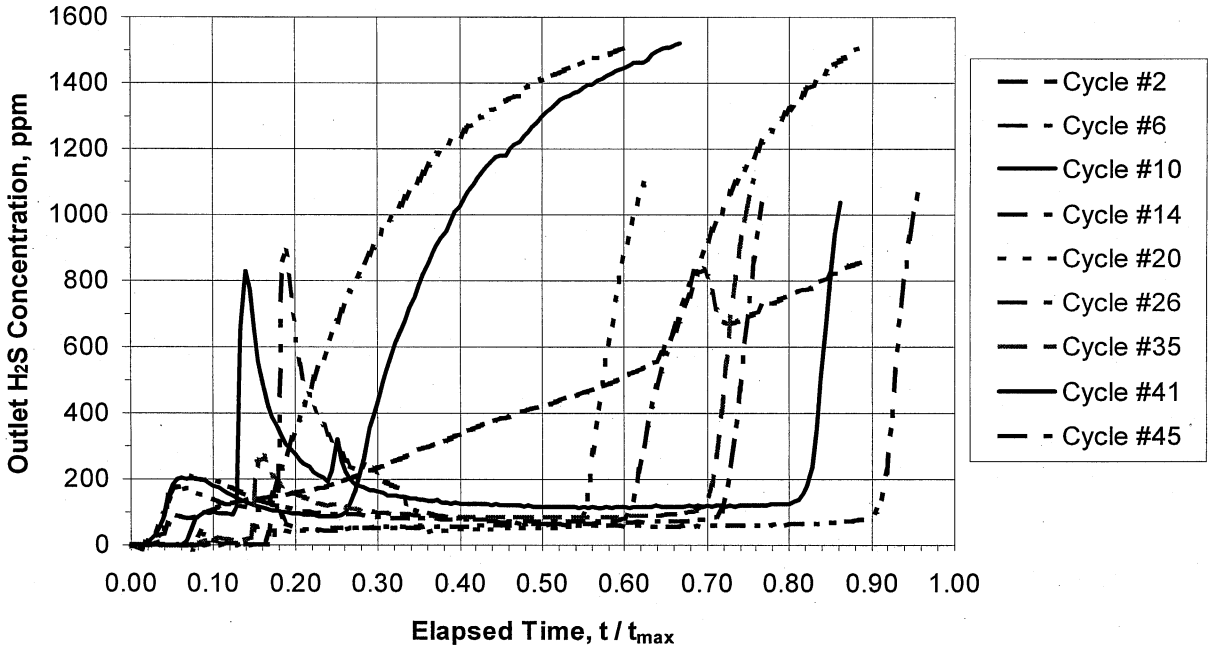

Figure 4. Sulfidation breakthrough curves.

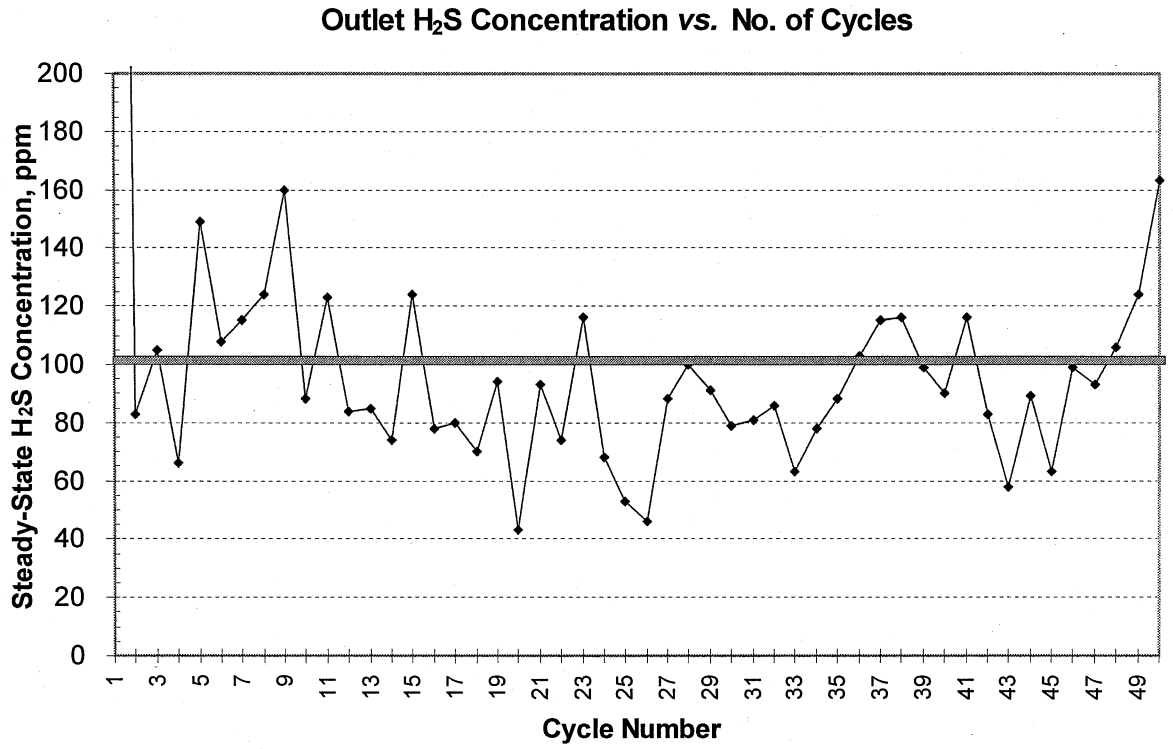

Figure 5. Sulfidation activity—sorbent R-5-58.

Reasonable sulfur balances were obtained by comparing the gas compositions and flow rates with the solid sulfur recovered. Figure 6 shows the total regeneration of the sorbent (SO_2 regeneration calculated by sulfur recovery, and O_2 regeneration calculated by gas analysis) for those cycles for which complete data are available. In most cases, the resulting value is approximately 100 percent of the sulfur that was loaded, confirming that the experimental protocol is yielding a sulfur balance.

In addition to durability testing of the sorbent, one main objective of the 50-cycle test program was to determine the effects of three primary variables: SO_2 concentration in the regeneration gas, temperature of the regeneration gas, and duration of the SO_2-regeneration half-cycle. Statistical analysis was applied to the results to generate an empirical second-order polynomial fit. The statistical model shows that duration of regeneration is the most important variable, percent regeneration is directly proportional to temperature, and SO_2 concentration has a small effect. Figure 7 shows a plot of the calculated percent regeneration (model values) as a function of duration for one SO_2 concentration value. The actual data points are also shown for comparison. Because an empirical model based on a small data set was used, there are obvious limitations to its application. However, the model is useful for guiding thinking on the process simulation and economic analysis.

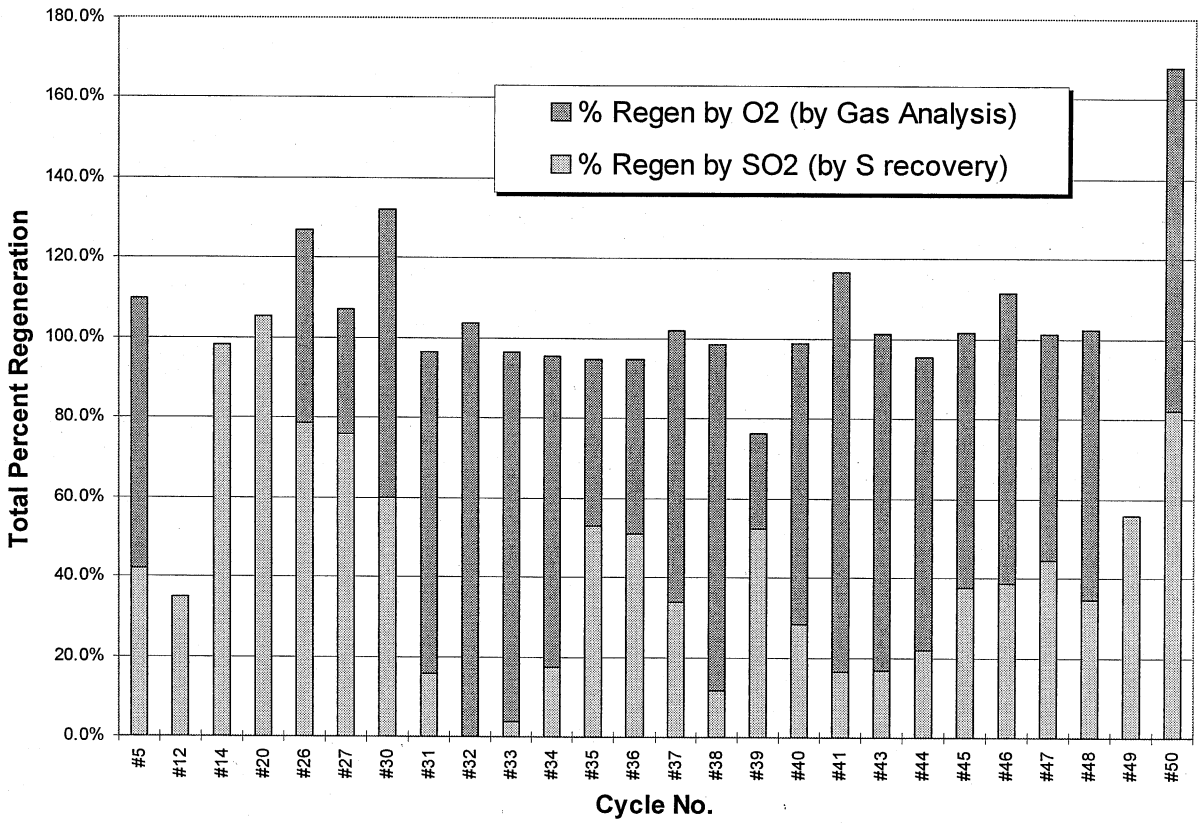

Figure 6. Sulfur balance.

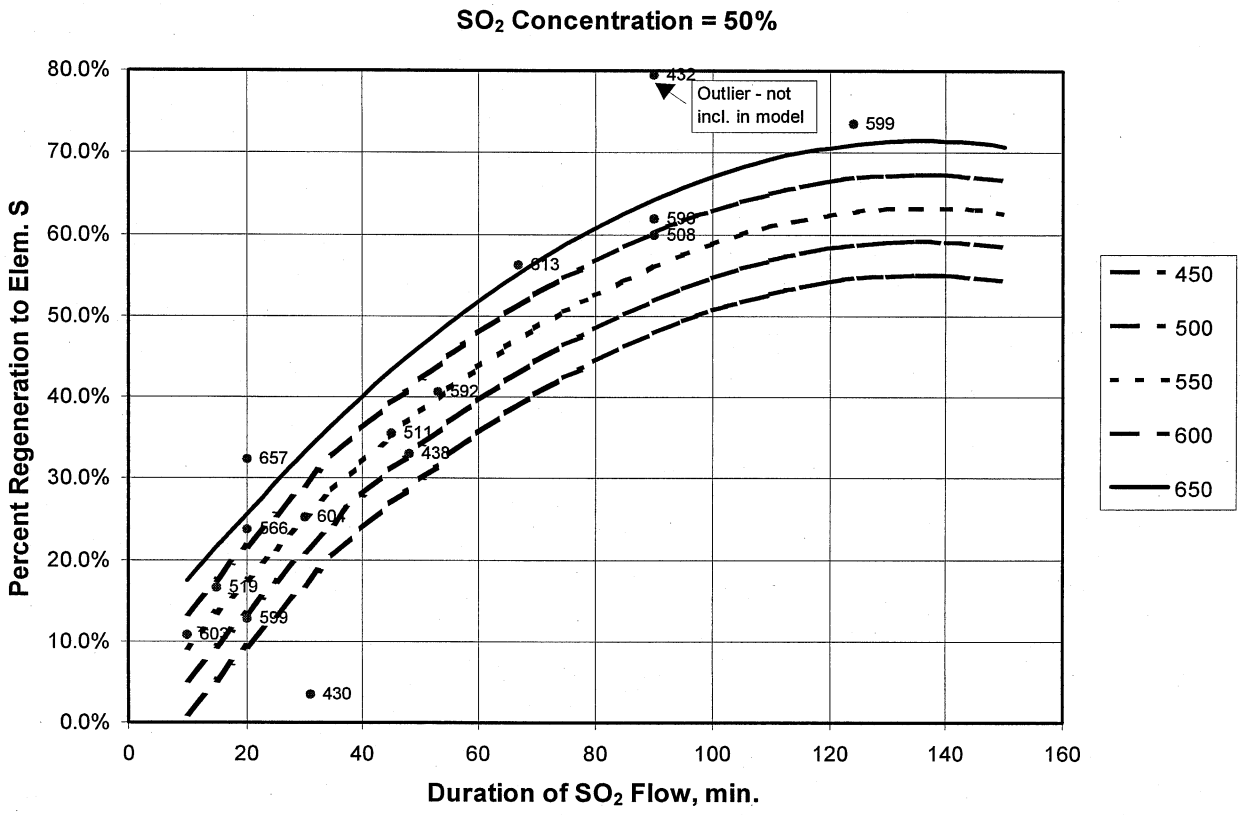

Figure 7. Statistical model of R-5-58 regeneration.

Characterization tests were run on the sorbent before and after the 50-cycle test run; Table 2 reports the results. The attrition losses were very low, as expected for this highly attrition-resistant formulation; the values are comparable to those for fluid catalytic cracking (FCC) catalysts. There was little change in the BET surface area and mercury pore volume measurements, attesting to the relative ruggedness of the candidate sorbent.

Table 2. Characterization of Sorbent R-5-58

	Fresh (%)	50-Cycle used (%)
BET surface area (m^2/g)	100	94
Hg pore volume (mL/g)	100	89
Attrition test:		
5-h loss	3.6	1.2
20-h loss	6.8	5.0

Process Simulation/Economic Analysis

The nominal plant size of 250 MW_e (net) was chosen as the design basis for the process simulations (material and energy balances) that are being conducted using the ASPEN PLUS software. Table 3 lists the flow rate, composition, and conditions of the clean coal gas exiting the simulations of both processes; the basis is an O_2-blown gasifier. One advantage of the ASPEN PLUS simulation software is the large built-in physical property database. The heat capacities, heats of reaction, reaction equilibrium based on Gibbs free energy minimization, and vapor-liquid equilibrium data based on Peng-Robinson

equation-of-state allowed for accurate accounting of the heat effects and phase changes. Selection of appropriate tear streams and convergence criteria resulted in consistently converged material and energy balances for a given set of conditions.

Table 3. Clean Coal Gas

Composition (vol %)	
H_2	27
CO	35.5
CO_2	12.5
H_2O	19
N_2	6
H_2S	20 ppm
Flow rate (lb/h)	450,000
Pressure (psia)	275
Temperature (°C)	460

The AdvHGD process scheme schematically shown in Figure 2 was modeled by the flow sheet simulator using appropriate fluidized-bed reactors, gas/solid phase separators, sulfur condenser, and heat exchanger blocks. The assumptions involved in the AdvHGD simulation have been described above. Pure O_2 is assumed to be available for adding to the recycle SO_2 stream to balance the sulfur being removed continuously as a liquid product. The simulation used the reactions presented above in the Approach section. The simulation further assumed that the consumption of SO_2 in Stage 2 was balanced by that produced in the air regeneration stage with no net generation of SO_2 within the system. As Figure 2 indicates, heat is released during desulfurization, cooling of the hot regenerated sorbent, and sulfur condensation. This available heat is assumed to produce high pressure (850 psig) steam from the high-temperature sources, and low-pressure steam from the sulfur condenser. In addition, the heat content of the regenerator off-gas is used to preheat the sulfided sorbent and the SO_2 recycle stream for in-plant heat integration.

The DSRP-based HGD simulated by ASPEN PLUS is shown schematically in Figure 3. The simulation assumed a fluidized-bed desulfurizer with zinc-based sorbent, fluidized-bed/transport reactor for air regeneration, and a fluidized-bed/transport reactor for DSRP reaction. A small slipstream of clean coal gas is used in the DSRP reactor for direct conversion of SO_2 to sulfur. This slipstream can essentially be viewed as a penalty experienced by the DSRP approach when compared with the AdvHGD scheme. Consequently, the DSRP releases considerably more heat in the air regenerator, DSRP reactor, and condenser units. The ASPEN simulation again assumed that this heat would be used to produce high-pressure stream (and low-pressure steam from the sulfur condenser). In addition, gas-gas heat exchangers are employed for in-plant heat integration similar to the AdvHGD simulation.

A preliminary comparison of the two process schemes, based on the ASPEN PLUS simulations, suggests the following: The DSRP uses approximately 2.2 percent more raw coal gas (about 10,000 lb/h) to produce an equivalent amount of clean fuel gas. As a consequence, the DSRP route releases about 27 million Btu/h more heat (potentially as high-pressure steam) than the AdvHGD route. The clean fuel gas from the AdvHGD route is more concentrated because it is not diluted with nitrogen from the air regeneration, but the process heat integration is more complicated with the AdvHGD route.

Application/Benefits

An AdvHGD process, such as that conceptualized in Figure 2, that results in the direct production of elemental sulfur during regeneration has potential advantages over existing process options if it can be economically integrated with IGCC. The existing process options are production of undesirable calcium waste, production of sulfuric acid, or production of elemental sulfur using DSRP. Production of sulfuric acid is attractive if a market is readily available nearby. It may be difficult to find several such sites for IGCC plants. Elemental sulfur is the preferred option, and DSRP is a highly efficient process but, as discussed earlier, requires the use of a small portion of the coal gas that results in an energy penalty to the power plant. Application of a reactive and attrition-resistant sorbent such as R-5-58 to an IGCC with the capability to undergo direct SO_2 regeneration to elemental sulfur is a process option that needs to be developed further.

Future Activities

The simulation work will continue; the converged heat and mass balances by ASPEN PLUS will provide the input to the planned economic analysis: preliminary equipment sizing, preliminary capital costs, and operating cost comparisons.

Additional sorbent modification and testing to demonstrate H_2S control to under 20 ppmv in the AdvHGD process is planned for FY97-98. Bench-scale testing with actual coal gas using the RTI/FETC Mobile Laboratory at the Power Systems Development Facility (PSDF) is planned for FY98-99.

Acknowledgments

This research is sponsored by the U.S. Department of Energy's Federal Energy Technology Center, under Contract No. DE-AC21-94MC31258 with Research Triangle Institute (fax: 919-541-8000). The authors gratefully acknowledge the guidance of the FETC Contracting Officer's Representative, Mr. Thomas P. Dorchak. United Catalysts, Inc. assisted with preparation of iron- and zinc-based sorbents. Mr. Steven C. Kozup, a graduate student at North Carolina State University working under the supervision of Dr. George Roberts on a subcontract with RTI, prepared the ASPEN PLUS process simulations. Texaco is following this project's progress and will review the simulation and economic evaluation. The contract period of performance is from March 21, 1994, to September 30, 1999.

References

Dorchak, T.P., S.K. Gangwal, and W.J. McMichael. 1991. "The Direct Sulfur Recovery Process." *Environmental Progress* 10(2):68.

Gangwal, S.K., B.S. Turk, and R.Gupta. 1995. "Advanced Sulfur Control Concepts." In *Proceedings of the Advanced Coal-Fired Power Systems '95 Review Meeting*, pp. 622-630, DOE/METC-95/1018, Vol. 2, NTIS/DE 95009733. Springfield, VA.

Gangwal, S.K., J.W. Portzer, B.S. Turk, and R.Gupta. 1996. "Advanced Sulfur Control Processing." In *Proceedings of the Advanced Coal-Fired Systems Review Meeting July 16–19, 1996.* (CD-ROM). U.S. Department of Energy, Morgantown, WV.

Portzer, J.W., and S.K. Gangwal. 1995. "Slipstream Testing of Hot Gas Desulfurization with Sulfur Recovery." In *Proceedings of the Advanced Coal-Fired Power Systems '95 Review Meeting*, pp. 220-228. DOE/METC-95/1018, Vol. 1, NTIS/DE 95009732. Springfield, VA.

Portzer, J.W., B.S. Turk, and S.K. Gangwal. 1996. "Durability Testing of the Direct Sulfur Recovery Process." In *Proceedings of the Advanced Coal-Fired Power Systems Review Meeting July 16–18, 1996*. (CD-ROM). U.S. Department of Energy. Morgantown, WV.

APPENDIX D Advanced Hot Gas Desulfurization Process with Sulfur Recovery: Proceedings of the International Symposium on "Gas Cleaning at High Temperatures", University of Karlsruhe, 1999

Advanced Hot Gas Desulfurization Process with Sulfur Recovery

S.K. Gangwal[1], J.W. Portzer[1], T.P. Dorchak[2], and K. Jothimurugesan[3]

[1]Research Triangle Institute, Research Triangle Park, NC 27709, USA
[2]Department of Energy, Federal Energy Technology Center,
Morgantown, WV 26505, USA
[3]Department of Chemical Engineering, Hampton University,
Hampton, VA 23668, USA

Abstract

Advanced integrated gasification combined cycle (IGCC) power plants employ a hot-gas desulfurization (HGD) process, typically involving a zinc oxide-based sorbent that efficiently removes H_2S from coal gas down to less than 20 ppmv and that can be regenerated using air for multicycle operation. However, an inherent complication in this air-regeneration-based HGD process is the disposal of the problematic dilute SO_2 containing regeneration tail gas. Some H_2S sorbents based on metal oxides other than zinc oxide, such as iron oxide, can be regenerated using SO_2 to produce a desirable elemental sulfur byproduct via the direct reaction of FeS and SO_2 ($2FeS + SO_2 - 2FeO + 3/2\ S_2$). The objective of this study is to develop an advanced hot-gas process (AHGP) that can eliminate the problematic SO_2 tail gas and yield elemental sulfur directly using a sorbent containing a combination of zinc and iron oxides. AHGP uses a two-stage regeneration reactor in which the sulfided sorbent flows down countercurrent to a regenerating gas containing a dilute mixture of O_2 in SO_2. The iron sulfide portion of the sorbent is regenerated by SO_2 in the upper stage whereas the zinc sulfide portion of the sorbent is regenerated using O_2 in the lower stage. The effluent SO_2 and S_2 mixture is cooled to condense elemental sulfur, and the SO_2 is recycled. Following lab-scale feasibility studies of AHGP, a 50-cycle bench-scale test was conducted at high-temperature, high-pressure conditions to demonstrate quantitative elemental sulfur recovery. A field test of the process is currently planned to take place in late 1999. Further work that will be described focuses on sorbent improvements using metallic additives to the zinc-iron sorbent to produce advanced attrition-resistant sorbents that can consistently reduce the H_2S during sulfidation to less than 20 ppmv.

Key words: IGCC, desulfurization, zinc oxide, iron oxide, sorbent, regeneration, sulfur

1. Introduction

Hot-gas desulfurization (HGD) of coal gas in IGCC power systems has received a great deal of attention over the past two decades due to the potential for high thermal efficiency (up to 47%) and low environmental impact of these advanced power systems. Research on HGD methods for coal gas in IGCC systems has concentrated on the use of regenerable metal oxide sorbents (Gangwal, 1991, 1996; Harrison, 1995; Jalan, 1985; Thambimuthu, 1993). This research and development effort has been spearheaded by Department of Energy's (DOE) Federal Energy Technology Center (FETC) and its predecessor agencies since 1975.

The HGD process typically uses a regenerable zinc-oxide-based sorbent and is carried out in a two-reactor system consisting of a desulfurizer and an air regenerator:

$$ZnO + H_2S \rightarrow ZnS + H_2O \qquad \text{(desulfurizer)}$$
$$ZnS + (3/2)\, O_2 \rightarrow ZnO + SO_2\,. \qquad \text{(regenerator)}$$

Early developments emphasized fixed bed reactors for HGD. The highly exothermic regeneration led to a move away from fixed beds toward moving beds (Ayala et al., 1995; Cook et al., 1992) and fluidized beds (Gupta and Gangwal, 1992). Fluidized-bed HGD systems are receiving a lot of emphasis due to several potential advantages over fixed- and moving-bed reactors, including excellent gas-solid contact, fast kinetics, pneumatic transport, ability to handle particles in gas, and ability to control the highly exothermic regeneration process. However, an attrition-resistant sorbent that can withstand stresses induced by fluidization, transport, chemical transformation, and rapid temperature swings must be developed.

Air regeneration leads to a problematic SO_2 tail gas that must be disposed. Converting to a salable product—sulfuric acid or elemental sulfur—is an attractive option. Elemental sulfur is particularly attractive because it is the smallest volume sulfur product and because it can be stored easily, transported over long distances, readily disposed, or sold. DSRP, a promising process, is currently in an advanced development stage to treat the SO_2 tail gas (Portzer et al., 1996, 1997). In this process the SO_2 is catalytically reduced to elemental sulfur at the pressure and temperature condition of the tail gas using a slipstream of the fuel gas

$$SO_2 + 2\, H_2 \text{ (or CO)} \rightarrow 1/2\, S_2 + 2\, H_2O \text{ (or } 2\, CO_2)$$

The process has undergone testing with actual coal gas from a gasifier and is being scaled up to a small pilot-scale stage.

The problematic SO_2 tail gas produced by air regeneration not only needs disposal but also consumes 2 mol of valuable reducing components in fuel gas for every mole of sulfur dioxide treated if elemental sulfur is to be produced using DSRP. Novel regeneration processes that could lead to elemental sulfur with limited use of fuel gas are being developed (Gangwal et al., 1996; Harrison et al., 1996). KEMA's hot-gas cleanup process (Meijer et al., 1996) uses a proprietary fluidized-bed sorbent that can remove H_2S to below 20 ppmv and can be regenerated using SO_2, O_2 mixtures to directly produce elemental sulfur. Along similar lines as above, RTI is developing an advanced HGD process (AHGP) that uses a zinc-iron sorbent (Portzer et al., 1997).

2. AHGP Process Concept

AHGP is a second-generation HGD process that regenerates the sulfided sorbent directly to elemental sulfur using SO_2. SO_2 regeneration involves the reaction of nearly pure SO_2 with sulfided sorbent at elevated temperature and pressure. Under these conditions, elemental sulfur is the only product predicted from thermodynamics. Some H_2S sorbents based on metal oxides other than zinc oxide—iron oxide, for example—can be regenerated following sulfidation using SO_2 to directly produce the desirable elemental sulfur byproduct according to the following sulfidation and regeneration reactions:

$$FeO + H_2S \rightarrow FeS + H_2O$$
$$2FeS + SO_2 \rightarrow 2FeO + 3/2\ S_2$$

Based on a theoretical evaluation of a number of potential sorbent candidates, iron- and zinc-based regenerable sorbents were chosen for experimental evaluation (Gangwal et al., 1995). Iron oxide was considered the most promising candidate based on a combination of factors—desulfurization efficiency, SO_2 regenerability, cost, and knowledge base. Zinc oxide is a leading candidate due to its excellent desulfurization efficiency, its extensive knowledge base, and its low cost. Although zinc sulfide (ZnS) shows essentially no SO_2 regenerability at temperatures of interest, zinc oxide can act as a polishing agent when combined with iron oxide to remove H_2S down to very low levels. Advantageously, the ZnS can be regenerated using air to produce the SO_2 needed for regeneration of the iron sulfide (FeS).

3. AHGP Process Description

Based on a feasibility study, initial laboratory testing, and successful bench-scale testing of several sorbent formulations, AHGP was conceptualized as shown in Figure 1. The primary elements of the process are a single

desulfurization reaction stage, but two stages of regeneration: an SO_2 regeneration stage, and an oxygen regeneration stage. The sulfided sorbent flows countercurrently to an internally recirculating regeneration gas (high concentration SO_2). The desulfurization of the coal gas (sulfidation of the sorbent) takes place at about 450°C at the pressure of the coal gas (typically 2.0 MPa) in the desulfurization reactor. This would most likely be a "transport" type fluidized-bed reactor, resulting in a research focus on attrition-resistant sorbents.

The sulfided sorbent enters a multistage reaction vessel to be heated to 600°C using waste heat from the regenerated sorbent. This reactor is envisioned to be a bubbling-type fluidized bed. The heated sorbent passes to Stage 2 of the regenerator to contact the recirculating SO_2 gas stream. The elemental sulfur formed exits in the gaseous state. The partially regenerated sorbent then passes into Stage 1 (the lowest stage) of the regenerator, where oxygen is added to the regeneration gas. In this heat-integrated process, the energy from the exothermic O_2 regeneration is used to drive the endothermic SO_2 regeneration. The regenerated sorbent is then cooled and recirculated to the desulfurization reactor.

The regeneration off-gas exiting from Stage 2 is cooled to condense out the sulfur, which is removed as a molten product. The exit gas from the sulfur condenser is then compressed slightly (to recover the pressure drop losses from recirculation) and is reheated by countercurrent exchange with the hot regeneration off-gas. With control of the ratio of iron and zinc in the sorbent, and by balancing the amount of oxygen supplied to Stage 1 with the amount of elemental sulfur that is actually being produced, the SO_2 material balance of the recirculation loop can be maintained. For startup purposes, an external supply of liquid SO_2 could be used to charge the recirculation loop.

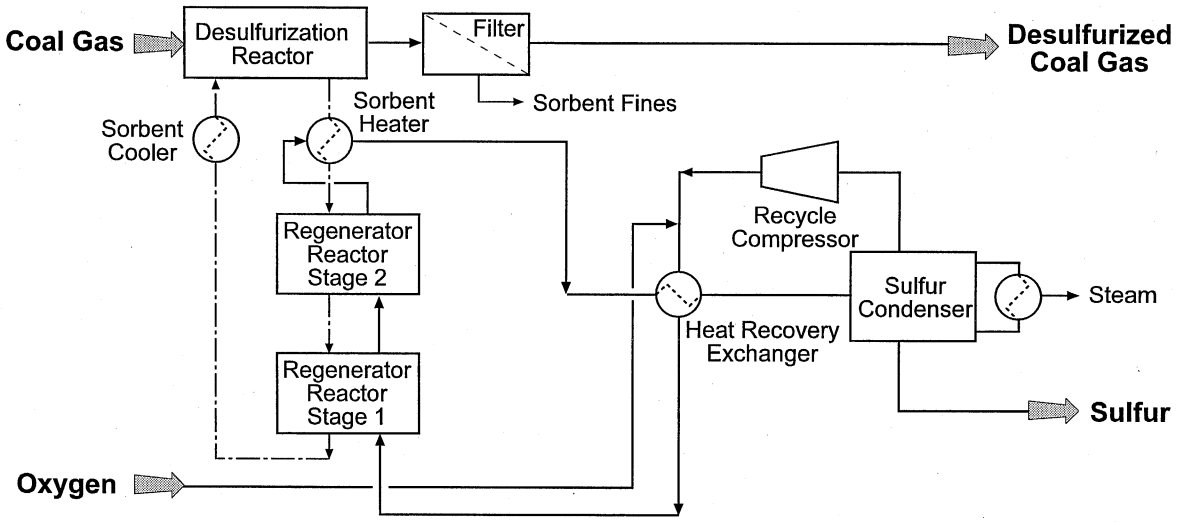

Figure 1. Conceptualized advanced hot-gas process (AHGP).

4. Experimental

a. Lab-scale feasibility studies

Laboratory experiments to test the SO_2 regeneration concept were carried out using a high-pressure thermogravimetric analyzer (TGA) and a high-pressure lab-scale reactor (Gangwal, et al., 1995). The reactor was made of a 1.25-cm stainless steel tube capable of operation at 750°C and 1.5 MPa. Provision was made for sulfiding up to 10 g of sorbent with simulated coal gas and regenerating the sulfided sorbent with up to 15 vol% SO_2. The gas exiting the reactor passed through heated tubing into a 130°C convective oven where a 0.1-m filter was used to collect sulfur. The gas vented through a back pressure regulator.

b. Bench-scale testing (50-cycle test)

An existing 10-cm diameter, high-temperature, high-pressure (HTHP), bench-scale sorbent test reactor system was modified to enable SO_2 regeneration plus elemental sulfur recovery (Figure 2). The reactor could operate in either the fluidized-bed or fixed-bed mode using an internal sorbent cage of up to 7.5 cm inside diameter. The reactor vessel was rated for operation at temperatures up to 800°C and pressures up to 3.0 MPa.

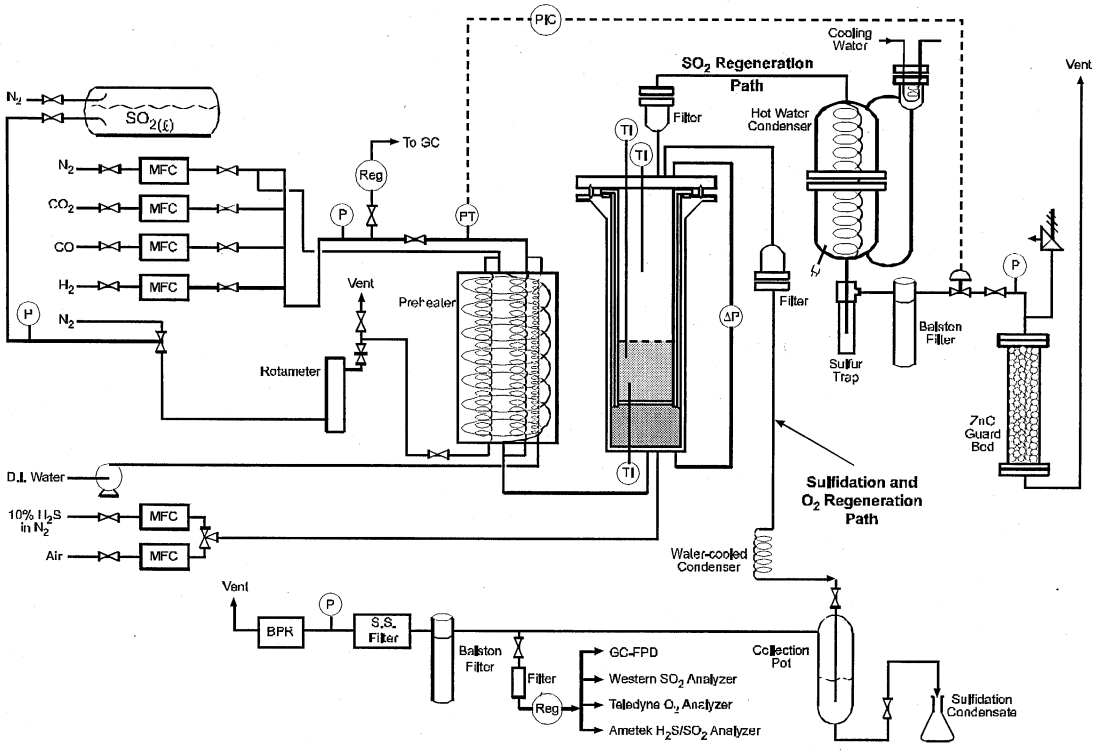

Figure 2. Bench-scale sorbent test facility.

Reactor throughput up to 24 Nm^3/h can be processed, and sorbent volumes up to 1,000 cm^3 could be tested.

The bench-scale test unit was used for screening tests (10 cycles or less) of several fluidized-bed sorbents (Gangwal et al.,1996) and for a long duration test (50 cycles; Portzer et al., 1997) of one highly attrition-resistant formulation. For each test cycle (of the 50-cycle test series conducted at 2.0 MPa), sulfidation of the sorbent at 450°C was accomplished using a synthetic coal-gas mixture containing 3,000 ppm of H_2S. For SO_2 regeneration, a metered flow of liquid SO_2 under pressure was fed to the reactor system by displacement of liquid SO_2 from a pressurized supply tank. The liquid SO_2 was vaporized into a heated nitrogen stream (at 450°C to 630°C); concentrations up to 75 vol% were achieved. What is designated as the "oxygen regeneration" step was in actuality dilute-air regeneration, and was accomplished by introducing a small air stream into the hot reactor through which was flowing a preheated nitrogen stream.

The SO_2 regeneration was conducted through a hot exit line with a sulfur condenser, catch pot, and a heated back pressure control valve. Sulfidation and air regeneration were conducted through a separate exit line. Reactor outlet gas samples were analyzed continuously for H_2S during sulfidation and for SO_2 during air regeneration using continuous analyzers. Oxygen concentration during the O_2 regeneration was measured continuously. H_2S, COS, and SO_2 were measured intermittently during sulfidation using a gas chromatograph with a flame photometric detector.

A major goal of the bench-scale experiments, in which gram quantities of elemental sulfur could be recovered, was to achieve a sulfur mass balance. With the instrumentation described above, it was possible to compare the amount of physically recovered elemental sulfur with a value calculated on the basis of the gas analyses.

c. Sorbent improvement studies

Sorbent improvement studies were undertaken to enable consistent reduction of H_2S to less than 20 ppmv during sulfidation. These studies followed two avenues: the replacement of zinc with molybdenum, and the use of other proprietary metals and stabilizers as an addition to the iron-zinc formulation. Other researchers have reported success with SO_2 regeneration using sorbents containing molybdenum (deWild et al., 1996). Therefore, several small batches of sorbent containing iron and molybdenum on γ-alumina were prepared and tested (one cycle each of sulfidation) in a fixed-bed lab-scale reactor at 450°C and 0.1 MPa. A large batch of the most active of the three

was prepared and tested in the bubbling fluid-bed bench-scale unit for eight cycles.

The second avenue of sorbent improvement research involved preparing small batches of the attrition-resistant zinc-iron formulation with the addition of other metal species, with stabilizer additives, and at varying calcination temperatures. The details of this experimental program are proprietary, at this time, pending potential patent activity. Multiple cycle screening tests were conducted in a 1-cm diameter microreactor at 0.1 MPa pressure and 480°C for sulfidation, and 630°C for dilute-air regeneration.

Two variations of the best-performing material from this second line of research were prepared in larger quantities and were tested in a 1-cm diameter lab-scale reactor at 0.1 MPa for six cycles (sulfidation at 480°C and dilute-air regeneration at 630°C). The better of the two was selected for multicycle testing including SO_2 regeneration at 0.1 MPa with 10% SO_2 in nitrogen.

d. Field test plans

Associated with a related process development project, RTI (with DOE support) outfitted a modified office trailer as a Mobile Laboratory (Portzer and Gangwal, 1998). The 3.65 m by 15.25 m trailer is divided into a control room/analytical lab and an equipment room that houses a bench-scale AHGP test unit that is essentially a duplicate of the one described above. The concept is to conduct long duration testing of candidate sorbents using a slip stream of actual coal gas by moving the Mobile Laboratory to the site of an operating gasifier. The immediate plan is to relocate the lab trailer to Wilsonville, Alabama, the site of DOE/FETC's Power Systems Development Facility (PSDF) for testing to be conducted in the late 1999, early 2000 time frame.

5. Results and Discussion

a. Feasibility studies

A number of proprietary sorbents based on iron and zinc oxides were prepared and tested for SO_2 regeneration. They were compared with benchmark zinc titanate and zinc ferrite sorbents developed for fluidized-bed desulfurization with air regeneration as part of a previous project with the DOE. The sulfided sorbent that was based purely on ZnO as the active sorbent showed essentially no rengeration with 3.3% SO_2 in N_2 at up to 800°C and 1.0 MPa. However, sulfided iron- and zinc-based sorbents showed good regeneration with SO_2. TGA rates of SO_2 regeneration ranged

from 1.3 x 10^{-2} to 3.6 x 10^{-2} g sulfur/g sorbent/h with 3.3 vol% SO_2 at 700°C and 1.0 MPa.

A zinc-iron sorbent designated R-5 showed promising results and was tested further using the high-pressure lab-scale reactor. Atmospheric TGA analysis showed that the zinc portion of the sorbent was not regenerated, but the iron portion of the sorbent regenerated at a rate of 1.2 x 10^{-2} g sulfur/g sorbent/h, similar to the rates achieved with the high-pressure TGA. Solid yellow sulfur was recovered from the experimental apparatus, giving a visual, qualitative confirmation of direct regeneration to elemental sulfur.

The R-5 sorbent was also tested for SO_2 regeneration as a function of SO_2 concentration and for O_2 (dilute air) regeneration. The SO_2 regeneration rate, as measured by the high pressure TGA increased from 1.3 x 10^{-3} to 2.2 x 10^{-2} g sulfur/g sorbent/h at 650°C and 1.0 MPa when SO_2 concentration was increased from 3.3 to 15 vol%. The O_2 regeneration rate at 700°C and 1.0 MPa was about 3 x 10^{-2} g sulfur/g sorbent/h with 2 vol% O_2 in N_2.

The R-5 sorbent recipe was scaled up to kilogram quantities of a fluidizable form. Two different scale-up procedures were tried. One formulation had poor attrition resistance and was immediately rejected. Four others were tested with the HTHP bench-scale apparatus for varying numbers of cycles. Generally, each of the sorbents was able to reduce the outlet H_2S to below 100 ppmv and was regenerable over multiple cycles. Also, measureable (several grams) quantities of elemental sulfur were produced during SO_2 regeneration of each of the sorbents. As much as 60 to 80% of the sulfur absorbed during sulfidation was recovered as elemental sulfur.

However, the materials produced by the first scale-up procedure experienced excessive loss in reactivity with multiple cycles. As well, their attrition, as measured by a three-hole attrition tester (similar to ASTM test method 5757), increased significantly following cyclic testing. On the other hand, the sorbents prepared by the second procedure showed no loss in reactivity over the cyclic operation, and in fact, the reactivity improved with cycling. These sorbents also had very low attrition, comparable to that of fluid catalytic cracking (FCC) catalysts, as measured both before and after cyclic testing. The best material prepared by the second procedure, R-5-58, was selected for a 50-cycle, long duration test.

b. 50-cycle test

In the 50-cycle, HTHP testing, sorbent R-5-58 demonstrated H_2S removal down to the 50 to 100 ppm level with stable desulfurization activity over the

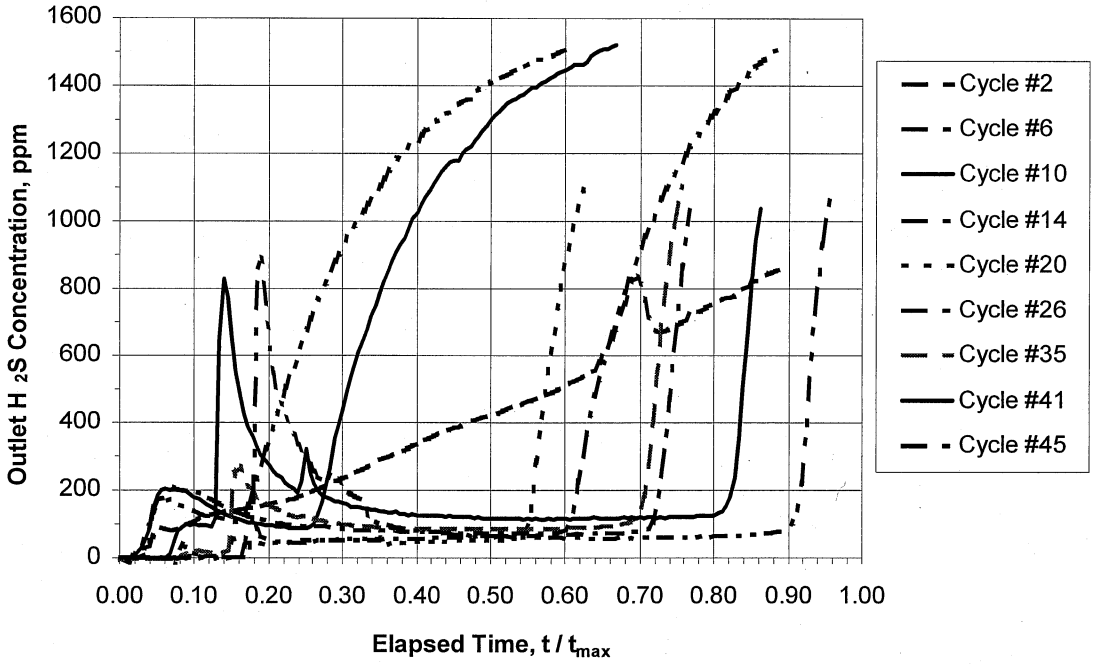

Figure 3. Sulfidation breakthrough curves from 50-cycle test of promising Zn-Fe sorbent.

duration. Figure 3 shows the sulfidation breakthrough curves for selected cycles covering the full test period. Interestingly, the sulfidation performance, as measured by time to breakthrough, improved considerably after the first few cycles.

In several cycles the concentration was less than 50 ppm and in general, the concentration was 100 ppm or lower. However, a successful commercial embodiment would require consistent removal of H_2S to 20 ppm or less. Sorbent improvement studies as described in the next section are being carried out to achieve this level of performance while maintaining the ability to be regenerated with SO_2.

Based on the "gas analysis difference" methodology described in the Experimental section above, the SO_2 regeneration step accounted for as much as 55 to 70% of the total regeneration of the sorbent. This compares to a theoretical limit of approximately 80%, assuming complete regeneration by SO_2 of the iron component. Many of the cycles had lower% regeneration because the test conditions were intentionally set at nonoptimal levels.

The observed rates of SO_2 regeneration in the 50-cycle bench-scale testing ranged from approximately 1.2×10^{-2} to 4.2×10^{-2} g S/g sorbent/h, consistent with the earlier TGA and microreactor studies. There is significant scatter in these data, but it appears that there is only a modest temperture dependency

for this process step. More precise data will be required for optimization of the regeneration reactor design.

The observed rates of the O_2 regeneration cannot be analyzed in detail, since there was an unexpected correlation of rate with cycle number; the later cycles had generally higher rates, apparently independent of operating conditions. The values fell in the range of 1.2×10^{-2} to 1.8×10^{-1} g S/g sorbent/h, much higher than was observed in the small-scale testing.

Figure 4 presents sulfur balance data in the form of a stacked-bar chart for those cycles for which complete data are available. In this chart, the total regeneration is the sum of SO_2 regeneration calculated by sulfur recovery, and O_2 regeneration calculated by gas analysis. In most cases, the resulting value is approximately 100% of the sulfur that was loaded, confirming that the experimental protocol yielded a sulfur balance.

In addition to durability (*i.e.,* multicycle regenerability) testing of the sorbent, another objective of the 50-cycle test program was to determine the effects of three primary variables: SO_2 concentration in the regeneration gas,

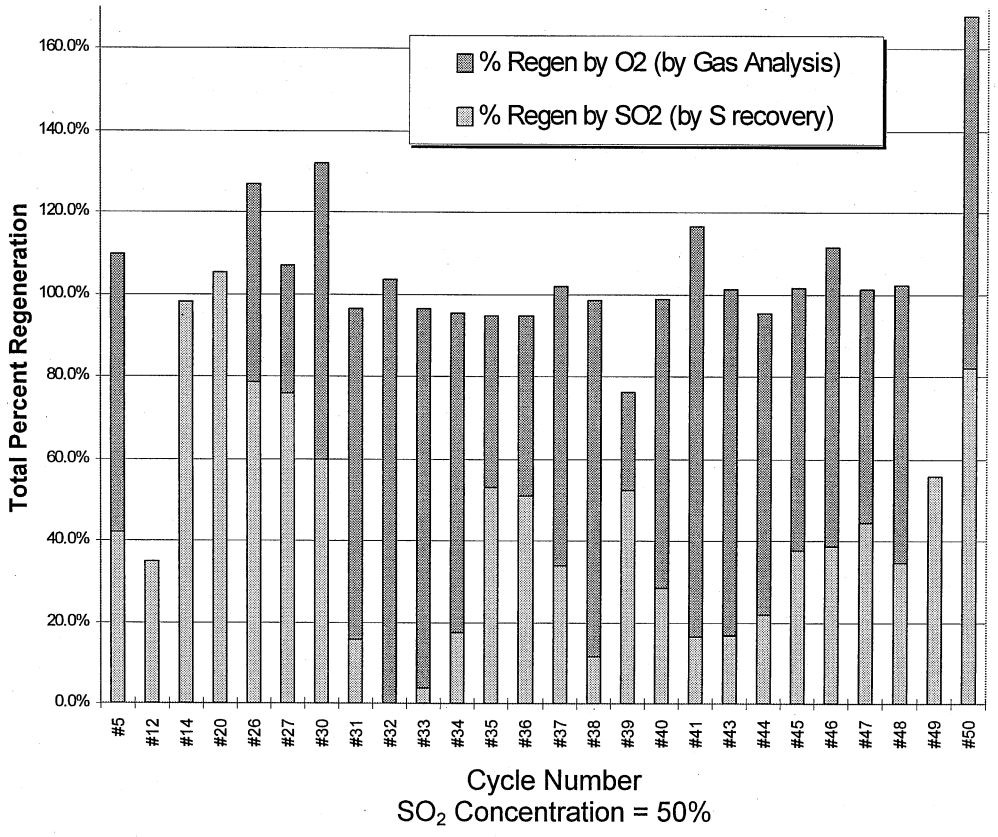

Figure 4. Sulfur balance of the combination of SO_2 and O_2 regeneration.

temperature of the regeneration gas, and duration of the SO_2-regeneration half-cycle. Statistical analysis was applied to the results to generate an empirical second-order polynomial fit. The statistical model shows that duration of regeneration is the most important variable,% regeneration is directly proportional to temperature, and SO_2 concentration has a small effect. Figure 5 shows a plot of the calculated % regeneration (model

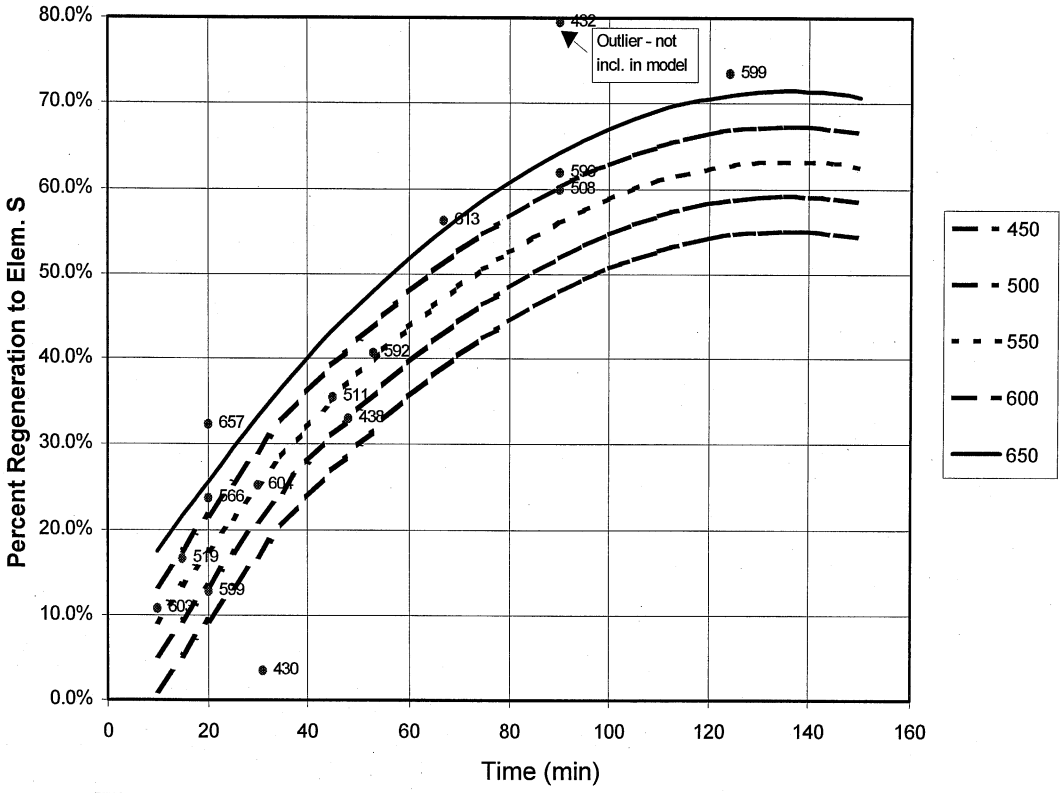

Figure 5. Empirical model of SO_2 regeneration operating parameters.

values) as a function of duration for one SO_2 concentration value. The actual data points are also shown for comparison. Because an empirical model based on a small data set was used, there are obvious limitations to its application. However, the model is useful for guiding thinking on the process simulation and economic analysis.

c. Sorbent improvement studies

The attempts to produce an iron-moly-based sorbent were disappointing. Although the initial activity of the materials, as tested in the microreactor, was promising—the outlet H_2S concentration was well below 20 ppmv—the multicycle performance of a larger sorbent batch (FHR-4) during the multicycle test was poor, as shown in Figure 6.

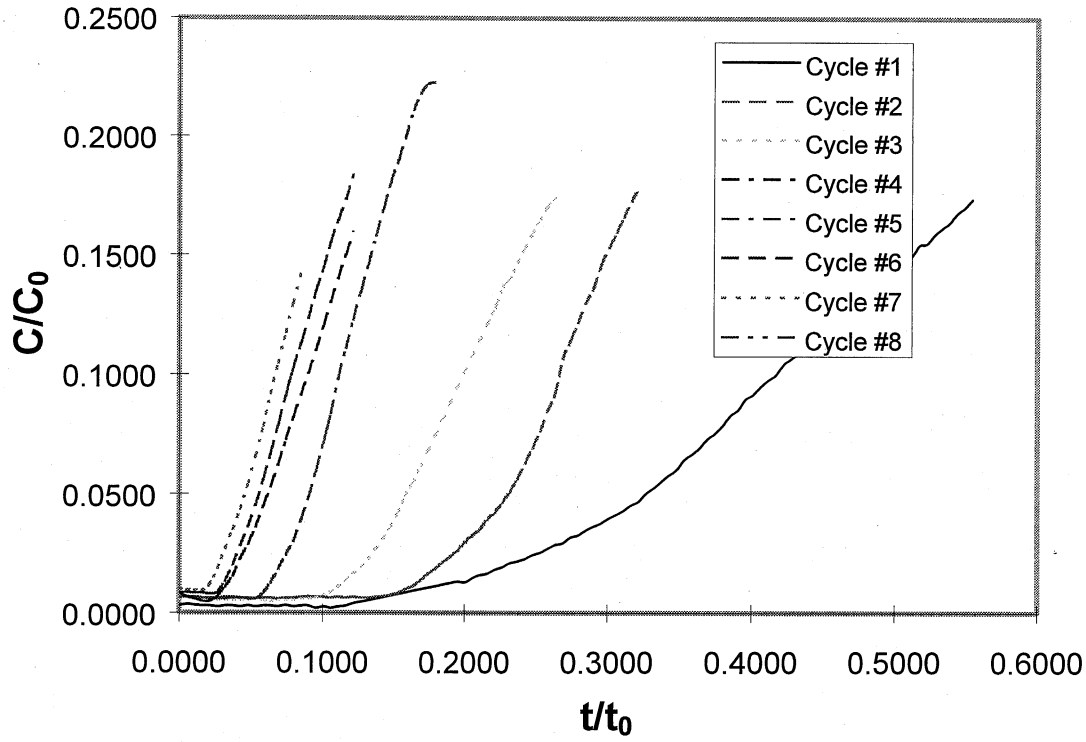

Figure 6. Dimensionless breakthrough curves for sorbent FHR-4.

By monitoring of the SO_2 evolved during the air-regeneration half cycles, it appeared that the reason for the capacity decline was that a significant portion of the absorbed sulfur was not released during regeneration; the formation of sulfate was suspected. This idea was at least partially confirmed when reductive regeneration conditions at the start of subsequent sulfidation half cycles resulted in H_2S evolution. The capacity of the sorbent could not be fully restored, however. No further work with the iron-moly combination was attempted.

The next phase of sorbent material development work was aimed at determining the conditions that result in sulfate formation (sulfation), and to determine the effect of multiple cycles of sulfidation and regeneration. The sorbent calcination temperature, additives, and additive content were evaluated using the atmospheric pressure microreactor. In particular, runs with sorbents FHR-6 and FHR-8 showed that using a higher calcination temperature resulted in stable capacity from cycle to cycle after the third cycle. However, sulfation continued to occur on the sorbent as evidenced by the evolution of SO_2 during sulfidation. Sorbent FHR-8 had superior performance in terms of reduced outlet H_2S concentration—less than 10 ppmv—and was selected for subsequent testing. A sample of R-5-58 (the sorbent used for the 50-cycle test) was tested with the same1-atm test protocol; FHR-8 showed superior H_2S removal activity.

The formulation for FHR-8 was used as the basis for preparation of two attrition-resistant candidate materials in larger batches, designated AHI-1 and AHI-2. Both samples were tested in the atmospheric TGA using a combination of gases and temperatures that simulated the complete AHGP: sulfidation, SO_2 regeneration, and O_2 regeneration. Variations in specific conditions and multiple cycles with constant conditions were run in the TGA in order to determine the preferred conditions to use for further testing. The microreactor setup was modified to include SO_2 regeneration, as well as sulfidation and air regeneration.

The initial testing did not include SO_2 regeneration. Promising reductions of H_2S concentration in the outlet gas were obtained, with AHI-2 performing slightly better and achieving approximately 10 ppmv. AHI-1 generally achieved better than 20 ppm H_2S outlet concentration, and always less than 40 ppm. A longer test program, 27 cycles, was conducted with the addition of the SO_2 regeneration step on the more promising sorbent formulation – AHI-2.

The protocol for the sulfidation at 480°C using simulated coal gas consisted of a 20-minute initial reductive regeneration, with no H_2S present, followed by the introduction of 4000 ppm of H_2S into the feed gas. Excellent activity in terms of low outlet H_2S concentration was observed; concentrations below 20 ppmv were consistently obtained, with many runs below 10 ppmv. Interestingly, the later runs showed higher activity than the initial runs; starting at cycle 19, the initial concentrations were undetectable (below 1 ppmv). No H_2S or SO_2 was detected during reductive regeneration indicating the absence of sulfation.

The SO_2 regeneration consisted of 3.5 hours of 10% SO_2 in nitrogen at 630°C. There are no analytic data from this step, nor was elemental sulfur recovered from the small-scale apparatus involved. The amount of regeneration accomplished with the SO_2 was estimated by difference from the O_2 regeneration data. Integration of the values for outlet SO_2 concentration (obtained by GC) gave an estimate of the amount of residual sulfur in the sorbent that was regenerated by the dilute air stream. By these calculations, the SO_2 regeneration resulted in up to 50% regeneration to elemental sulfur.

The AHI series of sorbents was designed to be highly attrition-resistant. The attrition indices for AHI-1 and -2 were 0.5 and 1.2, respectively—similar to the values for the benchmark FCC catalysts. These sorbents have been scaled up to 500 g quantity and are due to be tested at bench-scale at elevated pressure. Eventually one of these sorbents will be selected for the field test of the AHGP to be conducted in early 2000.

6. Conclusions

Conceptual and process development of AHGP, an advanced HGD process, has been carried out. AHGP uses a proprietary Zn-Fe sorbent. It requires two regeneration stages (SO_2 and O_2) but uses significantly less coal gas compared to DSRP for elemental sulfur recovery. The feasibility of AHGP as a promising alternative to DSRP has been demonstrated at bench-scale. Attrition-resistant Zn-Fe sorbent formulations have been prepared that can remove H_2S to below 20 ppmv from coal gas and can be regenerated using SO_2 to produce elemental sulfur.

7. Acknowledgments

The research is sponsored by the DOE/FETC, under Contract No. DE-AC21-94MC31258, with Research Triangle Institute and Contract No. DE-FG26-97FT97276 with Hampton University.

8. References

Ayala, R.E., A.S. Feitelberg, and A.H. Furman. 1995. "Development of a High-Temperature Moving-Bed Coal Gas Desulfurization System." In *Proceedings of 12th Ann. Int. Pittsburgh Coal Conf.*, p. 1053, September 11-15, Pittsburgh.

Cook, C.S., et al. 1992. "Integrated Operation of a Pressurized Fixed Bed Gasifier and Hot Gas Desulfurization System." In *Proceedings of 12th Annual Gasif. Gas Stream Cleanup Systems Contractor's Review Meeting*, Volume 1, DE93000228, p. 84.

deWild, P.J., J.H.A. Kiel, and E. Schenk. "Iron Oxide/Molybdenum Oxide Sorbents for High Temperature Fuel Gas Desulfurization." In *Procedings of the Thirteenth Annual International Pittsburgh Coal Conference (1996).*

Gangwal, S.K. 1991. "Hot-Gas Desulfurization Sorbent Development for IGCC Systems." IChemE Symposium Series No. 123. Sheffield, UK, pp. 159-170.

Gangwal, S.K. 1996. "Sulfur Removal from Gas Streams at High Temperature," 3rd International Symposium on Gas Cleaning at High Temperature. University of Karlsruhe, Karlsruhe, Germany, September.

Gangwal, S.K., J.W. Portzer, B.S. Turk, and R.Gupta. 1996. "Advanced Sulfur Control Processing." In *Proceedings of the Advanced Coal-Fired*

Systems Review Meeting July 16-19, 1996. (CD-ROM). U.S. Department of Energy, Morgantown, WV.

Gupta, R., and S.K. Gangwal. 1992. "Enhanced Durability of Desulfurization Sorbents for Fluidized Bed Applications—Development and Testing of Zinc Titanate Sorbents." DOE/MC/25006-3271.

Harrison, D.P. 1995. "Control of Gaseous Contaminants in IGCC Processes, An Overview," In *Proceedings of 12th Ann. Int. Pittsburgh Coal Conference*, p. 1047, September 11-15, Pittsburgh.

Harrison, D.P., F.R. Groves, J.D. White, W. Huang, and A. Lopez-Oritz. 1996. "Advanced Sulfur Control Processing." In *Proceedings of Advanced Coal-Fired Power Systems '96 Review Meeting*, Morgantown Energy Technology Center, Morgantown, WV, July.

Jalan, V. 1985. "High-Temperature Desulfurization of Coal Gases." In *Acid and Sour Gas Treating Processes*, Gulf Publishing Co., Houston, TX, Nov. 7.

Meijer, R., F.J.J.G. Janssen, G.L. Faring, and J.W. H. Hellendoorn. 1996. "KEMA's Hot Gas Cleanup Process." *In Proceedings of 3rd International Symposium on Gas Cleaning at High Temperature*. University of Karlsruhe, Karlsruhe, Germany, September.

Portzer, J.W., and S.K. Gangwal. 1998. "Bench-Scale Demonstration of Hot-Gas Desulfurization Technology." In *Proceedings of the Advanced Coal-Based Power and Environmental Systems '98 Conference*. July 21-23, 1998. Available on the U.S. Department of Energy, Federal Energy Technology Center Web site. (http://apis.fetc.doe.gov/publications/proceedings/98/98ps/pspb-1.pdf)

Portzer, J.W., A.S. Damle, and S.K. Gangwal. 1997. "Hot-Gas Desulfurization with Sulfur Recovery." In *Proceedings of Advanced Coal-Based Power and Environmental Systems '97 Conference*, Federal Energy Technology Center, Pittsburgh, PA, July.

Portzer, J.W., B.S. Turk, and S.K. Gangwal. 1996. "Durability Testing of the Direct Sulfur Recovery Process." In *Proceedings of the Advanced Coal-Fired Power Systems Review Meeting July 16-18, 1996.* (CD-ROM). U.S. Department of Energy. Morgantown, WV.

Thambimuthu, K.V. 1993. Gas Cleaning for Advanced Coal-Based Power Generation. Report by IEA Coal Research, IEACR/53, London, UK.

APPENDIX E Engineering Evaluation of Hot-Gas Desulfurization with Sulfur Recovery, Topical Report, May 1998

May 1998

Engineering Evaluation of Hot-Gas Desulfurization with Sulfur Recovery

Topical Report

Work performed under
Contract No. DE-AC21-94MC31258

for
U.S. Department of Energy
Federal Energy Technology Center
3610 Collins Ferry Road
Morgantown, WV 26505

by
S.K. Gangwal
J.W. Portzer
Research Triangle Institute
P.O. Box 12194
Research Triangle Park, NC 27709

and
G.W. Roberts
S.C. Kozup
North Carolina State University
Raleigh, NC 27695

This report was prepared by the Research Triangle Institute (RTI) as an account of work sponsored by the U.S. Department of Energy. RTI makes no warranty or representation, expressed or implied, with respect to the information contained in this report, or that the use of any apparatus, method or process disclosed in this report may not infringe privately owned rights. Furthermore, RTI assumes no liability with respect to the use of, or for damages resulting from the use of, any information, apparatus, method, or process disclosed in this report.

Engineering Evaluation of Hot-Gas Desulfurization with Sulfur Recovery

Topical Report

Work performed under
Contract No. DE-AC21-94MC31258

for
U.S. Department of Energy
Federal Energy Technology Center
3610 Collins Ferry Road
Morgantown, WV 26505

by
S.K. Gangwal
J.W. Portzer
Research Triangle Institute
3040 Cornwallis Road
Research Triangle Park, NC 27709

and
G.W. Roberts
S.C. Kozup
Chemical Engineering Department
North Carolina State University
Raleigh, NC 27695

May 1998

ABSTRACT

Engineering evaluations and economic comparisons of two hot-gas desulfurization (HGD) processes with elemental sulfur recovery, being developed by Research Triangle Institute, are presented. In the first process, known as the Direct Sulfur Recovery Process (DSRP), the SO_2 tail gas from air regeneration of zinc-based HGD sorbent is catalytically reduced to elemental sulfur with high selectivity using a small slipstream of coal gas. DSRP is a highly efficient first-generation process, promising sulfur recoveries as high as 99% in a single reaction stage. In the second process, known as the Advanced Hot Gas Process (AHGP), the zinc-based HGD sorbent is modified with iron so that the iron portion of the sorbent can be regenerated using SO_2. This is followed by air regeneration to fully regenerate the sorbent and provide the required SO_2 for iron regeneration. This second-generation process uses less coal gas than DSRP. Commercial embodiments of both processes were developed. Process simulations with mass and energy balances were conducted using ASPEN Plus. Results show that AHGP is a more complex process to operate and may require more labor cost than the DSRP. Also capital costs for the AHGP are higher than those for the DSRP.

However, annual operating costs for the AHGP appear to be considerably less than those for the DSRP with a potential break-even point between the two processes after just 2 years of operation for an integrated gasification combined cycle (IGCC) power plant using 3 to 5 wt% sulfur coal. Thus, despite its complexity, the potential savings with the AHGP encourage further development and scaleup of this advanced process.

TABLE OF CONTENTS

LIST OF FIGURES

LIST OF TABLES

ACKNOWLEDGMENTS

This research was sponsored by the Federal Energy Technology Center of the U.S. Department of Energy. Valuable guidance and suggestions provided by the Contracting Officer's Representative, Mr. Thomas P. Dorchak, are sincerely acknowledged.

EXECUTIVE SUMMARY

INTRODUCTION

Hot-gas desulfurization (HGD) of coal gas in integrated gasification combined cycle (IGCC) power systems has received a great deal of attention over the past two decades due to the potential for high thermal efficiency (up to 47%) and low environmental impact of these advanced power systems. In an advanced IGCC system, coal is gasified at elevated pressures, typically 20 to 30 atm, to produce a low-volume fuel gas which is desulfurized prior to burning in a combustion turbine to produce electricity. Higher efficiency and lower cost are achieved by efficient air and steam integration, and modular designs of the gasification, hot-gas cleanup, and turbine subsystems (Figure E-1). Hot gas cleanup primarily involves removal of particulates and sulfur—mostly hydrogen sulfide (H_2S) and some carbonyl sulfide (COS). H_2S and COS can be efficiently removed to less than 20 ppmv at 350 to 650 °C using zinc-based metal oxide sorbents that can be regenerated for multicycle operation.

Air regeneration of these sorbents results in a dilute sulfur dioxide (SO_2)-containing tail gas that needs to be disposed. Options include conversion of the SO_2 to calcium sulfate using lime (or limestone) for landfilling or conversion to saleable products such as sulfuric acid or elemental sulfur. Elemental sulfur, an essential industrial commodity, is an attractive option because it is the lowest volume product and can be readily stored, disposed, transported, and/or sold.

Research Triangle Institute (RTI), with U.S. Department of Energy (DOE) sponsorship, is pursuing the development of two processes for elemental sulfur production in conjunction with

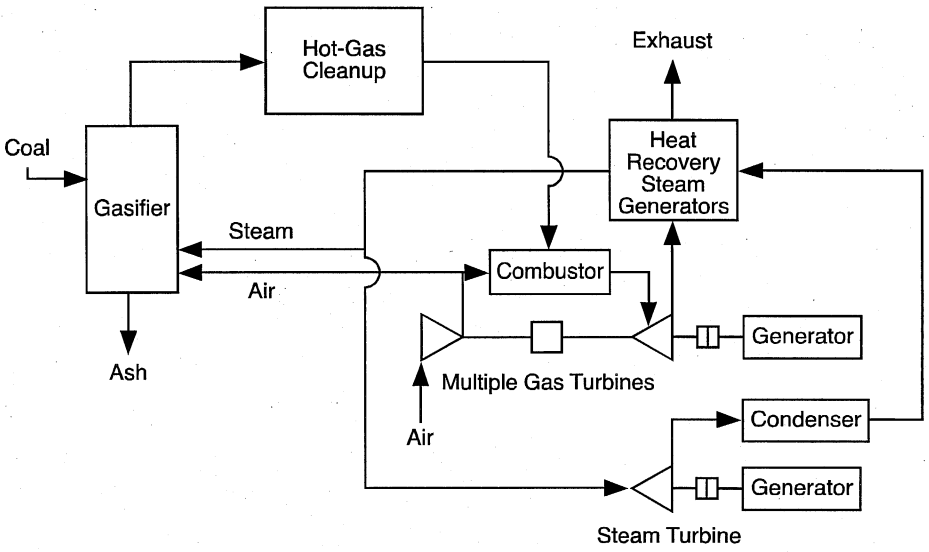

Figure E-1. Advanced IGCC system.

hot-gas desulfurization. The first process, called the Direct Sulfur Recovery Process (DSRP), involves the selective catalytic reduction of the SO_2 tail gas to sulfur using a small slipstream of the coal gas. DSRP is a highly efficient process that can recover up to 99% of SO_2 as elemental sulfur in a single catalytic reactor. However, for every mole of sulfur produced two moles of hydrogen (H_2) and/or carbon monoxide (CO) are consumed in DSRP and this represents an energy penalty for the IGCC plant. DSRP is currently in an advanced state of development.

A second-generation process being pursued by RTI involves the use of a modified zinc-based sorbent (containing zinc and iron). This sorbent can be regenerated using SO_2 and O_2 to directly produce sulfur. This process, called the Advanced Hot-Gas Process (AHGP), is expected to use much less coal gas than DSRP. DSRP is currently at the pilot-plant scale development stage, whereas AHGP has been demonstrated at small bench-scale. Both DSRP and AHGP are scheduled for slipstream testing at DOE's Power Systems Development Facility (PSDF), Wilsonville, Alabama, in 1999.

OBJECTIVE

The objective of this report is to develop process simulations with mass and heat balances for the DSRP and AHGP and to provide a **preliminary** economic comparison of the two processes in conjunction with an IGCC power plant employing HGD. The process simulation and economic evaluation were carried out by RTI's subcontractor, North Carolina State University (NCSU). NCSU's report of this work in its entirety is attached as an appendix. Background, brief process description, and important results and conclusions are provided below as a stand-alone executive summary.

BACKGROUND

Sorbent Development

Research on HGD methods for coal gas in IGCC systems has concentrated on the use of regenerable metal oxide sorbents (Gangwal, 1991, 1996; Gangwal et al., 1993, 1995; Harrison, 1995; Jalan, 1985; Thambimuthu, 1993). This research and development effort has been spearheaded by DOE's Federal Energy Technology Center (FETC) and its predecessor agencies since 1975.

The HGD process using a regenerable metal oxide (MO) sorbent is typically carried out in a two-reactor system consisting of a desulfurizer and an air regenerator

$$MO + H_2S \rightarrow MS + H_2O \quad \text{(desulfurizer)}$$
$$MS + (3/2)\, O_2 \rightarrow MO + SO_2 \quad \text{(regenerator).}$$

The main requirement of the metal oxide sorbent is that it should selectively react with H_2S and COS in a reducing fuel gas at desired conditions (2 to 3 Mpa, 350 to 750 °C). The thermodynamics of the reaction should be favorable enough to achieve the desired level of H_2S and COS removal (as much as 99% or more). The metal oxide should be stable in the reducing gas environment, i.e., reduction of MO to M should be slow or thermodynamically unfavorable since

it leads to loss of valuable fuel gas and could also lead to volatile metal evaporation and decrepitation of sorbent structure.

The principle requirement during air regeneration is that the sorbent should predominantly revert back to its oxide rather than to sulfate ($MO + SO_2 + 1/2\ O_2 \rightarrow MSO_4$). Air regeneration is highly exothermic and requires tight temperature control using large quantities of diluent (N_2) or other means to prevent sorbent sintering and sulfate formation.

The bulk of research on regenerable sorbents has been on zinc-based sorbents because sorbents based on zinc oxide appear to have the fewest technical problems among all sorbents. Zinc oxide (ZnO) has highly attractive thermodynamics for H_2S adsorption and can reduce the H_2S to parts-per-million levels over a very wide temperature range. Iron oxide appears to be the most popular sorbent for use at around 400 °C.

A combined ZnO-iron oxide (Fe_2O_3) sorbent, namely, zinc ferrite ($ZnFe_2O_4$) was developed by Grindley and Steinfeld (1981) to combine the advantages of ZnO and Fe_2O_3. A temperature range of 550 to 750 °C received the major research emphasis in the United States during the 1980s and early 1990s. Because of zinc oxide's potential for reduction ($ZnO + H_2 \rightarrow Zn + H_2O$) at >600 °C followed by evaporation, a zinc oxide-titanium oxide sorbent, namely zinc titanate sorbent, was developed and tested at high temperature and high pressure (HTHP) (Gangwal et al., 1988). Zinc titanate is currently one of the leading sorbents.

During recent years, research emphasis has shifted toward lower temperatures (350 to 550 °C) based on a study in the Netherlands (NOVEM, 1991). According to this study, the thermal efficiency of an 800-MWe IGCC plant increased from 42.75% using cold-gas cleanup to 45.14% using HGD at 350 °C and to 45.46% using HGD at 600 °C. The small efficiency increase from 350 to 600 °C suggested that temperature severity of HGD could be significantly reduced without much loss of efficiency.

Reactor and Systems

A two-reactor configuration is necessary for HGD due to its cyclic nature. Early developments emphasized fixed beds. The highly exothermic regeneration led to a move away from fixed beds toward moving beds (Ayala et al., 1995; Cook et al., 1992) and fluidized beds (Gupta and Gangwal, 1992). Two DOE Clean Coal Technology IGCC demonstration plants, namely TECO and Sierra-Pacific, employing General Electric's (GE's) moving-bed HGD reactor system and M.W. Kellogg's transport reactor HGD system, respectively, are scheduled to begin operation this year. Fluidized-bed HGD systems are receiving a lot of emphasis due to several potential advantages over fixed- and moving-bed reactors, including excellent gas-solid contact, fast kinetics, pneumatic transport, ability to handle particles in gas, and ability to control the highly exothermic regeneration process. However, an attrition-resistant sorbent that can withstand stresses induced by fluidization, transport, chemical transformation, and rapid temperature swings must be developed.

Development of an iron-oxide sorbent-based fluidized-bed HGD reactor system has been carried out in Japan over the past several years (Sugitani, 1989). The process is now up to 200 tons of

coal per day. The sorbent is prepared by crushing raw Australian iron oxide which is inexpensive, but attrition is a big problem with this sorbent. Durable zinc titanate and other zinc-based sorbent development is ongoing for application at the Sierra-Pacific plant for Kellogg's transport reactor (Gupta et al., 1996, 1997; Jothimurugesan et al., 1997; Khare et al., 1996).

A schematic of Kellogg's transport reactor system at Sierra-Pacific is shown in Figure E-2. This technology represents a significant development in HGD because it allows regeneration with neat air. Neat air regeneration produces a more concentrated SO_2 tail-gas stream containing around 14 vol% SO_2.

The initial sorbent tested at Sierra-Pacific was Phillips Z-Sorb III. Its attrition resistance was not acceptable. Phillips is continuing efforts to improve their sorbent. Recently RTI and Intercat have provided a much more attrition-resistant zinc titanate sorbent, EX-SO3, to Sierra-Pacific for testing after qualifying it through a series of bench- and process development unit (PDU)-scale tests (Gupta et al., 1997). This sorbent has been circulated in the system and has demonstrated satisfactory attrition resistance. Chemical reactivity tests with the sorbent are to be conducted shortly after the Sierra coal gasifier is fully commissioned and begins smooth operation.

Direct Sulfur Recovery Process

The patented DSRP being developed by RTI is a highly attractive option for recovery of sulfur from regeneration tail gas. Using a slipstream of coal gas as a reducing agent, it efficiently converts the SO_2 to elemental sulfur, an essential industrial commodity that is easily stored and transported. In the DSRP (Dorchak et al., 1991), the SO_2 tail gas is reacted with a slipstream of coal gas over a fixed bed of a selective catalyst to directly produce elemental sulfur at the HTHP conditions of the tail gas and coal gas. Overall reactions involved are shown below:

$$2\ H_2 + SO_2 \rightarrow (1/n)\ S_n + 2\ H_2O$$

$$2\ CO + SO_2 \rightarrow (1/n)\ S_n + 2\ CO_2$$

$$CO + H_2O \rightarrow H_2 + CO_2$$

$$H_2 + (1/n)\ S_n \rightarrow H_2S$$

$$2\ H_2S + SO_2 \rightarrow (3/n)\ S_n + 2\ H_2O\ .$$

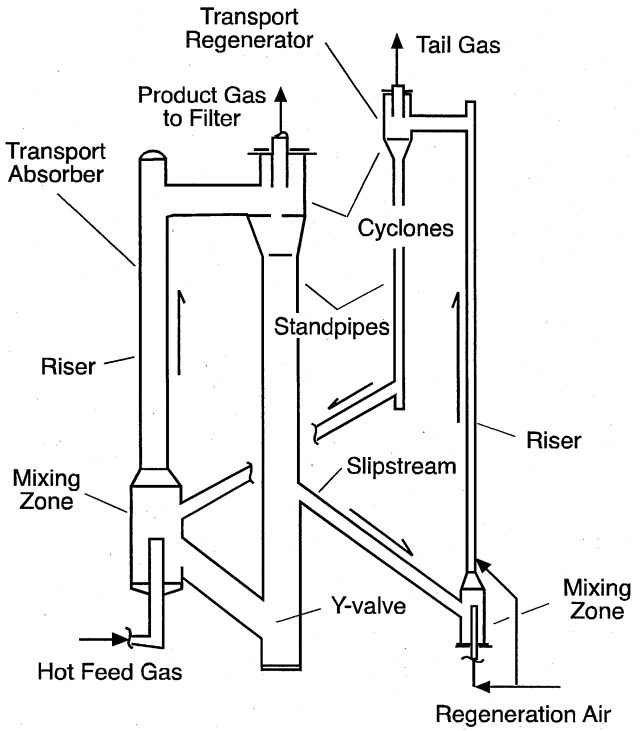

Figure E-2. Schematic of Sierra hot-gas desulfurization system.

RTI constructed and commissioned a mobile laboratory for DSRP demonstration with actual coal gas from the DOE-Morgantown coal gasifier. Slipstream testing using a 1-L fixed-bed of DSRP catalyst with actual coal gas (Portzer and Gangwal, 1995; Portzer et al., 1996) demonstrated that, with careful control of the stoichiometric ratio of the gas input, sulfur recovery of 96% to 98% can be consistently achieved in a single DSRP stage. The single-stage process, as it is proposed to be integrated with a metal oxide sorbent regenerator, is shown in Figure E-3. With the tail-gas recycle stream shown in the figure, there are no sulfur emissions from the DSRP. RTI also demonstrated the ruggedness of the DSRP catalyst by exposing it to coal gas for over 250 hours in a canister test.

The results show that, after a significant exposure time to actual coal gas, the DSRP catalyst continues to function in a highly efficient manner to convert SO_2 in a simulated regeneration tail gas to elemental sulfur. This demonstration of a rugged, single-stage catalytic process resulted in additional online experience and the assembling of more process engineering data. The development of the DSRP continues to look favorable as a feasible commercial process for the production of elemental sulfur from hot-gas desulfurizer regeneration tail gas.

Canisters of fixed-bed DSRP catalyst have been prepared for another exposure test with actual coal gas, this time at FETC's PSDF at Wilsonville, Alabama. Exposure is expected to take place sometime during FY 2000.

Additional development and testing of a fluidized-bed process is planned, capable of producing elemental sulfur from 14 vol% SO_2 at HTHP. These tests intend to demonstrate the use of DSRP in conjunction with the Kellogg transport regenerator producing 14 vol% SO_2. Due to the exothermic nature of the DSRP reactions, a fluidized-bed reactor is a preferred configuration at these high SO_2 concentrations. Two candidate attrition-resistant fluidizable DSRP catalysts have been prepared in cooperation with a catalyst manufacturer. A series of tests was conducted using these catalysts with up to 14 vol% SO_2 tail gas, at pressures from 1.0 to 2.0 Mpa, temperatures

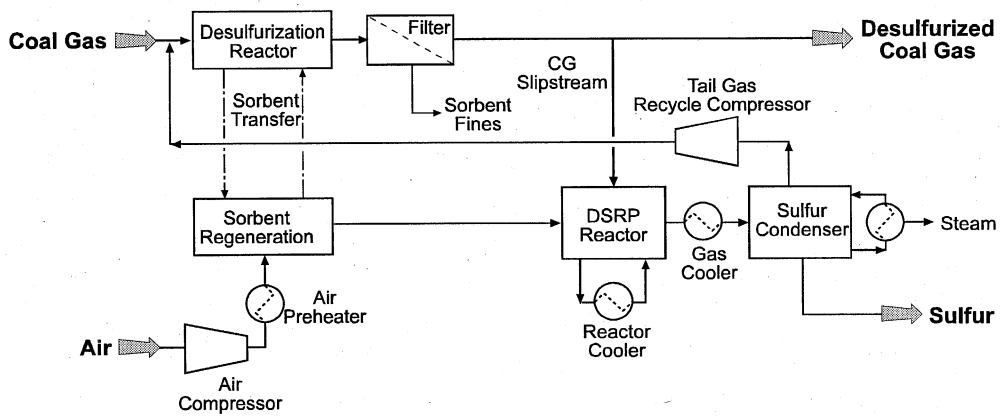

Figure E-3. Hot-gas desulfurization with DSRP.

from 500 to 600 °C, and space velocities from 3,000 to 6,000 stdcm^3/cm^3. Sulfur recoveries up to 98.5% were achieved during steady-state operation, and no attrition of the catalyst occurred in the fluidized-bed tests.

Planning is underway to conduct a long-duration field test using a skid-mounted six-fold larger (based on reactor volume) (6X) DSRP unit with a slipstream of actual coal gas at PSDF. The mobile laboratory will be refitted at RTI as a control room for the 6X unit and will be moved along with the skid-mounted 6X unit to Wilsonville, Alabama, for the testing to be conducted in FY 2000. This larger unit will utilize a fluidized-bed reactor and will be designed for production of up to 22 times more sulfur than the 7.5-cm I.D. bench-scale unit used in the previous slipstream tests.

Advanced Hot-Gas Process

In the DSRP, for every mole of SO_2, 2 mol of reducing components are used, leading to a small but noticeable consumption of coal gas. Novel regeneration processes that could lead to elemental sulfur without use of coal gas or with limited use of coal gas are being developed (Gangwal et al., 1996; Harrison et al. 1996). KEMA's hot-gas cleanup process (Meijer et al., 1996) uses a proprietary fluidized-bed sorbent which can remove H_2S to below 20 ppmv and can be regenerated using SO_2, O_2 mixtures to directly produce elemental sulfur. Along similar lines, a second-generation process, known as the Advanced Hot-Gas Process (AHGP), is being developed by RTI to regenerate the desulfurization sorbent directly to elemental sulfur with minimal consumption of coal gas. In this process (Figure E-4), a zinc-iron sorbent is used and the regeneration is carried out in two stages with SO_2 and O_2, respectively. The iron sulfide is regenerated by SO_2 in one stage to elemental sulfur. In the other stage, zinc sulfide and any remaining iron sulfide are regenerated by O_2 to provide the required SO_2. The sorbent is then returned to the desulfurizer.

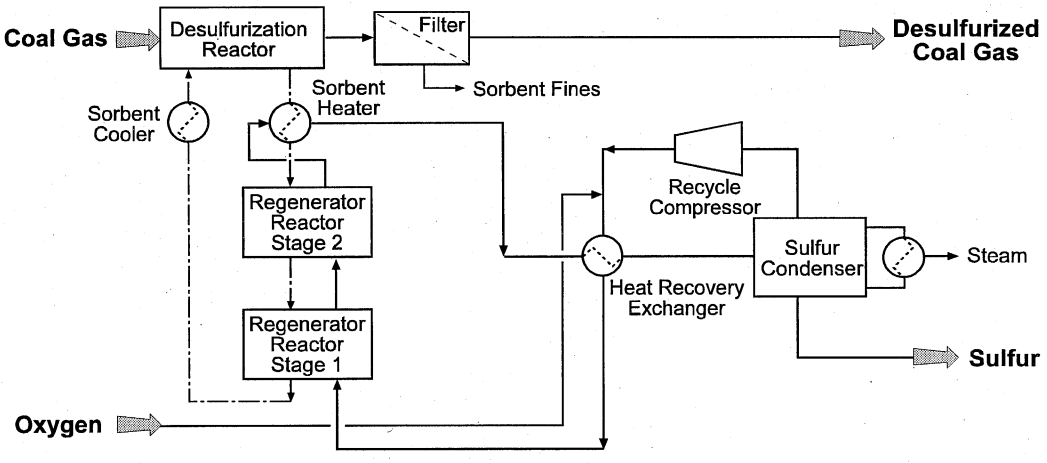

Figure E-4. Advanced hot-gas process.

The key chemical reactions of interest are as follows:

1. Sulfidation

$$Fe_2O_3 + 2H_2S + H_2 \rightarrow 2FeS + 3H_2O$$
$$ZnO + H_2S \rightarrow ZnS + H_2O$$

2. SO_2 regeneration

$$4FeS + 3SO_2 \rightarrow 2Fe_2O_3 + 7/2\ S_2$$

3. O_2 regeneration

$$2FeS + 7/2\ O_2 \rightarrow Fe_2O_3 + 2SO_2$$
$$ZnS + 3/2\ O_2 \rightarrow ZnO + SO_2.$$

The feasibility of SO_2 regeneration of combined zinc-iron sorbents was demonstrated using a thermogravimetric analyzer and high-pressure microreactor. Zinc sulfide shows essentially no SO_2 regeneration at temperatures of interest (500 to 600 °C), but zinc is needed to act as a polishing agent in the desulfurizer. A number of sorbents were prepared and tested at the bench scale over multiple cycles. Based on these tests, a highly attrition-resistant sorbent (R-5-58) was prepared and the process was demonstrated over 50 cycles in a 5.0-cm I.D. bench-scale reactor.

The results showed that R-5-58 removed H_2S down to 50 to 100 ppm levels with stable desulfurization activity over the duration. The surface area and pore volume of the sorbent did not change appreciably and the attrition index before and after the test was 3.6% and 1.2%, respectively. Sulfur balances were adequate and the SO_2 regeneration step accounted for up to 70% of the total regeneration of the sorbent. This compares to a theoretical limit of approximately 80%, assuming complete regeneration by SO_2 of the iron component.

The sorbent is being optimized further to increase its desulfurization efficiency. The goal is to develop a sorbent that can remove H_2S below 20 ppmv. Plans call for demonstrating the process at PSDF with a slipstream of actual coal gas in FY 1999 in conjunction with the DSRP field test at PDSF.

APPROACH

An engineering and economic evaluation of the DSRP (Figure E-3) and AHGP (Figure E-4) for large-scale IGCC plants was conducted using ASPEN PLUS® computer process simulation software by NCSU. The NCSU report is attached in its entirety as an appendix. Here we present a summary of the approach, key results, and conclusions.

Base case simulations of both processes assumed 0.85 mol% H_2S in the coal-gas feed. Such an H_2S concentration in the coal gas would be produced by an oxygen-blown Texaco gasification using roughly a 3.6 wt% sulfur-containing coal. Both base cases generate 260 MWe from the clean coal gas. Simulations that deviate from the base cases use suffixes to denote the changes. Table E-1 displays the significance of the suffixes. In all cases a coal-gas feed pressure and

temperature of 275 psia and 482 °C, respectively, was used. However, H_2S concentration was varied from 0.25 to 2.5 mol% and power produced was varied from 110 to 540 MWe. Table E-2 shows the composition and flow rate of the raw coal gas feed to the base case HGD processes. The requirement of a higher amount of coal gas to produce the same 260 MW power by DSRP versus the AHGP is noteworthy. The DSRP was assumed to use the standard Sierra-Pacific dual transport reactor configuration shown in Figure E-2 for HGD. The DSRP reactor used for the 14% SO2 tail gas was a fast fluidized bed with an alumina-based catalyst. The AHGP reactor configuration on the other hand used a transport sulfider and a bubbling multistage fluidized-bed regenerator as shown in Figure E-5. The large bubbling reactor was required to provide a greater residence time for the slow SO_2 regeneration stage.

Table E-1. Simulation Cases Considered

Simulations	H_2S feed concentration (mol%)	MW produced
DSRP, AHGP (base cases)	0.85	260
DSRP-b, AHGP-b	2.50	260
DSRP-c, AHGP-c	0.25	260
DSRP-100, AHGP-100	0.85	110
DSRP-500, AHGP-500	0.85	540

Table E-2. Raw Gas Feed to Base Case Simulations

Component	DSRP (lb/h)	AHGP (lb/h)
H_2S	6,300	6,100
H_2O	70,500	69,000
H_2	11,800	11,500
CO	218,200	213,400
CO_2	117,400	114,800
N_2	36,300	35,500
Total	460,500	450,300

RESULTS

The preliminary process and economic evaluations conducted using ASPEN Plus are summarized. Figure E-6 compares key elements using a simple method in which each parameter for the DSRP-based process is arbitrarily assigned the value of 1.0. A range of values is produced for AHGP to cover the various cases being considered. The big advantage of the AHGP is clearly the reduced parasitic consumption of coal gas. The other operating cost elements are also lower for AHGP, because that process has a considerably lower compression power requirement. A desulfurization process based on the DSRP requires a large flow of compressed air to provide the oxygen necessary to regenerate the sulfided sorbent, and thus has a large compressor horsepower duty. By comparison, the AHGP uses oxygen only for a smaller, polishing regeneration and, by using pure oxygen, the compression duty is lowered further. The AHGP also has the SO_2 loop recycle compressor, but its duty is quite small compared to the DSRP air compressor.

[It should be noted that in the NCSU economic analysis (Appendix) the AHGP recycle compressor duty may be understated, as the calculation was based on a rough estimate for pressure drop, not a calculated value based on a piping design. By comparison, the duty for the DSRP air compressor is primarily a function of the head pressure of the system, which is well defined.]

The value of "capital cost of all equipment" for the AHGP is higher than for the DSRP-based process, as Figure E-5 shows. The higher equipment cost is primarily due to the higher cost of the AHGP reactor vessel(s). Although there are three separate reactor steps required with the DSRP-based process, the single AHGP multistage reactor vessel(s) is larger. The larger size is primarily due to the longer residence time required for the SO_2 regeneration. [It should be noted that the NCSU cost estimates (Appendix) do not include piping costs, so that the total plant capital costs will be higher than the installed equipment costs. However, since piping costs are often estimated as a direct function of the equipment cost numbers, the ratio of the installed equipment costs for the two processes shown in the figure will approximate the ratio of the total plant costs.]

Another advantage of the DSRP is that it is the easier, more understood, process to operate. This is because balancing the SO_2 production and consumption in the AHGP may be difficult.

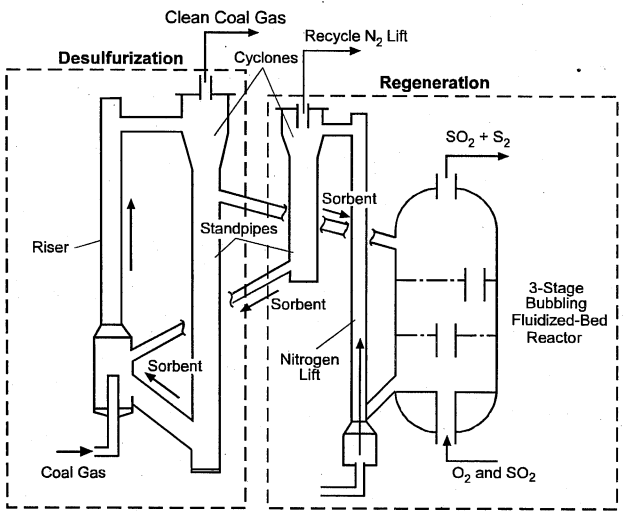

Figure E-5. Schematic of AHGP desulfurization and regeneration reactors.

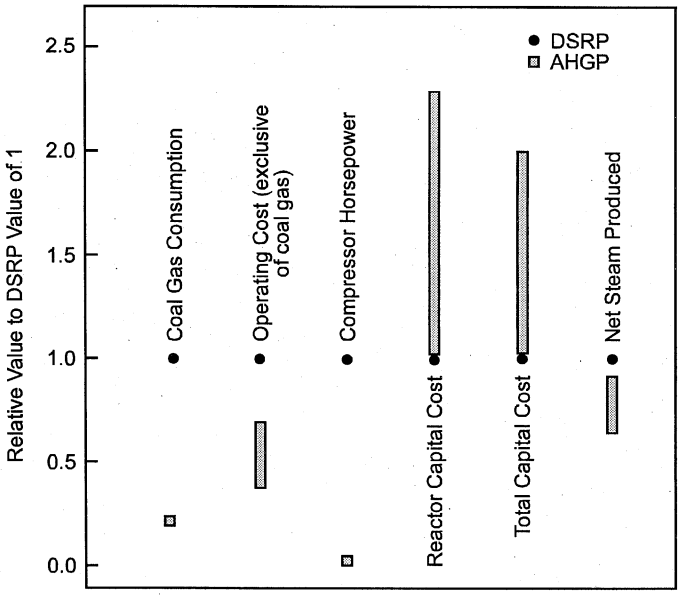

Figure E-6. Comparison of key elements of DSRP and AHGP.

Although the AHGP has a higher initial cost, indicated by its larger capital requirements, it has a significantly lower annual operating cost than DSRP. As shown in Figure E-7, the operating cost advantage of the AHGP increases as the sulfur to be recovered increases. The negative annual costs of AHGP at higher sulfur feed result from the sulfur credit with less consumption of coal gas. The operating cost difference is large enough to offset the installation cost of AHGP. As shown in Figure E-8, AHGP has a lower cumulative HGD investment after only 2 years of operation. Both Figures E-7 and E-8 are presented to illustrate only cost comparison of the two processes. Emphasis should not be placed on the accuracy of the absolute cost numbers presented in these figures.

CONCLUSIONS

ASPEN simulations of DSRP and AHGP revealed the complexity of both HGD processes. The AHGP appears to be the more difficult process to operate and may require more employees than

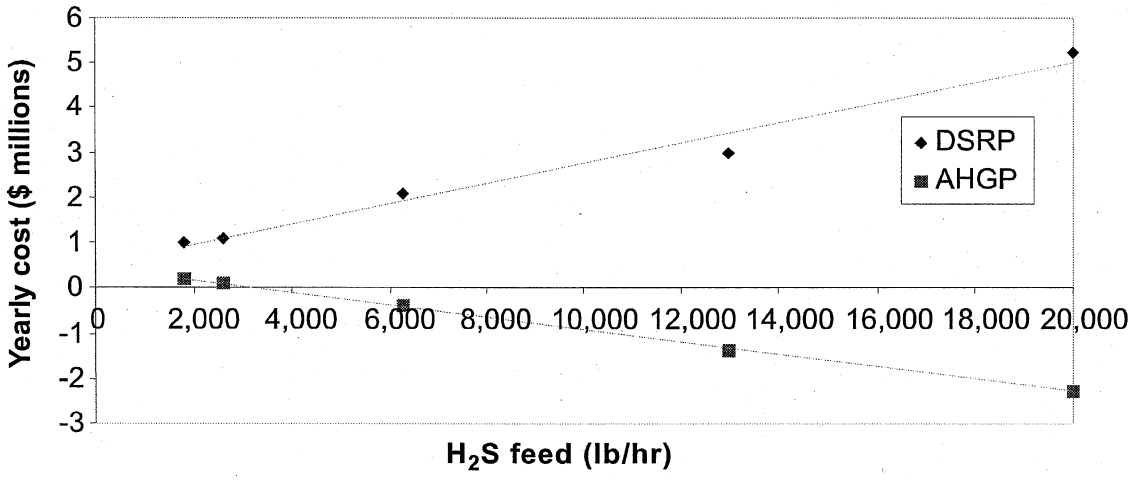

Figure E-7. Annual costs as a function of sulfur feed.

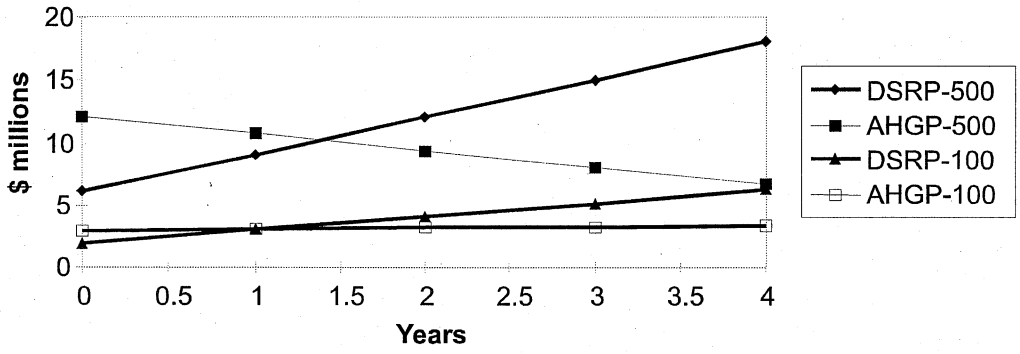

Figure E-8. Cumulative HGD investment.

the DSRP. Capital costs for the AHGP are higher than those for the DSRP—development of DSRP is also much closer to commercialization than AHGP. However, annual operating costs for the AHGP appear to be considerably less than those of the DSRP. Preliminary economic comparison shows that the total cost of implementing AHGP will be less than that of implementing DSRP after as little as 2 years of operation. Thus, despite its greater complexity, the potential savings with the AHGP encourage further development and scaleup of this advanced process.

REFERENCES

Ayala, R.E., A.S. Feitelberg, and A.H. Furman. 1995. "Development of a High-Temperature Moving-Bed Coal Gas Desulfurization System." In *Proceedings of 12th Ann. Int. Pittsburgh Coal Conf.*, p. 1053, September 11-15, Pittsburgh.

Cook, C.S., et al. 1992. "Integrated Operation of a Pressurized Fixed Bed Gasifier and Hot Gas Desulfurization System." In *Proceedings of 12th Annual Gasif. Gas Stream Cleanup Systems Contractor's Review Meeting*, Volume 1, DE93000228, p. 84.

Dorchak, T.P., S.K. Gangwal, and W.J. McMichael. 1991. The Direct Sulfur Recovery Process. *Environmental Progress* 19(2):68.

Gangwal, S.K. 1991. "Hot-Gas Desulfurization Sorbent Development for IGCC Systems." IChemE Symposium Series No. 123. Sheffield, UK, pp. 159-170.

Gangwal, S.K. 1996. "Sulfur Removal from Gas Streams at High Temperature," 3rd International Symposium on Gas Cleaning at High Temperature. University of Karlsruhe, Karlsruhe, Germany, September.

Gangwal, S.K., et al. 1988. "Bench-Scale Testing of Novel High-Temperature Desulfurization Sorbents." Report No. DOE/MC/23126-2662 (DE89000935).

Gangwal, S.K., R. Gupta, and W.J. McMichael. 1993. "Sulfur Control Options for IGCC Systems." In *Proceedings of 17th Biennial Low-Rank Fuels Symposium*, University of North Dakota, Energy and Environmental Research Center, St. Louis, MO, May 10-13.

Gangwal, S.K., R. Gupta, and W.J. McMichael. 1995. "Hot-Gas Cleanup-Sulfur Recovery-Technical, Environmental, and Economic Issues," *Heat Recovery Systems and CHP*. Vol. 15, No. 2, p. 205-214, Elsevier Science Limited.

Grindley, T., and G. Steinfeld. 1981. "Development and Testing of Regenerable Hot Coal-Gas Desulfurization Sorbents." DOE/MC/16545-1125.

Gupta, R., and S.K. Gangwal. 1992. "Enhanced Durability of Desulfurization Sorbents for Fluidized Bed Applications—Development and Testing of Zinc Titanate Sorbents." DOE/MC/25006-3271.

Gupta, R., B.S. Turk, and S.K. Gangwal. 1996. "Bench-Scale Development of Fluid-Bed Spray Dried Sorbents." In *Proceedings of Advanced Coal-Fired Power Systems '96 Review Meeting*, Morgantown Energy Technology Center, Morgantown, WV, July.

Gupta, R., B.S. Turk, and Albert A. Vierheilig. 1997. "Desulfurization Sorbents for Transport-Bed Applications." In *Proceedings of 1997 FETC Power Systems and Environmental Control Contractor's Meeting*, Pittsburgh, PA, July.

Harrison, D.P. 1995. "Control of Gaseous Contaminants in IGCC Processes, An Overview," In *Proceedings of 12th Ann. Int. Pittsburgh Coal Conference*, p. 1047, September 11-15, Pittsburgh.

Harrison, D.P., F.R. Groves, J.D. White, W. Huang, and A. Lopez-Oritz. 1996. "Advanced Sulfur Control Processing." In *Proceedings of Advanced Coal-Fired Power Systems '96 Review Meeting*, Morgantown Energy Technology Center, Morgantown, WV, July.

Jalan, V. 1985. "High-Temperature Desulfurization of Coal Gases." In *Acid and Sour Gas Treating Processes*, Gulf Publishing Co., Houston, TX, Nov. 7.

Jothimurugesan, K., S.K. Gangwal, R. Gupta, and B.S. Turk. 1997. "Advanced Hot-Gas Desulfurization Sorbents." In *Proceedings of 1997 FETC Power Systems and Environmental Control Contractor's Meeting*, Pittsburgh, PA, July.

Khare, G.P., G.A. Delzer, G.J. Greenwood, and D.H. Kunbicek. 1996. "Phillips Sorbent Development for Tampa Electric and Sierra Pacific." In *Proceedings of Advanced Coal-Fired Power Systems '96 Review Meeting*, Morgantown Energy Technology Center, Morgantown, WV, July.

Meijer, R., F.J.J.G. Janssen, G.L. Faring, and J.W. H. Hellendoorn. 1996. "KEMA's Hot Gas Cleanup Process." *In Proceedings of 3rd International Symposium on Gas Cleaning at High Temperature*. University of Karlsruhe, Karlsruhe, Germany, September.

NOVEM. 1991. "System Study High Temperature Gas Cleaning at IGCC Systems." Netherlands Agency for Energy and the Environment.

Portzer, J.W., and S.K. Gangwal. 1995. "Slipstream Testing of Hot Gas Desulfurization with Sulfur Recovery." In *Proceedings of the Advanced Coal-Fired Power Systems '95 Review Meeting*, pp. 220-228. DOE/METC-95/1018, Vol. 1, NTIS/DE 95009732. Springfield, VA: National Technical Information Service.

Portzer, J.W., B.S. Turk, and S.K. Gangwal. 1996. "Durability Testing of the Direct Sulfur Recovery Process." In *Proceedings of the Advanced Coal-Fired Power Systems Review Meeting July 16 B18, 1996*. (CD-ROM). U.S. Department of Energy. Morgantown, WV.

Sugitani, T. 1989. Development of Hot-Gas Desulfurization Process. *Journal of the Fuel Society of Japan* 68(9):787.

Thambimuthu, K.V. 1993. Gas Cleaning for Advanced Coal-Based Power Generation. Report by IEA Coal Research, IEACR/53, London, UK.

Appendix

Process Modeling of Hot-Gas Desulfurization

Steve C. Kozup
George W. Roberts
North Carolina State University

TABLE OF CONTENTS

LIST OF TABLES

LIST OF FIGURES

EXECUTIVE SUMMARY

This report summarizes the process simulation work and economic evaluations that were done under contract to Research Triangle Institute to aid in the design of hot gas desulfurization (HGD) processes. Two processes were evaluated for the removal of sulfur (as H_2S) from coal gas at high temperatures, that produce elemental sulfur as a byproduct. Complete mass and energy balances were accomplished for the Direct Sulfur Recovery Process (DSRP) -based process, for various feed conditions. The Advanced Hot Gas Desulfurization Process (AHGP) was also simulated for various feed conditions. ASPEN PLUS 9.3-1 was used for simulating the processes. The mass and energy balances were used in determining the equipment requirements. Equipment requirements were used for the estimation of capital costs and yearly operating costs.

The technical feasibility of the two processes was briefly evaluated. Operating the DSRP is less complicated than operating the AHGP. The AHGP contains a SO_2 loop that is balanced by reactions that consume and generate SO_2. The reaction that consumes SO_2 is equilibrium limited, and its equilibrium fractional conversion varies substantially over the range of possible reactor temperatures.

The economic evaluation shows that the AHGP has higher capital costs than the DSRP. However, the savings the AHGP provides with lower operating costs makes it the more attractive process. The economics in this report use two key assumptions: that there is a market credit for recovered elemental sulfur, and that the coal gas consumed by the HGD has an operating cost equal to the cost of the electricity that could have been generated from it. Using these and other assumptions, the analysis shows that, after only two years the AHGP should make up for its higher capital cost. After four years, AHGP could save millions over the DSRP (savings depend on plant size and the coal's sulfur concentration).

I. INTRODUCTION

1. Background

Integrated gasification combined cycle (IGCC) power plants gasify coal and then combust the coal gas to generate power. All new power plants are required to meet federal SO_X emission limitations, currently limited to 1.2 lbs per million BTU (Jaffee). Hot-gas desulfurization (HGD) removes sulfur from coal gas before combustion. HGD has the potential of reducing the cost of electricity (COE) in IGCC plants, compared to conventional liquid absorption desulfurization.

IGCC plants gasify coal using steam and either air or oxygen. The coal gas is then combusted and passes through a gas turbine, generating power. The hot exhaust gas from the turbine is then used to generate steam, which is used for additional power generation. Coal gas is produced at high temperatures and high pressures (HTHP), typically 450 to 800°C and 145 to 580 psia (Gangwal). HGD reduces the coal gas sulfur content before combustion while maintaining the coal gas at HTHP conditions. Currently, IGCC plants remove sulfur with liquid phase scrubbing. The scrubbing process cools the coal gas stream below 150°C. The temperature drop reduces thermal efficiency and limits the potential electricity cost reduction that is theoretically possible with IGCC power plants. IGCC power plants using liquid phase scrubbing have COE's equivalent to those of pulverized coal-based power plants (Gangwal). HGD would give IGCC power plants a competitive advantage. Implementing HGD will increase thermal efficiency, reduce the COE, and ensure SO_2 emissions are acceptable.

Another benefit of HGD is that the sulfur removed from the coal gas would be recovered as elemental sulfur, a valuable byproduct and easily stored material. This report describes work subcontracted to North Carolina State University (NCSU) from Research Triangle Institute (RTI). Two HGD processes that produce elemental sulfur were simulated using ASPEN PLUS 9.3-1. This work contributes to RTI efforts towards developing HGD technology. RTI research and development work includes sorbents development, characterization and a pilot-scale desulfurization testing.

Coal gas HGD and sulfur recovery could also be implemented in non-power producing applications. Although not the focus of this report, coal gas is used in methanation and Fischer-Tropsh synthesis. Methanation and Fisher-Tropsh catalysts require H_2S concentrations below 1 ppm (Cusumano) because H_2S and SO_2 poison catalysts with the formation of elemental sulfur.

2. Sulfur Production

The main purpose of the two desulfurization processes investigated is to remove sulfur from the coal gas prior to combustion, thereby reducing stack emissions. An advantage of these two processes is that elemental sulfur, which has commercial value, will be generated. Such "recovered sulfur" has been steadily replacing Frasch sulfur as a sulfur source (Figure 1). Frasch sulfur is obtained by drilling into sulfur deposits and injecting hot water, pushing molten sulfur to the surface.

Figure 1: U.S. Sulfur Production

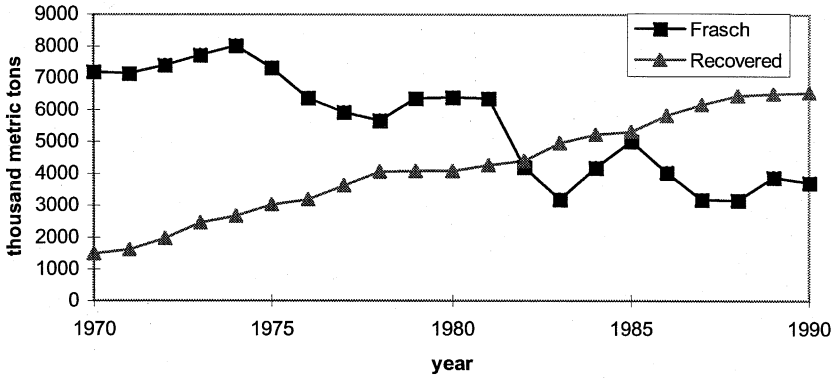

-Data from U.S. Geological Survey

Sulfur is used in both industrial and agricultural applications. In the U.S., the majority of sulfur is used for agricultural purposes (U.S. Geological).

Recovered sulfur can be sold for $50 to $150/ton (Caruanan). Since sulfur purification was not modeled, a $50/ton credit was assigned to the recovered sulfur for the economic evaluation.

II. BASIC PROCESS DESCRIPTIONS

Two distinct desulfurization processes where simulated, the Direct Sulfur Recovery Process (DSRP) -based process and the Advanced Hot-Gas Process (AHGP). A complete collection of process flowsheets and stream summaries is contained in Appendix E. The defining characteristic of the DSRP -based process is that a slipstream of clean coal gas is used to produce the elemental sulfur from an intermediate regeneration off-gas stream containing sulfur dioxide (SO_2). The defining characteristic of AHGP is that a SO_2 stream (in a recycle loop) is used to regenerate the sorbent and produce elemental sulfur. Base case simulations for both HGD processes, referred to as "DSRP" and "AHGP", have 0.85 mol% H_2S in the coal gas feed. Both base cases also generate 260 MW from the clean coal gas. Simulations that deviate from the base cases use suffixes to denote the changes. Table 1 displays the significance of the suffixes. In all cases the coal gas feed pressure is 275 psia and its temperature is 482°C. Simulations changes were strongly dependent on the quantity of sulfur removed from the coal gas. There is little distinction between HGD processes deviating the total sulfur removal by changing H_2S concentration and those changing sulfur removal by varying the power production.

Table 1: Coal Gas Characteristics of Simulations

Simulations	H_2S Feed Molar Concentration	MW Produced
DSRP, AHGP (base cases)	0.85 %	260
DSRP-**b**, AHGP-**b**	**2.50 %**	260
DSRP-**c**, AHGP-**c**	**0.25 %**	260
DSRP-**100**, AHGP-**100**	0.85 %	**110**
DSRP-**500**, AHGP-**500**	0.85 %	**540**

Table 2 shows the composition and flow rate of the "raw" coal gas feed to the base case HGD processes. After sulfur is removed from the streams the coal gas can produce 260 MW.

Table 2 : Raw Coal Gas Feed to Base Case Simulations

Component	DSRP (lb/hr)	AHGP (lb/hr)
H_2S	6,300	6,100
H_2O	70,500	69,000
H_2	11,800	11,500
CO	218,200	213,400
CO_2	117,400	114,800
N_2	36,300	35,500
Total	460,500	450,500

1. Direct Sulfur Recovery Process Sorbent Cycle

The term DSRP, strictly speaking , refers only to that part of the entire HGD process that produces elemental sulfur. For convenience, the process simulations were made by assuming a kind of "generic" process (Figure 2) utilizing a ZnO sorbent, with Al_2O_3 support, to remove sulfur (present in the form of H_2S) via reaction 1. The reader should note that in this report "DSRP" is often used as shorthand for the entire "DSRP-based HGD process," while the novel DSRP reactions to form elemental sulfur occur in what this report refers to as the "DSRP Reactor." Reaction 1 occurs in the desulfurization reactor (DESULF, Figure 2).

$$ZnO + H_2S \rightarrow ZnS + H_2O \qquad (1)$$

The spent sorbent is regenerated in an oxidizing environment, forming SO_2. Reaction 2 occurs in the regenerator reactor (REGEN, Figure 2), it is driven to completion by oxygen.

$$ZnS + 3/2\ O_2 \rightarrow ZnO + SO_2 \qquad (2)$$

The SO_2 exits the regenerator in a stream designated regenerator off-gas (ROG). The ROG flows to the DSRP Reactor. A slipstream of clean coal gas is also fed to the DSRP Reactor. The H_2 and CO in the coal gas slipstream participate in catalyzed reactions (3 and 4), converting SO_2

into elemental sulfur. The reactions 3 and 4 are the simplified overall reactions of a more complex series of reactions.

$$H_2 + 1/2\ SO_2 \rightarrow H_2O + 1/4\ S_2 \qquad (3)$$

$$CO + 1/2\ SO_2 \rightarrow CO_2 + 1/4\ S_2 \qquad (4)$$

The heats of reaction for converting SO_2 to elemental sulfur have been calculated by RTI (Portzer, 1996). Comparing RTI calculated values with experimental results indicated the RTI values were reasonable. Table 2 shows that ASPEN calculated heats of reaction are in general agreement with those calculated by RTI. The ASPEN model does an accurate job determining the heat evolved during reactions and therefore will predict correct heat transfer requirements in the process simulations.

Table 3: Heats of Reaction Calculated by RTI and ASPEN Model

Reaction	Temp (°C)	ΔH_{RTI} (BTU/mole)	ΔH_{ASPEN} (BTU/mole)	difference
3	550	- 28,000	- 28,700	2.5 %
3	650	- 28,300	- 29,000	2.5 %
3	750	- 28,600	- 29,200	2.1 %
4	550	- 43,900	- 44,100	0.5 %
4	650	- 43,700	- 44,000	0.7 %
4	750	- 43,800	- 43,600	0.5 %

-Heat of reaction values adjusted to match stoichiometry written, P=300 psig for calculations

2. Sorbent Composition - DSRP

The oxidized sorbent, a mixture of ZnO and Al_2O_3, was assumed to contain 15 wt% zinc metal. This distribution is based on an assumed, "generic" sorbent defined by RTI, and results in an oxidized sorbent containing 18.671 wt% ZnO with the balance as inert Al_2O_3 support. While developing the process model and adjusting the stream flow rates to achieve the desired heat balance, it became desirable to increase sorbent circulation rates above the stoichiometric requirements. For these models, the ratio of Zn to Al remained unchanged. The excess Zn sorbent circulating through the system was assumed to remain in the sulfide state (ZnS).

DSRP - based Desulfurization

12/20/97 DSRP

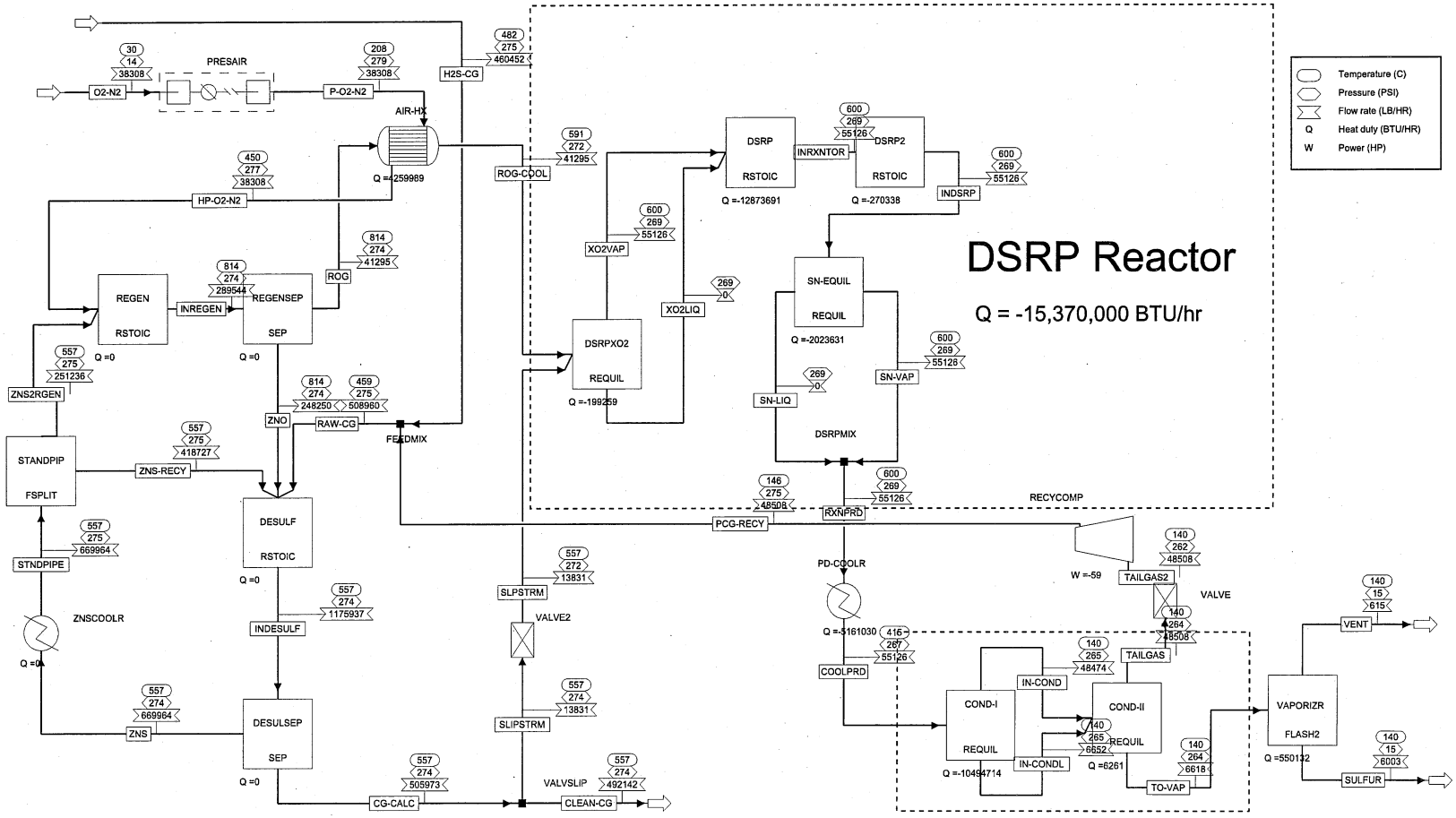

High Pressure Condenser Q = -10,500,000 BTU/hr

3. Advanced Hot Gas Process Sorbent Cycle

The AHGP (Figure 3) uses a sorbent containing a mixture of ZnO and Fe_2O_3 on Al_2O_3 support for removing H_2S from the coal gas and converting it into elemental sulfur. Both zinc and iron components react with the H_2S present in the coal gas. The desulfurization reactions are represented below.

$$ZnO + H_2S \rightarrow H_2O + ZnS \qquad (5)$$

$$Fe_2O_3 + 2\,H_2S + H_2 \rightarrow 2\,FeS + 3\,H_2O \qquad (6)$$

The sulfided sorbent is sent to a three-stage regenerating reactor that reoxidizes the sorbent and generates elemental sulfur. Sorbent and a SO_2 gas stream flow counter-currently through the regenerator (Figure 3) (Figure 6). The sorbent enters the regenerator at the HX-STAGE (the third and highest elevated stage) where the sorbent is heated by the effluent gas stream. Sorbent descends to REGEN2 (the second stage) where SO_2 , present in great excess, oxidizes the majority of the FeS sorbent.

$$3\,SO_2 + 4\,FeS \rightleftharpoons 7/2\,S_2 + 2\,Fe_2O_3 \qquad (7)$$

It has been assumed that two-thirds of the FeS oxidizes in REGEN2. Calculated equilibrium conversions for reaction 7 are listed in table 4. Sorbent enters the second stage of the regenerator at 512°C and gas enters the second stage at 715°C. Table 3 shows equilibrium conversions varies significantly over the range of temperatures possible in stage 2, a stage for which it is unclear what value represents its temperature the best. Simulated stage 2 exit temperatures were 580°C, this exit temperature assumes perfectly mixed behavior in the stage 2. In reality there will likely be higher temperatures at lower elevations in the stage. The ASPEN model uses an RSTOICH block to simulate this stage so that the conversion can be arbitrarily fixed at 67%. This value was defined by RTI, based on experimental data. The information in Table 4 suggests that the assumed two-thirds conversion probably overestimates the actual conversion. In commercial practice, increasing the Fe:Zn ratio could compensate for lower than simulated reaction 7 conversions (conversion written in terms of FeS). Another aspect of this reactor stage is that the

extent that FeS oxidizes by SO_2 will vary with temperature fluctuations and increase the difficulty in balancing SO_2 consumption and generation.

Table 4: Equilibrium Conversion for FeS Oxidation by SO_2

Regenerator Temperature (°C)	Equilibrium Fractional Conversion
500	0.43
550	0.53
600	0.65
650	0.77
700	0.90

Equilibrium calculated from ASPEN REQUIL block, P = 275 psia

Sorbent oxidization approaches completion in the bottom regenerator stage (REGEN1, Figure 3). REGEN1 oxidizes the sorbent using pure oxygen (reactions 8 and 9). The oxidation generates SO_2, making up for SO_2 used in reaction 7.

$$7/2\ O_2 + 2\ FeS \rightarrow 2\ SO_2 + Fe_2O_3 \qquad (8)$$

$$3/2\ O_2 + ZnS \rightarrow SO_2 + ZnO \qquad (9)$$

This modeling assumes that SO_2 does not oxidize sorbent in REGEN1, since equilibrium conversion for SO_2 oxidation is approached in REGEN2. The equilibrium regeneration of sorbent by SO_2 will be quickly superseded by oxygen regeneration.

4. Sorbent Composition - AHGP

AHGP sorbent composition was defined by RTI to contain 3 wt% Zn and 12 wt% Fe, which corresponds to 3.734 wt% ZnO and 17.154 wt% Fe_2O_3. The balance, 79.109 wt%, was inert Al_2O_3. As discussed above, the ratio of Fe to Zn will need to be increased if the actual conversion for reaction 7 is lower than 0.667, its assumed value.

AHGP Advanced Hot Gas Process

AHGP 1/19/98

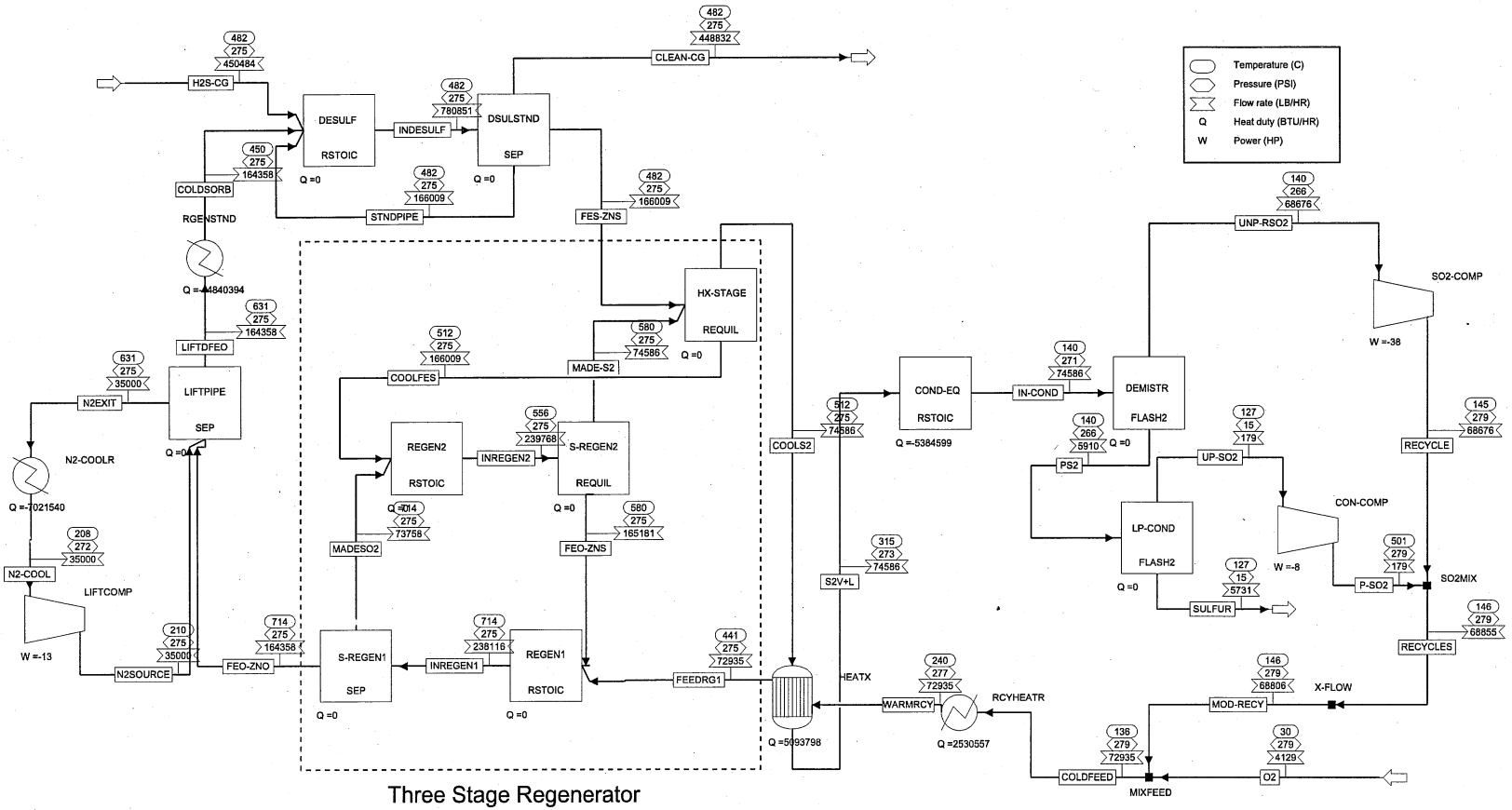

Three Stage Regenerator

During subsequent simulation development and adjustment of stream flow rates to achieve the desired heat balance, it became apparent the defined sorbent composition was not optimal. To run the reactors adiabatically, it was necessary to increase sorbent flow. Circulating more sorbent increased the heat capacity of the reactive stream and reduced the adiabatic temperature rise. Such a sorbent increase required an increase in Al_2O_3 flow. Increasing Fe or Zn flow would have upset the SO_2 generation and consumption balance created by reactions 7, 8 and 9. Therefore, alumina flow was increased. The effect would be the same as adding pure alumina sorbent to the reactor system, or by manufacturing a sorbent that has a lower active metal content and increasing the total flow to match the amount of alumina added.

The Al_2O_3 circulation was increased until an adiabatic regenerating reactor would operate below 716°C. The effects of changing Al_2O_3 circulation ripple through the process. The required SO_2 circulation rate was affected by varying the Al_2O_3 flow. The desired SO_2 volumetric flow rate increased with increasing sorbent flow rate because of increased reactor size. Increasing the SO_2 circulation helped reduce the adiabatic temperature rise, lessening the need to increase sorbent flow. Table 5 shows how Al_2O_3 flow was increased until an acceptable adiabatic regeneration temperature was achieved. The table displays the stepwise approach used to determine the Al_2O_3 circulation needed in the AHGP-b simulation (-b signifies a 2.5 mol% H_2S in the feed). In the simulation, ZnS and FeS flow rates (leaving the desulfurization reactor) were constant at 7,600 lb/hr and 41,000 lb/hr, respectively.

Table 5: Al_2O_3 Circulation Rate Effect on Regenerator Stage 1 Temperature

Al_2O_3 (lb/hr)	T_{REGEN1} (°C)	Desired SO_2 flow (ft^3/hr)
165,297	1025	102,000
330,594	787	181,000
400,000	759	214,000
450,000	715	238,000

III. PHYSICAL PROPERTIES

1. Equation of State

All simulations discussed in this report used the Peng Robinson cubic equation of state with the Boston-Mathias alpha function (PR-BM).

1.a. *Equation of State's Importance*

Modeling unit operations requires physical property information for all compounds present. In calculating thermodynamic equilibrium, fugacity coefficients are used to determine phase equilibrium. An equation of state can be used for the calculation of fugacity, as well as other important physical properties. The equation of state also relates pressure, temperature, and molar volume so that only two need to be specified and the third can be calculated. Phase equilibrium is established when the fugacity of each component is the same in all phases.
A two-phase (vapor and liquid) system is at equilibrium when:

$$f^{v}_{i} = f^{l}_{i} \qquad i = 1,2,...N \text{ where N is the number of compounds}$$

Where:

f^{v}_{i}	=	$\varphi^{v}_{i} y_i P$	Fugacity of component *i* in the vapor phase
f^{l}_{i}	=	$\varphi^{l}_{i} x_i P$	Fugacity of component *i* in the liquid phase

$$\ln \varphi^{\alpha}_{i} = -\frac{1}{RT}\int_{\infty}^{V^{\alpha}} \left[\left(\frac{\partial P}{\partial n_i} \right)_{T,V,n_{i \neq j}} - \frac{RT}{V} \right] dV - \ln Z^{\alpha}_{m}$$

Notation:

α	=	vapor or liquid (v or l)	P	=	Pressure
n_i	=	Mole number of component *i*	T	=	Temperature
x_i	=	Liquid mole faction of component *i*	R	=	Gas Constant
y_i	=	Vapor mole faction of component *i*	V	=	Total volume
Z	=	Compressibility factor			

The equation of state also is used to determine other properties via departure functions.

- Enthalpy departure:

$$(H_m - H_m^{ig}) = -\int_{\infty}^{V}\left(P - \frac{RT}{V}\right)dV - RT\ln\left(\frac{V}{V^{ig}}\right) + T(S_m - S_m^{ig}) + RT(Z_m - 1)$$

- Entropy departure:

$$(S_m - S_m^{ig}) = -\int_{\infty}^{V}\left[\left(\frac{\partial P}{\partial T}\right)_V - \frac{R}{V}\right]dV + R\ln\left(\frac{V}{V^{ig}}\right)$$

- Gibbs Free Energy departure:

$$(G_m - G_m^{ig}) = -\int_{\infty}^{V}\left(P - \frac{RT}{V}\right)dV - RT\ln\left(\frac{V}{V^{ig}}\right) + RT(Z_m - 1)$$

Notation:

H = Enthalpy S = Entropy G = Gibbs Free Energy

ig (superscript) denotes variable's value for ideal gas

m (subscript) denotes variable's value for the mixture

1.b. *Selection*

The Peng Robinson cubic equation of state with the Boston-Mathias alpha function (PR-BM) was used in these simulations because it was recommended for gas-processing, refinery, and petrochemical applications (ASPEN PLUS- Reference Manual 2). It was recommend for modeling nonpolar and mildly polar mixtures, including hydrocarbons and light gases like: carbon dioxide, hydrogen sulfide, and hydrogen. Reasonable results can be expected for all temperatures and pressures. The Peng-Robinson equation of state is:

$$P = \frac{RT}{V_m - b} - \frac{a}{V_m(V_m + b) + b(V_m - b)}$$

Variables 'a' and 'b' account for attractive forces and the space occupied by all species present, R is the ideal gas constant, T is temperature and V_m is the mixture's specific molar volume.

The Boston Mathias extrapolation is used for supercritical components. Boston and Mathias derived an alpha function that is particularly good at modeling decreasing attraction between molecules at high temperatures (ASPEN PLUS- Reference Manual 2).

The above descriptions also apply to the Redlich-Kwong-Soave cubic equation of state with Boston-Mathias alpha function (RKS-BM). The decision to use the PR-BM over RKS-BM was made after comparing literature phase data (Braker) with simulations using both property option sets. Figure 4 shows the fractional deviation of simulated vapor pressures compared to literature values. Both equations of state calculate values in good agreement with actual values, and the Peng-Robinson equation of state gives the best results.

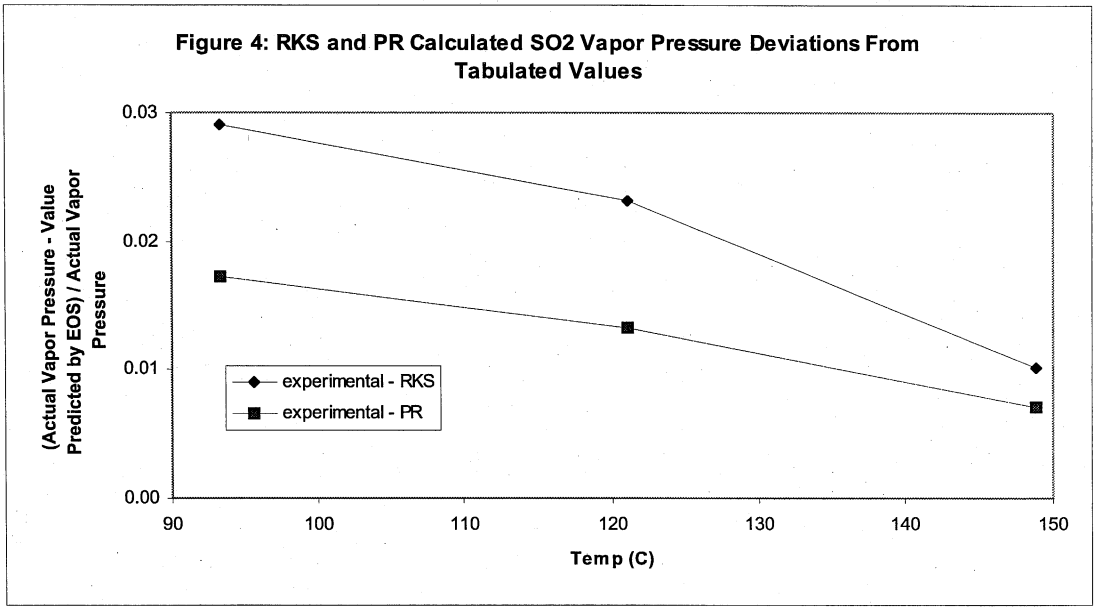

2. Elemental Sulfur

Accurately predicting elemental sulfur properties requires knowing which allotropes of sulfur will be formed. For the conditions occurring in the HGD process S_8, S_6, and S_2 are the predominant allotropes (Barnett; Cotton). Temperature is the dominant variable affecting the equilibrium sulfur distribution. The ASPEN simulations concurred with literature distributions, predicting S_2 predominance at high temperatures (reactor temperatures), and a shift towards S_8 and S_6 at lower temperatures (condenser temperatures). Accurate sulfur distributions are important for the integrity of phase equilibrium predictions. In addition, correctly simulating sulfur equilibrium increases the accuracy of energy balances.

It is worth noting some unusual properties of liquid elemental sulfur. Recovered sulfur should not be raised to temperatures above 159°C, as above that temperature the liquid sulfur becomes increasingly viscous (Cotton). Sulfur melts around 114°C; it does not have a sharp melting point due to the presence of various allotropes (Barnett).

IV. EQUIPMENT

1. DSRP- Based Process Equipment

For the purposes of this process simulation and economic evaluation, the DSRP - based HGD process was defined to have a desulfurization and regeneration transport reactor network as shown in Figure 5. Sulfur is removed from coal gas (Reaction 1) in the desulfurization reactor and sorbent regeneration (Reaction 2) takes place in the regeneration reactor. There is also a DSRP Reactor in which the elemental sulfur is formed via Reactions 3 and 4. Other major pieces of equipment in the DSRP include compressors, condensers, and heat exchangers.

$$ZnO + H_2S \rightarrow ZnS + H_2O \quad (1)$$

$$ZnS + 3/2\ O_2 \rightarrow ZnO + SO_2 \quad (2)$$

$$H_2 + 1/2\ SO_2 \rightarrow H_2O + 1/4\ S_2 \quad (3)$$

$$CO + 1/2\ SO_2 \rightarrow CO_2 + 1/4\ S_2 \quad (4)$$

In addition to Reactions 3 and 4, intermediate and side reactions occur in the DSRP Reactor. They are discussed later in the report.

1.a. *Desulfurization and Regeneration Transport Reactors - DSRP*

The DSRP - based HGD process is assumed to use transport reactors for the desulfurization and regeneration reactions. The Sierra Pacific hot-gas desulfurization system (Cambell) has been the basis for the reactor system design (Figure 5). Cyclones separate the sorbent from the exiting gas streams. Sorbent settles from the cyclones into standpipes. The sorbent has a relatively high residence time in the standpipes. Standpipe residence times are several minutes while reactor residence times are only several seconds long. Standpipe heat exchangers remove heat from the reactor system. During startup, sending steam through the standpipe heat exchanger could heat the sorbent partially up to reactor temperatures.

The regeneration reaction releases a substantial amount of heat. Feeding a stoichiometric amount of sorbent in the ASPEN simulation to an adiabatic regeneration reactor results in predicted temperatures surpassing 1,000°C (DSRP base case). RTI guidelines stated that HGD sorbents would experience substantial sintering at temperatures above 815°C. The strategy adopted to control reactor temperature is recycling excess sorbent. The additional sorbent increases the total heat capacity of the reactive streams. The additional sorbent will not result in additional reactions and the increased heat capacity will decrease the adiabatic temperature rise. The adiabatic temperature rise can be expressed by the following relationship:

$$\Delta T_{adiabatic} \approx \frac{\Delta H_{rxn}}{Cp_{stream}}$$

Increased sorbent flow was selected as the preferred strategy over that of using a reactor heat exchanger, since it simplifies reactor design. Furthermore, hot spots are more likely to occur in a reactor containing a heat exchanger. Limiting reactor temperature by reducing reactor feed stream temperatures (without additional sorbent circulation) was also investigated. This approach was discarded because the reactions would be extinguished at feed temperatures low enough to keep the reactor temperature below 815°C.

Figure 5: Schematic of DSRP - Based HGD Process Desulfurization and Regeneration Reactors

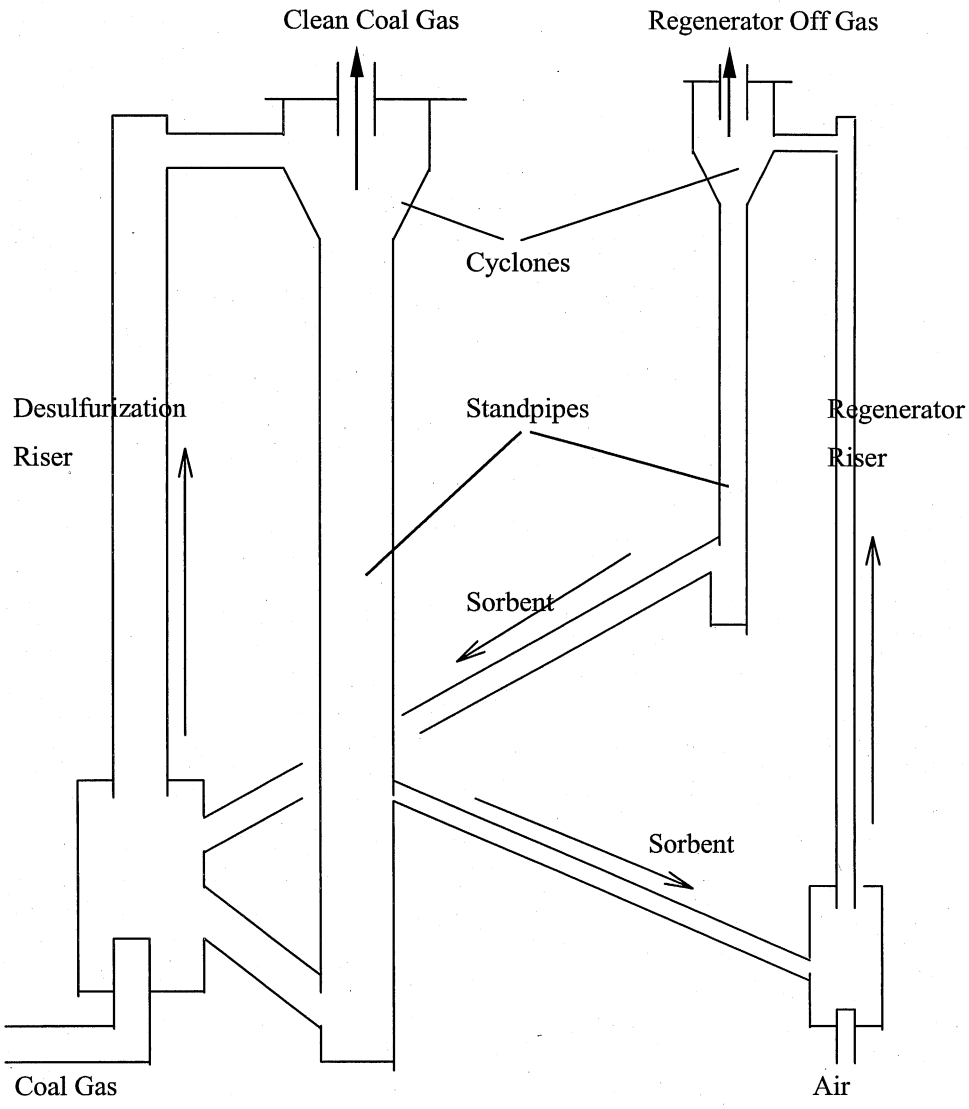

The transport reactors exhibit numerous advantages over fixed-bed, fluid-bed and moving-bed reactors. The transport reactor has lower capital cost, its high flowrate of sorbent controls reactor temperatures, and the high velocities prevent hot spots from occurring on the sorbent (Campbell). The transport reactor's superior temperature control allows undiluted air to be used during regeneration.

The equations used for sizing and costing the DSRP - based process desulfurization and regeneration transport reactor system are described in Appendix G-Calculation of Reactor Size. The actual calculations can be found in Appendix H-Sizing Reactors for the DSRP.

1.b. *DSRP Reactor - DSRP*

The DSRP Reactor itself is a fast fluidized bed reactor with its catalyst modeled as Al_2O_3. There are several ASPEN blocks used to model what will be only one DSRP Reactor, a dashed box has been drawn around the series of blocks used (Figure 2). The catalyst is circulated through the reactor and an external heat exchanger. Heat is removed by cooling the catalyst while it is outside the reactor. The heat exchanger cools the catalyst to 500°C and the catalyst is then reintroduced to the reactor at a rate that is high enough to keep the DSRP Reactor effluent near 600°C. (Appendix D- Calculation of DSRP Catalyst Cycling Rate)

Figure 2 shows that several blocks were used for the simulation of the DSRP Reactor: DSRPXO2, DSRP, DSRP2, and SN-EQUIL.

In DSRPXO2, any oxygen that enters the DSRP as a contaminant in the ROG consumes coal gas by a conventional combustion reaction. The oxygen combines with CO forming CO_2. It is not necessary to model combustion of H_2 since the ratio of CO to H_2 will be set by the Water Gas Shift (WGS) reaction. Also in DSRPXO2 the WGS reaches equilibrium. The WGS reaction is known to reach equilibrium before the reactions of SO_2 with H_2 or CO begin (Chen,

1994). DSRPXO2 uses a Gibbs Free Energy calculation to establish equilibrium for reactions 10 and 11.

DSRPXO2	$CO + 1/2\ O_2 \rightarrow CO_2$	$X_{O2} = 1$	(10)
	$H_2O + CO = CO_2 + H_2$	$K_C(600^\circ C) = 2.6$	(11)

The key DSRP reactions have been modeled in the following blocks.

DSRP	$2\ H_2 + SO_2 \rightarrow 0.5\ S_2 + 2\ H_2O$	$X_{H2} = 0.99$	(3)
	$3\ CO + SO_2 \rightarrow COS + 2\ CO_2$	$X_{CO} = 0.9995$	(12)
	$H_2 + 0.5\ S_2 \rightarrow H_2S$	$X_{H2} = 0.01$	(13)
DSRP2	$SO_2 + 2\ COS \rightarrow 1.5\ S_2 + 2\ CO_2$	$X_{COS} = 0.9999$	(14)

SN-EQUIL establishes the allotropic distribution of elemental sulfur using a Gibbs Free Energy calculation. Including this block more accurately models the heat generated inside the DSRP Reactor.

SN-EQUIL	$4\ S_2 \rightarrow S_8$	$X_{S2} = 0.23$	(15)
	$3\ S_2 \rightarrow S_6$	$X_{S2} = 0.32$	(16)

1.c. *PRESAIR - DSRP*

The transport reactor design for the regenerator in the DSRP - base HGD process model allows the use of undiluted air ("neat air") to regenerate the desulfurization sorbent. Introducing air at the required pressure can be accomplished using either an axial-flow or centrifugal compressor. In most applications, including this process simulation, it is preferable to use a centrifugal compressor. Centrifugal compressors have the advantage of a larger operating range (Dimoplom). Centrifugal compressors typically operate below 225°C (Brown; Dimoplon) in order to avoid equipment damage.

The large increase in pressure (ambient to 275+ psia) in the PRESAIR air compressor generates a considerable temperature rise. Interstage cooling, between the compressor's 6 stages, is necessary to maintain an air temperature below 225°C and to prevent mechanical damage to the compressor (Brown; Dimoplon). The temperature increase across the first stage does not require cooling stage 1 effluent and there is no need to cool the effluent of the final stage as well. Therefore, there will be four interstage coolers needed for the six-stage compressor. Pressure drop during interstage cooling can be approximated as 2% of the pressure entering the cooler or 2 psia, whichever is larger (Brown). For pressuring to 280 psia estimating a 2 psia drop for each cooler is reasonable; these pressure losses are included in the ASPEN PLUS compressor block calculations.

Significant capital will be spent on the purchase of an air compressor. Increasing pressure to 280 psia for an feed of 8,800 ft^3/min (DSRP base case) requires a compressor made of steel as opposed to cast iron (Bloch). Compressors made of low value steel should be both mechanically durable and economical. For simplicity, the cost estimates in this report assume electric drive.

Steam turbines could drive the compressors. Steam turbines are historically the most popular means of driving centrifugal compressors. They have the ability to operate over a wide speed range. Electric motors have experienced increasing favor due to a typically lower operating cost. Buying electricity is more economical than small scale steam generation for a specific piece of equipment (Brown). However, with the desulfurization processes generating steam and with steam available from the power plant, a steam turbine may be the best means of driving the compressors.

Air Compressor Costs

Compressor costs were determined from a budgetary quotation obtained from Ingersoll-Rand. Ingersoll-Rand stated a cost of $241,000 for the Centac Model 2CV23M3EEPF. This model Centac is a centrifugal air compressor (drive and motor) capable of raising 2,250 acfm to

280 psia. Extrapolation was used to determine the cost of compressors needed for the different flow rates. Figures in Peters and Timmerhaus (1991) were used to determine the rate at which compressor costs change with varying flow rates.

The compressor, PRESAIR, is modeled as a six stage compressor. It has been assumed that the interstage coolers lower the air temperature to 115°C. Calculation of stage efficiency was performed using a procedure outlined in Brown (1986). The polytropic efficiencies calculated range from 0.65 to 0.787, which are consistent with other values found in literature (Brown; Dimoplon). PRESAIR pressurizes 8,800 acfm (in the DSRP base case); for such a flow ASPEN predicts a 3,280 HP power requirement. Directly scaling up the Centac (2,250 acfm, 800 HP) compressor predicts a 3,130 HP power requirement. The similar horsepower requirements suggest that ASPEN is realistically simulating the air compressor.

1.d. *RECYCOMP - DSRP*

The compressor RECYCOMP repressurizes the vapor stream leaving the sulfur condenser (the tailgas of the DSRP reaction) and sends it back to the desulfurization reactor. Recycling this stream eliminates an emissions stream while causing a minor load increase for the reactor network. The pressure increase between the condenser and the desulfurization reactor should be within the capabilities of a single stage centrifugal compressor, and RECYCOMP was modeled as such.

1.e. *High Pressure Condenser - DSRP*

The High Pressure Condenser condenses sulfur out of the DSRP Reactor effluent stream. It is high pressure in the sense that it operates near the pressure of the DSRP Reactor. Reducing the temperature to 140°C condenses the sulfur. At this temperature, the vast majority of sulfur condenses, and there is no risk of freezing.

The High Pressure Condenser is simulated using two blocks (Figure 2). The first, COND-I, is an equilibrium block that establishes equilibrium between S_2 and S_8. At high temperatures like those in the DSRP reactor, sulfur is predominately in the S_2 form (Barnett; Chen; Cotton). At the cooler condensation temperatures, the S_8 and S_6 sulfur species predominate. The second block, COND-II, establishes equilibrium between the S_8 and S_6 sulfur species and phase equilibrium. The S_8 and S_6 sulfur species are easier to condense. Calculation of the sulfur equilibrium, in addition to more accurately simulating the phase equilibrium, also increases the accuracy of the heat transfer requirements. The low temperature in the condenser makes it unsuitable for the direct production of high pressure steam. The condenser could be used to preheat the feedwater to other steam-generation units (Appendix F).

1.f. *VAPORIZR - DSRP*

Reducing the sulfur product stream's pressure to ambient will cause the water present in the stream to vaporize. The vaporizing water can cool the sulfur stream enough to cause freezing. The VAPORIZR accomplishes three tasks: a) it reduces sulfur pressure to ambient; b) it supplies heat to the sulfur stream so that the temperature will be maintained at 140°C and sulfur will remain molten; and, c) it also helps purify the product stream by removing water from the sulfur.

1.g. *PD-COOLR - DSRP*

Prior to entering the condenser, the DSRP Reactor effluent ("RXNPRD") is sent through the Product Cooler (PD-COOLR) heat exchanger. Cooling the reactor products in this heat exchanger reduces the condenser heat duty and PD-COOLR operates at temperatures suitable for generating high pressure steam. Sulfur condensation inside the PD-COOLR should be avoided. Condensation would create the undesirable situation of two phase flow and would require removing the sulfur during shutdown so that it will not freeze inside the heat exchanger. Operating the PD-COOLR above the product stream's dew point would prevent sulfur condensation. Dew point calculations were made for the various reactor effluent distributions.

The allotropic sulfur distribution (S_2, S_6, S_8) changes with temperature, however the speed at which equilibrium is reached is unknown. It is not known how closely sulfur allotrope distribution will approach equilibrium in the cooler. Therefore, calculations were made for the dew point temperatures at both the equilibrium distribution of sulfur allotropes, and at the allotrope distribution that leaves the reactor (Table 6).

For the simulations, the PD-COOLR was defined to cool reaction products to 415°C. Table 6 shows that at 415°C sulfur condensation will not occur if the sulfur allotrope equilibrium is reached instantaneously (Sulfur Equilibrium = yes) and also will not occur if the sulfur allotrope distribution is still at the DSRP Reactor temperature distribution (Sulfur Equilibrium = no).

Table 6: Dew Point Temperatures for DSRP Product Distributions

Product distribution	Sulfur Equilibrium	Pressure (psia)	Temperature (°C)
DSRP	yes	275	360
DSRP	no	275	405
DSRP-b	yes	275	357
DSRP-b	no	275	402
DSRP-c	yes	275	362
DSRP-c	no	275	406

1.h. *AIR-HX - DSRP*

The AIR-HX heat exchanger utilizes the hot regenerator off gas ("ROG") stream to raise the temperature of the high pressure air stream ("P-O2-N2"). Heating the air is required to achieve a sufficiently high temperature to initiate the regeneration reaction. Cooling the ROG reduces the heat removal required to keep the DSRP reactor at 600°C. The hot (above 800°C) ROG stream contains SO_2. The presence of hot SO_2 requires that the AIR-HX heat exchanger tubes be constructed from type 310 stainless steel (SS 310).

2. AHGP Equipment

The AHGP consists of a desulfurization transport reactor and a 3-stage bubbling bed regeneration reactor. The reactions that remove sulfur from coal gas (Reactions 5 and 6) proceed in the desulfurization reactor. In the regenerator the sorbent is regenerated with SO_2, to generate elemental sulfur (reaction 7), and is subsequently regenerated with O_2 to produce SO_2 (reactions 8 & 9). Forming elemental sulfur during regeneration eliminates the need a for third reactor, as the DSRP based process requires. Other major pieces of equipment in the AHGP include compressors, condensers, a demister, and heat exchangers.

2.a. *Desulfurization and Regeneration Reactors - AHGP*

There are several differences between the AHGP desulfurization and regenerator reactor designs (Figure 6) and those envisioned for the DSRP -based process (Figure 5). For example, in the AHGP sorbent descends counter-currently against the rising SO_2 in the regeneration reactor. Sorbent descending through the regenerator makes it necessary to re-elevate sorbent into a standpipe located upstream of the desulfurization reactor. A heat exchanger in the standpipe enables cooling of the sorbent before it re-enters the desulfurization reactor.

The top stage of the regenerator (HX-STAGE, Figure 3) heats the entering sorbent by direct contact with the exiting SO_2 stream. The second stage of the regenerator is modeled with REGEN2 and S-REGEN2. REGEN2 models the following equilibrium reaction:

$$3\ SO_2 + 4\ FeS = 7/2\ S_2 + 2\ Fe_2O_3 \qquad (7)$$

This equilibrium reaction is modeled with an RSTOICH block, assuming a 0.667 fractional conversion of FeS. An RSTOICH block is used due to the difficulty of balancing SO_2 consumption and generation. As discussed earlier in the report (Section II.4), assuming a 0.667

Figure 6: Schematic of AHGP Desulfurization and Regeneration Reactors

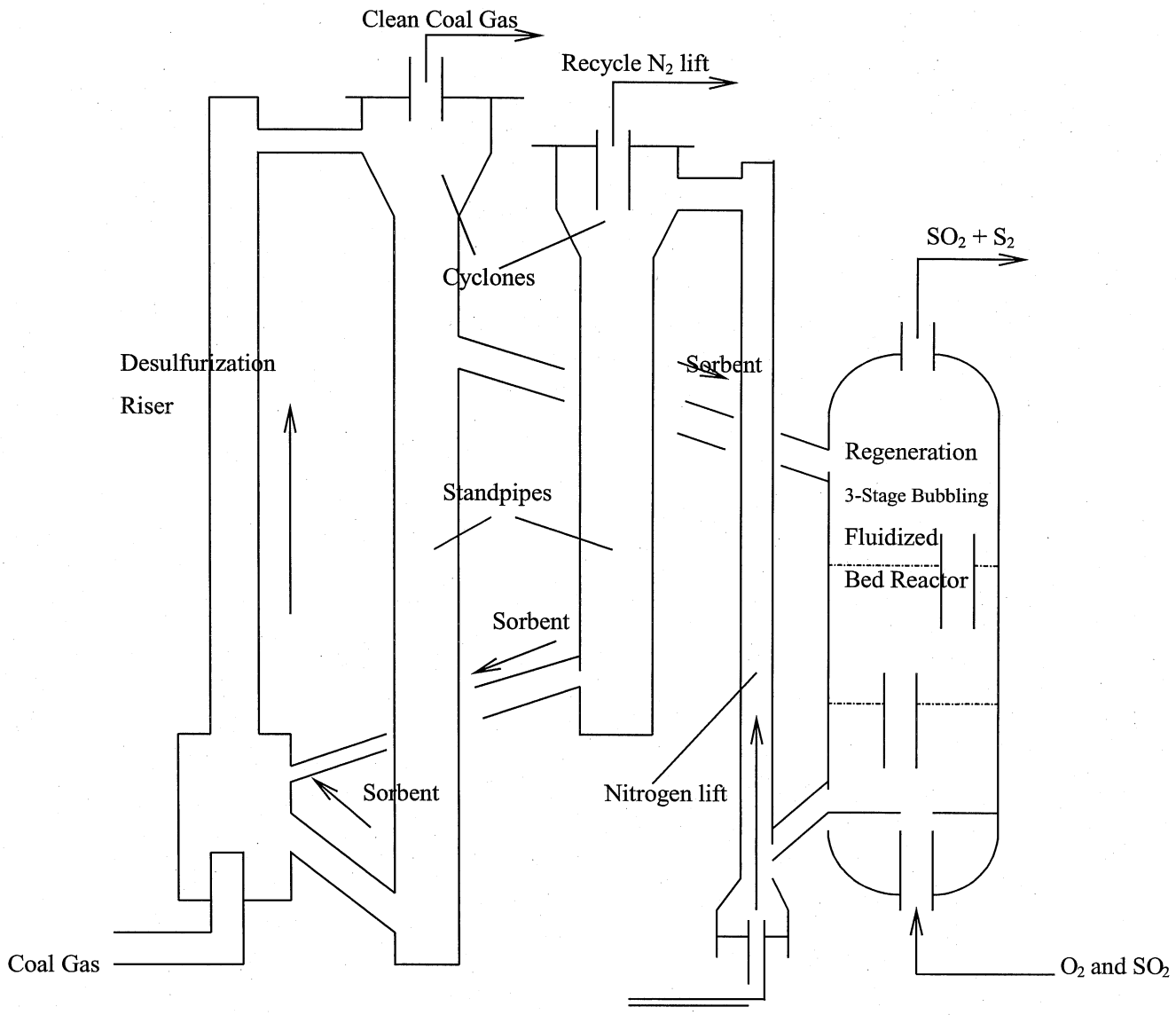

fractional conversion may be an optimistically high assumption. If so, more Fe will need to be circulated to make up for the discrepancy. The S-REGEN2 block establishes the equilibrium distribution of sulfur allotropes.

The bottom stage is modeled with the REGEN1 and S-REGEN1 blocks. Oxygen feed to REGEN1 oxidizes the sorbent. Although there is SO_2 present in large quantities in REGEN1, it is assumed not to oxidize any sorbent. Equilibrium conversion for SO_2 oxidation is assumed to be reached in the second stage. Any unreacted FeS present in the sorbent coming from the second stage is expected to react very quickly with oxygen present (reactions 17 & 18). The ZnS is expected to regenerate less rapidly than the iron compound. Uncondensed sulfur recycling back to REGEN1 will quickly oxidize. These reactions are modeled to occur in the following order:

$$S_8 + 8\,O_2 \rightarrow 8\,SO_2 \qquad (17)$$

$$S_6 + 6\,O_2 \rightarrow 6\,SO_2 \qquad (18)$$

$$2\,FeS + 3.5\,O_2 \rightarrow Fe_2O_3 + 2\,SO_2 \qquad (8)$$

$$ZnS + 1.5\,O_2 \rightarrow ZnO + SO_2 \qquad (9)$$

The bottom stage is simulated to operate with all oxygen being consumed in REGEN1, and a small portion of ZnS remaining unoxidized.

More than one regeneration reactor maybe used in parallel for the AHGP. Sizing the reactor (Appendix I) revealed that to achieve the desired superficial velocity for removing the larger sulfur quantities requires undesirably large reactor diameters (25+ ft). The larger reactor diameters will require thicker reactor walls (4.5+ in) to contain the high pressures. Reactors in parallel reduce reactor diameter and the required wall thickness resulting in less steel required. A maximum reactor diameter of 13 feet was the guideline used during sizing. The 3-stage regenerator heights were set at 45 feet. It is expected that 5 ft will be needed for the heat exchanging stage, 10 ft for the middle stage, and 2.5 ft for the bottom stage. The rest of the reactor height will be used for phase separation.

The equations used for sizing and costing the AHGP desulfurization and regeneration transport reactor system are described in Appendix G-Calculation of Reactor Size. The actual calculations can be found in Appendix I-Sizing Reactors for the AHGP.

2.b. *LIFTCOMP - AHGP*

The AHGP desulfurization - regeneration transport reactor system requires a means of elevating the sorbent exiting the regeneration reactor. This will be accomplished using a nitrogen lift (Figure 3 and Figure 6). LIFTCOMP increases the pressure of the nitrogen recycle before it enters the nitrogen lift. A cyclone and filters placed upstream of LIFTCOMP and N2-COOLR will prevent sorbent from damaging the compressor.

2.c. *SO2-COMP - AHGP*

SO2-COMP recompresses the SO_2 loop. It is advantageous to recompress the SO_2 loop after the condenser because the lower gas temperature will increase the compressor efficiency and reduce wear on the compressor. The pressure increase required will be obtainable using a single stage centrifugal compressor.

2.d. *CON-COMP - AHGP*

The CON-COMP compressor is used to reintroduce the SO_2 that vaporizes when the sulfur stream is reduced to ambient pressures (LP-COND, Figure 3). The small flow rate means a single stage reciprocating compressor can be used to pressure the SO_2 stream. The pulsing flow of SO_2 coming from CON-COMP will not have a significant effect on the large SO_2 loop.

2.e. *COND-EQ - AHGP*

The condenser, COND-EQ, cools down the SO_2 loop so that sulfur can be condensed out. The stream temperature is reduced to 140°C, and sulfur distribution is established in COND-EQ. It was initially intended that sulfur equilibrium would be calculated using a REQUIL block; however, this caused convergence problems. Using the RSTOIC block eliminates the convergence problem and does not compromise the validity of the results. The sulfur equilibrium distribution was determined in a separate simulation.

$$4\ S_2 \text{ --> } S_8 \qquad X_{S2} = 0.98 \qquad (15)$$

$$3\ S_2 \text{ --> } S_6 \qquad X_{S2} = 0.02 \qquad (16)$$

The large vapor stream containing a small volume of molten sulfur will make a demister necessary to isolate the small liquid flow.

2.f. *DEMISTR - AHGP*

The large gas stream of SO_2 will suspend the relatively small flow of condensed sulfur. The demister (DEMISTR) will be necessary for collecting the sulfur. The liquid sulfur accounts for 8 wt% of the stream ("IN-COND"), but only 0.1 vol% of the SO_2 - sulfur flow.

2.g. *LP-COND - AHGP*

Sulfur leaving the demister needs to be brought to ambient pressure for storage. This can be accomplished in a flash tank (LP-COND, Figure 3). The pressure drop vaporizes much of the SO_2 that co-condenses with the sulfur. The temperature drop caused by SO_2 vaporization is not enough to freeze the sulfur. Vaporizing off the SO_2 decreases the sulfur stream temperature to 127°C, well above the melting temperature of sulfur (114°C). The volumetric flow of SO_2 vaporized is 47 times larger than the condensed sulfur flow. The tank should contain a demister pad or some other separation device to prevent sulfur from being entrained with the SO_2 vaporized.

2.h. *HEATX - AHGP*

The HEATX heat exchanger transfers heat from the warm regenerator effluent (SO_2 and sulfur) to preheat the cool regenerator feed stream of recycled SO_2 and oxygen. Sulfur condensation in the heat exchanger should be avoided. If sulfur condenses, the system would have to handle two phase flow from HEATX to the condenser. Shutdown procedures would also require removing sulfur from the heat exchanger to prevent sulfur from freezing inside. Assuming the sulfur allotrope distribution is at equilibrium when condensation occurs, the SO_2 - sulfur stream's dew point is 310°C. Cooling the SO_2 - sulfur stream to no lower than 315°C should prevent condensation from occurring.

2.i. *N2-COOLR - AHGP*

The N2-COOLR cools the nitrogen stream prior to its recompression in LIFTCOMP. Cooling the stream decreases the power required for recompression and reduces the possibility of damaging the compressor. The cool nitrogen stream contributes to reducing the temperature of sorbent feed to the desulfurization reactor. Sorbent entering the compressor would cause damage. Therefore, filters should be installed upstream of the compressor. The filters will also be placed upstream of the heat exchanger (N2-COOLR) to prevent build up of sorbent in the heat exchanger.

2.j. *RCYHEATR - AHGP*

The RCYHEATR was incorporated to ensure that the SO_2 - oxygen feed to the regenerator would be hot enough to initiate the regeneration reactions. Superheated steam is used to raise the SO_2 - oxygen stream temperature, as the separate steam generation process flow sheets show (Appendix F). RCYHEATR works with the HEATX heat exchanger to raise the SO_2 - oxygen stream temperature above 400°C. The RCYHEATR is needed because, HEATX heat transfer is limited to insure no condensation occurs upstream of the condenser.

V. PARAMETRIC STUDIES

Parametric studies were performed to determine how HGD requirements were affected by various coal gas feeds. Inlet H_2S concentrations were varied to simulate variation in sulfur content with different types of coal. Therefore, H_2S concentrations will vary between plants using different coal sources. The effect of power generation capacity was also simulated. Finally, different oxygen sources (air vs. pure oxygen) were investigated. Flow sheets and stream summaries for variations of both processes can be found in appendix H.

1. H_2S Inlet Concentration

DSRP and AHGP simulations were performed using a base case coal gas feed containing 0.85 mol% H_2S and a base case power production of 260 megawatts, after sulfur removal. Additional simulations were performed to determine the effect of H_2S inlet concentration on the amount of coal gas that had to be produced. Table 7 shows how varying H_2S inlet concentration requires increasing the gasification of coal to maintain 260 MW generation.

Table 7: Coal Gas Fed to and Consumed by HGD for Various H_2S Concentrations

Simulation	H_2S inlet conc. (mol%)	Coal Gas Fed (lb/hr)	Consumed H_2 (lb/hr)	Consumed CO (lb/hr)
DSRP	0.85	460,000	320	6,000
DSRP-b	2.50	501,000	1,000	19,000
DSRP-c	0.25	447,000	90	1,700
AHGP	0.85	450,000	160	0
AHGP-b	2.50	468,000	470	0
AHGP-c	0.25	444,000	46	0

The sulfur concentration has a profound effect on DSRP flow requirements because of the coal gas slipstream used in the DSRP reactor. The coal gas slipstream increases as the amount of sulfur converted in the DSRP reactor increases.

The small increase in required coal gas for the AHGP can be attributed to the consumption of H_2 in the desulfurization reaction:

$$Fe_2O_3 + 2\,H_2S + H_2 \rightarrow 2\,FeS + 3\,H_2O \qquad (6)$$

The higher sulfur concentrations also require more sorbent circulation to dissipate the heat evolved during reactions. Increased sulfur concentrations require larger reactors. Increasing sulfur also increases the heat removal requirements.

2. Power Generation

Parametric studies were performed to determine the influence of power plant capacity; power generation is 260 MW in the base case. Inlet flows were altered to generate 110 MW and 540 MW. The power level adjustments resulted in flow rates and energy transfer that both scale directly with the change in power generation. The effect of the varying coal gas feed rate was similar to the effect of changing H_2S feed concentrations. An economic comparison shows that the process costs depend on the total sulfur removal requirements. Variations in the flow rates of the other coal gas components do not have a significant effect on the HGD.

3. Pure Oxygen vs. Air Oxidation

Sulfur is removed from the coal gas stream by the reaction of H_2S with the active components of the sorbent to form metal sulfides. Regenerating the sorbent allows it to be reused for removing more sulfur. Sorbent regeneration occurs by exposing the sulfurized sorbent to an oxidizing environment. Pure oxygen and air are both capable of performing the oxidation. Implications of using oxygen and air follow.

3.a. *DSRP*

Pure oxygen is an impractical oxidizing medium for sorbent regeneration. In the DSRP - based process, regenerating with pure oxygen would result in such high temperatures that the sorbent would sinter. By comparison, the nitrogen present in air dilutes the oxygen and serves as

a heat sink for the highly exothermic regeneration reactions. What is not intuitively obvious is that it is more expensive to supply air to the system than to supply oxygen. For DSRP - based process conditions it is more expensive to compress air than to separate oxygen and then compress only the oxygen (Hvizdos).

3.b. *AHGP*

Air is not a viable oxidizing medium for use in the Advanced Hot Gas Desulfurization Process. The use of air would require separating nitrogen from sulfur dioxide. The AHGP process has a large SO_2 stream that circulates through the regeneration reactor and the sulfur condenser. In the AHGP, oxygen enters the SO_2 loop as a pure oxygen feed and leaves with the sorbent. Sulfur enters the SO_2 loop on the sorbent and leaves as condensed sulfur. Feeding air instead of oxygen would provide a steady flow of nitrogen into the SO_2 loop. Maintaining steady state would require removing nitrogen at the rate it is introduced.

The concept of adding a condenser to the SO_2 loop was investigated for separating nitrogen from SO_2 (Figure 7). ASPEN simulations were performed to determine the condenser conditions necessary for removing nitrogen at the rate it enters the system. The idea was to condense the SO_2 in the loop and vent only nitrogen. Table 8 shows that this concept is impractical. When the ratio of SO_2: N_2 is large the SO_2 is more prone to condense. This can be seen in table 8 where for the same temperature and pressure, uncondensed SO_2 (SO_2 vented) decreases as the mass fraction of SO_2 increases. Therefore, the most efficient condenser will have the minimum amount of N_2 feed to it. The minimum N_2 fed to the condenser will be equal to the rate at which nitrogen enters the system via the air steam. The minimum corresponds to a case where no N_2 condenses (N_2 unpurged). Table 8 shows that even with the very low N_2 concentration there is an unreasonable amount of SO_2 vented.

Figure 7: Condenser for Removal of Nitrogen

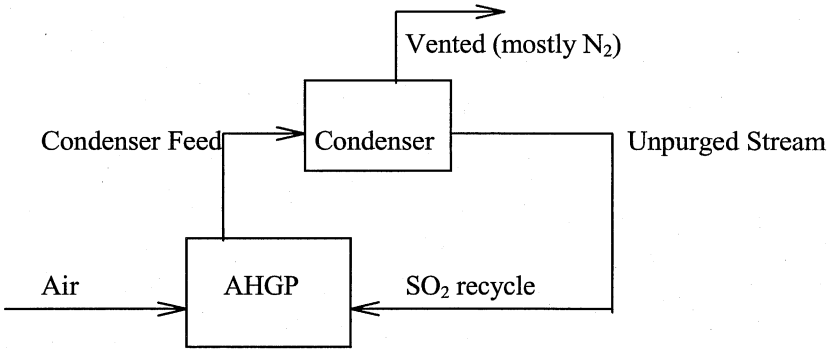

The simulations assumed that the total SO_2 loop flow would be 260,000 lbs/hr and 13,500 lbs N_2/hr would need to be removed.

Table 8: N_2 Removal at Various N_2 Concentrations, Condenser Temperatures and Pressures

Condenser Fed: SO_2 mass fraction	Condenser Pressure (psia)	Condenser Temperature (^oC)	N_2 unpurged (lbs/hr)	SO_2 vented (lbs/hr)	N_2 vented (lbs/hr)
0.100	275	50	0	26,000	234,000
0.900	275	50	418	58,200	25,600
0.946	275	50	511	30,800	13,500
0.946	400	50	1,010	16,800	13,000
0.940	275	-20	716	1,540	14,900

Furthermore, nitrogen is not needed as a heat sink in the AHGP. The SO_2 stream is a sufficient gas phase heat sink to carry away the heat of the regeneration reaction. The economic analysis showed it is actually desirable to feed oxygen instead of air. The cost of compressing air is higher than the cost of separating out oxygen and then compressing only the oxygen.

VI. ADDITIONAL PROCESS CONSIDERATIONS

1. Steam Generation

The coal gas desulfurization with sulfur production overall process is exothermic. DSRP and AHGP both require heat removal for condensation and to maintain reaction temperatures. The heat removal requirements create the opportunity to generate high pressure steam that could drive plant equipment or be incorporated into the plant's power generation steam cycle.

Steam generation has been modeled as a closed loop. Steam is generated by removing heat from the desulfurization process. The steam is then utilized, by undefined means, condensed, cooled and the condensate is reused. Cooling tower water is used to cool the steam-condensate loop (Figure 8). There are benefits to having a self-contained loop for steam production. First, it makes it easy to maintain steam-condensate purity, which reduces fouling and corrosion. It also allows for higher cool water feed temperatures (~ 90°C), which increases steam production.

Figure 8: Schematic for HGD Steam Generation

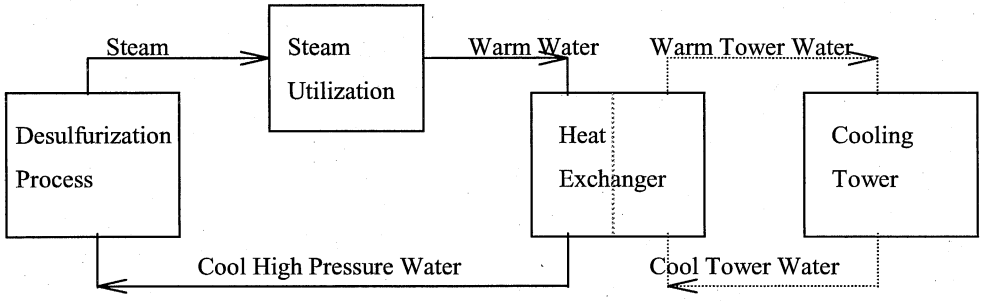

The steam generated from the HGD process was assumed to be at 950 psia and 441°C (Appendix F). Since desulfurization would be incorporated into a larger power generating plant, it is not possible to discern the most useful steam conditions without knowledge of the power generation facility. It is likely that steam generated from the HGD would be utilized by existing power plant equipment. Since the end use of the steam generated is unknown a generic dollar

credit for the steam generated was used for the economic analysis. Peters and Timmerhaus (1991) state that 500 psig steam was worth $ 0.0039/lb in 1990; this value was used during the economic assessment. The benefit calculated should be a conservative value since the simulated steam produced is at a higher pressure (950 psia) and the economic calculations use 1996 as a basis. However, another source notes that for 900 psi and 441°C steam, 1 kWh power generation can be expected per 22.44 pounds of steam (Noyes). The economic credit from the conversion of steam to power according to this relationship was less than the credit obtained using the Peters and Timmerhaus relationship. Since the Peters and Timmerhaus credit value is conservative and still predicts a larger benefit, the Peters and Timmerhaus value was used.

2. Material of Construction

Type 310 stainless steel (25%Cr - 20%Ni) should be used for the construction of equipment that contacts sulfur species. Type 310 stainless steel (SS 310) will be more durable than type 316 stainless steel (SS 316) (17%Cr - 8% Ni - 2%Mo). Higher chromium content gives SS310 greater oxidation resistance, and the higher nickel concentration gives improved resistance to carburization (EPRI). Cost data for SS310 is not contained in ASPEN so SS316 material cost factors were used.

3. Sulfur Storage

Transporting molten sulfur is preferred over solid sulfur. Liquid sulfur is easier to transport and reduces handling losses. It will be necessary to store the molten sulfur before it is shipped out by train. The storage tank should be capable of storing several days worth of recovered sulfur. It should also be equipped with a heat exchanger to keep sulfur molten. The costs of the sulfur storage tanks were calculated using ASPEN assuming SS 310 was used to construct storage for seven days of sulfur production (SS 316 was entered in ASPEN due to lack of data for SS 310).

4. Process Operation

The DSRP should be the easier process to operate. Balancing the SO_2 production and consumption in the AHGP appears to be particularly difficult. The difficulty arises from the reaction of FeS with SO_2 to form elemental sulfur. The reaction's equilibrium varies significantly with temperature. If the reactants are too thermodynamically favored, less SO_2 will be consumed than expected. However, SO_2 production will remain constant (sorbent oxidation being driven to completion by oxygen). Thus, if the reaction:

$$3\ SO_2 + 4\ FeS \ <\!\!=\!\!=\!\!> \ 7/2\ S_2 + 2\ Fe_2O_3 \qquad (7)$$

does not reach design conversions, SO_2 flow will increase and sulfurized sorbent will be returned to the desulfurization reactor. With SO_2 already present in great excess the increased SO_2 flow will not significantly shift equilibrium towards the products.

It is recommended that the AHGP be operated at conditions that will cause a net consumption of SO_2. Replenishing depleted SO_2 levels can easily be accomplished by increasing the oxygen feed. Excess oxygen will convert elemental sulfur into SO_2.

Preventing the build up of impurities in the SO_2 loop contributes to the complexity of the AHGP. Venting a portion of the loop is undesirable since it contains mostly SO_2. Venting would release SO_2, emissions the system is designed to eliminate. Operating the AHGP requires determining the rate at which impurities build up in the recycle loop and the appropriate purge stream for the rate of build up. The purge stream should be fed to the desulfurization reactor, reducing the release of SO_2.

VII. ECONOMIC ANALYSIS

1. Capital Expenditures

The AHGP requires more capital investment than the DSRP. Reactors account for over half of the capital investment. The higher cost of AHGP reactors results in an higher overall capital investment necessary for the AHGP (Figure 9). The majority of equipment was costed using ASPEN. Equipment costed by ASPEN has a purchase date set at June, 1996. Equipment contacting sulfur will experience less corrosion when constructed of stainless steel 310 (SS310). Since ASPEN lacks material of construction correction factors for SS310, SS316 values were used. While the majority of equipment was costed using ASPEN, the equipment that comprises the majority of the capital expenditures, such as the reactors, were estimated by other means.

The reactor costs were calculated using a procedure outlined in Peters and Timmerhaus (1991). The reactor costs were determined using the amount of steel required for their construction. The procedure is described in appendix G, and the calculations are contained in appendix H and appendix I. The reactor cost includes the cost of installation.

Another piece of equipment not costed by ASPEN is the PRESAIR - air compressor used in the DSRP. PRESAIR costs were determined by scaling a price quote for the Ingersoll-Rand Centac air compressor. The Centac Model 2CV23M3EEPF, capable of raising 2,250 acfm to 280 psia, was quoted at $241,000. Extrapolation was used in determining the cost of compressors needed for the different flow rates. Figures in Peters and Timmerhaus (1990) were used to determine the rate at which compressor costs change with varying flow rates.

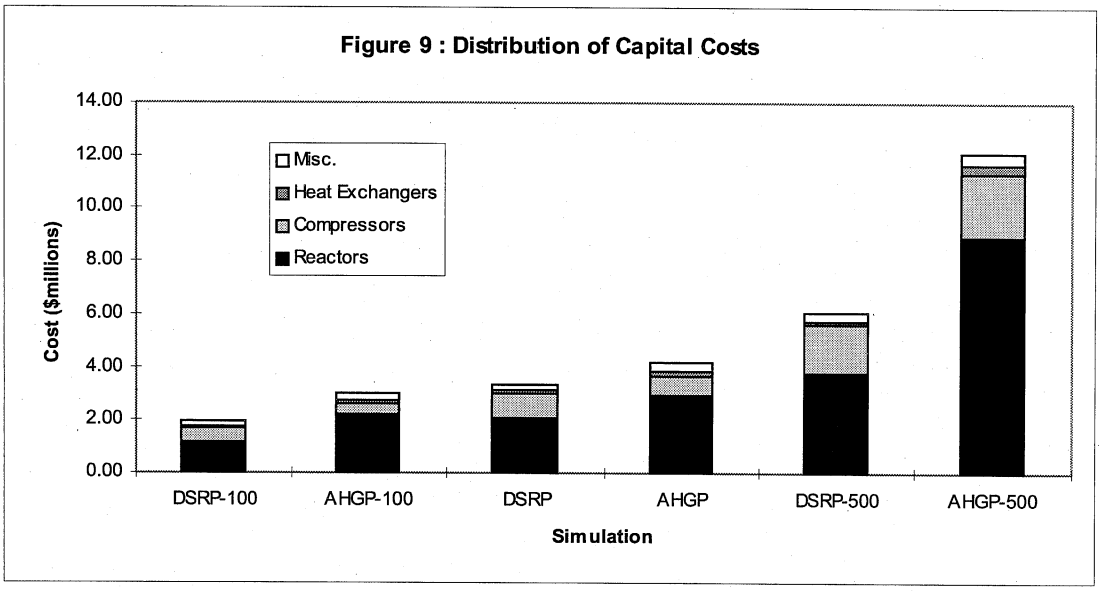

There are additional capital costs not included in this report, two of which, piping costs and sorbent/catalyst costs, will probably be significant. There will be other expenses, like additional office space for employees, which are site dependent. The site dependent expenses should not have an significant effect on the total capital investment calculations. At this stage of investigation the piping and sorbent/catalyst cost are assumed identical for both HGD process. If this assumption is valid than a comparison of the overall capital costs for the AHGP and the DSRP will not be affected by their absence.

2. Yearly Operating Costs

The AHGP has a lower yearly operating cost than the DSRP. Figures 10 and 11 show the distribution of the major yearly expenditures for both processes.

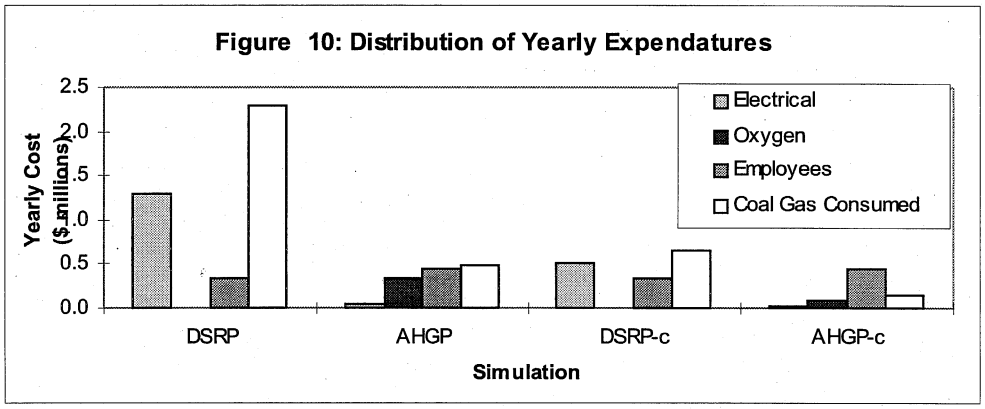

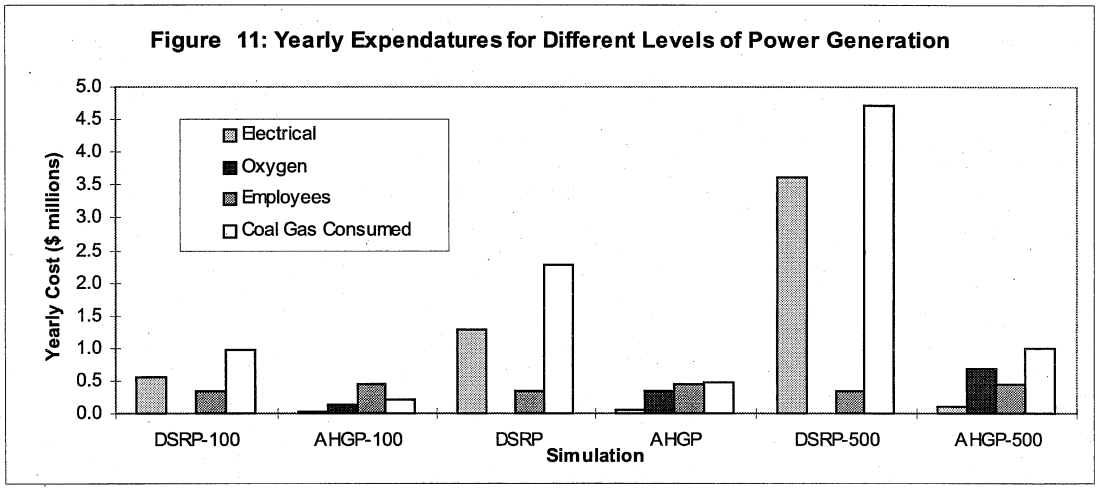

The bases cases (DSRP and AHGP) have coal gas feeds containing 0.85 mol% H_2S and produce 260 MW. Most of the yearly expenditures decline as the amount sulfur in the coal gas is decreased (DSRP-c and AHGP-c have feeds containing 0.25 mol% H_2S). The exception is the yearly costs of additional employees, which have been assumed to be dependent on the complexity of the HGD process and not its size. As the sulfur concentration decreases both the absolute expenditure difference (DSRP cost - AHGP cost) and the relative expenditure difference ([DSRP cost - AHGP cost] / AHGP cost) decrease. This decrease indicates that the competitive advantage of the AHGP is smaller for cleaning a coal gas stream containing a low H_2S concentration. The same trend exists comparing the economics of different levels of power generation: the AHGP's yearly economic advantage over the DSRP declines as the overall power generation is decreased.

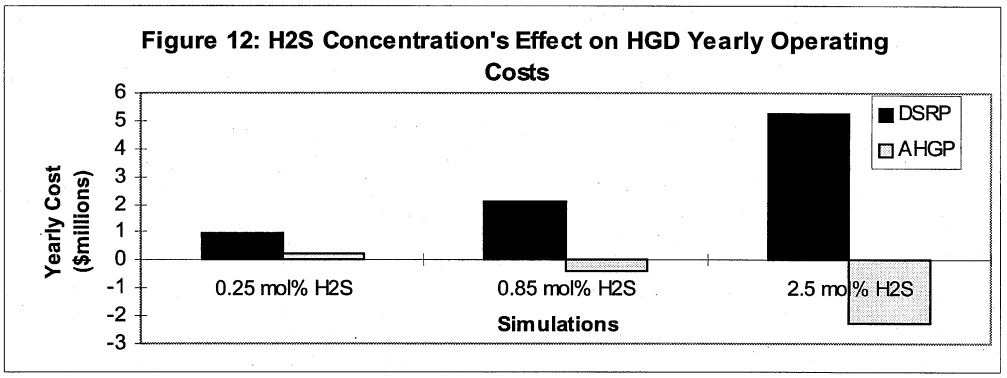

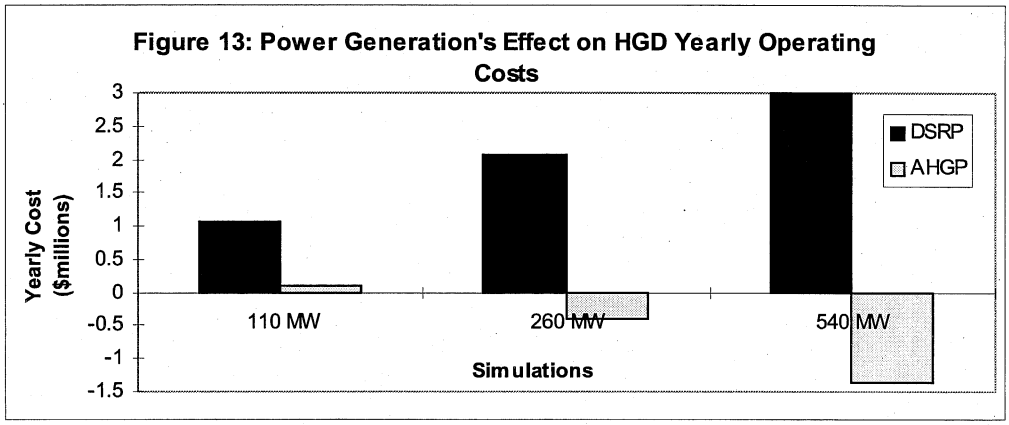

In assessing the yearly cost of maintaining HGD, benefits of the process should also be accounted for. Two sources of credit were observed: the recovery of sulfur and the production of steam. Sulfur credits where consistently larger than steam credits within the same simulation. The sulfur credits remained virtually unchanged between corresponding DSRP and AHGP simulations. Figure 12 and 13 show that for several AHGP conditions the credits are larger than the expenditures. This results in negative yearly operating costs. When larger amounts of sulfur are removed, the yearly expenditures combined with the sulfur and steam credits result in negative yearly costs for the AHGP. In such cases it is more profitable to use the AHGP, then to leave the coal gas stream untreated (if Federal Regulations allowed). The profit that results from the sale of recovered sulfur (Appendix M) allows the AHGP to be more profitable than generating power without desulfurization.

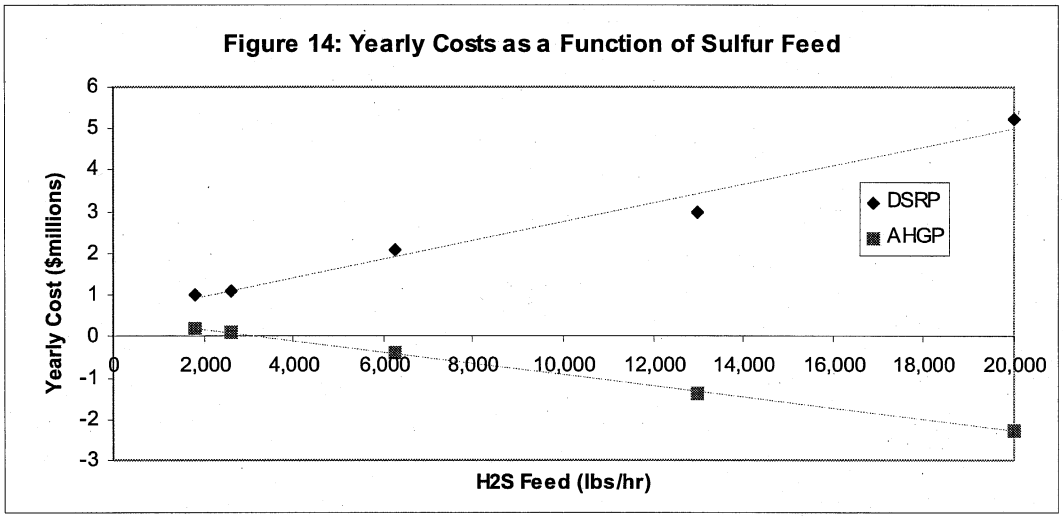

The yearly costs have a linear dependence on the amount of sulfur being processed. This can be seen by comparing all simulations (DSRP, DSRP-b, DSRP-c, DSRP-100, DSRP-500, AHGP, AHGP-b, AHGP-c, AHGP-100, AHGP-500). Figure 14 shows that regardless of how the sulfur feed is varied (changing concentration vs. changing power generation), the yearly costs scale directly with sulfur removed.

2.a. *Electrical*

The pumps and compressors have been assumed to account for the majority of the electrical requirements for the HGD processes. The additional power requirements for lighting and instrumentation have been assumed to be 20% of the compressor and pump requirements for the base case of each HGD. It is assumed that the additional power requirements will not vary significantly with plant size.

The DSRP power requirement is significantly higher than that of the AHGP. The PRESAIR air compressor is the reason for the high DSRP power requirement. The air compressor supplies air to the regenerator for the oxidation of sulfurized sorbent. It is interesting to note that the cost of supplying oxygen by compressing air is more than the cost of separating oxygen and then compressing the pure oxygen. The phenomenon is not unprecedented; it has

been observed that as the pressure of injection is raised the cost of compressing air increases faster than the cost of separating oxygen and pressuring only oxygen (Hvizdos).

The compressed nitrogen feed to the DSRP - based process regenerator that is included in the air stream will increase the total volumetric flow to the turbine. This would indicate that there should be a power credit associated with the nitrogen's introduction, offsetting some of the compression costs. However, nitrogen will also increase the heat capacity of the stream, lowering the combustion temperature, thus lowering the power production. These competing effects have been assumed to cancel each other out. The design work assumes there is no change in power production attributed to the introduction of nitrogen.

2.b. *Cooling Water*

The steam generation/cooling loop is closed; maintaining water purity is not difficult for a self-contained loop. Furthermore, makeup water requirements will be negligible, for the detail level of this report. The is no debit calculated for the HGD steam system water because of the above mentioned reasons.

The steam condensate is assumed to be cooled to 90°C by cooling tower water. Tower water is exposed to the atmosphere, which means maintaining water purity will be an issue. There will also be makeup water requirements. Therefore a yearly debit has been calculated for the use of tower water. The tower water flow rates have been calculated in the Complete Steam Generation Scheme simulations (Appendix F). The tower water cools the steam stream that is considered "utilized." Utilized steam is a stream that was steam (441°C, 950 psia) but has been reduced to 30 psia and the corresponding bubble point temperature. Tower water cools the utilized steam stream to 90°C, before its reuse. The cost of the tower water is $\$2.6 \times 10^{-5}$/lb (Peters). The cost of the tower water is insignificant compared to the other yearly capital expenditures.

The cost of the tower is not an issue as there will already be a tower on site. HGD water sent to it will represent only a minor increase in load.

2.c. *Oxygen*

The cost of supplying oxygen has been assessed as a yearly expenditure with no capital cost. Dr. George Roberts indicated that its reasonable to expect oxygen to cost $20/ton. The value is reasonable when compared with a dated guideline (Chilton, 1960) stating 99.5% pure oxygen at 450 psig would sell at $8 to $15/ton. There are no capital costs associated with the supplied oxygen assuming the oxygen will be bought from a gas supplier, in which only a usage charge is assigned. The price has been assumed to be set at $20/ton, the price will actually be dependent on usage. The unit cost of oxygen decreases as quantity purchased increases.

There are oxygen costs only for the AHGP, since air is used to oxidize the sorbent in the DSRP.

2.d. *Additional Employees*

The number of additional employees required to operate the HGD processes have been assumed constant with process size. The additional employees required will depend more upon the complexity of the process than its size. The hiring of two additional engineers and two maintenance personal have been assigned to the DSRP. The AHGP has the hiring of three engineers accounted for. An additional engineer is hired since the AHGP is a more complex process to control because SO_2 production and consumption must be balanced. Furthermore, the purity of the SO_2 loop must be maintained. Two maintenance personnel are also accounted for in AHGP costs. The unit cost for an engineer is assumed to be $100,000/year, and maintenance personnel are assumed to cost $70,000/year. These numbers include the base salary and benefits.

2.e. *Consumed Coal Gas*

Coal gas (H_2 and CO) is consumed in both HGD processes. The consumption reduces the amount power that can be produced. The cost of consumed coal gas is calculated from the CO and H_2 lost during HGD, and calculating the value of the energy that the CO and H_2 could have produced. Calculation of power generation is described in Appendix J.

The DSRP consumes substantially more coal gas then the AHGP; this is the major factor in the lower yearly operating cost of the AHGP.

2.f. *Additional Yearly Expenditures*

Sorbent and catalyst attrition have not been accounted for in this report. The rate at which sorbent and catalyst need to be replaced times their unit cost will represent another yearly expenditure. Assuming the attrition costs for both processes are identical a comparison of the process economics will be unaffected by the absence of attrition costs in this report.

Maintenance charges have not be fully accounted for in this report. While the cost of additional employees to maintain equipment has been included, the cost of the replacement parts and equipment have not. Yearly maintenance costs should increase with years of service as well as with the size of the HGD process.

3. Economic Summary

The AHGP has a higher initial startup costs, indicated by its larger capital requirements. However, the AHGP has lower yearly expenditures then the DSRP. The operating cost difference is large enough to offset the initial startup cost difference within a few years.

Figure 15: Cumulative HGD Investment

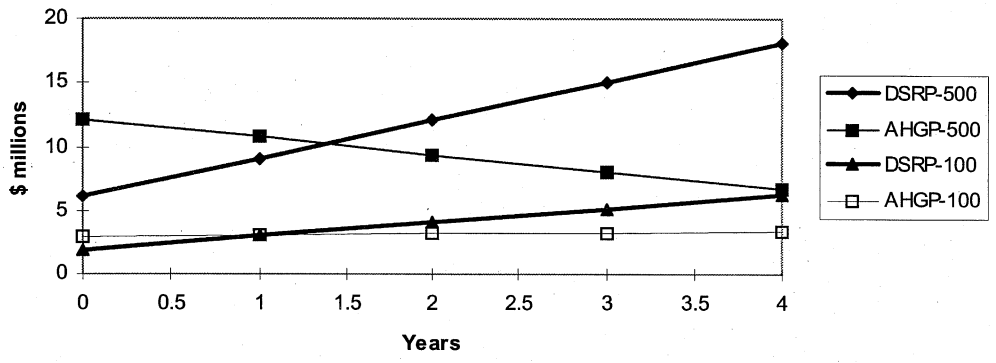

Figure 15 shows that despite an higher initial investment, within two years the AHGP can financially outperform the DSRP.

VIII. SUMMARY

Mass and energy balances were calculated for the Direct Sulfur Recovery Process - based Hot Gas Desulfurization and the Advanced Hot Gas Process. Establishing the balances has helped determine the equipment requirements for both processes. The specifications for the major pieces of equipment have been described in this report.

Simulating the HGD processes revealed the complexity of both processes. The AHGP appears to be the more difficult of the two processes to operate. More employees may be needed to operate the AHGP process than the DSRP -based process.

Capital costs for the AHGP are higher than those for the DSRP. However, yearly operating costs for the AHGP are considerably less than those of the DSRP. After two years of operation the total cost of implementing an AHGP will be less then the cost of a DSRP -based process. It will be more difficult to operate an AHGP but the substantial savings the process delivers makes it the more desirable process to implement.

REFERENCES

ASPEN PLUS, *Reference Manual - Volume 2 Physical Property Methods and Models*, Release 9, Aspen Technology, INC, 1994

Barnett, E. B., Wilson, C. L., *Inorganic Chemistry - A Text-book For Advanced Students*, 2nd Edition, John Wiley & Sons Inc., New York, 1957

Bird, R.B., Stewart, W.E., Lightfoot, E.N., *Transport Phenomena*, John Wiley & Sons, New York, 1960

Bloch, H. P., *A Practical Guide to Compressor Technology,* McGraw-Hill, New York 1996

Braker, W., Mossman, A. L., *Matheson Gas Data Book*, 5th Edition, Matheson Gas Products, Milwaukee, 1971

Brown, R. N., *Compressors - Selection & Sizing*, Gulf Publishing Company, Houston 1986

Campbell, W. M., and Henningsen, G. B., "Hot Gas Desulfurization Using Transport Reactors" *Proceedings of the Twelfth Annual International Pittsburgh Coal Conference,* Pittsburgh, 1995

Caruanan, C. M., "Processes Aim to Improve Sulfur Recovery From Gases," *Chemical Engineering Progress*, February 1996, pp. 11-17

Chen, D. H., *Kinetically Modified Equilibrium Calculation and Thermodynamic Analysis for the DSRP Hot Gas Sulfur Recovery Process,* Final Report to Research Triangle Institute, March 10, 1994 report 1994

Chilton, C. H., Cost Engineering In the Process Industries, McGraw-Hill Company, New York, 1960, pg. 302-303

Cootner, P. H., Lof, G. O., *Water Demand for Steam Electric Generation*, John Hopkins Press, Baltimore, 1965

Cotton, F. S., Wilkinson, G., *Advanced Inorganic Chemistry - A Comprehensive Text*, 2nd Edition, Interscience Publishers, New York 1966

Cusumano, J. A., Dalla Betta, and R. A., Levy R. B., *Catalysis in Coal Conversion*, Academic Press, Inc. New York 1978

Dimoplon, W., "What Process Engineers Need to Know About Compressors," *Hydrocarbon Processing* May 1978, pp. 221-227

EPRI CS-4035, "Continuous Testing of the Resox Process," Project 1257-2, Final Report, May 1985

Gangwal, S. K., Hot-Gas Desulphurisation Sorbent Development for IGCC Systems, "Desulphurisation 2 Technologies and Strategies for Reducing Sulphur Emissions" *Institution of Chemical Engineers*, New York 1991

Hvizdos, L. J., Howard, J. V., Roberts, G. W., "Enhanced Oil Recovery Through Oxygen Enriched In-Situ Combustion: Test Results From the Forest Hill Field in Texas" *Journal of Petroleum Technology* June 1983, pp. 1061-1070

Jaffee, R. I., "Advances in Materials for Fossil Power Plants," *Advances in Material Technology for Fossil Power Plant - Proceedings of an International Conference on Advances in Material Technology for Fossil Power Plants,* ASM International, Chicago, 1987

Kern, D. Q., *Process Heat Transfer*, McGraw-Hill Book Company, New York, 1950

Noyes, R. Cogeneration of Steam and Electric Power, Noyes Data Corporation Park Ridge, Park Ridge, NJ, 1978

Perry, R.H., Green, D.W., Maloney, J.O., *Perry's Chemical Engineers' Handbook*, 6th Edition, McGraw Hill Inc., New York, 1984

Peters, M. S., Timmerhaus, K. D., *Plant Design and Economics for Chemical Engineers*, 4th Edition, McGraw Hill Inc. New York, 1991

Portzer, J. W., Research Triangle Institute internal memo, November 26, 1996

Ulrich, G. D., A Guide to Chemical Engineering Process Design And Economics, John Wiley & Sons, Inc. New York 1984

U.S. Geological Survey, Minerals Information, *http://minerals.er.usgs.gov/minerals/pubs/commodity/sulfur/stat/*

Welty, J.R., Wicks, C.E., Wilson, R.E., *Fundamentals of Momentum, Heat, and Mass Transfer*, 3rd Edition, John Wiley & Sons, New York, 1984

Appendix A
Calculation of the SO_2 Circulation Rate for AHGP

SO_2 circulation rates are set to create the desired flow conditions in the regenerating reactor. First the sorbent flow rate through the regenerator must be determined. Al_2O_3 must pass through the reactor in large quantities to keep the adiabatic temperature raise small. The sorbent flow is used to determine the reactor's cross sectional area. The SO_2 circulation rate necessary to provide a 2.5 cm/s upwards velocity is then calculated. Calculation results follow:

SO2 Regenerator Sizing - Commercial Embodiment

Givens:	AGHP (SO2 Regen) Case E-2	AHGP-b (SO2 Regen) Case E-2	AHGP-c
Sorbent circulation rate, lb/hr	166010	496000	48000
Sorbent bulk density, lb/ft3	62.4	62.4	62.4
Req'd rxtr residence time, hr	1	1	1
Regen Gas v_{super}, cm/sec	2.5	2.5	2.5
Desired H/D	2	2	2
Adjusted values:			
Assumed Bed Depth, ft	10	10	10
SO2 needed ft3/hr	**79,813**	**238,462**	**23,077**
Calculated values:			
Hold-up volume, ft3	2660	7949	769
Diameter, ft	18	32	9.9
X-section area, ft2	266	795	77
Calculated H/D	0.54	0.31	1.01
RG Vol. flow rate, acf/sec	21.8	65.2	6.3
RG flow rate, lb/hr	86366	258043	24972
Ratio of RG flow/sorbent, lb/lb	0.52	0.52	0.52
Calculated Bed Depth, ft			
Operating conditions/Gas Density Calc'ns:			
Pressure, psig	275	275	275
Pressure, psia	289.7	289.7	289.7
MW of gas	64	64	64
Bed Temp., C	600	600	600
Bed Temp., R	1571.67	1571.67	1571.67
R, gas constant,	10.73	10.73	10.73
Gas density, lb/ft3	1.1	1.1	1.1

Appendix B
Heat Transfer Coefficients

The following approximate overall heat transfer coefficients were found in the literature. The values were in used estimating the heat exchangers' overall heat transfer coefficients.

Coolers

Hot Fluid	Cold Fluid	Overall U_D, BTU/hr ft^2 °F
Water	Water	250 - 500
Gases	Water	2 - 50

Heaters

Hot Fluid	Cold Fluid	Overall U_D, BTU/hr ft^2 °F
Steam	Water	200 - 700
Steam	Gases	5 - 50

Values above found in Kern (1950).

Fluid combination	U, BTU/hr ft^2 °F
Water to compressed air	10 - 30
Water to water	150-275
Steam to aqueous solutions	100-600
Steam to gases	5 - 50

Values above found in Welty, Wicks, and Wilson (1984).

Appendix C
Determination of Catalyst Velocity in DSRP Reactor

In order to determine whether the catalyst in the DSRP Reactor (a fast fluid-bed reactor) will be transported to the top of the reactor by the gas feed, the following calculation was performed. A terminal velocity calculation was performed on a catalyst particle. This calculation will approximate the catalyst's velocity relative to the gas phase. The gas velocity through the DSRP will be 3 ft/s (0.9 m/s). The catalyst's relative velocity needs to be less than the gas velocity in order for the catalyst to be elevated.

Terminal velocity is determined from a force balance on the particle.

$$m\frac{dv}{dt} = F_g - F_d - F_b$$

$$m\frac{dv}{dt} = mg - \frac{C_D v^2 \rho(\pi D_p^2 / 4)}{2} - \frac{m\rho g}{\rho_p}$$

At steady state the left side equals zero and the equations simplify to give the steady state (terminal) velocity:

$$v_{ss} = \sqrt{\frac{4}{3}\left(\frac{D_p g}{C_D \rho}\right)(\rho_p - \rho)}$$

The catalyst size is 160 micron.

$D_p = 1.6 \times 10^{-4}$ m $\qquad \rho_p = 1.2$ g/cm^3 $\qquad g = 9.8$ m/s^2

Bulk samples of the catalyst have a density (ρ_{bulk}) of 0.9 g/cm^3. The bulk catalyst is assumed to have a packing fraction of 0.74, the highest packing fraction possible for spheres. Assuming the packing fraction enables calculation of the individual catalyst density (ρ_p).

$\rho_p = \rho_{bulk}$ /(packing fraction) $\qquad \rho_p = 1.2$ g/cm^3 = (0.9 g/cm^3) / (0.74)

The gas density is taken as a weighted average of the feeds ROG-COOL and SLIPSTRM.

$\rho = 0.50$ lb/ft^3 x (1,000 gr) / (2.205 lb) x (1 ft^3) / (30.48 cm)^3 = 0.008 g/cm^3 = 8 kg/m^3

Inserting the values gives:

$$v_{ss} = \sqrt{\frac{0.3136 \frac{m^2}{s^2}}{C_D}}$$

The drag coefficient C_D is correlated with the Reynolds number (N_{Re})of the gas phase. After determining the Reynolds number C_D can be determined from charts in Bird (1960).

$$N_{Re} = D_p \, v_{ss} \, \rho / \mu$$

The steady state velocity is determined iteratively. That leaves μ, viscosity of the gas, the only other unknown.

For viscosity calculations, the gas will been assumed to have the properties of nitrogen (N_2 represents over 50 wt% of reactor gas).

Reactor conditions T = 600°C and P = 275 psia.

The Reichenberg correlation was used for the determination of the high pressure viscosity (Perry's 3-279). The correlation typically has errors of less than 10 percent.

Equations

$$(\mu - \mu^o)/(\mu^o \rho) = A \, P_r^{1.5} / [\, B \, P_r + (1 + C \, P_r^D)^{-1}]$$

$$A = 1.9824 \times 10^{-3} \, T_r^{-1} \exp (5.2683 \, T_r^{-0.5767})$$

$$B = A \, (1.6552 \, T_r - 1.2760)$$

$$C = 0.1319 \, T_r^{-1} \exp (3.7035 \, T_r^{-79.8678})$$

$$D = 2.9496 \, T_r^{-1} \exp (2.9190 \, T_r^{-16.6169})$$

Nitrogen Properties

$T_r = T / T_c = 873 \text{ K} / 126.2 \text{ K} = 6.91$ $\quad P_r = P / P_c = 275 \text{ psia} / 492 \text{ psia} = 0.559$

$\mu^o = \mu \, (1 \text{ atm}, 873 \text{ K}) = 3.8 \times 10^8$ Poise

And for nonpolar molecules: $\rho = 1$

Calculated Values

A = 0.001615 B = 0.0164 C = 0.01909 D = 0.4269

$$(\mu - \mu^o) / (\mu^o) = 6.7498 \times 10^{-4} / 0.9945 = 6.787 \times 10^{-4}$$

$$\mu = 3.8 \times 10^{-4} + (3.8 \times 10^{-4})(6.787 \times 10^{-4}) \text{ Poise}$$

$$\mu = 3.8 \times 10^{-4} \text{ Poise} = 3.8 \times 10^{-5} \text{ Pa s} = 3.8 \times 10^{-5} \text{ kg/(m s)}$$

The Reynolds number is can now be expressed:

$$N_{Re} = (1.6 \times 10^{-4} \text{ m}) (v_{ss}) (8 \text{ kg/m}^3) / [3.8 \times 10^{-5} \text{ kg/(m s)}]$$

$$N_{Re} = (v_{ss}) \, 33.68 \text{ s/m}$$

And our velocity equation is: $v_{ss} = \sqrt{\dfrac{0.3136 \dfrac{m^2}{s^2}}{C_D}}$

First Iteration, take $v_{ss} = 0.9$ m/s then $N_{Re} = 30$ (above equation)
For the above Reynolds number $C_D = 2.4$ (Fig. 6.3-1 in Bird)
Velocity equation gives $v_{ss} = 0.36$ m/s

The calculations are repeated.

Second iteration:	$v_{ss} = 0.36$ m/s	$N_{Re} = 12$
	$C_D = 4.2$	$v_{ss} = 0.27$ m/s
Third iteration:	$v_{ss} = 0.27$ m/s	$N_{Re} = 9.09$
	$C_D = 4.9$	$v_{ss} = 0.252$ m/s
Fourth iteration:	v_{ss} 0.252 m/s	$N_{Re} = 8.49$
	$C_D = 5.13$	$v_{ss} = 0.247$ m/s
Fifth iteration:	v_{ss} 0.247 m/s	$N_{Re} = 8.33$
	$C_D = 5.19$	$v_{ss} = 0.246$ m/s

The velocity of falling catalyst is 0.25 m/s. Thus in a gas stream flowing up at 0.9 m/s the catalyst will rise at 0.65 m/s (2.1 ft/s).

CONCLUSION: The gas stream will be capable of elevating the catalyst.
Sorbent in the risers will be elevated at approximately the same velocity (20 ft/s) as the gas lifting it.

Appendix D
Calculation of DSRP Catalyst Cycling Rate

The rate at with catalyst is fed to the DSRP was determined by the heat removal requirements of the DSRP reactor. Heat is removed from the reactor by cooling the catalyst effluent and reintroducing that catalyst. Exiting catalyst temperature is set at 600°C and the catalyst is cooled to 500°C.

Catalyst Properties

The DSRP reactor catalyst is a porous aluminum oxide catalyst modeled as Al_2O_3. Catalyst density at ambient conditions is 56.18 lb/ft^3. This density includes the void space filled by air. ASPEN was utilized to determine the void space in the settled catalyst, assuming nitrogen fills the voids in the solid catalyst. At ambient conditions 1 lb of Al_2O_3 and 0.00095 lb of N_2 have a combined density of 55.6 lb/ft^3.

The similar densities allow us to assume that there is roughly 0.00095 lb of nitrogen present for every 1 lb of solid Al_2O_3 (at ambient conditions). That quantity of nitrogen occupies 0.0132 ft^3 (at ambient conditions). This represents the catalyst void volume and is expected to remain constant.

$V_{void} = 0.0132 \text{ ft}^3 / 1 \text{ lb } Al_2O_3$

The density of the gas in the reactor was taken as the average of nitrogen's density at 600°C (275 psia) and 500°C (275 psia).

$$\rho_{gas} = 0.483 \text{ lb/ft}^3$$

Therefore the mass of gas (in the settled catalyst) per pound Al_2O_3 can be calculated.

$$M_{gas} = 0.483 \text{ lb/ft}^3 \text{ x } 0.0132 \text{ ft}^3 = 0.0064 \text{ lbs}$$

The heat transfer requirements for cooling Al_2O_3 were than simulated (including cooling nitrogen contained in the catalyst voids).

$$Q(600°C \rightarrow 500°C) = -51.239 \text{ BTU/lb } Al_2O_3$$

Calculation of necessary catalyst circulation rate:

$$(\text{circulation rate } \{lb/hr\}) = (Q_{DSRP}) / (-51.239 \text{ BTU/lb } Al_2O_3)$$

DSRP (circulation rate {lb/hr}) = (-15,340,000 BTU/hr) / (-51.239 BTU/lb Al_2O_3)
= 300,000 lb Al_2O_3 / hr

DSRP-b (circulation rate {lb/hr}) = (-51,320,000 BTU/hr) / (-51.239 BTU/lb Al_2O_3)
= 1,000,000 lb Al_2O_3 / hr

DSRP-c (circulation rate {lb/hr}) = (-4,029,000 BTU/hr) / (-51.239 BTU/lb Al_2O_3)
= 79,000 lb Al_2O_3 / hr

DSRP-100 (circulation rate {lb/hr}) = (-6,459,000 BTU/hr) / (-51.239 BTU/lb Al_2O_3)
= 130,000 lb Al_2O_3 / hr

DSRP-500 (circulation rate {lb/hr}) = (-31,370,000 BTU/hr) / (-51.239 BTU/lb Al_2O_3)
= 610,000 lb Al_2O_3 / hr

Appendix E
Process Flowsheets and Stream Summaries

Direct Sulfur Recovery Process Simulations

DSRP (base case)	0.85 mole% H_2S	260 MW generated
DSRP-b	2.50 mole% H_2S	260 MW generated
DSRP-c	0.25 mole% H_2S	260 MW generated
DSRP-100*	0.85 mole% H_2S	110 MW generated
DSRP-500	0.85 mole% H_2S	540 MW generated

Advanced Hot Gas Process Simulations

AHGP (base case)	0.85 mole% H_2S	260 MW generated
AHGP-b	2.50 mole% H_2S	260 MW generated
AHGP-c	0.25 mole% H_2S	260 MW generated
AHGP-100*	0.85 mole% H_2S	110 MW generated
AHGP-500*	0.85 mole% H_2S	540 MW generated

*DSRP-100, AHGP-100, and AHGP-500 were not simulated. The flowrates and heat duties will scale directly from the base cases (DSRP and AHGP). DSRP-100 and AHGP-100 values equal DSRP and AHGP values scaled by 0.4211. AHGP-500 values equal AHGP values scaled by 2.1055.

DSRP - based Desulfurization

12/20/97 DSRP

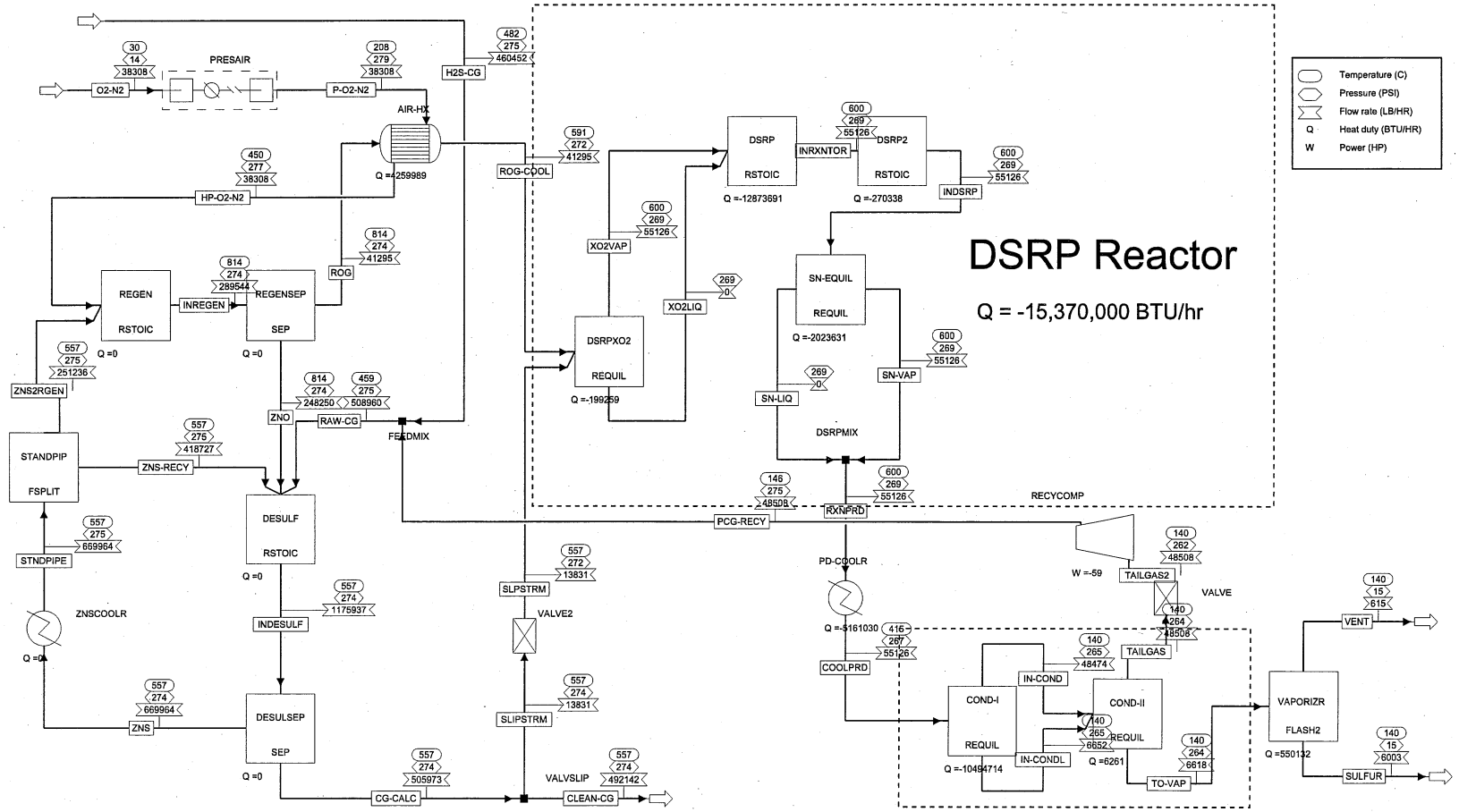

High Pressure Condenser Q = -10,500,000 BTU/hr

DSRP 12/20/97 pg1

Display ALLS Units: Format: SOLI	TREAMS From DS To Phas	CG-CALC DESULSEP VALVSLIP VAPOR	CLEAN-CG VALVSLIP VAPOR	COOLPRD PD-COOLR COND-I VAPOR	H2S-CG FEEDMIX VAPOR	HP-O2-N2 AIR-HX REGEN VAPOR	IN-COND COND-I COND-II VAPOR	IN-CONDL COND-I COND-II LIQUID	INDESULF DESULF DESULSEP VAPOR	INDSRP DSRP2 SN-EQUIL VAPOR	INREGEN REGEN REGENSEP VAPOR	INRXNTOR DSRP DSRP2 VAPOR	O2-N2 PRESAIR VAPOR	Display ALLS Units: Format: SOLI	TREAMS From DS To Phas
Temperature	[C]	557.2	557.2	415	482.2	450	140	140	557.2	600	814.4	600	30	Temperature	[C]
Pressure	[PSI]	274.4	274.4	266.6	275	276.9	264.6	264.6	274.4	268.6	273.6	268.6	13.7	Pressure	[PSI]
Mass VFrac		1	1	1	1	1	1	0	0.43	1	0.143	1	1	Mass VFrac	
Mass SFrac		0	0	0	0	0	0	0	0.57	0	0.857	0	0	Mass SFrac	
*** ALL PHAS	ES ***													*** ALL PHAS	ES ***
Mass Flow	[LB/HR]	505972.781	492141.531	55125.902	460451.688	38308.016	48474.25	6651.654	1.18E+06	55125.902	289544.469	55126.063	38308.016	Mass Flow	[LB/HR]
Volume Flow	[CUFT/HR]	1.37E+06	1.33E+06	87129.523	1.15E+06	67432.328	49166.316	48.953	1.37E+06	112094.914	96496.891	111308.695	567372.75	Volume Flow	[CUFT/HR]
Enthalpy	[BTU/HR]	-1.15E+09	-1.11E+09	-6.57E+07	-1.09E+09	7.31E+06	-7.15E+07	-4.68E+06	-4.84E+09	-5.85E+07	-1.38E+09	-5.82E+07	79241.141	Enthalpy	[BTU/HR]
Density	[LB/CUFT]	0.37	0.37	0.633	0.399	0.568	0.986	135.877	0.857	0.492	3.001	0.495	0.068	Density	[LB/CUFT]
Mass Flow	[LB/HR]													Mass Flow	[LB/HR]
O2S		63.71	61.968	63.879			63.7	0.18	63.71	63.879	11909.276	1787.733		O2S	
H2S		6.82	6.634	72.073	6270.481		71.958	0.116	6.82	72.072		72.072		H2S	
H2O		78082.43	75947.969	4963.325	70525.25		4175.116	788.209	78082.43	4963.325		4963.325		H2O	
S2		< 0.001	< 0.001	2631.176			< 0.001	0.212	< 0.001	5861.615		3273.283		S2	
S6		0.39	0.38	1891.255			0.965	1890.29	0.39	0.011		0.011		S6	
S8		2.764	2.688	1339.271			2.025	3968.209	2.764	0.076		0.076		S8	
CO		218164.266	212200.516	2.262	218162		2.262	< 0.001	218164.266	2.262		2.262		CO	
CO2		130332.672	126769.898	12929.425	117407.195		12925.243	4.181	130332.672	12929.425		10560.996		CO2	
H2		11766.221	11444.579	0.85	11765.37		0.85	< 0.001	11766.221	0.85		0.85		H2	
O2						8922.588							8922.588	O2	
N2		67553.203	65706.57	31232.063	36321.383	29385.428	31231.807	0.256	67553.203	31232.063	29385.428	31232.063	29385.428	N2	
COS		0.323	0.314	0.323			0.323	< 0.001	0.323	0.323		3233.392		COS	
ZNO											15129.819			ZNO	
ZNS									144457.359		36055			ZNS	
AL2O3									525506.5		197064.938			AL2O3	

DSRP 12/20/97 pg.2

Display ALLS Units: Format: SOLI	TREAMS From DS To Phas	P-O2-N2 PRESAIR AIR-HX VAPOR	PCG-RECY RECYCOMP FEEDMIX VAPOR	RAW-CG FEEDMIX DESULF VAPOR	ROG REGENSEP AIR-HX VAPOR	ROG-COOL AIR-HX DSRPXO2 VAPOR	RXNPRD DSRPMIX PD-COOLR VAPOR	SLIPSTRM VALVSLIP VALVE2 VAPOR	SLPSTRM VALVE2 DSRPXO2 VAPOR	SN-LIQ SN-EQUIL DSRPMIX MISSING	SN-VAP SN-EQUIL DSRPMIX VAPOR	STNDPIPE ZNSCOOLR STANDPIP MISSING	SULFUR VAPORIZR LIQUID	Display ALLS Units: Format: SOLI	TREAMS From DS To Phas
Temperature	[C]	207.6	146.5	458.8	814.4	590.7	600	557.2	557.2		600	557.2	140	Temperature	[C]
Pressure	[PSI]	278.9	275	275	273.6	271.6	268.6	274.4	271.6		268.6	275	14.7	Pressure	[PSI]
Mass VFrac		1	1	1	1	1	1	1	1		1	0	0	Mass VFrac	
Mass SFrac		0	0	0	0	0	0	0	0		0	1	0	Mass SFrac	
*** ALL PHAS	ES ***													*** ALL PHAS	ES ***
Mass Flow	[LB/HR]	38308.016	48507.805	508959.5	41294.703	41294.703	55125.902	13831.278	13831.278	0	55125.902	669963.875	6002.956	Mass Flow	[LB/HR]
Volume Flow	[CUFT/HR]	44510.953	48127.191	1.20E+06	95300.984	76325.195	109933.391	37429.125	37813.297		109933.273	3189.083	33.124	Volume Flow	[CUFT/HR]
Enthalpy	[BTU/HR]	3.05E+06	-7.15E+07	-1.16E+09	-9.58E+06	-1.38E+07	-6.05E+07	-3.13E+07	-31319000	0.00E+00	-6.05E+07	-3.69E+09	-4.57E+05	Enthalpy	[BTU/HR]
Density	[LB/CUFT]	0.861	1.008	0.423	0.433	0.541	0.501	0.37	0.366		0.501	210.08	181.225	Density	[LB/CUFT]
Mass Flow	[LB/HR]													Mass Flow	[LB/HR]
O2S			63.71	63.71	11909.276	11909.276	63.879	1.742	1.742		63.879		0.001	O2S	
H2S			71.964	6342.445			72.073	0.186	0.186		72.072		< 0.001	H2S	
H2O			4208.244	74733.492			4963.325	2134.462	2134.462		4963.325		146.193	H2O	
S2			< 0.001	< 0.001			2631.176	trace	trace		2631.176		0.212	S2	
S6			0.39	0.39			1891.255	0.011	0.011		1891.255		724.696	S6	
S8			2.764	2.764			1339.271	0.076	0.076		1339.271		5131.851	S8	
CO			2.262	218164.266			2.262	5963.741	5963.741		2.262		trace	CO	
CO2			12925.476	130332.672			12929.425	3562.775	3562.775		12929.425		0.002	CO2	
H2			0.85	11766.221			0.85	321.642	321.642		0.85		trace	H2	
O2		8922.588												O2	
N2		29385.428	31231.822	67553.203	29385.428	29385.428	31232.063	1846.635	1846.635		31232.063		trace	N2	
COS			0.323	0.323			0.323	0.009	0.009		0.323		trace	COS	
ZNO														ZNO	
ZNS												144457.359		ZNS	
AL2O3												525506.5		AL2O3	

DSRP 12/20/97 pg.3

Display ALLS	TREAMS	TAILGAS	TAILGAS2	TO-VAP	VENT	XO2LIQ	XO2VAP	ZNO	ZNS	ZNS-RECY	ZNS2RGEN			Display ALLS	TREAMS
Units:	From	COND-II	VALVE	COND-II	VAPORIZR	DSRPXO2	DSRPXO2	REGENSEP	DESULSEP	STANDPIP	STANDPIP			Units:	From
Format: SOLI	DS To	VALVE	RECYCOMP	VAPORIZR		DSRP	DSRP	DESULF	ZNSCOOLR	DESULF	REGEN			Format: SOLI	DS To
	Phas	VAPOR	VAPOR	LIQUID	VAPOR	MISSING	VAPOR	MISSING	MISSING	MISSING	MISSING				Phas
Temperature	[C]	140	139.9	140	140		600	814.4	557.2	557.2	557.2			Temperature	[C]
Pressure	[PSI]	264.4	262	264.4	14.7		268.6	273.6	274.4	275	275			Pressure	[PSI]
Mass VFrac		1	1	0	1		1	0	0	0	0			Mass VFrac	
Mass SFrac		0	0	0	0		0	1	1	1	1			Mass SFrac	
*** ALL PHAS	ES ***													*** ALL PHAS	ES ***
Mass Flow	[LB/HR]	48507.805	48507.805	6618.099	615.143	0	55126.27	248249.766	669963.875	418727.406	251236.453			Mass Flow	[LB/HR]
Volume Flow	[CUFT/HR]	49255.441	49703.582	46.323	18288.283		118222.719	1195.906	3189.083	1993.177	1195.906			Volume Flow	[CUFT/HR]
Enthalpy	[BTU/HR]	-7.17E+07	-7.17E+07	-4482800	-3.48E+06	0.00E+00	-4.54E+07	-1.37E+09	-3.69E+09	-2307300000	-1.38E+09			Enthalpy	[BTU/HR]
Density	[LB/CUFT]	0.985	0.976	142.868	0.034		0.466	207.583	210.08	210.08	210.08			Density	[LB/CUFT]
Mass Flow	[LB/HR]													Mass Flow	[LB/HR]
O2S		63.71	63.71	0.17	0.169		11911.018							O2S	
H2S		71.964	71.964	0.109	0.109		0.186							H2S	
H2O		4208.244	4208.244	755.081	608.888		1209.115							H2O	
S2		< 0.001	< 0.001	0.212	< 0.001		trace							S2	
S6		0.39	0.39	724.917	0.221		0.011							S6	
S8		2.764	2.764	5133.418	1.567		0.076							S8	
CO		2.262	2.262	< 0.001	< 0.001		4524.921							CO	
CO2		12925.476	12925.476	3.95	3.948		5823.677							CO2	
H2		0.85	0.85	< 0.001	< 0.001		425.192							H2	
O2														O2	
N2		31231.822	31231.822	0.241	0.241		31232.063							N2	
COS		0.323	0.323	< 0.001	< 0.001		0.009							COS	
ZNO								15129.819						ZNO	
ZNS								36055	144457.359	90285.852	54171.508			ZNS	
AL2O3								197064.938	525506.5	328441.563	197064.938			AL2O3	

DSRP-b - based Desulfurization

12/20/97 DSRP-b

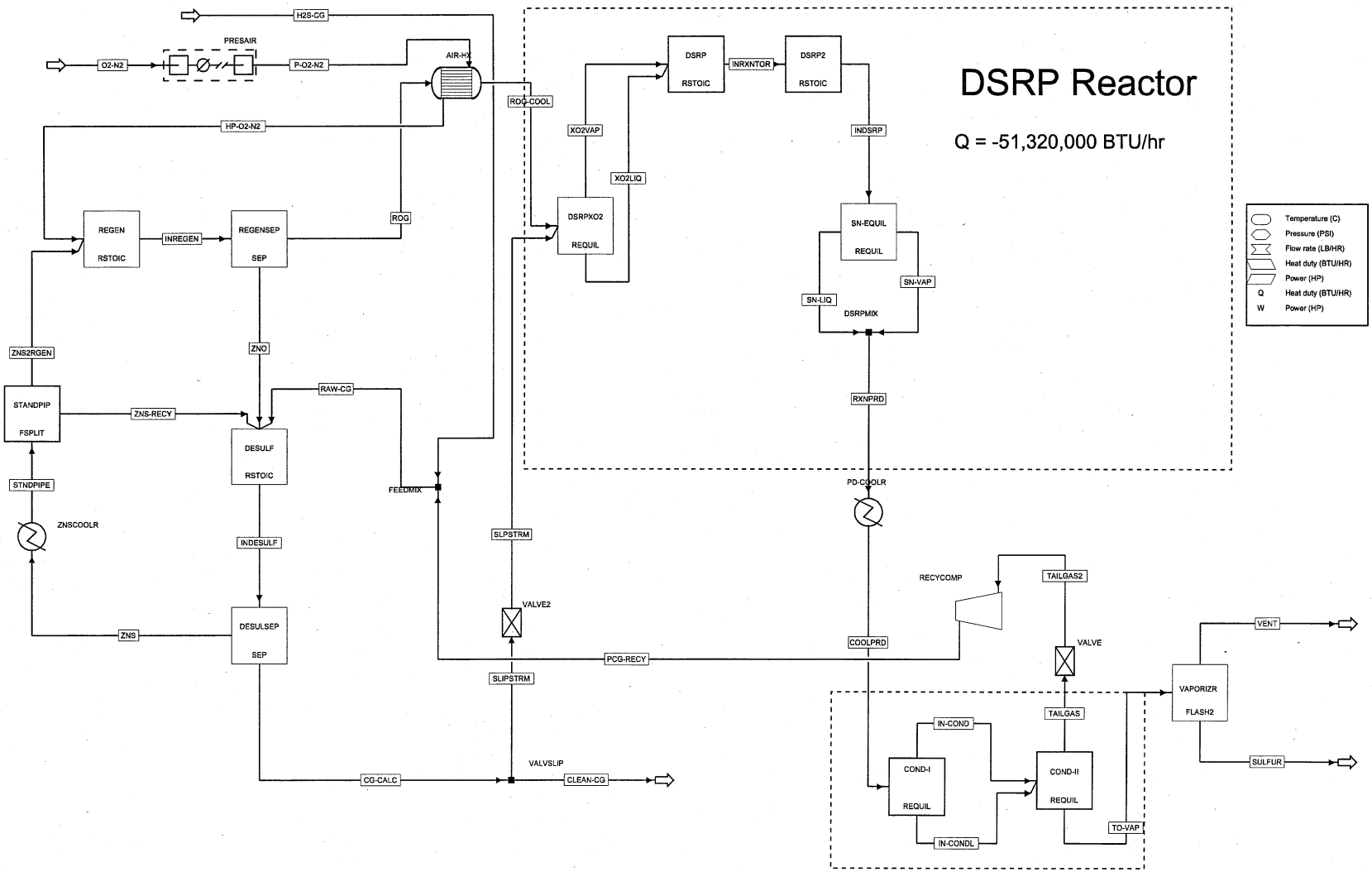

High Pressure Condenser Q = -35,100,000 BTU/hr

DSRP-b 12/20/97 pg1

Display ALLS Units: Format: SOLI	TREAMS From DS To Phas	CG-CALC DESULSEP VALVSLIP VAPOR	CLEAN-CG VALVSLIP VAPOR	COOLPRD PD-COOLR COND-I VAPOR	H2S-CG FEEDMIX VAPOR	HP-O2-N2 AIR-HX REGEN VAPOR	IN-COND COND-I COND-II VAPOR	IN-CONDL COND-I COND-II LIQUID	INDESULF DESULF DESULSEP VAPOR	INDSRP DSRP2 SN-EQUIL VAPOR	INREGEN REGEN REGENSEP VAPOR	INRXNTOR DSRP DSRP2 VAPOR	O2-N2 PRESAIR VAPOR	Display ALLS Units: Format: SOLI	TREAMS From DS To Phas
Temperature	[C]	647.5	647.5	415	482.2	450	140	140	647.5	600	810	600	30	Temperature	[C]
Pressure	[PSI]	273.6	273.6	265.6	275	277.4	263.6	263.6	273.6	267.6	272.6	267.6	13.7	Pressure	[PSI]
Mass VFrac		1	1	1	1	1	1	0	0.197	1	0.099	1	1	Mass VFrac	
Mass SFrac		0	0	0	0	0	0	0	0.803	0	0.901	0	0	Mass SFrac	
*** ALL PHAS	ES ***													*** ALL PHAS	ES ***
Mass Flow	[LB/HR]	655189.75	601554.75	184610.219	501234.031	121500	163323.219	21287.002	3324180	184607.219	1322550	184607.719	121500	Mass Flow	[LB/HR]
Volume Flow	[CUFT/HR]	1887870	1733330	294846.875	1244460	213489.484	166528.75	159.053	1900580	378670.75	307882.375	376264.813	1799510	Volume Flow	[CUFT/HR]
Enthalpy	[BTU/HR]	-1.36E+09	-1.24E+09	-2.24E+08	-1.16E+09	2.32E+07	-2.43E+08	-1.61E+07	-1.60E+10	-2.00E+08	-6.55E+09	-1.99E+08	2.51E+05	Enthalpy	[BTU/HR]
Density	[LB/CUFT]	0.347	0.347	0.626	0.403	0.569	0.981	133.836	1.749	0.488	4.296	0.491	0.068	Density	[LB/CUFT]
Mass Flow	[LB/HR]													Mass Flow	[LB/HR]
O2S		194.606	178.675	195.105			194.579	0.526	194.606	195.105	37772.176	5444.741		O2S	
H2S		62.453	57.341	240.342	19916.91		239.971	0.371	62.453	240.342		240.342		H2S	
H2O		99935.453	91754.563	17155.324	74738.914		14470.859	2684.464	99935.453	17155.324		17155.324		H2O	
S2		< 0.001	< 0.001	8658.119			< 0.001	0.695	< 0.001	18593.258		10711.036		S2	
S6		1.28	1.175	5885.709			3.086	5882.623	1.28	0.105		0.105		S6	
S8		8.967	8.233	4053.262			6.665	12704.021	8.967	0.734		0.734		S8	
CO		231203.391	212276.672	6.89	231196.5		6.89	< 0.001	231203.391	6.89		6.89		CO	
CO2		167878.578	154135.734	43469.434	124421.914		43455.953	13.482	167878.578	43469.434		36256.879		CO2	
H2		12471.098	11450.191	2.783	12468.315		2.783	< 0.001	12471.098	2.783		2.783		H2	
O2						28299.416							28299.416	O2	
N2		143432.969	131691.281	104942.266	38491.473	93200.586	104941.445	0.818	143432.969	104942.266	93200.586	104942.266	93200.586	N2	
COS		0.984	0.904	0.985			0.984	< 0.001	0.984	0.985		9846.616		COS	
ZNO											47986.641			ZNO	
ZNS									576614.875		202017.281			ZNS	
AL2O3									2092380		941570.188			AL2O3	

DSRP-b 12/20/97 pg.2

Display ALLS	TREAMS	P-O2-N2	PCG-RECY	RAW-CG	ROG	ROG-COOL	RXNPRD	SLIPSTRM	SLPSTRM	SN-LIQ	SN-VAP	STNDPIPE	SULFUR	Display ALLS	TREAMS
Units:	From	PRESAIR	RECYCOMP	FEEDMIX	REGENSEP	AIR-HX	DSRPMIX	VALVSLIP	VALVE2	SN-EQUIL	SN-EQUIL	ZNSCOOLR	VAPORIZR	Units:	From
Format: SOLI	DS To	AIR-HX	FEEDMIX	DESULF	AIR-HX	DSRPXO2	PD-COOLR	VALVE2	DSRPXO2	DSRPMIX	DSRPMIX	STANDPIP		Format: SOLI	DS To
	Phas	VAPOR	VAPOR	VAPOR	VAPOR	VAPOR	VAPOR	VAPOR	VAPOR	MISSING	VAPOR	MISSING	LIQUID		Phas
Temperature	[C]	207.7	147.5	418.7	810	586.3	600	647.5	647.5		600	640	140	Temperature	[C]
Pressure	[PSI]	279.4	275	275	272.6	270.6	267.6	273.6	270.6		267.6	275	14.7	Pressure	[PSI]
Mass VFrac		1	1	1	1	1	1	1	1		1	0	0	Mass VFrac	
Mass SFrac		0	0	0	0	0	0	0	0		0	1	0	Mass SFrac	
*** ALL PHAS	ES ***													*** ALL PHAS	ES ***
Mass Flow	[LB/HR]	121500	163428.5	664662.5	130972.758	130972.758	184610.219	53635.004	53635.004	0	184610.219	2668990	19044.756	Mass Flow	[LB/HR]
Volume Flow	[CUFT/HR]	140938.547	162790.359	1410320	302165.188	241725.797	372001.438	154544.391	156250.734		372001.031	12704.87	105.13	Volume Flow	[CUFT/HR]
Enthalpy	[BTU/HR]	9691570	-2.43E+08	-1.40E+09	-3.07E+07	-4.42E+07	-2.06E+08	-1.11E+08	-1.11E+08	0	-2.06E+08	-1.46E+10	-1.45E+06	Enthalpy	[BTU/HR]
Density	[LB/CUFT]	0.862	1.004	0.471	0.433	0.542	0.496	0.347	0.343		0.496	210.076	181.154	Density	[LB/CUFT]
Mass Flow	[LB/HR]													Mass Flow	[LB/HR]
O2S			194.606	194.606	37772.176	37772.176	195.105	15.931	15.931		195.105		0.002	O2S	
H2S			239.99	20156.9			240.342	5.113	5.113		240.342		0.001	H2S	
H2O			14574.853	89313.766			17155.324	8180.895	8180.895		17155.324		464.116	H2O	
S2			< 0.001	< 0.001			8658.119	< 0.001	< 0.001		8658.119		0.695	S2	
S6			1.28	1.28			5885.709	0.105	0.105		5885.709		2321.039	S6	
S8			8.967	8.967			4053.262	0.734	0.734		4053.262		16258.897	S8	
CO			6.89	231203.391			6.89	18926.723	18926.723		6.89		trace	CO	
CO2			43456.652	167878.578			43469.434	13742.839	13742.839		43469.434		0.006	CO2	
H2			2.783	12471.098			2.783	1020.906	1020.906		2.783		trace	H2	
O2		28299.416												O2	
N2		93200.586	104941.492	143432.969	93200.586	93200.586	104942.266	11741.678	11741.678		104942.266		< 0.001	N2	
COS			0.984	0.984			0.985	0.081	0.081		0.985		trace	COS	
ZNO														ZNO	
ZNS												576614.875		ZNS	
AL2O3												2092380		AL2O3	

Display ALLS	TREAMS	TAILGAS	TAILGAS2	TO-VAP	VENT	XO2LIQ	XO2VAP	ZNO	ZNS	ZNS-RECY	ZNS2RGEN			Display ALLS	TREAMS
Units:	From	COND-II	VALVE	COND-II	VAPORIZR	DSRPXO2	DSRPXO2	REGENSEP	DESULSEP	STANDPIP	STANDPIP			Units:	From
Format: SOLI	DS To Phas	VALVE VAPOR	RECYCOMP VAPOR	VAPORIZR LIQUID	VAPOR	DSRP MISSING	DSRP VAPOR	DESULF MISSING	ZNSCOOLR MISSING	DESULF MISSING	REGEN MISSING			Format: SOLI	DS To Phas
Temperature	[C]	140	139.9	140	140		600	810	647.5	640	640			Temperature	[C]
Pressure	[PSI]	263.6	261	263.6	14.7		267.6	272.6	273.6	275	275			Pressure	[PSI]
Mass VFrac		1	1	0	1		1	0	0	0	0			Mass VFrac	
Mass SFrac		0	0	0	0		0	1	1	1	1			Mass SFrac	
*** ALL PHAS	ES ***													*** ALL PHAS	ES ***
Mass Flow	[LB/HR]	163428.5	163428.5	21181.719	2136.962	0	184608.375	1191570	2668990	1467950	1201050			Mass Flow	[LB/HR]
Volume Flow	[CUFT/HR]	166691.297	168340.75	150.956	63551.742		398196.594	5717.191	12704.87	6987.678	5717.191			Volume Flow	[CUFT/HR]
Enthalpy	[BTU/HR]	-2.43E+08	-2.43E+08	-1.54E+07	-1.21E+07	0	-1.59E+08	-6.52E+09	-1.46E+10	-8.03E+09	-6.57E+09			Enthalpy	[BTU/HR]
Density	[LB/CUFT]	0.98	0.971	140.317	0.034		0.464	208.419	210.076	210.076	210.076			Density	[LB/CUFT]
Mass Flow	[LB/HR]													Mass Flow	[LB/HR]
O2S		194.606	194.606	0.499	0.497		37788.105							O2S	
H2S		239.99	239.99	0.353	0.352		5.113							H2S	
H2O		14574.853	14574.853	2580.471	2116.355		4870.572							H2O	
S2		< 0.001	< 0.001	0.695	< 0.001		< 0.001							S2	
S6		1.28	1.28	2321.814	0.776		0.105							S6	
S8		8.967	8.967	16264.332	5.434		0.734							S8	
CO		6.89	6.89	< 0.001	< 0.001		13779.622							CO	
CO2		43456.652	43456.652	12.781	12.774		21830.447							CO2	
H2		2.783	2.783	< 0.001	< 0.001		1391.339							H2	
O2														O2	
N2		104941.492	104941.492	0.773	0.773		104942.266							N2	
COS		0.984	0.984	< 0.001	< 0.001		0.081							COS	
ZNO								47986.641						ZNO	
ZNS								202017.281	576614.875	317138.188	259476.688			ZNS	
AL2O3								941570.188	2092380	1150810	941570.188			AL2O3	

DSRP-c - based Desulfurization

12/21/97 DSRP-c

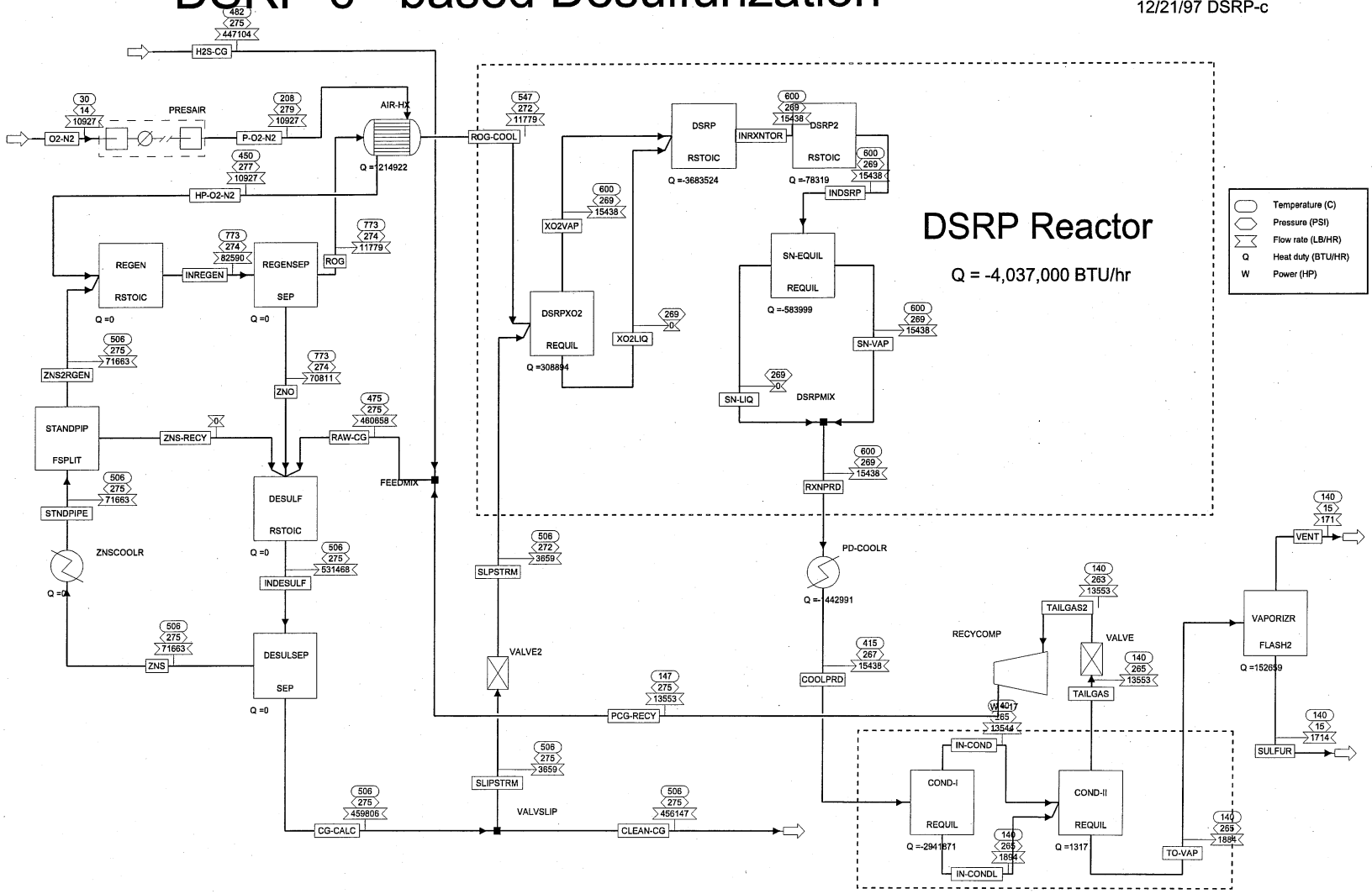

High Pressure Condenser Q = -2,940,000 BTU/hr

DSRP-c 12/21/97 pg.1

Display ALLS	TREAMS	CG-CALC	CLEAN-CG	COOLPRD	H2S-CG	HP-O2-N2	IN-COND	IN-CONDL	INDESULF	INDSRP	INREGEN	INRXNTOR	O2-N2	Display ALLS	TREAMS
Units:	From	DESULSEP	VALVSLIP	PD-COOLR		AIR-HX	COND-I	COND-I	DESULF	DSRP2	REGEN	DSRP		Units:	From
Format: SOLI	DS To	VALVSLIP		COND-I	FEEDMIX	REGEN	COND-II	COND-II	DESULSEP	SN-EQUIL	REGENSEP	DSRP2	PRESAIR	Format: SOLI	DS To
	Phas	VAPOR	VAPOR	VAPOR	VAPOR	VAPOR	VAPOR	LIQUID	VAPOR	VAPOR	VAPOR	VAPOR	VAPOR		Phas
Temperature	[C]	506.4	506.4	415	482.2	450	140	140	506.4	600	772.6	600	30	Temperature	[C]
Pressure	[PSI]	274.9	274.9	267.1	275	277.3	265.1	265.1	274.9	269.1	274.1	269.1	13.7	Pressure	[PSI]
Mass VFrac		1	1	1	1	1	1	0	0.865	1	0.143	1	1	Mass VFrac	
Mass SFrac		0	0	0	0	0	0	0	0.135	0	0.857	0	0	Mass SFrac	
*** ALL PHAS	ES ***													*** ALL PHAS	ES ***
Mass Flow	[LB/HR]	459805.594	456146.75	15437.757	447104.125	10927	13544.205	1893.551	531468.188	15437.757	82589.578	15437.803	10927	Mass Flow	[LB/HR]
Volume Flow	[CUFT/HR]	1187320	1177870	24296.518	1125490	19206.873	13705.025	13.869	1187660	31278.654	26436.727	31051.443	161837.719	Volume Flow	[CUFT/HR]
Enthalpy	[BTU/HR]	-1.08E+09	-1.08E+09	-1.83E+07	-1.07E+09	2.09E+06	-1.99E+07	-1.30E+06	-1.48E+09	-1.63E+07	-3.94E+08	-1.62E+07	2.26E+04	Enthalpy	[BTU/HR]
Density	[LB/CUFT]	0.387	0.387	0.635	0.397	0.569	0.988	136.533	0.447	0.494	3.124	0.497	0.068	Density	[LB/CUFT]
Mass Flow	[LB/HR]													Mass Flow	[LB/HR]
O2S		15.704	15.579	15.747			15.702	0.045	15.704	15.747	3397.009	515.087		O2S	
H2S		14.867	14.749	20.399	1801.676		20.366	0.033	14.867	20.399		20.399		H2S	
H2O		71265.617	70698.523	1374.565	69146.555		1154.749	219.816	71265.617	1374.565		1374.565		H2O	
S2		< 0.001	< 0.001	741.13			< 0.001	0.06	< 0.001	1673.231		923.483		S2	
S6		0.11	0.109	543.432			0.274	543.158	0.11	0.001		0.001		S6	
S8		0.78	0.774	388.677			0.57	1129.177	0.78	0.006		0.006		S8	
CO		213897.828	212195.766	0.655	213897.172		0.655	trace	213897.828	0.655		0.655		CO	
CO2		118728.914	117784.148	3618.024	115112.016		3616.834	1.189	118728.914	3618.024		2931.973		CO2	
H2		11535.61	11443.817	0.24	11535.37		0.24	trace	11535.61	0.24		0.24		H2	
O2						2545.084							2545.084	O2	
N2		44346.063	43993.184	8734.794	35611.336	8381.916	8734.721	0.073	44346.063	8734.794	8381.916	8734.794	8381.916	N2	
COS		0.094	0.093	0.094			0.094	< 0.001	0.094	0.094		936.6		COS	
ZNO											4315.638			ZNO	
ZNS									15452.001		10284.438			ZNS	
AL2O3									56210.578		56210.578			AL2O3	

DSRP-c 12/21/97 pg.2

Display ALLS	TREAMS	P-O2-N2	PCG-RECY	RAW-CG	ROG	ROG-COOL	RXNPRD	SLIPSTRM	SLPSTRM	SN-LIQ	SN-VAP	STNDPIPE	SULFUR	Display ALLS	TREAMS
Units:	From	PRESAIR	RECYCOMP	FEEDMIX	REGENSEP	AIR-HX	DSRPMIX	VALVSLIP	VALVE2	SN-EQUIL	SN-EQUIL	ZNSCOOLR	VAPORIZR	Units:	From
Format: SOLI	DS To	AIR-HX	FEEDMIX	DESULF	AIR-HX	DSRPXO2	PD-COOLR	VALVE2	DSRPXO2	DSRPMIX	DSRPMIX	STANDPIP		Format: SOLI	DS To
	Phas	VAPOR	VAPOR	VAPOR	VAPOR	VAPOR	VAPOR	VAPOR	VAPOR	MISSING	VAPOR	MISSING	LIQUID		Phas
Temperature	[C]	207.7	146.8	475.2	772.6	547.5	600	506.4	506.4		600	506.4	140	Temperature	[C]
Pressure	[PSI]	279.3	275	275	274.1	272.1	269.1	274.9	272.1		269.1	275	14.7	Pressure	[PSI]
Mass VFrac		1	1	1	1	1	1	1	1		1	0	0	Mass VFrac	
Mass SFrac		0	0	0	0	0	0	0	0		0	1	0	Mass SFrac	
*** ALL PHAS	ES ***													*** ALL PHAS	ES ***
Mass Flow	[LB/HR]	10927	13553.382	460657.5	11778.925	11778.925	15437.757	3658.844	3658.844	0	15437.757	71662.578	1713.577	Mass Flow	[LB/HR]
Volume Flow	[CUFT/HR]	12679.411	13452.904	1139190	26095.605	20645.352	30656.066	9447.959	9544.736		30656.035	341.12	9.454	Volume Flow	[CUFT/HR]
Enthalpy	[BTU/HR]	871552.063	-1.99E+07	-1.09E+09	-2.96E+06	-4.18E+06	-1.68E+07	-8.63E+06	-8.63E+06	0	-1.68E+07	-3.97E+08	-1.30E+05	Enthalpy	[BTU/HR]
Density	[LB/CUFT]	0.862	1.007	0.404	0.451	0.571	0.504	0.387	0.383		0.504	210.08	181.246	Density	[LB/CUFT]
Mass Flow	[LB/HR]													Mass Flow	[LB/HR]
O2S			15.704	15.704	3397.009	3397.009	15.747	0.125	0.125		15.747		< 0.001	O2S	
H2S			20.368	1822.044			20.399	0.118	0.118		20.399		< 0.001	H2S	
H2O			1163.806	70310.359			1374.565	567.087	567.087		1374.565		41.723	H2O	
S2			< 0.001	< 0.001			741.13	trace	trace		741.13		0.06	S2	
S6			0.11	0.11			543.432	0.001	0.001		543.432		206.281	S6	
S8			0.78	0.78			388.677	0.006	0.006		388.677		1465.512	S8	
CO			0.655	213897.828			0.655	1702.064	1702.064		0.655			CO	
CO2			3616.9	118728.914			3618.024	944.77	944.77		3618.024		0.001	CO2	
H2			0.24	11535.61			0.24	91.793	91.793		0.24		trace	H2	
O2		2545.084												O2	
N2		8381.916	8734.726	44346.063	8381.916	8381.916	8734.794	352.878	352.878		8734.794		trace	N2	
COS			0.094	0.094			0.094	0.001	0.001		0.094		trace	COS	
ZNO														ZNO	
ZNS												15452.001		ZNS	
AL2O3												56210.578		AL2O3	

DSRP-c 12/21/97 pg.3

Display ALLS	TREAMS	TAILGAS	TAILGAS2	TO-VAP	VENT	XO2LIQ	XO2VAP	ZNO	ZNS	ZNS-RECY	ZNS2RGEN			Display ALLS	TREAMS
Units:	From	COND-II	VALVE	COND-II	VAPORIZR	DSRPXO2	DSRPXO2	REGENSEP	DESULSEP	STANDPIP	STANDPIP			Units:	From
Format: SOLI	DS To	VALVE	RECYCOMP	VAPORIZR		DSRP	DSRP	DESULF	ZNSCOOLR	DESULF	REGEN			Format: SOLI	DS To
	Phas	VAPOR	VAPOR	LIQUID	VAPOR	MISSING	VAPOR	MISSING	MISSING	MISSING	MISSING				Phas
Temperature	[C]	140	139.9	140	140		600	772.6	506.4		506.4			Temperature	[C]
Pressure	[PSI]	265.1	262.5	265.1	14.7		269.1	274.1	274.9		275			Pressure	[PSI]
Mass VFrac		1	1	0	1		1	0	0		0			Mass VFrac	
Mass SFrac		0	0	0	0		0	1	1		1			Mass SFrac	
*** ALL PHAS	ES ***													*** ALL PHAS	ES ***
Mass Flow	[LB/HR]	13553.382	13553.382	1884.374	170.798	0	15437.86	70810.656	71662.578	0	71662.578			Mass Flow	[LB/HR]
Volume Flow	[CUFT/HR]	13719.107	13854.065	13.12	5077.429		33024.156	341.12	341.12		341.12			Volume Flow	[CUFT/HR]
Enthalpy	[BTU/HR]	-2.00E+07	-2.00E+07	-1.25E+06	-9.65E+05	0	-1.25E+07	-3.91E+08	-3.97E+08	0.00E+00	-3.97E+08			Enthalpy	[BTU/HR]
Density	[LB/CUFT]	0.988	0.978	143.629	0.034		0.467	207.583	210.08		210.08			Density	[LB/CUFT]
Mass Flow	[LB/HR]													Mass Flow	[LB/HR]
O2S		15.704	15.704	0.043	0.042		3397.134							O2S	
H2S		20.368	20.368	0.031	0.031		0.118							H2S	
H2O		1163.806	1163.806	210.759	169.036		315.4							H2O	
S2		< 0.001	< 0.001	0.06	< 0.001		trace							S2	
S6		0.11	0.11	206.342	0.061		0.001							S6	
S8		0.78	0.78	1465.947	0.435		0.006							S8	
CO		0.655	0.655	trace	trace		1310.713							CO	
CO2		3616.9	3616.9	1.124	1.123		1559.735							CO2	
H2		0.24	0.24	trace	trace		119.958							H2	
O2														O2	
N2		8734.726	8734.726	0.069	0.069		8734.794							N2	
COS		0.094	0.094	< 0.001	< 0.001		0.001							COS	
ZNO								4315.638						ZNO	
ZNS								10284.438	15452.001		15452.001			ZNS	
AL2O3								56210.578	56210.578		56210.578			AL2O3	

DSRP-500 - based Desulfurization

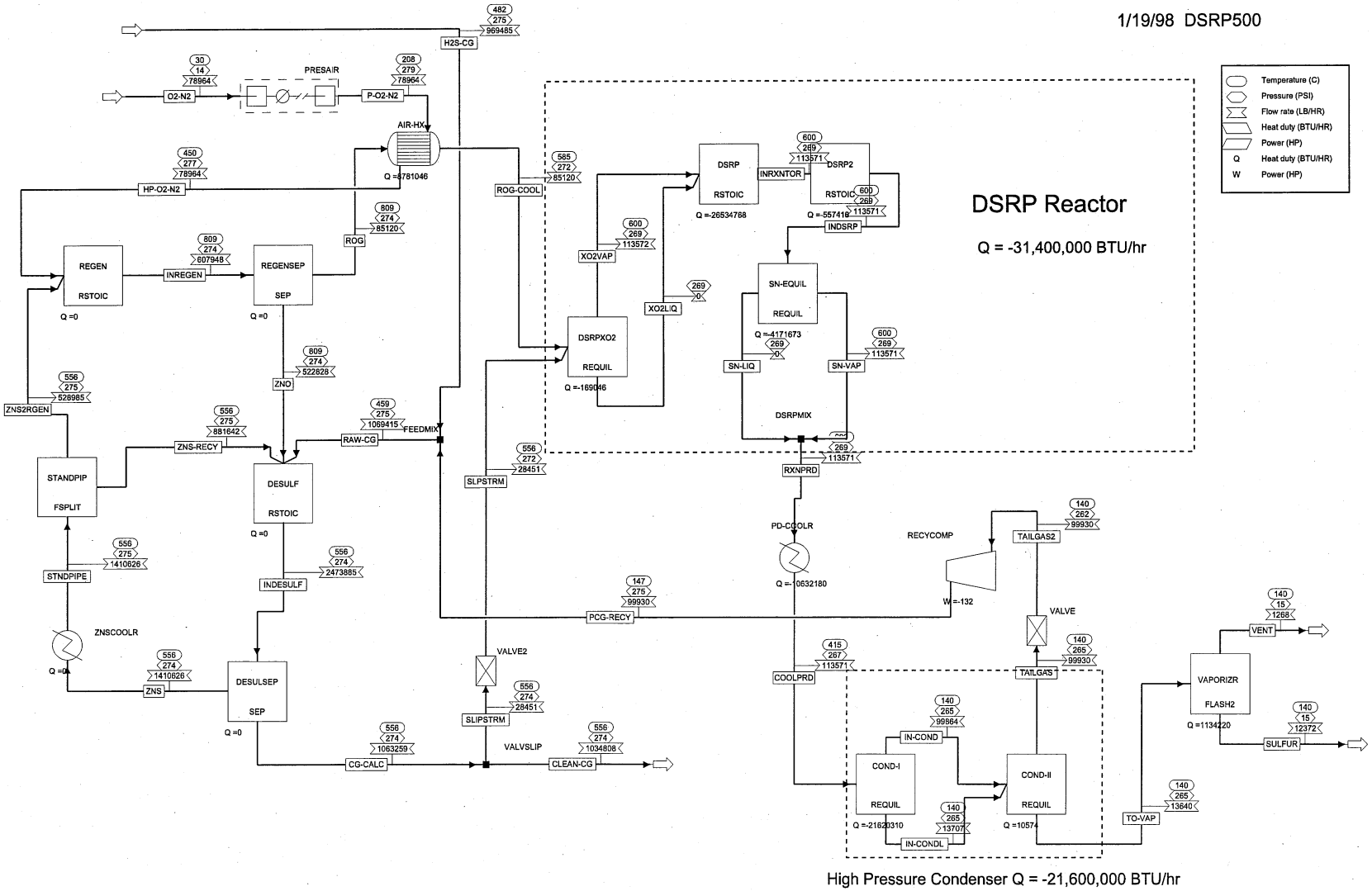

DSRP-500 1/19/98 pg.1

Display ALLS Units: Format: SOLI	TREAMS From DS To Phas	CG-CALC DESULSEP VALVSLIP VAPOR	CLEAN-CG VALVSLIP VAPOR	COOLPRD PD-COOLR COND-I VAPOR	H2S-CG FEEDMIX VAPOR	HP-O2-N2 AIR-HX REGEN VAPOR	IN-COND COND-I COND-II VAPOR	IN-CONDL COND-I COND-II LIQUID	INDESULF DESULF DESULSEP VAPOR	INDSRP DSRP2 SN-EQUIL VAPOR	INREGEN REGEN REGENSEP VAPOR	INRXNTOR DSRP DSRP2 VAPOR	O2-N2 PRESAIR VAPOR	Display ALLS Units: Format: SOLI	TREAMS From DS To Phas
Temperature	[C]	556.1	556.1	415	482.2	450	140	140	556.1	600	808.9	600	30	Temperature	[C]
Pressure	[PSI]	274.4	274.4	266.6	275	276.9	264.6	264.6	274.4	268.6	273.6	268.6	13.7	Pressure	[PSI]
Mass VFrac		1	1	1	1	1	1	0	0.43	1	0.14	1	1	Mass VFrac	
Mass SFrac		0	0	0	0	0	0	0	0.57	0	0.86	0	0	Mass SFrac	
*** ALL PHAS	ES ***													*** ALL PHAS	ES ***
Mass Flow	[LB/HR]	1063260	1034810	113570.906	969485	78963.703	99863.633	13707.267	2.47E+06	113570.898	607948.188	113571.234	78963.703	Mass Flow	[LB/HR]
Volume Flow	[CUFT/HR]	2.87E+06	2.80E+06	179490.672	2.43E+06	138997.172	101285.656	100.854	2.88E+06	230923.609	197974.375	229302.5	1169520	Volume Flow	[CUFT/HR]
Enthalpy	[BTU/HR]	-2.41E+09	-2.35E+09	-1.35E+08	-2.30E+09	1.51E+07	-1.47E+08	-9.63E+06	-1.02E+10	-1.20E+08	-2.90E+09	-1.20E+08	163338.5	Enthalpy	[BTU/HR]
Density	[LB/CUFT]	0.37	0.37	0.633	0.399	0.568	0.986	135.912	0.859	0.492	3.071	0.495	0.068	Density	[LB/CUFT]
Mass Flow	[LB/HR]													Mass Flow	[LB/HR]
O2S		134.563	130.963	134.922			134.543	0.379	134.563	134.922	24548.4	3689.37		O2S	
H2S		298.899	290.901	156.105	13202.553		155.855	0.25	298.899	156.105		156.105		H2S	
H2O		164058.219	159668.297	10220.242	148491.516		8597.656	1622.586	164058.219	10220.242		10220.242		H2O	
S2		< 0.001	< 0.001	5421.442			< 0.001	0.438	< 0.001	12080.898		6743.967		S2	
S6		0.803	0.782	3898.438			1.989	3896.449	0.803	0.021		0.021		S6	
S8		5.689	5.537	2761.193			4.175	8178.022	5.689	0.152		0.152		S8	
CO		459346.656	447055.344	4.665	459341.969		4.665	< 0.001	459346.656	4.665		4.665		CO	
CO2		273825.563	266498.469	26631.824	247201.875		26623.211	8.614	273825.563	26631.824		21748.314		CO2	
H2		24773.842	24110.938	1.752	24772.09		1.752	< 0.001	24773.842	1.752		1.752		H2	
O2						18391.988							18391.988	O2	
N2		140814.141	137046.203	64339.652	76474.984	60571.711	64339.125	0.528	140814.141	64339.652	60571.711	64339.652	60571.711	N2	
COS		0.666	0.649	0.667			0.666	< 0.001	0.666	0.667		6666.993		COS	
ZNO											31186.855			ZNO	
ZNS									304172		76721.18			ZNS	
AL2O3									1106450		414920.063			AL2O3	

DSRP-500 1/19/98 pg.2

Display ALLS	TREAMS	P-O2-N2	PCG-RECY	RAW-CG	ROG	ROG-COOL	RXNPRD	SLIPSTRM	SLPSTRM	SN-LIQ	SN-VAP	STNDPIPE	SULFUR	Display ALLS	TREAMS
Units:	From	PRESAIR	RECYCOMP	FEEDMIX	REGENSEP	AIR-HX	DSRPMIX	VALVSLIP	VALVE2	SN-EQUIL	SN-EQUIL	ZNSCOOLR	VAPORIZR	Units:	From
Format: SOLI	DS To	AIR-HX	FEEDMIX	DESULF	AIR-HX	DSRPXO2	PD-COOLR	VALVE2	DSRPXO2	DSRPMIX	DSRPMIX	STANDPIP		Format: SOLI	DS To
	Phas	VAPOR	VAPOR	VAPOR	VAPOR	VAPOR	VAPOR	VAPOR	VAPOR	MISSING	VAPOR	MISSING	LIQUID		Phas
Temperature	[C]	207.6	147.1	459.3	808.9	585.1	600	556.1	556.1		600	556.1	140	Temperature	[C]
Pressure	[PSI]	278.9	275	275	273.6	271.6	268.6	274.4	271.6		268.6	275	14.7	Pressure	[PSI]
Mass VFrac		1	1	1	1	1	1	1	1		1	0	0	Mass VFrac	
Mass SFrac		0	0	0	0	0	0	0	0		0	1	0	Mass SFrac	
*** ALL PHAS	ES ***													*** ALL PHAS	ES ***
Mass Flow	[LB/HR]	78963.703	99930.422	1069420	85120.109	85120.109	113570.906	28450.951	28450.951	0	113570.906	1410630	12372.203	Mass Flow	[LB/HR]
Volume Flow	[CUFT/HR]	91749.711	99302.75	2.53E+06	195456.375	156297.594	226467.672	76921.539	77711.063		226467.438	6714.697	68.27	Volume Flow	[CUFT/HR]
Enthalpy	[BTU/HR]	6.30E+06	-1.47E+08	-2.44E+09	-2.00E+07	-2.88E+07	-1.25E+08	-6.45E+07	-64473000	0.00E+00	-1.25E+08	-7.77E+09	-9.42E+05	Enthalpy	[BTU/HR]
Density	[LB/CUFT]	0.861	1.006	0.422	0.435	0.545	0.501	0.37	0.366		0.501	210.08	181.225	Density	[LB/CUFT]
Mass Flow	[LB/HR]													Mass Flow	[LB/HR]
O2S			134.563	134.563	24548.4	24548.4	134.922	3.601	3.601		134.922		0.002	O2S	
H2S			155.868	13358.421			156.105	7.998	7.998		156.105		0.001	H2S	
H2O			8663.586	157155.109			10220.242	4389.911	4389.911		10220.242		301.303	H2O	
S2			< 0.001	< 0.001			5421.442	trace	trace		5421.442		0.437	S2	
S6			0.803	0.803			3898.438	0.021	0.021		3898.438		1493.655	S6	
S8			5.689	5.689			2761.193	0.152	0.152		2761.193		10576.802	S8	
CO			4.665	459346.656			4.665	12291.313	12291.313		4.665		trace	CO	
CO2			26623.678	273825.563			26631.824	7327.093	7327.093		26631.824		0.005	CO2	
H2			1.752	24773.842			1.752	662.905	662.905		1.752		trace	H2	
O2		18391.988												O2	
N2		60571.711	64339.152	140814.141	60571.711	60571.711	64339.652	3767.94	3767.94		64339.652		trace	N2	
COS			0.666	0.666			0.667	0.018	0.018		0.667		trace	COS	
ZNO														ZNO	
ZNS												304172		ZNS	
AL2O3												1106450		AL2O3	

DSRP-500 1/19/98 pg.3

Display ALLS Units: Format: SOLI	TREAMS From DS To Phas	P-O2-N2 PRESAIR AIR-HX VAPOR	PCG-RECY RECYCOMP FEEDMIX VAPOR	RAW-CG FEEDMIX DESULF VAPOR	ROG REGENSEP AIR-HX VAPOR	ROG-COOL AIR-HX DSRPXO2 VAPOR	RXNPRD DSRPMIX PD-COOLR VAPOR	SLIPSTRM VALVSLIP VALVE2 VAPOR	SLPSTRM VALVE2 DSRPXO2 VAPOR	SN-LIQ SN-EQUIL DSRPMIX MISSING	SN-VAP SN-EQUIL DSRPMIX VAPOR	STNDPIPE ZNSCOOLR STANDPIP MISSING	SULFUR VAPORIZR LIQUID	Display ALLS Units: Format: SOLI	TREAMS From DS To Phas
Temperature	[C]	207.6	147.1	459.3	808.9	585.1	600	556.1	556.1		600	556.1	140	Temperature	[C]
Pressure	[PSI]	278.9	275	275	273.6	271.6	268.6	274.4	271.6		268.6	275	14.7	Pressure	[PSI]
Mass VFrac		1	1	1	1	1	1	1	1		1	0	0	Mass VFrac	
Mass SFrac		0	0	0	0	0	0	0	0		0	1	0	Mass SFrac	
*** ALL PHAS	ES ***													*** ALL PHAS	ES ***
Mass Flow	[LB/HR]	78963.703	99930.422	1069420	85120.109	85120.109	113570.906	28450.951	28450.951	0	113570.906	1410630	12372.203	Mass Flow	[LB/HR]
Volume Flow	[CUFT/HR]	91749.711	99302.75	2.53E+06	195456.375	156297.594	226467.672	76921.539	77711.063		226467.438	6714.697	68.27	Volume Flow	[CUFT/HR]
Enthalpy	[BTU/HR]	6.30E+06	-1.47E+08	-2.44E+09	-2.00E+07	-2.88E+07	-1.25E+08	-6.45E+07	-64473000	0.00E+00	-1.25E+08	-7.77E+09	-9.42E+05	Enthalpy	[BTU/HR]
Density	[LB/CUFT]	0.861	1.006	0.422	0.435	0.545	0.501	0.37	0.366		0.501	210.08	181.225	Density	[LB/CUFT]
Mass Flow	[LB/HR]													Mass Flow	[LB/HR]
O2S			134.563	134.563	24548.4	24548.4	134.922	3.601	3.601		134.922		0.002	O2S	
H2S			155.868	13358.421			156.105	7.998	7.998		156.105		0.001	H2S	
H2O			8663.586	157155.109			10220.242	4389.911	4389.911		10220.242		301.303	H2O	
S2			< 0.001	< 0.001			5421.442	trace	trace		5421.442		0.437	S2	
S6			0.803	0.803			3898.438	0.021	0.021		3898.438		1493.655	S6	
S8			5.689	5.689			2761.193	0.152	0.152		2761.193		10576.802	S8	
CO			4.665	459346.656			4.665	12291.313	12291.313		4.665		trace	CO	
CO2			26623.678	273825.563			26631.824	7327.093	7327.093		26631.824		0.005	CO2	
H2			1.752	24773.842			1.752	662.905	662.905		1.752		trace	H2	
O2		18391.988												O2	
N2		60571.711	64339.152	140814.141	60571.711	60571.711	64339.652	3767.94	3767.94		64339.652		trace	N2	
COS			0.666	0.666			0.667	0.018	0.018		0.667		trace	COS	
ZNO														ZNO	
ZNS												304172		ZNS	
AL2O3												1106450		AL2O3	

AHGP Advanced Hot Gas Process

AHGP 1/19/98

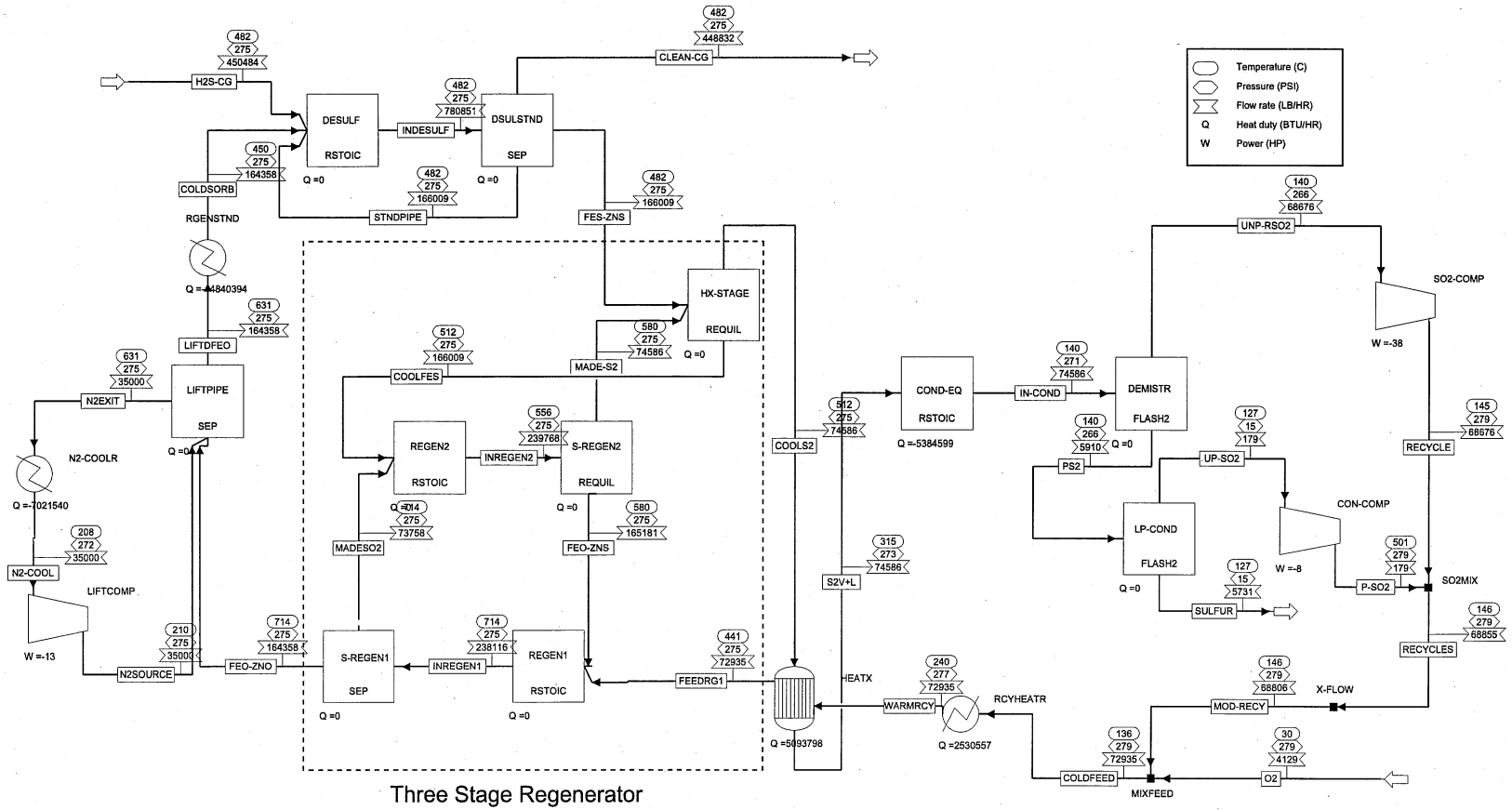

Three Stage Regenerator

AHGP 1/19/98 pg1

Display ALLS TREAMS		CLEAN-CG	COLDFEED	COLDSORB	COOLFES	COOLS2	FEEDRG1	FEO-ZNO	FEO-ZNS	FES-ZNS	H2S-CG	IN-COND	Display ALLS TREAMS	
Units:	From	DSULSTND	MIXFEED	RGENSTND	HX-STAGE	HX-STAGE	HEATX	S-REGEN1	S-REGEN2	DSULSTND		COND-EQ	Units:	From
Format: SOLI	DS To		RCYHEATR	DESULF	REGEN2	HEATX	REGEN1	LIFTPIPE	REGEN1	HX-STAGE	DESULF	DEMISTR	Format: SOLI	DS To
	Phas	VAPOR	MIXED	MISSING	MISSING	VAPOR	VAPOR	MISSING	MISSING	MISSING	VAPOR	MIXED		Phas
Temperature	[C]	482.4	136.5	450	512.3	512.3	440.6	713.9	580.4	482.4	482.2	140	Temperature	[C]
Pressure	[PSI]	274.7	279.2	275	274.7	274.7	275.2	274.7	274.7	274.7	275	270.7	Pressure	[PSI]
Mass VFrac		1	1	0	0	1	1	0	0	0	1	0.921	Mass VFrac	
Mass SFrac		< 0.001	0	1	1	0	0	1	1	1	0	0	Mass SFrac	
*** ALL PHAS ES ***													*** ALL PHAS ES ***	
Mass Flow	[LB/HR]	448832.344	72935.094	164357.922	166009.453	74586.227	72935.094	164357.922	165181.094	166009.453	450483.875	74586.227	Mass Flow	[LB/HR]
Volume Flow	[CUFT/HR]	1.13E+06	30858.555	756.208	793.141	60581.492	59761.762	756.208	768.468	793.141	1.13E+06	2.82E+04	Volume Flow	[CUFT/HR]
Enthalpy	[BTU/HR]	-1.09E+09	-1.35E+08	-1.06E+09	-1.03E+09	-1.25E+08	-1.28E+08	-1.04E+09	-1.04E+09	-1.04E+09	-1.07E+09	-1.35E+08	Enthalpy	[BTU/HR]
Density	[LB/CUFT]	0.397	2.364	217.345	209.306	1.231	1.22	217.345	214.949	209.306	0.399	2.645	Density	[LB/CUFT]
Mass Flow	[LB/HR]												Mass Flow	[LB/HR]
O2S			68800			68860.266	68800					68860.266	O2S	
H2S		23.01									6134.738		H2S	
H2O		73613.648									68998.523		H2O	
S2						519.707							S2	
S6			2.397			2171.238	2.397					2181.632	S6	
S8			3.894			3035.012	3.894					3544.325	S8	
CO		213439.25									213439.25		CO	
CO2		114865.578									114865.578		CO2	
H2		11355.747									11510.675		H2	
O2			4128.805				4128.805						O2	
N2		35535.098									35535.098		N2	
COS													COS	
ZNO				2084.988				2084.988					ZNO	
ZNS					2496.573				2496.573	2496.573			ZNS	
FE2O3				12272.938				12272.938	8199.015				FE2O3	
FEO													FEO	
FES		0.001			13512.88				4485.513	13512.88			FES	
AL2O3				150000	150000			150000	150000	150000			AL2O3	

AHGP 1/19/98 pg2

Display ALLS TREAMS Units: From Format: SOLI DS To Phas	INDESULF DESULF DSULSTND VAPOR	INREGEN1 REGEN1 S-REGEN1 VAPOR	INREGEN2 REGEN2 S-REGEN2 VAPOR	LIFTDFEO LIFTPIPE RGENSTND MISSING	MADE-S2 S-REGEN2 HX-STAGE VAPOR	MADESO2 S-REGEN1 REGEN2 VAPOR	MOD-RECY X-FLOW MIXFEED VAPOR	N2-COOL N2-COOLR LIFTCOMP VAPOR	N2EXIT LIFTPIPE N2-COOLR VAPOR	N2SOURCE LIFTCOMP LIFTPIPE VAPOR	O2 MIXFEED VAPOR	Display ALLS TREAMS Units: From Format: SOLI DS To Phas
Temperature [C]	482.4	713.9	556.4	631	580.4	713.9	146.1	208	631	210.1	30	Temperature [C]
Pressure [PSI]	274.7	274.7	274.7	274.7	274.7	274.7	279.2	272	274.7	275	279.2	Pressure [PSI]
Mass VFrac	0.575	0.31	0.311	0	1	1	1	1	1	1	1	Mass VFrac
Mass SFrac	0.425	0.69	0.689	1	0	0	0	0	0	0	0	Mass SFrac
*** ALL PHASES ***												*** ALL PHASES ***
Mass Flow [LB/HR]	780850.875	238116.203	239767.375	164357.922	74586.227	73758.273	68806.289	35000	35000	35000	4128.805	Mass Flow [LB/HR]
Volume Flow [CUFT/HR]	1132710	8.08E+04	68028.672	756.208	66784.258	80083.75	27821.109	43008.844	79902.289	42726.648	2669.199	Volume Flow [CUFT/HR]
Enthalpy [BTU/HR]	-3.16E+09	-1.17E+09	-1.16E+09	-1.05E+09	-1.22E+08	-1.30E+08	-1.35E+08	2866710	9.89E+06	2899740	-1712.78	Enthalpy [BTU/HR]
Density [LB/CUFT]	0.689	2.946	3.525	217.345	1.117	0.921	2.473	0.814	0.438	0.819	1.547	Density [LB/CUFT]
Mass Flow [LB/HR]												Mass Flow [LB/HR]
O2S		73722.469	68860.266		68860.266	73722.469	68800					O2S
H2S	23.01											H2S
H2O	73613.648											H2O
S2			5726		1563.893							S2
S6					2146.613		2.397					S6
S8					2015.451		3.894					S8
CO	213439.25											CO
CO2	114865.578											CO2
H2	11355.747											H2
O2		35.801				35.801					4128.805	O2
N2	35535.098							35000	35000	35000		N2
COS												COS
ZNO		2084.988		2084.988								ZNO
ZNS	4993.106		2496.573									ZNS
FE2O3		12272.938	8199.016	12272.938								FE2O3
FEO												FEO
FES	27025.441		4485.513									FES
AL2O3	300000	150000	150000	150000								AL2O3

AHGP 1/19/98 pg3

Display ALLS Units: Format: SOLI	TREAMS From DS To Phas	P-SO2 CON-COMP SO2MIX VAPOR	PS2 DEMISTR LP-COND LIQUID	RECYCLE SO2-COMP SO2MIX VAPOR	RECYCLES SO2MIX X-FLOW VAPOR	S2V+L HEATX COND-EQ VAPOR	STNDPIPE DSULSTND DESULF MISSING	SULFUR LP-COND LIQUID	UNP-RSO2 DEMISTR SO2-COMP VAPOR	UP-SO2 LP-COND CON-COMP VAPOR	WARMRCY RCYHEATR HEATX VAPOR	Display ALLS Units: Format: SOLI	TREAMS From DS To Phas
Temperature	[C]	500.6	139.6	145.1	146.1	315	482.4	127.1	139.6	127.1	240	Temperature	[C]
Pressure	[PSI]	279.2	265.7	279.2	279.2	272.7	274.7	14.7	265.7	14.7	277.2	Pressure	[PSI]
Mass VFrac		1	0	1	1	1	0	0	1	1	1	Mass VFrac	
Mass SFrac		0	0	0	0	0	1	0	0	0	0	Mass SFrac	
*** ALL PHAS ES ***												*** ALL PHAS ES ***	
Mass Flow	[LB/HR]	179.039	5910.173	68676.164	68855.203	74586.227	166009.094	5731.134	68676.133	179.039	72935.094	Mass Flow	[LB/HR]
Volume Flow	[CUFT/HR]	148.551	33.732	27679.805	27840.887	44448.238	793.139	31.631	28725.764	1460.365	41204.621	Volume Flow	[CUFT/HR]
Enthalpy	[BTU/HR]	-3.30E+05	120743.211	-1.35E+08	-135330000	-1.30E+08	-1.04E+09	472141.281	-135100000	-351400	-132710000	Enthalpy	[BTU/HR]
Density	[LB/CUFT]	1.205	175.208	2.481	2.473	1.678	209.307	181.187	2.391	0.123	1.77	Density	[LB/CUFT]
Mass Flow	[LB/HR]											Mass Flow	[LB/HR]
O2S		178.945	190.34	68669.961	68848.906	68860.266		11.396	68669.93	178.945	68800	O2S	
H2S												H2S	
H2O												H2O	
S2						519.707						S2	
S6		0.036	2179.265	2.363	2.398	2171.238		2179.229	2.363	0.036	2.397	S6	
S8		0.058	3540.567	3.838	3.897	3035.012		3540.509	3.838	0.058	3.894	S8	
CO												CO	
CO2												CO2	
H2												H2	
O2											4128.805	O2	
N2												N2	
COS												COS	
ZNO												ZNO	
ZNS							2496.533					ZNS	
FE2O3												FE2O3	
FEO												FEO	
FES							13512.56					FES	
AL2O3							150000					AL2O3	

AHGP-b Advanced Hot Gas Process

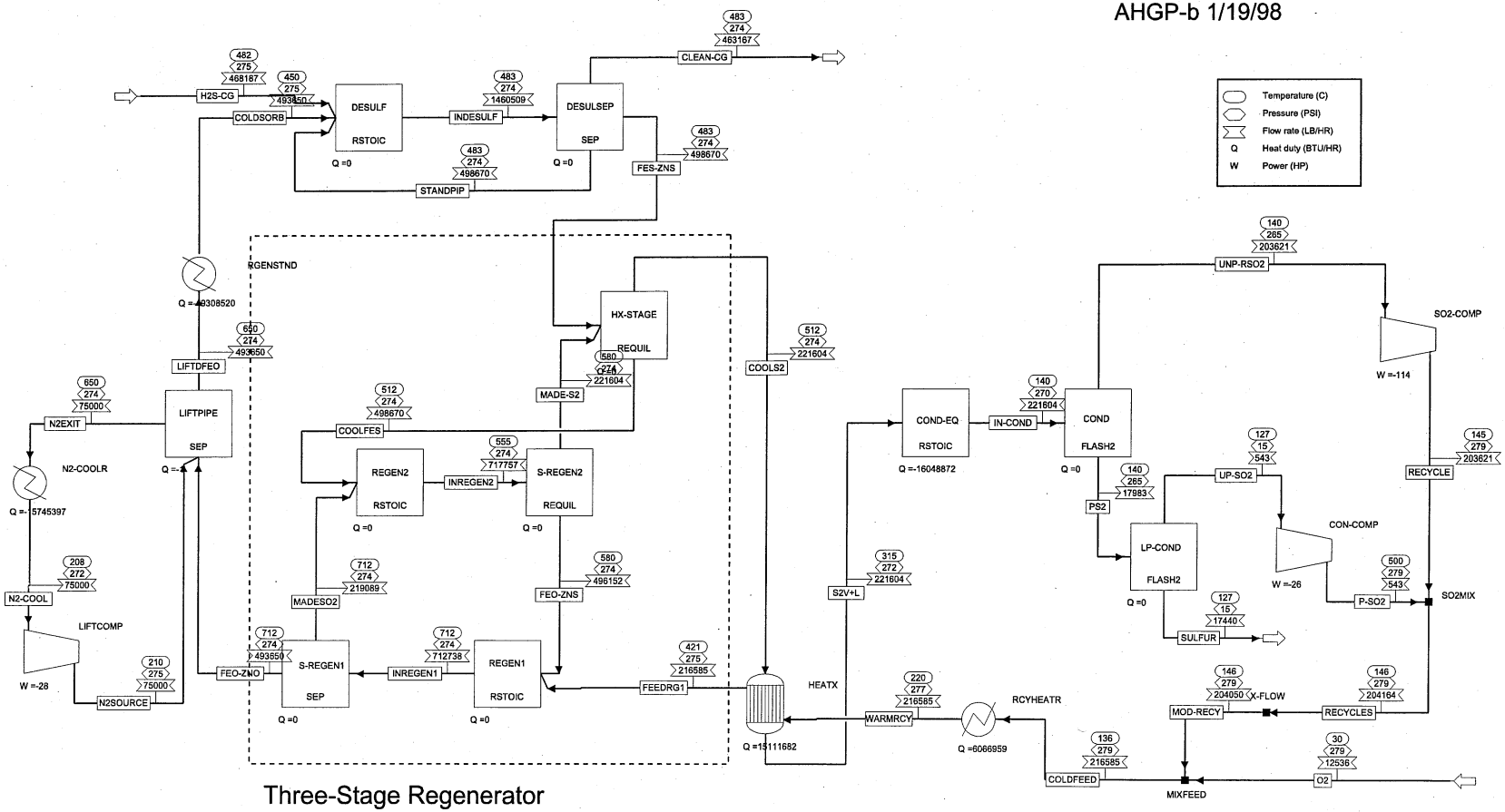

AHGP-b 1/19/98 pg1

Display ALLS TREAMS	CLEAN-CG	COLDFEED	COLDSORB	COOLFES	COOLS2	FEEDRG1	FEO-ZNO	FEO-ZNS	FES-ZNS	H2S-CG	IN-COND	Display ALLS TREAMS
Units: From	DESULSEP	MIXFEED	RGENSTND	HX-STAGE	HX-STAGE	HEATX	S-REGEN1	S-REGEN2	DESULSEP		COND-EQ	Units: From
Format: SOLI DS To Phas	VAPOR	RCYHEATR MIXED	DESULF MISSING	REGEN2 MISSING	HEATX VAPOR	REGEN1 VAPOR	LIFTPIPE MISSING	REGEN1 MISSING	HX-STAGE MISSING	DESULF VAPOR	COND MIXED	Format: SOLI DS To Phas
Temperature [C]	482.7	136.3	450	512.1	512.1	421.5	711.6	579.5	482.7	482.2	140	Temperature [C]
Pressure [PSI]	274.1	278.6	275	274.1	274.1	274.6	274.1	274.1	274.1	275	270.1	Pressure [PSI]
Mass VFrac	1	1	0	0	1	1	0	0	0	1	0.919	Mass VFrac
Mass SFrac	0	0	1	1	0	0	1	1	1	0	0	Mass SFrac
*** ALL PHAS ES ***												*** ALL PHAS ES ***
Mass Flow [LB/HR]	463167.313	216585.75	493649.531	498669.813	221603.984	216585.75	493649.531	496152.125	498669.813	468187.563	221603.984	Mass Flow [LB/HR]
Volume Flow [CUFT/HR	1.17E+06	91955.008	2270.583	2382.878	180074.938	173024.047	2270.583	2307.888	2382.878	1.16E+06	8.38E+04	Volume Flow [CUFT/HR]
Enthalpy [BTU/HR]	-1.16E+09	-4.01E+08	-3.18E+09	-3.10E+09	-3.69E+08	-3.80E+08	-3.12E+09	-3.13E+09	-3.11E+09	-1.08E+09	-4.00E+08	Enthalpy [BTU/HR]
Density [LB/CUFT]	0.397	2.355	217.411	209.272	1.231	1.252	217.411	214.981	209.272	0.403	2.643	Density [LB/CUFT]
Mass Flow [LB/HR]												Mass Flow [LB/HR]
O2S		204031.219			204180.078	204031.219					204180.078	O2S
H2S	23.471									18603.785		H2S
H2O	83842.484									69811.359		H2O
S2					1549.572							S2
S6		7.099			6588.625	7.099					6619.617	S6
S8		11.587			9285.715	11.587					10804.296	S8
CO	215953.672									215953.672		CO
CO2	116218.758									116218.758		CO2
H2	11175.208									11646.276		H2
O2		12535.85				12535.85						O2
N2	35953.723									35953.723		N2
COS												COS
ZNO			6332.866				6332.866					ZNO
ZNS				7583				7583	7583			ZNS
FE2O3			37316.672				37316.672	24919.895				FE2O3
FEO												FEO
FES				41086.797				13649.23	41086.797			FES
AL2O3			450000	450000			450000	450000	450000			AL2O3

AHGP-b 1/19/98 pg2

Display ALLS TREAMS		INDESULF	INREGEN1	INREGEN2	LIFTDFEO	MADE-S2	MADESO2	MOD-RECY	N2-COOL	N2EXIT	N2SOURCE	O2	Display ALLS TREAMS
Units:	From	DESULF	REGEN1	REGEN2	LIFTPIPE	S-REGEN2	S-REGEN1	X-FLOW	N2-COOLR	LIFTPIPE	LIFTCOMP		Units: From
Format: SOLI	DS To Phas	DESULSEP VAPOR	S-REGEN1 VAPOR	S-REGEN2 VAPOR	RGENSTND MISSING	HX-STAGE VAPOR	REGEN2 VAPOR	MIXFEED VAPOR	LIFTCOMP VAPOR	N2-COOLR VAPOR	LIFTPIPE VAPOR	MIXFEED VAPOR	Format: SOLI DS To Phas
Temperature [C]		482.7	711.6	554.9	649.8	579.5	711.6	146.1	208	649.8	210.1	30	Temperature [C]
Pressure [PSI]		274.1	274.1	274.1	274.1	274.1	274.1	278.6	272	274.1	275	278.6	Pressure [PSI]
Mass VFrac		0.317	0.307	0.309	0	1	1	1	1	1	1	1	Mass VFrac
Mass SFrac		0.683	0.693	0.691	1	0	0	0	0	0	0	0	Mass SFrac
*** ALL PHAS	ES ***												*** ALL PHAS ES ***
Mass Flow	[LB/HR]	1460510	712737.875	717757.063	493649.531	221603.984	219088.344	204049.906	75000	75000	75000	12535.85	Mass Flow [LB/HR]
Volume Flow	[CUFT/HR]	1171290	2.40E+05	202161.641	2270.583	198350.969	237827.297	82715.25	92161.805	175148.922	91557.102	8121.884	Volume Flow [CUFT/HR]
Enthalpy	[BTU/HR]	-7.37E+09	-3.51E+09	-3.49E+09	-3.13E+09	-3.62E+08	-3.87E+08	-4.01E+08	6142950	2.19E+07	6213730	-5136.922	Enthalpy [BTU/HR]
Density	[LB/CUFT]	1.247	2.969	3.55	217.411	1.117	0.921	2.467	0.814	0.428	0.819	1.543	Density [LB/CUFT]
Mass Flow	[LB/HR]												Mass Flow [LB/HR]
O2S			219000	204180.953		204180.078	219000	204031.219					O2S
H2S		23.471											H2S
H2O		83842.484											H2O
S2				17423.979		4630.148							S2
S6						6555.111		7.099					S6
S8						6238.653		11.587					S8
CO		215953.672											CO
CO2		116218.758											CO2
H2		11175.208											H2
O2			88.344				88.344					12535.85	O2
N2		35953.723							75000	75000	75000		N2
COS													COS
ZNO			6332.866		6332.866								ZNO
ZNS		15166		7583									ZNS
FE2O3			37316.672	24919.895	37316.672								FE2O3
FEO													FEO
FES		82173.594		13649.23									FES
AL2O3		900000	450000	450000	450000								AL2O3

AHGP-b 1/19/98 pg3

Display ALLSTREAMS	P-SO2	PS2	RECYCLE	RECYCLES	S2V+L	STANDPIP	SULFUR	UNP-RSO2	UP-SO2	WARMRCY		Display ALLSTREAMS
Units: From	CON-COMP	COND	SO2-COMP	SO2MIX	HEATX	DESULSEP	LP-COND	COND	LP-COND	RCYHEATR		Units: From
Format: SOLIDS To Phas	SO2MIX VAPOR	LP-COND LIQUID	SO2MIX VAPOR	X-FLOW VAPOR	COND-EQ VAPOR	DESULF MISSING	LIQUID	SO2-COMP VAPOR	CON-COMP VAPOR	HEATX VAPOR		Format: SOLIDS To Phas
Temperature [C]	500.4	139.6	145.1	146.1	315	482.7	127.2	139.6	127.2	220		Temperature [C]
Pressure [PSI]	278.6	265.1	278.6	278.6	272.1	274.1	14.7	265.1	14.7	276.6		Pressure [PSI]
Mass VFrac	1	0	1	1	1	0	0	1	1	1		Mass VFrac
Mass SFrac	0	0	0	0	0	1	0	0	0	0		Mass SFrac
*** ALL PHASES ***												*** ALL PHASES ***
Mass Flow [LB/HR]	543.2	17983.422	203620.531	204163.734	221603.984	498669.813	17440.221	203620.938	543.2	216585.75		Mass Flow [LB/HR]
Volume Flow [CUFT/HR]	451.514	102.6	82271.875	82761.391	132160.859	2382.878	96.225	85387.891	4431.133	117188.945		Volume Flow [CUFT/HR]
Enthalpy [BTU/HR]	-1.00E+06	370562.063	-4.00E+08	-401270000	-3.84E+08	-3.11E+09	1436680	-400560000	-1066100	-394990000		Enthalpy [BTU/HR]
Density [LB/CUFT]	1.203	175.276	2.475	2.467	1.677	209.272	181.244	2.385	0.123	1.848		Density [LB/CUFT]
Mass Flow [LB/HR]												Mass Flow [LB/HR]
O2S	542.913	577.553	203602.125	204145.031	204180.078		34.64	203602.531	542.913	204031.219		O2S
H2S												H2S
H2O												H2O
S2					1549.572							S2
S6	0.109	6612.687	6.994	7.103	6588.625		6612.578	6.994	0.109	7.099		S6
S8	0.178	10793.182	11.415	11.593	9285.715		10793.004	11.415	0.178	11.587		S8
CO												CO
CO2												CO2
H2												H2
O2										12535.85		O2
N2												N2
COS												COS
ZNO												ZNO
ZNS						7583						ZNS
FE2O3												FE2O3
FEO												FEO
FES						41086.797						FES
AL2O3						450000						AL2O3

AHGP-c Advanced Hot Gas Process

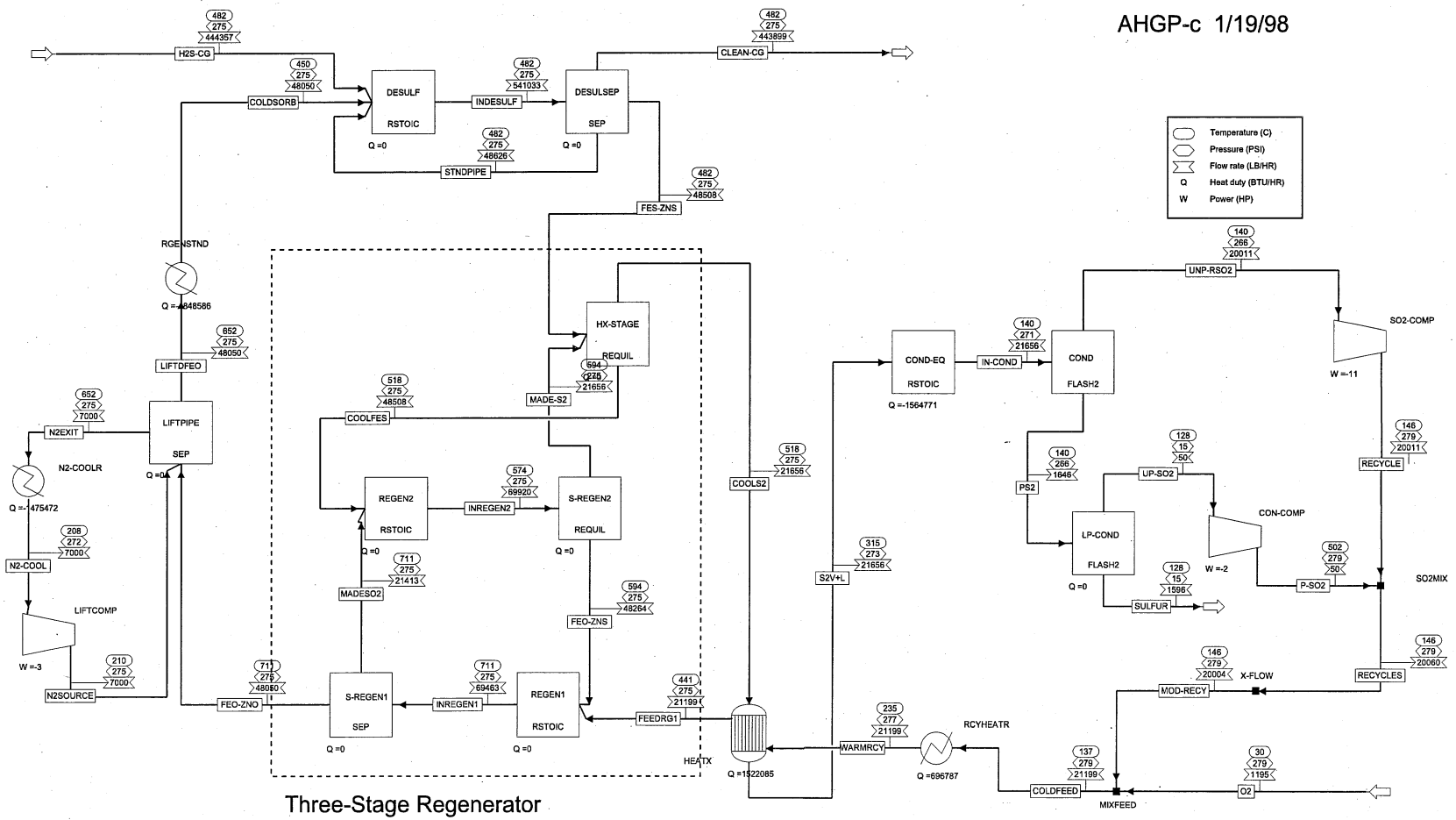

Three-Stage Regenerator

AHGP-c 1/19/98 pg1

Display ALLS TREAMS	CLEAN-CG	COLDFEED	COLDSORB	COOLFES	COOLS2	FEEDRG1	FEO-ZNO	FEO-ZNS	FES-ZNS	H2S-CG	IN-COND	Display ALLS TREAMS
Units: From	DESULSEP	MIXFEED	RGENSTND	HX-STAGE	HX-STAGE	HEATX	S-REGEN1	S-REGEN2	DESULSEP		COND-EQ	Units: From
Format: SOLI DS To		RCYHEATR	DESULF	REGEN2	HEATX	REGEN1	LIFTPIPE	REGEN1	HX-STAGE	DESULF	DEMISTR	Format: SOLI DS To
Phas	VAPOR	MIXED	MISSING	MISSING	VAPOR	VAPOR	MISSING	MISSING	MISSING	VAPOR	MIXED	Phas
Temperature [C]	482.1	136.9	450	517.8	517.8	441.4	711	594.5	482.1	482.2	140	Temperature [C]
Pressure [PSI]	274.9	279.4	275	274.9	274.9	275.4	275.4	275.4	274.9	275	270.9	Pressure [PSI]
Mass VFrac	1	1	0	0	1	1	0	0	0	1	0.924	Mass VFrac
Mass SFrac	0	0	1	1	0	0	1	1	1	0	0	Mass SFrac
*** ALL PHAS ES ***												*** ALL PHAS ES ***
Mass Flow [LB/HR]	443898.906	21199.451	48050.277	48507.699	21656.5	21199.451	48050.277	48263.68	48507.699	444356.313	21656.5	Mass Flow [LB/HR]
Volume Flow [CUFT/HR	1.12E+06	8971.891	221.013	231.696	17760.699	17373.199	221.013	224.428	231.696	1.12E+06	8.21E+03	Volume Flow [CUFT/HR]
Enthalpy [BTU/HR]	-1.07E+09	-3.93E+07	-3.11E+08	-3.03E+08	-3.62E+07	-3.71E+07	-3.05E+08	-3.05E+08	-3.04E+08	-1.06E+09	-3.93E+07	Enthalpy [BTU/HR]
Density [LB/CUFT]	0.397	2.363	217.409	209.359	1.219	1.22	217.409	215.052	209.359	0.397	2.638	Density [LB/CUFT]
Mass Flow [LB/HR]												Mass Flow [LB/HR]
O2S		20002.434			20061.83	20002.434					20061.83	O2S
H2S	65.815									1790.604		H2S
H2O	70033.773									68721.594		H2O
S2					164.784							S2
S6		0.719			612.014	0.719					615.31	S6
S8		1.144			817.872	1.144					979.36	S8
CO	212582.609									212582.609		CO
CO2	114404.563									114404.563		CO2
H2	11419.664									11464.477		H2
O2		1195.155				1195.155						O2
N2	35392.48									35392.48		N2
COS												COS
ZNO			500.379				500.379					ZNO
ZNS				599.156				599.156	599.156			ZNS
FE2O3			3549.896				3549.896	2415.33				FE2O3
FEO												FEO
FES				3908.545				1249.193	3908.545			FES
AL2O3			44000	44000			44000	44000	44000			AL2O3

AHGP-c 1/19/98 pg2

Display ALLS Units: Format: SOLI	TREAMS From DS To Phas	INDESULF DESULF DESULSEP VAPOR	INREGEN1 REGEN1 S-REGEN1 VAPOR	INREGEN2 REGEN2 S-REGEN2 VAPOR	LIFTDFEO LIFTPIPE RGENSTND MISSING	MADE-S2 S-REGEN2 HX-STAGE VAPOR	MADESO2 S-REGEN1 REGEN2 VAPOR	MOD-RECY X-FLOW MIXFEED VAPOR	N2-COOL N2-COOLR LIFTCOMP VAPOR	N2EXIT LIFTPIPE N2-COOLR VAPOR	N2SOURCE LIFTCOMP LIFTPIPE VAPOR	O2 MIXFEED VAPOR	Display ALLS Units: Format: SOLI	TREAMS From DS To Phas
Temperature	[C]	482.1	711	573.5	651.5	594.5	711	146.5	208	651.5	210.1	30	Temperature	[C]
Pressure	[PSI]	274.9	275.4	275.4	275	275.4	275.4	279.4	272	275	275	279.4	Pressure	[PSI]
Mass VFrac		0.82	0.308	0.31	0	1	1	1	1	1	1	1	Mass VFrac	
Mass SFrac		0.18	0.692	0.69	1	0	0	0	0	0	0	0	Mass SFrac	
*** ALL PHAS	ES ***												*** ALL PHAS	ES ***
Mass Flow	[LB/HR]	541032.563	69463.133	69920.453	48050.277	21656.5	21412.854	20004.297	7000	7000	7000	1195.155	Mass Flow	[LB/HR]
Volume Flow	[CUFT/HR]	1119290	2.34E+04	20135.34	221.013	19779.051	23221.412	8092.941	8601.769	16324.121	8545.33	772.086	Volume Flow	[CUFT/HR]
Enthalpy	[BTU/HR]	-1.68E+09	-3.42E+08	-3.41E+08	-3.06E+08	-3.54E+07	-3.76E+07	-3.93E+07	573341.625	2.05E+06	579948.125	-497.809	Enthalpy	[BTU/HR]
Density	[LB/CUFT]	0.483	2.963	3.473	217.409	1.095	0.922	2.472	0.814	0.429	0.819	1.548	Density	[LB/CUFT]
Mass Flow	[LB/HR]												Mass Flow	[LB/HR]
O2S			21310.348	20062.115		20061.83	21310.348	20002.434					O2S	
H2S		65.815											H2S	
H2O		70033.773											H2O	
S2				1594.662		542.278							S2	
S6						569.93		0.719					S6	
S8						482.462		1.144					S8	
CO		212582.609											CO	
CO2		114404.563											CO2	
H2		11419.664											H2	
O2			102.507				102.507					1195.155	O2	
N2		35392.48							7000	7000	7000		N2	
COS													COS	
ZNO			500.379		500.379								ZNO	
ZNS		1316.587		599.156									ZNS	
FE2O3			3549.896	2415.33	3549.896								FE2O3	
FEO													FEO	
FES		7817.09		1249.193									FES	
AL2O3		88000	44000	44000	44000								AL2O3	

AHGP-c 1/19/98 pg3

Display ALLS	TREAMS	P-SO2	PS2	RECYCLE	RECYCLES	S2V+L	STNDPIPE	SULFUR	UNP-RSO2	UP-SO2	WARMRCY		Display ALLS	TREAMS
Units:	From	CON-COMP	DEMISTR	SO2-COMP	SO2MIX	HEATX	DESULSEP	LP-COND	DEMISTR	LP-COND	RCYHEATR		Units:	From
Format: SOLI	DS To	SO2MIX	LP-COND	SO2MIX	X-FLOW	COND-EQ	DESULF		SO2-COMP	CON-COMP	HEATX		Format: SOLI	DS To
	Phas	VAPOR	LIQUID	VAPOR	VAPOR	VAPOR	MISSING	LIQUID	VAPOR	VAPOR	VAPOR			Phas
Temperature	[C]	501.6	140	145.5	146.5	315	482.1	127.7	140	127.7	235		Temperature	[C]
Pressure	[PSI]	279.4	265.9	279.4	279.4	272.9	274.9	14.7	265.9	14.7	277.4		Pressure	[PSI]
Mass VFrac		1	0	1	1	1	0	0	1	1	1		Mass VFrac	
Mass SFrac		0	0	0	0	0	1	0	0	0	0		Mass SFrac	
*** ALL PHAS	ES ***												*** ALL PHAS	ES ***
Mass Flow	[LB/HR]	49.58	1645.675	20010.68	20060.26	21656.5	48625.977	1596.094	20010.973	49.58	21199.451		Mass Flow	[LB/HR]
Volume Flow	[CUFT/HR]	41.161	9.405	8070.953	8115.582	12934.794	232.279	8.823	8375.842	404.953	11828.04		Volume Flow	[CUFT/HR]
Enthalpy	[BTU/HR]	-9.14E+04	34663.465	-3.93E+07	-39425000	-3.78E+07	-3.04E+08	131964.156	-39363000	-97300.727	-38619000		Enthalpy	[BTU/HR]
Density	[LB/CUFT]	1.205	174.979	2.479	2.472	1.674	209.343	180.904	2.389	0.122	1.792		Density	[LB/CUFT]
Mass Flow	[LB/HR]												Mass Flow	[LB/HR]
O2S		49.553	52.704	20008.838	20058.391	20061.83		3.15	20009.131	49.553	20002.434		O2S	
H2S													H2S	
H2O													H2O	
S2						164.784							S2	
S6		0.01	614.651	0.711	0.721	612.014		614.641	0.711	0.01	0.719		S6	
S8		0.016	978.32	1.131	1.148	817.872		978.303	1.131	0.016	1.144		S8	
CO													CO	
CO2													CO2	
H2													H2	
O2											1195.155		O2	
N2													N2	
COS													COS	
ZNO													ZNO	
ZNS							717.431						ZNS	
FE2O3													FE2O3	
FEO													FEO	
FES							3908.545						FES	
AL2O3							44000						AL2O3	

Appendix F
Steam Generation Process Flowsheets

The following flowsheets represent possible design schemes for producing high pressure steam. Desulfurization units that require heat removal are utilized for producing the steam. The steam generated will result in an economic credit for the process. The steam generation simulations will help determine the equipment necessary for cooling the desulfurization process.

DSRP Complete Steam Generation Scheme

DSTEAM 11/26/97

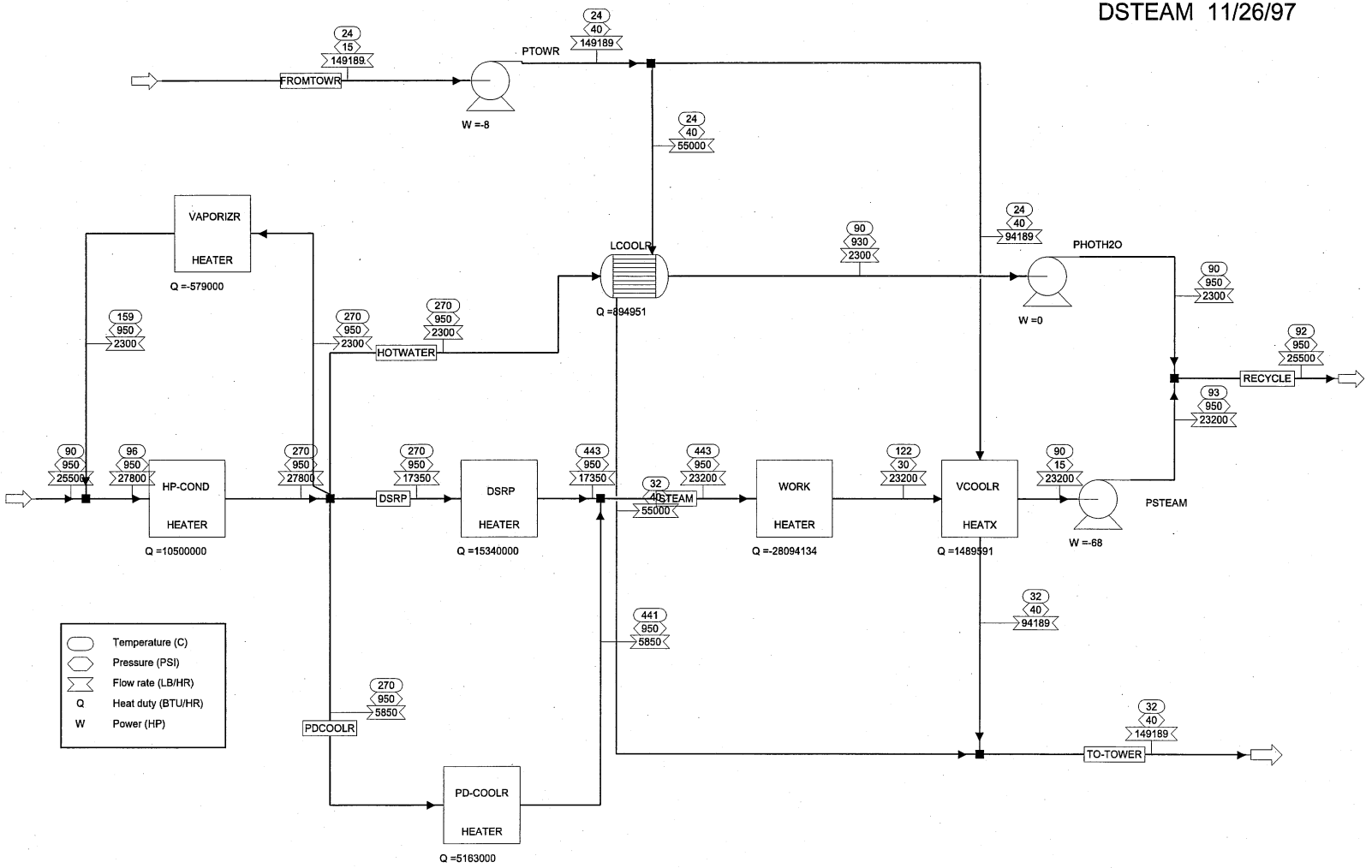

DSRP-b Complete Steam Generation Scheme

DBSTEAM 11/26/97

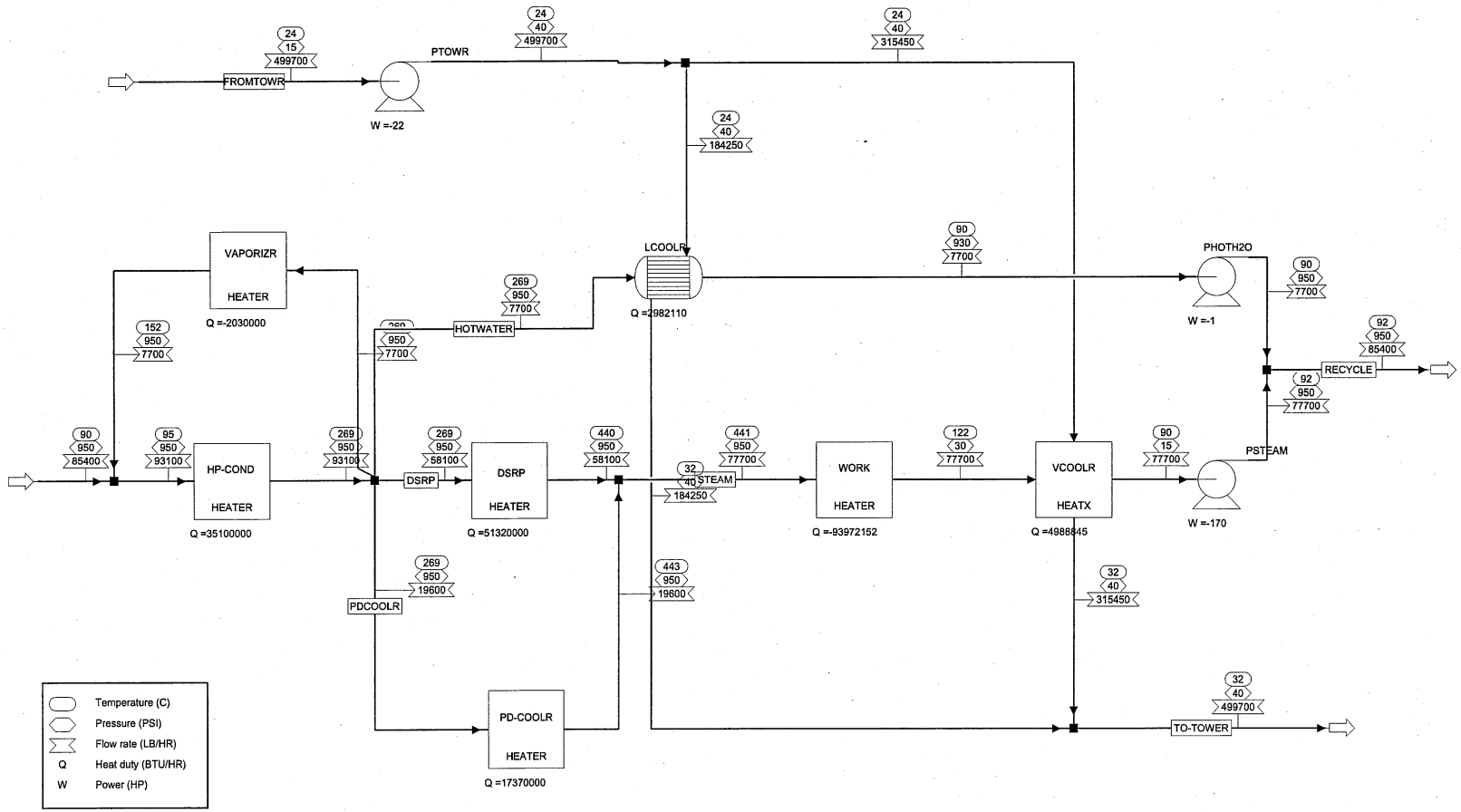

DSRP-c Complete Steam Generation Scheme

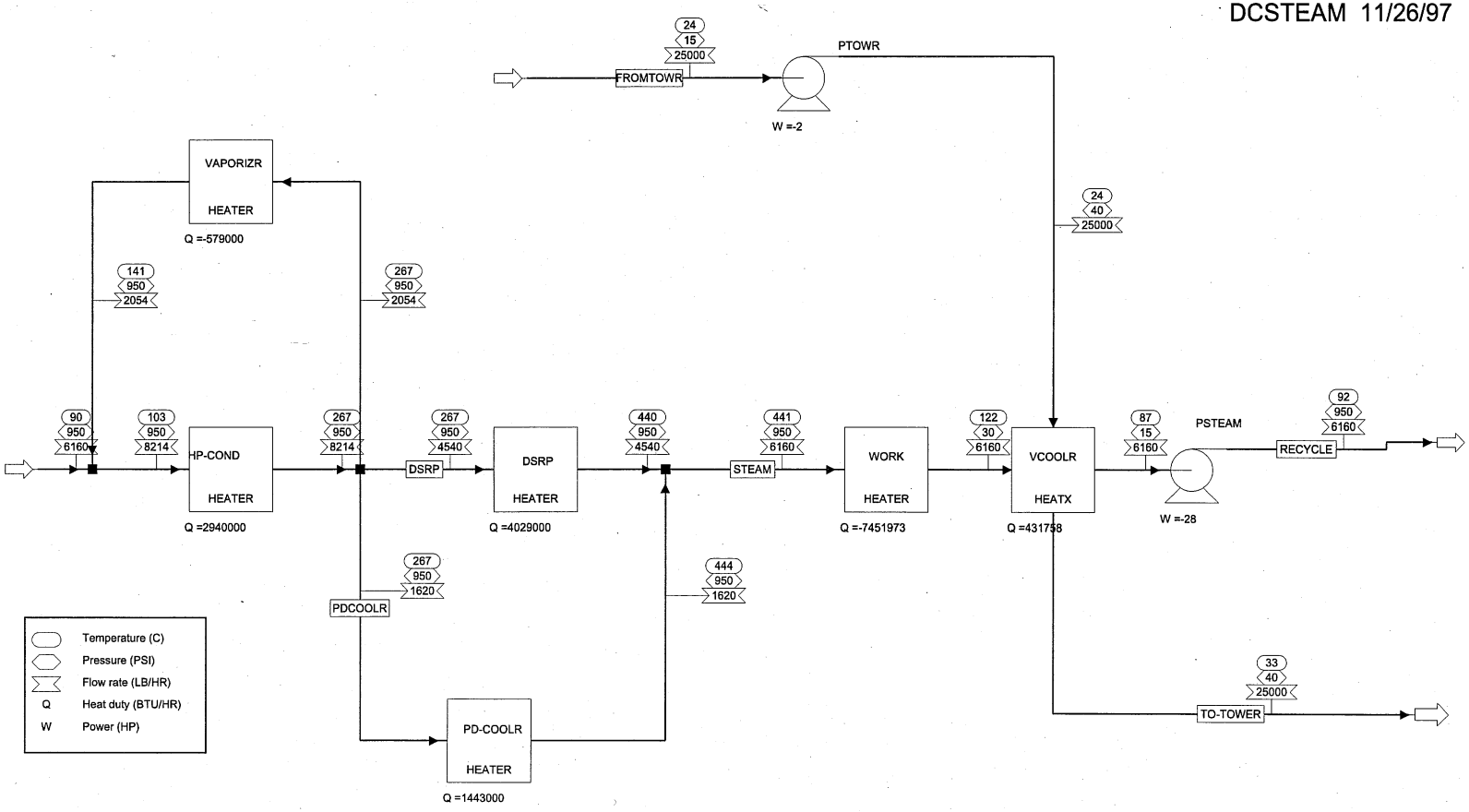

AHGP Complete Steam Generation Scheme

ASTEAM 1/22/98

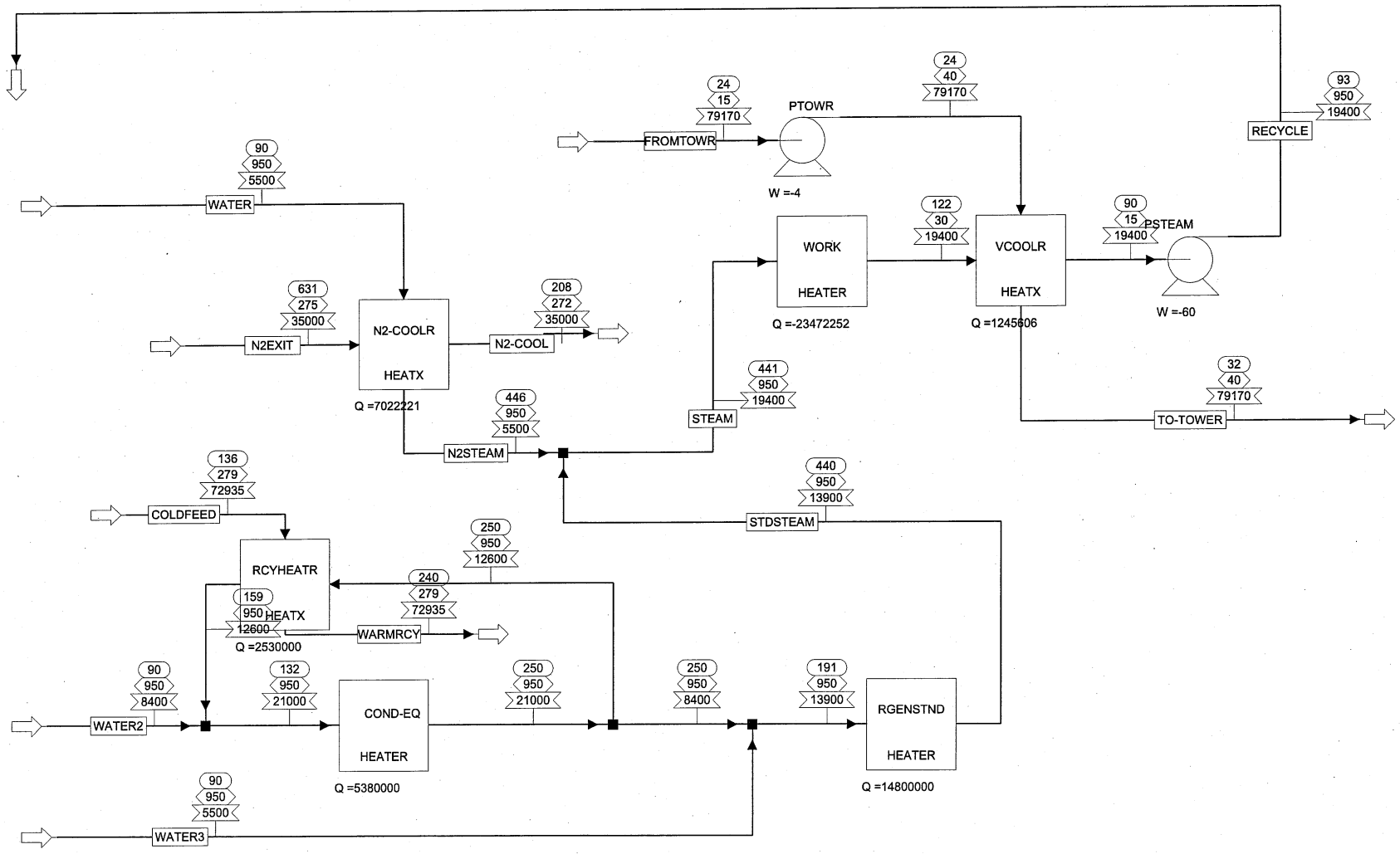

E-116

Temperature (C)

Pressure (PSI)

AHGP-b Complete Steam Generation Scheme

ABSTEAM 1/22/98

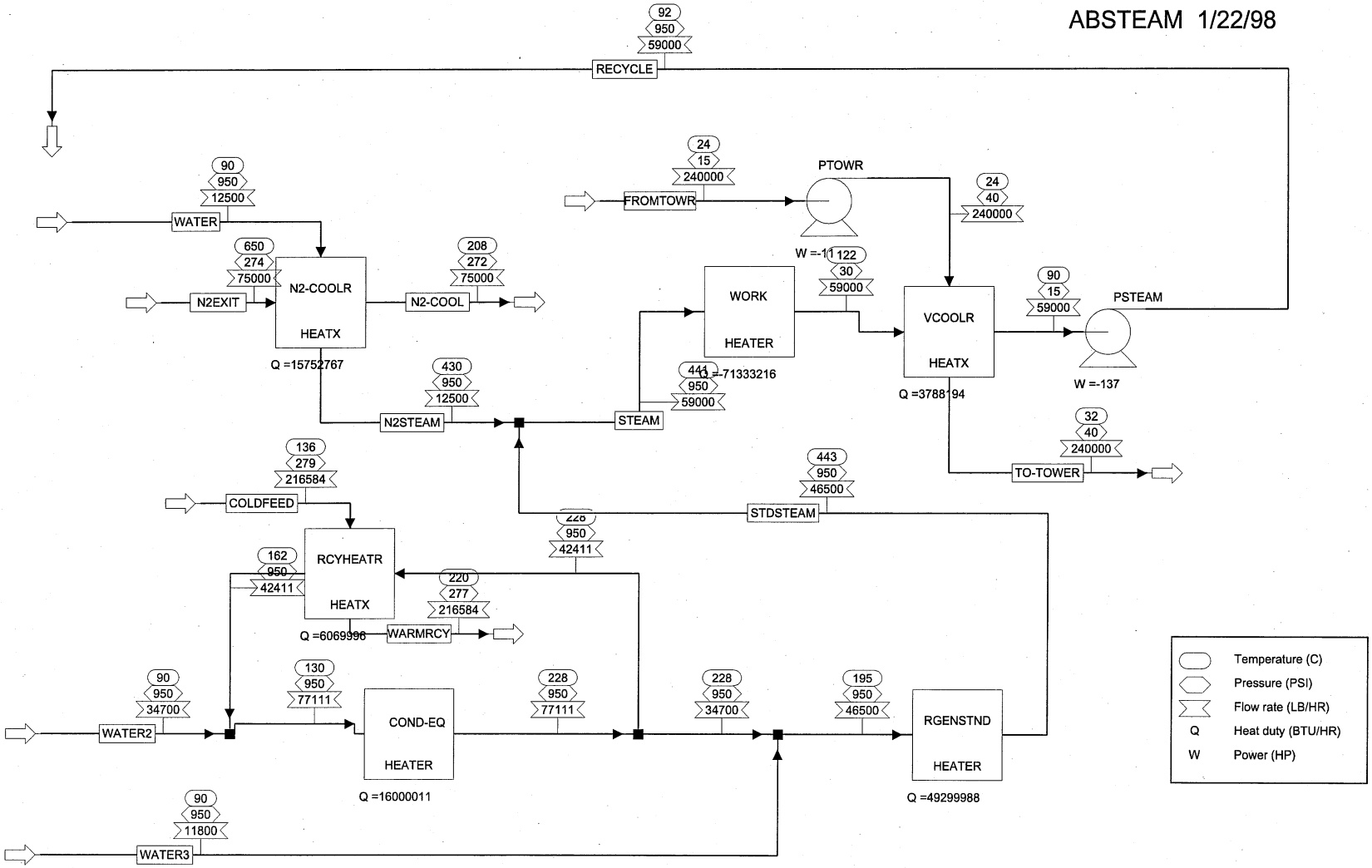

AHGP-c Complete Steam Generation Scheme

ACSTEAM 1/23/98

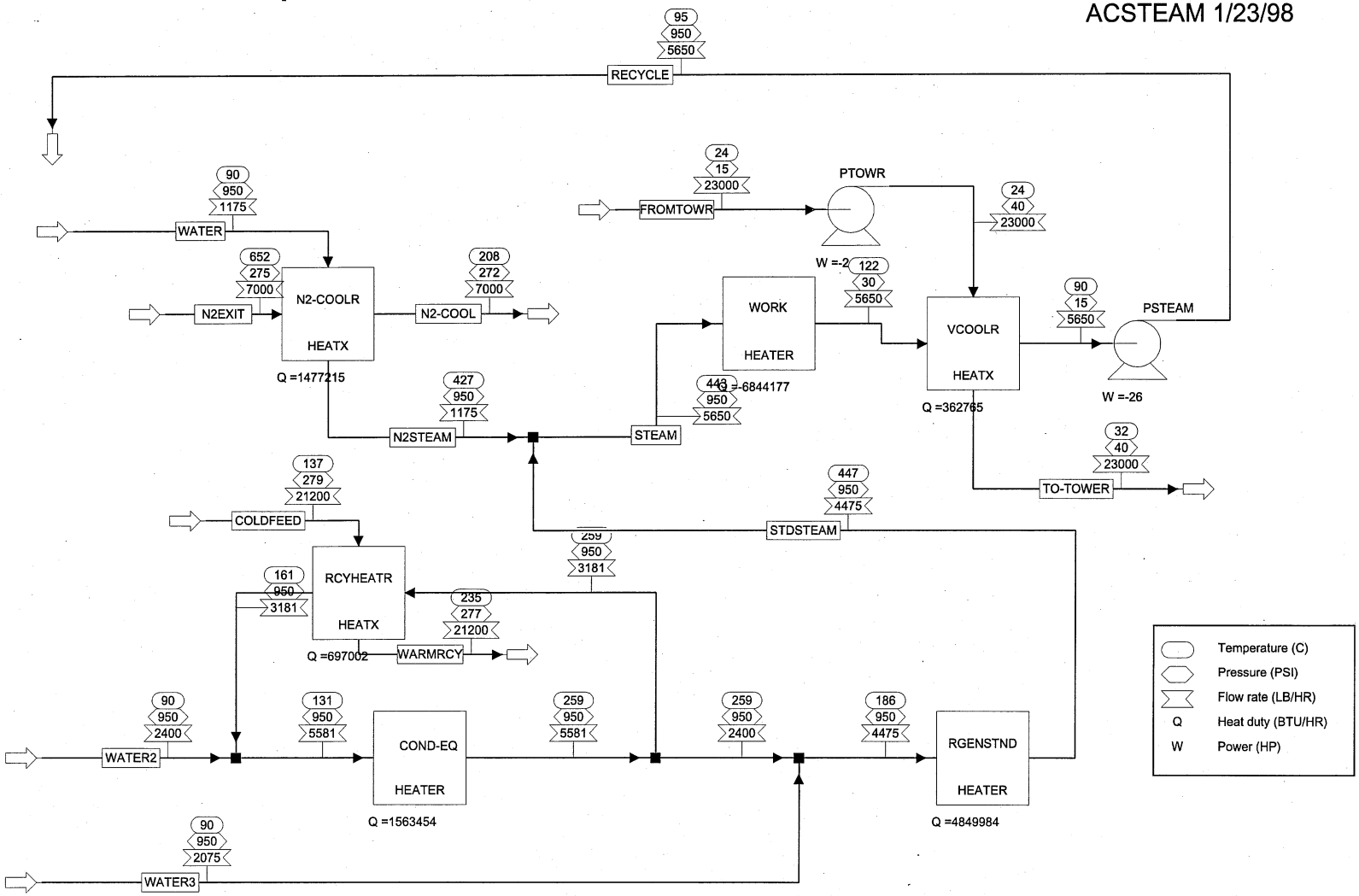

Appendix G
Calculation of Reactor Size

The reactor's diameter is determined from the average volumetric flow rate and the linear velocity.

$v = 20$ ft/sec $= 72{,}000$ ft/hr

$V = [(\text{gas volume entering}) + (\text{gas volume leaving})]/2 + (\text{sorbent mass flow}) (60 \text{ lb/ft}^3)^{-1}$

$\text{Area} = V/v = (\text{Volumetric flow rate ft}^3\text{/hr}) / 72{,}000 \text{ ft/hr}$ {ft^2}

Calculating the area allows for the calculation of the reactor inside diameter.

$\text{Area} = \pi (\text{I.D.})^2 / (4 \times 144 \text{ in}^2/\text{ft}^2)$

$\text{I.D.} = [(\text{Area}) (4 \times 144) / \pi]^{0.5}$ {in}

The reactor cost will be based on the material of construction costs. The reactor wall thickness and height are necessary for such a calculation. The reactor system cost will be calculated to include installation costs.

The reactor will be cylindrical. The wall and heads will be assumed to have the same thickness. The following equation was used for determining wall thickness (Peters & Timmerhaus, 1991).

$\text{Thickness} = P (\text{I.D.}) / [2 (\text{Max. allowable working stress psia}) (\text{Efficiency of joints}) - 0.6 P] + C_c$

P = pressure {psia} C_c = corrosion losses {in}

$\text{Thickness} = 275 (\text{I.D.})/ [2 (12{,}000) (0.85) - 0.6 (275)] + 0.125$ {in}

Taking steel density to be 489 lb/ft^3, the reactor weight is calculated with the equations below.

$\text{Weight of shell} = \pi (\text{I.D.}/12) (\text{height}) (\text{Thickness}/12)(489)$ {lbs}

$\text{Weight of heads} = 2 \pi [12 \text{ I.D.}/ 2]^2 (\text{Thickness}) (489/12^3) (2)$ {lbs}

$\text{Total weight} = 1.15 (\text{weight of shell} + \text{weight of heads})$ {lbs}

The total weight is increased 15% to account of nozzles, manholes, ect.

The cost of carbon steel can be calculated by the equation below.

$$(\text{Cost per lb}) = 80\ (\text{total weight})^{-0.34}$$

The equation above in applicable for 800 lb to 100,000 lb vessels (Peters and Timmerhaus 1991). Estimates for weights over 100,000 lbs could not be found. Therefore, in such cases the unit cost for carbon steel was taken as an average of the above equation calculated for 100,000 lb and the above equation calculated for the total weight. The unit cost is expected to continue to decrease at larger quantities but the decrease should become less pronounced.

Unit cost of carbon steel (weight > 100,000 lbs)

$$(\text{Cost per lb}) = 80\ [(\text{total weight})^{-0.34} + (100{,}000)^{-0.34}] / 2$$

The cost of installation will be twice of the cost of the reactor if it were constructed of carbon steel.

$$(\text{Cost of installation}) = 2\ (\text{Cost per lb})\ (\text{total weight})$$

The total cost of the reactor system includes installation and material costs. Material cost is multiplied by 3.5 to account for using stainless steel 310 instead of carbon steel.

$$(\text{Total cost for reactor}) = (\text{Cost of installation}) + 3.5\ (\text{Cost per lb})\ (\text{total weight})$$

Appendix H
Sizing Reactors for the DSRP

Copies of the reactor system sizing calculations follow. They include estimates of the reactor system costs. The equations describe in *Appendix G - Calculation of Reactor Size* where used in the spreadsheet.

Desulf and Regen transport reactor price calculation

DSRP

Regenerator Reactor

v (ft/sec) =	20	72000 ft/hr	air volume	67,895	cfh	HP-O2-N2
V (cfh) =	85,541		ROG volume	94,813	cfh	ROG
Area =	1.188 ft^2		regen sorbent flow	251,240	lb/hr	ZNS2RGEN
I.D.	15.068 in		regen sorbent vol.	4,187	cfh	
			sorbent vol%	4.90%		
thickness=	0.330					
shell wt.=	5,302 lbs		Corrosion depth	0.125	in	
heads wt.=	67 lbs		reactor height	100	ft	

total wt. 6,174 lbs (includes additional 15% for nozzles, manholes, etc.)

Regenerator Standpipe

size vs. regen size 1

total wt. 6,174 lbs

Desulfurization Reactor

v (ft/sec) =	20	72000 ft/hr	coal gas in volume	1,200,000	cfh	RAW-CG
V (cfh) =	1,296,166		cg out volume	1,370,000	cfh	CG-CALC
Area =	18.002 ft^2		regen sorbent flow	669,972	lb/hr	ZNS
I.D.	58.653 in		regen sorbent vol.	11,166	cfh	
			sorbent vol%	0.86%		
thickness=	0.922					
shell wt.=	57,707 lbs		Corrosion depth	0.125	in	
heads wt.=	2,821 lbs		reactor height	100	ft	

total wt. 69,607 lbs (includes additional 15% for nozzles, manholes, etc.)

Desulfurization Standpipe

size vs. desulf size 1

total wt. 69,607 lbs

total wt. 151,561 lbs weight for desulfurization and regeneration transport reactors

COST

			>100,000 lb calc	
C.S. unit price for quantiy needed	1.491 $/lb	1990 $	1.490988	1.386
	1.593 $/lb	1996 $		<100,000 lb calc

Cost of installation $482,917

Total reactor cost $1,328,020 includes cost of installation

DSRP reactor

DSRP Reactor Cost

DSRP

DSRP Reactor

v (ft/sec) gas =	3	10800 ft/hr	slipstream	37,342	cfh	SLIPSTREAM
V (cfh) =	114,923		ROG volume	75,166	cfh	ROG-COOL
space time -gas	33.33 seconds		reactor effluent	107,359	cfh	RXNPRD
v (ft/sec) cat =	2.3	8280 ft/hr	DSRP reactor Q	-15,340,000	BTU/hr	
			catalyst flow	299,381	lb/hr	
Area =	10.782 ft^2		catalyst vol.	4,990	cfh	
I.D.	45.391 in		catalyst vol%	5.59%		
thickness=	0.742 in					
shell wt.=	35,930 lbs		Corrosion depth	0.125	in	
heads wt.=	1,359 lbs		reactor height	100	ft	

total wt. 42,882 lbs (includes additional 15% for nozzles, manholes, etc.)

DSRP Standpipe

Cyclone (20% of reactor size)	8,576	Area =	10.78	ft^2
		I.D.	45.39	in
standpipe height	40 ft	thickness=	0.74	in
		shell wt.=	14,372	lbs
residense time	10.81 minutes	heads wt.=	1,359	lbs

total wt. 26,667 lbs (includes additional 15% on standpipe weight + Cyclone weight)

Heat Exchanger

Heat Exchanger Area (ft^2) 1063 heat exchanger pipe thickness 0.25 in

volume of steel 22

total weight 10,829 lbs

total wt. **80,379 lbs** weight for DSRP reactor system

COST

			>100,000 lb calc	
C.S. unit price for quantiy needed	1.719 $/lb	1990 $	1.657735955	1.719
	1.837 $/lb	1996 $		<100,000 lb calc

Cost of installation $295,320

Total reactor cost **$812,129** includes cost of installation

Desulf and Regen transport reactor price calculation

DSRP

Regenerator Reactor			air volume	215,340	cfh	HP-O2-N2
v (ft/sec) =	20	72000 ft/hr	ROG volume	299,541	cfh	ROG
V (cfh) =	277,458		regen sorbent flow	1,201,050	lb/hr	ZNS2RGEN
Area =	3.854 ft^2		regen sorbent vol.	20,018	cfh	
I.D.	27.137 in					
			sorbent vol%	7.21%		
thickness=	0.494					
shell wt.=	14,298 lbs		Corrosion depth	0.125	in	
heads wt.=	323 lbs		reactor height	100	ft	

total wt. 16,814 lbs (includes additional 15% for nozzles, manholes, etc.)

Regenerator Standpipe

size vs. regen size 1

total wt. 16,814 lbs

Desulfurization Reactor			coal gas in volume	1,409,220	cfh	RAW-CG
v (ft/sec) =	20	72000 ft/hr	cg out volume	1,877,650	cfh	CG-CALC
V (cfh) =	1,687,918		regen sorbent flow	2,669,000	lb/hr	ZNS
Area =	23.443 ft^2		regen sorbent vol.	44,483	cfh	
I.D.	66.933 in					
			sorbent vol%	2.64%		
thickness=	1.035					
shell wt.=	73,889 lbs		Corrosion depth	0.125	in	
heads wt.=	4,121 lbs		reactor height	100	ft	

total wt. 89,711 lbs (includes additional 15% for nozzles, manholes, etc.)

Desulfurization Standpipe

size vs. desulf size 1

total wt. 89,711 lbs

total wt. 213,051 lbs weight for desulfurization and regeneration transport reactors

COST

				>100,000 lb calc	
C.S. unit price for quantiy needed	1.415 $/lb	1990 $	1.4152335	1.234	
	1.512 $/lb	1996 $		<100,000 lb calc	

Cost of installation $644,349

Total reactor cost **$1,771,959** includes cost of installation

DSRP-b reactor

DSRP-b Reactor Cost

DSRP

DSRP Reactor

v (ft/sec) gas =	3	10800	ft/hr	slipstream	153,708	cfh	SLIPSTREAM
V (cfh) =	393,089			ROG volume	237,184	cfh	ROG-COOL
space time -gas	33.33	seconds		reactor effluent	361,900	cfh	RXNPRD
v (ft/sec) cat =	2.3	8280	ft/hr	DSRP reactor Q	-51,320,000	BTU/hr	
				catalyst flow	1,001,581	lb/hr	
				catalyst vol.	16,693	cfh	
Area =	36.868	ft^2					
I.D.	83.936	in		catalyst vol%	5.47%		
thickness=	1.266	in					
shell wt.=	113,355	lbs		Corrosion depth	0.125	in	
heads wt.=	7,929	lbs		reactor height	100	ft	

total wt. 139,477 lbs (includes additional 15% for nozzles, manholes, etc.)

DSRP Standpipe

Cyclone (20% of reactor size)		27,895	Area =	36.87	ft^2
			I.D.	83.94	in
standpipe height	40	ft	thickness=	1.27	in
			shell wt.=	45,342	lbs
residense time	11.05	minutes	heads wt.=	7,929	lbs

total wt. 89,157 lbs (includes additional 15% on standpipe weight + Cyclone weight)

Heat Exchanger

Heat Exchanger Area (ft^2) 3556 heat exchanger pipe thickness 0.25 in

volume of steel 74

total weight 36,229 lbs

total wt. 264,863 lbs weight for DSRP reactor system

COST

				>100,000 lb calc	
C.S. unit price for quantiy needed	1.371	$/lb	1990 $	1.371208108	1.146
	1.465	$/lb	1996 $		<100,000 lb calc

Cost of installation $776,129

Total reactor cost **$2,134,355** includes cost of installation

Desulf and Regen transport reactor price calculation

DSRP

Regenerator Reactor			air volume	19,366	cfh	HP-O2-N2
v (ft/sec) =	20	72000 ft/hr	ROG volume	26,009	cfh	ROG
V (cfh) =	23,882		regen sorbent flow	71,663	lb/hr	ZNS2RGEN
Area =	0.332 ft^2		regen sorbent vol.	1,194	cfh	
I.D.	7.962 in					
			sorbent vol%	5.00%		
thickness=	0.233					
shell wt.=	1,981 lbs		Corrosion depth	0.125	in	
heads wt.=	13 lbs		reactor height	100	ft	
total wt.	2,293 lbs	(includes additional 15% for nozzles, manholes, etc.)				
Regenerator Standpipe						
			size vs. regen size	1		
total wt.	2,293 lbs					
Desulfurization Reactor			coal gas in volume	1,139,050	cfh	RAW-CG
v (ft/sec) =	20	72000 ft/hr	cg out volume	1,186,750	cfh	CG-CALC
V (cfh) =	1,164,094		regen sorbent flow	71,663	lb/hr	ZNS
Area =	16.168 ft^2		regen sorbent vol.	1,194	cfh	
I.D.	55.585 in					
			sorbent vol%	0.10%		
thickness=	0.880					
shell wt.=	52,215 lbs		Corrosion depth	0.125	in	
heads wt.=	2,419 lbs		reactor height	100	ft	
total wt.	62,829 lbs	(includes additional 15% for nozzles, manholes, etc.)				
Desulfurization Standpipe						
			size vs. desulf size	1		
total wt.	62,829 lbs					

total wt. **130,244 lbs** weight for desulfurization and regeneration transport reactors

COST

			>100,000 lb calc	
C.S. unit price for quantiy needed	1.528 $/lb	1990 $	1.5276336	1.459
	1.632 $/lb	1996 $		<100,000 lb calc

Cost of installation $425,193

Total reactor cost **$1,169,282** includes cost of installation

DSRP-c reactor

DSRP-c Reactor Cost

DSRP

DSRP Reactor

v (ft/sec) gas =	3	10800 ft/hr	slipstream	9,443	cfh	SLIPSTREAM
V (cfh) =	31,212		ROG volume	20,364	cfh	ROG-COOL
space time -gas	33.33 seconds		reactor effluent	29,995	cfh	RXNPRD
v (ft/sec) cat =	2.3	8280 ft/hr	DSRP reactor Q	-4,029,000	BTU/hr	
			catalyst flow	78,632	lb/hr	
			catalyst vol.	1,311	cfh	
Area =	2.93 ft^2					
I.D.	23.650 in		catalyst vol%	5.41%		
thickness=	0.446 in					
shell wt.=	11,265 lbs		Corrosion depth	0.125	in	
heads wt.=	222 lbs		reactor height	100	ft	

total wt. 13,210 lbs (includes additional 15% for nozzles, manholes, etc.)

DSRP Standpipe

Cyclone (20% of reactor size)	2,642	Area =	2.93	ft^2
		I.D.	23.65	in
standpipe height	40 ft	thickness=	0.45	in
		shell wt.=	4,506	lbs
residense time	11.17 minutes	heads wt.=	222	lbs

total wt. 8,079 lbs (includes additional 15% on standpipe weight + Cyclone weight)

Heat Exchanger

Heat Exchanger Area (ft^2) 279 heat exchanger pipe thickness 0.25 in

volume of steel 6

total weight 2,844 lbs

total wt. 24,133 lbs weight for DSRP reactor system

COST

				>100,000 lb calc	
C.S. unit price for quantiy needed	2.588 $/lb	1990 $	2.092218539	2.588	
	2.766 $/lb	1996 $		<100,000 lb calc	

Cost of installation $133,482

Total reactor cost **$367,075** includes cost of installation

Desulf and Regen transport reactor price calculation

DSRP

Regenerator Reactor

v (ft/sec) =	20	72000 ft/hr	air volume	28,592	cfh	HP-O2-N2
V (cfh) =	36,020		ROG volume	39,921	cfh	ROG
Area =	0.500 ft^2		regen sorbent flow	105,797	lb/hr	ZNS2RGEN
I.D.	9.778 in		regen sorbent vol.	1,763	cfh	
			sorbent vol%	4.90%		
thickness=	0.258					
shell wt.=	2,690 lbs		Corrosion depth	0.125	in	
heads wt.=	22 lbs		reactor height	100	ft	

total wt. 3,119 lbs (includes additional 15% for nozzles, manholes, etc.)

Regenerator Standpipe

size vs. regen size 1

total wt. 3,119 lbs

Desulfurization Reactor

v (ft/sec) =	20	72000 ft/hr	coal gas in volume	506,745	cfh	RAW-CG
V (cfh) =	545,644		cg out volume	575,144	cfh	CG-CALC
Area =	7.58 ft^2		regen sorbent flow	281,971	lb/hr	ZNS
I.D.	38.06 in		regen sorbent vol.	4,700	cfh	
			sorbent vol%	0.86%		
thickness=	0.642					
shell wt.=	26,075 lbs		Corrosion depth	0.125	in	
heads wt.=	827 lbs		reactor height	100	ft	

total wt. 30,938 lbs (includes additional 15% for nozzles, manholes, etc.)

Desulfurization Standpipe

size vs. desulf size 1

total wt. 30,938 lbs

total wt. 68,113 lbs weight for desulfurization and regeneration transport reactors

COST

				>100,000 lb calc	
C.S. unit price for quantiy needed	1.819 $/lb	1990 $	1.7075181	1.819	
	1.943 $/lb	1996 $		<100,000 lb calc	

Cost of installation $264,748

Total reactor cost **$728,057** includes cost of installation

DSRP-100 reactor

DSRP-100 Reactor Cost

DSRP

DSRP Reactor

v (ft/sec) gas =	3	10800 ft/hr		slipstream	15,723	cfh	SLIPSTREAM
V (cfh) =	48,391			ROG volume	31,647	cfh	ROG-COOL
space time -gas	33.33 seconds			reactor effluent	45,210	cfh	RXNPRD
v (ft/sec) cat =	2.3	8280 ft/hr		DSRP reactor Q	-6,459,000	BTU/hr	
				catalyst flow	126,056	lb/hr	
				catalyst vol.	2,101	cfh	
Area =	4.540 ft^2						
I.D.	29.454 in			catalyst vol%	5.59%		
thickness=	0.525 in						
shell wt.=	16,508 lbs			Corrosion depth	0.125	in	
heads wt.=	405 lbs			reactor height	100	ft	

total wt. 19,451 lbs (includes additional 15% for nozzles, manholes, etc.)

DSRP Standpipe

Cyclone (20% of reactor size)	3,890		Area =	4.54	ft^2
			I.D.	29.45	in
standpipe heigh	40 ft		thickness=	0.53	in
			shell wt.=	6,603	lbs
residense time	10.81 minutes		heads wt.=	405	lbs

total wt. 11,950 lbs (includes additional 15% on standpipe weight + Cyclone weight)

Heat Exchanger

Heat Exchanger Area (ft^2) 448 heat exchanger pipe thickness 0.25 in

volume of steel 9

total weight 4,560 lbs

total wt. 35,960 lbs weight for DSRP reactor system

COST

				>100,000 lb calc	
C.S. unit price for quantiy needed	2.260 $/lb	1990 $		1.928109822	2.26
	2.415 $/lb	1996 $			<100,000 lb calc

Cost of installation $173,677

Total reactor cost **$477,612** includes cost of installation

Desulf and Regen transport reactor price calculation

DSRP

Regenerator Reactor			air volume	139,951	cfh	HP-O2-N2
v (ft/sec) =	20	72000 ft/hr	ROG volume	194,430	cfh	ROG
V (cfh) =	176,007		regen sorbent flow	528,985	lb/hr	ZNS2RGEN
Area =	2.445 ft^2		regen sorbent vol.	8,816	cfh	
I.D.	21.614 in					
			sorbent vol%	5.01%		
thickness=	0.419					
shell wt.=	9,656 lbs		Corrosion depth	0.125	in	
heads wt.=	174 lbs		reactor height	100	ft	

total wt. 11,305 lbs (includes additional 15% for nozzles, manholes, etc.)

Regenerator Standpipe

size vs. regen size 1

total wt. 11,305 lbs

Desulfurization Reactor			coal gas in volume	2,531,530	cfh	RAW-CG
v (ft/sec) =	20	72000 ft/hr	cg out volume	2,867,390	cfh	CG-CALC
V (cfh) =	2,722,971		regen sorbent flow	1,410,630	lb/hr	ZNS
Area =	37.82 ft^2		regen sorbent vol.	23,511	cfh	
I.D.	85.01 in					
			sorbent vol%	0.86%		
thickness=	1.280348					
shell wt.=	116,135 lbs		Corrosion depth	0.125	in	
heads wt.=	8,227 lbs		reactor height	100	ft	

total wt. 143,017 lbs (includes additional 15% for nozzles, manholes, etc.)

Desulfurization Standpipe

size vs. desulf size 1

total wt. 143,017 lbs

total wt. 308,644 lbs weight for desulfurization and regeneration transport reactors

COST

				>100,000 lb calc	
C.S. unit price for quantiy needed	1.342 $/lb	1990 $	1.3421617	1.088	
	1.434 $/lb	1996 $		<100,000 lb calc	

Cost of installation $885,263

Total reactor cost **$2,434,474** includes cost of installation

DSRP-500 reactor

DSRP-500 Reactor Cost

DSRP

DSRP Reactor

v (ft/sec) gas =	3	10800 ft/hr		slipstream	76,726	cfh	SLIPSTREAM
V (cfh) =	236,095			ROG volume	153,894	cfh	ROG-COOL
space time -gas	33.33 seconds			reactor effluent	221,163	cfh	RXNPRD
v (ft/sec) cat =	2.3	8280 ft/hr		DSRP reactor Q	-31,370,000	BTU/hr	
				catalyst flow	612,229	lb/hr	
				catalyst vol.	10,204	cfh	
Area =	22.148 ft^2						
I.D.	65.058 in			catalyst vol%	5.56%		
thickness=	1.009 in						
shell wt.=	70,050 lbs			Corrosion depth	0.125	in	
heads wt.=	3,798 lbs			reactor height	100	ft	

total wt. 84,925 lbs (includes additional 15% for nozzles, manholes, etc.)

DSRP Standpipe

Cyclone (20% of reactor size)		16,985	Area =	22.15	ft^2
			I.D.	65.06	in
standpipe height	40 ft		thickness=	1.01	in
			shell wt.=	28,020	lbs
residense time	10.86 minutes		heads wt.=	3,798	lbs

total wt. 53,575 lbs (includes additional 15% on standpipe weight + Cyclone weight)

Heat Exchanger

Heat Exchanger Area (ft^2) 2174 heat exchanger pipe thickness 0.25 in

volume of steel 45

total weight 22,146 lbs

total wt. **160,646 lbs** weight for DSRP reactor system

COST

				>100,000 lb calc	
C.S. unit price for quantiy needed	1.477 $/lb	1990 $		1.477409568	1.359
	1.579 $/lb	1996 $			<100,000 lb calc

Cost of installation $507,200

Total reactor cost **$1,394,800** includes cost of installation

Appendix I
Sizing Reactors for the AHGP

Copies of the reactor system sizing calculations follow. They include estimates of the reactor system costs. The equations describe in *Appendix G - Calculation of Reactor Size* where used in the spreadsheet.

Desulf and Regen transport reactor price calculation

AHGP

N2 lift

v (ft/sec) =	50	180000 ft/hr	N2 in volume	42,761	cfh	N2SOURCE
V (cfh) =	64,033		N2 out volume	79,826	cfh	N2EXIT
Area =	0.356 ft^2		regen sorbent flow	164,358	lb/hr	FEO-ZNO
I.D.	8.245 in		regen sorbent vol.	2,739	cfh	
			sorbent vol%	4.28%		
thickness=	0.237					
shell wt.=	2,085 lbs		Corrosion depth	0.125	in	
heads wt.=	14 lbs		reactor height	100	ft	

key
caculated or constant values
inputed variables

total wt. 2,415 lbs (includes additional 15% for nozzles, manholes, etc.)

Regenerator Standpipe

			residence time	10	min	
volume -sorbent	457 ft^3					
			heat removal	14,850,494	BTU/hr	RGENSTND
Heat Exchanger Area	1,029 ft^2		heat exchanger pipe thickness	0.25	in	
length of pipe	2,620 ft		heat exchanger pipe I.D.	1	in	
volume -heat exchanger	32 ft^3					
necessary standpipe volum	489 ft^3		standpipe height	60	ft	
Area =	8 ft^2					
I.D. =	39 in					
			Corrosion depth	0.125	in	
thickness=	0.650 in					
shell wt. =	16,085 lbs					
heads wt. =	863 lbs					

total wt. 19,491 lbs (includes additional 15% for nozzles, manholes,etc.

Desulfurization Reactor

v (ft/sec) =	20	72000 ft/hr	coal gas in volume	1,130,000	cfh	H2S-CG
V (cfh) =	1,135,506		cg out volume	1,130,000	cfh	CLEAN-CG
Area =	15.77 ft^2			164,358	lb/hr	COLDSORB
I.D.	54.90 in			166,009	lb/hr	STNDPIPE
			regen sorbent flow	330,367	lb/hr	
			regen sorbent vol.	5,506	cfh	
thickness=	0.871 in		sorbent vol%	0.48%		
shell wt.=	51,023 lbs		Corrosion depth	0.125	in	
heads wt.=	2,334 lbs		reactor height	100	ft	

total wt. 61,361 lbs (includes additional 15% for nozzles, manholes, etc.)

Desulfurization Standpipe

			residence time	1	min	
volume -sorbent	2,767 ft^3					
Area =	28 ft^2		standpipe height	100	ft	
I.D. =	71 in					
			Corrosion depth	0.125	in	
thickness=	1.093 in					
shell wt. =	83,058 lbs					
heads wt. =	4,930 lbs					

total wt. 101,186 lbs (includes additional 15% for nozzles, manholes,etc.

Three Stage Regenerator

			number of reactors	2		
I.D. =	13.01 ft		standpipe height	45	ft	
I.D. =	156 in					
thickness=	2.247 in					
shell wt. =	168,516 lbs		Corrosion depth	0.125	in	
heads wt. =	48,735 lbs					

total wt. 260,701 lbs (includes additional 20% for cyclones, nozzles, manholes,etc.

total wt. 383,793 lbs weight for desulfurization and regeneration transport reactors

COST

				>100,000 lb calc	
C.S. unit price for quantiy needed	1.303 $/lb	1990 $	1.30330926	1.01	
	1.393 $/lb	1996 $		<100,000 lb calc	

Cost of installation $1,068,941

Total reactor cost **$2,939,588** includes cost of installation

SO2 Regenerator Sizing - Commercial Embodiment

Givens:	Revised (SO2 Regen) Case E-2
Sorbent circulation rate, lb/h	166010
Sorbent bulk density, lb/ft3	62.4
Req'd rxtr residence time, h	1
Regen Gas v_{super}, cm/sec	2.5
Desired H/D	2
Adjusted values:	
Assumed Bed Depth, ft	10
SO2 needed ft3/hr	79812.5

Calculated values:	
Hold-up volume, ft3	2660.41667
Diameter, ft	18.4047564
X-section area, ft2	266.041667
Calculated H/D	0.54333781
RG Vol. flow rate, acf/sec	21.8210028
RG flow rate, lb/hr	86366.3549
Ratio of RG flow/sorbent, lb/lb	0.52024791
Calculated Bed Depth, ft	

Operating conditions/Gas Density Calc'ns:	
Pressure, psig	275
Pressure, psia	289.7
MW of gas	64
Bed Temp., C	600
Bed Temp., R	1571.67
R, gas constant,	10.73
Gas density, lb/ft3	1.099429

Desulf and Regen transport reactor price calculation

AHGP

N2 lift

v (ft/sec) =	50	180000 ft/hr	N2 in volume	91,631	cfh	N2SOURCE
V (cfh) =	141,578		N2 out volume	175,069	cfh	N2EXIT
Area =	0.787 ft^2		regen sorbent flow	493,650	lb/hr	FEO-ZNO
I.D.	12.260 in		regen sorbent vol.	8,228	cfh	
			sorbent vol%	5.81%		
thickness=	0.292					
shell wt.=	3,815 lbs		Corrosion depth	0.125	in	
heads wt.=	39 lbs		reactor height	100	ft	

key
caculated or constant values
inputed variables

total wt. 4,432 lbs (includes additional 15% for nozzles, manholes, etc.)

Regenerator Standpipe

			residence time	10	min	
volume -sorbent		1371 ft^3				
			heat removal	49,966,040	BTU/hr	RGENSTND
Heat Exchanger Area		3,462 ft^2	heat exchanger pipe thickness	0.25	in	
length of pipe		8,817 ft	heat exchanger pipe I.D.	1	in	
volume -heat exchanger		108 ft^3				
necessary standpipe volum		1,479 ft^3	standpipe height	60	ft	
Area =	24.7 ft^2					
I.D. =	67.2 in					
			Corrosion depth	0.125	in	
thickness=	1.039 in					
shell wt. =	44,713 lbs					
heads wt. =	4,176 lbs					

total wt. 56,222 lbs (includes additional 15% for nozzles, manholes,etc.

Desulfurization Reactor

v (ft/sec) =	20	72000 ft/hr	coal gas in volume	1,160,000	cfh	H2S-CG
V (cfh) =	1,176,539		cg out volume	1,160,000	cfh	CLEAN-CG
Area =	16.341 ft^2			493,650	lb/hr	COLDSORB
I.D.	55.881 in			498,670	lb/hr	STANDPIP
			regen sorbent flow	992,320	lb/hr	
			regen sorbent vol.	16,539	cfh	
thickness=	0.884 in		sorbent vol%	1.41%		
shell wt.=	52,734 lbs		Corrosion depth	0.125	in	
heads wt.=	2,456 lbs		reactor height	100	ft	

total wt. 63,468 lbs (includes additional 15% for nozzles, manholes, etc.)

Desulfurization Standpipe

			residence time	1	min	
volume -sorbent		8,311 ft^3				
Area =	83 ft^2		standpipe height	100	ft	
I.D. =	123 in					
			Corrosion depth	0.125	in	
thickness=	1.803 in					
shell wt. =	237,425 lbs					
heads wt. =	24,424 lbs					

total wt. 301,127 lbs (includes additional 15% for nozzles, manholes,etc.

Three Stage Regenerators

		number of reactors	6		
I.D. =	12.99 ft	standpipe height	45	ft	
I.D. =	156 in				
thickness=	2.243 in				
shell wt. =	167,848 lbs	Corrosion depth	0.125	in	
heads wt. =	48,443 lbs				

total wt. 1,557,295 lbs (includes additional 20% for cyclones, nozzles, manholes,etc.

total wt. 1,919,076 lbs weight for desulfurization and regeneration transport reactors

COST

				>100,000 lb calc	
C.S. unit price for quantiy needed	1.090 $/lb	1990 $	1.09039137	0.585	
	1.165 $/lb	1996 $		<100,000 lb calc	

Cost of installation $4,471,817

Total reactor cost **$12,297,497** includes cost of installation

SO2 Regenerator Sizing - Commercial Embodiment

AHGP-b
(SO2 Regen)

Givens:	**Case E-2**
Sorbent circulation rate, lb/h	496000
Sorbent bulk density, lb/ft3	62.4
Req'd rxtr residence time, h	1
Regen Gas v_{super}, cm/sec	2.5
Desired H/D	2
Adjusted values:	
Assumed Bed Depth, ft	10
SO2 needed ft3/hr	238461.5385

Calculated values:	
Hold-up volume, ft3	7948.71795
Diameter, ft	31.8129385
X-section area, ft2	794.871795
Calculated H/D	0.31433751
RG Vol. flow rate, acf/sec	65.1961774
RG flow rate, lb/hr	258042.961
Ratio of RG flow/sorbent, lb/lb	0.52024791
Calculated Bed Depth, ft	

Operating conditions/Gas Density Calc'ns:	
Pressure, psig	275
Pressure, psia	289.7
MW of gas	64
Bed Temp., C	600
Bed Temp., R	1571.67
R, gas constant,	10.73
Gas density, lb/ft3	1.099429

AHGP-c
Desulf and Regen transport reactor price calculation

AHGP

N2 lift

v (ft/sec) =	50	180000 ft/hr	N2 in volume	8,552	cfh	N2SOURCE
V (cfh) =	13,240		N2 out volume	16,326	cfh	N2EXIT
Area =	0.074 ft^2		regen sorbent flow	48,050	lb/hr	FEO-ZNO
I.D. =	3.749 in		regen sorbent vol.	801	cfh	
			sorbent vol%	6.05%		
thickness=	0.176					
shell wt.=	704 lbs		Corrosion depth	0.125	in	
heads wt.=	2 lbs		reactor height	100	ft	

key
caculated or constant values
inputed variables

total wt. 812 lbs (includes additional 15% for nozzles, manholes, etc.)

Regenerator Standpipe

			residence time	10	min	
volume -sorbent	133 ft^3					
			heat removal	48,050	BTU/hr	RGENSTND
Heat Exchanger Area	3.25 ft^2		heat exchanger pipe thickness	0.25	in	
length of pipe	8.27 ft		heat exchanger pipe I.D.	1	in	
volume -heat exchanger	0.10 ft^3					
necessary standpipe volume	134 ft^3		standpipe height	60	ft	
Area =	2.2 ft^2					
I.D. =	20.2 in					
			Corrosion depth	0.125	in	
thickness=	0.400 in					
shell wt. =	5,168 lbs					
heads wt. =	145 lbs					

total wt. 6,110 lbs (includes additional 15% for nozzles, manholes,etc.

Desulfurization Reactor

v (ft/sec) =	20	72000 ft/hr	coal gas in volume	1,120,000	cfh	H2S-CG
V (cfh) =	1,121,611		cg out volume	1,120,000	cfh	CLEAN-CG
Area =	15.58 ft^2			48,050	lb/hr	COLDSORB
I.D. =	54.56 in			48,626	lb/hr	STANDPIP
			regen sorbent flow	96,676	lb/hr	
			regen sorbent vol.	1,611	cfh	
thickness=	0.867 in		sorbent vol%	0.14%		
shell wt.=	50,444 lbs		Corrosion depth	0.125	in	
heads wt.=	2,294 lbs		reactor height	100	ft	

total wt. 60,648 lbs (includes additional 15% for nozzles, manholes, etc.)

Desulfurization Standpipe

		residence time	1	min	
volume -sorbent	810 ft^3				
Area =	8.10 ft^2	standpipe height	100	ft	
I.D. =	38.55 in				
		Corrosion depth	0.125	in	
thickness=	0.649 in				
shell wt. =	26,687 lbs				
heads wt. =	857 lbs				

total wt. 31,676 lbs (includes additional 15% for nozzles, manholes,etc.

Three Stage Regenerator

		number of reactors	1		
I.D. =	9.90 ft	standpipe height	45	ft	
I.D. =	119 in				
thickness=	1.739 in				
shell wt. =	99,156 lbs	Corrosion depth	0.125	in	
heads wt. =	21,807 lbs				

total wt. 145,156 lbs (includes additional 20% for cyclones, nozzles, manholes,etc.

total wt. 183,754 lbs weight for desulfurization and regeneration transport reactors

COST

				>100,000 lb calc	
C.S. unit price for quantiy needed	1.447 $/lb	1990 $	1.44706713	1.298	
	1.546 $/lb	1996 $		<100,000 lb calc	

Cost of installation $568,244

Total reactor cost **$1,562,672** includes cost of installation

SO2 Regenerator Sizing - Commercial Embodiment

	AHGP-c (SO2 Regen)
Givens:	**Case E-2**
Sorbent circulation rate, lb/h	48000
Sorbent bulk density, lb/ft3	62.4
Req'd rxtr residence time, hr	1
Regen Gas v_{super}, cm/sec	2.5
Desired H/D	2
Adjusted values:	
Assumed Bed Depth, ft	10
SO2 needed ft3/hr	23077

Calculated values:	
Hold-up volume, ft3	769.23
Diameter, ft	9.90
X-section area, ft2	76.92
Calculated H/D	1.01
RG Vol. flow rate, acf/sec	6.31
RG flow rate, lb/hr	24971.90
Ratio of RG flow/sorbent, lb/lb	0.52
Calculated Bed Depth, ft	

Operating conditions/Gas Density Calc'ns:	
Pressure, psig	275
Pressure, psia	289.7
MW of gas	64
Bed Temp., C	600
Bed Temp., R	1571.67
R, gas constant,	10.73
Gas density, lb/ft3	1.10

AHGP-100

Desulf and Regen transport reactor price calculation (0.4211 the size of the AHGP case)

AHGP

N2 lift

v (ft/sec) =	50	180000 ft/hr	N2 in volume	18,007	cfh	N2SOURCE
V (cfh) =	26,964		N2 out volume	33,615	cfh	N2EXIT
Area =	0.150 ft^2		regen sorbent flow	69,211	lb/hr	FEO-ZNO
I.D.	5.350 in		regen sorbent vol.	1,154	cfh	
			sorbent vol%	4.28%		
thickness=	0.198					
shell wt.=	1,129 lbs		Corrosion depth	0.125	in	
heads wt.=	5 lbs		reactor height	100	ft	

key
caculated or constant values
inputed variables

total wt. 1,304 lbs (includes additional 15% for nozzles, manholes, etc.)

Regenerator Standpipe

			residence time	10	min	
volume -sorbent		192 ft^3				
			heat removal	6,253,543	BTU/hr	RGENSTND
Heat Exchanger Area		433 ft^2	heat exchanger pipe thickness	0.25	in	
length of pipe		1,103 ft	heat exchanger pipe I.D.	1	in	
volume -heat exchanger		14 ft^3				
necessary standpipe volume		206 ft^3	standpipe height	60	ft	
Area =	3.43 ft^2					
I.D. =	25.08 in					
			Corrosion depth	0.125	in	
thickness=	0.466 in					
shell wt. =	7,478 lbs					
heads wt. =	260 lbs					

total wt. 8,899 lbs (includes additional 15% for nozzles, manholes,etc.

Desulfurization Reactor

			coal gas in volume	475,843	cfh	H2S-CG
v (ft/sec) =	20	72000 ft/hr	cg out volume	475,843	cfh	CLEAN-CG
V (cfh) =	478,162			69,211	lb/hr	COLDSORB
Area =	6.64 ft^2			69,906	lb/hr	STNDPIPE
I.D.	35.62 in		regen sorbent flow	139,118	lb/hr	
			regen sorbent vol.	2,319	cfh	
thickness=	0.609 in		sorbent vol%	0.48%		
shell wt.=	23,154 lbs		Corrosion depth	0.125	in	
heads wt.=	687 lbs		reactor height	100	ft	

total wt. 27,418 lbs (includes additional 15% for nozzles, manholes, etc.)

Desulfurization Standpipe

		residence time	1	min	
volume -sorbent	1,165 ft^3				
Area =	11.7 ft^2	standpipe height	100	ft	
I.D. =	46.2 in				
		Corrosion depth	0.125	in	
thickness=	0.753 in				
shell wt. =	37,140 lbs				
heads wt. =	1,430 lbs				

total wt. 44,356 lbs (includes additional 15% for nozzles, manholes,etc.

Three Stage Regenerators

		number of reactors	1		
I.D. =	11.94 ft	standpipe height	45	ft	
I.D. =	143 in				
thickness=	2.073 in				
shell wt. =	142,638 lbs	Corrosion depth	0.125	in	
heads wt. =	37,858 lbs				

total wt. 216,595 lbs (includes additional 20% for cyclones, nozzles, manholes,etc.

total wt. 271,154 lbs weight for desulfurization and regeneration transport reactors

COST

				>100,000 lb calc	
C.S. unit price for quantiy needed	1.367 $/lb	1990 $	1.36665221	1.137	
	1.460 $/lb	1996 $		<100,000 lb calc	

Cost of installation $791,924

Total reactor cost **$2,177,791** includes cost of installation

SO2 Regenerator Sizing - Commercial Embodiment

AHGP-100
(SO2 Regen)

Givens:	**Case E-2**
Sorbent circulation rate, lb/h	69910
Sorbent bulk density, lb/ft3	62.4
Req'd rxtr residence time, hr	1
Regen Gas v_{super}, cm/sec	2.5
Desired H/D	2

Adjusted values:

Assumed Bed Depth, ft	10.00
SO2 needed ft3/hr	33611

Calculated values:	
Hold-up volume, ft3	1,120.35
Diameter, ft	11.94
X-section area, ft2	112.04
Calculated H/D	0.84
RG Vol. flow rate, acf/sec	9.19
RG flow rate, lb/hr	36,370.53
Ratio of RG flow/sorbent, lb/lb	0.520
Calculated Bed Depth, ft	

Operating conditions/Gas Density Calc'ns:	
Pressure, psig	275
Pressure, psia	289.7
MW of gas	64
Bed Temp., C	600
Bed Temp., R	1571.67
R, gas constant,	10.73
Gas density, lb/ft3	1.099429

AHGP-500

Desulf and Regen transport reactor price calculation (2.1055 the size of the AHGP case)

AHGP

N2 lift

v (ft/sec) =	50	180000 ft/hr	N2 in volume	90,033	cfh	N2SOURCE
V (cfh) =	134,821		N2 out volume	168,074	cfh	N2EXIT
Area =	0.75 ft^2		regen sorbent flow	346,056	lb/hr	FEO-ZNO
I.D.	11.96 in		regen sorbent vol.	5,768	cfh	
			sorbent vol%	4.28%		
thickness=	0.287592409					
shell wt.=	3,671 lbs		Corrosion depth	0.125	in	
heads wt.=	37 lbs		reactor height	100	ft	

key
caculated or constant values
inputed variables

total wt. 4,264 lbs (includes additional 15% for nozzles, manholes, etc.)

Regenerator Standpipe

		residence time	10	min	
volume -sorbent	961 ft^3				
		heat removal	31,267,715	BTU/hr	RGENSTND
Heat Exchanger Area	2,167 ft^2	heat exchanger pipe thickness	0.25	in	
length of pipe	5,517 ft	heat exchanger pipe I.D.	1	in	
volume -heat exchanger	68 ft^3				
necessary standpipe volume	1,029 ft^3	standpipe height	60	ft	
Area =	17 ft^2				
I.D. =	56 in				
		Corrosion depth	0.125	in	
thickness=	0.887 in				
shell wt. =	31,844 lbs				
heads wt. =	2,480 lbs				

total wt. 39,472 lbs (includes additional 15% for nozzles, manholes,etc.

Desulfurization Reactor

			coal gas in volume	2,379,215	cfh	H2S-CG
v (ft/sec) =	20	72000 ft/hr	cg out volume	2,379,215	cfh	CLEAN-CG
V (cfh) =	2,390,808			346,056	lb/hr	COLDSORB
Area =	33.21 ft^2			349,532	lb/hr	STNDPIPE
I.D.	79.66 in		regen sorbent flow	695,588	lb/hr	
			regen sorbent vol.	11,593	cfh	
thickness=	1.208 in		sorbent vol%	0.48%		
shell wt.=	102,638 lbs		Corrosion depth	0.125	in	
heads wt.=	6,813 lbs		reactor height	100	ft	

total wt. 125,868 lbs (includes additional 15% for nozzles, manholes, etc.)

Desulfurization Standpipe

		residence time	1	min	
volume -sorbent	5,826 ft^3				
Area =	58 ft^2	standpipe height	100	ft	
I.D. =	103 in				
		Corrosion depth	0.125	in	
thickness=	1.530 in				
shell wt. =	168,662 lbs				
heads wt. =	14,526 lbs				

total wt. 210,666 lbs (includes additional 15% for nozzles, manholes,etc.

Three Stage Regenerators

		number of reactors	5		
I.D. =	11.94 ft	standpipe height	45	ft	
I.D. =	143 in				
thickness=	2.073 in				
shell wt. =	142,618 lbs	Corrosion depth	0.125	in	
heads wt. =	37,850 lbs				

total wt. 1,082,809 lbs (includes additional 20% for cyclones, nozzles, manholes,etc.

total wt. 1,337,211 lbs weight for desulfurization and regeneration transport reactors

COST

				>100,000 lb calc	
C.S. unit price for quantiy needed	1.129 $/lb	1990 $	1.12859015	0.661	
	1.206 $/lb	1996 $		<100,000 lb calc	

Cost of installation $3,225,118

Total reactor cost **$8,869,074** includes cost of installation

SO2 Regenerator Sizing - Commercial Embodiment

	AHGP-500 (SO2 Regen) Case E-2	Calculated values:		Operating conditions/Gas Density Calc'ns:	
Givens:		Hold-up volume, ft3	5,600.96	Pressure, psig	275
		Diameter, ft	26.70	Pressure, psia	289.7
Sorbent circulation rate, lb/h	349500	X-section area, ft2	560.10	MW of gas	64
Sorbent bulk density, lb/ft3	62.4	Calculated H/D	0.37	Bed Temp., C	600
Req'd rxtr residence time, hr	1	RG Vol. flow rate, acf/sec	45.94	Bed Temp., R	1571.67
Regen Gas v_{super}, cm/sec	2.5	RG flow rate, lb/hr	181,826.64	R, gas constant,	10.73
Desired H/D	2	Ratio of RG flow/sorbent, lb/lb	0.520	Gas density, lb/ft3	1.099429
		Calculated Bed Depth, ft			
Adjusted values:					
Assumed Bed Depth, ft	10.00				
SO2 needed ft3/hr	168,029				

Appendix J
Power Generation Achievable from Clean Coal Gas

Two sources where used in determining the power generated by the clean coal gas. The Sierra power generating facility was used as the basis for determining the power generating capacity coal gas.

Sierra Clean Coal Gas Feed		
H_2 (lbmole/hr)	CO (lbmole/hr)	Power Generation (MW)
5760	7570	260

The individual contribution of the H_2 and CO where determined assuming there relative contribution was consistent with their standard heats of combustion.

Standard heat of combustion (Felled & Rousseau):
ΔH°_{comb} (H_2) = -3.605E-2 MW hr/ lbmole ΔH°_{comb} (CO) = -3.569E-2 MW hr/ lbmole

Power generation can be expressed:

$$E\,[5760\,\Delta H_C\,(H_2) + 7570\,\Delta H_C\,(CO)] = 260\ MW$$

where:

E = Efficiency of power generation

assuming:

ΔH_C (CO) = 0.99 ΔH_C (H_2)

and substituting gives:

$$13{,}254\ E\ \Delta H_C(H_2) = 260\ MW$$

$$E\ \Delta H_C(H_2) = 0.0196\ MW\ hr\ /\ lbmole$$

therefore

$$E\ \Delta H_C(CO) = 0.0194\ MW\ hr\ /\ lbmole$$

The values calculated above can be used to write a power generation expression.

Power Generation {MW} = 0.0196 (H_2 {lbmoles/hr}) + 0.0194 (CO {lbmoles/hr})

The plants power generation is determined by inserting the clean coal gas flows for H_2 and CO into the above equation. HGD coal gas consumption is assessed as a debit equivalent to the cost of the lost power generation. The power generation lost is determined by inserting the difference in the dirty coal gas and clean coal gas molar flow rates into the above equation. The cost of the electricity is taken as $0.04 per kWh. The plant has been assumed to be in operation 90% of the year.

Summary of Power Generation Calculations

simulation	H_2 clean	H_2 in	CO clean	CO in	MW made	MW lost
DSRP	11,444.58	11,765.37	212,200.52	218,162.00	258.25	7.248
DSRP-b	11,450.19	12,468.32	212,276.67	231,196.50	258.35	23.003
DSRP-c	11,443.82	11,535.37	212,195.77	213,897.17	258.24	2.069
DSRP-100	4,819.31	4,954.40	89,357.59	91,868.05	108.75	3.052
DSRP-500	24,110.94	24,772.09	447,055.34	459,341.97	544.06	14.938
AHGP	11,355.75	11,510.68	213,439.25	213,439.25	258.24	1.506
AHGP-b	11,175.21	11,646.28	215,953.67	215,953.67	258.23	4.580
AHGP-c	11,419.66	11,464.48	212,582.61	212,582.61	258.27	0.436
AHGP-100	4,781.91	4,847.15	89,879.27	89,879.27	108.74	0.634
AHGP-500	23,909.53	24,235.73	449,396.34	449,396.34	543.72	3.172

Appendix K
Calculation of Reactor Pressure Drops

Pressure drops for transport reactors have been calculated assuming the pressure drops are related to the energy required to lift the sorbent / catalyst to the top of the reactor.

Energy balance for lifting solid to top of reactor:

$$\Delta E_{PART} = \Delta E_{GAS}$$

$$m_{PART} (g / g_C) h = \Delta P \, m_{GAS} / \rho_{GAS}$$

$$\Delta P = m_{PART} (g / g_C) h \, \rho_{GAS} / m_{GAS}$$

$$\Delta P_{REACTOR} = 1.5 \text{ (Energy to lift particle)}$$

DSRP Regeneration Reactor

$$\Delta P = 1.5 \, m_{PART} (g / g_C) h \, \rho_{GAS} / m_{GAS}$$

m_{PART} = sorbent mass flow, ZNS2RGEN & ZNO average

$(g / g_C) = 1$ lb_f/lb_m

h = reactor height, defined in Appendix H

ρ_{GAS} = gas density, HP-O2-N2 & ROG average

m_{GAS} = gas mass flow, HP-O2-N2 & ROG average

DSRP Regeneration Reactor (DSRP)

$$\Delta P = 1.5 \, (250{,}000 \text{ } lb_m/hr) \, (1 \text{ } lb_f/lb_m) \, (100 \text{ ft}) \, (0.5 \text{ } lb_m/ft^3) / (40{,}000 \text{ } lb_m/hr) \, (1 \text{ } ft^3 / 144 \text{ } in^2)$$

$$\Delta P = 3.32 \text{ psi}$$

DSRP Regeneration Reactor (DSRP-b)

$$\Delta P = 1.5 \, (1{,}200{,}000 \text{ } lb_m/hr) \, (1 \text{ } lb_f/lb_m) \, (100 \text{ ft}) \, (0.5 \text{ } lb_m/ft^3) / (130{,}000 \text{ } lb_m/hr) (1 \text{ } ft^3 / 144 \text{ } in^2)$$

$$\Delta P = 4.8 \text{ psi}$$

DSRP Regeneration Reactor (DSRP-c)

$$\Delta P = 1.5 \, (71{,}000 \text{ } lb_m/hr) \, (1 \text{ } lb_f/lb_m) \, (100 \text{ ft}) \, (0.5 \text{ } lb_m/ft^3) / (12{,}000 \text{ } lb_m/hr) (1 \text{ } ft^3 / 144 \text{ } in^2)$$

$$\Delta P = 3.2 \text{ psi}$$

DSRP Regeneration Reactor (DSRP-100) (DSRP-500)

same as base case $\Delta P = 3.3$ psi

DSRP Reactor

$$\Delta P = 1.5\ m_{PART}\ (g / g_C)\ h\ \rho_{GAS} / m_{GAS}$$

m_{PART} = catalyst mass flow, Appendix H

$(g / g_C) = 1\ lb_f/lb_m$

h = reactor height, defined in Appendix H

ρ_{GAS} = gas density, ROG-COOL & RXNPRD average

m_{GAS} = gas mass flow, RXNPRD

DSRP Reactor (DSRP)

$\Delta P = 1.5\ (300{,}000\ lb_m/hr)\ (1\ lb_f/lb_m)\ (100\ ft)\ (0.53\ lb_m/ft^3) / (55{,}000\ lb_m/hr)\ (1\ ft^3 / 144\ in^2)$

$\Delta P = 3.0$ psi

DSRP Reactor (DSRP-b)

$\Delta P = 1.5\ (1{,}000{,}000\ lb_m/hr)(1\ lb_f/lb_m)\ (100\ ft)\ (0.53\ lb_m/ft^3) / (185{,}000\ lb_m/hr)(1\ ft^3/ 144\ in^2)$

$\Delta P = 3.0$ psi

DSRP Reactor (DSRP-c)

$\Delta P = 1.5\ (79{,}000\ lb_m/hr)(1\ lb_f/lb_m)\ (100\ ft)\ (0.55\ lb_m/ft^3) / (15{,}000\ lb_m/hr)(1\ ft^3/ 144\ in^2)$

$\Delta P = 3.0$ psi

DSRP Reactor (DSRP-100) (DSRP-500)

same as base case $\Delta P = 3.0$ psi

DSRP Desulfurization Reactor

$$\Delta P = 1.5\ m_{PART}\ (g / g_C)\ h\ \rho_{GAS} / m_{GAS}$$

m_{PART} = sorbent mass flow, ZNS

$(g / g_C) = 1\ lb_f/lb_m$

h = reactor height, defined in Appendix H

ρ_{GAS} = gas density, RAW-CG & CG-CALC average

m_{GAS} = gas mass flow, CG-CALC

DSRP Desulfurization Reactor (DSRP)

$\Delta P = 1.5\ (670{,}000\ lb_m/hr)\ (1\ lb_f/lb_m)\ (100\ ft)\ (0.4\ lb_m/ft^3) / (510{,}000\ lb_m/hr)\ (1\ ft^3 / 144\ in^2)$

$\Delta P = 0.6$ psi

DSRP Desulfurization Reactor (DSRP-b)

$\Delta P = 1.5\ (2{,}700{,}000\ lb_m/hr)(1\ lb_f/lb_m)\ (100\ ft)\ (0.4\ lb_m/ft^3) / (660{,}000\ lb_m/hr)\ (1\ ft^3 / 144\ in^2)$

$\Delta P = 1.6$ psi

DSRP Desulfurization Reactor (DSRP-c)

$\Delta P = 1.5\ (72{,}000\ lb_m/hr)(1\ lb_f/lb_m)\ (100\ ft)\ (0.4\ lb_m/ft^3) / (460{,}000\ lb_m/hr)\ (1\ ft^3 / 144\ in^2)$

$\Delta P = 0.06$ psi

DSRP Desulfurization Reactor (DSRP-100) (DSRP-500)

same as base case $\Delta P = 0.6$ psi

AHGP Desulfurization Reactor

$\Delta P = 1.5\ m_{PART}\ (g / g_C)\ h\ \rho_{GAS} / m_{GAS}$

m_{PART} = sorbent mass flow, STNDPIPE + COLDSORB

$(g / g_C) = 1\ lb_f/lb_m$

h = reactor height, defined in Appendix I

ρ_{GAS} = gas density, H2S-CG & CLEAN-CG average

m_{GAS} = gas mass flow, CLEAN-CG

AHGP Desulfurization Reactor (AHGP-100 and AHGP-500 results will be consistent)

$\Delta P = 1.5\ (330{,}000\ lb_m/hr)\ (1\ lb_f/lb_m)\ (100\ ft)\ (0.4\ lb_m/ft^3) / (450{,}000\ lb_m/hr)\ (1\ ft^3 / 144\ in^2)$

$\Delta P = 0.3$ psi

AHGP-b Desulfurization Reactor

$\Delta P = 1.5\ (990{,}000\ lb_m/hr)\ (1\ lb_f/lb_m)\ (100\ ft)\ (0.4\ lb_m/ft^3) / (460{,}000\ lb_m/hr)\ (1\ ft^3 / 144\ in^2)$

$\Delta P = 0.9$ psi

AHGP-c Desulfurization Reactor

$\Delta P = 1.5\ (97{,}000\ lb_m/hr)\ (1\ lb_f/lb_m)\ (100\ ft)\ (0.4\ lb_m/ft^3) / (440{,}000\ lb_m/hr)\ (1\ ft^3 / 144\ in^2)$

$\Delta P = 0.09$ psi

The pressure drop through the bubble bed regenerator is calculated as the sum of the static head in each stage times 1.3.

AHGP 3-Stage Regenerator Reactor

$$\Delta P = 1.3\ g/g_C\ (\rho\ h_{top\text{-}stage} + \rho\ h_{stage2} + \rho\ h_{bottom\text{-}stage})\ (1/144)$$

m_{PART} = sorbent mass flow, FES-ZNS

$(g / g_C) = 1\ lb_f/lb_m$

h = reactor stage height,

ρ_{GAS} = average of density of streams entering and exiting the reactor stage

AHGP 3-Stage Regenerator Reactors

$\Delta P = 1.3\ (1\ lb_f/lb_m)\ [\ (3.66\ lb_m/ft^3)\ (5.0\ ft) + (3.20\ lb_m/ft^3)\ (10\ ft) + (3.40\ lb_m/ft^3)\ (2.5\ ft)]\ (\ 1\ ft^3 / 144\ in^2)$

$\Delta P = 0.5$ psi

Appendix L
Summary of the Process Pressure Drops

This appendix contains lists of the calculated pressure drops for the DSRP and AHGP at the various feed conditions.

DSRP pressure drops are used to determine the pressure rise needed from the RECYCOMP (sends tailgas to the Desulfurization reactor) and PRESAIR (pressurizes the air fed to the regenerator) Reactor pressure drops are calculated in Appendix H. Pressure drops in other equipment has been assigned without calculations.

Having streams enter the DSRP Reactor at the same pressure (bold pressures) was the starting point for the calculations.

DSRP (base case) & DSRP-100 & DSRP-500

Equipment	ΔP drop (psi)	P_{EXIT} (psia)
PRESAIR	13.7 psia inlet P	278.9
pipe [P-02-N2]	0	278.9
AIR-HX (shell)	2.0	276.9
pipe [HP-O2-N2]	0	276.9
REGENERATOR	3.3	273.6
pipe [ROG]	0	273.6
AIR-HX (tube)	2.0	271.6
pipe [ROG-COOL]	0	**271.6**
DSRP	2.0	268.6
pipe [RXNPRD]	0	268.6
PD-COOLR	2.0	266.6
pipe [COOLPRD]	0	266.6
High Press. Cond.	2.0	264.6
pipe [TAILGAS]	0	264.6
VALVE	2.6	262.0
pipe [TAILGAS2]	0	262.0
RECYCOMP		275

Coal Gas Slipstream Pressure

Equipment	ΔP drop (psi)	P_{EXIT} (psia)
Desulfurization Reactor	0.6	274.4
pipe [SLIPSTRM]	0	274.4
VALVE2	2.8	271.6
pipe [SLPSTRM]	0	**271.6**

DSRP-b

Equipment	ΔP drop (psi)	P_{EXIT} (psia)
PRESAIR	13.7 psia inlet P	279.4
pipe [P-O2-N2]	0	279.4
AIR-HX (shell)	2.0	277.4
pipe [HP-O2-N2]	0	277.4
REGENERATOR	4.8	272.6
pipe [ROG]	0	272.6
AIR-HX (tube)	2.0	270.6
pipe [ROG-COOL]	0	**270.6**
DSRP	3.0	267.6
pipe [RXNPRD]	0	267.6
PD-COOLR	2.0	265.6
pipe [COOLPRD]	0	265.6
High Press. Cond.	2.0	263.6
pipe [TAILGAS]	0	263.6
VALVE	2.6	261.0
pipe [TAILGAS2]	0	261.0
RECYCOMP		275

Coal Gas Slipstream Pressure

Equipment	ΔP drop (psi)	P_{EXIT} (psia)
Desulfurization Reactor	1.6	273.4
pipe [SLIPSTRM]	0	273.4
VALVE2	2.8	270.6
pipe [SLPSTRM]	0	**270.6**

DSRP-c

Equipment	ΔP drop (psi)	P_{EXIT} (psia)
PRESAIR	13.7 psia inlet P	279.3
pipe [P-O2-N2]	0	279.3
AIR-HX (shell)	2.0	277.3
pipe [HP-O2-N2]	0	277.3
REGENERATOR	3.2	274.1
pipe [ROG]	0	274.1
AIR-HX (tube)	2.0	272.1
pipe [ROG-COOL]	0	**272.1**
DSRP	3.0	269.1
pipe [RXNPRD]	0	269.1
PD-COOLR	2.0	267.1
pipe [COOLPRD]	0	267.1
High Press. Cond.	2.0	265.1
pipe [TAILGAS]	0	265.1
VALVE	2.6	262.5
pipe [TAILGAS2]	0	262.5
RECYCOMP		275

DSRP-c

Coal Gas Slipstream Pressure

Equipment	ΔP drop (psi)	P_{EXIT} (psia)
Desulfurization Reactor	0.06	274.9
pipe [SLIPSTRM]	0	274.9
VALVE2	2.8	272.1
pipe [SLPSTRM]	0	**272.1**

AHGP pressure drop calculations determine the required ΔP for the SO2-COMP, compressor. The pressure drop balance is done to insure the SO_2 loop with maintain desired pressure. The set pressure (bold) in the SO_2 loop is the pressure at the 3-Stage Regenerator exit. This pressure is set to equal the calculated exit pressure of the AHGP Desulfurization reactor (Appendix K).

AHGP (base case), & AHGP-100 & AHGP-500

Equipment	ΔP drop (psi)	P_{EXIT} (psia)
3-Stage Regenerator	0.5 (Append. K)	**274.7**
pipe [COOLS2]	0	274.7
HEATX (tube)	2.0	272.7
pipe [S2V+L]	0	272.7
COND-EQ	2.0	270.7
pipe [IN-COND]	0	270.7
DEMISTR	5	265.7
pipe [UNP-RSO2]	0	265.7
SO2-COMP		279.2
pipe [RCYHEATR]	0	279.2
RCYHEATR	2.0	277.2
pipe [WARMRCY]	0	277.2
HEATX (shell)	2.0	275.2
pipe [FEEDRG1]	0	275.2 to 3-Stage Regenerator

AHGP-b

Equipment	ΔP drop (psi)	P_{EXIT} (psia)
3-Stage Regenerator	0.5 (Append. K)	**274.1**
pipe [COOLS2]	0	274.1
HEATX (tube)	2.0	272.1
pipe [S2V+L]	0	272.1
COND-EQ	2.0	270.1
pipe [IN-COND]	0	270.1
DEMISTR	5	265.1
pipe [UNP-RSO2]	0	265.1
SO2-COMP		278.6
pipe [RCYHEATR]	0	278.6
RCYHEATR	2.0	276.6
pipe [WARMRCY]	0	276.6
HEATX (shell)	2.0	274.6
pipe [FEEDRG1]	0	274.6 to 3-Stage Regenerator

AHGP-c

Equipment	ΔP drop (psi)	P_{EXIT} (psia)
3-Stage Regenerator	0.5 (Append. K)	**274.9**
pipe [COOLS2]	0	274.9
HEATX (tube)	2.0	272.9
pipe [S2V+L]	0	272.9
COND-EQ	2.0	270.9
pipe [IN-COND]	0	270.9
DEMISTR	5	265.9
pipe [UNP-RSO2]	0	265.9
SO2-COMP		279.4
pipe [RCYHEATR]	0	279.4
RCYHEATR	2.0	277.4
pipe [WARMRCY]	0	277.4
HEATX (shell)	2.0	275.4
pipe [FEEDRG1]	0	275.4 to 3-Stage Regenerator

Appendix M
Summary of Major HGD Equipment

The following tables list equipment required for both HGD processes under various feed conditions. Equipment specifications are also listed in the tables.

DSRP - base Process Equipment Specifications

		DSRP	DSRP-b	DSRP-c	DSRP-100	DSRP-500
REACTORS						
Desulfurization reactor						
	height (ft)	100	100	100	100	100
	diameter (ft)	4.9	5.6	4.6	3.2	7.1
	weight (lbs)	70,000	90,000	63,000	31,000	140,000
Desulf. standpipe						
	height (ft)	100	100	100	100	100
	diameter (ft)	4.9	5.6	4.6	3.2	7.1
	weight (lbs)	70,000	90,000	63,000	31,000	140,000
Regeneration reactor						
	height (ft)	100	100	100	100	100
	diameter (ft)	1.3	2.3	0.66	0.82	1.8
	weight (lbs)	6,000	17,000	2,000	3,000	11,000
Regen. standpipe						
	height (ft)	100	100	100	100	100
	diameter (ft)	1.3	2.3	0.66	0.82	1.8
	weight (lbs)	6,000	17,000	2,000	3,000	11,000
DSRP Reactor						
	height (ft)	100	100	100	100	100
	diameter (ft)	3.8	7.0	2.0	2.5	5.4
	weight (lbs)	43,000	140,000	13,000	19,000	85,000
DSRP standpipe						
	height (ft)	40	40	40	40	40
	diameter (ft)	3.8	7.0	2.0	2.5	5.4
	weight (lbs)	27,000	89,000	8,000	12,000	540,000
COMPRESSORS						
PRESAIR						
	acfh	570,000	1,800,000	160,000	240,000	1,200,000
	Pin (psia)	13.7	13.7	13.7	13.7	13.7
	Pout (psia)	278.9	279.4	279.3	278.9	278.9
	power (hp)	3,300	10,000	900	1,400	6,900
	stages	6	6	6	6	6
RECOMP						
	acfh	49,000	170,000	14,000	21,000	100,000
	Pin (psia)	264.4	261	262.5	264.4	264.4
	Pout (psia)	275	275	275	275	275
	power (hp)	59	227	17	25	124
	stages	1	1	1	1	1
HEAT EXCHANGERS						
AIRHX						
	Duty (BTU/hr)	4,300,000	14,000,000	1,200,000	1,900,000	9,600,000
	Area (ft^2)	700	2,200	200	300	1,400
	tube mat.	SS 310	SS 310	SS 310	SS 310	SS 310
	shell mat.	SS 304	SS 304	SS 304	SS 304	SS 304
DSRP						
	Duty (BTU/hr)	15,000,000	51,000,000	4,000,000	6,500,000	31,000,000
	Area (ft^2)	1,000	3,600	280	450	2,200
	tube mat.	SS 310	SS 310	SS 310	SS 310	SS 310
PDCOOLR						
	Duty (BTU/hr)	5,200,000	17,000,000	1,400,000	2,200,000	11,000,000
	Area (ft^2)	1,000	3,200	300	300	2,000
	tube mat.	SS 310	SS 310	SS 310	SS 310	SS 310
	shell mat.	SS 310	SS 310	SS 310	SS 310	SS 310
MISC.						
High Pressure Condenser						
	Duty (BTU/hr)	10,500,000	35,100,000	2,940,000	4,320,000	21,600,000
	Material	SS 310	SS 310	SS 310	SS 310	SS 310
VAPORIZR						
	Duty (BTU/hr)	550,000	1,900,000	150,000	230,000	1,100,000
	Material	SS 310	SS 310	SS 310	SS 310	SS 310
Storage Tank						
	vol. (ft^3)	5,600	18,000	1,600	2,400	11,000
	Material	SS 310	SS 310	SS 310	SS 310	SS 310

EQPTSPEC.XLS

AHGP Process Equipment Specifications

	AHGP	AHGP - b	AHGP - c	AHGP - 100	AHGP -500
REACTORS					
Desulfurization reactor					
height (ft)	100	100	100	100	100
diameter (ft)	4.58	4.66	4.55	2.97	6.64
weight (lbs)	61,361	63,000	61,000	27,000	130,000
Desulf. standpipe					
height (ft)	100	100	100	100	100
diameter (ft)	5.92	10.25	3.21	3.85	8.58
weight (lbs)	100,000	300,000	32,000	44,000	210,000
Regeneration reactor					
# of reactors	2	6	1	1	5
height (ft)	45	45	45	45	45
diameter (ft)	13.0	13.0	0.8	11.9	11.9
weight (lbs)	260,000	1,600,000	150,000	270,000	1,000,000
Regen. standpipe & RGENSTAND					
height (ft)	60	60	60	60	60
diameter (ft)	3.25	5.6	1.68	2.1	4.7
weight (lbs)	19,000	56,000	6,100	8,900	39,000
Duty (BTU/hr)	15,000,000	50,000,000	48,000	6,300,000	31,000,000
N2 Lift					
height (ft)	100	100	100	100	100
diameter (ft)	0.69	1.02	0.31	0.45	1.00
weight (lbs)	2,400	4,400	800	1,300	4,300
COMPRESSORS					
CON-COMP					
acfh	1,500	4,400	400	600	3,200
Pin (psia)	15	15	15	15	15
Pout (psia)	279	279	279	279	279
power (hp)	8	26	2	3	17
stages	1	1	1	1	1
LIFTCOMP					
acfh	43,000	92,000	8,600	18,000	91,000
Pin (psia)	272	272	272	272	272
Pout (psia)	275	275	275	275	275
power (hp)	13	28	3	5	27
stages	1	1	1	1	1
SO2-COMP					
acfh	29,000	85,000	8,400	12,000	61,000
Pin (psia)	266	265	266	266	266
Pout (psia)	279	279	279	279	279
power (hp)	38	114	11	16	80
stages	1	1	1	1	1
HEAT EXCHANGERS					
N2-COOLR					
Duty (BTU/hr)	7,020,000	15,800,000	1,480,000	3,130,000	15,700,000
Area (ft^2)	1,100	2,600	210	470	2,300
tube mat.	SS 304	SS 304	SS 304	SS 304	SS 304
shell mat.	SS 304	SS 304	SS 304	SS 304	SS 304
HEATX					
Duty (BTU/hr)	5,100,000	15,000,000	1,500,000	2,100,000	11,000,000
Area (ft^2)	1,600	3,600	500	700	3,500
tube mat.	SS 310	SS 310	SS 310	SS 310	SS 310
shell mat.	SS 310	SS 310	SS 310	SS 310	SS 310
RCYHEATR					
Duty (BTU/hr)	2,530,000	6,070,000	697,000	1,070,000	5,330,000
Area (ft^2)	3,200	7,800	570	1,300	6,700
tube mat.	SS 310	SS 310	SS 310	SS 310	SS 310
shell mat.	SS 310	SS 310	SS 310	SS 310	SS 310
MISC.					
COND-EQ					
Duty (BTU/hr)	5,380,000	16,000,000	1,560,000	2,400,000	12,000,000
Material	SS 310	SS 310	SS 310	SS 310	SS 310
DEMISTR					
Duty (BTU/hr)	0	0	0	0	0
Material	SS 310	SS 310	SS 310	SS 310	SS 310
LP-COND					
vol. (ft^3)	30	100	10	10	70
Material	SS 310	SS 310	SS 310	SS 310	SS 310
Storage Tank					
vol. (ft^3)	5,600	18,000	1,600	2,400	11,000
Material	SS 310	SS 310	SS 310	SS 310	SS 310

EQPTSPEC.XLS

Appendix N
Summary of HGD Costs

The following pages are taken from an Excel spreadsheet containing the culmination of all costs and benefits for all simulated Hot Gas Desulfurization processes.

DSRP costs

Equipment -Sulfur side

Type	unit	DSRP Price	DSRP-b Price	DSRP-c Price	DSRP-100 Price	DSRP-500 Price	Mat. of Construction	Purchase date	Purchase price ref.	date of calculation
Heat Exchangers										
	AIRHX	$33,500	$71,500	$17,900	$19,400	$55,300	SS304 / SS310 tubes	June, 1996	aspen DAIRHX	1/22/98
	PDCOOLR	$63,400	$126,600	$25,200	$42,000	$90,400	SS310 (calc w SS316)	June, 1996	aspen	1/22/98
Tanks										
7 days	Sulfur Storage	$125,500	$205,400	$65,000	$80,000	$171,000	SS310 (calc w SS316)	June, 1996	aspen	11/6/97
Condenser										
	High Pressure	$40,400	$82,200	$18,500	$21,900	$59,600	SS310 (calc w SS316)	June, 1996	aspen	
Vaporiser										
	VAPORIZR	$16,100	$17,800	$15,900	$15,200	$16,700	SS310 (calc w SS316)	June, 1996	aspen	
Compressor										
	RECOMP	$52,900	$52,900	$52,900	$52,900	$52,900	Carbon Steel	June, 1996	aspen	
	PRESAIR	$844,000	$2,680,000	$241,000	$416,000	$1,740,000		1997 Ingesoll-Rand Centac Pricing		10/20/97
Reactors										
	Desulf & Regen	$1,328,000	$1,772,000	$1,169,000	$728,000	$2,434,000	SS310 (calc w SS316)	June, 1996 (w install)	P&T calc	10/7/97
	DSRP reactor	$812,129	$2,134,355	$367,075	$477,612	$1,394,800	SS310 (calc w SS316)	June, 1996 (w install)	P&T calc	10/16/97
Pipes										
	pipe lines									
	totals	$3,315,929	$7,142,755	$1,972,475	$1,853,012	$6,014,700				

Equipment -Steam side

Type	unit	DSRP Price	DSRP-b Price	DSRP-c Price	DSRP-100 Price	DSRP-500 Price	Mat. of Construction	date		Purchase price ref.
Heat Exchangers										
	LCOOLR	$7,600	$8,100	$0	$6,800	$7,600		June, 1996	aspen	11/26/97
	VCOOLR	$7,000	$8,400	$6,700	$6,800	$7,600		June, 1996	aspen	11/26/97
Pumps										
	PTOWR	$4,200	$8,000	$2,800	$3,200	$5,500		June, 1996	aspen	11/26/97
	PHOTH2O	$1,000	$3,500	$0	$400	$3,500		price quote from General Pumps		
	PSTEAM	$57,400	$75,100	$57,400	$57,400	$59,300		June, 1996	aspen	11/26/97
	totals	$77,200	$103,100	$66,900	$74,600	$83,500				

Expendatures

		DSRP	DSRP-b	DSRP-c	DSRP-100	DSRP-500	cost ref.		
Electrical									
Pumps & Compressors									
kW	RECYCOMP	59	227	5	7	37	ASPEN generated power requirements		
kW	PRESAIR	3282	10414	900	999	4889	ASPEN generated power requirements		
kW	Steam pumps	76	193	30	32	160	ASPEN steam simulations		11/26/97
Light & instruments									
kW	misc.	683	683	683	683	683	20% base case pump & compressor requirements		
TOTAL	kW	4100.4	11517.4	1618.4	1721	5769			
	unit cost $/kWh	0.04	0.04	0.04	0.04	0.04	Self-gen. (Jan. 1990)	Peters & Timmeraus	
90 % op	Cost $/yr	$1,293,988	$3,634,615	$510,728	$543,234	$1,820,690			
Cooling Water									
	lbs/hr	149,000	500,000	25,000	62,744	313,720	ASPEN Complete Steam Generation Scheme simulations		
	unit value $/lb	2.6E-05	2.6E-05	2.6E-05	2.6E-05	2.6E-05	Tower (Jan. 1990)	Peters & Timmeraus	
90 % op	Cost $/yr	$21,854	$73,336	$3,667	$9,203	$46,014			
Oxygen									
	lbs/hr	0	0	0	0	0			
	unit value $/lb								
	Cost $/yr								
Addtional Employees									
	Engineers	2	2	2	2	2			
	unit cost	$100,000	$100,000	$100,000	$100,000	$100,000			
	Maintenance	2	2	2	2	2			
	unit cost	$70,000	$70,000	$70,000	$70,000	$70,000			
	Cost $/yr	$340,000	$340,000	$340,000	$340,000	$340,000			
Consumed Coal Gas									
	MW lost	7	23	2	3	15	Appendix J		
	unit cost $/MWh	40	40	40	40	40	Self-gen. (Jan. 1990)	Peters & Timmeraus	
	Cost $/yr	$2,287,295	$7,259,195	$652,927	$963,138	$4,714,074			
	totals (yearly)	$3,943,137	$11,307,146	$1,507,322	$1,855,574	$6,920,778			

Benefits

		DSRP	DSRP-b	DSRP-c	DSRP-100	DSRP-500	Condition	value ref.	date of calc.
Sulfur Recovered									
	lbs/hr	5,840	18,590	1,667	2,460	12,300			
90% op	tons/year	23,037	73,332	6,576	9,704	48,520			11/4/97
	unit value $/ton	50	50	50	50	50	low purity	Chem. Eng. Progress 1996	
	Revenue $/yr	$1,151,852	$3,666,599	$328,791	$485,198	$2,425,991			
Steam Generation									
	lbs/hr	23,200	77,700	6,160	9,800	48,800	950 psia, 441 C		11/4/97
	unit value $/lb	0.0039	0.0039	0.0039	0.0039	0.0039	500 psig, (Jan. 1990)	Peters and Timmeraus	
90% op	Revenue $/yr.	$713,833	$2,390,725	$189,535	$301,533	$1,501,511			
	totals (yearly)	$1,865,685	$6,057,324	$518,326	$786,731	$3,927,501			

	DSRP	DSRP-b	DSRP-c	DSRP-100	DSRP-500
YEARLY COST	$2,077,452	$5,249,823	$988,996	$1,068,843	$2,993,277
EQUIPMENT COSTS	$3,393,129	$7,245,855	$2,039,375	$1,927,612	$6,098,200

DSRP costs

Equipment -Sulfur side

Type	unit	DSRP Price	DSRP-b Price	DSRP-c Price	DSRP-100 Price	DSRP-500 Price	Mat. of Construction	Purchase date	Purchase price ref.	date of calculation
Heat Exchangers										
	AIRHX	$33,500	$71,500	$17,900	$19,400	$55,300	SS304 / SS310 tubes	June, 1996	aspen DAIRHX	1/22/98
	PDCOOLR	$63,400	$126,600	$25,200	$42,000	$90,400	SS310 (calc w SS316)	June, 1996	aspen	1/22/98
Tanks										
7 days	Sulfur Storage	$125,500	$205,400	$65,000	$80,000	$171,000	SS310 (calc w SS316)	June, 1996	aspen	11/6/97
Condenser										
	High Pressure	$40,400	$82,200	$18,500	$21,900	$59,600	SS310 (calc w SS316)	June, 1996	aspen	
Vaporiser										
	VAPORIZR	$16,100	$17,800	$15,900	$15,200	$16,700	SS310 (calc w SS316)	June, 1996	aspen	
Compressor										
	RECOMP	$52,900	$52,900	$52,900	$52,900	$52,900	Carbon Steel	June, 1996	aspen	
	PRESAIR	$844,000	$2,680,000	$241,000	$416,000	$1,740,000		1997 Ingesoll-Rand	Centac Pricing	10/20/97
Reactors										
	Desulf & Regen	$1,328,000	$1,772,000	$1,169,000	$728,000	$2,434,000	SS310 (calc w SS316)	June, 1996 (w install)	P&T calc	10/7/97
	DSRP reactor	$812,129	$2,134,355	$367,075	$477,612	$1,394,800	SS310 (calc w SS316)	June, 1996 (w install)	P&T calc	10/16/97
Pipes										
	pipe lines									
	totals	$3,315,929	$7,142,755	$1,972,475	$1,853,012	$6,014,700				

DSRP costs

Equipment -Steam side

Type	unit	DSRP Price	DSRP-b Price	DSRP-c Price	DSRP-100 Price	DSRP-500 Price	Mat. of Construction	date		Purchase price ref.
Heat Exchangers										
	LCOOLR	$7,600	$8,100	$0	$6,800	$7,600		June, 1996	aspen	11/26/97
	VCOOLR	$7,000	$8,400	$6,700	$6,800	$7,600		June, 1996	aspen	11/26/97
Pumps										
	PTOWR	$4,200	$8,000	$2,800	$3,200	$5,500		June, 1996	aspen	11/26/97
	PHOTH2O	$1,000	$3,500	$0	$400	$3,500		price quote from General Pumps		
	PSTEAM	$57,400	$75,100	$57,400	$57,400	$59,300		June, 1996	aspen	11/26/97
	totals	$77,200	$103,100	$66,900	$74,600	$83,500				

DSRP costs

Expendatures

		DSRP	DSRP-b	DSRP-c	DSRP-100	DSRP-500	cost ref.	
Electrical								
Pumps & Compressors								
kW	RECYCOMP	59	227	5	7	37	ASPEN generated power requirements	
kW	PRESAIR	3282	10414	900	999	4889	ASPEN generated power requirements	
kW	Steam pumps	76	193	30	32	160	ASPEN steam simulations	11/26/97
Light & instruments								
kW	misc.	683	683	683	683	683	20% base case pump & compressor requirements	
TOTAL	kW	4100.4	11517.4	1618.4	1721	5769		
	unit cost $/kWh	0.04	0.04	0.04	0.04	0.04	Self-gen. (Jan. 1990) Peters & Timmeraus	
90 % op	Cost $/yr	$1,293,988	$3,634,615	$510,728	$543,234	$1,820,690		
Cooling Water								
	lbs/hr	149,000	500,000	25,000	62,744	313,720	ASPEN Complete Steam Generation Scheme simulations	
	unit value $/lb	2.6E-05	2.6E-05	2.6E-05	2.6E-05	2.6E-05	Tower (Jan. 1990) Peters & Timmeraus	
90 % op	Cost $/yr	$21,854	$73,336	$3,667	$9,203	$46,014		
Oxygen								
	lbs/hr	0	0	0	0	0		
	unit value $/lb							
	Cost $/yr							
Addtional Employees								
	Engineers	2	2	2	2	2		
	unit cost	$100,000	$100,000	$100,000	$100,000	$100,000		
	Maintenance	2	2	2	2	2		
	unit cost	$70,000	$70,000	$70,000	$70,000	$70,000		
	Cost $/yr	$340,000	$340,000	$340,000	$340,000	$340,000		
Consumed Coal Gas								
	MW lost	7	23	2	3	15	Appendix J	
	unit cost $/MWh	40	40	40	40	40	Self-gen. (Jan. 1990) Peters & Timmeraus	
	Cost $/yr	$2,287,295	$7,259,195	$652,927	$963,138	$4,714,074		
	totals (yearly)	$3,943,137	$11,307,146	$1,507,322	$1,855,574	$6,920,778		

DSRP costs

Benefits

		DSRP	DSRP-b	DSRP-c	DSRP-100	DSRP-500	Condition	value ref.	date of calc.
Sulfur Recovered									
	lbs/hr	5,840	18,590	1,667	2,460	12,300			
90% op	tons/year	23,037	73,332	6,576	9,704	48,520			11/4/97
	unit value $/ton	50	50	50	50	50	low purity	Chem. Eng. Progress 1996	
	Revenue $/yr	$1,151,852	$3,666,599	$328,791	$485,198	$2,425,991			
Steam Generation									
	lbs/hr	23,200	77,700	6,160	9,800	48,800	950 psia, 441 C		11/4/97
	unit value $/lb	0.0039	0.0039	0.0039	0.0039	0.0039	500 psig, (Jan. 1990)	Peters and Timmeraus	
90% op	Revenue $/yr.	$713,833	$2,390,725	$189,535	$301,533	$1,501,511			
	totals (yearly)	$1,865,685	$6,057,324	$518,326	$786,731	$3,927,501			

	DSRP	DSRP-b	DSRP-c	DSRP-100	DSRP-500
YEARLY COST	$2,077,452	$5,249,823	$988,996	$1,068,843	$2,993,277
EQUIPMENT COSTS	$3,393,129	$7,245,855	$2,039,375	$1,927,612	$6,098,200

AHGP Costs

Equipment

Type	unit	AHG Price	AHG-b Price	AHG-c Price	AHG-100 Price	AHG-500 Price	Mat. of Construction	Purchase date	price ref.	date of calculation
Heat Exchangers										
	HEATX	$64,900	$125,700	$32,900	$39,600	$107,300	SS310 (SS 316)	June, 1996	aspen	12/3/97 AHGPcosts
	RCYHEATR	$102,800	$162,900	$35,300	$60,500	$181,000	SS310 (SS 316)	June, 1996	aspen	1/22/98 steam
	N2-COOLR	$42,000	$72,200	$16,800	$26,500	$66,400	SS304	June, 1996	aspen	1/22/98 steam
Condensers										
	COND	$82,200	$177,000	$41,000	$51,400	$138,500	SS310-heat exchanger	June, 1996	aspen	1/22/98 steam
	LP-COND	$8,200	$11,100	$6,200	$7,000	$10,000	SS310 tank (τ = 1min)	June, 1996	aspen	12/3/97 AHGPcosts
Demister										
	DEMISTR	$53,100	$109,000	$30,600	$35,000	$83,700	SS310 1.5tank (τ =1mir	June, 1996	aspen	12/3/97 AHGPcosts
Compressor										
	CON-COMP	$201,100	$203,300	$200,900	$200,900	$202,100	3 x (Carbon Steel)	June, 1996	aspen	12/3/97 AHGPcosts
	LIFTCOMP	$485,000	$820,000	$161,600	$161,600	$820,000	3 x (Carbon Steel)	June, 1996	aspen mod.	12/3/97 AHGPcosts
	SO2-COMP	$53,900	$66,200	$53,900	$53,900	$1,410,000	3 x (Carbon Steel)	June, 1996	aspen	12/3/97 AHGPcosts
Tanks										
7 days	storage	$125,500	$205,400	$65,000	$80,000	$171,000	SS316	June, 1996	aspen	11/6/97
Reactors										
		$2,939,588	$12,297,497	$1,562,672	$2,177,791	$8,869,074	SS310	June, 1996 (w install)	P&T calc	11/20/97
Pipes										
	pipe lines									
	totals	$4,158,288	$14,250,297	$2,206,872	$2,894,191	$12,059,074				

Equipment -Steam side

Type	unit	AHGP Price	AHGP-b Price	AHGP-c Price	AHGP-100 Price	AHGP-500 Price	Mat. of Construction	date		Purchase price ref.
pumps										
	PTOWR	$3,400	$5,000	$2,800	$2,800	$4,300		June, 1996	aspen	11/26/97 steam
	PSTEAM	$57,400	$63,300	$57,400	$57,400	$59,300		June, 1996	aspen	11/26/97 steam
Heat Exchangers										
	VCOOLR	$7,000	$8,000	$6,700	$6,800	$7,600	shell CS / tube 304	June, 1996	aspen	11/26/97 steam
	totals	$67,800	$76,300	$66,900	$67,000	$71,200				

Expendatures

		AHGP	AHGP-b	AHGP-c	AHGP-100	AHGP-500		cost ref.	
Electrical						1 kW = 1.341 hp			
Pumps & Compressors									
kW	CON-COMP	8	26	2	3	17	ASPEN generated power requirements		1/22/98
kW	LIFTCOMP	13	28	3	5	27	ASPEN generated power requirements		1/22/98
kW	SO2-COMP	38	114	11	16	80	ASPEN generated power requirements		1/22/98
kW	Steam pumps	64	148	28	27	135	ASPEN generated power requirements		
Light & instruments									
kW	misc.	25	25	25	25	25	20% base case pump & compressor requirements		
TOTAL	kW	148	341	68	76	284			
	unit cost $/kWh	0.04	0.04	0.04	0.04	0.04	Self-gen. (Jan. 1990)	Peters & Timmeraus	
90 % op	Cost $/yr	$46,579	$107,485	$21,491	$24,109	$89,490			
Cooling Water									
	lbs/hr	79,200	4,530	434	33,351	166,756			
	unit value $/lb	2.6E-05	2.6E-05	2.6E-05	2.6E-05	2.6E-05	Tower (Jan. 1990)	Peters & Timmeraus	
90 % op	Cost $/yr	$29,041	$1,661	$159	$12,229	$61,146			
Oxygen									
	lbs/hr	4,129	12,536	1,195	1,739	8,694			
	unit value $/ton	$20	$20	$20	$20	$20	Increased O2 plant production	Dr. Roberts	
90 %op	Cost $/yr	$325,753	$989,015	$94,278	$137,175	$685,874			
Additional Employees									
	Engineers	3	3	3	3	3			
	unit cost	$100,000	$100,000	$100,000	$100,000	$100,000			
	Maintenance	2	2	2	2	2			
	unit cost	$70,000	$70,000	$70,000	$70,000	$70,000			
	Cost $/yr	$440,000	$440,000	$440,000	$440,000	$440,000			
Consumed Coal Gas									
	MW lost	1.506	4.580	0.436	0.634	3.172	Appendix J		
	unit cost $/MWh	40	40	40	40	40	Self-gen. (Jan. 1990)	Peters & Timmeraus	
	Cost $/yr	$475,257	$1,445,338	$137,591	$200,075	$1,001,007			
	totals (yearly)	$1,316,631	$2,983,500	$693,519	$813,588	$2,277,517			

Benefits

		AHGP	AHGP-b	AHGP-c	AHGP-100	AHGP-500	Condition	value ref.	date of calc.
Sulfur Recovered									
	lbs/hr	5,731	17,440	1,593	2,413	12,067			
90% op	tons/year	22,607	68,796	6,284	9,520	47,599			11/4/97
	unit value $/ton	50	50	50	50	50	low purity	Chem. Eng. Progress 1996	
	Revenue $/yr	$1,130,354	$3,439,778	$314,195	$475,992	$2,379,960			
Steam Generation									
	lbs/hr	19,400	59,000	5,650	8,169	40,847	950 psia, 441 C		11/4/97
	unit value $/lb	0.0039	0.0039	0.0039	0.0039	0.0039	500 psig, (Jan. 1990)	Peters and Timmeraus	
90% op	Revenue $/yr.	$596,912	$1,815,351	$173,843	$251,360	$1,256,798			
	totals (yearly)	$1,727,266	$5,255,129	$488,038	$727,352	$3,636,758			

	AHGP	AHGP-b	AHGP-c	AHGP-100	AHGP-500
YEARLY COST	-$410,635	-$2,271,630	$205,481	$86,236	-$1,359,241
EQUIPMENT COSTS	$4,226,088	$14,326,597	$2,273,772	$2,961,191	$12,130,274

AHGP Costs

Equipment

Type	unit	AHG Price	AHG-b Price	AHG-c Price	AHG-100 Price	AHG-500 Price	Mat. of Construction	Purchase date	price ref.	date of calculation
Heat Exchangers										
	HEATX	$64,900	$125,700	$32,900	$39,600	$107,300	SS310 (SS 316)	June, 1996	aspen	12/3/97 AHGPcosts
	RCYHEATR	$102,800	$162,900	$35,300	$60,500	$181,000	SS310 (SS 316)	June, 1996	aspen	1/22/98 steam
	N2-COOLR	$42,000	$72,200	$16,800	$26,500	$66,400	SS304	June, 1996	aspen	1/22/98 steam
Condensers										
	COND	$82,200	$177,000	$41,000	$51,400	$138,500	SS310-heat exchanger	June, 1996	aspen	1/22/98 steam
	LP-COND	$8,200	$11,100	$6,200	$7,000	$10,000	SS310 tank (τ = 1min)	June, 1996	aspen	12/3/97 AHGPcosts
Demister										
	DEMISTR	$53,100	$109,000	$30,600	$35,000	$83,700	SS310 1.5tank (τ =1min	June, 1996	aspen	12/3/97 AHGPcosts
Compressor										
	CON-COMP	$201,100	$203,300	$200,900	$200,900	$202,100	3 x (Carbon Steel)	June, 1996	aspen	12/3/97 AHGPcosts
	LIFTCOMP	$485,000	$820,000	$161,600	$161,600	$820,000	3 x (Carbon Steel)	June, 1996	aspen mod.	12/3/97 AHGPcosts
	SO2-COMP	$53,900	$66,200	$53,900	$53,900	$1,410,000	3 x (Carbon Steel)	June, 1996	aspen	12/3/97 AHGPcosts
Tanks										
7 days	storage	$125,500	$205,400	$65,000	$80,000	$171,000	SS316	June, 1996	aspen	11/6/97
Reactors										
		$2,939,588	$12,297,497	$1,562,672	$2,177,791	$8,869,074	SS310	June, 1996 (w install)	P&T calc	11/20/97
Pipes										
	pipe lines									
	totals	$4,158,288	$14,250,297	$2,206,872	$2,894,191	$12,059,074				

AHGP Costs

Equipment -Steam side

Type	unit	AHGP Price	AHGP-b Price	AHGP-c Price	AHGP-100 Price	AHGP-500 Price	Mat. of Construction	date		Purchase price ref.
pumps										
	PTOWR	$3,400	$5,000	$2,800	$2,800	$4,300		June, 1996	aspen	11/26/97 steam
	PSTEAM	$57,400	$63,300	$57,400	$57,400	$59,300		June, 1996	aspen	11/26/97 steam
Heat Exchangers										
	VCOOLR	$7,000	$8,000	$6,700	$6,800	$7,600	shell CS / tube 304	June, 1996	aspen	11/26/97 steam
	totals	$67,800	$76,300	$66,900	$67,000	$71,200				

AHGP Costs

Expendatures

		AHGP	AHGP-b	AHGP-c	AHGP-100	AHGP-500	cost ref.		
Electrical						1 kW = 1.341 hp			
Pumps & Compressors									
kW	CON-COMP	8	26	2	3	17	ASPEN generated power requirements		1/22/98
kW	LIFTCOMP	13	28	3	5	27	ASPEN generated power requirements		1/22/98
kW	SO2-COMP	38	114	11	16	80	ASPEN generated power requirements		1/22/98
kW	Steam pumps	64	148	28	27	135	ASPEN generated power requirements		
Light & instruments									
kW	misc.	25	25	25	25	25	20% base case pump & compressor requirements		
TOTAL	kW	148	341	68	76	284			
	unit cost $/kWh	0.04	0.04	0.04	0.04	0.04	Self-gen. (Jan. 1990)	Peters & Timmeraus	
90 % op	Cost $/yr	$46,579	$107,485	$21,491	$24,109	$89,490			
Cooling Water									
	lbs/hr	79,200	4,530	434	33,351	166,756			
	unit value $/lb	2.6E-05	2.6E-05	2.6E-05	2.6E-05	2.6E-05	Tower (Jan. 1990)	Peters & Timmeraus	
90 % op	Cost $/yr	$29,041	$1,661	$159	$12,229	$61,146			
Oxygen									
	lbs/hr	4,129	12,536	1,195	1,739	8,694			
	unit value $/ton	$20	$20	$20	$20	$20	Increased O2 plant production	Dr. Roberts	
90 %op	Cost $/yr	$325,753	$989,015	$94,278	$137,175	$685,874			
Additional Employees									
	Engineers	3	3	3	3	3			
	unit cost	$100,000	$100,000	$100,000	$100,000	$100,000			
	Maintenance	2	2	2	2	2			
	unit cost	$70,000	$70,000	$70,000	$70,000	$70,000			
	Cost $/yr	$440,000	$440,000	$440,000	$440,000	$440,000			
Consumed Coal Gas									
	MW lost	1.506	4.580	0.436	0.634	3.172	Appendix J		
	unit cost $/MWh	40	40	40	40	40	Self-gen. (Jan. 1990)	Peters & Timmeraus	
	Cost $/yr	$475,257	$1,445,338	$137,591	$200,075	$1,001,007			
	totals (yearly)	$1,316,631	$2,983,500	$693,519	$813,588	$2,277,517			

AHGP Costs

Benefits

		AHGP	AHGP-b	AHGP-c	AHGP-100	AHGP-500	Condition	value ref.	date of calc.
Sulfur Recovered									
	lbs/hr	5,731	17,440	1,593	2,413	12,067			
90% op	tons/year	22,607	68,796	6,284	9,520	47,599			11/4/97
	unit value $/ton	50	50	50	50	50	low purity	Chem. Eng. Progress 1996	
	Revenue $/yr	$1,130,354	$3,439,778	$314,195	$475,992	$2,379,960			
Steam Generation									
	lbs/hr	19,400	59,000	5,650	8,169	40,847	950 psia, 441 C		11/4/97
	unit value $/lb	0.0039	0.0039	0.0039	0.0039	0.0039	500 psig, (Jan. 1990)	Peters and Timmeraus	
90% op	Revenue $/yr.	$596,912	$1,815,351	$173,843	$251,360	$1,256,798			
	totals (yearly)	$1,727,266	$5,255,129	$488,038	$727,352	$3,636,758			

	AHGP	AHGP-b	AHGP-c	AHGP-100	AHGP-500
YEARLY COST	-$410,635	-$2,271,630	$205,481	$86,236	-$1,359,241
EQUIPMENT COSTS	$4,226,088	$14,326,597	$2,273,772	$2,961,191	$12,130,274

Appendix O
Reaction Data Obtained from RTI

The following data was obtained during correspondence with RTI.

DSRP reactions at 300 psi

Reaction	ΔH at 550°C (J/mol)	ΔH at 650°C (J/mol)	ΔH at 750°C (J/mol)
$0.5\ SO_2 + H_2 = (1/4)S_2 + H_2O$	-65128	-65795	-66436
$0.5\ SO_2 + CO = (1/4)S_2 + CO_2$	-101938	-101629	-101295

$ZnO + H_2S(g) = ZnS + H_2O(g)$

Temp. °C	ΔH kcal	ΔS cal	ΔG kcal	K
400	-17.079	-0.071	-17.031	3.387E+5
500	-17.056	-0.040	-17.025	6.502E+4
600	-17.047	-0.029	-17.022	1.824E+4
700	-17.050	-0.032	-17.019	6.645E+3

$ZnS + 1.5\ O_2(g) = ZnO + SO_2(g)$

Temp. °C	ΔH kcal	ΔS cal	ΔG kcal	K
500	-107.110	-18.940	-92.467	1.381E+26
550	-107.135	-18.971	-91.519	1.999E+24
600	-107.155	-18.995	-90.570	4.694E+22
650	-107.172	-19.013	-89.620	1.654E+21
700	-107.185	-19.027	-88.669	8.220E+19
750	-107.195	-19.038	-87.717	5.474E+18
800	-107.204	-19.046	-86.765	4.692E+17

APPENDIX F Advances in Hot Gas Desulfurization with Elemental Sulfur Recovery: Proceedings of the 15th Annual International Pittsburgh Coal Conference, Sept. 1998

Advances in Hot Gas Desulfurization with Elemental Sulfur Recovery

Jeffrey W. Portzer (jwp@rti.org; 919-541-8025)
Santosh K. Gangwal (skg@rti.org; 919-541-8033)
Research Triangle Institute
3040 Cornwallis Road
Research Triangle Park, NC 27709

T.P. Dorchak (Thomas.Dorchak@fetc.doe.gov; 304-285-4305)
Federal Energy Technology Center
U.S. Department Of Energy
3610 Collins Ferry Road
Morgantown, WV 26505

INTRODUCTION

Hot-gas desulfurization (HGD) of coal gas in integrated gasification combined cycle (IGCC) power systems has received a great deal of attention over the past two decades due to the potential for high thermal efficiency (up to 47%) and low environmental impact of these advanced power systems. In an advanced IGCC system, coal is gasified at elevated pressures, typically 20 to 30 atm, to produce a low-volume fuel gas that is desulfurized prior to burning in a combustion turbine to produce electricity. Higher efficiency and lower cost are achieved by efficient air and steam integration, and modular designs of the gasification, hot-gas cleanup, and turbine subsystems (Figure 1). Hot gas cleanup primarily involves removal of particulates and sulfur—mostly hydrogen sulfide (H_2S) and some carbonyl sulfide (COS). H_2S and COS can be efficiently removed to less than 20 ppmv at 350 to 650 °C using zinc-based metal oxide sorbents that can be regenerated for multicycle operation.

Air regeneration of these sorbents results in a dilute sulfur dioxide (SO_2)-containing tail gas that needs to be disposed. Options include conversion of the SO_2 to calcium sulfate using lime (or limestone) for landfilling or conversion to saleable products such as sulfuric acid or elemental sulfur. Elemental sulfur, an essential industrial commodity, is an attractive option because it is the lowest volume product and can be readily stored, disposed, transported, and/or sold.

Research Triangle Institute (RTI), with U.S. Department of Energy (DOE) sponsorship, is pursuing the development of two processes for elemental sulfur production in conjunction with hot-gas desulfurization. The first process, called the Direct Sulfur Recovery Process (DSRP), involves the selective catalytic reduction of the SO_2 tail gas to sulfur using a small slipstream of the coal gas. DSRP is a highly efficient process that can recover up to 99% of SO_2 as elemental

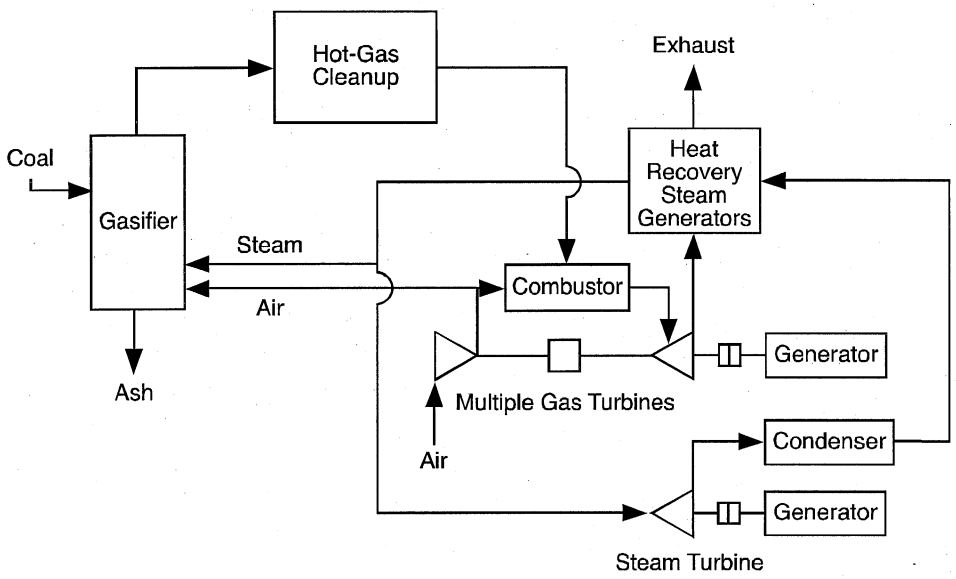

Figure 1. Advanced IGCC system.

sulfur in a single catalytic reactor. However, for every mole of sulfur produced two moles of hydrogen (H_2) and/or carbon monoxide (CO) are consumed in DSRP and this represents an energy penalty for the IGCC plant. DSRP is currently in an advanced state of development.

A second-generation process being pursued by RTI involves the use of a modified zinc-based sorbent (containing zinc and iron). This sorbent can be regenerated using SO_2 and O_2 to directly produce sulfur. This process, called the Advanced Hot-Gas Process (AHGP), is expected to use much less coal gas than DSRP. DSRP is currently at the pilot-plant scale development stage, whereas AHGP has been demonstrated at small bench-scale. Both DSRP and AHGP are scheduled for slipstream testing at DOE's Power Systems Development Facility (PSDF), Wilsonville, Alabama, in 1999.

This paper summarizes the results of DSRP field testing and the recent laboratory development efforts for the DSRP and the AHGP. In addition, this paper presents the results of a preliminary engineering and economic evaluation of the two processes used in conjunction with an IGCC power plant employing HGD. The computer process simulations used to develop the mass and energy balances, and economic evaluations were carried out by RTI's subcontractor, North Carolina State University (NCSU).

BACKGROUND

Sorbent Development

Research on HGD methods for coal gas in IGCC systems has concentrated on the use of regenerable metal oxide sorbents (Gangwal, 1991, 1996; Gangwal et al., 1993, 1995; Harrison, 1995; Jalan, 1985; Thambimuthu, 1993). This research and development effort has been spearheaded by DOE's Federal Energy Technology Center (FETC) and its predecessor agencies since 1975.

The HGD process using a regenerable metal oxide (MO) sorbent is typically carried out in a two-reactor system consisting of a desulfurizer and an air regenerator

$$MO + H_2S \rightarrow MS + H_2O \quad \text{(desulfurizer)}$$
$$MS + (3/2)\ O_2 \rightarrow MO + SO_2 \quad \text{(regenerator).}$$

The main requirement of the metal oxide sorbent is that it should selectively react with H_2S and COS in a reducing fuel gas at desired conditions (2 to 3 Mpa, 350 to 750 °C). The thermodynamics of the reaction should be favorable enough to achieve the desired level of H_2S and COS removal (as much as 99% or more). The metal oxide should be stable in the reducing gas environment, i.e., reduction of MO to M should be slow or thermodynamically unfavorable since it leads to loss of valuable fuel gas and could also lead to volatile metal evaporation and decrepitation of sorbent structure.

The principle requirement during air regeneration is that the sorbent should predominantly revert back to its oxide rather than to sulfate ($MO + SO_2 + 1/2\ O_2 \rightarrow MSO_4$). Air regeneration is highly exothermic and requires tight temperature control using large quantities of diluent (N_2) or other means to prevent sorbent sintering and sulfate formation.

The bulk of research on regenerable sorbents has been on zinc-based sorbents because sorbents based on zinc oxide appear to have the fewest technical problems among all sorbents. Zinc oxide (ZnO) has highly attractive thermodynamics for H_2S adsorption and can reduce the H_2S to parts-per-million levels over a very wide temperature range. Iron oxide appears to be the most popular sorbent for use at around 400 °C.

A combined ZnO-iron oxide (Fe_2O_3) sorbent, namely, zinc ferrite ($ZnFe_2O_4$) was developed by Grindley and Steinfeld (1981) to combine the advantages of ZnO and Fe_2O_3. A temperature range of 550 to 750 °C received the major research emphasis in the United States during the 1980s and early 1990s. Because of zinc oxide's potential for reduction ($ZnO + H_2 \rightarrow Zn + H_2O$) at >600 °C followed by evaporation, a zinc oxide-titanium oxide sorbent, namely zinc titanate sorbent, was developed and tested at high temperature and high pressure (HTHP) (Gangwal et al., 1988). Zinc titanate is currently one of the leading sorbents.

During recent years, research emphasis has shifted toward lower temperatures (350 to 550 °C) based on a study in the Netherlands (NOVEM, 1991). According to this study, the thermal efficiency of an 800-MWe IGCC plant increased from 42.75% using cold-gas cleanup to 45.14% using HGD at 350 °C and to 45.46% using HGD at 600 °C. The small efficiency increase from 350 to 600 °C suggested that temperature severity of HGD could be significantly reduced without much loss of efficiency.

Reactor and Systems

A two-reactor configuration is necessary for HGD due to its cyclic nature. Early developments emphasized fixed beds. The highly exothermic regeneration led to a move away from fixed beds toward moving beds (Ayala et al., 1995; Cook et al., 1992) and fluidized beds (Gupta and Gangwal, 1992). Two DOE Clean Coal Technology IGCC demonstration plants, namely Tampa Electric and Sierra-Pacific, employing General Electric's (GE's) moving-bed HGD reactor system and M.W. Kellogg's transport reactor HGD system, respectively, are scheduled to begin operation this year. Fluidized-bed HGD systems are receiving a lot of emphasis due to several potential advantages over fixed- and moving-bed reactors, including excellent gas-solid contact, fast kinetics, pneumatic transport, ability to handle particles in gas, and ability to control the highly exothermic regeneration process. However, an attrition-resistant sorbent that can withstand stresses induced by fluidization, transport, chemical transformation, and rapid temperature swings must be developed.

Development of an iron-oxide sorbent-based fluidized-bed HGD reactor system has been carried out in Japan over the past several years (Sugitani, 1989). The process is now up to 200 tons of coal per day. The sorbent is prepared by crushing raw Australian iron oxide which is inexpensive, but attrition is a big problem with this sorbent. Durable zinc titanate and other zinc-based sorbent development is ongoing for application at the Sierra-Pacific plant for Kellogg's transport reactor (Gupta et al., 1996, 1997; Jothimurugesan et al., 1997; Khare et al., 1996).

A schematic of Kellogg's transport reactor system at Sierra-Pacific is shown in Figure 2. This technology represents a significant development in HGD because it allows regeneration with neat air. Neat air regeneration produces a more concentrated SO_2 tail-gas stream containing around 14 vol% SO_2.

The initial sorbent tested at Sierra-Pacific was Phillips Z-Sorb III. Its attrition resistance was not acceptable. Phillips is continuing efforts to improve their sorbent. Recently RTI and Intercat have provided a much more attrition-resistant zinc titanate sorbent, EX-SO3, to Sierra-Pacific for testing after qualifying it through a series of bench- and process development unit (PDU)-scale tests (Gupta et al., 1997). This sorbent has been circulated in the system and has demonstrated satisfactory attrition resistance. Chemical reactivity tests with the sorbent are to be conducted shortly after the Sierra coal gasifier is fully commissioned and begins smooth operation.

SULFUR RECOVERY PROCESSES AND RECENT DEVELOPMENT

Direct Sulfur Recovery Process

The patented DSRP being developed by RTI is a highly attractive option for recovery of sulfur from regeneration tail gas. Using a slipstream of coal gas as a reducing agent, it efficiently converts the SO_2 to elemental sulfur, an essential industrial commodity that is easily stored and transported. In the DSRP (Dorchak et al., 1991), the SO_2 tail gas is reacted with a slipstream of coal gas over a fixed bed of a selective catalyst to directly produce elemental sulfur at the HTHP conditions of the tail gas and coal gas. Overall reactions involved are shown below:

$$2\ H_2 + SO_2 \rightarrow (1/n)\ S_n + 2\ H_2O$$

$$2\ CO + SO_2 \rightarrow (1/n)\ S_n + 2\ CO_2$$

$$CO + H_2O \rightarrow H_2 + CO_2$$

$$H_2 + (1/n)\ S_n \rightarrow H_2S$$

$$2\ H_2S + SO_2 \rightarrow (3/n)\ S_n + 2\ H_2O\ .$$

RTI constructed and commissioned a mobile laboratory for DSRP demonstration with actual coal gas from the DOE-Morgantown coal gasifier. Slipstream testing using a 1-L fixed-bed of DSRP catalyst with actual coal gas (Portzer and Gangwal, 1995; Portzer et al., 1996) demonstrated that, with careful control of the stoichiometric ratio of the gas input, sulfur recovery of 96% to 98% can be consistently achieved in a single DSRP stage. The single-stage process, as it is proposed to be integrated with a metal oxide sorbent regenerator, is shown in Figure 3. With the tail-gas recycle stream shown in the figure, there are no sulfur emissions from the DSRP.

RTI also demonstrated the ruggedness of the DSRP catalyst by exposing it to

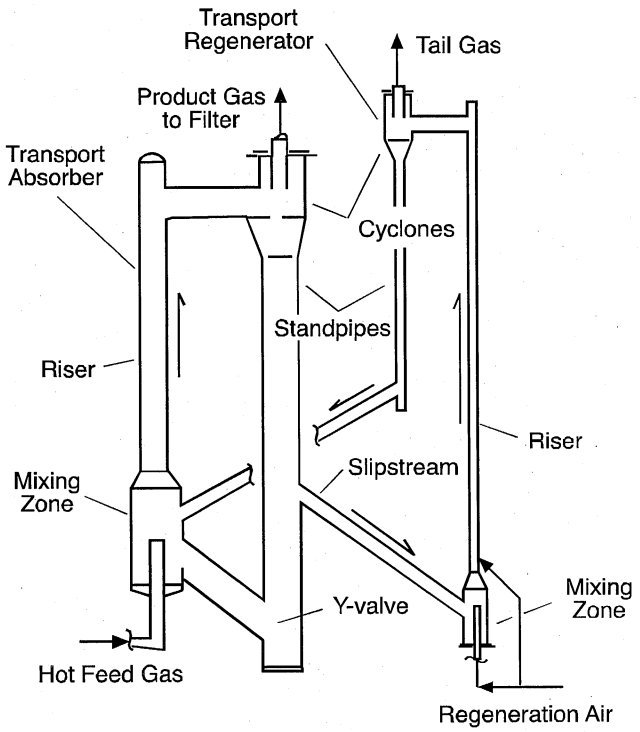

Figure 2. Schematic of Sierra hot-gas desulfurization system.

coal gas for over 250 hours in a canister test. The results show that, after a significant exposure time to actual coal gas, the DSRP catalyst continues to function in a highly efficient manner to convert SO_2 in a simulated regeneration tail gas to elemental sulfur. This demonstration of a rugged, single-stage catalytic process resulted in additional online experience and the assembling of more process engineering data. The development of the DSRP continues to look favorable as a feasible commercial process for the production of elemental sulfur from hot-gas desulfurizer regeneration tail gas.

Canisters of fixed-bed DSRP catalyst have been prepared for another exposure test with actual coal gas, this time at FETC's Power Systems Development Facility (PSDF) at Wilsonville, Alabama. Exposure is expected to take place in the 1999-2000 time frame.

Additional development and testing of a fluidized-bed process is planned, capable of producing elemental sulfur from 14 vol% SO_2 at HTHP. These tests intend to demonstrate the use of DSRP in conjunction with the Kellogg transport regenerator that produces 14 vol% SO_2. Due to the exothermic nature of the DSRP reactions, a fluidized-bed reactor is a preferred configuration at these high SO_2 concentrations. Two candidate attrition-resistant fluidizable DSRP catalysts have been prepared in cooperation with a catalyst manufacturer. A series of tests was conducted using these catalysts with up to 14 vol% SO_2 tail gas, at pressures from 1.0 to 2.0 Mpa, temperatures from 500 to 600 °C, and space velocities from 3,000 to 6,000 std cm^3/cm^3. Sulfur recoveries up to 98.5% were achieved during steady-state operation, and no attrition of the catalyst occurred in the fluidized-bed tests.

Planning is underway to conduct a long-duration field test using a skid-mounted six-fold larger (based on reactor volume) (6X) DSRP unit with a slipstream of actual coal gas at PSDF. The

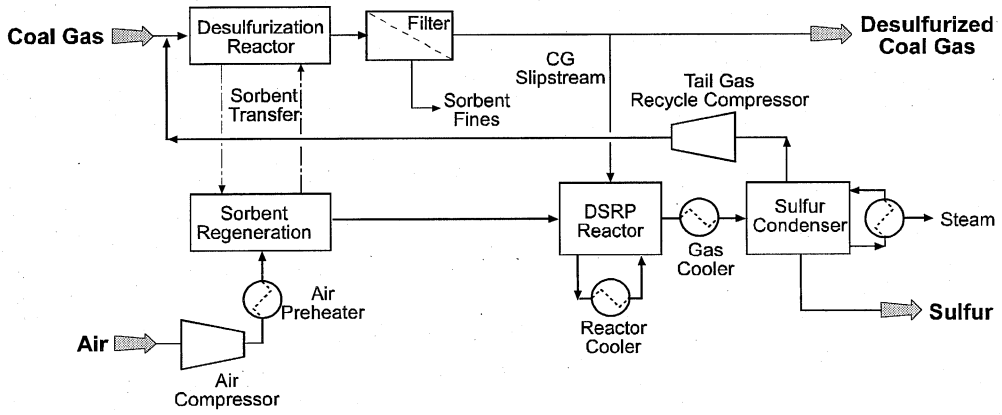

Figure 3. Hot-gas desulfurization with DSRP.

mobile laboratory will be refitted at RTI as a control room for the 6X unit and will be moved along with the skid-mounted 6X unit to Wilsonville, Alabama, for the testing to be conducted in the 1999-2000 time frame. This larger unit will utilize a fluidized-bed reactor and will be designed for production of up to 22 times more sulfur than the 7.5-cm I.D. bench-scale unit used in the previous slipstream tests.

Advanced Hot-Gas Process

In the DSRP, for every mole of SO_2, 2 mol of reducing components are used, leading to a small but noticeable consumption of coal gas. Novel regeneration processes that could lead to elemental sulfur without use of coal gas or with limited use of coal gas are being developed (Gangwal et al., 1996; Harrison et al. 1996). KEMA's hot-gas cleanup process (Meijer et al., 1996) uses a proprietary fluidized-bed sorbent that can remove H_2S to below 20 ppmv and that can be regenerated using SO_2-O_2 mixtures to produce elemental sulfur directly. Along similar lines, a second-generation process, known as the Advanced Hot-Gas Process (AHGP), is being developed by RTI to regenerate the desulfurization sorbent directly to elemental sulfur with minimal consumption of coal gas. In this process (Figure 4), a zinc-iron sorbent is used and the regeneration is carried out in two stages with SO_2 and O_2, respectively. The iron sulfide is regenerated by SO_2 in one stage to elemental sulfur. In the other stage, zinc sulfide and any remaining iron sulfide are regenerated by O_2 to provide the required SO_2. The sorbent is then returned to the desulfurizer.

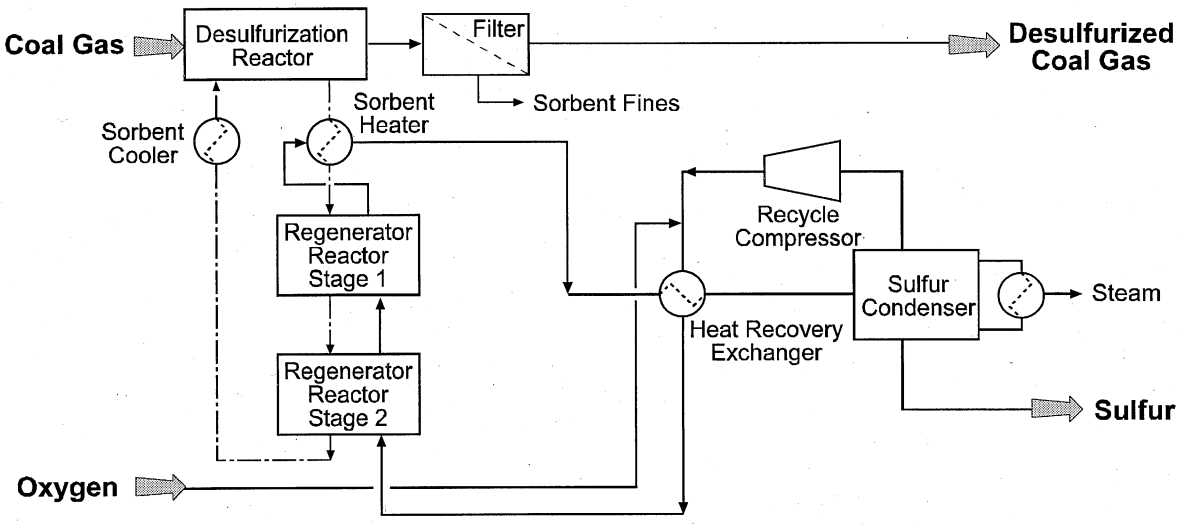

Figure 4. Advanced hot-gas process.

The key chemical reactions of interest are as follows:

1. Sulfidation

$$Fe_2O_3 + 2H_2S + H_2 \rightarrow 2FeS + 3H_2O$$
$$ZnO + H_2S \rightarrow ZnS + H_2O$$

2. SO_2 regeneration

$$4FeS + 3SO_2 \rightarrow 2Fe_2O_3 + 7/2\ S_2$$

3. O_2 regeneration

$$2FeS + 7/2\ O_2 \rightarrow Fe_2O_3 + 2SO_2$$
$$ZnS + 3/2\ O_2 \rightarrow ZnO + SO_2.$$

The feasibility of SO_2 regeneration of combined zinc-iron sorbents was demonstrated using a thermogravimetric analyzer and high-pressure microreactor. Zinc sulfide shows essentially no SO_2 regeneration at temperatures of interest (500 to 600 °C), but zinc is needed to act as a polishing agent in the desulfurizer. A number of sorbents were prepared and tested at the bench scale over multiple cycles. Based on these tests, a highly attrition-resistant sorbent (R-5-58) was prepared and the process was demonstrated over 50 cycles in a 7.5-cm I.D. bench-scale reactor.

The results showed that R-5-58 removed H_2S down to 50 to 100 ppm levels with stable desulfurization activity over the duration. The surface area and pore volume of the sorbent did not change appreciably and the attrition index before and after the test was 3.6% and 1.2%, respectively. Sulfur balances were adequate and the SO_2 regeneration step accounted for up to 70% of the total regeneration of the sorbent. This compares to a theoretical limit of approximately 80%, assuming complete regeneration by SO_2 of the iron component.

The sorbent is being optimized further to increase its desulfurization efficiency. The goal is to develop a sorbent that can remove H_2S below 20 ppmv. Plans call for demonstrating the process at PSDF with a slipstream of actual coal gas in FY 1999 in conjunction with the DSRP field test at PDSF.

ENGINEERING EVALUATION/COMPARISON

Approach

An engineering and economic evaluation of the DSRP (Figure 3) and AHGP (Figure 4) for large-scale IGCC plants was conducted by NCSU using ASPEN PLUS® computer process simulation software and published generalized cost estimating methods (Gangwal, *et al*, 1998) . For both processes the scope of the equipment and process steps included in the simulations were the same: coal gas desulfurization (but not the high temperature particulate removal), regeneration of the desulfurizing sorbent, and production, isolation, and short term storage of elemental sulfur. The recovered sulfur was assumed to have a market value, and thus generate a cost credit. Coal gas consumed in the process was evaluated at a cost based on the potential power generation that was lost. High pressure steam generated in the process was assumed to provide a cost credit based on the power that could be recovered from it.

Base case simulations of both processes assumed 0.85 mol% H_2S in the coal-gas feed. Such an H_2S concentration in the coal gas would be produced by an oxygen-blown Texaco gasification using a roughly 3.6 wt% sulfur-containing coal. Both base cases generate 260 MWe from the clean coal gas. Simulations that deviate from the base cases use suffixes to denote the changes. Table 1 displays the significance of the suffixes. In all cases a coal-gas feed pressure and temperature of 275 psia and 482 °C, respectively, was used. However, H_2S concentration was varied from 0.25 to 2.5 mol% and power produced was varied from 110 to 540 MWe. Table 2 shows the composition and flow rate of the raw coal gas feed to the base case HGD processes. The requirement of a higher amount of coal gas to produce the same 260 MW power by DSRP versus the AHGP is noteworthy. The DSRP was assumed to use the standard Sierra-Pacific dual transport reactor configuration shown in Figure 2 for HGD. The DSRP reactor used for the 14% SO2 tail gas was a fast fluidized bed with an alumina-based catalyst.

Table E-1. Simulation Cases Considered

Simulations	H_2S feed concentration (mol%)	MW produced
DSRP, AHGP (base cases)	0.85	260
DSRP-b, AHGP-b	2.50	260
DSRP-c, AHGP-c	0.25	260
DSRP-100, AHGP-100	0.85	110
DSRP-500, AHGP-500	0.85	540

Table E-2. Raw Gas Feed to Base Case Simulations

Component	DSRP (lb/h)	AHGP (lb/h)
H_2S	6,300	6,100
H_2O	70,500	69,000
H_2	11,800	11,500
CO	218,200	213,400
CO_2	117,400	114,800
N_2	36,300	35,500
Total	460,500	450,300

The AHGP reactor configuration on the other hand used a transport sulfider and a bubbling multistage fluidized-bed regenerator as shown in Figure 5. This vessel combines two stages of regeneration with one stage of heat transfer (to recover a portion of the heat of reaction as preheat for the sorbent). The large cross-sectional area bubbling reactor was required to provide a greater residence time for the slow SO_2 regeneration stage.

Results

The preliminary process and economic evaluations conducted using ASPEN PLUS are

summarized. Figure 6 compares key elements using a simple method in which each parameter for the DSRP-based process is arbitrarily assigned the value of 1.0. A range of values is produced for AHGP to cover the various cases being considered. The big advantage of the AHGP is clearly the reduced parasitic consumption of coal gas. The other operating cost elements are also lower for AHGP, because that process has a considerably lower compression power requirement. A desulfurization process based on the DSRP requires a large flow of compressed air to provide the oxygen necessary to regenerate the sulfided sorbent, and thus has a large compressor horsepower duty. By comparison, the AHGP uses oxygen only for a smaller, polishing regeneration and, by using pure oxygen, the compression duty is lowered further. The AHGP also has the SO_2 loop recycle compressor, but its duty is quite small compared to the DSRP air compressor.

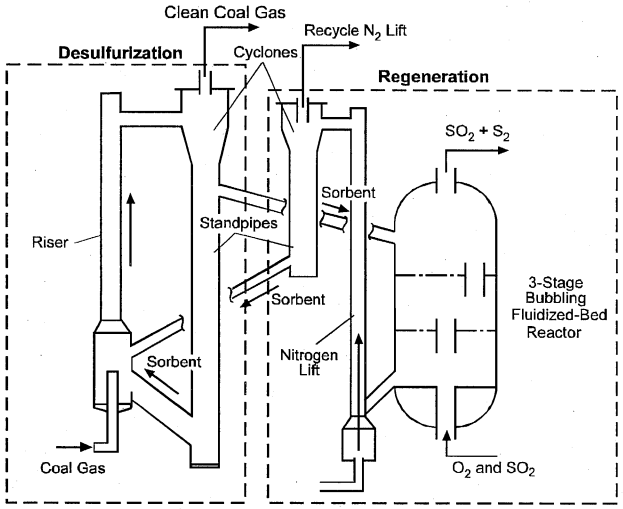

Figure 5. Schematic of AHGP desulfurization and regeneration reactors.

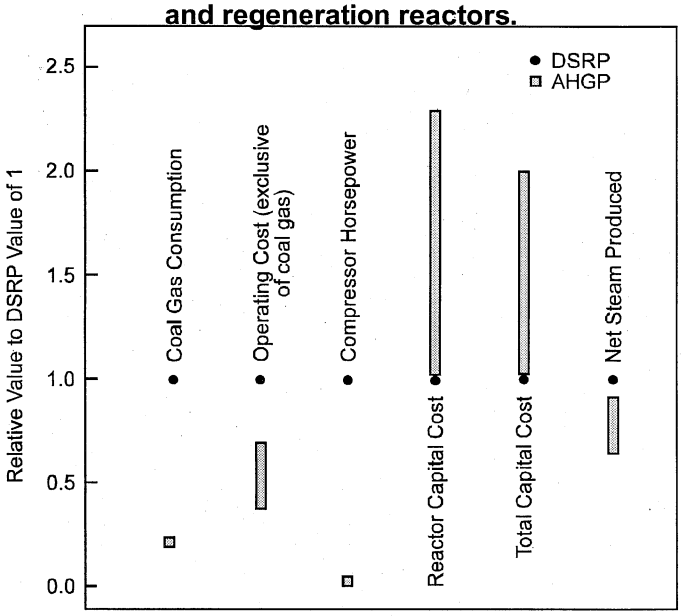

Figure 6. Comparison of key elements of DSRP and AHGP.

The value of "capital cost of all equip ment" for the AHGP is higher than for the DSRP-based process, as Figure 5 shows. The higher equipment cost is primarily due to the higher cost of the AHGP reactor vessel(s). Although there are three separate reactor steps required with the DSRP-based process, the single AHGP multistage reactor vessel(s) is larger. The larger size is primarily due to the longer residence time required for the SO_2 regeneration.

Another advantage of the DSRP is that it is the easier, more understood, process to operate. This is because balancing the SO_2 production and consumption in the AHGP may be difficult.

Presumably a simpler process would have lower operating labor costs.

Although the AHGP has a higher initial cost, indicated by its larger capital requirements, it has a significantly lower annual operating cost than DSRP. As Figure 7 shows, the operating cost advantage of the AHGP increases as the sulfur to be recovered increases. The negative annual costs of AHGP at higher sulfur feed result from the sulfur credit with less consumption of coal gas. The operating cost difference is large enough to offset the installation cost of AHGP. As Figure 8 shows, AHGP has a lower cumulative HGD investment after only 2 years of operation. Both Figures 7 and 8 are presented to illustrate only cost comparison of the two processes. Emphasis should not be placed on the accuracy of the absolute cost numbers presented in these figures.

CONCLUSIONS

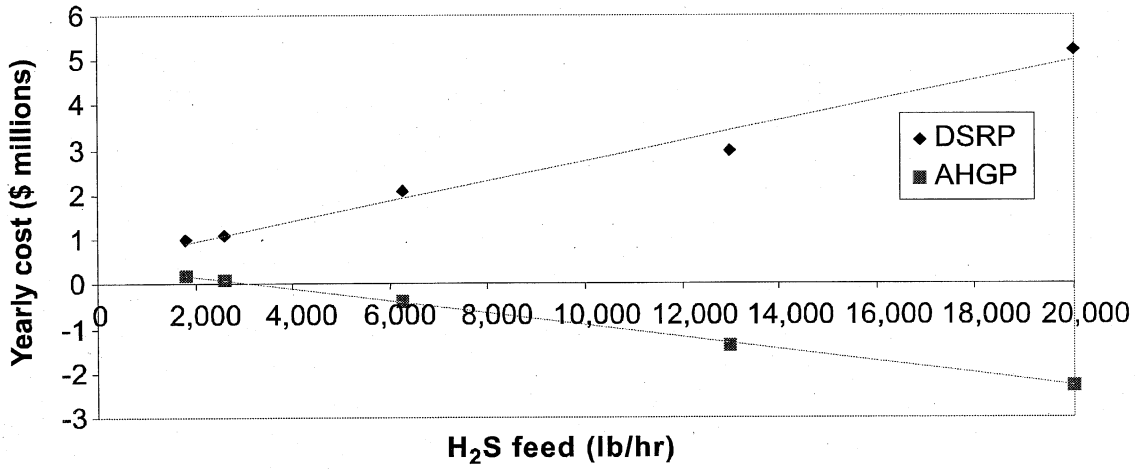

Figure 7. Annual costs as a function of sulfur feed.

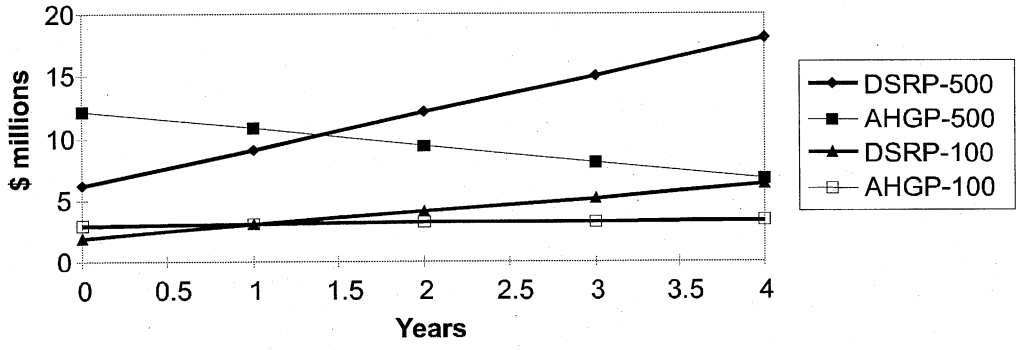

Figure 8. Cumulative HGD investment.

ASPEN simulations of DSRP and AHGP revealed the complexity of both HGD processes. The AHGP appears to be the more difficult process to operate and may require more employees than the DSRP. Capital costs for the AHGP are higher than those for the DSRP—development of DSRP is also much closer to commercialization than AHGP. However, annual operating costs for the AHGP appear to be considerably less than those of the DSRP. Preliminary economic comparison shows that the total cost (capital plus cumulative operating cost) of implementing AHGP will be less than that of implementing DSRP after as little as 2 years of operation. Thus, despite its greater complexity, the potential savings with the AHGP encourage further development and scaleup of this advanced process.

REFERENCES

Ayala, R.E., A.S. Feitelberg, and A.H. Furman. 1995. "Development of a High-Temperature Moving-Bed Coal Gas Desulfurization System." In *Proceedings of 12th Ann. Int. Pittsburgh Coal Conf.*, p. 1053, September 11-15, Pittsburgh.

Cook, C.S., et al. 1992. "Integrated Operation of a Pressurized Fixed Bed Gasifier and Hot Gas Desulfurization System." In *Proceedings of 12th Annual Gasif. Gas Stream Cleanup Systems Contractor's Review Meeting*, Volume 1, DE93000228, p. 84.

Dorchak, T.P., S.K. Gangwal, and W.J. McMichael. 1991. The Direct Sulfur Recovery Process. *Environmental Progress* 19(2):68.

Gangwal, S.K. 1991. "Hot-Gas Desulfurization Sorbent Development for IGCC Systems." IChemE Symposium Series No. 123. Sheffield, UK, pp. 159-170.

Gangwal, S.K. 1996. "Sulfur Removal from Gas Streams at High Temperature," 3rd International Symposium on Gas Cleaning at High Temperature. University of Karlsruhe, Karlsruhe, Germany, September.

Gangwal, S.K., et al. 1988. "Bench-Scale Testing of Novel High-Temperature Desulfurization Sorbents." Report No. DOE/MC/23126-2662 (DE89000935).

Gangwal, S.K., R. Gupta, and W.J. McMichael. 1993. "Sulfur Control Options for IGCC Systems." In *Proceedings of 17th Biennial Low-Rank Fuels Symposium*, University of North Dakota, Energy and Environmental Research Center, St. Louis, MO, May 10-13.

Gangwal, S.K., R. Gupta, and W.J. McMichael. 1995. "Hot-Gas Cleanup-Sulfur Recovery-Technical, Environmental, and Economic Issues," *Heat Recovery Systems and CHP*. Vol. 15, No. 2, p. 205-214, Elsevier Science Limited.

Gangwal, S.K., J.W. Portzer, G.W. Roberts, and S.C. Kozup. 1998. "Engineering Evaluation of Hot-Gas Desulfurization with Sulfur Recovery." Topical Report. DOE Contract No. DE-

AC21-94MC31258. Research Triangle Institute. Research Triangle Park, NC.
Grindley, T., and G. Steinfeld. 1981. "Development and Testing of Regenerable Hot Coal-Gas Desulfurization Sorbents." DOE/MC/16545-1125.

Gupta, R., and S.K. Gangwal. 1992. "Enhanced Durability of Desulfurization Sorbents for Fluidized Bed Applications—Development and Testing of Zinc Titanate Sorbents." DOE/MC/25006-3271.

Gupta, R., B.S. Turk, and S.K. Gangwal. 1996. "Bench-Scale Development of Fluid-Bed Spray Dried Sorbents." In *Proceedings of Advanced Coal-Fired Power Systems '96 Review Meeting*, Morgantown Energy Technology Center, Morgantown, WV, July.

Gupta, R., B.S. Turk, and Albert A. Vierheilig. 1997. "Desulfurization Sorbents for Transport-Bed Applications." In *Proceedings of 1997 FETC Power Systems and Environmental Control Contractor's Meeting*, Pittsburgh, PA, July.

Harrison, D.P. 1995. "Control of Gaseous Contaminants in IGCC Processes, An Overview," In *Proceedings of 12th Ann. Int. Pittsburgh Coal Conference*, p. 1047, September 11-15, Pittsburgh.

Harrison, D.P., F.R. Groves, J.D. White, W. Huang, and A. Lopez-Oritz. 1996. "Advanced Sulfur Control Processing." In *Proceedings of Advanced Coal-Fired Power Systems '96 Review Meeting*, Morgantown Energy Technology Center, Morgantown, WV, July.

Jalan, V. 1985. "High-Temperature Desulfurization of Coal Gases." In *Acid and Sour Gas Treating Processes*, Gulf Publishing Co., Houston, TX, Nov. 7.

Jothimurugesan, K., S.K. Gangwal, R. Gupta, and B.S. Turk. 1997. "Advanced Hot-Gas Desulfurization Sorbents." In *Proceedings of 1997 FETC Power Systems and Environmental Control Contractor's Meeting*, Pittsburgh, PA, July.

Khare, G.P., G.A. Delzer, G.J. Greenwood, and D.H. Kunbicek. 1996. "Phillips Sorbent Development for Tampa Electric and Sierra Pacific." In *Proceedings of Advanced Coal-Fired Power Systems '96 Review Meeting*, Morgantown Energy Technology Center, Morgantown, WV, July.

Meijer, R., F.J.J.G. Janssen, G.L. Faring, and J.W. H. Hellendoorn. 1996. "KEMA's Hot Gas Cleanup Process." *In Proceedings of 3rd International Symposium on Gas Cleaning at High Temperature*. University of Karlsruhe, Karlsruhe, Germany, September.

NOVEM. 1991. "System Study High Temperature Gas Cleaning at IGCC Systems." Netherlands Agency for Energy and the Environment.

Portzer, J.W., and S.K. Gangwal. 1995. "Slipstream Testing of Hot Gas Desulfurization with Sulfur Recovery." In *Proceedings of the Advanced Coal-Fired Power Systems '95 Review Meeting*, pp. 220-228. DOE/METC-95/1018, Vol. 1, NTIS/DE 95009732. Springfield, VA: National Technical Information Service.

Portzer, J.W., B.S. Turk, and S.K. Gangwal. 1996. "Durability Testing of the Direct Sulfur Recovery Process." In *Proceedings of the Advanced Coal-Fired Power Systems Review Meeting July 16 B18, 1996.* (CD-ROM). U.S. Department of Energy. Morgantown, WV.

Sugitani, T. 1989. Development of Hot-Gas Desulfurization Process. *Journal of the Fuel Society of Japan* 68(9):787.

Thambimuthu, K.V. 1993. Gas Cleaning for Advanced Coal-Based Power Generation. Report by IEA Coal Research, IEACR/53, London, UK.

APPENDIX G Candidate Processes and Materials for the Direct Oxidation of H_2S in Coal Gas: A Literature Review

CANDIDATE PROCESSES AND MATERIALS FOR THE DIRECT OXIDATION OF H_2S IN COAL GAS

prepared by *James J. Spivey*[1] and *S.K. Gangwal*[2], Research Triangle Institute
[1]e-mail jjs@rti.org, ph 919-541-8033, fax 919-541-8000;
[2]e-mail skg@rti.org, ph 919-541-8033, fax 919-541-8000.
January 20, 2000

Task 1: Literature Review

Scope: This review focuses on homogeneous and heterogeneous catalytic processes and liquid phase processes to oxidize H_2S in coal gas to elemental sulfur at temperatures below 200□C and pressures near 20 atm. Although the exact inlet gas composition will depend on the type of gasifier, Table 1 shows the general range of compositions considered in this review.

Table 1. Composition of Coal Gas*

Component	Concentration range
CO	30-50%
H_2	20-40%
CO_2	2-3%
H_2O	10-15%
H_2S	1,000-4,000 ppm

* Does not include trace compounds (NH_3, alkali metals, etc.)

SO_2, obtained by burning the required portion of elemental sulfur, is used as the oxidant. The ultimate goal is to recover elemental sulfur from coal gasification in a process such as that shown in Figure 1.

In this process, coal gas containing H_2S is brought into contact with a catalyst or absorber in which H_2S is removed and converted to elemental sulfur. Variations of this general process are discussed below in considering the three options for sulfur removal and recovery:

- Heterogeneous catalysts
- Liquid phase absorption/reaction
- Supported liquid phase catalysts

The scope of this literature review is to identify candidate materials and processes that can be tested experimentally for H_2S oxidation to elemental sulfur at the conditions shown in Figure 1.

Summary of the Literature

Three types of catalysts and processes were examined: heterogeneous catalysts, liquid phase absorption/reaction, and supported liquid catalysts.

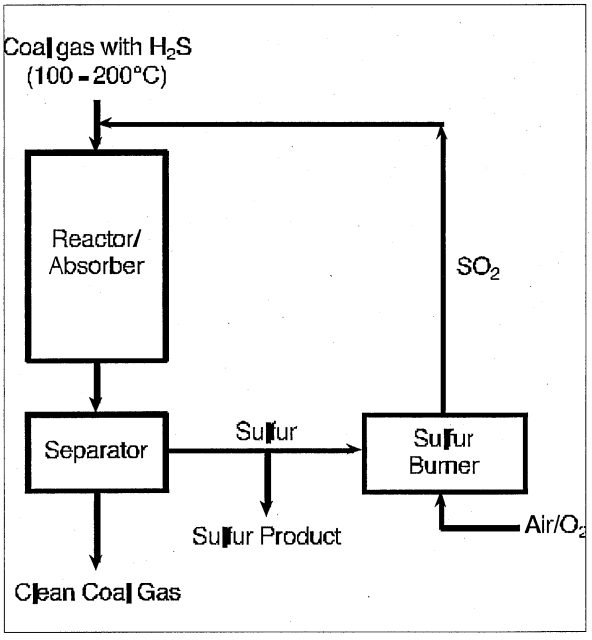

Figure 1. Schematic of the sulfur recovery process.

Section 1—Heterogeneous Catalysts

When using heterogeneous catalysts, the solid catalyst promotes the gas phase reaction of H_2S and SO_2 to produce elemental sulfur, which is recovered as a liquid. The reaction would be carried out in a fixed bed, as shown in Figure 2.

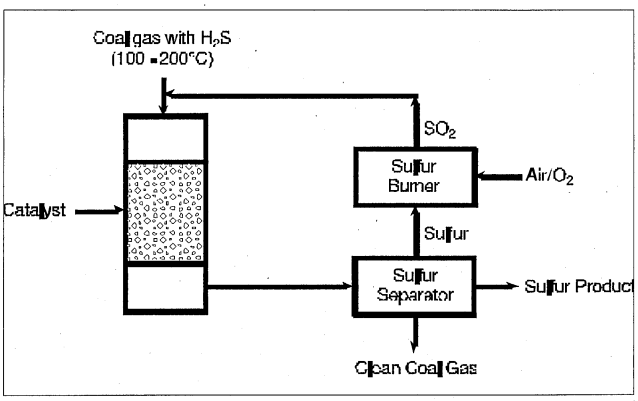

Figure 2. Heterogeneous catalyst for the Claus reaction.

Overall Process. The coal gas containing H_2S is contacted with a reactor in which gaseous SO_2 is also introduced from a recycle burner. A portion of the sulfur produced is passed through a burner to form SO_2, which is recycled to the top of the reactor.

Despite the possibility that the liquid sulfur could plug the pores of the catalyst, the process is similar in principle to Fischer Tropsch (FT) synthesis, in which waxes are produced from gaseous reactants. In FT synthesis, the catalyst in this process continues to promote the gas phase reaction for long periods of time while the liquid product is collected downstream. This suggests the possibility of a continuous process in which liquid sulfur is formed and collected downstream of the catalyst bed, just as waxes are collected in FT synthesis. However, if the catalyst loses activity rapidly, parallel beds would be needed to enable periodic regeneration and recovery of the sulfur. This would be both cumbersome and costly. Thus, a key challenge would be to find a catalyst with long life in the presence of molten sulfur.

Catalysts. Although the Claus reaction is carried out industrially at temperatures between 200□C and 280□C, the inlet gas to the catalytic reactor in that process does not contain CO and H_2. This is a key difference between the commercial Claus process and conditions shown in Figure 2. These reducing gases may cause undesirable reactions, such as the formation of COS, and may affect the modified alumina catalysts used industrially for the Claus reaction. In addition, reactions between CO/H_2 and any of the reactants or products of the Claus reaction must be avoided in order to minimize the consumption of these valuable fuel gases. The challenge is thus to selectively promote the Claus reaction when the H_2S and SO_2 reactants are in dilute concentrations in the presence of large concentrations of CO and H_2.

Table 2. Inlet Gas Composition Studied by Pearson (1975)*

Component	Concentration, %
CO	1.2
H_2	2.4
CO_2	6
H_2O	33.8
H_2S	0.75
SO_2	0.375
N_2	55

* Catalysts were tested a GHSV of 550 h^{-1}.

A review of the literature did not identify any directly related studies in which the Claus reaction was carried out in the presence of large concentrations of CO and H_2. However, closely related studies suggest that alumina catalysts related to those used for commercial Claus catalysis should be tested, after modifications that avoid deactivation due to sulfur deposition in catalyst pores over sulfate formation. Pearson (1975) studied the Claus reaction at temperatures between 135°C and 175°C using a gas composition corresponding to a Claus tail gas, which contained low levels of CO and H_2 (Table 2).

The catalyst tested most extensively was described only as an "active" alumina, with a surface area of 300 m^2/g. In all tests, conversion of H_2S/SO_2 was about 96 to 98 percent and remained at this level until the catalyst reached 60 to 70 wt% sulfur loading, after which the conversion declined rapidly. With a sulfur loading of about 92 wt%, the conversion was only 31 percent, and calculations showed that this corresponded to completely full pores. Tests comparing the sulfate tolerance of these materials showed that the promoted alumina, described only as "S-501," was most tolerant to sulfate formation.

One further study of the low-temperature Claus reaction in the presence of reducing gases showed that iron-based materials are active, though it is doubtful that iron catalysts can be used in the presence of the high levels of CO and H_2 that are of interest here. Smith et al. (1978) studied "commercial hematite ore pellets" to form sulfur from the off-gas produced in a metallurgical cupola. When the cupola was operated at reducing conditions, the off-gas contained the components shown in Table 3.

Table 3. Cupola Off-Gas Composition—Inlet Gas for Claus Reactor (Smith et al., 1978)

Component	Concentration, %
CO	0.9-1.9 %
H_2	(not measured)
CO_2	1.1-1.5 %
H_2O	0.47-2.26 %
H_2S	128-227 ppm
SO_2	77-339 ppm
N_2	(not measured)

The values reported in Table 3 span the range of concentrations reported for a series of six tests. The oxygen content was not reported, though presumably it was negligible when the cupola was operated at reducing conditions.

Interestingly, separate lab tests on the iron pellets showed that the pellets alone had no Claus activity, which means that the active catalyst was not the iron. Further analysis showed that traces of "silicates and halides of Mg, Al, Mn, Fe, Ca, and Na" had deposited on the pellets during the tests, which changed the pellets' composition and catalytic activity. Unfortunately, the exact composition of these apparently effective Claus catalysts is not further described, making it impossible to duplicate them. However, these results suggest that "silicates and halides" of these metals may be active low-temperature Claus catalysts. Unfortunately, no further information is given that would enable candidate catalysts to be suggested.

Finally, a series of papers show that sepiolite, a naturally occurring magnesium silicate ($Si_{12}Mg_8O_{30}$ $(OH)_4 \cdot 8H_2O$), and faujasite are active low temperature Claus catalysts, but no studies were carried out in the presence of CO or H_2 (Alvarez et al., 1996; Guijarro et al., 1995; Alvarez et al., 1993). Only one test of faujasite is reported, but in a direct comparison to two sepiolites and -alumina, it maintained a slightly higher level of conversion (see Figure 3).

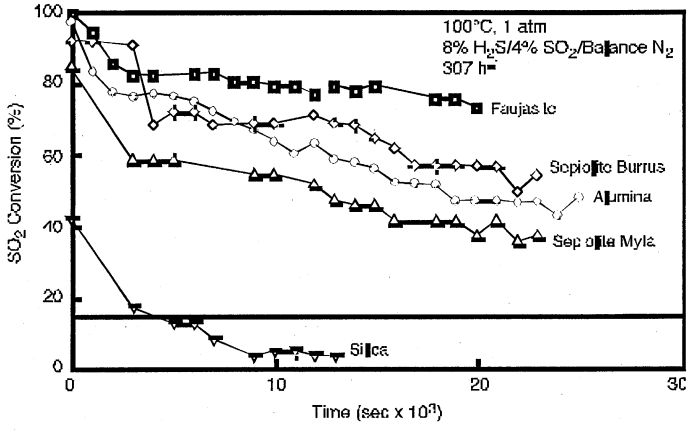

Figure 3. SO_2 conversion in the Claus reactions as a function of time for various heterogeneous catalysts (Alvarez et al., 1993)

Much more extensive tests on sepiolites were carried out using 0.4 to 8 percent H_2S and near-stoichiometric amounts of SO_2 (in nitrogen) at temperatures between 70°C and 200°C, which spans the ~120°C melting point of sulfur. Deactivation tests at 100°C show that sulfur accumulates primarily in the micropores of the catalyst, as expected, leading to steady deactivation. However, the authors show that the deactivation is less rapid than would be expected because of the loss of surface area to deposited sulfur, leading them to conclude that the "...sulfur formed ...is solely responsible for the catalysis [of the Claus reaction]." Even if this conclusion is questionable, this experimental result is significant, because it suggests that a heterogeneous catalyst can remain relatively active despite the inevitable accumulation of sulfur. This could be even more important at temperatures above the melting point of sulfur, because liquid sulfur may be more catalytically active than solid sulfur. Finally, despite the uncertain effect of CO and H_2 on conventional alumina catalysts used for the Claus process, these materials with some modifications should be considered candidates for further study.

These modifications include the addition of metals that have been shown to be active for the selective oxidation of H_2S to elemental sulfur in the presence of syngas or hydrocarbons. Although it is uncertain whether these catalysts would also promote the Claus reaction in the presence of these compounds, the milder oxidation potential of SO_2 (versus oxygen) suggests that they be evaluated.

Several studies show that vanadium may be such a candidate [Haas, 1979; Li and Shyn, 1997]. Using a gas containing 6,600 to 12,000 ppm sulfur in various mixtures of hydrogen (up to 12 percent), CO (<1 percent), and methane (up to 80 percent), Haas (1979) showed that a 10 percent V_2O_5/alumina catalyst selectivity oxidized H_2S to sulfur at temperatures between 315□C and 482□C. Although these are higher temperatures than those of interest here, the selective formation of sulfur in the presence of high levels of hydrogen suggests that these catalysts be tested. Tests on a vanadium/mordenite catalyst showed similar results to those on vanadium/alumina, but with slightly higher H_2S conversion at temperatures near 260°C, and more tolerance of HN_3, which may be important in coal gas applications. [Though not carried out in the presence of CO, H_2, or hydrocarbons, Li and Shyn (1997) show that bulk vanadium/antimony catalysts are active for H_2S oxidation to sulfur at 250°C, approximately the temperatures of interest here.]

Supported Liquid Phase Catalysts. In addition to the conventional heterogeneous catalysts considered above, a more exploratory class of catalysts can be envisioned. These are catalysts in which the active component from homogeneous Claus catalysts is supported on a solid material. Despite extensive study on the general concept of supporting homogeneous catalysts on solid supports, few reports are available in which a commercially practical catalyst of this type has been developed. We are aware of no reports in which a Claus catalyst has been prepared and tested at conditions of interest here.

The general problem in supporting homogeneous catalysts has been that the catalysts are easily leached from the support, lose their high activity or selectivity when supported on solid carriers, or decompose at the higher temperatures needed to operate at industrially practical reaction rates. Nevertheless, Rossarie and Maurie (1978a) show that various salts of weak acids are active homogeneous Claus catalysts (e.g., potassium and sodium benzoate). We suggest preparing and testing two exploratory solid catalysts composed of these two salts on non-acidic alumina supports that are comparable to those used for commercial Claus catalysis but do not contain added alkalis (other than those in the salt).

Summary. Five heterogeneous catalysts, including a commercial alumina as baseline catalyst, are recommended for study of the low-temperature Claus reaction, as shown in Table 4.

However, specific materials and preparation procedures need to be further defined. For the first three catalysts shown in Table 4, preference will be given to testing existing commercial materials that have known properties and that can be readily obtained for any scale-up that may be needed.

Table 4. Heterogeneous Catalysts Recommended for Low-Temperature Claus Reaction

Catalyst	Rationale
Sepiolite	has low temperature Claus activity, but the effect of CO and H_2 at the levels of interest here is not known.
Faujasite	has slightly higher reported activity than sepiolite and is not likely to be affected by CO and H_2.
commercial alumina Claus catalysts	active for the reaction, but like the sepiolite, the effect of CO and H_2 at the levels of interest here is not known.
sodium and potassium benzoate on alumina	active low-temperature homogeneous Claus catalysts, and alumina supports are tolerant of the required reaction conditions
vanadium/ alumina	vanadium selectivity oxidizes H_2S to sulfur in the presence of CO and H_2, and aluminas are active for the Claus reaction

Section 2—Liquid Phase Absorption/ Reaction

Despite the desirability of a gas phase catalytic process, the low concentrations of H_2S and SO_2 in the coal gas, coupled with the need for high conversions to meet environmental requirements, suggest that these reactants may have to be separated from the coal gas as absorbed liquids and reacted in a separate step. Several reports show the feasibility of such processes, which are especially applicable to the low temperatures of interest here, because the absorbent can be easily maintained as a liquid.

There are many variations on these processes in the literature, but we have focused on two processes that exemplify the two principle approaches to the liquid phase route of interest here: homogeneous catalysis of the Claus reaction and liquid phase stoichiometric reaction of H_2S and SO_2 to produce sulfur. Both processes can be represented as shown in Figure 4.

In both processes, H_2S is contacted with a liquid absorbent that contains SO_2, which appears in most cases to enhance the absorption of H_2S. Sulfur is formed in the liquid phase and separated from the absorbent, with a portion of it being recovered as product and a portion being sent to a burner to produce SO_2.

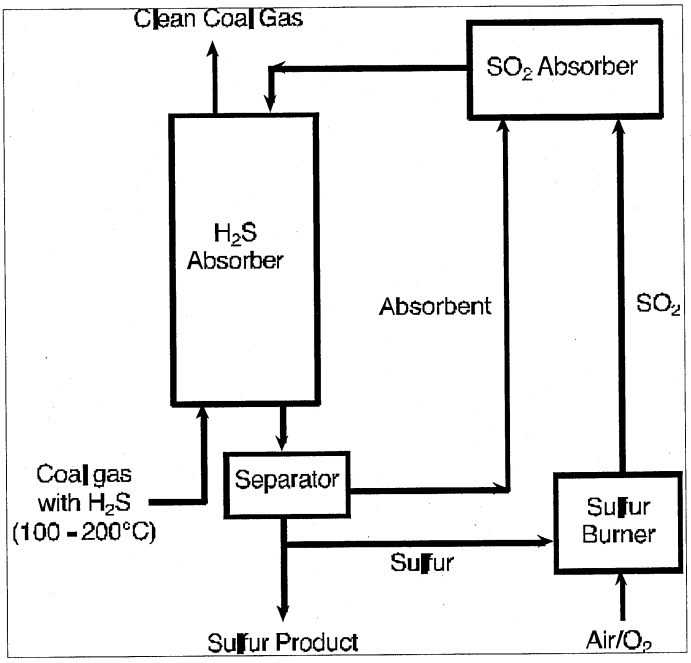

Figure 4. Liquid phase processes for sulfur recovery.

The liquid absorbent is recycled to an absorber in which SO_2 is recovered. In the homogeneous catalytic process, this liquid also contains a catalyst. In the case of a stoichiometric reaction, the liquid reacts with the two gases in a self-regenerating cycle, such as the following (Sherif et al., 1975):

$$NaHSO_4 + SO_2 + H_2O \rightarrow NaHSO_3 + NaH_2PO_4 \quad (1)$$

$$NaHSO_3 + 2H_2S + NaH_2PO_4 \rightarrow Na_2HPO_4 + 3S + 3H_2O \quad (2)$$

$$2H_2S + SO_2 \rightarrow 3S + 2H_2O \quad (3)$$

In a number of references, the distinction between processes that are in fact catalytic and those that involve a stoichiometric reaction is unclear. This is because in some cases the catalyst is not identified. The situation is further complicated by the fact that the water produced in the reaction can serve as the catalyst (German Patent 2,001,284). In summarizing the literature below, we have focused on those studies in which sufficient information is given to provide guidance on candidate processes, as well as catalysts and absorbent liquids, that are applicable to the conditions of interest here—especially the presence of CO and H_2.

Homogeneous Catalysis of the Claus Reaction. Rossarie and Maurie (1978a) describe such a process in which H_2S is absorbed from a gas stream containing 65 percent H_2, 31 percent CO_2, 3.4 percent CO, and 0.7 percent H_2S into a solution containing SO_2 flowing countercurrently. The reaction was carried out at 55 atm and 115°C. The liquid is "diethylene glycol monomethyl ether or monomethyl ether" and 0.5 percent potassium benzoate and is used as the homogeneous catalyst. Sulfur yield was 99+ percent in the two examples given. Other homogeneous catalysts that are claimed include "...salts of weak acids such as sodium benzoate, or nitrogen compounds such as amines." This example provides an absorbent/catalyst system that functions in the presence of significant concentrations of CO and H_2, though these compounds were not present at concentrations typical of coal gas.

Liquid Phase Stoichiometric Reaction. Sherif et al. (1975) describe a process involving the absorption of H_2S from the coal gas into a liquid, forming sulfur in the liquid phase, and recovering sulfur from the resulting mixture. SO_2 is absorbed in an aqueous alkali metal phosphate. An example of the reaction sequence is show in Reactions (1) through (3). The process is claimed to operate best around 66°C to 77°C and is designed primarily for flue gas desulfurization. Optimum concentrations of SO_2 are below 15 percent.

Candidate Liquid Absorbents. Many of the studies for both the catalytic process and the liquid phase stoichiometric process use liquids that are similar or identical to those used in conventional acid gas removal processes, for example, the "amines" claimed by Rossarie and Maurie (1978). This has led us to review the potential use of various liquids as candidates for the absorbent needed by both processes considered here.

There are a wide range of alkanolamines and other absorbents for removal of H_2S from a range of gas streams, primarily natural gas. The most widely used absorbents are monoethanol amine, diethanol amine, and mixtures of various glycols (Kohl and Nielsen, 1997a). Although we did not identify literature discussing the specific effects of high levels of CO and H_2 on the absorption of H_2S in these amines, we would expect that H_2S absorption would not be significantly affected. These amines would be expected to absorb SO_2, but no literature was identified showing this, although closely related aromatic amines are used to remove dilute levels of SO_2

(Kohl and Nielsen, 1997b). Additional selective absorbents for SO_2 include various glycol ethers (Kohl and Nielsen, 1997c). Additional absorbents reported for H_2S include alkali phosphates and carbonates (German Patent 2,001,284; U.S. Patent 2,368,595) and aluminum sulfate/sulfuric acid (U.S. Patent 2,563,437).

For the purpose of this review, the candidate absorbents include those shown in Table 5, which have been reported for absorption of H_2S, SO_2, or both. For those that have been reported only for H_2S or SO_2 absorption, a cursory examination of their chemical properties does not appear to preclude their being used in the process of Figure 4.

Table 5. Candidate Liquid Absorbents

Absorbents for H_2S		**Absorbents for SO_2**		**Absorbents for H_2S and SO_2**	
Absorbent	Reference	Absorbent	Reference	Absorbent	Reference
alkanolamines (MEA, DEA, etc.)	Kohl and Nielsen, 1997a	$Al_2(SO_4)_3$/ sulfuric acid	U.S. Patent 2,563,437	"aqueous citrate"	George et al., 1969
alkali carbonates (K_2CO_3)	German Patent 2,001,284	tetraethylene glycol dimethyl ether	Kohl and Nielsen, 1997c	K_3PO_4	German Patent 2,001,284; U.S. Patent 2,368,595
		monobasic phosphates and sodium citrate	U.S. Patent 2,031,802; U.S. Patent 2,729,543		

Section 3—Liquid Phase Claus Catalyst Supported on a Solid

A third class of materials considered here are solids composed of a microporous material in which a liquid phase catalyst or liquid absorbent/reactant is retained (as a liquid) in the micropores. This has the advantage of concentrating the H_2S and SO_2 reactants from the gas phase. The overall process would be carried out as shown in Figure 2. As in Figure 2, the sulfur may, in principle, be collected as a liquid downstream of the reactor. However, it is also possible that as sulfur accumulates in the pores, the activity will decrease and periodic regeneration would be needed.

In this type of catalyst, the support does not need to be catalytically active, but should have a high microporosity and be tolerant of sulfur, H_2S, SO_2, and coal gas components at the temperatures of interest. All else being equal, the smaller the pores, the lower the vapor pressure of the liquid (due to the Kelvin effect), and the less the loss of liquid due to the inevitable process of vaporization.

Candidate support materials include activated carbon, high surface area silica, and perhaps alumina (though its inherent acidity may limit the rates of reaction or cause it to react with H_2S or SO_2). Liquids include those discussed above in Section 2—both homogeneous liquid phase catalysts and liquid phase absorbent/reactants (see Table 6).

Table 6. Candidate Supported Liquids for the Claus Reaction*

Liquid	Rationale	Support	Rationale
"diethylene glycol monomethyl ether or monomethyl ether" and 0.5% potassium benzoate	reported homogeneous Claus catalyst (Rossarie and Maurie, 1978a)	activated carbon	high microporosity and tolerance to sulfur and coal gas
aqueous alkali metal phosphate	reported liquid phase absorbent/reactant (Sherif et al., 1975)	high surface area silica	

* Note that either of the candidate liquids could be used with either of the supports, making a total of four candidate materials

References

Alvarez, E., S Mendioroz, V. Munoz, J.M. Palacios, Appl. Catal.B, 9, 1996, 179-199.
Alvarez, E., S Mendioroz, J.M. Palacios, Appl. Catal. A, 93, 1993, 231-244.
George,....., et al., presented at the Mining Society, AIME Fall Meeting, Salt Lake City, UT, Sept. 17-19, 1969.
German Patent 2,001,284
Guijarro, M.I., S. Mendioroz, V. Munoz, Appl. Catal. A, 132, 1995, 335-351.
Haas, R.H., U.S. Patent 4,171,347, Oct. 16, 1979.
Kohl, A.L. and R. Nielsen, Gas Purification, Gulf Publishing, Houston, TX, 1997, (a) p. 40-186, (b) p.590-593, (c) p. 602.
Li and Shyn.
Pearson, M.J., Energy Processing/Canada, July-August 1976, 38-42.
Rossarie, J. and J. Maurin, US Patent 4,107,269, Aug. 15, 1978, (a) Example 2, (b) Example 1.
Sherif, F.G., J.S. Hayford, J.E. Blanch, US Patent 3,911,093, Oct. 7, 1975.
Smith, J.W., C. Knight, W.H. Powlesland, P.H.I. Harper, "Dry Desulfurization of Industrial Process Gases by Low Temperature Catalytic Oxidation", in Treatment of Coke Oven Gas, Dept. of Metallurgy and Material Science, McMaster University, Ontario, Canada, 1978, 14-1 to 14-16.
U.S. Patent 2,563,437
U.S. Patent 2,368,595

APPENDIX H Single-step Sulfur Recovery Process (SSRP): Proceedings of the 19th Annual International Pittsburgh Coal Conference, Sept. 2002

Single-step Sulfur Recovery Process (SSRP)

Apostolos A. Nikolopoulos and Santosh K. Gangwal

Center for Energy Technology, RTI International
3040 Cornwallis Road, Research Triangle Park, NC 27709-2194
Tel: (919) 990-8406, (919) 541-8030; Fax: (919) 541-8000; E-mail: nik@rti.org, skg@rti.org

The direct catalytic oxidation of H_2S in the presence of great excess (> 60%) H_2 and CO was examined on a commercial alumina catalyst at 125-160°C and 200-350psig. Total sulfur (H_2S + SO_2) conversions of 98.5% or higher were achieved, with the undesirable formation of carbonyl sulfide limited to below 40ppm. SO_2 is much more selective than oxygen for the catalytic oxidation of H_2S to high-purity sulfur by the Single-step Sulfur Recovery Process (SSRP).

INTRODUCTION

Gasification of heavy feeds (e.g., coal, pet coke, resid, biomass) produces a raw fuel gas that requires cleaning before its use to produce electricity and/or synthetic liquid fuels (e.g., using Fischer-Tropsch synthesis). The current commercial process for gas cleaning involves quenching the gas to remove particulates and trace contaminants. Then, a complex multi-step amine-based process to remove hydrogen sulfide (H_2S) follows. The fuel gas is first contacted by an amine solution using a gas-liquid scrubber. The spent amine is then regenerated using steam and the regeneration off-gas containing H_2S is sent to a Claus plant. An H_2S burner oxidizes 1/3 of H_2S to SO_2, which then reacts with the remaining H_2S to form sulfur:

$$\mathbf{2\ H_2S + SO_2 \rightarrow 3/n\ S_n + 2\ H_2O} \qquad \text{(Claus reaction)}$$

The Claus reaction uses a series of up to three catalytic reactors, and yet its tail gas still contains about 2% of the inlet H_2S – SO_2 mixture, which is then sent to a tail gas treatment plant. To reduce the numerous steps in conventional sulfur removal and recovery processes, RTI with DOE/NETL funding is developing the **Single-step Sulfur Recovery Process (SSRP)**. The SSRP consists of injecting SO_2 directly into the quenched fuel gas to oxidize H_2S selectively on a suitable catalyst to both remove and recover sulfur in a single step. The key differences between SSRP and the traditional Claus process are: a) in SSRP the catalytic oxidation of H_2S by SO_2 (Claus reaction) occurs selectively in a highly reducing atmosphere containing the highly reactive H_2 and CO fuel gas components, and b) the reaction is carried out at the pressure of the fuel gas (300-1200 psig). The temperature of the SSRP reactor is within 125°C (257°F, where sulfur liquefies) and 160°C (320°F, where liquid sulfur viscosity starts to increase rapidly). The SSRP uses a catalyst that is highly selective for the oxidation of H_2S as opposed to the undesirable oxidation of H_2 and CO that are present in great excess in the fuel gas (ca. 60vol% vs. less than 1vol% H_2S).

A review of the literature did not identify any studies in which the Claus reaction was carried out in the presence of large concentrations of CO and H_2. Pearson (1976) studied the Claus reaction at temperatures between 135°C and 175°C using a Claus tail gas containing ca. 3vol% CO+H_2. Conversion of H_2S+SO_2 was 96 to 98% until his active alumina catalyst reached 60% sulfur loading in the pores. The conversion then declined rapidly to 31%.

The scope of this work is to determine the feasibility of the SSRP for the selective catalytic oxidation of H_2S in the presence of excess amounts (> 30vol%) of highly reactive gases such as H_2 and CO. Also, it is to evaluate the performance of commercial catalysts to selectively remove and recover high-purity sulfur under commercially applicable process conditions.

EXPERIMENTAL

The SSRP reaction was studied in a 0.5-inch fixed-bed micro-reactor at 125-160°C (257-320°F) and 200-350 psig, over a commercial high-surface-area (227m^2/g) alumina catalyst. The stainless steel reactor was coated with silica to minimize reactions on its walls. The reactant feed consisted of a simulated Texaco coal gas stream containing 50.8% CO, 35.7% H_2, 12.5% CO_2, and 1.0% H_2S, and a 2.5% SO_2/N_2 stream. A syringe pump provided a constant flow of steam (through water evaporation) into the coal gas line. A typical reaction composition included ca. 8400ppm H_2S, ca. 4200ppm SO_2, 10% steam, and a balance of simulated Texaco gasifier gas (N_2, CO_2, H_2, and CO). The steam condensed into a condensation pot past the reactor outlet. A back-pressure-control valve, located downstream of the condenser, controlled the reactor and condenser pressure. The outlet gases were analyzed in a gas chromatograph with a thermal conductivity detector (TCD) and a flame photometric detector (FPD), for high (above 500ppm) and low (down to single-digit ppm) sulfur-gas concentrations, respectively. A schematic of the SSRP reaction system is shown in Figure 1.

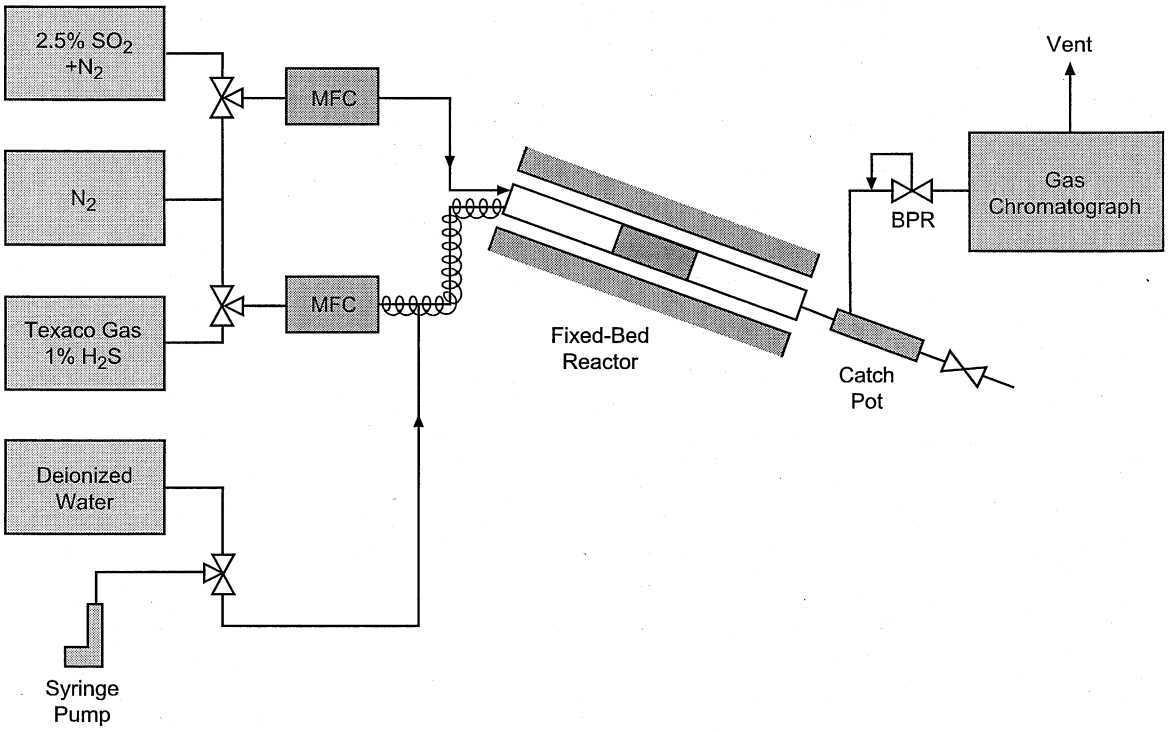

Figure 1. Schematic of the SSRP reaction system

RESULTS AND DISCUSSION

The SSRP reaction experiments were conducted by loading the silica-coated reactor with 5 cm^3 of alumina catalyst, then heating to 154°C (309°F) and pressurizing to 200psig (14.4 bar) under an inert gas flow of 100sccm. 15sccm SO_2/N_2 (corresponding to ca. 3800ppm SO_2) were fed into the reactor, followed by feeding 10sccm steam, substituting an equal flow of N_2. Upon reaching a pseudo steady state, simulated coal gas with H_2S was fed into the reactor (giving ca. 8400ppm H_2S), at a constant total feed flow of 100sccm. The total sulfur (H_2S+SO_2) conversion was 86.5%, with less than 20ppm COS (carbonyl sulfide) formation.

The effect varying the inlet SO_2 concentration was examined by increasing the SO_2/N_2 flow from 15 to 18 to 20sccm while keeping the coal gas and steam flows constant, thus increasing the total flow from 100 to 103 to 105sccm, respectively. The results are shown in Figure 2. Upon increasing the SO_2 inlet concentration the conversion of H_2S increased up to 99.5%, while the conversion of SO_2 decreased from essentially 100% down to ca. 87%. Thus the H_2S+SO_2 conversion showed a maximum at an intermediate SO_2 concentration. This implies reaction of SO_2 with H_2S only, and not with H_2 or CO which are in great excess, at least to any appreciable rate. The COS formation was only about 20ppm.

The effect of space velocity was studied by varying the total feed flow from 100sccm to 500sccm while keeping the other reaction parameters (temperature, pressure, feed composition) constant. A fivefold increase in space velocity resulted in only a minor decrease (from 98.5% to 96%) in H_2S+SO_2 conversion (Figure 3). The formation of COS was again only about 20ppm. Thus the SSRP reaction is very active and selective even at significantly small contact times.

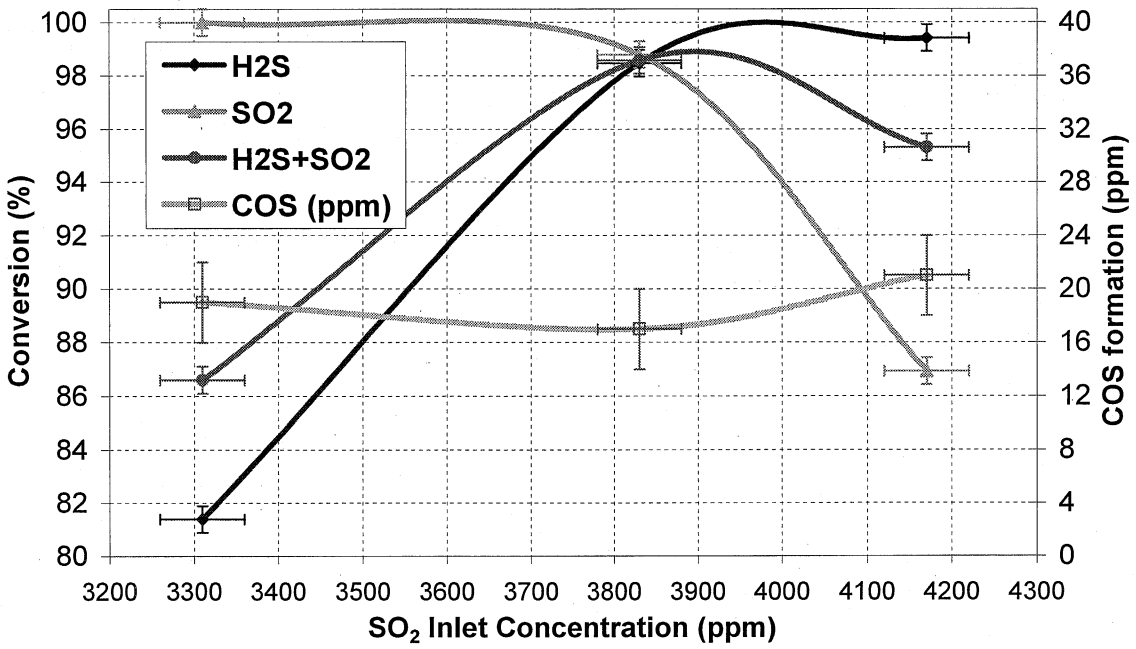

Figure 2. Effect of SO_2 inlet concentration on H_2S, SO_2, and H_2S+SO_2 conversion, and COS formation, for SSRP on alumina; T: 154°C, P: 200psig; SV: 1200 (1230) (1260) h^{-1}; H_2S: 8400-8000ppm; steam: 10%

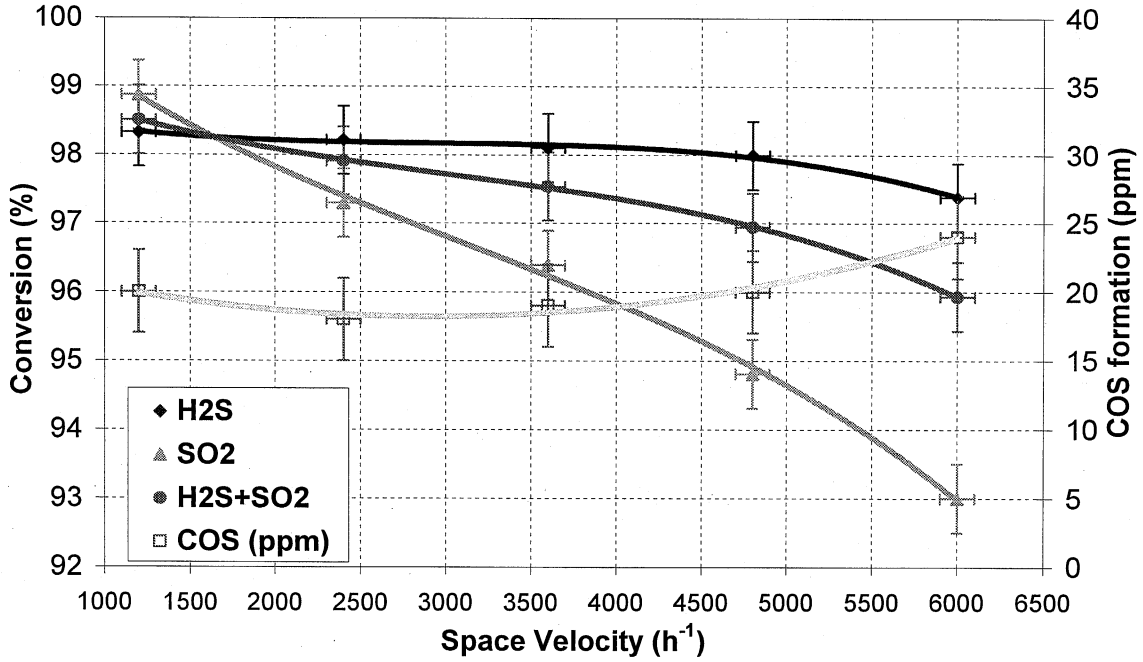

Figure 3. Effect of space velocity on H_2S, SO_2, and H_2S+SO_2 conversion, and COS formation, for SSRP on alumina; T: 154°C, P: 200psig; H_2S: 8400pm; SO_2: 4200ppm; steam: 10%

The effect of pressure was examined by increasing the reaction pressure from 200psig (12.4 bar) to 350psig (25.8 bar) at a total feed flow of 300sccm while keeping the other reaction parameters (temperature, feed composition) constant. The results are given in Table 1. The combined H_2S+SO_2 conversion was found to increase up to 99.0%. Higher pressures favor the reaction in terms of thermodynamic equilibrium, so they would be expected to further increase the measured conversion. The amount of formed COS was below 40ppm.

Table 1. Effect of pressure on H_2S, SO_2, and H_2S+SO_2 conversion, and COS formation, for SSRP on alumina; T: 154°C, H_2S: 8400ppm; SO_2: 4200ppm; steam: 10%

	Conversion (%)			COS formation
Pressure (psig)	H_2S	SO_2	H_2S+SO_2	(ppmv)
200	98.9	97.3	98.4	34
240	98.9	98.4	98.7	34
300	99.0	99.0	99.0	36
350	98.8	99.3	99.0	38

The effect of catalytically oxidizing H_2S in the presence of excess H_2 and CO by an oxidant other than SO_2 (such as O_2) was also examined on alumina at 154°C, 200psig, and a total flow of 100sccm. After addition of 10% steam for 30min, $2\%O_2/N_2$ was fed into the reactor,

producing ca. 4300ppm O_2 in the feed, at a total flow of 105sccm. Then, coal gas was fed to get a ratio of H_2S/O_2 of ca. 2 and the reaction reached a pseudo steady state. Finally, the O_2 flow was substituted by a flow of SO_2 producing ca. 4300ppm of SO_2 in the feed (H_2S/SO_2 ratio of ca. 2) and the reaction reached a new pseudo steady state.

The results for the effect of O_2 vs. SO_2 in the feed are given in Figure 4. Oxygen is much less selective for the oxidation of H_2S compared to SO_2 and also allows for enhanced undesirable formation of COS. There appears to be a clear unselective consumption of O_2 by the H_2 and/or CO of the coal gas, thus limiting its availability for the desirable selective reaction with H_2S.

The sulfur that was generated on the catalyst during the SSRP was retained within the catalyst pores (the collected water condensate was clear). Normally in low temperature fixed-bed Claus-type processes, the catalyst is reversibly poisoned by the sulfur plugging its pores, as shown by Pearson (1975). The catalyst would have to be heated to high temperatures to remove the sulfur.

A commercial embodiment of the SSRP involving a liquid phase of molten sulfur with dispersed catalyst in a slurry bubble column reactor (SBCR) is currently under development (Gangwal et al, 2002). A schematic of this embodiment is given in Figure 5. The sulfur that is generated during the SSRP dissolves into the molten sulfur, in analogy to the wax formed and removed by the liquid wax medium in a slurry-bubble column Fischer-Tropsch reactor. Therefore, recovery of the product sulfur as well as a shift in thermodynamic equilibrium limitations on sulfur formation can be accomplished.

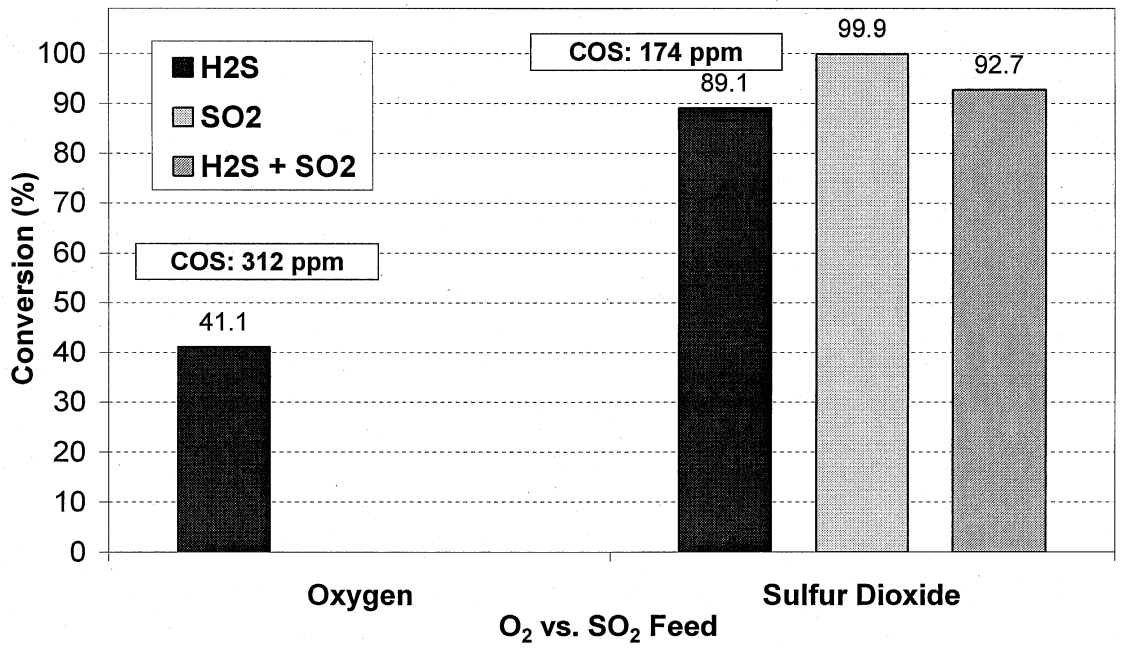

Figure 4. Effect of O_2 vs. SO_2 feed on H_2S, SO_2, and H_2S+SO_2 conversion, and COS formation, for SSRP on alumina; T: 125°C, P: 200psig; H_2S: 8400pm; O_2 (SO_2): 4300ppm; steam: 10%

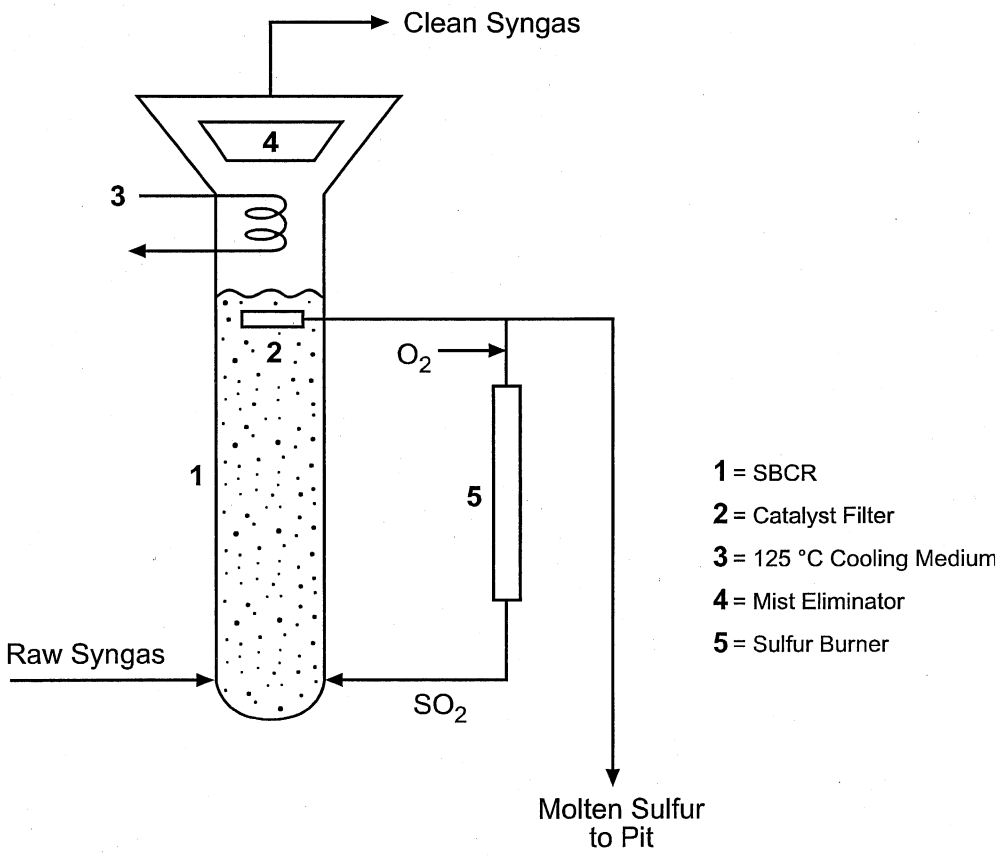

Figure 5. Proposed commercial embodiment of the Single-step Sulfur Recovery Process (SSRP)

CONCLUSIONS

The results of this work have clearly demonstrated that the direct catalytic oxidation of H_2S by SO_2 can be successfully performed even in the presence of great excess of highly reactive reducing species such as H_2 and CO. The combined H_2S+SO_2 conversion on an alumina catalyst is 98.5% at 154°C and 200psig and further increases with increasing pressure (99% at 300psig), being limited only by thermodynamic equilibrium from attaining 100%. Furthermore, higher pressures would shift the equilibrium limitations towards higher conversion, thus the SSRP is favored by using high-pressure fuel gas (300-1200psig). SO_2 is a much more selective oxidant compared to oxygen for selectively oxidizing H_2S in the presence of excess H_2 and CO. Under the examined experimental conditions, the undesirable formation of COS was limited to 40ppm or lower.

REFERENCES

Gangwal, S.K., Nikolopoulos, A.A., and Dorchak, T.P., "Method of Removing and Recovering Elemental Sulfur from Highly Reducing Gas Streams Containing Sulfur Gases", US Patent applied for, July 2002.

Pearson, M.J., "Catalyst Performance in Low-Temperature Claus Process", Energy Processing/ Canada, July-August 1976, 38-42.

APPENDIX I SSRP Micro-Reactor Processed Data

Norton Alumina

NAL01 **W+G+S** **D'**

In (ppm): 9200 4350

F (cc/min)	P (psig)	H2S (ppm)	SO2 (ppm)	X(H2S)%	X(SO2)%	Error-Y
101	70	5850	2650	36.4	39.1	1
101	50	6450	2950	29.9	32.2	1

NAL02 **W+G+S** **D'**

In (ppm): 9100 4000

F (cc/min)	P (psig)	H2S (ppm)	SO2 (ppm)	X(H2S)%	X(SO2)%	Error-Y
100	80	5350	2150	41.2	46.3	1
150	80	6475	2600	28.8	35.0	1
100	70	5750	2400	36.8	40.0	1
50	70	2000	800	78.0	80.0	3

NAL06

H2S in:	9100
SO2 in:	4000
F (cc/min)	100
G+W+S	**C'**

NAL03 **G+W+S** **C'**

In (ppm): 9000 3900

F (cc/min)	P (psig)	H2S (ppm)	SO2 (ppm)	X(H2S)%	X(SO2)%	Error-Y
100	60	6000	2400	33.3	38.5	1
100	90	4800	1900	46.7	51.3	1
100	105	4100	1500	54.4	61.5	2

NAL04 **S+W+G** **C** **W+S+G** **D** **NAL05**

P (psig): 95

H2S in (ppm)	SO2 in (ppm)	H2S (ppm)	SO2 (ppm)	X(H2S)%	X(SO2)%	Error-Y	X(tot)%	COS
9000	3900	4650	1750	48.3	55.1	1	50.4	70
8900	4400	4400	2200	50.6	50.0	1	50.4	65
8700	4850	3950	2500	54.6	48.5	3	52.4	80
8550	5200	3850	2850	55.0	45.2	3	51.3	110

NAL04 **NAL05**

P (psig): 95

H2S in (ppm)	SO2 in (ppm)	H2S (ppm)	SO2 (ppm)	DH2S/2	Delta SO2	Error-Y
9000	3900	4650	1750	2175.0	2150.0	100
8900	4400	4400	2200	2250.0	2200.0	100
8700	4850	3950	2500	2375.0	2350.0	100
8550	5200	3850	2850	2350.0	2350.0	100

F (cc/min)	SV (h-1)	P (psig)	H2S (ppm)	SO2 (ppm)	X(H2S)%	X(SO2)%	Error-Y
50	600	70	2000	800	78.0	80.0	3
100	1200	75	5650	2400	38.1	41.8	3
150	1800	80	6475	2600	28.8	35.0	1

F (cc/min)	P (psig)	H2S (ppm)	SO2 (ppm)	X(H2S)%	X(SO2)%	Error-Y
101	50	6450	2950	29.9	32.2	1
100	60	6000	2350	33.3	38.5	1
100	70	5800	2525	36.6	40.0	1
100	80	5350	2150	41.2	46.3	1
100	90	4800	1900	46.7	51.3	1
100	105	4100	1500	54.4	61.5	2

E-alumina

EAL02 125°C

H2S in (ppm)	SO2 in (ppm)	P (psig): H2S (ppm)	200 SO2 (ppm)	D(H2S)/2	D(SO2)	Error-Y
9350	3400	2300	0	3525	3400	100
9100	3900	500	50	4300	3850	100
8900	4400	150	550	4375	3850	100
8700	4850	100	950	4300	3900	100
8550	5200	0	1650	4275	3550	100

EAL04 125°C

H2S in (ppm)	SO2 in (ppm)	P (psig): H2S (ppm)	200 SO2 (ppm)	P (psig): X(H2S)%	300 X(SO2)%	Error-Y	X(tot)%
9300	3900	90	550	99.0	85.9	0.2	95.2
9200	4200	100	350	98.9	91.7	0.2	96.6
9100	4500	180	150	98.0	96.7	0.2	97.6
9100	4500	150	25	98.4	99.4	0.2	98.7

125°C P (psig)	H2S (ppm)	SO2 (ppm)	X(H2S)%	X(SO2)%	Error-Y	X(tot)%
200	190	150	97.9	96.7	0.5	97.5
250						
300	150	25	98.4	99.4	0.5	98.7

EAL05 125°C 139°C

H2S in (ppm)	SO2 in (ppm)	P (psig): H2S (ppm)	300 SO2 (ppm)	X(H2S)%	X(SO2)%	Error-Y	X(tot)%
9100	4500	200	150	97.8	96.7	0.2	97.4
9100	4500	300	100	96.7	97.8	0.2	97.1

EAL06 139°C

F (cc/min)	In (ppm): P (psig)	9100 H2S (ppm)	4500 SO2 (ppm)	X(H2S)%	X(SO2)%	Error-Y	X(tot)%
86	200	650	0	92.9	100.0	0.2	95.2
86	250	550	0	94.0	100.0	0.2	96.0
86	300	400	0	95.6	100.0	0.2	97.1

139°C P (psig)	H2S (ppm)	SO2 (ppm)	X(H2S)%	X(SO2)%	Error-Y	X(tot)%
200	650	0	92.9	100.0	0.5	95.2
250	550	0	94.0	100.0	0.5	96.0
300	350	50	96.2	98.9	1	97.1

Blank (no catalyst)

BLN01	156°C	**High W**	**22.5%**		**W+G+S**	**D'**		
	In (ppm):	9300	4500					
F (sccm)	P (psig)	H2S (ppm)	SO2 (ppm)	X(H2S)%	X(SO2)%	Error-Y	X(tot)%	COS(ppm)
100	200	2800	1100	69.9	75.6	1	71.7	350
100	250	1950	800	79.0	82.2	1	80.1	450
100	300	1500	550	83.9	87.8	1	85.1	550

BLN01	86sccm	**Low W**	**10%**		**W+G+S**	**D'**		
	In (ppm):	9300	4500					
P (psig)	T (°C)	H2S (ppm)	SO2 (ppm)	X(H2S)%	X(SO2)%	Error-Y	X(tot)%	COS(ppm)
300	156	1650	700	82.3	84.4	1	83.0	550
300	140	1450	700	84.4	84.4	1	84.4	300
300	125	1050	700	88.7	84.4	1	87.3	200

BLN02	86sccm	**Low W**	**10%**		**S+W+G**	**C**		
	In (ppm):	9300	4500					
P (psig)	T (°C)	H2S (ppm)	SO2 (ppm)	X(H2S)%	X(SO2)%	Error-Y	X(tot)%	COS(ppm)
200	125	2490	1190	73.2	73.6	1	73.3	130
250	125	1700	870	81.7	80.7	1	81.4	500
300	125	1360	780	85.4	82.7	1	84.5	600
300	140	1395	735	85.0	83.7	2	84.6	730

BLN03	200psig	77/86sccm	**S+G**	**A**	**S+G+W**	**B**	**Low W**	**10%**	
	In (ppm):	9300	4500		9300	4500			
Parameter	T (°C)	H2S (ppm)	SO2 (ppm)	X(H2S)%	X(SO2)%	Error-Y	X(tot)%	COS(ppm)	**H2O**
-W -H	125	7625	3675	18.0	18.3	1	18.1	50	0%
-H2O	125	5100	2330	45.2	48.2	1	46.2	100	**0%**
+H2O	125	2800	1380	69.9	69.3	1	69.7	1300	**10%**

BLN04	200psig	86sccm	**W+O+G**	**O**	**W+G+S**	**D'**	**Low W**	**10%**
	In (ppm):	9500	4500					
Parameter	T (°C)	H2S (ppm)	SO2 (ppm)	X(H2S)%	X(SO2)%	Error-Y	X(tot)%	COS(ppm)
Oxygen	140	6050	0	37.1		1		150
Sulfur Dioxide	140	3400	920	63.4	79.6	1	68.7	240

E-alumina

EAL03 **200 psig** **154°C** **10% W**

F(SO2)	In (ppm):	8500							
(cc/min)	SO2 (ppm)	H2S (ppm)	SO2 (ppm)	X(H2S)%	X(SO2)%	Error-Y	X(tot)%	COS (ppm)	H2O
15	3310	1582	0	81.4	100.0	0.5	86.6	19	10%
18	3830	130	46	98.5	98.8	0.5	98.6	17	10%
20	4170	50	545	99.4	86.9	0.5	95.3	21	10%

EAL04 **200 psig** **154°C** **10% W**

	In (ppm):	8965	4430						
F (sccm)	SV (h-1)	H2S (ppm)	SO2 (ppm)	X(H2S)%	X(SO2)%	Error-Y	X(tot)%	COS (ppm)	H2O
100	1200	150	50	98.3	98.9	0.5	98.5	20	10%
200	2400	160	120	98.2	97.3	0.5	97.9	18	10%
300	3600	170	160	98.1	96.4	0.5	97.5	19	10%
400	4800	180	230	98.0	94.8	0.5	96.9	20	10%
500	6000	235	310	97.4	93.0	0.5	95.9	24	10%

EAL05 **154°C** **10% W**

	In (ppm):	8550	4358						
F (sccm)	P (psig)	H2S (ppm)	SO2 (ppm)	X(H2S)%	X(SO2)%	Error-Y	X(tot)%	COS (ppm)	H2O
300	200	94	116	98.9	97.3	0.5	98.4	34	10%
300	240	98	71	98.9	98.4	0.5	98.7	34	10%
300	300	89	45	99.0	99.0	0.5	99.0	36	10%
300	350	106	30	98.8	99.3	0.5	98.9	38	10%
300	200	104	86	98.8	98.0	0.5	98.5	46	10%

EAL06 **200 psig** **10% W**

	In (ppm):	8550	4275						
F (sccm)	T (°C)	H2S (ppm)	SO2 (ppm)	X(H2S)%	X(SO2)%	Error-Y	X(tot)%	COS (ppm)	H2O
300	154	111	68	98.7	98.4	0.5	98.6	85	10%
300	140	70	113	99.2	97.4	0.5	98.6	45	10%
300	125	90	163	98.9	96.2	0.5	98.0	31	10%
300	154	137	112	98.4	97.4	0.5	98.1	86	10%

EAL09 **200 psig** **154°C** **10% W**

	In (ppm):	8500	4300						
F (sccm)	Oxidizer	H2S (ppm)	SO2 (ppm)	X(H2S)%	X(SO2)%	Error-Y	X(tot)%	COS (ppm)	H2O
100	Oxygen	5009	0	41.1		0.5		312	10%
100	Sulfur Dioxide	928	3	89.1	99.9	0.5	92.7	174	10%

P3-alumina

P3AL01	200 psig	154°C	G+S	A'		G+S+W	B'	
	In (ppm):	8500	4350					
H2O	F (sccm)	H2S (ppm)	SO2 (ppm)	X(H2S)%	X(SO2)%	Error-Y	X(tot)%	COS(ppm)
0%	270	8450	0	0.6	100.0	0.5	34.2	1950
10%	300	6470	0	23.9	100.0	0.5	49.6	5300

P3AL02	200 psig	154°C	W+S+G	D				
	In (ppm):	8500	4350					
H2S	F (sccm)	H2S (ppm)	SO2 (ppm)	X(H2S)%	X(SO2)%	Error-Y	X(tot)%	COS(ppm)
8500	300	750	950	91.2	78.2	0.5	86.8	250
8550	305	890	650	89.6	85.1	0.5	88.0	380

P3AL03	300sccm	154°C	W+S+G	D				
	In (ppm):	8500	4350					
P (psig)	F (sccm)	H2S (ppm)	SO2 (ppm)	X(H2S)%	X(SO2)%	Error-Y	X(tot)%	COS(ppm)
200	300	65	560	99.2	87.1	0.5	95.1	235
290	300	50	230	99.4	94.7	0.5	97.8	310

P3AL04	300sccm	154°C	S+W+G	C				
	In (ppm):	8500	4600					
P (psig)	F (sccm)	H2S (ppm)	SO2 (ppm)	X(H2S)%	X(SO2)%	Error-Y	X(tot)%	COS(ppm)
200	300	40	530	99.5	88.5	0.5	95.6	45
275	300	20	400	99.8	91.3	0.5	96.8	45

200psig	300sccm	154°C	S+W+G	C				
	In (ppm):							
Alumina	F (sccm)	H2S (ppm)	SO2 (ppm)	X(H2S)%	X(SO2)%	Error-Y	X(tot)%	COS(ppm)
P	300			99.5	88.5	0.5	95.6	45
E	300			98.9	97.3	0.5	98.4	34

Sulfided Iron Oxide

FeS01 **200 psig** **154°C** **10% W**

F	In (ppm):		Out(ppm):						
(cc/min)	H2S (ppm)	SO2 (ppm)	H2S (ppm)	SO2 (ppm)	X(H2S)%	X(SO2)%	Error-Y	X(tot)%	COS (ppm)
300	8500	0	4282	0	49.6	#DIV/0!	0.5	49.6	303
300	8500	4300	208	0	97.6	100.0	0.5	98.4	8578
295	8650	4000	352	0	95.9	100.0	0.5	97.2	8868
285	8950	3300	1020	0	88.6	100.0	0.5	91.7	7594
265	9600	1750	3457	0	64.0	100.0	0.5	69.5	4130
265	9600	0	6667	0	30.6	#DIV/0!	0.5	30.6	798

Procedure	SUM In	SUM Out	Delta S	Effic. (%)
W+G	8500	4585	3915	46.1
W+G+S	12800	8786	4014	31.4
W+G+S	12650	9220	3430	27.1
W+G+S	12250	8614	3636	29.7
W+G+S	11350	7587	3763	33.2
W+G	9600	7465	2135	22.2

FeS02 **200 psig** **154°C** **10% W**

F	In (ppm):		Out(ppm):						
(cc/min)	H2S (ppm)	SO2 (ppm)	H2S (ppm)	SO2 (ppm)	X(H2S)%	X(SO2)%	Error-Y	X(tot)%	COS (ppm)
300	8500	0	7099	0	16.5	#DIV/0!	0.5	16.5	706
300	8500	4300	913	0	89.3	100.0	0.5	92.9	13139
310	8250	4900	264	140	96.8	97.1	0.5	96.9	13705
320	7950	5500	158	580	98.0	89.5	0.5	94.5	14190
340	7500	6550	49	1679	99.3	74.4	0.5	87.7	14215
340	0	6550	0	5124	#DIV/0!	21.8	0.5	21.8	13

Procedure	SUM In	SUM Out	Delta S	Effic. (%)
W+G	8500	7805	695	8.2
W+G+S	12800	14052	-1252	-9.8
W+G+S	13150	14109	-959	-7.3
W+G+S	13450	14928	-1478	-11.0
W+G+S	14050	15943	-1893	-13.5
W+S	6550	5137	1413	21.6

(cc/min)	H2S (ppm)	SO2 (ppm)	H2S (ppm)	SO2 (ppm)	X(H2S)%	X(SO2)%	Error-Y	X(tot)%	COS (ppm)
340	7500	6550	49	1679	99.3	74.4	10	87.7	14215
320	7950	5500	158	580	98.0	89.5	10	94.5	14190
310	8250	4900	264	140	96.8	97.1	10	96.9	13705
300	8500	4300	208	0	97.6	100.0	1300	98.4	10858.5
295	8650	4000	352	0	95.9	100.0	10	97.2	8868
285	8950	3300	1020	0	88.6	100.0	10	91.7	7594
265	9600	1750	3457	0	64.0	100.0	10	69.5	4130
265	9600	0	6667	0	30.6		10	30.6	798

Procedure	SUM In	SUM Out	Delta S	Effic. (%)
W+G+S	14050	15943	-1893	-13.5
W+G+S	13450	14928	-1478	-11.0
W+G+S	13150	14109	-959	-7.3
W+G+S	12800	11067	1734	13.5
W+G+S	12650	9220	3430	27.1
W+G+S	12250	8614	3636	29.7
W+G+S	11350	7587	3763	33.2
W+G	9800	7465	2335	23.8

FeS02	200 psig	154°C	10% W						
1750 ppm	9600	**1750**	3457	0	**64.0**	**100.0**	0.5	**69.5**	4130
0 ppm	9600	**0**	6667	0	**30.6**		0.5		798

Procedure	SUM In	SUM Out	Delta S	Effic. (%)
W+G+S	11350	7587	3763	33.2
W+G	9800	7465	2335	23.8

Silica gel

SIL01	300sccm	154°C	10% W	W+G+S	D'				
		In (ppm)		Out (ppm)					
	P (psig)	H2S (ppm)	SO2 (ppm)	H2S (ppm)	SO2 (ppm)	X(H2S)%	X(SO2)%	H2S-2SO2	X(tot)%
W+G	200	8200		7787		5.0		413	5.0
W+G+S	200	8200	4400	736	847	91.0	80.8	358	87.4
W+G+S	250	8200	4400	213	442	97.4	90.0	71	94.8
W+G+S	300	8200	4400	130	351	98.4	92.0	-28	96.2
W+G	300	8200		7603		7.3		597	7.3

COS (ppm)	SUM In	SUM Out	Delta S	Effic. (%)
47	8200	7834	366	4.5
172	12600	1755	10845	86.1
146	12600	801	11799	93.6
159	12600	640	11960	94.9
85	8200	7688	512	6.2

SIL02	200psig	154°C	10% W	W+S+G	D	W+S+O	O	W+G+S	D'
		In (ppm)		Out (ppm)					
		H2S (ppm)	SO2 (ppm)	H2S (ppm)	SO2 (ppm)	X(H2S)%	X(SO2)%	H2S-2SO2	X(tot)%
W+S			4450		4458		-0.2	16	-0.2
Sulfur Dioxide		8200	4450	506	669	93.8	85.0	132	90.7
Oxygen		8200		5593		31.8		2607	
Sulfur Dioxide		8200	4450	597	743	92.7	83.3	189	89.4
W+G		8200		7375		10.1		825	10.1

COS (ppm)	SUM In	SUM Out	Delta S	Effic. (%)
0	4450	4458	-8	-0.2
138	12650	1313	11337	89.6
512	8200	6105	2095	25.5
183	12650	1523	11127	88.0
125	8200	7500	700	8.5

SIL11	200psig	154°C	0/10% W	G+S	A'	G+S+W	B'	G+W	G'
		In (ppm)		Out (ppm)					
	H2O	H2S (ppm)	SO2 (ppm)	H2S (ppm)	SO2 (ppm)	X(H2S)%	X(SO2)%	H2S-2SO2	X(tot)%
G		8200		7827		4.5		373	
G+S	**0%**	8200	4400	284	833	96.5	81.1	782	91.1
G+S+W	**10%**	8200	4400	598	877	92.7	80.1	556	88.3
G+W		8200		7954		3.0		246	

COS (ppm)	SUM In	SUM Out	Delta S	Effic. (%)
293	8200	8120	80	1.0
80	12600	1197	11403	90.5
114	12600	1589	11011	87.4
87	8200	8041	159	1.9

SIL12	100psig	154°C	0/10% W	G+S	A'	G+S+W	B'	G+S	A'
		In (ppm)		Out (ppm)					
	H2O	H2S (ppm)	SO2 (ppm)	H2S (ppm)	SO2 (ppm)	X(H2S)%	X(SO2)%	H2S-2SO2	X(tot)%
G		8200		7838		4.4		362	
G+S	0%	8200	4400	719	1072	91.2	75.6	825	85.8
G+S+W	10%	8200	4400	1445	1325	82.4	69.9	605	78.0
G+S	0%	8200	4400	1036	1181	87.4	73.2	726	82.4
G		8200		7700		6.1		500	

COS (ppm)	SUM In	SUM Out	Delta S	Effic. (%)
298	8200	8136	64	0.8
116	12600	1907	10693	84.9
135	12600	2905	9695	76.9
116	12600	2333	10267	81.5
110	8200	7810	390	4.8

	300sccm	154°C	10% W	200psig					
		In (ppm)		Out (ppm)					
Silica	Procedure	H2S (ppm)	SO2 (ppm)	H2S (ppm)	SO2 (ppm)	X(H2S)%	X(SO2)%	H2S-2SO2	X(tot)%
W+G+S	D'	8200	4400	736	847	91.0	80.8	358	87.4
W+S+G	D	8200	4450	506	669	93.8	85.0	132	90.7
W+G+S	D'	8200	4450	597	743	92.7	83.3	189	89.4
G+S+W	B'	8200	4400	598	877	92.7	80.1	556	88.3
Avg						92.6	82.3	309	89.0

COS (ppm)	SUM In	SUM Out	Delta S	Effic. (%)
172	12600	1755	10845	86.1
138	12650	1313	11337	89.6
183	12650	1523	11127	88.0
114	12600	1589	11011	87.4
152	12625	1545	11080	88

Avg

	300sccm	154°C	10% W	200psig					
		In (ppm)		Out (ppm)					
Catalyst	Procedure	H2S (ppm)	SO2 (ppm)	H2S (ppm)	SO2 (ppm)	X(H2S)%	X(SO2)%	H2S-2SO2	X(tot)%
Silica	D'	8200	4400	736	847	91.0	80.8	358	87.4
E-Alumina	D'	8550	4350	70	68	99.2	98.4	-84	98.9

COS (ppm)	SUM In	SUM Out	Delta S	Effic. (%)
172	12600	1755	10845	86.1
85	12900	223	12677	98.3

APPENDIX J SSRP Micro-Bubbler Processed Data

Molten Sulfur + E-alumina

MSAL01 150 psig 60/120scc 10% W W+G+S D'

	In (ppm):		Out (ppm):						
T(°C)	H2S (ppm)	SO2 (ppm)	H2S (ppm)	SO2 (ppm)	COS (ppm)	X(H2S)%	X(SO2)%	X(tot)%	H2O
154	8900	0	11119	0	1825	-24.9	#DIV/0!	-24.9	10%
154	8900	4200	3141	0	2644	64.7	100.0	76.0	10%
140	8900	4200	2130	69	2012	76.1	98.4	83.2	10%

MSAL01 150 psig 140°C 10% W

	In (ppm):		Out (ppm):						
F (sccm)	H2S (ppm)	SO2 (ppm)	H2S (ppm)	SO2 (ppm)	COS (ppm)	X(H2S)%	X(SO2)%	X(tot)%	H2O
60	8900	4200	2130	69	2012	76.1	98.4	83.2	10%
120	8900	4200	2694	641	1331	69.7	84.7	74.5	10%

MSAL09 300 psig 154°C 0/10% W S+C S+C+W S+W

	In (ppm):		Out (ppm):						
Switch	H2S (ppm)	SO2 (ppm)	H2S (ppm)	SO2 (ppm)	COS (ppm)	X(H2S)%	X(SO2)%	X(tot)%	H2O
-CO	0	5850	0	5810	0		0.7	0.7	**0%**
+CO	0	5850	0	5880	230		-0.5	-0.5	**0%**
+CO	0	4500	0	4580	420		-1.8	-1.8	**0%**
+CO	0	4500	0	4520	440		-0.4	-0.4	**10%**
+CO	0	5850	0	5420	200		7.4	7.4	**10%**
-CO	0	5850	0	5450	12		6.8	6.8	**10%**
-CO	0	5850	0	5900	3		-0.9	-0.9	**0%**

MSAL02 150 psig 140°C 10% W W+(G+S) D*
MSAL05 150 psig 140°C 10% W W+(G+S) D*

	In (ppm):		Out (ppm):						
F(SO2)	H2S (ppm)	SO2 (ppm)	H2S (ppm)	SO2 (ppm)	COS (ppm)	X(H2S)%	X(SO2)%	X(tot)%	H2O
20	8900	3800	2826	630	424	68.2	83.4	72.8	10%
24	8630	4420	1869	783	441	78.3	82.3	79.7	10%
25	8565	4570	1633	894	395	80.9	80.4	80.8	10%
26	8500	4720	1590	969	422	81.3	79.5	80.6	10%
27	8440	4860	1494	1248	407	82.3	74.3	79.4	10%
27.5	8400	4940	1453	1554	430	82.7	68.5	77.5	10%

MSAL05 127 sccm 140°C 10% W

	In (ppm):		Out (ppm):						
P (psig)	H2S (ppm)	SO2 (ppm)	H2S (ppm)	SO2 (ppm)	COS (ppm)	X(H2S)%	X(SO2)%	X(tot)%	H2O
150	8400	4900	1494	1048	407	82.2	78.6	80.9	10%
200	8400	4900	1108	808	416	86.8	83.5	85.6	10%
250	8400	4900	839	502	459	90.0	89.8	89.9	10%
300	8400	4900	640	318	475	92.4	93.5	92.8	10%

MSAL06 300 psig 140°C 10% W W+(G+S) D*

	In (ppm):		Out (ppm):						
F(sccm)	H2S (ppm)	SO2 (ppm)	H2S (ppm)	SO2 (ppm)	COS (ppm)	X(H2S)%	X(SO2)%	X(tot)%	**SV (h-1)**
64	8400	5300	316	465	1062	96.2	91.2	94.3	3840
128	8400	5300	550	578	662	93.5	89.1	91.8	7680
192	8400	5300	584	684	639	93.0	87.1	90.7	11520
256	8400	5300	857	1135	414	89.8	78.6	85.5	15360

MSAL07	**300 psig**	**140/154°C**	**0/10% W**		**W+S+G**	**D**	**S+G**	**S+G+W**	**B**
	In (ppm):		Out (ppm):						
T (°C)	H2S (ppm)	SO2 (ppm)	H2S (ppm)	SO2 (ppm)	COS (ppm)	X(H2S)%	X(SO2)%	X(tot)%	H2O
140	0	**5850**	0	5849	0	#DIV/0!	0.0	0.0	10%
140	8400	**5850**	950	981	360	88.7	83.2	86.4	10%
154	8400	**5850**	465	358	1330	94.5	93.9	94.2	**10%**
154	8400	**5850**	439	235	1632	94.8	96.0	95.3	**0%**
154	8400	**5850**	611	100	780	92.7	98.3	95.0	**10%**

MSAL08	**300 psig**	**154°C**	**0% W**		**C+S**				
	In (ppm):		Out (ppm):						
Switch	H2S (ppm)	SO2 (ppm)	H2S (ppm)	SO2 (ppm)	COS (ppm)	X(H2S)%	X(SO2)%	X(tot)%	H2O
-SO2	0	0	92	0	10900				0%
+SO2	0	5850	0	5870	1250		-0.3	-0.3	0%

Blank (no Molten Sulfur, no catalyst)

BLN0	300 psig	154°C	10% W		S+W	S+W+C	S+W		
	In (ppm):		Out (ppm):						
Switch	H2S (ppm)	SO2 (ppm)	H2S (ppm)	SO2 (ppm)	COS (ppm)	X(H2S)%	X(SO2)%	F (sccm)	X(tot)%
-H2O	0	**5850**	0	**5850**	0		0.0	128	0.0
-CO	0	**5850**	0	**5800**	0		0.9	128	0.9
+CO	0	5850	0	5600	70		4.3	128	4.3
-CO	0	**5850**	0	**5800**	0		0.9	**128**	0.9
-CO	0	**4400**	0	**4350**	0		1.1	**125**	1.1

BLN1	300 psig	154/140°C	10% W		S+W	S+W+G			
	In (ppm):		Out (ppm):						
Switch	H2S (ppm)	SO2 (ppm)	H2S (ppm)	SO2 (ppm)	COS (ppm)	X(H2S)%	X(SO2)%	T (°C)	X(tot)%
-H2O	0	**5850**	0	**5900**	0		-0.9	154°C	-0.9
+H2O	0	**5850**	0	**5850**	0		0.0	154°C	0.0
+G	8800	5850	166	1036	400	98.1	82.3	154°C	91.8
+G	9000	5300	225	643	400	97.5	87.9	**154°C**	93.9
+G	9000	5300	220	634	410	97.6	88.0	**140°C**	94.0

BLN2	300 psig	140/154°C	10/0% W		W+G	W+G+S	G+S	G	
	In (ppm):		Out (ppm):						
Switch	H2S (ppm)	SO2 (ppm)	H2S (ppm)	SO2 (ppm)	COS (ppm)	X(H2S)%	X(SO2)%	T (°C)	X(tot)%
-SO2	8800	0	8461	0	289	3.9		140°C	3.9
+SO2	8800	5300	329	579	691	96.3	89.1	**140°C**	93.6
+SO2	8800	5300	399	763	881	95.5	85.6	**154°C**	91.8
+SO2-W	8800	5300	498	831	1077	94.3	84.3	154°C	90.6
-SO2	8800	0	8307	0	588	5.6	#DIV/0!	154°C	5.6

BLN3	300 psig	154/140°C	0/10% W		S+G	S+G+W			
	In (ppm):		Out (ppm):						
Switch	H2S (ppm)	SO2 (ppm)	H2S (ppm)	SO2 (ppm)	COS (ppm)	X(H2S)%	X(SO2)%	Variable	X(tot)%
-H2O	0	5500	0	5496	0		0.1	**154°C**	0.1
+G	8800	5500	752	899	1003	91.5	83.7	**154°C**	88.5
+G	8800	5500	899	962	985	89.8	82.5	**140°C**	87.0
+G	8800	5500	899	962	985	89.8	82.5	**300 psig**	87.0
+G	8800	5500	2884	2379	893	67.2	56.7	**200 psig**	63.2
+G	8800	5500	899	962	985	89.8	82.5	**125 sccm**	87.0
+G	8800	5500	7345	5301	546	16.5	3.6	**250 sccm**	11.6
+H2O	8800	5500	3392	2253	466	61.5	59.0	250 sccm	60.5

APPENDIX K SSRP CSTR Processed Data

Blank (no Molten Sulfur, no catalyst)

BLR01 **1.5 LPM** **155°C** **0% W** **G** **G+S** **S**

		In (ppm)		Out (ppm)					
	P (psig)	H2S (ppm)	SO2 (ppm)	H2S (ppm)	SO2 (ppm)	X(H2S)%	X(SO2)%	H2S-2SO2	X(tot)%
-SO2	200	8000		7970		0.4		30	0.4
+SO2	200	8000	5450	7515	5360	6.1	1.7	305	4.3
+SO2	200	8200	4850	7730	4785	5.7	1.3	340	4.1
+SO2	200	8320	4360	7940	4300	4.6	1.4	260	3.5
+SO2	200	8450	3920	8140	3870	3.7	1.3	210	2.9
+Coal Gas	200	8640	3270	8390	3250	2.9	0.6	210	2.3
-Coal Gas	200		3280		3280		0.0	0	0.0

	COS (ppm)	SUM In	SUM Out	Delta S	Effic. (%)
-SO2	5	8000	7975	25	0.3
+SO2	165	13450	13040	410	3.0
+SO2	175	13050	12690	360	2.8
+SO2	180	12680	12420	260	2.1
+SO2	180	12370	12190	180	1.5
+Coal Gas	180	11910	11820	90	0.8
-Coal Gas	0	3280	3280	0	0.0

BLR02 **1.5 LPM** **155°C** **0% W** **G** **G+S** **S**

		In (ppm)		Out (ppm)					
	P (psig)	H2S (ppm)	SO2 (ppm)	H2S (ppm)	SO2 (ppm)	X(H2S)%	X(SO2)%	H2S-2SO2	X(tot)%
-SO2	200	6400		6308		1.4		92	1.4
+SO2	200	6400	8300	5670	8283	11.4	0.2	696	5.1
+SO2	200	6400	7500	6100	7493	4.7	0.1	286	2.2
+Coal Gas	250	2700	6100	2035	4700	24.6	23.0	-2135	23.5
-Coal Gas	250		6100		6083		0.3	-34	0.3

	COS (ppm)	SUM In	SUM Out	Delta S	Effic. (%)
-SO2	60	6400	6368	32	0.5
+SO2	270	14700	14223	477	3.2
+SO2	260	13900	13853	47	0.3
+Coal Gas	275	8800	7010	1790	20.3
-Coal Gas	0	6100	6083	17	0.3

BLR03 **1.5 LPM** **155°C** **0/10% W** **G** **G+S** **G+S+W** **S+W**

		In (ppm)		Out (ppm)					
	H2O	H2S (ppm)	SO2 (ppm)	H2S (ppm)	SO2 (ppm)	X(H2S)%	X(SO2)%	H2S-2SO2	X(tot)%
-SO2	0%	8350		8318		0.4		32	0.4
+SO2	0%	8350	4800	8038	4637	3.7	3.4	-14	3.6
+W	10%	8350	4800	4075	2371	51.2	50.6	-583	51.0
S+W	10%		4800		4838		-0.8	76	-0.8

	COS (ppm)	SUM In	SUM Out	Delta S	Effic. (%)
-SO2	14	8350	8332	18	0.2
+SO2	73	13150	12748	402	3.1
+W	56	13150	6502	6648	50.6
S+W	0	4800	4838	-38	-0.8

Molten Sulfur + E-alumina

TST02 1.0 LPM 155°C 0% W S S+G

		In (ppm)		Out (ppm)					
	H2O	H2S (ppm)	SO2 (ppm)	H2S (ppm)	SO2 (ppm)	X(H2S)%	X(SO2)%	H2S-2SO2	X(tot)%
-Coal Gas	0%	0	4600	0	4600		0.0	0	0.0
+Coal Gas	0%	8500	4600	324	755	96.2	83.6	486	91.8

	COS (ppm)	SUM In	SUM Out	Delta S	Effic. (%)
-Coal Gas	0	4600	4600	0	0.0
+Coal Gas	767	13100	1846	11254	85.9

TST03 1.0 LPM 155°C 10% W S S+W S+W+G

	In (ppm)		Out (ppm)					
RPM	H2S (ppm)	SO2 (ppm)	H2S (ppm)	SO2 (ppm)	X(H2S)%	X(SO2)%	H2S-2SO2	X(tot)%
	0	3800	0	3784		0.4	-32	0.4
500	8500	3800	615	765	92.8	79.9	1815	88.8
750	8500	3800	562	711	93.4	81.3	1760	89.7
1000	8500	3800	454	707	94.7	81.4	1860	90.6
1250	8500	3800	448	698	94.7	81.6	1848	90.7
1500	8500	3800	470	684	94.5	82.0	1798	90.6

RPM	COS (ppm)	SUM In	SUM Out	Delta S	Effic. (%)
	0	3800	3784	16	0.4
500	780	12300	2160	10140	82.4
750	824	12300	2097	10203	83.0
1000	829	12300	1990	10310	83.8
1250	822	12300	1968	10332	84.0
1500	843	12300	1997	10303	83.8

TST04 300psig 155°C 10% W W W+(S+G)

	In (ppm)		Out (ppm)					
F (SLPM)	H2S (ppm)	SO2 (ppm)	H2S (ppm)	SO2 (ppm)	X(H2S)%	X(SO2)%	H2S-2SO2	X(tot)%
1.0	8500	4600	140	1050	98.4	77.2	1260	90.9
0.5	8500	4600	80	700	99.1	84.8	620	94.0

F (SLPM)	COS (ppm)	SUM In	SUM Out	Delta S	Effic. (%)
1.0	745	13100	1935	11165	85.2
0.5	950	13100	1730	11370	86.8

TST05 1.0 LPM 155°C 10% W W W+(S+G)

	In (ppm)		Out (ppm)					
P(psig)	H2S (ppm)	SO2 (ppm)	H2S (ppm)	SO2 (ppm)	X(H2S)%	X(SO2)%	H2S-2SO2	X(tot)%
375	8500	4600	135	350	98.4	92.4	-135	96.3
350	8500	4600	145	370	98.3	92.0	-105	96.1
300	8500	4600	190	430	97.8	90.7	-30	95.3
250	8500	4600	200	640	97.6	86.1	380	93.6
250	8500	0	8500	0	0.0		0	

P(psig)	COS (ppm)	SUM In	SUM Out	Delta S	Effic. (%)
375	630	13100	1115	11985	91.5
350	625	13100	1140	11960	91.3
300	550	13100	1170	11930	91.1
250	530	13100	1370	11730	89.5
250	800	8500	9300	-800	-9.4

TST06	1.0 LPM	155°C	10% W	W	W+(S+G)				
		In (ppm)		Out (ppm)					
P(psig)		H2S (ppm)	SO2 (ppm)	H2S (ppm)	SO2 (ppm)	X(H2S)%	X(SO2)%	H2S-2SO2	X(tot)%
300		8800	3800	272	291	96.9	92.3	1510	95.5
350		8800	3800	241	135	97.3	96.4	1229	97.0
400		8800	3800	221	64	97.5	98.3	1107	97.7
250		8800	3800	272	415	96.9	89.1	1758	94.5
250		8800		8762		0.4		38	

P(psig)	COS (ppm)	SUM In	SUM Out	Delta S	Effic. (%)
300	660	12600	1223	11377	90.3
350	707	12600	1083	11517	91.4
400	733	12600	1018	11582	91.9
250	598	12600	1285	11315	89.8
250	928	8800	9690	-890	-10.1

Molten Sulfur + E-alumina

EAL01 1.0 LPM 155°C 10% W 300psig S+W+G

	In (ppm)		Out (ppm)					
	H2S (ppm)	SO2 (ppm)	H2S (ppm)	SO2 (ppm)	X(H2S)%	X(SO2)%	H2S-2SO2	X(tot)%
-Coal Gas		**4700**	0	4674		0.6	-52	0.6
+Coal Gas	**8100**	**4700**	76	1546	99.1	67.1	1716	87.3
+Coal Gas	**8400**	**4000**	175	964	97.9	75.9	2153	90.8
+Coal Gas	**8600**	**3500**	408	495	95.3	85.9	2182	92.5
-Coal Gas		**3500**	4	3485		0.4	-34	0.3

	COS (ppm)	SUM In	SUM Out	Delta S	Effic. (%)
-Coal Gas	0	4700	4674	26	0.6
+Coal Gas	473	12800	2095	10705	83.6
+Coal Gas	517	12400	1656	10744	86.6
+Coal Gas	573	12100	1476	10624	87.8
-Coal Gas	4	3500	3493	7	0.2

EAL02 300psig 155°C 10% W W+S+G

	In (ppm)		Out (ppm)					
F (SLPM)	H2S (ppm)	SO2 (ppm)	H2S (ppm)	SO2 (ppm)	X(H2S)%	X(SO2)%	H2S-2SO2	X(tot)%
1.0		3900	0	3898		0.1	-4	0.1
1.0	8400	3900	121	1063	98.6	72.7	2605	90.4
2.0	8400	3900	186	1187	97.8	69.6	2788	88.8
3.0	8400	3900	417	1238	95.0	68.3	2659	86.5

F (SLPM)	COS (ppm)	SUM In	SUM Out	Delta S	Effic. (%)
1.0	0	3900	3898	2	0.1
1.0	643	12300	1827	10473	85.1
2.0	410	12300	1783	10517	85.5
3.0	267	12300	1922	10378	84.4

EAL03 2.8 LPM 155°C 10% W W+S+G

		In (ppm)		Out (ppm)					
P(psig)		H2S (ppm)	SO2 (ppm)	H2S (ppm)	SO2 (ppm)	X(H2S)%	X(SO2)%	H2S-2SO2	X(tot)%
300			4550	5	4554		-0.1	3	-0.2
300		8200	4550	485	1120	94.1	75.4	855	87.4
350		8400	4500	389	911	93.9	81.3	833	89.9
400		8800	4400	429	739	95.1	83.2	1049	91.2
300		8800	4400	647	867	92.6	80.3	1087	88.5
275		8800	4400	747	890	91.5	79.8	1033	87.6
250	**+ SO2**	8800	4400	785	927	91.1	78.9	1069	87.0
250	**- SO2**	8800		8350	0	5.1		450	

P(psig)		COS (ppm)	SUM In	SUM Out	Delta S	Effic. (%)
300		0	4550	4559	-9	-0.2
300		301	12750	1906	10844	85.1
350		325	12900	1625	11275	87.4
400		344	13200	1512	11688	88.5
300		317	13200	1831	11369	86.1
275		290	13200	1927	11273	85.4
250	**+ SO2**	**290**	13200	2002	11198	84.8
250	**- SO2**	**410**	8800	8760	40	0.5

EAL04 **2.8 LPM** **350psig** **10% W** **W+S+G**

		In (ppm)		Out (ppm)					
T(°C)		H2S (ppm)	SO2 (ppm)	H2S (ppm)	SO2 (ppm)	X(H2S)%	X(SO2)%	H2S-2SO2	X(tot)%
155			4400	6	4371		0.7	-64	0.5
155		8250	4400	327	1503	96.0	65.8	2129	85.5
140		8350	4150	373	1168	94.0	73.4	2013	87.7
125	**+ SO2**	8450	3900	537	857	93.6	78.0	1827	88.7
125	**- SO2**	8450		8355	0	1.1		95	

T(°C)		COS (ppm)	SUM In	SUM Out	Delta S	Effic. (%)
155		0	4400	4377	23	0.5
155		330	12650	2160	10490	82.9
140		193	12500	1734	10766	86.1
125	**+ SO2**	**95**	12350	1489	10861	87.9
125	**- SO2**	**85**	8450	8440	10	0.1

EAL05 **300psig** **125°C** **2.3 LPM** **W+(S+G)**

		In (ppm)		Out (ppm)					
H2O (%)		H2S (ppm)	SO2 (ppm)	H2S (ppm)	SO2 (ppm)	X(H2S)%	X(SO2)%	H2S-2SO2	X(tot)%
10.0		8480	3800	833	313	90.2	91.8	673	90.7
14.3		8480	3800	823	342	90.3	91.0	741	90.5
18.2		8480	3800	810	357	90.4	90.6	784	90.5

H2O (%)		COS (ppm)	SUM In	SUM Out	Delta S	Effic. (%)
10.0		115	12280	1261	11019	89.7
14.3		93	12280	1258	11022	89.8
18.2		74	12280	1241	11039	89.9

EAL06 **2.8 LPM** **155°C** **10% W** **W+S+G**

		In (ppm)		Out (ppm)					
P(psig)	**H2O (%)**	H2S (ppm)	SO2 (ppm)	H2S (ppm)	SO2 (ppm)	X(H2S)%	X(SO2)%	H2S-2SO2	X(tot)%
270	**10%**	7900		7805		1.2	#DIV/0!	95	1.2
250	15%	7900		7763		1.7	#DIV/0!	137	1.7
220	**10%**	7900		7775		1.6	#DIV/0!	125	1.6

P(psig)		COS (ppm)	SUM In	SUM Out	Delta S	Effic. (%)
270		112	7900	7917	-17	-0.2
250		63	7900	7826	74	0.9
220		41	7900	7816	84	1.1

Molten Sulfur only (no catalyst)

MS01 300psig 155°C W+G

		In (ppm)		Out (ppm)					
F (SLPM)	H2O (%)	H2S (ppm)	SO2 (ppm)	H2S (ppm)	SO2 (ppm)	X(H2S)%	X(SO2)%	H2S-2SO2	X(tot)%
1.0	10	9000		8397		6.7		603	6.7
2.0	10	9000		8501		5.5		499	5.5
3.0	10	9000		8453		6.1		547	6.1
4.0	10	9000		8556		4.9		444	4.9
1.0	**10.0**	9000		8397		6.7		603	6.7
1.0	**10.0**	9000		8459		6.0		541	6.0
1.1	**18.2**	9000		8384		6.8		616	6.8
1.3	**30.8**	9000		8657		3.8		343	3.8

F (SLPM)	H2O (%)	COS (ppm)	SUM In	SUM Out	Delta S	Effic. (%)
1.0	10	521	9000	8918	82	0.9
2.0	10	256	9000	8757	243	2.7
3.0	10	159	9000	8612	388	4.3
4.0	10	115	9000	8671	329	3.7
1.0	**10.0**	521	9000	8918	82	0.9
1.0	**10.0**	520	9000	8979	21	0.2
1.1	**18.2**	460	9000	8844	156	1.7
1.3	**30.8**	418	9000	9075	-75	-0.8

MS02 300psig 155°C 10% W W+G+S

		In (ppm)		Out (ppm)					
F (SLPM)	H2O (%)	H2S (ppm)	SO2 (ppm)	H2S (ppm)	SO2 (ppm)	X(H2S)%	X(SO2)%	H2S-2SO2	X(tot)%
1.0	10	9000		8388		6.8		612	6.8
1.0	10	9000	4400	822	123	90.9	97.2	-376	92.9
2.0	10	9000	4400	1056	647	88.3	85.3	438	87.3
3.0	10	9000	4400	1249	883	86.1	79.9	717	84.1
1.0	**10.0**	9000	4400	822	123	90.9	97.2	-376	92.9
1.2	**25.0**	9000	4400	984	17	89.1	99.6	-750	92.5

F (SLPM)	H2O (%)	COS (ppm)	SUM In	SUM Out	Delta S	Effic. (%)
1.0	10	664	9000	9052	-52	-0.6
1.0	10	831	13400	1776	11624	86.7
2.0	10	421	13400	2124	11276	84.1
3.0	10	255	13400	2387	11013	82.2
1.0	**10.0**	830	13400	1775	11625	86.8
1.2	**25.0**	620	13400	1621	11779	87.9

MS03 300psig 155°C 10% W 2.0 SLPM W+G+S

	In (ppm)		Out (ppm)					
	H2S (ppm)	SO2 (ppm)	H2S (ppm)	SO2 (ppm)	X(H2S)%	X(SO2)%	H2S-2SO2	X(tot)%
	8500		8036		5.5		464	5.5
	5667		5293		6.6		374	6.6
	4250		4081		4.0		169	4.0
	8500		8127		4.4		373	4.4
-SO2	**8500**		8127		4.4		373	
+SO2	**8500**	**4330**	639	576	92.5	86.7	353	90.5
		4330		4323		0.2	-14	0.2

	H2S (ppm)	SO2 (ppm)	COS (ppm)	SUM In	SUM Out	Delta S	Effic. (%)
	8500		395	8500	8431	69	0.8
	5667		215	5667	5508	159	2.8
	4250		157	4250	4238	12	0.3
	8500		385	8500	8512	-12	-0.1
-SO2	**8500**		385	8500	8512	-12	-0.1
+SO2	**8500**	**4330**	475	12830	1690	11140	86.8
		4330	6	4330	4329	1	0.0

MS04 **300psig** **155°C** **W+S** **W+S+G**

		In (ppm)		Out (ppm)					
F (SLPM)	H2O (%)	H2S (ppm)	SO2 (ppm)	H2S (ppm)	SO2 (ppm)	X(H2S)%	X(SO2)%	H2S-2SO2	X(tot)%
2.0	**10.0**		4400	4	4384		0.4	-36	0.3
1.7	**11.8**	7140	5240	237	2068	96.7	60.5	559	81.4
1.8	**16.7**	6740	4940	258	2159	96.2	56.3	920	79.3
1.9	**21.1**	6380	4680	295	2071	95.4	55.7	867	78.6
Rs (RPM)	H2O (%)	H2S (ppm)	SO2 (ppm)	H2S (ppm)	SO2 (ppm)	X(H2S)%	X(SO2)%	H2S-2SO2	X(tot)%
1500	21.1	6380	4680	272	1833	95.7	60.8	414	81.0
1000	21.1	6380	4680	295	2071	95.4	55.7	867	78.6
750	21.1	6380	4680	250	1773	96.1	62.1	316	81.7
500	21.1	6380	4680	253	2013	96.0	57.0	793	79.5

F (SLPM)	H2O (%)	COS (ppm)	SUM In	SUM Out	Delta S	Effic. (%)
2.0	**10.0**	0	4400	4388	12	0.3
1.7	**11.8**	530	12380	2835	9545	77.1
1.8	**16.7**	475	11680	2892	8788	75.2
1.9	**21.1**	482	11060	2848	8212	74.2
Rs (RPM)	H2O (%)	COS (ppm)	SUM In	SUM Out	Delta S	Effic. (%)
1500	21.1	495	11060	2600	8460	76.5
1000	21.1	482	11060	2848	8212	74.2
750	21.1	485	11060	2508	8552	77.3
500	21.1	481	11060	2747	8313	75.2

MS05 **300psig** **155°C** **W+(S+G)**

		In (ppm)		Out (ppm)					
Feed	F (SLPM)	H2S (ppm)	SO2 (ppm)	H2S (ppm)	SO2 (ppm)	X(H2S)%	X(SO2)%	H2S-2SO2	X(tot)%
+SO2	1.8	7500	5000	193	2937	97.4	41.3	3181	75.0
-SO2	**1.8**	7500		6909		7.9		591	
-SO2	**2.2**	9330		8844		5.2		486	
+SO2	2.2	9330	4000	1014	383	89.1	90.4	1082	89.5

Feed	F (SLPM)	COS (ppm)	SUM In	SUM Out	Delta S	Effic. (%)
+SO2	1.8	660	12500	3790	8710	69.7
-SO2	**1.8**	585	7500	7494	6	0.1
-SO2	**2.2**	480	9330	9324	6	0.1
+SO2	2.2	535	13330	1932	11398	85.5

MS06 **300psig** **10% W** **W+S+G**

		In (ppm)		Out (ppm)					
T (°C)	F (SLPM)	H2S (ppm)	SO2 (ppm)	H2S (ppm)	SO2 (ppm)	X(H2S)%	X(SO2)%	H2S-2SO2	X(tot)%
155	2.2		4000		3997		0.1	-6	
155	2.0	8500	4380	1318	790	84.5	82.0	2	83.6
145	2.0	8500	4380	1427	876	83.2	80.0	65	82.1
136	2.0	8500	4380	1493	989	82.4	77.4	225	80.7
128	2.0	8500	4380	1591	1018	81.3	76.8	185	79.7

T (°C)	COS (ppm)	SUM In	SUM Out	Delta S	Effic. (%)
155	0	4000	3997	3	0.1
155	493	12880	2601	10279	79.8
145	305	12880	2608	10272	79.8
136	275	12880	2757	10123	78.6
128	167	12880	2776	10104	78.4

Molten Sulfur + Double Load of E-alumina

DAL02	300psig	155°C	10% W	W+S	W+S+G				
		In (ppm)		Out (ppm)					
	F (SLPM)	H2S (ppm)	SO2 (ppm)	H2S (ppm)	SO2 (ppm)	X(H2S)%	X(SO2)%	H2S-2SO2	X(tot)%
	1.0		3200		3197		0.1	-6	
	1.0	7500	3200	186	787	97.5	75.4	2488	90.9
	F (SLPM)				COS (ppm)	SUM In	SUM Out	Delta S	Effic. (%)
	1.0				0	3200	3197	3	0.1
	1.0				783	10700	1756	8944	83.6

DAL03	300psig	155°C		W+S	W+S+G				
		In (ppm)		Out (ppm)					
F (SLPM)	H2O (%)	H2S (ppm)	SO2 (ppm)	H2S (ppm)	SO2 (ppm)	X(H2S)%	X(SO2)%	H2S-2SO2	X(tot)%
1.0	**10.0**		3640		3637		0.1	-6	
1.0	**10.0**	8500	3640	334	506	96.1	86.1	1898	93.1
1.1	**18.2**	8500	3640	434	350	94.9	90.4	1486	93.5
1.0	10.0	8500	3640	334	506	96.1	86.1	1898	93.1
2.0	10.0	8500	3640	493	789	94.2	78.3	2305	89.4
	RPM								
2.0	**1000**	8500	3640	493	789	94.2	78.3	2305	89.4
2.0	**750**	8500	3640	526	780	93.8	78.6	2254	89.2
F (SLPM)	H2O (%)				COS (ppm)	SUM In	SUM Out	Delta S	Effic. (%)
1.0	**10.0**				0	3640	3637	3	0.1
1.0	**10.0**				953	12140	1793	10347	85.2
1.1	**18.2**				709	12140	1493	10647	87.7
1.0	10.0				953	12140	1793	10347	85.2
2.0	10.0				541	12140	1823	10317	85.0
	RPM								
2.0	**1000**				541	12140	1823	10317	85.0
2.0	**750**				554	12140	1860	10280	84.7

DAL04	300psig	155°C		W+S	W+S+G				
		In (ppm)		Out (ppm)					
F (SLPM)	H2O (%)	H2S (ppm)	SO2 (ppm)	H2S (ppm)	SO2 (ppm)	X(H2S)%	X(SO2)%	H2S-2SO2	X(tot)%
2.0	**10.0**		4040		4039		0.0	-2	
2.0	**10.0**	8500	4040	404	597	95.2	85.2	1210	92.0
1.0	**10.0**	8500	4040	498	61	94.1	98.5	44	95.5
1.1	**18.2**	8500	4040	380	143	95.5	96.5	326	95.8
1.2	**25.0**	8500	4040	475	91	94.4	97.7	127	95.5
F (SLPM)	H2O (%)				COS (ppm)	SUM In	SUM Out	Delta S	Effic. (%)
2.0	**10.0**				0	4040	4039	1	0.0
2.0	**10.0**				576	12540	1577	10963	87.4
1.0	**10.0**				629	12540	1188	11352	90.5
1.1	**18.2**				655	12540	1178	11362	90.6
1.2	**25.0**				536	12540	1102	11438	91.2

DAL05 10% H2O 155°C 2 SLPM W+S W+S+G

		In (ppm)		Out (ppm)					
	P (psig)	H2S (ppm)	SO2 (ppm)	H2S (ppm)	SO2 (ppm)	X(H2S)%	X(SO2)%	H2S-2SO2	X(tot)%
	300		3300		3299		0.0	-2	
	300	8500	3300	347	113	95.9	96.6	1779	96.1
	350	8500	3300	453	16	94.7	99.5	1479	96.0
	350	8500	3300	438	14	94.8	99.6	1490	96.2
	400	8500	3300	664	0	92.2	100.0	1236	94.4

P (psig)	COS (ppm)	SUM In	SUM Out	Delta S	Effic. (%)
300	0	3300	3299	1	0.0
300	567	11800	1027	10773	91.3
350	586	11800	1055	10745	91.1
350	564	11800	1016	10784	91.4
400	533	11800	1197	10603	89.9

DAL06 300psig 155°C W+S W+S+G

		In (ppm)		Out (ppm)					
F (SLPM)	H2O (%)	H2S (ppm)	SO2 (ppm)	H2S (ppm)	SO2 (ppm)	X(H2S)%	X(SO2)%	H2S-2SO2	X(tot)%
2.0	**10.0**		4550		4553		-0.1	6	
2.0	**10.0**	8500	4550	295	578	96.5	87.3	261	93.3
1.9	**10.5**	9000	3200	2244	0	75.1	100.0	356	81.6
1.95	**10.26**	8750	3900	776	22	91.1	99.4	218	93.7
2.05	**9.76**	8270	5150	192	855	97.7	83.4	-512	92.2

F (SLPM)	H2O (%)	COS (ppm)	SUM In	SUM Out	Delta S	Effic. (%)
2.0	**10.0**	0	4550	4553	-3	-0.1
2.0	**10.0**	463	13050	1336	11714	89.8
1.9	**10.5**	570	12200	2814	9386	76.9
1.95	**10.26**	533	12650	1331	11319	89.5
2.05	**9.76**	481	13420	1528	11892	88.6

DAL07 300psig 10% W 18.2% W W+G W+G+S

		In (ppm)		Out (ppm)					
T (°C)	F (SLPM)	H2S (ppm)	SO2 (ppm)	H2S (ppm)	SO2 (ppm)	X(H2S)%	X(SO2)%	H2S-2SO2	X(tot)%
155	2.0	8760		8199		6.4		561	6.4
155	2.0	8760	4400	300	698	96.6	84.1	1056	92.4
155	1.1	8760	4400	273	209	96.9	95.3	105	96.3
145	1.1	8760	4400	334	63	96.2	98.6	-248	97.0
135	1.1	8760	4400	269	99	96.9	97.8	-111	97.2

T (°C)	F (SLPM)	COS (ppm)	SUM In	SUM Out	Delta S	Effic. (%)
155	2.0	559	8760	8758	2	0.0
155	2.0	465	13160	1463	11697	88.9
155	1.1	721	13160	1203	11957	90.9
145	1.1	588	13160	985	12175	92.5
135	1.1	508	13160	876	12284	93.3

DAL08	300psig	135°C		S+G	S+G+W				
		In (ppm)		Out (ppm)					
F (SLPM)	H2O (%)	H2S (ppm)	SO2 (ppm)	H2S (ppm)	SO2 (ppm)	X(H2S)%	X(SO2)%	H2S-2SO2	X(tot)%
0.9	**0.0**	8760	4700	104	682	98.8	85.5	620	94.2
1.1	**18.2**	8760	4700	150	461	98.3	90.2	132	95.5
2.0	**10.0**	8760	4700	265	705	97.0	85.0	505	92.8
2.10	**9.5**	8760	4700	295	624	96.6	86.7	313	93.2
2.10	**9.5**		4700	3	4733		-0.7	63	

F (SLPM)	H2O (%)	COS (ppm)	SUM In	SUM Out	Delta S	Effic. (%)
0.9	**0.0**	452	13460	1238	12222	90.8
1.1	**18.2**	406	13460	1017	12443	92.4
2.0	**10.0**	214	13460	1184	12276	91.2
2.10	**9.5**	234	13460	1153	12307	91.4
2.10	**9.5**	5	4700	4741	-41	-0.9

DAL09	10% H2O	135°C	2 SLPM	W+S	W+S+G				
		In (ppm)		Out (ppm)					
	P (psig)	H2S (ppm)	SO2 (ppm)	H2S (ppm)	SO2 (ppm)	X(H2S)%	X(SO2)%	H2S-2SO2	X(tot)%
	300		4040		4039		0.0	-2	
	300	8700	4040	383	175	95.6	95.7	587	95.6
	350	8700	4040	551	7	93.7	99.8	83	95.6
	350	8700	4040	321	25	96.3	99.4	349	97.3

P (psig)	COS (ppm)	SUM In	SUM Out	Delta S	Effic. (%)
300	0	4040	4039	1	0.0
300	367	12740	925	11815	92.7
350	463	12740	1021	11719	92.0
350	440	12740	786	11954	93.8

DAL10	10% H2O	135°C	2 SLPM	W+S	W+S+G				
		In (ppm)		Out (ppm)					
	P (psig)	H2S (ppm)	SO2 (ppm)	H2S (ppm)	SO2 (ppm)	X(H2S)%	X(SO2)%	H2S-2SO2	X(tot)%
	300		4200		4207		-0.2	14	
	300	8700	4200	290	615	96.7	85.4	1240	93.0
	350	8700	4200	210	529	97.6	87.4	1148	94.3
	400	8700	4200	166	509	98.1	87.9	1152	94.8
	450	8700	4200	148	504	98.3	88.0	1160	94.9
	375	8700	4200	178	595	98.0	85.8	1312	94.0
	325	8700	4200	250	675	97.1	83.9	1400	92.8

P (psig)	COS (ppm)	SUM In	SUM Out	Delta S	Effic. (%)
300	0	4200	4207	-7	-0.2
300	233	12900	1138	11762	91.2
350	213	12900	952	11948	92.6
400	211	12900	886	12014	93.1
450	218	12900	870	12030	93.3
375	202	12900	975	11925	92.4
325	192	12900	1117	11783	91.3

DAL11 **300psig** **135°C** **W+G** **W+G+S**

		In (ppm)		Out (ppm)					
F (SLPM)	H2O (%)	H2S (ppm)	SO2 (ppm)	H2S (ppm)	SO2 (ppm)	X(H2S)%	X(SO2)%	H2S-2SO2	X(tot)%
2.0	**10.0**	9200		9030		1.8		170	
1.8	**11.1**	9200		8977		2.4		223	
1.5	**13.3**	9200		8944		2.8		256	
1.5	**13.3**	9200	3000	3945	0	57.1	100.0	-745	67.7
1.2	**16.7**	7670	3750	2145	0	72.0	100.0	-1975	81.2
1.0	**20.0**	6440	5400	399	2	93.8	100.0	-4755	96.6

F (SLPM)	H2O (%)
2.0	**10.0**
1.8	**11.1**
1.5	**13.3**
1.5	**13.3**
1.2	**16.7**
1.0	**20.0**

COS (ppm)	SUM In	SUM Out	Delta S	Effic. (%)
160	9200	9190	10	0.1
170	9200	9147	53	0.6
172	9200	9116	84	0.9
184	12200	4129	8071	66.2
249	11420	2394	9026	79.0
388	11840	789	11051	93.3

DAL12 **300psig** **135°C** **W+S** **W+S+G**

		In (ppm)		Out (ppm)					
F (SLPM)	H2O (%)	H2S (ppm)	SO2 (ppm)	H2S (ppm)	SO2 (ppm)	X(H2S)%	X(SO2)%	H2S-2SO2	X(tot)%
1.35	**14.8**		3300		3272		0.8	-56	
1.35	**14.8**	8800	3300	1567	0	82.2	100.0	633	87.0
0.85	**23.5**	7800	5850	33	582	99.6	90.1	-2769	95.5
1.05	**19.05**	8330	4450	243	305	97.1	93.1	-203	95.7

F (SLPM)	H2O (%)
1.35	**14.8**
1.35	**14.8**
0.85	**23.5**
1.05	**19.05**

COS (ppm)	SUM In	SUM Out	Delta S	Effic. (%)
0	3300	3272	28	0.8
265	12100	1832	10268	84.9
568	13650	1183	12467	91.3
407	12780	955	11825	92.5

DAL13 **18.2% W** **135°C** **1 SLPM** **W+S** **W+S+G**

		In (ppm)		Out (ppm)					
	P (psig)	H2S (ppm)	SO2 (ppm)	H2S (ppm)	SO2 (ppm)	X(H2S)%	X(SO2)%	H2S-2SO2	X(tot)%
	300		4400		4412		-0.3	24	
	300	8400	4400	202	251	97.6	94.3	-100	96.5
	350	8400	4400	256	130	97.0	97.0	-396	97.0
	400	8400	4400	284	36	96.6	99.2	-612	97.5
	400	8400		4947		41.1		3453	41.1

P (psig)
300
300
350
400
400

COS (ppm)	SUM In	SUM Out	Delta S	Effic. (%)
0	4400	4412	-12	-0.3
402	12800	855	11945	93.3
373	12800	759	12041	94.1
367	12800	687	12113	94.6
172	8400	5119	3281	39.1

DAL14	300psig	135°C		W+S	W+S+G				
		In (ppm)		Out (ppm)					
F (SLPM)	H2O (%)	H2S (ppm)	SO2 (ppm)	H2S (ppm)	SO2 (ppm)	X(H2S)%	X(SO2)%	H2S-2SO2	X(tot)%
1.10	**18.2**	7500	5100	268	116	96.4	97.7	-2736	97.0
1.10	**18.2**		5100		5120		-0.4	40	
1.10	**18.2**	7500	5100	232	200	96.9	96.1	-2532	96.6

F (SLPM)	H2O (%)	COS (ppm)	SUM In	SUM Out	Delta S	Effic. (%)
1.10	**18.2**	509	12600	893	11707	92.9
1.10	**18.2**	13	5100	5133	-33	-0.6
1.10	**18.2**	469	12600	901	11699	92.8

DAL15	300psig	135°C		S+G	S+G+W				
		In (ppm)		Out (ppm)					
F (SLPM)	H2O (%)	H2S (ppm)	SO2 (ppm)	H2S (ppm)	SO2 (ppm)	X(H2S)%	X(SO2)%	H2S-2SO2	X(tot)%
0.90	**0.0**	7500	5100	238	199	96.8	96.1	-2540	96.5
1.00	**10.0**	8800	5100	296	150	96.6	97.1	-1396	96.8
1.10	**18.2**	7500	5100	262	182	96.5	96.4	-2598	96.5
1.20	**25.0**	7500	5100	327	123	95.6	97.6	-2781	96.4
2.10	**14.3**	7500	5100	244	697	96.7	86.3	-1550	92.5

F (SLPM)	H2O (%)	COS (ppm)	SUM In	SUM Out	Delta S	Effic. (%)
0.90	**0.0**	687	12600	1124	11476	91.1
1.00	**10.0**	696	13900	1142	12758	91.8
1.10	**18.2**	664	12600	1108	11492	91.2
1.20	**25.0**	548	12600	998	11602	92.1
2.10	**14.3**	286	12600	1227	11373	90.3

DAL16	300psig	18.2% W		W+S	W+S+G				
		In (ppm)		Out (ppm)					
T (°C)	F (SLPM)	H2S (ppm)	SO2 (ppm)	H2S (ppm)	SO2 (ppm)	X(H2S)%	X(SO2)%	H2S-2SO2	X(tot)%
135	1.1	7500	5100	220	273	97.1	94.6	-2374	96.1
125	1.1	7500	5100	246	362	96.7	92.9	-2222	95.2
	125°C								
F (SLPM)	W (%)	H2S (ppm)	SO2 (ppm)	H2S (ppm)	SO2 (ppm)	X(H2S)%	X(SO2)%	H2S-2SO2	X(tot)%
1.1	**18.2**	7500	5100	246	362	96.7	92.9	-2222	95.2
1.2	**16.7**	8400	4550	304	295	96.4	93.5	-414	95.4
1.3	**15.4**	9300	4150	328	226	96.5	94.6	1124	95.9
1.3	15.4	9300		6369		31.5		2931	

T (°C)	F (SLPM)	COS (ppm)	SUM In	SUM Out	Delta S	Effic. (%)
135	1.1	681	12600	1174	11426	90.7
125	1.1	448	12600	1056	11544	91.6
	125°C					
F (SLPM)	W (%)	COS (ppm)	SUM In	SUM Out	Delta S	Effic. (%)
1.1	**18.2**	448	12600	1056	11544	91.6
1.2	**16.7**	419	12950	1018	11932	92.1
1.3	**15.4**	386	13450	940	12510	93.0
1.3	15.4	261	9300	6630	2670	28.7

DAL17	300psig	125°C		W+S	W+S+G				
		In (ppm)		Out (ppm)					
F (SLPM)	H2O (%)	H2S (ppm)	SO2 (ppm)	H2S (ppm)	SO2 (ppm)	X(H2S)%	X(SO2)%	H2S-2SO2	X(tot)%
1.0	**10.0**	7500	5100	106	634	98.6	87.6	-1538	94.1
1.1	**9.1**	8400	4550	223	446	97.3	90.2	-31	94.8
1.2	**8.3**	9300	4150	582	78	93.7	98.1	574	95.1
1.1 SLPM	**8.3% W**								
	P (psig)	H2S (ppm)	SO2 (ppm)	H2S (ppm)	SO2 (ppm)	X(H2S)%	X(SO2)%	H2S-2SO2	X(tot)%
	300	9300	4150	582	78	93.7	98.1	574	95.1
	350	8400	4550	342	78	95.9	98.3	-886	96.8
	400	8400	4550	320	27	96.2	99.4	-966	97.3
	300	8400	4550	379	168	95.5	96.3	-743	95.8

F (SLPM)	H2O (%)	COS (ppm)	SUM In	SUM Out	Delta S	Effic. (%)
1.0	**10.0**	619	12600	1359	11241	89.2
1.1	**9.1**	605	12950	1274	11676	90.2
1.2	**8.3**	556	13450	1216	12234	91.0
1.1 SLPM	**8.3% W**					
	P (psig)	COS (ppm)	SUM In	SUM Out	Delta S	Effic. (%)
	300	556	13450	1216	12234	91.0
	350	607	12950	1027	11923	92.1
	400	662	12950	1009	11941	92.2
	300	604	12950	1151	11799	91.1